Chronologie et dynamique de la formation des terrasses fluviales dans des chaînes des montagnes avec une surrection modéré : l'exemple du Vénézuéla et de l'Albanie

Oswaldo Guzman Gutierrez Guzman Gutierrez

UNIVERSITÉ DE GRENOBLE

THÈSE

Pour obtenir le grade de

DOCTEUR DE L'UNIVERSITÉ DE GRENOBLE

Spécialité : **Sciences de la Terre, de l'Univers et de l'Environnement**

Arrêté ministériel : 7 août 2006

Présentée par

Oswaldo José GUZMAN GUTIERREZ

Thèse dirigée par **Jean-Louis MUGNIER** et
codirigée par **Riccardo VASSALLO et Franck AUDEMARD**

préparée au sein de **L'Institut des Sciences de la Terre** (ISTerre)
dans **l'École Doctorale Terre, Univers, Environnement**

Timing and dynamics of river terraces formation in moderate uplifted ranges: the example of Venezuela and Albania

Thèse soutenue publiquement le **30 octobre 2013**
devant le jury composé de :

Mr Bernard DELCAILLAU
Professeur, Université de Caen, Rapporteur

Mr Vincent REGARD
M. de Conf. - HDR, Université de Toulouse, Rapporteur

Mr Christian BECK
Professeur, Université de Savoie, Président du jury

Mr François ROURE
Professeur, IFP-Paris, Examinateur

Mr Stéphane DOMINGUEZ
Chargé de recherche, Geosciences Montpellier, Examinateur

Mr Jean-Louis MUGNIER
Directeur de recherche, CNRS - Université de Savoie, Directeur de thèse

Mr Riccardo VASSALLO
M. de conf., Université de Savoie, Co-directeur de thèse

Mr Franck AUDEMARD
Professeur, FUNVISIS - Universidad Central de Venezuela, Co-directeur de thèse

Acknoledgments

The completion of this thesis required long hours of work, it would have been impossible to carry out without the help and support of many people and institution; here I would like to thank some of them.

Firstly, I want to thank my three advisors: Jean-Louis Mugnier, Riccardo Vassallo and Franck Audemard for the help they have given me throughout these four long years. Jean-Louis thank for having proposed me this thesis, for having confidence in me and for listening from the first day. Riccardo thank for your full availability, for helping me considerably to improve my ideas and to have been able to send me your optimism during my moments of doubts. Franck thank for our precise-productive technical and personal discussion.

The Albania research was in large part because of Jean-Louis Mugnier and François Jouanne's prior researches and their ongoing interest in the geology of the Balkan region. The generosity and logistical support during each of my two research trips of Reshep Koçi of the Institute of Seismology of Albania will never be forgotten. The research was funded by the NATO and the Science for Peace team throught the project SFP 977993.

The research in Venezuela was intellectually and logistically supported by a number of folks very deserving of recognition. Franck thanks to guide us in the reconignition of the Southeastern flank of the Mérida Andes. Javier, Miguel I am grateful for your help during the field work. Javi thank again for the technical and logistical contribution about the Venezuelan terraces. Santiago I am thankful for supporting in the construction of the DEM of the study areas and for your help in the use of satellites images. Enzo thank for introduce me ArcGIS. Field work was funded by ECOS Nord project PI-2007001823, and was also posibble by the logistical support provided by the Fundación Venezolana de Investigaciones Sismológicas (FUNVISIS). I want to thank FUNVISIS for provide us aerial photographs and topographic maps of the study area

I wish to give an especial thankful to Riccardo Vassallo and Julien Carcaillet to guide me in the world of ^{10}Be dating. Both took a considerable amount of personal time to assist me in the samples preparation, chemichal treatment and attainment of ^{10}Be exposure age.

I want to thank the members of the jury, Bernard Delcaillau, Vincent Regard, François Roure, Stephane Dominguez and Christian Beck for accepting to review my work.

Finally, I would like to thank to Universidad Simon Bolivar and specifically the department of earth sciences, for giving me permission to conduct this thesis and for financial

aid to cover administrative costs of my stay in France. I also thanks to IRD-DPF for financial support provide me during the first three monts of the last year.

Abstract

This research addresses interactions between tectonics, climate and geomorphic processes at the surface of the Earth through the study of river terraces in Venezuela and Albania. Both areas have been exposed to moderate uplift, to Quaternary climatic variations and provide a wide record of river terraces. These contexts furnish opportunities to investigate the dynamics of terraces formation at 10^2-10^5 year time scale. Thus, a morphochronologic approach was applied in order to achieve greater understanding about this issue for the Venezuelan and Albanian rivers.

In the Pueblo Llano and Santo Domingo rivers system located in the Southeastern flank of the Mérida Andes in Venezuela, twelve river terraces were identified for the last 200 ka. Analysis of ^{10}Be concentration provides for the first time exposure ages for seven terraces and for one frontal moraine complex. A terraces model supported by these dating and geomorphologic, stratigraphic and sedimentologic data indicates that the formation of terraces was mainly controlled by high frequency (10^3-10^4 years) worldwide climatic variations through unsteady discharge of water and sediments. Nevertheless, the type of response was highly related to the altitude of the site and the influence of usptreams glaciers. As a matter of fact, in the upper reaches of the system, the succession of aggradation and incision phases were synchronized with the succession of cold-dry and warm-humid periods, while the lower reaches of the system show the opposite pattern. Based on the temporal restoration of the incision rate of the lower reaches of the system an uplift rate at 1.1 mm/a for the last 70 ka was estimated for the Southeastern flank of the MA. Additionally, the identification and dating of a frontal moraine complex located at elevation of 2300 m a.s.l. in the Pueblo Llano valley highlights the fact that the glacier advance during the Last Glacial Maximum, in other areas of the MA could have also reached lower elevation than those reported between 2900 and 3500 m a.s.l.

In the Albania domain, the terrace records of the six main Albanian rivers were analyzed. New geomorphologic and geochronological data were integrated with published data in order to propose a regional homogeneous stratigraphic/chronologic framework for the last 200 ka. Based on this framework the timing of formation of eleven regional river terraces was established. In Albania, the processes of terraces formation were also mainly controlled by high frequency (10^3-10^4 years) worldwide climatic variations. Nonetheless, the results also show that the geomorphic responses of the fluvial systems were probably modulated by the

size of the catchments and by eustatic variations. Indeed, for the period before the Marine Isotope Stage 2 (MIS 2), fill and strath terraces were formed in the large and small catchments, respectively. After the beginning of the MIS 2, a complex relation between climatic and eustatic variations only favored the development of strath terraces in large and small catchments. Despite of the differences between the rivers responses, the succession of aggradation or lateral erosion and incision phases were synchronized with the succession of cold-dry and warm-humid periods in all the rivers of Albania. The restoration of spatial and temporal variation of incision rate allowed: 1) identify the spatial variation of the mean long-term incision rate. It varies from less than 0.1 mm/a in Southern Albania to 1 mm/a in Northern Albania; 2) estimate vertical slip rates for eight active faults for the last 19 ka in Southern Albania. These vertical slip rates appear to decrease from ~2 to ~0.1 mm/a from the extensional domain in the Eastern Albania to the compressional domain in Western Albania.

All our results put in evidence that the worldwide climate variation was the main external force that controlled the process and timing of terraces formation, while the local climatic context had weak impact on the type of river response. Indeed, the type of river response was influenced by other variables such as: size of the catchment, altitude, glacial activity, eustatism and internal processes of the river. Finally, this research also shows that a moderate uplift context allowed recording low and high frequency climatic signal on different climatic cycles.

Résumé

Cette recherche porte sur les interactions entre la tectonique, le climat et les processus géomorphologiques de la surface de la Terre à travers l'étude des terrasses fluviales au Venezuela et l'Albanie. Ces deux domaines ont été soumis à une surrection modérée, aux variations climatiques du Quaternaire et fournissent un large registre de terrasses fluviales. Ces contextes donnent l'opportunité d'étudier la dynamique de la formation des terrasses fluviales à l'échelle de temps 10^2-10^5 ans. Ainsi, une approche morpho-chronologique a été appliquée afin de parvenir à une meilleure compréhension de cette dynamique dans les rivières du Venezuela et de l'Albanie.

Dans le système des rivières Pueblo Llano et Santo Domingo situé sur le flanc sud-est des Andes de Mérida au Venezuela, douze terrasses fluviales ont été identifiées pour les derniers 200 ka. Les mesures des concentrations du ^{10}Be réalisées sur les dépôts fluviatiles et glaciaires ont permis d'estimer l'âge d'exposition de sept terrasses et d'un complexe de moraines frontales. Un modèle dynamique de terrasses soutenues par ces datations et des données géomorphologiques, stratigraphiques et sédimentologiques, indique que la formation de terrasses est principalement contrôlée par des variations climatiques de haute fréquence (10^3 à 10^4 ans) qui induisent un déséquilibre entre capacité de transport de l'eau et apport des sédiments. Néanmoins, le type de réponse a été très lié à l'altitude du site et l'influence des glaciers en amont. En effet, dans la partie supérieure du système, la succession des phases d'aggradation et d'incision a été synchronisée avec la succession des périodes froides-sèches et chaudes-humides, tandis que la partie inférieure du système montre une tendance opposée. Basé sur la restauration temporelle du taux d'incision de la partie inférieure du système, un taux de surrection de 1.1 mm/an au cours des dernières 70 ka a été estimé pour le flanc sud-est des Andes de Mérida. En outre, l'identification et la datation d'un complexe de moraines frontales situé à l'altitude de 2300 m au dessus du niveau de la mer met en évidence le fait que l'avancée glaciaire au cours du Dernier Maximum Glaciaire, dans d'autres domaines des Andes de Mérida, pourrait également avoir atteint des élévations inférieures à celles déjà signalés entre 2900 et 3500 m au dessus du niveau de la mer.

En Albanie, les six principales rivières ont été analysées. De nouvelles données géomorphologiques et géochronologiques ont été intégrées aux données publiées afin de proposer un cadre stratigraphique et chronologique homogène à l'échelle régional pour les derniers 200 ka. Sur la base de ce cadre, l'âge de la formation de onze terrasses fluviales

régionales a été établi. En Albanie, les processus de formation des terrasses ont également été principalement contrôlés par des variations climatiques de haute fréquence (10^3 à 10^4 ans). Néanmoins, les résultats montrent également que la réponse géomorphologique du système fluvial était probablement modulée par la taille des bassins versants et par les variations eustatiques. En effet, pour la période précédant le MIS 2, les terrasses de remplissage et d'abrasion ont été formées repectivement dans les grands et petits bassins versants. Pour la période après le début du MIS 2, une relation complexe entre les variations climatiques et eustatiques a favorisé le développement de terrasses d'abrasion partout en Albanie. Malgré des différences entre les réponses des rivières, la succession de phases d'aggradation ou d'abrasion latérale et de phases d'incision a été synchronisée avec la succession des périodes froides-sèches et chaudes-humides dans toutes les rivières de l'Albanie. La reconstitution de la variation spatiale et temporelle des taux d'incision a permis: 1) d'identifier la variation spatiale du taux d'incision à long-terme, qui varie de moins de 0.1 mm/an dans le sud de l'Albanie à 1 mm/an dans le Nord de l'Albanie; 2) d'estimer la composante verticale de huit failles actives pour les dernières 19 ka dans le sud de l'Albanie. Ces taux de glissement verticaux semblent diminuer de ~2 à ~0.1 mm/an à partir du domaine d'extension de l'Albanie orientale au domaine de compression de l'Albanie occidentale.

Tous nos résultats mis en évidence que la variation du climat à travers le monde a été la principale force extérieure qui contrôlait le processus et le calendrier de la formation des terrasses, alors que le contexte climatique local a eu un impact faible sur le type de réponse de la rivière. En effet, le type de réponse de la rivière a été influencé par d'autres variables telles que la taille du bassin versant, l'altitude, l'activité glaciaire, l'eustatisme et les processus internes de la rivière. Enfin, cette recherche montre aussi qu'un contexte de soulèvement modéré permis enregistré des signaux climatiques de basse et haute fréquence sur différents cycles climatiques.

Table of Contents

Chapter I: General Introduction

River terraces are landforms underlain by alluvial deposits, located on the flanks of river valleys along a wide range of climatic and tectonic setting (**figure I.1**). They constitute a main target for geoscientists interested in fluvial processes, active tectonics and Quaternary paleoclimatology (e.g. Schumm, 1977; Bull, 1991; Pazzaglia, 2013).

River terraces represent the remnants of abandoned floodplains, stream bed or valley floor produced during a former stage of erosion or deposition. Thus, they are the morpho-sedimentologic expression of process adjustments in a river system (Schumm, 1977). These adjustments can be caused by a variety of mechanisms that occur on vastly different temporal and spatial scale. These mechanisms can be divided into intrinsic causes (internal fluvial system dynamical changes) and extrinsic causes (changes in external variables such as climate, tectonics, or base level). Intrinsic changes tend to occur on relatively short time scale and to produce small and localized landforms and deposits; extrinsic changes produce more continuous and valley scale river terraces (Schumm, 1977; Bull, 1990, 2009; Maddy et al., 2001). In this thesis, I am concerned for the main roles that play the external variables in the processes of river terraces formation. Thus, regional river terraces are the main objects to analyze in this study.

In order to address this task, here a brief synthesis about the knowledge of river terraces is presented. This synthesis is not intended to be a review and reconciliation of the wide literature on the subject of river terraces. Rather, it is evidence of the ongoing debate on the issue and justifies the problematic addressed in this work.

River terraces and the underlying alluvia are described as allostratigraphic units (Blum, 1993; Pazzaglia and Brandon, 2001). They consist of: 1) a relatively flat surface, called tread; 2) a steep slope, called riser, which separates the terrace from either adjacent floddplain, others terraces, or valley hillslopes, and 3) some terraces could have an erosional base, called strath (**figures I.1a, I.2**) (Fairbridge, 1968; Schumm, 1977; Bull, 1990; Blum and Tönqvist, 2000). The tread and the strath can be treated as paleogeodetic indicators of crustal deformation over geologic time scales (Burbank and Anderson, 2001; Bull, 2009). Geometry

of the terrace and the underlain alluvial deposit contains paleohydrologic information about hillslope erosion, fluvial transport, and catchment-scale climatic processes (Bull, 1991; Blum and Valastro, 1994; Paola and Mohrig, 1996; Maddy et al., 2001).

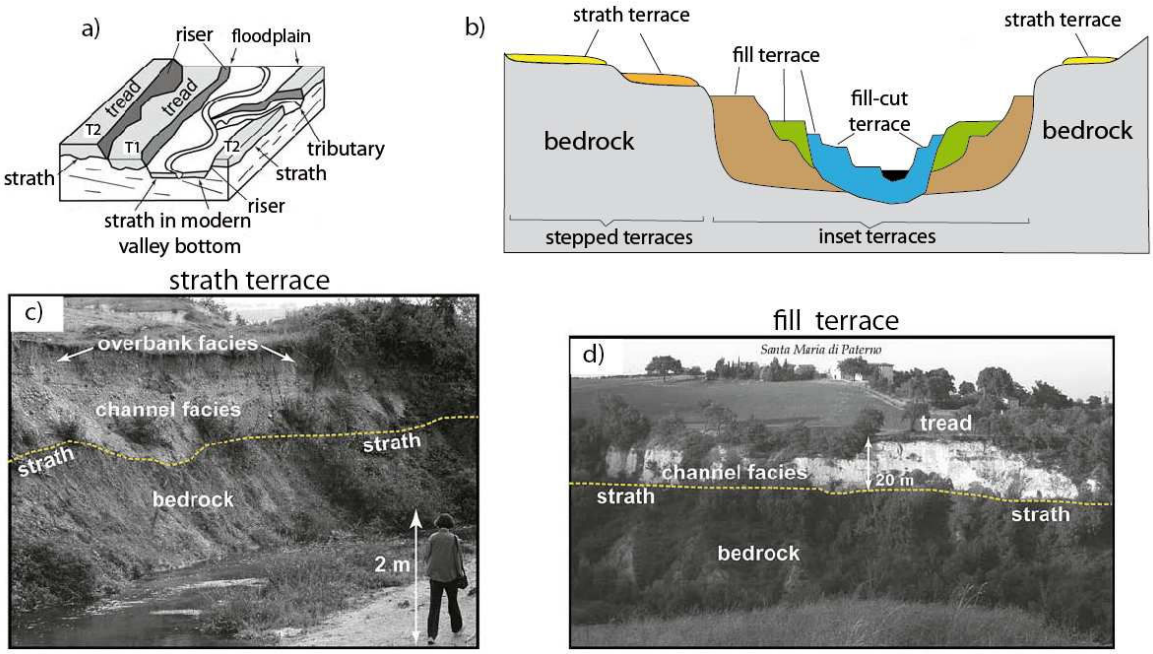

Figure I.1*. Cartoon and pictures showing river terraces morphology and the relationships between river terraces and their deposits (adapted from Wegmann and Pazzaglia, 2009).* ***a)*** *Schematic diagram illustrating the morphology of river terraces (T1, T2). Tread, riser and strath surfaces are shown.* ***b)*** *Schematical transversal cross-section through a river valley showing geometric differences between strath, fill and fill-cut terraces. An idealized complex of stepped and inset terraces is also shown (modified from Burbank and Anderson, 2001).* ***c)*** *Picture of an exposure of Late Holocene strath terrace in the Musone River basin – Italy.* ***d)*** *Picture of a fill terrace in the valley of the Torbido River – Italy.*

Based on the river terrace morphology and thickness of the underlain alluvial deposits, terraces are commonly organized into two main categories. A strath terrace is characterized by a distinct, subhorizontal erosional base, either carved into bedrock (i.e. rock substratum) or soft and poorly consolidated sediments. The strath is overlain by a relatively thin alluvial cover (≤ 5 m). This material represents the mobile alluvial cover of a river channel during a large discharge (**figure I.1.b, c**) (Easterbrook, 1999; Pazzaglia and Brandon, 2001; Pazzaglia, 2013). From a general point of view, a strath terrace represents periods of lateral erosion processes that widens valley bottom by syn-bedrock erosion and bedload transport. These processes can be followed by a subsequent vertical incision that deepens the river valley and

leads to the formation and preservation of the strath terrace (**figure I.2**) (Schumm, 1987; Ritter et al., 1995; Pazzaglia et al., 1998).

On the other hand, a fill terrace is characterized by a thick alluvial deposit that buried the river valley bottom. The base of a fill terrace can be sub-horizontal like a strath or it can also have irregularities linked to buried topography with local relief (**figure I.1.b, d**). Conversely to a strath terrace, a fill terrace represents a periods of valley aggradation. This aggradation is preserved as a fill terrace along the valley wall when the channel ceases aggrading and vertical incision affects the alluvial deposit. During the vertical incision of the alluvial deposit, several episodes of lateral erosion may occur, and multiple levels of terraces can be formed. The uppermost level is a fill terrace and the remaining lower terraces are called fill-cut or degradational terraces (Bull, 1990; Easterbrook, 1999; Burbank and Anderson, 2001; Pazzaglia, 2013).

Fill terraces may cover a substratum composed of alluvial material. This configuration (called inset terraces) suggests relatively strong aggradation phases with respect to weak vertical incision phases (**figure I.1b**). Instead, a configuration where the substratum is composed of bedrock, and the risers of recent alluvial material and bedrock (called stepped terraces), suggest the occurrence of a vertical surface motion (uplift) led by tectonics or glacioeustatism (**figure I.1b**). This vertical motion causes relatively strong vertical incision phases with respect to weak aggradations phases (Delcaillau, 2004).

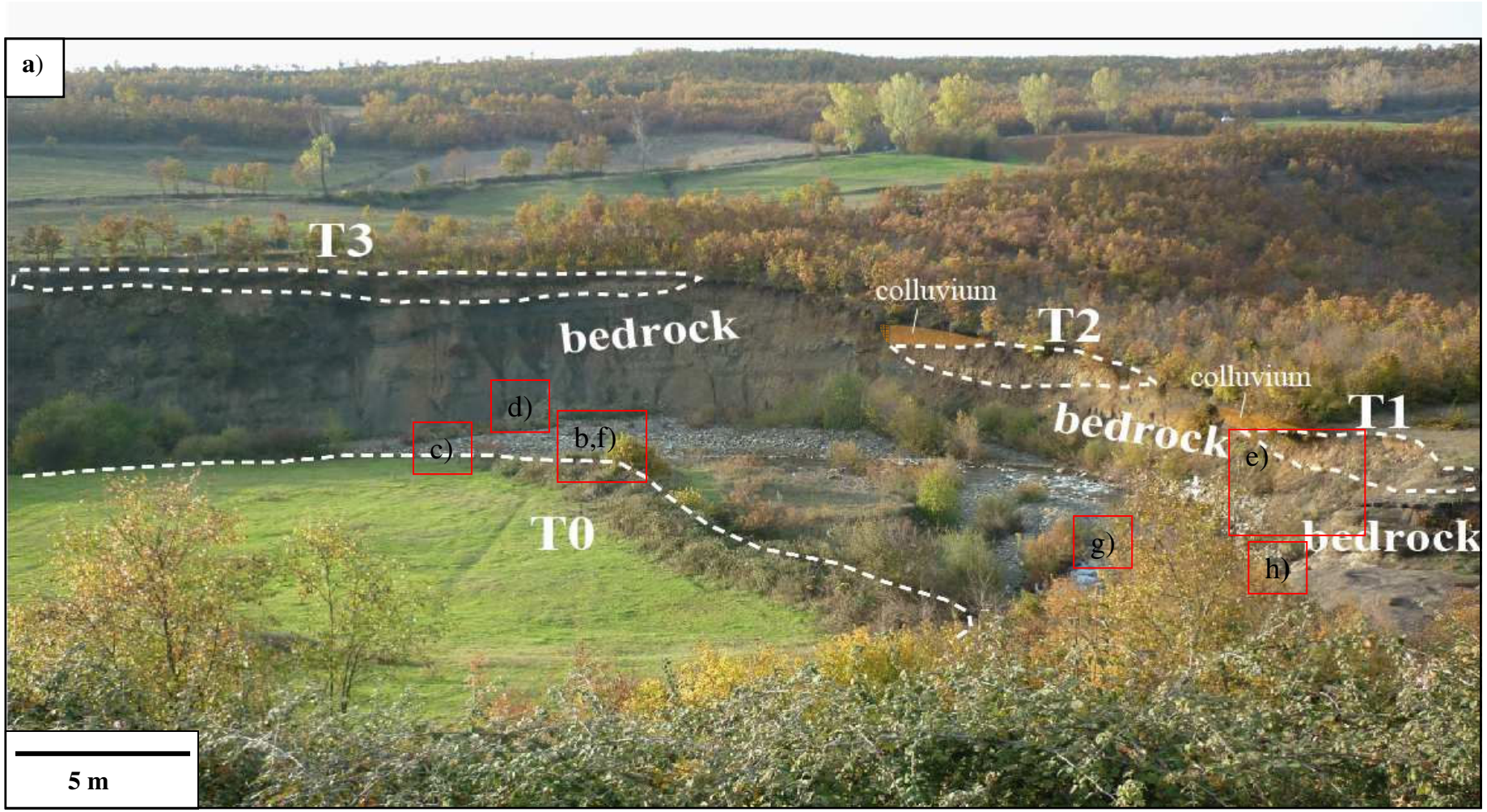

Figure I.2. *Description of main characteristics and dynamical processes in a river valley developing strath terraces. This example is observed in a tributary of the Mat river, Northern Albania.* ***a****) General context and pictures localization indicated by red squares. <u>Morphology of a bedrock river valley:</u>* ***b****) Bedrock channel with sediments being transported.* ***c****) The present floodplain (T0).* ***d****) Colluvial material burying fluvial facies.* ***e****) Abandoned river terrace. <u>Dynamical processes:</u>* ***f****) Motion of the bedload sediments that induce erosion of the substratum in the central part of the channel and widening of the active channel. Strath surface is thus formed.* ***h****) Regressive erosion affecting the bedrock channel.* ***i****) Vertical incision leads to the abandonment of a strath terrace.*

Morphology of a bedrock river valley:

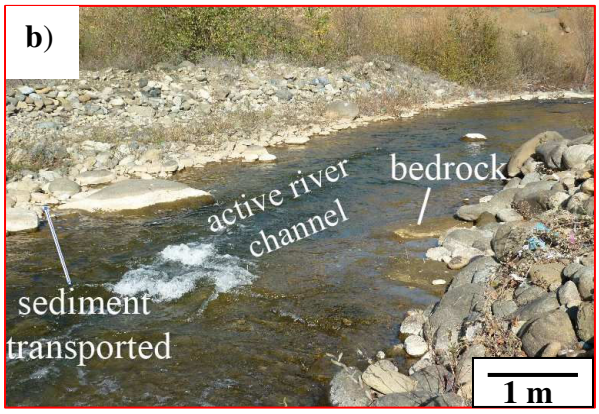

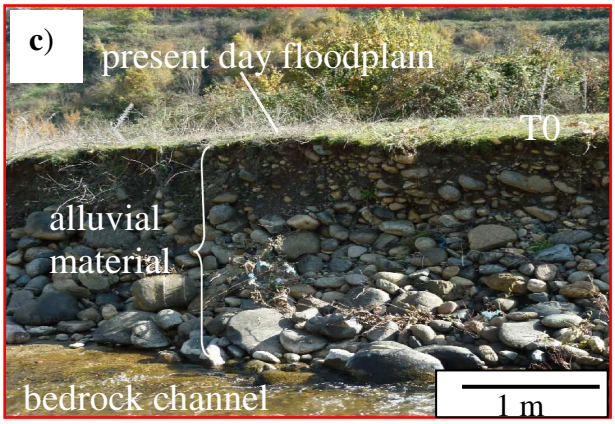

Dynamical processes:

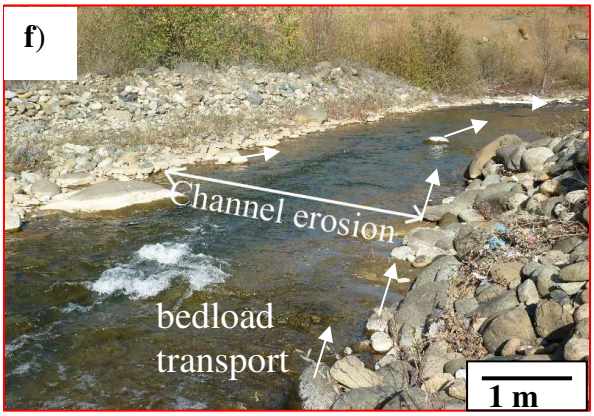

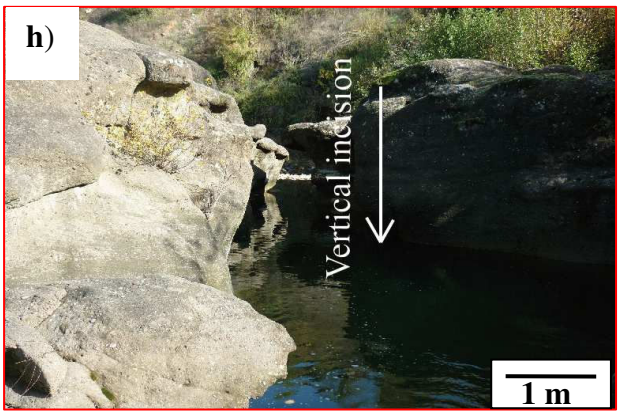

River terraces characteristics discussed above put in evidence that the terrace formation involves changes in the behaviour of a fluvial system. Channel lateral erosion, fluvial aggradation and vertical incision appear to occur as separate processes under certain circumstances over geomorphic time. Bull (1979, 1990) postulated that these behaviours are controlled by the critical power. This parameters is defined as a ratio, where the numerator (stream power) consists of those variables that increase the vertical incision, and the denominator (resisting power) consists of those variables that increase the fluvial aggradation:

$$Critical\ power = \frac{Stream\ power(\Omega)}{\mathrm{Re}\ sisting\ power} \tag{1}$$

Stream power (Ω) is the rate of energy dissipation against the bed and banks of a river or stream per unit downstream length. It is a function of the slope of the water surface (S) and the river discharge (Q) (Bagnold, 1960, 1977):

$$\Omega = \rho g Q S \tag{2}$$

where ρ is the density of water, and g the gravity. Resisting power is mainly controlled by bedload characteristics, channel morphology and bed roughness (Bull, 1991).

The case when the ratio of equation (1) is equal to one was primary envisioned by Gilbert (1877). This author proposed that when sediment load equals stream power, the river reaches stability in its vertical position with respect to a datum. Under these conditions, channel vertical incision and deposition are at a minimum (Knox, 1975; Leopold and Bull, 1979; Bull, 1990). Lateral migration and erosion of the river can nonetheless occur, thus wide and continuous erosional surface (strath) is developed. This stability condition later evolved to be the concept of graded or equilibrium condition of the river (Mackin, 1948; Knox, 1975; Leopold and Bull, 1979). From these graded conditions, strath terraces are abandoned when stream power becomes greater than the resisting power, leading to vertical incision and floodplain abandonment. When resisting power exceeds stream power, fluvial aggradations of bedload occur, and fill terraces are created with the following vertical incision phase (Bull, 1979, 1990).

Nowadays as equivalent of the equation (1), the relation of transport capacity (i.e. maximum amount of sediment of a given size that a river can transport in traction as bedload)

and sediment supply (i.e. amount and size of sediments avalaible to transport) is analysed in terms of river terraces formation. Some authors propose that fluvial aggradation is favoured during higher sediment supply relative to river transport capacity, whereas vertical incision is favoured when sediment supply is low relative to transport capacity (e.g. Fuller et al. 1998; Wegmann and Pazzaglia, 2009; Lewin and Gibbard, 2010).

In this conceptual model, switches between channel lateral erosion, fluvial aggradation and vertical incision states can occur by altering the available stream power (e.g. changing discharge or slope), and/or the resisting power (e.g. sediment load or size; Bull, 1979). Changes in these variables are mainly associated to climate and/or base level variations (caused by tectonic or eustatic perturbation), which are too abrupt or too great of magnitude for the river to internally adjust (e.g. Schumm, 1977; Van den Berg, 1996; Blum and Törnqvist, 2000). This statement bring us to the next question: what is the relationship between the climate and/or base level variations and the river system behaviour?

Leopold et al. (1964) proposed that climate variation (climate refers not only to mean annual temperature and moisture, but also to precipitation intensity, seasonality, and inter-annual variability) produces changes in the hydrology of the river system. Moreover, Bull and Knüpfer (1987) and Bull (1990, 1991) postulated that the river system should have responded to the climate change during the past 200 ka through vegetation-related variations in runoff and sediment supply. Recently, Macklin et al. (2012) proposed that a change in the frequency and magnitude of floods is the main direct driver that determines the response of river systems to climatic change. This results from altered precipitation and runoff regimes and it is coupled with variation in the input of sediments from channel-way and slope domains (**figure I.3**). Factors that alter erodibility and sediment supply, such as riverbank and catchment vegetation, frost action and permafrost melt, as well as the short- and long-term build-up and decay of glaciers and ice sheets, also play a key role in river system sediment dynamics. The geological and geomorphological characteristics of river catchments affected by climate change should be also considered, because their individual hydraulic systems and morphologies may process flood-producing events differently.

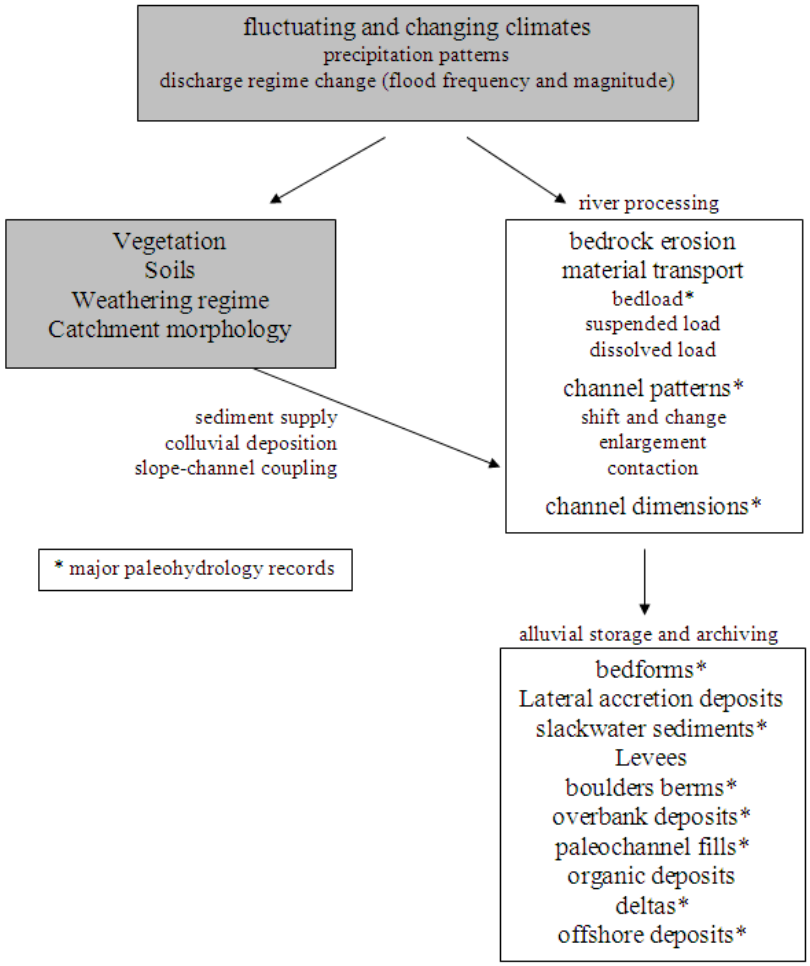

Figure I.3. *Diagram showing how rivers respond to and record the effects of climatic variation (from Macklin et al., 2012). The key controls on sediment supply are also shown. Sediments are transported in various forms by rivers. The dimensions and dynamics of river channels may also reflect climate controls. The sedimentary signals induced by climatic changes are recorded in a range of sedimentary environments.*

Several river terraces record coupled with geochronological data from around the world (e.g. Macklin et al., 2002; Bridgland and Westaway, 2008, Pazzaglia, 2013), and numerical modeling (e.g. Hancock and Anderson, 2002) suggest that the climatic variation is the main driving force of the terraces formation. Terraces analysis also show us that the variables of geography (e.g. latitude, elevation), geology (e.g. tectonic context, lithology characteristic of the basin), climatic context (e.g. temperate, mediterranean) and hydrology (e.g. presence or absence of glaciers) may play a role in the river response to climatic variation. Hence, different models to river formation in response to climatic variation have been proposed. These models were synthesised by Bridgland and Westaway (2008) (**figure I.4**), and they are described below taking Northwestern Europe as region of reference.

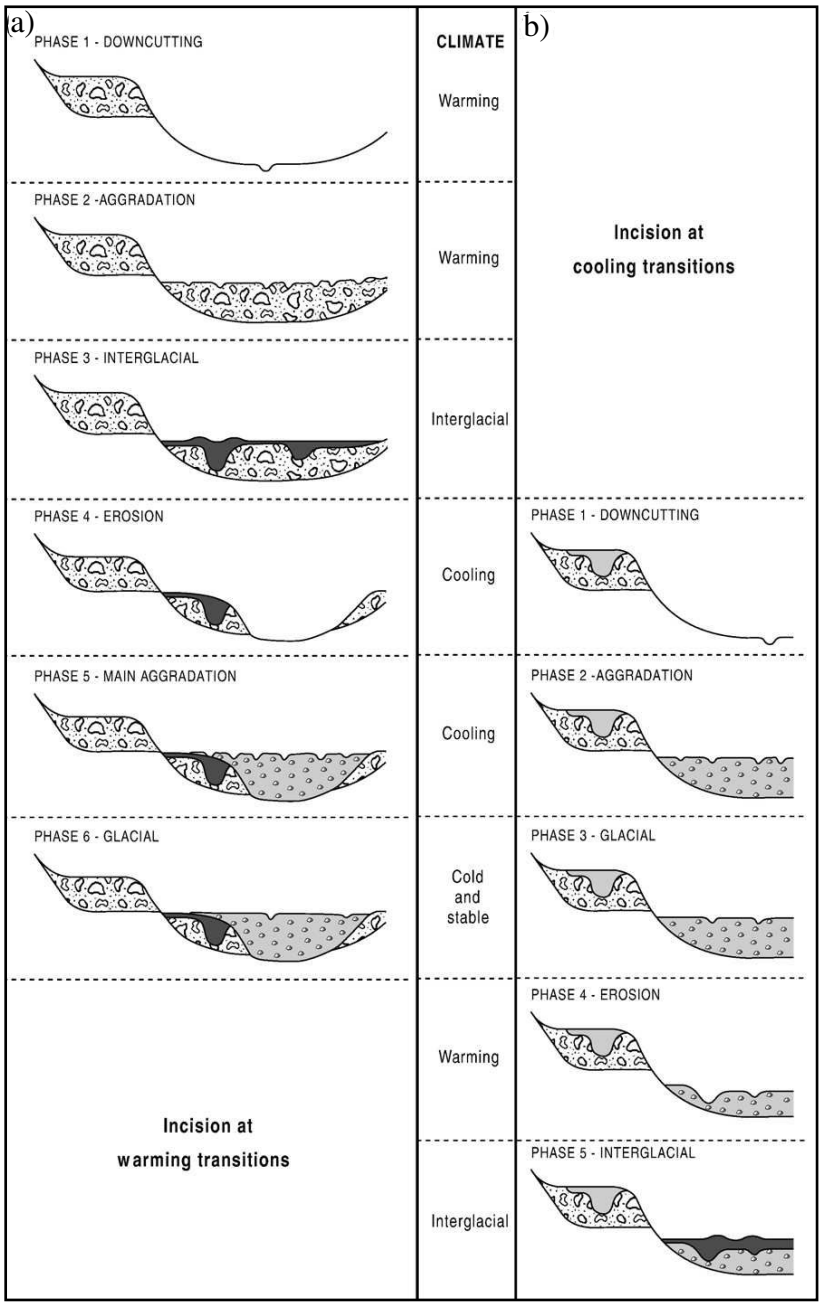

Figure. I.4. *Model for terrace formation in response to climatic forcing (from Bridgland and Westaway, 2008).* ***a****) Vertical incision at cold/warm transitions.* ***b****) Vertical incision at warm/cold transitions.*

In the temperate maritime climate of Northwestern Europe, the aggradation/incision phase of the Maas, lower Thames and Avon rivers are synchronized with the glacial and interglacial periods. Terrace alluvia were mainly aggraded during periods of cold, glacial climate, whereas river incision occurred during cold-to-warm transitions (**figure I.4**) (van der Berg, 1996, Bridgland, 2000; Bridgland et al., 2004). This river response is also reported for the temperate climate of Rocky Mountains in Western United States and the Southern Alps of

New Zealand (Bull and Knüpfer, 1987; Bull 1990), for the Mediterranean climate (e.g. Fuller et al., 1998; Macklin et al., 2002, Wegmann and Pazzaglia, 2009), for the semi arid climate of Central Asia in Mongolia (Vassallo et al., 2007) and for the sub-Saharan climate within the subtropical high pressure system of the central High Atlas mountains in Morocco (Arboleya et al., 2008; Delcaillau et al., 2010), among others regions. Nonetheless, in the Mediterranean region, the rivers seem also to respond to high frequency climatic variations (e.g. Heinrich event - Macklin et al., 2002). In the Somme and Moselle rivers also located in Northwestern Europe, terrace alluvia were mainly aggraded during the late phase of the glacial periods, whereas river incision occurred during warm-to-cold transitions (Antoine, 1994; Antoine et al., 2000, 2007, Cordier et al., 2004, 2006). In the Solent river located in Southern England, river terraces have been formed at both climatic transition episodes (Vandenberghe, 1995, 2008, Bridgland, 2001) (**figure I.4**). These results highlight the similarities between climate-driven terraces formation models for river valleys from all over the world, but put also in evidence the differences among terraces systems located in the same region.

In another way, an unsteady base level can also lead the formation of a river terrace. This instability may result from changing eustatic sea level, from changing uplift rate or active tectonics (Maddy et al., 2001). Particularly in the lower reaches of a river that drains to the sea, eustatic base level change can have dramatic effects on profile concavity. In general sea-level fall produce a vertical incision in the lower reaches of the river. It may progress upstream via knickpoint migration (Begin et al., 1981), resulting eventually in basin-wide terracing, although the absolute magnitude of incision may attenuate upstream, or incision may be stopped before complete recession has occurred. Conversely, sea-level rise generally results in aggradation. Nonetheless, the precise response of the shoreline to accommodation space, sediment flux, and discharge vary geographically and in concert with the ratio of the gradient of the coastal plain and gradient of the shelf (**figure I.5**) (Schumm, 1993; Blum and Törnqvist, 2000; Pazzaglia and Brandon, 2001).

Eustatic-driven river terraces have been documented from near the coast to at least 370 km upstream (e.g. Schumm, 1993, Ishihara et al., 2003). These terraces are associated to coastlines with high sediment fluxes, located within passive and active tectonics setting (e.g. Southern and Eastern United States, Northen Appenines and Eastern Japan) (Bull and Knüpfer, 1987; Autin et al., 1991; Pazzaglia and Brandon 2001; Nesci and Savelli, 2003, Ishihara et al., 2012). Schumm (1993) made an analysis of the main parameters (i.e.

characteristic of the eustatic change, geologic and geomorphic control) that play an important role in the river response due to eutatism. This author concluded that in most of the cases, large rivers are able to adjust to altered gradient caused by eustatic change, via adjustements of sinuosity, channel dimensions and/or roughness. Therefore, the effect of eustatic change is localized and minor; and except under extreme conditions, this effect would be limited to areas close to the sea. Hence the effect of eustatic changes on river behaviour is still controversial.

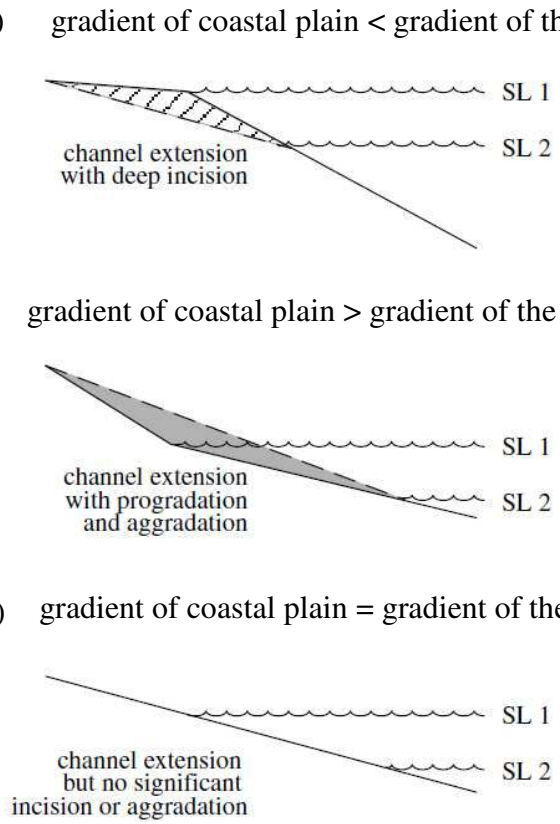

Figure I.5. *Models for fluvial response to eustatic fall as a function of coastal plain and shelf gradients (from Blum and Törnqvist, 2000).* ***a****) Incision through coastal plain is caused by knickpoint migration, due to steeper gradients of the shelf exposed by the sea level fall.* ***b****) Aggradation and progradation due to sea level fall across a shelf that has a gradient shallower than the coastal plain. This effect is produced because the channel needs to maintain a transport gradient for its bedload. Thus, the channel will have to rise as it progrades, resulting in aggradation at the coast.* ***c****) Channel extension with little incision, due to no differences between coastal plain and exposed shelf gradients during sea level fall.*

There is a general consensus that tectonic uplift provides the potential for vertical incision and preservation of river terraces (e.g. Maddy, 1997; Antoine et al., 2000, Bridgland,

2000; Wegmann and Pazzaglia, 2009). Additionally, tectonic perturbations may also lead to a base level change, and produce river terraces. For example, an increased uplift rate or a vertical movement of active fault may increase the river slope, and consequently the transport capacity would exceed the sediment supply, resulting in channel vertical incision that produces the abandonment of a terrace surface (Bull, 1991). This response has been specially documented in studies of coastal marine terraces, where impulsive tectonic uplift is recorded by marine terraces and upstream fluvial equivalent (e.g. Gardner et al., 1992; Molin et al., 2004; Sak et al., 2004, Pedoja et al., 2011).

The potential to create and preserve river terrace seem to be related to the uplift context. In tectonic regions with low uplift rate (e.g. Northwestern Europe) only the major and low frequency terrace formation events seem to be preserved (e.g. glacial/interglacial cycle) (e.g. Bridgland, 2000, Antoine et al., 2000; Bridgland et al., 2004). In areas with high uplift rates (e.g. Siwaliks piedmont - Himalaya region), younger terraces are preserved while older terraces are rapidly eroded (e.g. Delcaillau, 1986; Lavé and Avouac, 2000, Vignon, 2011). In region with moderate uplift (e.g. Mediterranean region), the response of the river to low and high frequency extrinsic changes seem to be preserved within the terraces record (e.g. Fuller et al., 1998; Macklin et al., 2002, 2012). Therefore, over different climate cycles, moderate uplift context seems to be the best to create and preserve a maximum of terraces through time.

The aim of this thesis is a better understanding of the impact of all these processes in river terraces formation. Specifically, the following questions are explored:

- Are the processes of terraces formation similar in different climatic setting?
- Are the high frequency and low frequency climatic variations globally recorded in the same manner by the river systems?
- Are the river terraces useful to determine tectonics rate and/or climatic variation in any geological, geomorphologic and climatic context?

In order to answer these questions, I applied a geomorphological and geochronological approach in two areas with different geological, geomorphological and climatic setting, both characterized by a moderate uplift such that the maximum number of terraces may be preserved: Venezuela and Albania.

- Venezuela

Venezuela is located North of the Equator between the latitude 0° and 12° N. Venezuelan climate varies from tropical humid conditions in the low elevation plains to glacier conditions in the highlands. No large glaciers are present nowadays, but they were well-developed in the high regions of the mountains ranges during the glacial periods. The climatic zonation is sensitive to the seasonal migration of the Intertropical Convergence Zone (ITCZ) that causes two distinct seasons: between December to March (when the ITCZ is South of the Equator) a relatively cool and dry season with winds from the North is installed over Venezuela, while a period of heavy rainfall and hot conditions occurs between June and November (when the ITCZ migrates Northward near to Venezuelan coast) (Hastenrath, 1984; Rull et al., 2010).

The Mérida Andes (MA) is an active orogen located in Western Venezuela, where several rivers (e.g. Chama, Pueblo Llano, Santo Domingo, Motatán, Guanare, Mocotíes, Tucaní) provide a wide record of river terraces. The origin of these terraces has been mainly associated with Pleistocene paleoclimatic fluctuations (e.g. Zinck, 1980; Vivas, 1984; Schubert and Vivas, 1993), in particular with glacial/interglacial cycle (Tricart and Millies-Lacroix, 1962; Tricart and Michel, 1965; Tricart, 1966). For the terraces located along the axial part of the chain, a tectonic origin associated with the uplift of the chain has also been proposed (Shagam, 1972; Giegengack, 1984; Audemard, 2003). Nonetheless the lack of numerical ages in the river terraces of the MA constitutes a weakness in the argumentation for the two hypotheses.

In this thesis, I studied the river terraces located along the Pueblo Llano and Santo Domingo rivers system (PLSDS), which flow across the Southeastern flank of the MA. This system of rivers is orthogonally oriented with respect to the structural trend of the chain; therefore the effect of localized active deformation tectonic in the process of terraces formation can be evaluated. Additionally, the river is far from the sea (more than 1500 km), then the effect of eustatic variation can be neglected.

- Albania

Albania is located in the Mediterranean region between 40 and 43° N. The climate is characterized by warm to hot, dry summers and mild to cool, wet winters. During summer, regions of Mediterranean climate are dominated by subtropical high pressure cells, with dry sinking air capping a surface marine layer of varying humidity and making rainfall unlikely

except for occasional storms. Instead, during winter the polar jet stream and associated periodic storms reach the lower latitudes of the Mediterranean zones, bringing rain, with snow at higher elevations. As a result, areas with this climate receive almost all of their precipitation during the winter season, while during the 4-6 months of summer no significant precipitations occur (Akin, 1991; Kottek, et al., 2006; Peel et al., 2007).

Several studies on Albanian rivers showed that uplifted Quaternary terraces of different ages are widely developed on a vast area from mountainous regions to coastal plains at less than 20 km from the sea (Melo, 1961; Prifti, 1984; Lewin et al., 1991; Koçi, 2007, Carcaillet et al., 2009). Albanian rivers are mainly oriented orthogonal to the structural trend and the rivers flow from the extensional domain in the East to the compressional domain in the West, crossing several active faults. For the previous reasons, Albanian rivers appear as one of the most suitable features in the Mediterranean domain to study the effect of the tectonic, climatic and eustatic variations in the processes of river terraces formation.

In this thesis, I studied three rivers located in central and Northern Albania (i.e. Shkumbin, Devoll and Mat rivers). Then, the new geomorphologic and geochonological data are integrated with published data coming from other rivers in order to propose a homogeneous stratigraphic/chronologic framework, applicable to terrace formation in Albania for the last 200 ka.

Chapter II: Methodology

In order to decipher the main role of external forces in the processes of river terraces formation, it is necessary to analyze the temporal and spatial relation between river terraces at a regional scale (1:100000 – 1:50000), catchment or local scale (1:50000 – 1:10000) and field scale (1:10000 – 1:1). This analysis should take into account the geologic and geomorphologic context of the study area. This morphological analysis, coupled with Quaternary geochronology allows reconstructing the chronology of the river terraces and the temporal and spatial evolution of the incision rate. These reconstructions and the correlation with global signals of climate and eustatic variations can be analysed in terms of impact of the different main forces.

In this chapter, I discuss firstly the principles of geomorphological analysis used to characterize the river valleys and to identify and map river terraces. Then, I present the ^{10}Be and ^{14}C dating methods used in this thesis to estimate ages of river terraces are presented.

2.1. Geomorphological analysis

2.2.1. Morphometric analysis

Morphometric analysis characterizes spatially the relief associated to actives structures (e.g. morphologic discontinuity associated to tectonic uplift, fault scarp, folding activity) and hydrographic objects (morphometric variation of the catchment and drainage network). These characteristics are associated to the spatial variation of tectonic and surface processes (Delcaillau, 2004). In this thesis, in order to analyze the relief and drainage evolution and their effect on the river terraces formation, three types of morphometric analyses were made: topographic profiles of the valleys, longitudinal profiles of the rivers and hypsometry.

- Valley profiles

The analysis of spatial elevation of the hillslopes along of river catchment allows distinguishing the morphologic discontinuity of the relief. In this thesis, crest profiles were made. These profiles were built extracting one maximum elevation point (orthogonal to the river) at each kilometer of the river (starting from the source and following the curvilinear distance of the river) from a 30–m digital elevation model (DEM) based on the Shuttle Radar

Topographic Mission (SRTM). This extraction was made using the "3D analyst" extension (within ArcMap) of the ArcGis software version 10.0. Then, a continue profile was made with a simple graph software (i.e. Excel) and using the same X values (distance from the source) as the longitudinal profile of the river (**figure II.1**). These profiles were thus analysed jointly with the geological features of the study area (geological and neotectonic maps), allowing the identification and characterization of morphostructural units.

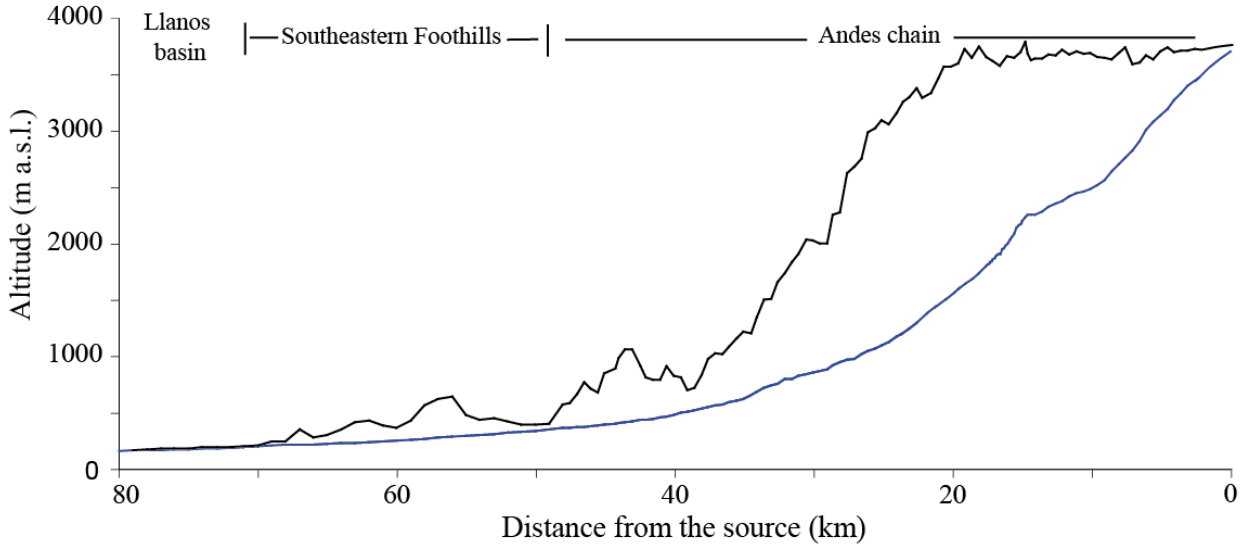

Figure II.1. *Example of morphometric curves of the PLSDS. Blue and black lines represent the longitudinal river profile and the right crest profile along the valley (valley profile), respectively.*

- Longitudinal profiles of the rivers

Rivers are linear systems that show a gradient of characters along their length. Ideally the longitudinal profile of a river is concave with a steep upper portion near the source, giving way progressively to reaches of less gradient as the mouth is approached. This profile could have steps, called knickpoints, which can be originated by differential erosion controlled by either lithological, flow regime contrasts or base level change (led by tectonic or eustatic variation). Knickpoint can migrate upstream and lead to the formation of a river terrace (e.g. Whipple, 2001; Zaprowski et al., 2001). In this thesis, longitudinal river profiles of the rivers were extracted from the 30–m DEM based on SRTM and topographic maps at 1:25000 scale. In the first case, the profiles were obtained by using the tool profile graph within the extension "3D analyst" of the ArcGis software version 10.0 (**figure II.1**). For the second case, the different elevations of the rivers and the curvilinear distance associated were digitalized from the topographic map, and then an x-y plot was made with the Excel software.

➢ Hypsometric curves

Hypsometric curve is the graphical representation of the area/elevation function of a drainage basin. This curve can be graphically displayed as an x-y plot with normalized elevation (ratio between of height of contour above base (h) and the maximum height of basin (H)) on the vertical (y axis) and normalized area (ratio of area enclosed between a given contour and the upper segment of the basin perimeter (a), and the total area of the basin (A)) on the horizontal (x axis) (**figure II.2**). Hypsometric integral (HI) is the area under the curve (Strahler, 1952). These parameters are commonly used to characterize the evolution degree of the relief. Concave hypsometric curve and low HI (≤ 0.3) are associated to stable and mature relief, while convex curve and high HI (≥ 0.6) indicate unstable and young relief (Stralher, 1957). These parameters are also used to identify the differences in the morphotectonic process between catchments (e.g. Delcaillau et al., 1998; Delcaillau, 2004). In this thesis, hypsometric parameters were extracted from the 30–m DEM based on SRTM, and using the extension CalHypso for ArcGis 10.0 (Perez-Peña et al., 2009). The results were used to compare the relative rates of surface processes in different river system.

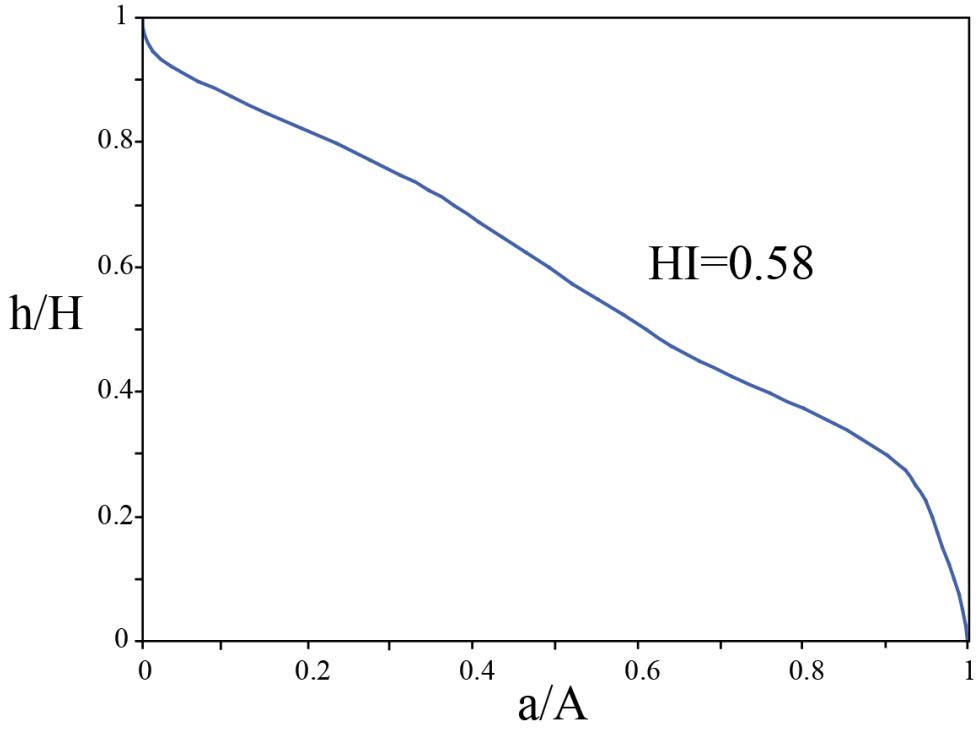

Figure II.2. *Example of the hypsometric curve of the Pueblo Llano drainage basin, located in Mérida Andes, Venezuela. The value of the hypsometric integral (HI) is also shown.*

2.2.2. Mapping of river terraces

The identification and mapping of river terraces require observations at different spatial scale. For this reason, a variety of tools and techniques were used during this thesis. In the following, I present a brief description of each tool together with the main results to obtain.

- Satellite imagery

In order to identify the regional morphologic units, to establish the regional relation between these units and the river terraces, and also to complete the field observation, we used three types of satellite images.

- **Landsat images:** Multispectral and panchromatic Landsat images with a spatial resolution of 30 m and 15 m, respectively, were freely obtained from Google earth software version 6.1.0.5001. These images are overlapping a 90–m DEM based on SRTM, allowing a 3D view of the area (**figure II.3**).

- **Spot images:** Pancromatic Spot 5 images with a spatial resolution of 2.5 m were provided by the Fundación Instituto de Ingeniería – Centro de Procesamiento Digital de Imagenes (CPDI) of Venezuela.

- **Aerial photography:** Photos obtained from airplane platform with a spatial scale of 1:20000 were provided by the Fundación Venezolana de Investigaciones Sismologicas (FUNVISIS) and interpreted with a stereoscope (**figure II.4**).

- Digital Elevation Model (DEM)

A 30-m of spatial resolution DEM based on SRTM was provided by the Fundación Instituto de Ingenieía – CDPI - of Venezuela. A shaded relief map based on this DEM, was performed using the tool "Topographic Modeling" of the ENVI 4.7 software (**figure II.5**). This shaded relief map is useful to identify, correlate and characterize the geometry of river terraces (e.g. gradient, incision) an also to analyze the morphologic characteristics of the studied area (see sub-section 2.1.1).

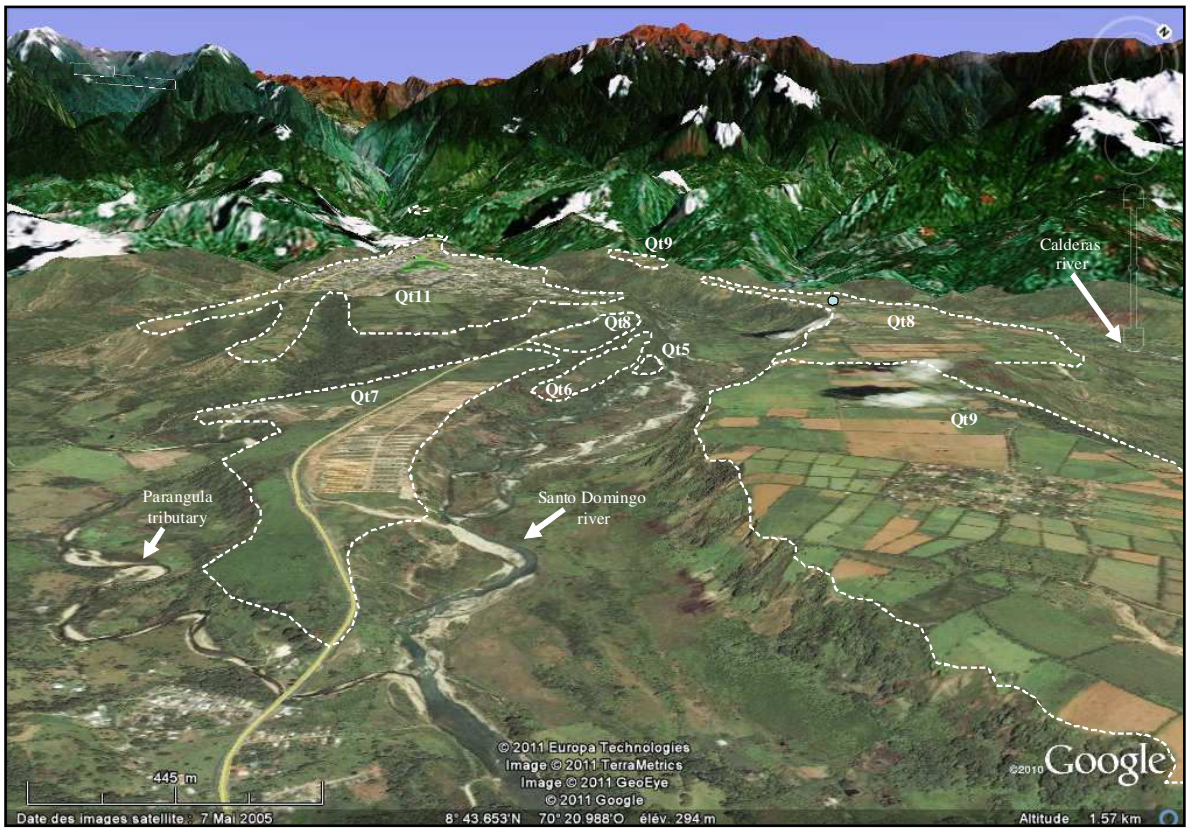

Figure II.3. *Landsat images of the lower reaches of Santo Domingo river in the Southeastern flank of the MA, Western Venezuela, obtained from Google Earth software. Shape of river terraces are identified with white dashed lines.*

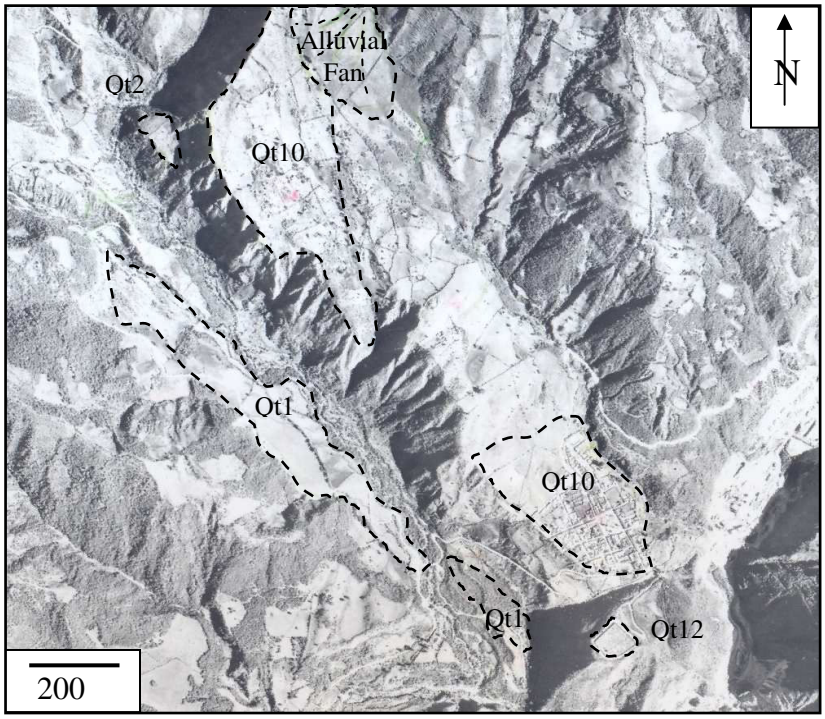

Figure II.4. *Aerial photograph of the lower reaches of Pueblo Llano river, Venezuela. Extension of river terraces is identified with black dashed lines. Aerial photograprah of Dirección de Cartografía Nacional – Venezuela (mission 01045, scale 1:20000, janvier 1973).*

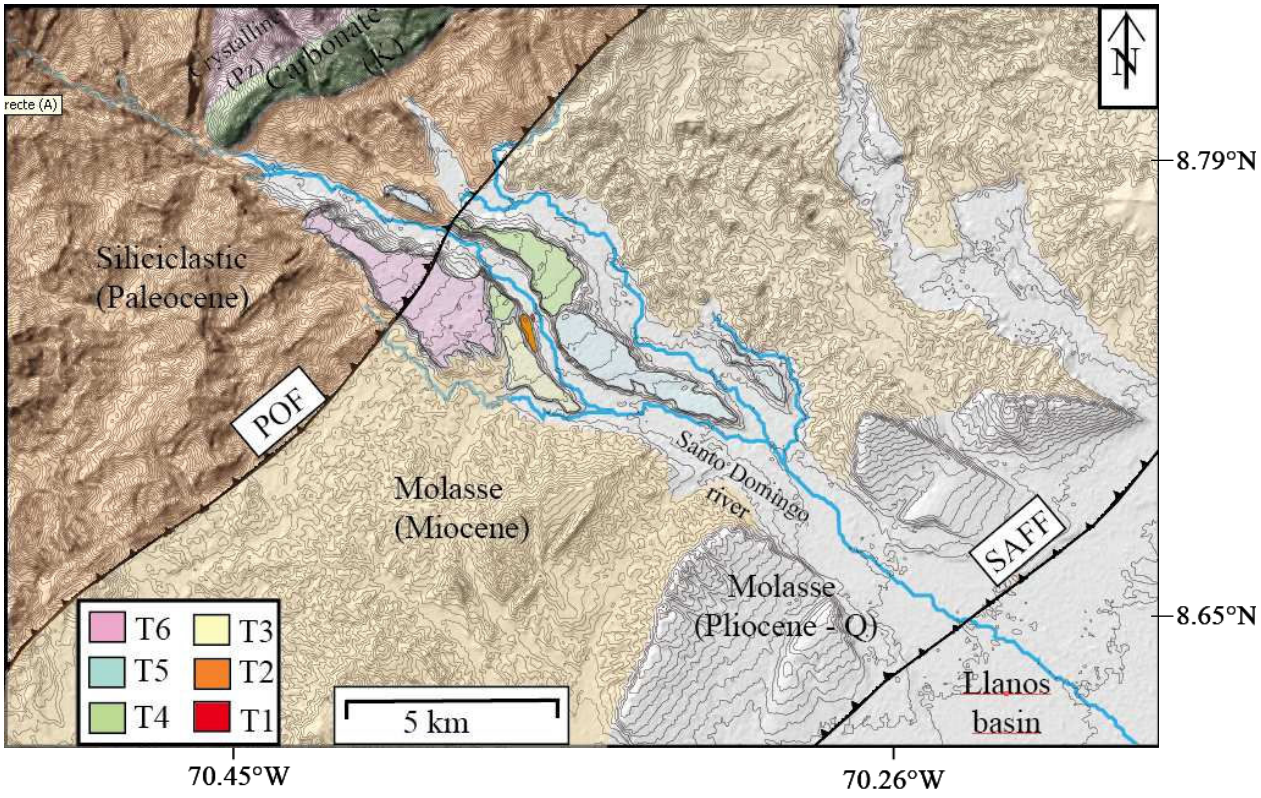

Figure II.5. *Shaded relief map of Southeastern flank of the Mérida Andes. River terraces are clearly visible in the central part of the map. Geological and neotectonic features also shown.*

- Topographic maps

Topographic maps at 1:25000 scale provided by the Institut of Seismology of Albania and FUNVISIS were georeferenced in ArcGIS 10.0. These maps were used together with the shaded relief map as the elevation base to map the river terraces, and to construct the longitudinal river profiles.

- Field observation

In order to verify, complete and detail the information acquired indirectly from the previous tool and techniques, a field work on the river terraces is required. In this way, sedimentologic, stratigraphic and morphologic data of river terrace can be collected, and also local relation between terraces and geological and geomorphologic characteristic can be analyzed. In this thesis, the thickness of the alluvial deposit and heights of the terraces above the current riverbed were measured using a measuring tape and a laser distancemeter (vertical accuracy ± 0.5 m). Aditionally, longitudinal terrace elevation profiles data were adquired using GPS navigator (Etrex®) (**figure II.6**).

Figure II.6. *Field work observations.* ***a)*** *Set of river terraces along of the Mat valley in Northern Albania. Relation between river terraces can be established at a local scale.* ***b)*** *Alluvial deposits that compose a terrace of the Shkumbin river in central Albania. Sedimentological and morphologic data can be obtained at 1:1 scale.* ***c)*** *Set of tools used in field work to describe and characterize river terraces.*

2.2. Dating of river terraces

The geochronology of river terraces can be determined using techniques that either date landforms surface or techniques that date the sediment of which the river terraces are composed. In this thesis, taking into consideration the geological, geomorphical and chronological setting, I used a combination of two dating methods. It allowed a coherent dating of a maximum number of river terraces.

One of these methods was the ^{10}Be dating. This technique allows dating the exposure of surface landforms to the cosmic radiation by measuring the concentration of ^{10}Be in the rocks or deposits exposed on the surface. An age of exposure to cosmic radiation, and in some cases erosion rates, can be estimated (Raisbeck et al., 1987). In this work, ^{10}Be concentrations are measured in quartz. It is a highly resistant mineral to weathering, abundant on the surface

of the Earth, and its crystalline structure minimizes the diffusion losses. The production rate of ^{10}Be in quartz is dependant of latitude and altitude (Lal, 1991; Stone, 2000; Balco et al., 2008; Dunai, 2010), and the half-life of ^{10}Be is 1.387 ± 0.012 Ma (Chmeleff et al., 2010; Korschinek et al., 2010). Potentially it allows the dating of landforms of hundreds of thousands of years, such as river terraces and moraines (e.g. Bierman, 1994; Ritz et al., 1995; Phillips et al., 1997; Hancock et al., 1999).

^{14}C dating was the other method used in this thesis. In this case, the estimations of ^{14}C (expressed as a ratio of ^{14}C/^{12}C) in an organic material of died organism indicate the time since the death of the organism. Assuming that the death of this organism was contemporaneous to the deposit that contains it, an age for this deposit can be estimated (Libby, 1955; Taylor and Lloyd, 1992). This technique is widely used for dating alluvial materials that composes river terraces (e.g. Rockwell et al., 1984; Personius, 1993; Meyer et al., 1995; Wegmann and Pazzaglia, 2002). However, due to the short half life of the ^{14}C (5730 ± 40 years) (Stuiver and Polach, 1977) and the avalaible technology to mesure the concentration of ^{14}C remain, the range of applicability of ^{14}C dating is fixed between > 300 years and < 55000 years (Trumbore, 2000).

During this thesis, I thus used ^{10}Be to date river terraces with deposits composed of siliceous rocks, and mainly with ages older than the upper limit of the ^{14}C dating. Indeed, in Albania previously published ages give an idea of the ages of the river terraces (e.g. Lewin et al., 1991, Carcaillet et al., 2009). Hence ^{10}Be dating was mainly used in the higher and older terraces, while ^{14}C was used in the lower terraces. Although no siliceous rocks are predominant in the source areas of Albanian rivers (mainly composed of ophiolites and carbonates rocks), some quartz-rich lithology can be found within the alluvial material (e.g. radiolarites, sandstones). In contrast, the source areas in Venezuela are composed of siliceous rocks (e.g. gneiss, granite), so the alluvial and glacial materials are mainly composed of quartz-rich lithologies. For these reasons, I applied ^{10}Be dating in the Venezuelan river terraces and moraines.

2.2.1. ^{10}Be dating

- **General principles**

The Earth is constantly bombed by galactic cosmic radiations, which consist mostly of high-energy (~1 - 10^{10} GeV) protons and alpha particles emanating from our galaxy. These

radiations interact with elements targets in the atmosphere (O, N) to produce atmospheric cosmogenic nuclides (e.g. ^{14}C and ^{10}Be) and a cascade of secondary particles, primarily neutrons and muons. They interact with target nucleides (e.g. Si, O, Mg, Fe, Al, Cl, K) within minerals such as quartz and olivine at the earth's surface, producing terrestrial cosmogenic nuclides (TCN), also called terrestrial *in situ* cosmogenic (e.g. ^{3}He, ^{21}Ne, ^{22}Ne, ^{36}Cl, ^{26}Al, ^{10}Be) (Bierman, 1994). In this work, we use the *in situ* ^{10}Be (following called ^{10}Be), which is mainly produced by spallation reactions between a low fraction of secondary cosmic-ray particles (~0.1%) and the atoms of Si and O present into the minerals in the first meters of the earth crust (**figure II.7**). Due to the attenuation of the incident particles in the soil, the production of ^{10}Be decreases exponentially with depth. At surface, most of this production (~98%) is due to neutrons. At depth, the neutron production becomes negligible and the production by muons becomes dominant (Braucher, 1998).

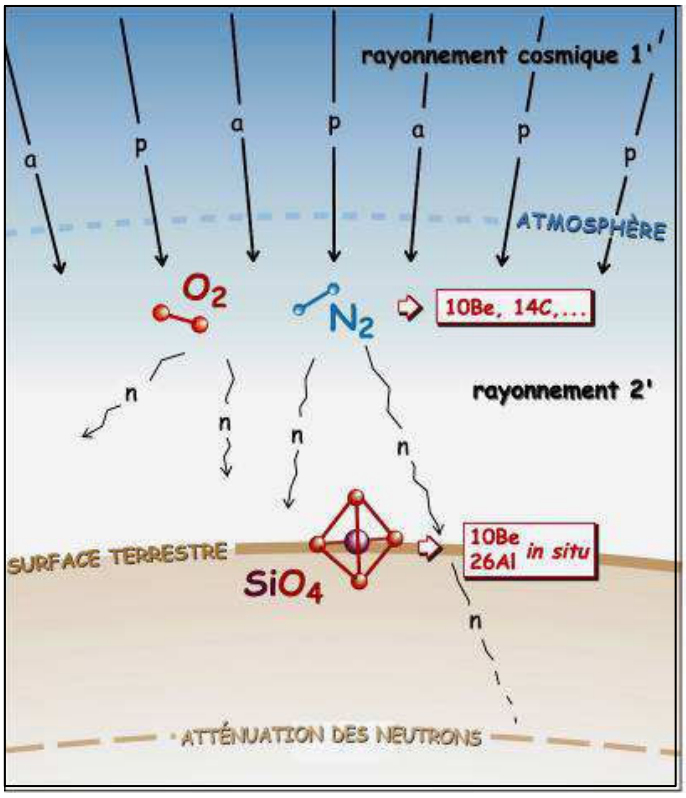

Figure II.7. *Scheme of ^{10}Be production by cosmic radiation in the first meters of earth crust (from Vassallo, 2006).*

- *Sampling*

In this work, I mainly used ^{10}Be dating with the aim to estimate exposure ages of river terraces and a frontal moraine. Ideally, the material collected for dating should be slightly or not eroded material with a negligible pre-exposure history. Hence, the sampling was made

taking into account the morphological conditions of the surface and the deposit. Aditionally, in order to determine the more favorable samples for dating the following four sampling strategies were applied:

- **Individual exposed boulders:** Samples were taken from siliceous rich boulders distributed along of the surface (**figure II.8a**). The sampled boulders should be partially embedded into the deposit and therefore not remobilized since their deposition, and they should have the least possible alteration to minimize the loss by erosion and the effect of any post-depositational processes. This strategy allowed having a statistical view of ^{10}Be concentration along the surface. However, information about ^{10}Be inherited concentration from prior exposure and erosion rate of the surface was not obtained.
- **Depth profile:** Samples were taken along a depth profile (**figure II.8b**), in order to compare the depth distribution of ^{10}Be with the exponential decay curve provided by the physical law (e.g. Brown et al., 1992). In the case of a low dispersion of the distribution of ^{10}Be in depth compared to theoretical model, the inversion of the data provides an estimate of the ^{10}Be inherited concentration, which allows a more precise dating.
- **Amalgam of exposed cobbles and pebbles:** Several individual exposed cobbles and/or pebbles were taken from the surface of the terrace, which were analyzed as a single sample (**figure II.8c**). In absence of boulders at surface, this strategy allowed homogenize the ^{10}Be concentrations, in a context where the dispersion of the concentrations may be due to problems of inheritance.
- **Stream river sediment:** Sediments were collected from the active stream bed (**figure II.8d**). They allowed the estimation of the average of ^{10}Be inherited from the catchment.

I personally treated and extracted the beryllium oxydum for sixty (60) samples in the Cosmogenic Laboratory of Institut de Sciences de la Terre (ISTerre, France), but only forty four (44) ^{10}Be concentrations are reported in this thesis. The chemical treatement was made following the procedures of Brown et al. (1991) and Merchel and Herpers (1999). ^{10}Be concentrations were measured at the accelerator mass spectrometry facility ASTER, Centre Européen de recherche et d'Enseignement des Geosciences de l'Environnement (CNRS, France) (Arnold et al., 2010), while the exposure ages estimation was also made by myself.

Figure II.8. *Pictures of sampling strategy of* ^{10}*Be dating.* ***a)*** *Individual exposed boulders.* ***b)*** *Depth profile.* ***c)*** *Amalgam of exposed cobbles and pebbles.* ***d)*** *Present river sediments. Pictures by R. Vassallo (a, d) and F. Audemard (b).*

- **Exposure age estimation**

The estimation of exposure age to cosmic rays from ^{10}Be dating involves the quantification of local production rate for each sample. It mainly depends on the intensity of cosmic radiation, which is influenced by the direction and intensity of the earth magnetic field and the thickness of atmosphere traversed. Hence, the production rate of ^{10}Be depends on the latitude and altitude of the sampling site.

The production rate for mineral quartz has been estimated empirically, comparing several ^{10}Be concentrations from different latitudes and altitudes with rocks of known ages (Lal, 1991). This estimation was improved by taking into account the atmospheric pressure (Stone, 2000). The production rate (*Po*) is expressed in at/g/a, and is estimated using the polynomial of Lal:

$$Po(L,z) = a(L) + b(L)z + c(L)z^2 + d(L)z^3 \quad (3)$$

where, L is the geomagnetic latitude; z is the altitude in km; and a, b, c, d are coefficients dependent of L. The Stone model is also based in this polynomial but Stone expresed the altitude of the sampling site in terms of atmospheric pressure.

The bombardment by cosmic radiation is isotropic and the production rate of ^{10}Be for one studied site is highly dependent on the geometry of the surrounding terrain. Hence, the production rate must be corrected by the geometric characteristics of the sampling site. The production rate is maximal when the sample is located on a surface where the sky is visible on 4 π steradian. In contrast, if any part of the sky is masked by terrain, the production is corrected by a shielding factor (*Sf*) which corresponds to the remaining part of cosmic radiation. The Sf is comprised between 1 and 0, and is estimated by the equation proposed by Dunne et al. (1999):

$$Sf = 1 - \frac{1}{360°} \sum_{i=1}^{n} \Delta\varphi_i \sin_{n+1}\theta \tag{4}$$

where, $\Delta\varphi_i$ is the azimuth of each mask zone; θi is the obstruction angle between the horizon and the topography.

Additionally, the absorption properties of the material traversed by the secondary particles and the sampling depth will be responsible for an attenuation of the production rate of ^{10}Be, given by the following law:

$$P(x) = Po.e^{(-\rho x/\Lambda)} \tag{5}$$

where, ρ is the rock density in g/cm^3; x is the depth of sampling in cm; Λ is the particles attenuation length, which is 150, 1500 and 5300 g/cm^2 for the neutrons (n), slow muons (μs) and fast muons (μf), respectively (e.g. Braucher et al., 2003).

Injecting into this expression the losses by radioactive decay and erosion of the surface portion of the profile, the concentration (C) ^{10}Be according to the depth (x) and time (t) is given by the following differential equation:

$$\frac{\partial C(x,t)}{\partial t} = \varepsilon . \frac{\partial C(x,t)}{\partial x} - \lambda C(x,t) + Po.e \frac{\rho x(t)}{\Lambda} \tag{6}$$

where, λ is the radioactive decay constants of ^{10}Be (4,62.10^{-7} yr^{-1}); and ε is the erosion rate in g/cm^2/yr.

To solve this equation, we consider the erosion and cosmic radiation constant through time, and by differentiating the contribution of neutron (97.85%) and muons (1.5% and 0.65%) of total production, the general equation becomes:

$$C(x,\varepsilon,t) = C_{inh}.e^{-\lambda t} + \frac{Po.Pn}{\frac{\varepsilon}{\Lambda_n}+\lambda}.e^{-\frac{x}{\Lambda_n}}\left[1-e^{-1\left(\frac{\varepsilon}{\Lambda_n}+\lambda\right)}\right] + \frac{Po.P\mu s}{\frac{\varepsilon}{\Lambda_{\mu s}}+\lambda}.e^{-\frac{x}{\Lambda_{\mu s}}}\left[1-e^{-1\left(\frac{\varepsilon}{\Lambda_{\mu s}}+\lambda\right)}\right] + \frac{Po.P\mu f}{\frac{\varepsilon}{\Lambda_{\mu f}}+\lambda}.e^{-\frac{x}{\Lambda_{\mu f}}}\left[1-e^{-1\left(\frac{\varepsilon}{\Lambda_{\mu f}}+\lambda\right)}\right] \quad (7)$$

where, C(x, ε, t) is the ^{10}Be concentration depending on the sampling depth, the erosion rate and the exposure time; C_{inh} is the ^{10}Be inherited concentration in at/g; Pn, $P\mu s$, $P\mu f$ are the relative contributions of neutrons, slow muons and fast muons, respectively.

^{10}Be concentration increases with time until it reaches a steady state balance between production and losses due to erosion and radioactive decay. This state is reached earlier when the erosion rate of the surface is high (**figure II.9**).

The distribution of ^{10}Be at depth describes an exponential decay, in accordance with theoretical laws. In this case, the ^{10}Be inherited concentration is constant for all samples and could be determined graphically from a concentration depth profile by taking the asymptotic value towards which the model tends (**figure II.10**). The erosion rate is more difficult to quantify, and can greatly affect the dating of surfaces.

Therefore, to solve the equation (5), we must make assumptions because there is only one equation with two unknowns (ε, t). Firstly, assuming that the surface reached the steady state, the erosion rate may be determined from the ^{10}Be concentration in surface by the following equation:

$$\varepsilon = \left(\frac{P_0}{C(0,\infty) - C_0} - \lambda\right) \times \Lambda \quad (8)$$

where, $C(0, \varepsilon, \infty)$ is the ^{10}Be concentration at steady state; C_0 is the initial ^{10}Be concentration. However, in most cases, the local and temporal variations of the erosion rates cannot be quantified and the lack of constraint on this parameter remains the main problem for ^{10}Be dating. Thus, the assumption of a negligible erosion is most used and a minimum exposure age of the surface can be estimated from the simplified equation (5):

$$t_{\min} = -\frac{1}{\lambda} \times Ln(1 - \frac{\lambda C(0,t)}{P_0}) \quad (9)$$

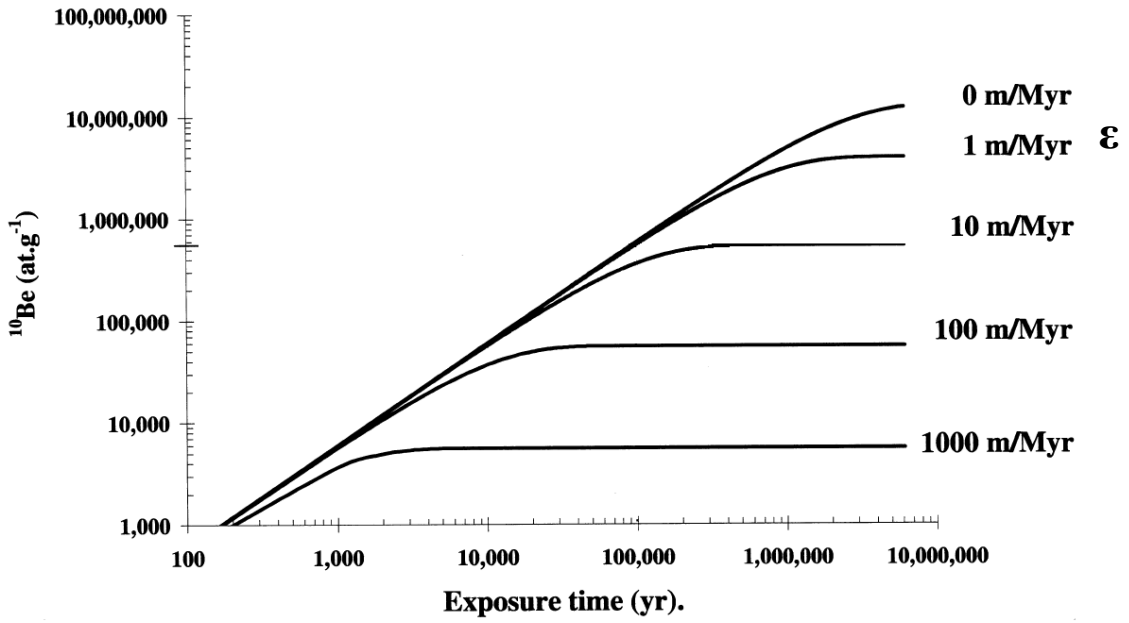

Figure II.9. *Theorical ^{10}Be concentrations evolutions with exposure time for different erosion rates (Brown et al., 1991).*

In this work, when a concentration depth profile was made, the Chi-square inversion method was used. This method allowed minimizing mathematically the differences between the analytical and theoretical ^{10}Be concentrations along the depth profile, and to estimate an age of exposure of the surface (e.g. Braucher et al., 2003, Ritz et al., 2006). The inversion is given by the following equation:

$$Chi - square = \sum_{i=1}^{n} \left[\frac{C_i - C_{(x,\varepsilon,t)}}{\sigma_i} \right]^2 \quad (10)$$

where, C_i is the analytical ^{10}Be concentration at depth x_i; $C(x, \varepsilon, t)$ is the theoretical ^{10}Be concentration, using the equation (4); σ is the analytical uncertainty.

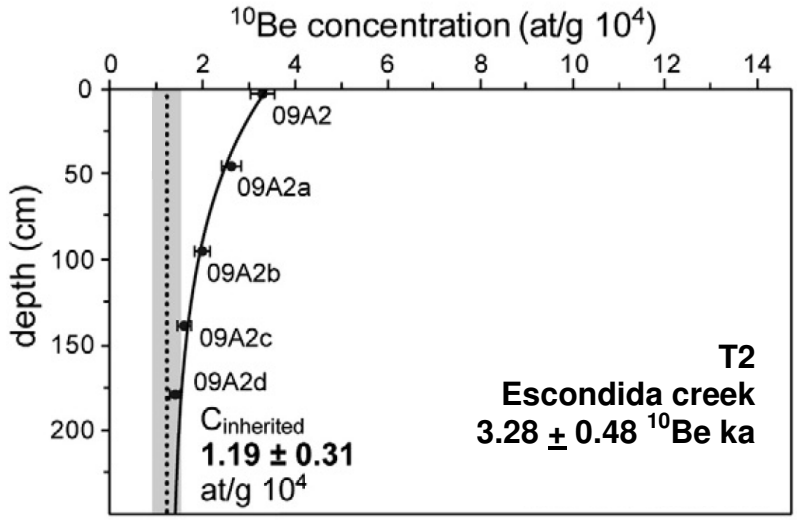

Figure II.10. *Example of evolution of ^{10}Be concentration along a depth profile with inherited concentration. The dotted vertical line represents the inherited ^{10}Be concentration estimated at 1.19 ± 0.31 at/g 10^4, gray field indicates its 1σ error. The black line represents the best fit for an exposure age of 3.20 ± 0.48 ^{10}Be ka with the assumption of no erosion (adapted from Schmidt et al., 2011).*

2.2.2. ^{14}C dating

- **General principles and age estimations**

Carbon has three naturally occurring isotopes. The two most abundant are the stable isotopes, ^{12}C (98.99 %) and ^{13}C (1.11 %). ^{14}C, with an abundance of less than 10^{-10} %, is unstable and undergoes β-decay with a half life of 5730 ± 40 years (Stuiver and Polach, 1977). This unstable isotope is produced by the interaction of cosmic rays with nitrogen and oxygen, with the majority formed by the ^{14}N (n,p) ^{14}C reaction in the atmosphere (**figure II.7**) (Kamen, 1963). The ^{14}C formed is rapidly oxidised to $^{14}CO_2$ and enters the earth's plant and animal lifeways through photosynthesis and the food chain. Thus, the level of ^{14}C in plants and animals when they died approximately equals the levels of ^{14}C in the atmosphere at that time (Taylor and Lloyd, 1992). After the death of an organism, the ^{14}C in its tissues is no longer refilled through direct or indirect exchange with atmospheric CO_2, and undergoes radioactive decay back to ^{14}N. If the plants or animals tissues remain intact and isolated from exchange, the decrease in its ^{14}C content (expressed as a ratio of $^{14}C/^{12}C$) from that in living organism, may be used to indicate the time since the death of the organism (**figure II.11**) (Trumbore, 2000).

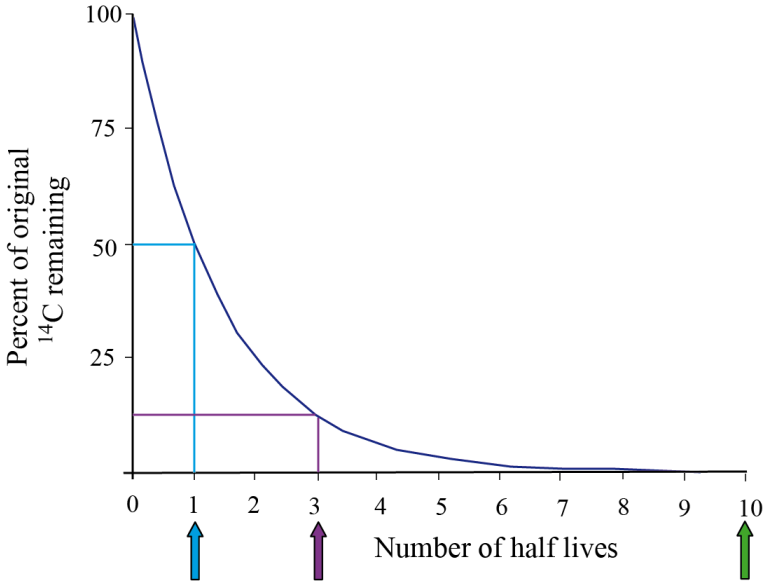

Figure II.11 *Decay curve for C14 showing the activity at different period. After one half life (~5730 years) (light blue arrow), only half of the original amount of ^{14}C remain. After three half lifes (magenta arrow), an eighth of the ^{14}C remains. After 57000 years (green arrow), less than 0.1 % of the ^{14}C remains. The limit of the technique is thus reached.*

Calculation of a radiocarbon age requires the assumption that the ^{14}C content of the carbon originally fixed in plant or animal tissues equalled that of the atmospheric CO_2 (Karlen et al., 1966). There are two major problems with this assumption. First, there is a difference between the ratio of $^{14}C/^{12}C$ present in the atmosphere and the carbon fixed in the living organism by photosynthesis. However, this is easily and frequently corrected in the radiocarbon laboratory by measuring the degree to which mass-dependant fractionation affects the stable ^{13}C isotopic content of a sample, and assuming that fractionation of ^{14}C will be approximately double that of ^{13}C (Craig, 1954; Trumbore, 2000). The second problem is that the production rates of ^{14}C in the atmosphere has varied, due to changes in cosmic rays flux, the variations in the earth magnetic field, and changes in the distribution of carbon among ocean, biosphere and atmospheric reservoirs (Stuiver et al., 1991). Additionally, open air nuclear testing between 1955-1964 dramatically increased the ^{14}C in the atmosphere (Trumbore, 2000). In order to solve the second problem, correction factors and curves corrections are used to determine calendar ages (calibrated ^{14}C dates) from conventional ^{14}C ages. They are based on the observed ^{14}C content of independently dated tree ring cellulose (Stuiver and Kra, 1986; Stuiver et al., 1993), macrofossils from varved lake sediments (Hajdas et al., 1993) and independently dated coral terraces (Bard et al., 1990; Reimer et al.,

2009). Nowaydays, calibrated curves reach more than 50000 years (Reimer et al., 2009), and they are specific for each hemisphere and origin data (e.g. marine, continental) (McCormac et al., 2004).

- Sampling

In order to date the fluvial sediments studied in this thesis, the hypothesis that the death of organism dated is contemporaneous to the associated sedimentary deposit was made. Care was taken to assure that the dated organic samples (e.g. charcoal, vegetal debris) were *in sit*u, fluvially deposited materials associated with terrace aggradation, and not linked to the subsequent emplacement of organic matter by penetrating tree roots or weathering profiles. Twenty two samples were collected from clay lenses, located close to the base of the fine sediment level standing above or within the conglomeratic material (**figure II.12**). This implies that most of the materials collected were deposited during the ultimate phase of river aggradation and these ages represent a maximum age of the abandonment of the river terraces.

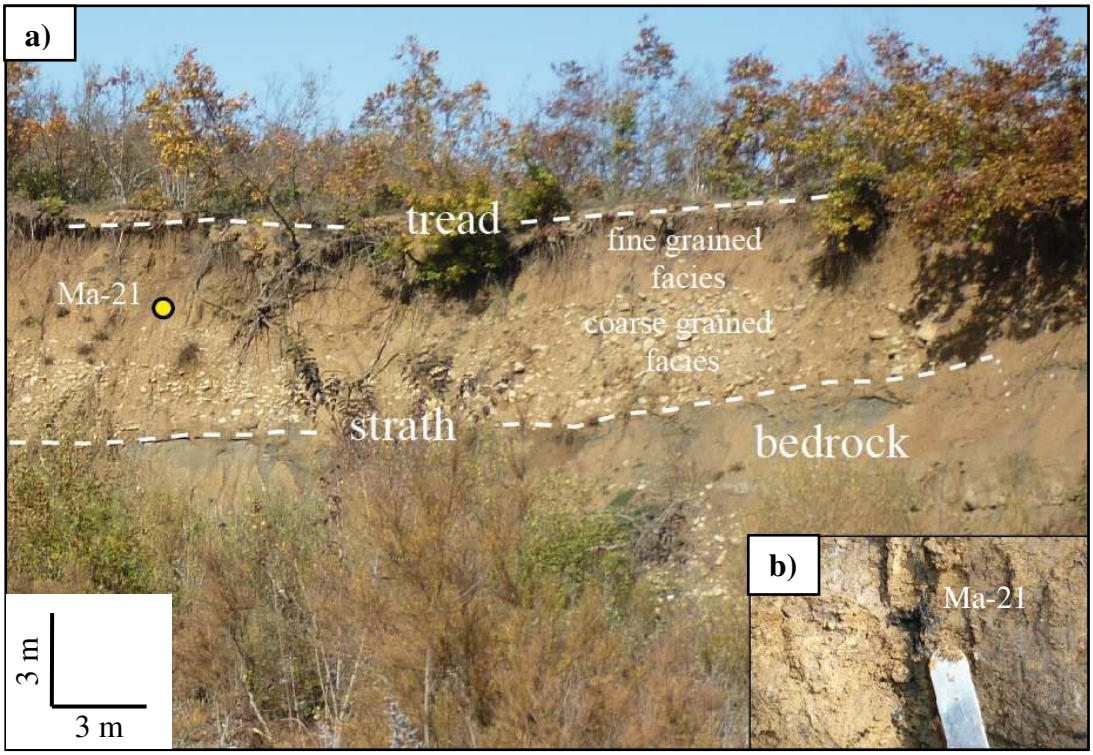

Figure II.12. a) *Stratigraphic position of ^{14}C sample (Ma-21), localized close to the base of the fine-grained facies.* ***b)*** *Detail of the organic material sampled.*

All the samples were sent to the Poznan radiocarbon Laboratory (Poland) or the ARTEMIS Insu facility, France - CNRS, where the analysis of ^{14}C dating were performed using accelerator mass spectrometer technology (AMS). Then, I calibrated the ^{14}C ages lower than ~40 ka using the OxCal program version 4.1 (Ramsey, 2009), based on the IntCal09 data

set (Reimer et al., 2009) and reported as intercept ages with two sigma (95%) (**figure II.13**). Calibrated ages (cal ka BP) are given as a time interval linked to the related probability. ^{14}C ages older than ~40 ka were corrected using the polynomial calibration of Bard et al. (2004). The previously published conventional ^{14}C ages (e.g. Lewin et al., 1991; Carcaillet et al., 2009) were recalibrated following the same procedure.

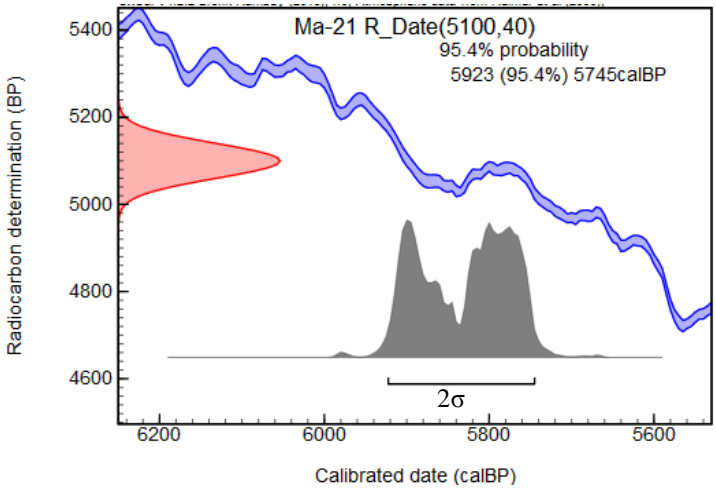

Figure II.13. *Calibration age of Ma-21 sample using the OxCal program version 4.1 (Ramsey, 2009). The not calibrated ^{14}C age given by the radiocarbon laboratory was 5.10 ± 0.04 ^{14}C ka BP. X axis is the calendar dates, while Y axis is "before present" dates. The pink envelop represents not calibrated ^{14}C age, while the blue curve is the IntCal09 calibration curve (Reimer et al., 2009). Gray envelop is the interception of pink evelop with blue curve, and represents the probability of ages. In this case, the age of the sample has a probability of 95.4% to be between 5.92 and 5.74 cal ka BP.*

2.2.3. Reconciling different dating methods

- **Meaning and correlation**

According to the sampling strategy applied in this study, ^{10}Be ages represent the surface exposure ages of the terraces (Gosse and Phillips, 2001). ^{14}C ages and the others ages achieved in previous studies, using others methods and strategies (U series (U/Th), electron spin resonance (ESR) and thermoluminescense (TL); Lewin et al., 1991; Woodward et al., 2001), represent the timing of deposition or formation of a particular sediment or material within the alluvial deposit of the terrace (Noller et al., 2000). Most of the ^{14}C samples collected in this thesis, and also the material used in previous dating studies (e.g. calcite cement, deer tooth) were taken from the sediment that corresponds to the ultimate phase of

river aggradation. These ages thus represent a maximum age of abandonment of the river terrace. Moreover, due to the closeness of the values of the available dating for each terrace and the uncertainty of the dating methods, we are not able to distinguish between the end of alluviation and the abandonment of the terraces, if they are separated by less than few thousand years (**figure II.14**). Hence, the ages reported in this thesis are analysed as ages of terraces abandonment.

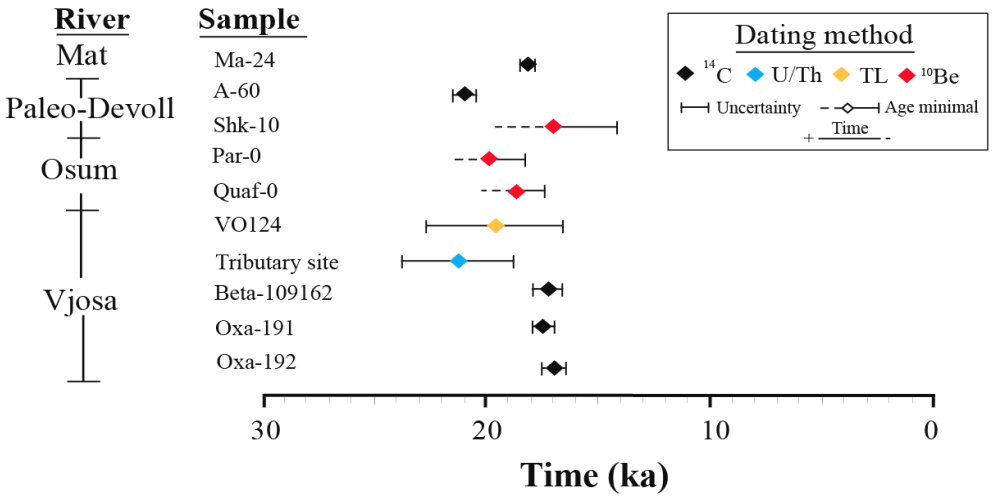

Figure II.14. *Plot of surface exposure ages (^{10}Be) and deposits ages of the last aggradation phase (^{14}C, U/Th and TL) (see text for discussion) that composes the T3 Albania river terrace. These ages were obtained in different rivers by different dating methods. Despite of this, a good agreement between the ages is found. It suggests that the exposition of the terraces (its abandonment) and the end of aggradation phase were likely separated by less than few thousand years. Therefore, we consider all these ages as the ages of abandonment of the river terraces.*

This assumption is validated by the good agreement between the majority of the ages analysed in this study, either new (performed in this thesis) or published (Lewin et al., 1991; Woodward et al., 2001, 2008; Hamlin et al., 2000; Koçi, 2007; Carcaillet et al., 2009) reported for alluvial sediments of Albania and Greece rivers (see Chapter IV, subsection 4.5).

The summation of the probability density plot of ages (Ramsey, 2009) is useful for river terraces chonostratigraphy analysis with abundant ages (e.g. Meyer et al., 1995; Wegmann and Pazzaglia, 2002, 2009). In this thesis, this approach was used to reconcile the different ages of Albanian terraces. Probability curves were thus produced by calculating calendar ages

and their two sigma (95%) analytical errors and then summing the normal probabilities distribution defined for individual ages. This summation has been performed with the OxCal program version 4.1 (**figure II.15**) (Ramsey, 2009). Due to the uncertainty associated to a minimum and maximum ages, these ages were not used in the construction of probability curves.

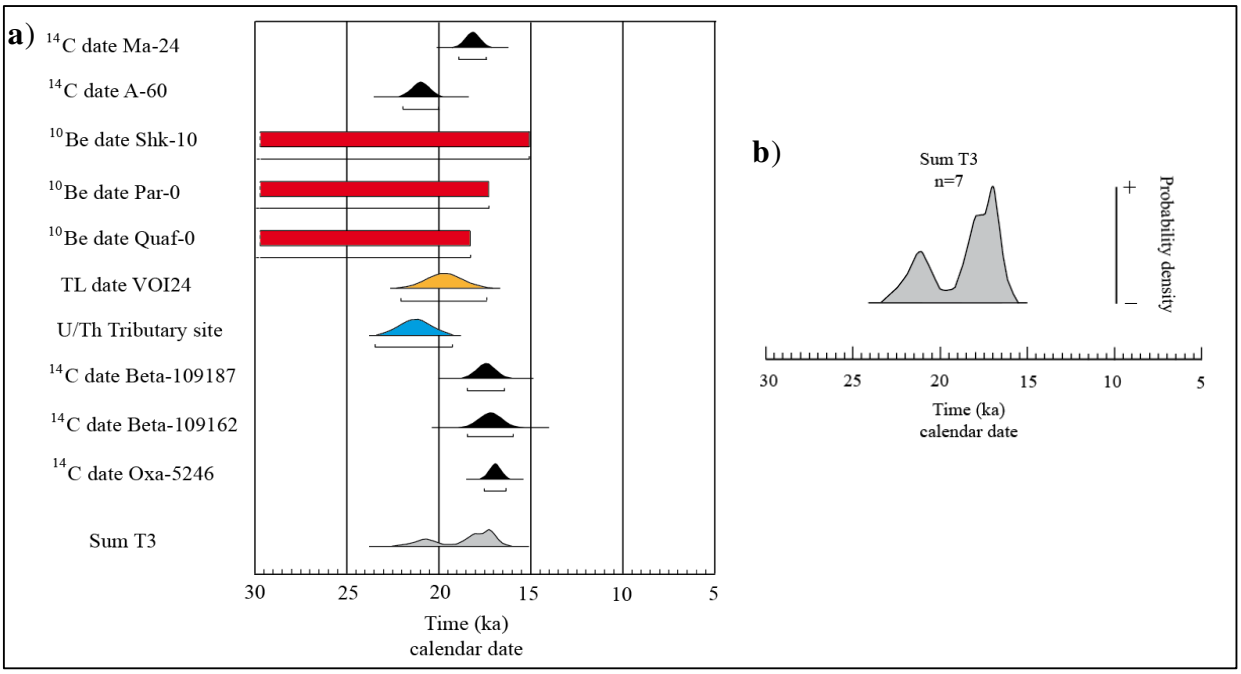

Figure II.15. *Probability density curves for abandonment of terrace T3 in Albania.* ***a)*** *Probabilities distribution defined for individual ages (same samples of* ***figure II.14****). Normal gaussian distributions were assigned to the ^{14}C, TL and U/Th dating. Continuous uniform distributions were assigned to the minimum ages achieved with ^{10}Be dating. These ages were not used to produce the probability curves (Sum T3). Nonetheless, they were used to define the younger limit of the probability density curves.* ***b)*** *Zoom of the probability density curve for abandonment of T3.*

- **Reporting dating ages**

In order to identify the origin and the meaning of the ages, the following conventions to report river terraces ages are adopted during this thesis.

Ages obtained by ^{10}Be dating are reported followed by the suffix "^{10}Be ka". Maximum and minimum ages performed with this dating method are plotted with their uncertainy associated and a dashed line toward younger and older times (maximum and minimum ages, respectively) (**figure II.14**). This convention is also valid for the other dating methods. The

published ages obtain by U series, electron spin resonance and thermoluminescense are reported by the suffixes “U/Th”, “ESR” and “TL ka”, repectively.

During the discussion of river terraces chronology, I use the calibrated radiocarbon ages, which are given as a time interval linked to the related probability (95%). These ages are reported followed by the suffix “cal ka BP”. However, not calibrated ages are also reported in the tables.

Chapter III:

Geomorphologic Analysis of river terraces on the Southeastern Flank of the Mérida Andes, Venezuela

Panoramic view of the lower reaches of the Pueblo Llano river in the Mérida Andes, Venezuela.

3.1. Overview and main results of chapter III

The Mérida Andes (MA) is an active orogen, located in Western Venezuela, where several rivers (e.g. Chama, Pueblo Llano, Santo Domingo, Motatán, Guanare, Mocotíes, Tucaní) provide a wide record of river terraces. The origin of these terraces have been mainly associated with Pleistocene paleoclimatic fluctuations (e.g. Tricart and Millies- Lacroix, 1962; Tricart and Michel, 1965; Tricart, 1966; Zinck, 1980; Vivas, 1984; Schubert and Vivas, 1993). However a tectonic origin associated with the uplift of the chain has also been proposed (Shagam, 1972; Giegengack, 1984; Audemard, 2003). Nonetheless the lack of numerical ages in the river terraces of MA constitutes a weakness in the argumentation for the two hypotheses.

The lower reaches of the Pueblo Llano and Santo Domingo rivers constitute a system of rivers that flow from the core of the range across the Southeastern flank of the MA. Along this system, several river terraces are preserved in landscape. Pueblo Llano and Santo Domingo rivers system is orthogonally oriented with respect to the structural trend of the chain. Additionally, the outlet of the system is far from the sea (more than 1500 km), then the effect of eustatic variation can be neglected. For these reasons, the Pueblo Llano and Santo Domingo rivers system appears a suitable context to study the effect of tectonic and climatic variations in the process of terrace formation. Thus, we apply a morphotectonic analysis coupled with *in situ* produced ^{10}Be dating in order to understand the process of terraces formation along this system.

In this chapter, firstly a brief synthesis of the geological, climatic and paleoclimatic setting of the study area is discussed. Then, I focus the analysis on the lower reaches of the system (Santo Domingo river), within the foothills unit, where six strath terraces were identified. Geomorphic observations and dating allowed the restoration of the temporal evolution of incision rate, which was analysed in terms of tectonic, climatic and geomorphic processes. It is found that the long-term incision rate averages 1.1 mm/a over the last 70 ka. Taking into account the geologic and geomorphologic setting, this value can be converted into the Late Pleistocene uplift rate of the Southeastern flank of the MA. The results show that the process of terraces formation in the lower reaches of the Santo Domingo river occurred at a higher frequency (10^3-10^4 years) than a glacial/interglacial cycle (10^4-10^5 years). According to the global and local climate curves, these terraces were abandoned during relatively warm to cold transition. The results obtained in this part of the system are presented in this chapter as an article published in Journal of South American Earth Sciences.

Then, the geomorphologic and dating results of the upper reaches of the rivers system (Pueblo Llano river) are discussed. In this part of the system, six fill terraces and a frontal moraine complex were identified. Four terraces and the moraine were dated. These results were integrated with the results obtained in the lower reaches of the system and allowed a better understanding of the processes of the river terraces formation at a catchment scale. The strong correlation between climatic variations and ages of abandonment of terraces of the whole system puts in evidence that the climate is the main force that controls the cycles of aggradation/incision, while a moderate uplift (~1.1 mm/a) provides the potential for vertical incision and preservation of the river responses to low and high frequency climatic variations. Nonetheless, the river responses to a climate variation in Venezuela seem to be highly controlled by altitude. As a matter of fact, in the upper reaches of the Santo Domingo and Pueblo Llano system, where the elevations vary between 2300 and 1600 m a.s.l. and only fill terraces are recognized, the ages of abandonment of the terraces correspond to transitions from cold and dry to warm and humid conditions. On the contray, in the lower reaches of the system, where the elevations are around 300 m a.s.l. and only strath terraces are identified, the ages of the abandonment of the terraces correspond to short period of cold and dry conditions (e.g. stadial), within a large relatively warm and humid period.

These results allowed proposing that in the upper reaches of the Pueblo Llano and Santo Domingo rivers system, cold and dry periods lead to aggradation phases, while warm and humid conditions cause the incision and abandonment of the terraces. During the warm and humid phase, the material eroded at the upper reaches is transported toward the lower reaches, where the increase in the sediment supply and water discharge makes the river attaining a graded condition (Mackin, 1948; Knox, 1975; Leopold and Bull, 1979). Under these conditions, channel vertical incision and deposition are at a minimum. Lateral erosion is more important, thus wide and continuous erosional surface (strath) is developed. This condition is interrupted by vertical fluvial incision triggered by the decrease in the transport capacity caused by short period of cold and dry conditions. Thus, in this moment, a strath terrace is formed at the lower reaches of the river.

Finally, the identification and dating of a frontal moraine complex located at elevation of 2300 m a.s.l in the upper reaches of the system highlights the fact that the glacier advance during the LGM, in other areas of the MA could have also reach elevation lower that those reported between 2900 and 3500 m a.s.l. It might have relevants implications in the paleoclimatic reconstruction of the MA. Our results also put in evidence that the morphological criteria (used alone up to present) are not enough to correlate glacial deposits

and landforms in the MA. Hence numerical dating in the lowest glacial deposits is needed to reconstruct the glacial history of the area.

3.2. Résumé et principaux résultats du chapitre

Les Andes de Mérida sont une chaîne de montagne tectoniquement active, située dans l'ouest du Vénézuéla, où plusieurs rivières offrent un large registre de terrasses fluviales. L'origine de ces terrasses a été principalement liée aux fluctuations paléoclimatiques du Pléistocène (e.g. Tricart et Millies-Lacroix, 1962; Tricart et Michel, 1965 ; Tricart, 1966; Zinck, 1980; Vivas, 1984; Schubert et Vivas, 1993), mais une origine tectonique associée à la surrection de la chaîne a également été proposée (Shagam, 1972; Giegengack, 1984; Audemard, 2003). Néanmoins, le manque d'âges numériques dans les terrasses fluviales des Andes de Mérida constitue une faiblesse dans l'argumentation de ces deux hypothèses.

Le cours inférieur des riviéres Pueblo Llano et Santo Domingo constitue un système de rivières qui coulent du centre de la chaîne vers le flanc sud-est des Andes de Mérida. Le long de ce système, plusieurs terrasses fluviales sont préservent dans le paysage. Le système des rivières Pueblo Llano et Santo Domingo est orthogonalement orienté par rapport à la fabrique structurale de la chaîne. En outre, l'exutoire du bassin versant est loin de la mer (plus de 1500 km), donc on peut consideres l'effet de la variation eustatique est négligeable. Pour ces raisons, le système Pueblo Llano et Santo Domingo apparaît comme un contexte adapté pour étudier l'effet des variations téctoniques et climatiques dans le processus de formation des terrasses. Ainsi, nous appliquons une analyse morphotectonique couplée avec des datations par ^{10}Be *in situ*, pour tenter de comprendre le processus de formation des terrasses le long de ce système.

Dans ce chapitre, une breve synthèse du contexte géologique, climatique et paléoclimatique de la zone d'étude est abordée dans un premier temps. Plus tard, je me concentre sur le cours inférieur du système (rivière Santo Domingo), où six terrasses d'abrasion ont été identifiées. Les observations géomorphologiques et les datations des terrasses ont permis la reconstruction de l'évolution temporelle des taux d'incision, qui a été analysée en termes de processus téctoniques, climatiques et géomorphologiques. Le taux d'incision au long-term dans la région a été autour de 1.1 mm/an au cours des dernières 70 ka. Compte tenu du contexte géologique et géomorphologique, cette valeur peut être convertie en taux de soulèvement durant le Pléistocene supérieur du flanc sud-est des Andes de Mérida. Les résultats montrent que le processus de formation des terrasses dans le cours inférieur de la rivière Santo Domingo s'est produit à une fréquence plus élevée (10^3 à 10^4 ans) que celle d'un cycle glaciaire/interglaciaire (de 10^4 à 10^5 ans). Selon les courbes climatiques globales et locales, ces terrasses ont été abandonnées lors des transitions de periodes chaudes à froides.

Les résultats obtenus dans cette partie du système sont présentés dans ce chapitre en tant qu'article publié au Journal of South American Earth Sciences.

Ensuite, les résultats géomorphologiques et les datations de la partie supérieure du système (rivière Pueblo Llano) sont discutées. Dans cette partie du système, six terrasses de remplissage et un complexe de moraine frontale ont été identifiés. Quatre terrasses et la moraine ont été datées. Ces résultats ont été intégrés aux résultats obtenus dans la partie inférieure du système et ont permis une meilleure compréhension des processus des formations des terrasses à l'échelle du bassin versant entier. La forte corrélation entre l'âge d'abandon des terrasses et les variations climatiques montre que le climat est la principale force qui contrôle les cycles d'aggradation / d'incision fluviales, alors qu'un soulèvement modéré (~1.1 mm/an) donne le potentiel pour l'incision verticale et la préservation des terrasses. Néanmoins, au Vénézuéla, le type de réponse de la rivière à une variation climatique semble être fortement contrôlé par l'altitude. En effet, dans la partie supérieure du système Pueblo Llano et Santo Domingo, où les altitudes varient entre 2300 et 1600 m au dessus du niveau de la mer et où des terrasses de remplissage sont reconnus, l'âge d'abandon des terrasses correspondant aux transitions froid-sec/chaud-humide. Alors que dans le cours inférieur du système, où les altitudes sont d'environ 300 m au dessus du niveau de la mer et où des terrasses d'abrasion sont identifiés, l'âge de l'abandon des terrasses correspondant à de courtes périodes froides et sèches (par exemple stadial conditions), au sein de longues periodes relativement chaudes et humides.

Ces résultats ont permis de proposer que dans la partie supérieure du système Pueblo Llano et Santo Domingo, les périodes froides et sèches produisent des phases d'aggradation fluviatile, tandis que des conditions chaudes et humides causent l'incision et l'abandon des terrasses. Au cours de la dernière phase, le matériau érodé dans la partie supérieure est transporté vers le cours inférieur, où l'augmentation simultanee du débit et de l'apport de sédiments mettent la rivière en condition d'equilibre (*graded condition*) (Mackin, 1948; Knox, 1975; Léopold et Bull, 1979). Dans ces conditions, l'incision verticale et le dépôt sont au minimum. L'érosion latérale est plus importante, donc une large et continue surface d'érosion (*strath*) est développée. Cette condition est interrompue par une incision fluviale verticale provoquée par la diminution de la capacité de transport lors des courts periodes froids et seches. Ainsi, à ces momens-là, une terrasse d'abrasion est formée dans la partie inférieure du système.

Enfin, l'identification et la datation d'un complexe de moraine frontale située à l'altitude de 2300 m au dessus du niveau de la mer dans la partie supérieure du système mets

en évidence le fait que l'avancée glaciaire pendant le Dernier Maximum Glaciaire (DGM ou *LGM*), dans d'autres domaines des Andes de Mérida, a pu atteindre des altitudes plus basses que celles signalées dans la litterature (entre 2900 et 3500 m d'altitude) Ce pourrait avoir des implications importantes dans la reconstruction paléoclimatique des Andes de Mérida. Nos résultats sont également la preuve que les critères morphologiques et sedimentologiques tous seuls ne suffisent pas pour correler les dépôts et les reliefs glaciaires. Ainsi, la datation numérique sur les autres dépôts glaciaires des Andes de Mérida est nécessaire pour reconstruire l'histoire paleogéographique de la région.

3.3. Geodynamics and structural setting of the Mérida Andes

3.3.1. Regional tectonic context of the Mérida Andes

The Mérida Andes (MA), also known as the Venezuelan Andes, is located in the Western part of Venezuela. This range is around 400 km long with a SW-NE direction from the Colombian-Venezuelan border in the Southwest to Barquisimeto city in the Northeast (**figure III.1**). The mean elevation of the MA is about 2024 m a.s.l. and culminates at 4978 m a.s.l. at Pico Bolivar, located in the central part of the chain. The range is bounded on both flanks by the lowlands of the Maracaibo and Llanos basins on the Northwest and Southeast, respectively. Two prominent forebergs are clearly distinguishable along both flanks even if the Southeastern one is better developed. The MA has a crystalline core of Precambrian gneiss and schist and Paleozoic to Mesozoic plutonic rocks, overlain by Jurassic and Cretaceous clastics and calcareous rocks, and flanked by Eocene to Pliocene molasse rocks and Quaternary sediments (**figure III.2**) (Hackley et al., 2005).

MA mountain belt results from a complex geodynamic interaction between the Caribbean, Nazca and South America plates and other minor continental blocks (**figure III.1)** (Taboada et al., 2000; Audemard and Audemard, 2002). This interaction of plates leads to the oblique convergence between the Maracaibo Triangular Block and South America Plate, and is responsible for the present MA buil-up (Kellogg and Bonini, 1982; Colletta et al., 1997; Audemard and Audemard, 2002; Bermudez, 2009, Monod et al., 2010).

Several tectonic models for the evolution of the MA have been proposed (e.g. Kellogg and Bonini, 1982; Colletta et al., 1997; Audemard and Audemard, 2002, Monod et al., 2010). However due to the lack of deep seismic reflection data, their crustal structure, symmetry and kinematics remain controversial. Audemard and Audemard (2002) separate these models in two groups: symmetric and asymmetric models. In the first group, the MA is conceived as a symmetric chain with a major axial strike slip fault in the centre (Boconó fault), and with bounding reverse faults on both sides of the mountain. The MA is interpreted as a positive flower structure and originates by pure transpression along of Boconó fault (e.g. Rod et al., 1958; Shagam, 1972; Stéphan, 1982). The second group of tectonics models takes into account the asymmetry of the MA revealed by the gravimetric survey of Hospers and Van Wijnen (1959). This asymmetry is explained by two types of subduction models. The first type proposes a doubly-vergent orogen (in sense of Willet et al., 1993), which is produced by the incipient continental subduction of the Maracaibo triangular block toward the Southeast

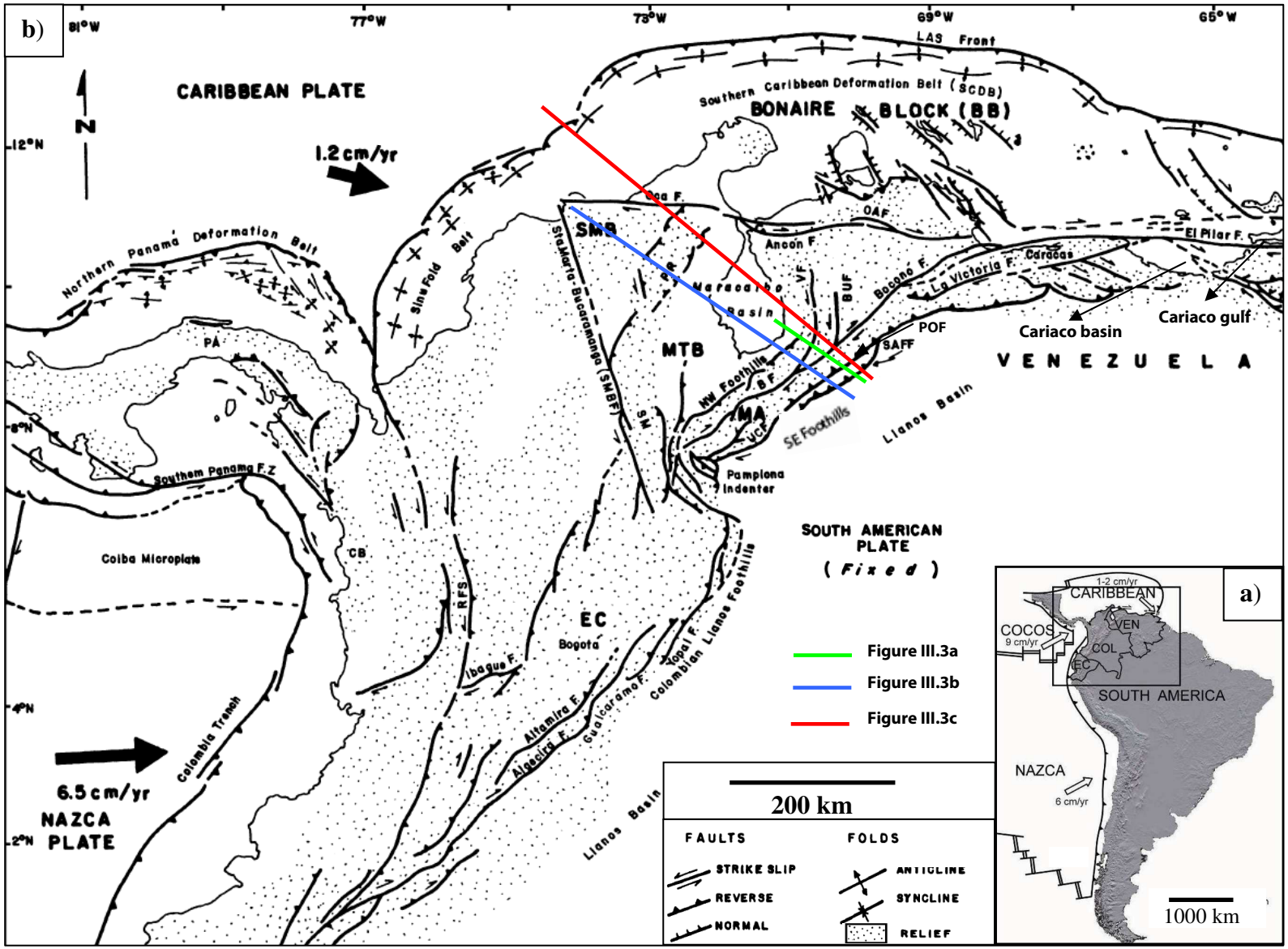
b)
81°W
77°W
73°W
69°W
65°W
12°N
8°N
4°N
2°N
N
CARIBBEAN PLATE
1.2 cm/yr
LAS Front
Southern Caribbean Deformation Belt (SCDB)
BONAIRE BLOCK (BB)
Northern Panama Deformation Belt
Sinu Fold Belt
Oca F.
OAF
Ancon F.
El Pilar F.
Caracas
La Victoria F.
Cariaco basin
Cariaco gulf
VENEZUELA
Santa Marta-Bucaramanga (SMBF)
SMB
Maracaibo Basin
BUF
Boconó F.
POF
SAFF
MTB
NW Foothills
BF
MA
SE Foothills
Llanos Basin
Pamplona Indenter
PA
Southern Panama F.Z
Coiba Microplate
CB
RFS
EC
Bogotá
Ibagué F.
Altamira F.
Algeciras F.
Guaicaramo F.
Topaipí F.
Colombian Llanos Foothills
SOUTH AMERICAN PLATE
(Fixed)
Figure III.3a
Figure III.3b
Figure III.3c
Colombia Trench
6.5 cm/yr
NAZCA PLATE
200 km
FAULTS
STRIKE SLIP
REVERSE
NORMAL
FOLDS
ANTICLINE
SYNCLINE
RELIEF
a)
1-2 cm/yr
CARIBBEAN
COCOS
9 cm/yr
VEN
COL
EC
SOUTH AMERICA
NAZCA
6 cm/yr
1000 km

***Figure III.1**. The MA with respect to the geodynamic setting of the Northern Andes, from Ecuador to Venezuela and Caribbean context. a) Shaded relief map of South America showing present-day plate configuration. The Northern Andes comprise mountain ranges in Ecuador (EC), Colombia (COL), and Venezuela (VEN). Black box is shows the location of the **figure III.1.b**. **b**) Major tectonic features of Northern South America (adapted from Audemard and Audemard, 2002). Original source: Stéphan (1982), Beltrán (1994), Audemard et al. (2000), Taboada et al. (2000). The locations of the cross section of the **figure III.3** are shown in the map. (BB) Bonaire Block; (BF) Boconó Fault; (BUF) Burbusay Fault; CB) Chocó Block; (EC) Esatern Cordillera of Colombia; (LAS) Lesser Antilles Subduction; (MTB) Maracaibo Triangular Block; (OAF) Oca-Ancón Fault; (PA) Panama Arc; (POF) Piedemonte Oriental Fault; (PR) Perija Range; (SAFF) South Andean Frontal Flexure; (SCDS) Southern Caribbean Deformation Belt; (SM) Santander Massif; (SMB) Santa Marta Block; (SMBF) Santa Marta-Bucaramanga Fault; (UCF) Uribante-Caparo Fault; (VF) Valera Fault.*

(e.g. Kellogg and Bonini, 1982; De Toni and Kellogg, 1993; Colletta et al., 1997) (**figure III.3a**). The other type applies an "orogenic float" model (in the sense of Oldow et al., 1990) to the whole of the Caribbean-South American plates boundary zone. In this case, a major mid-crustal detachment underlying the MA, Maracaibo basin, Perijá and Santa Marta ranges is proposed, with either north-west- or south-east-directed subduction of the underlying lower crust, and varying importance of strike-slip faults (e.g. Audemard, 1991; Jácome et al., 1995; Yoris and Ostos, 1997; Audemard and Audemard, 2002; Cediel et al., 2003; Monod et al., 2010) (**figure III.3b,c,d**).

The present-day kinematics of Northern Venezuela is dominated by relative Eastward advance of the Caribbean plate with respect to South America (**figure III.1**) (e.g. Molnar and Sykes, 1969; Bell, 1972; Malfait and Dinkelman, 1972; Jordan 1975; Pindell and Dewey 1982; Sykes et al., 1982; Wadge and Burke, 1983; Burke et al., 1984; Avé Lallemant, 1997; Villamil and Pindell, 1998; James, 2000; Colmenares and Zoback, 2003; Audemard et al., 2006). This Eastward motion is supported by results from GPS surveys, which put in evidence a rate between 12 mm/a in the West, and ~20 mm/a in the East (Freymueller et al., 1993; Kaniuth et al., 1999; Weber et al., 2001; Pérez et al., 2001; Trenkamp et al., 2002; Colmenares and Zoback, 2003; Jouanne et al., 2011). However this active boundary is not a simple dextral strike-slip type (Soulas, 1986; Beltran, 1994) since it is an over 100 km wide of active transpressional zone (Audemard, 1993, 1998; Singer and Audemard, 1997). In Western Venezuela the plate boundary covers a 600 km wide zone and comprises a set of discrete tectonic blocks or microplates (**figure III.1**), which move independently among the surrounding larger plates (Caribbean, South America and Nazca). The Maracaibo Triangular

Block is one of them, and is defined between the Bucaramanga-Santa Marta, Oca-Ancón and Boconó faults (Audemard, 1993, 1998; Dhont et al., 2005; Backé et al., 2006; Audemard et al., 2006). The kinematics of the bounding faults (sinistral for Bucaramanga - Santa Marta and dextral for Oca-Ancón and Boconó faults) has been used to propose a general North-Eastward escape of this block with respect to stable South America (Kellogg and Bonini, 1982; Dhont et al., 2005; Backé et al., 2006). Results of GPS plate motion studies confirm this hypothesis (Freymueller et al., 1993; Kellogg et al., 1995; Kaniuth et al., 1999; Trenkamp et al., 2002). This geodynamic setting produces strain partitioning along the MA, with NW-SE shortening component accommodated mostly along the two fronts of the chain, whereas the dextral component is accommodated along the axis of the range by the Boconó Fault (Audemard and Audemard, 2002; Pérez et al. 2011).

The current seismicity along the MA occurs within a broad zone, involving the main lineation of the Boconó Fault and the entire width of the MA (Audemard and Audemard, 2002). The seismicity along the main trace of the Boconó Fault occurs at depth lower than 40 km. The depths tend to increase for the biggest events to the Northwest (Maracaibo basin), Southwest (Pamplona) and Southeast (Llanos basin) to the surface trace of the Boconó Fault, reaching depths that can exceed 40 km (**figure III.4**). On the Southeastern flank of the MA, the Guanare March 05, 1975 (focal depth of 2.0 km) (Giraldo, 1985) and the Ospino December 11, 1977 (focal depth of 25 km) (Marín, 1982) earthquakes of magnitudes mb 5.5 and 5.6, respectively, are the largest events associated with the Southern Andean Foothills thrust system and specifically with the activity of the Piedemonte Oriental Fault (Audemard and Audemard, 2002).

Earthquake focal mechanism solutions show mainly a right - lateral faulting along the Boconó fault, left lateral faulting along the North –South trending fault to the North of the MA, and compression along the foothills thrust belts structures (**figure III.5**) (Audemard, 2003; Colmenares and Zoback, 2003; Corredor, 2003; Audemard et al., 2005; Cortés and Angelier, 2005). This compression can be distributed on different sub-parallels foothills thrust faults (e. g. Soulas, 1985; De Toni and Kellogg, 1993; Colletta et al., 1997; Duerto et al., 1998).

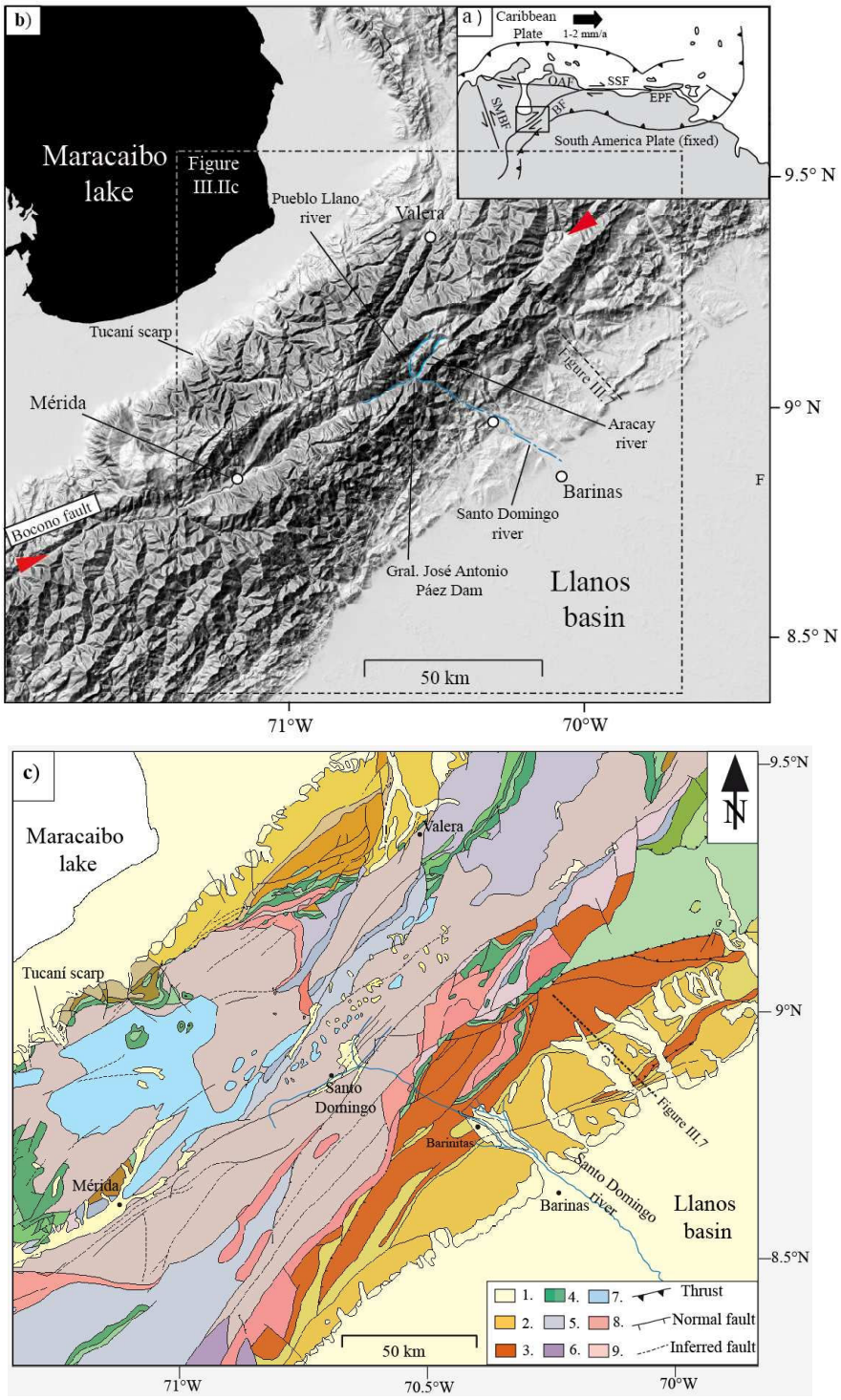

Figure III.2. *Geodynamic and morphological settings of the MA.* ***a****) simplified main present-day active tectonics of Northern South America (from Audemard and Audemard, 2002). (SMBF) Santa Marta Bucaramanga Fault; (OAF) Oca-Ancón Fault; SSF) San Sebastián Fault; (EPF) EL Pilar Fault; (BF) Boconó Fault.* ***b****) Shaded relief map of the central part of MA based on SRTM. Main active trace of the Boconó Fault is indicated by the two red arrows.* ***c****) Geological map of the central part of MA (from Hackley et al., 2005). 1. Pleistocene to Holocene alluvial sediments; 2. Oligocene, Miocene and Pliocene conglomerates and sandstones; 3. Paleocene to Eocene shales and sandstones;*

4. Jurassic to Cretaceous (Undifferentiated) limestones and sandstones; 5. Carboniferous to Permian phylites and limestones; 6. Ordovicician to Silurian shales and silstones; 7. Upper Paleozoic to Mesozoic intrusives rocks; 8. Upper to Lower Paleozoic intrusives rocks, phyllites, schists and gneiss; 9. Proterozoic gneiss, schists and granites. The location of Tucaní scarp (Wesnousky et al., 2012), Santo Domingo, Pueblo Llano and Aracay rivers are shown, as well as the location of the ***figure III.7****.*

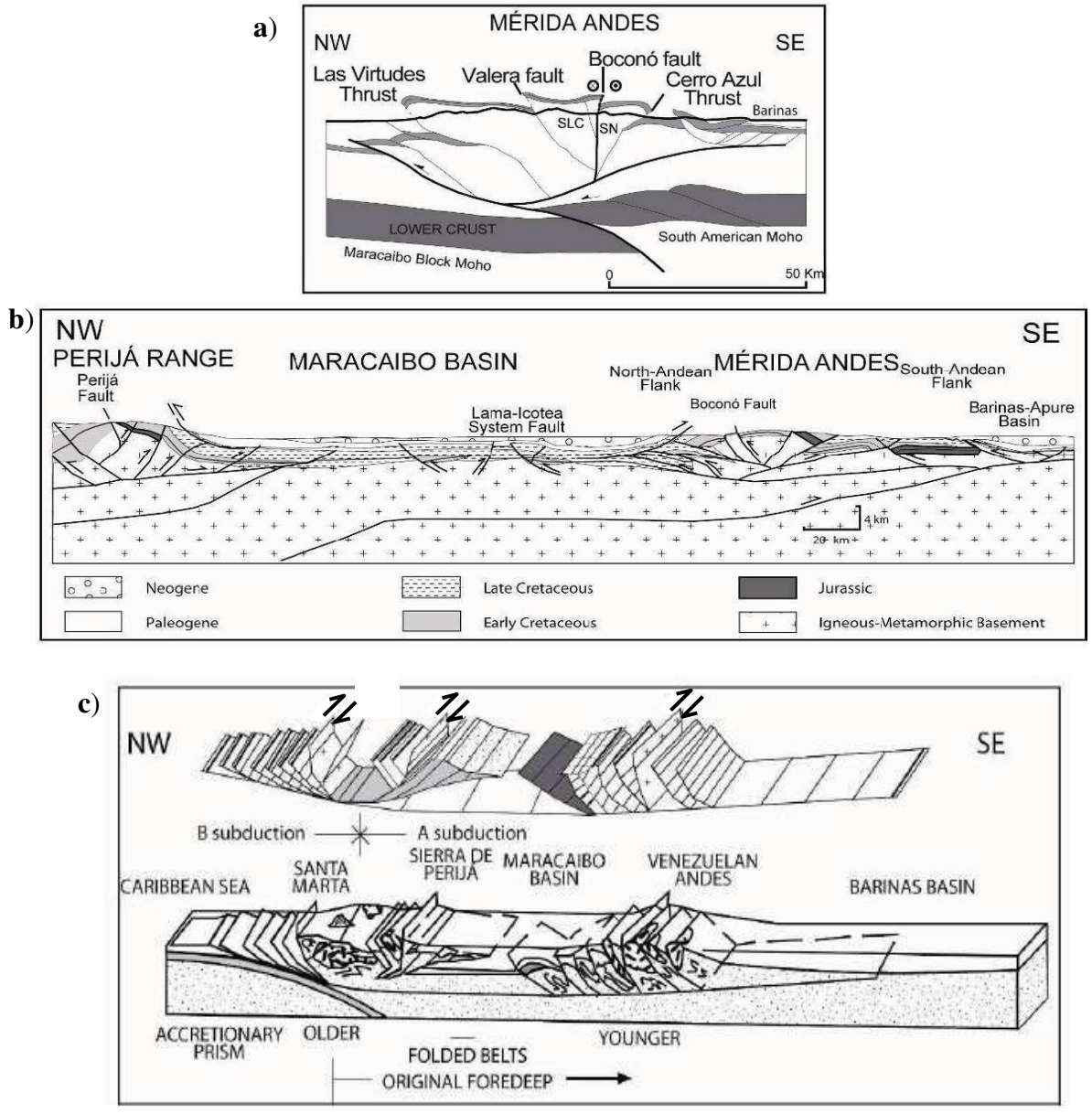

Figure III.3. *Crustal models for the MA.* ***a****) Intracontinental collision of Colletta et al. (1997). (SLC) Sierra La Culata block; (SN) Sierra Nevada block. Orogenic float models (in sense of Oldow et al. 1990):* ***b****) Yoris and Ostos (1997). (C&R basin) Cesar and Rancheria basin; (Lpz) lower Paleozoic; (Upz) upper Paleozoic; (Jr) Jurassic; (K) Cretaceous; (P) Paleogene; (N) Neogene.* ***c****) Audemard and Audemard (2002). The locations of these cross sections are shown in the* ***figure III.1b****.*

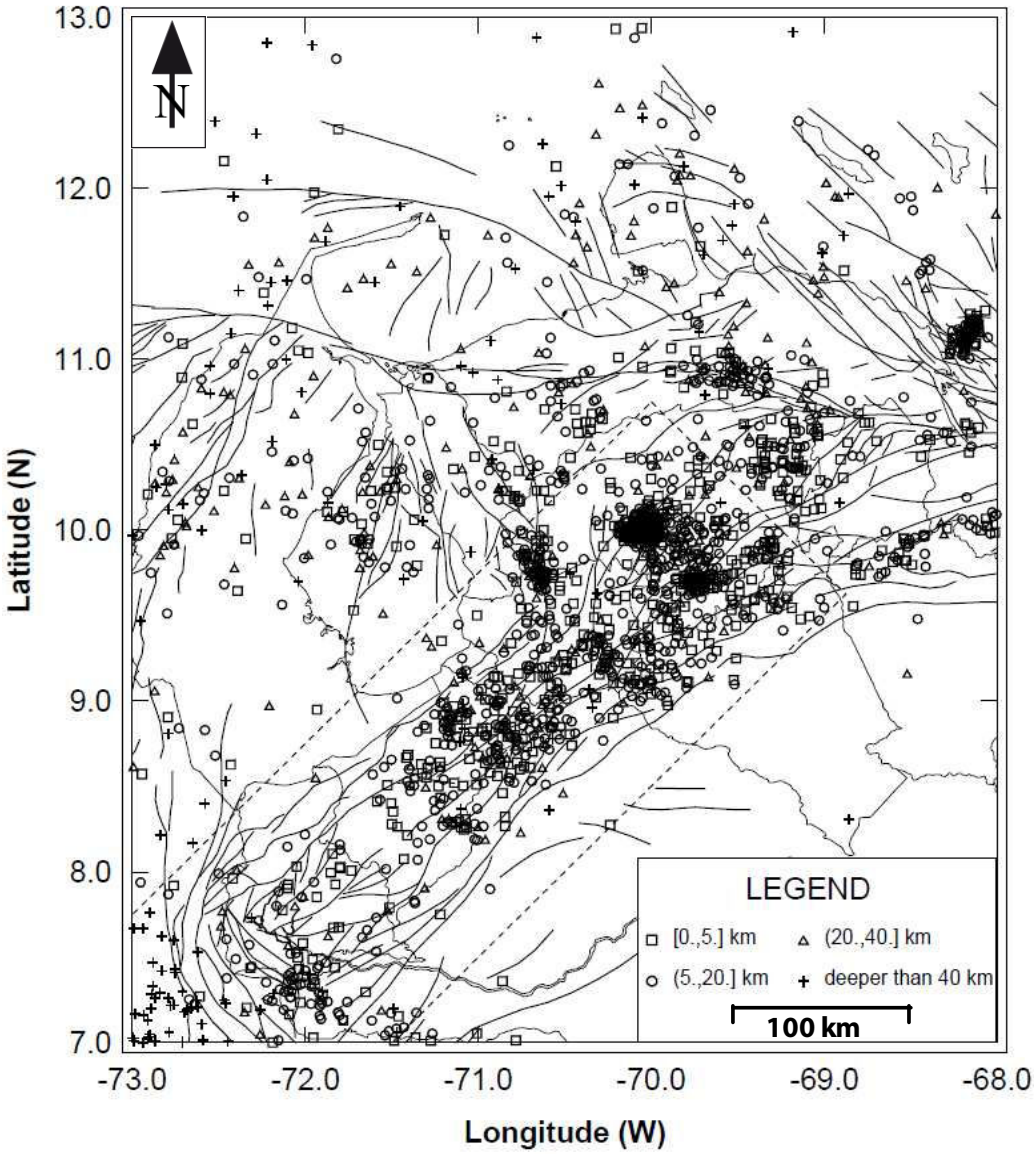

Figure III.4. *Depth distribution of the seismicity along the MA and surrounds (from Funvisis catalog).*

The MA uplift rate was roughly determined by Audemard (2003). This author used the depths of formation of the igneous and metamorphic rock (8-10 km), located in the highest summits of the chain (~5000 m a.s.l.), to propose a total uplift in the order of 12-15 km for the last 3-5 Ma, and to estimate an average uplift rate of 2 – 5 mm/a. Recently, ^{10}Be dating of boulders on a faulted alluvial fan along the Northwestern foothills (Tucaní scarp – **figure III.2b, c**) allowed to estimate a Late Pleistocene uplift rate of the Northwestern Andes at ~1.7 $\pm$ 0.7 mm/a (Wesnousky et al., 2012). Cooling ages derived from apatite fission track analysis of samples from different part of the chain suggest that the exhumation is diachronic across the MA from South-East to North-West (Kohn et al., 1984; Shagam et al., 1984, Bermudez,

2009; Bermudez et al., 2011). It is controlled by the reactivation of pre-existing faults and structures, and the inversion of Jurassic grabens (Kellogg and Bonini, 1982; Colletta et al., 1997; Audemard and Audemard, 2002; Bermudez, 2009).

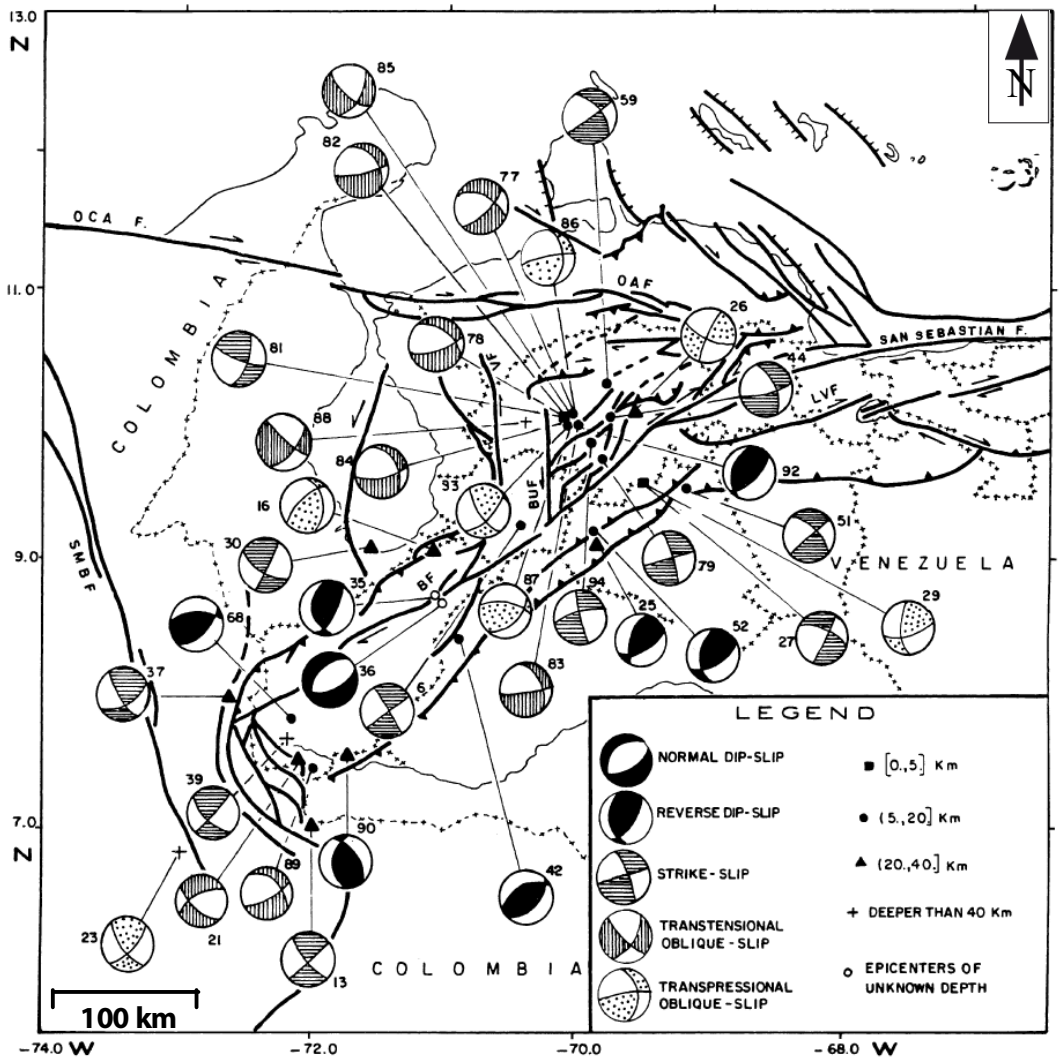

Figure III.5. *Focal mechanism solutions for earthquakes located within or near the MA, indicating the corresponding depth of the events (from Audemard et al., 1999a). Solutions are gathered based on their dominant slip.*

3.3.2. Southeastern flank of the Mérida Andes –Structural geology

As mentioned earlier, the core of the MA is characterized by strike-slip fault systems, while currently active fold and thrust belts are developed at each flank. This structural configuration allows the development of two prominent forebergs clearly distinguishable along both flanks, where the Southeastern one is better developed. During this thesis, the fluvial terraces located in the Southeastern flank and specifically among the Pueblo Llano and Santo Domingo rivers are analyzed. Therefore, a geological and geomorphological setting of

the central part of the Southeastern flank with emphasis in the Pueblo Llano - Barinitas area (study area – **figure III.6**) is discussed next.

- **Subsurface structure**

The deep structure of the MA through the Southeastern flank remains unknown. Indeed, there is no general agreement in the thrust vergenge, probably due to masking introduced by triangular zones and intracutaneous wedges, combined with important along-strike variations (Audemard and Audemard, 2002). However, the shallow subsurface structure of the Southeastern foothills can be observed in a seismic reflexion profile located relatively close to the study area (~30 km eastward) and with similar geologic surface characteristics (**figures III.2b, 6**). In the seismic profile, the Southeastern foothills exhibits a SE vergence, at least in the upper part crustal levels, as demonstrated by Funvisis (1997), Duerto et al. (1998) and Audemard (1999) (**figure III.7**). The subsurface is being affected by an active fold and thrust belt with ramp-flats geometry, where the thrusts have a gently dip at upper levels. A blind backthrust is identified in the front of the fold and thrust belt. This blind structure deforms the Plio-Quaternary molasses as indicated by a very prominent NE-SW-trending, SE-facing flexural scarp. It scarp is called South Andean Frontal Flexure (SAFF) (Audemard, 1999), and defines the boundary between the foothills unit and the Llanos basin (**figure III.7**) (Audemard, 1991, 1999; Funvisis, 1997). In this structural section, the thrust located further North is called Piedemonte Oriental fault (POF). This thrust finishes in a ramp that outcropps and forms La Antena range (**figure III.7**). This range is not present in the Barinitas area (**figure III.6)**, which suggests that the geometry of the POF is slightly different in the study area, where this fault does not exhibit the frontal ramp identified in the seismic profile (**figure III.7**). In this case, the upper detachment level probably continues with a very gentle dip until the frontal thrust. This geometry would cause a rising without tilting of the ground surface of the POF hangingwall block, where the river terraces located in the lower reaches of Santo Domingo river (object of this study) are located (**figures II. 3, 7**) (Audemard et al., 2007). Therefore these terraces will not suffer structural deformation in this part.

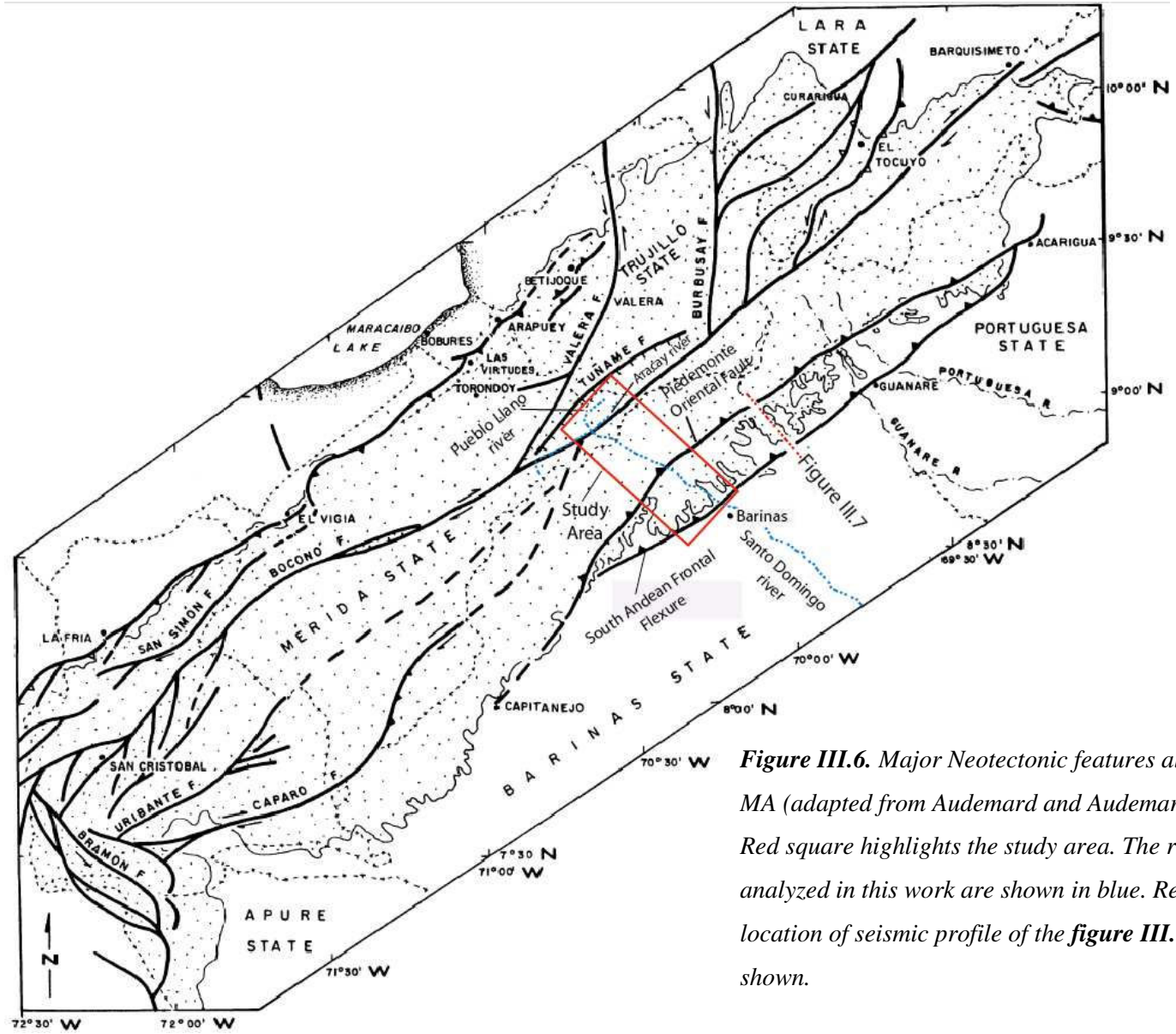

Figure III.6. *Major Neotectonic features along the MA (adapted from Audemard and Audemard, 2002). Red square highlights the study area. The rivers analyzed in this work are shown in blue. Relative location of seismic profile of the* ***figure III.7*** *is also shown.*

- **Active faults**

According to seismic activity and geomorphic evidence, the study area is affected by three active faults (Audemard et al., 2000 – **figure III.6**). At the core of the chain, the right-lateral Boconó Fault is traversed almost orthogonally by the Pueblo Llano and Santo Domingo rivers. The activity of this fault is largely evidenced by the current seismicity grouped along the main lineation of the Boconó Fault in the whole MA (Audemard et al., 1999a), as well as geomorphic evidence of right lateral offsets of Quaternary features (e.g. mountainous ridges, drainage channels, alluvial and glacial deposits) (e.g. Schubert, 1980a; 1980b; Soulas, 1985; Soulas et al., 1986; Ferrer, 1991; Audemard et al.,1999b). Slip rates of this fault have been estimated from moraine offset between 5.5 and 9 mm/a (e.g. Schubert and Sifontes, 1970; Schubert, 1980b; Schubert, 1982; Audemard et al., 2008; Wesnousky et al., 2011). These slip rates correlate with those given by geodetic measurements between 6.2 and 12 mm/a (Henneberg and Schubert, 1986; Pérez et al., 2001, 2011; Trenkamp et al., 2002).

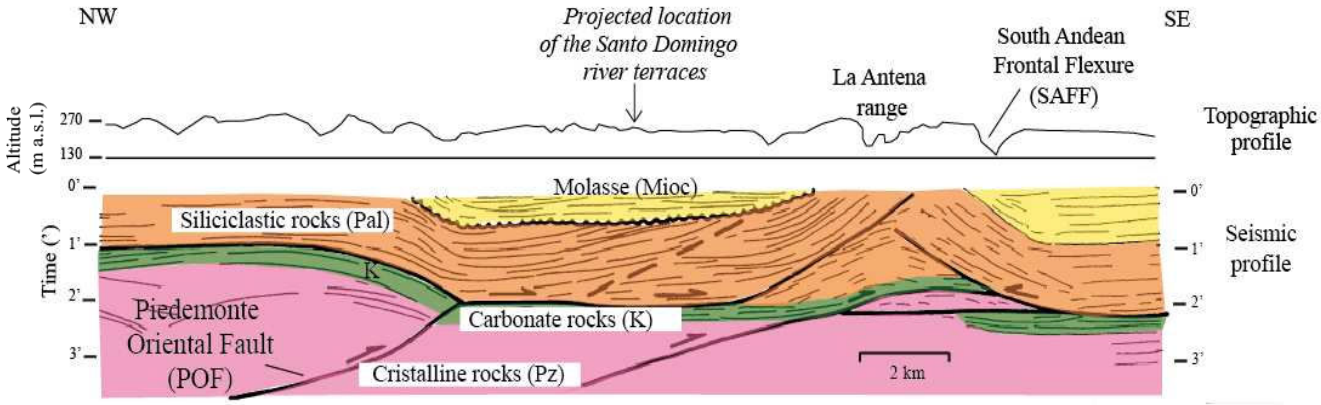

Figure III.7. *Structural interpretation from seismic and topographic profiles across the Southeastern foothills of the MA (Funvisis, 1997; Duerto et al., 1998; Audemard, 1999). The faults have ramp-flats geometry. Terraces located in the lower reaches of Santo Domingo river was projected in this section. Location of this figure is shown in* ***figures III.2b, 2c, 6****.*

The two other active thrust faults that affect the study area are the POF and the SAFF. These faults are present along the chain front (Audemard, 1999), both are blind faults and belong to the Southern Andean Foothills thrust system. The largest events associated with this system and specifically with the Piedemonte Oriental fault are the Guanare March 05, 1975 (focal depth of 2.0 km) (Giraldo, 1985) and the Ospino December 11, 1977 (focal depth of 25 km) (Marín, 1982) earthquakes of magnitudes mb 5.5 and 5.6, respectively. Geomorphic evidences like flexural scarps, tilting of river terraces and drainage patterns anomalies also put in evidence the active deformation of the Southern Andean Foothills thrust system (**figure**

III.8) (Audemard, 1999, 2003). Therefore this thrust system seems to be responsible for producing the uplift of the Southeastern flank of the MA. Hence in this thesis, I will use the river terraces located in the area to attempt quantifying the uplift rate of the MA.

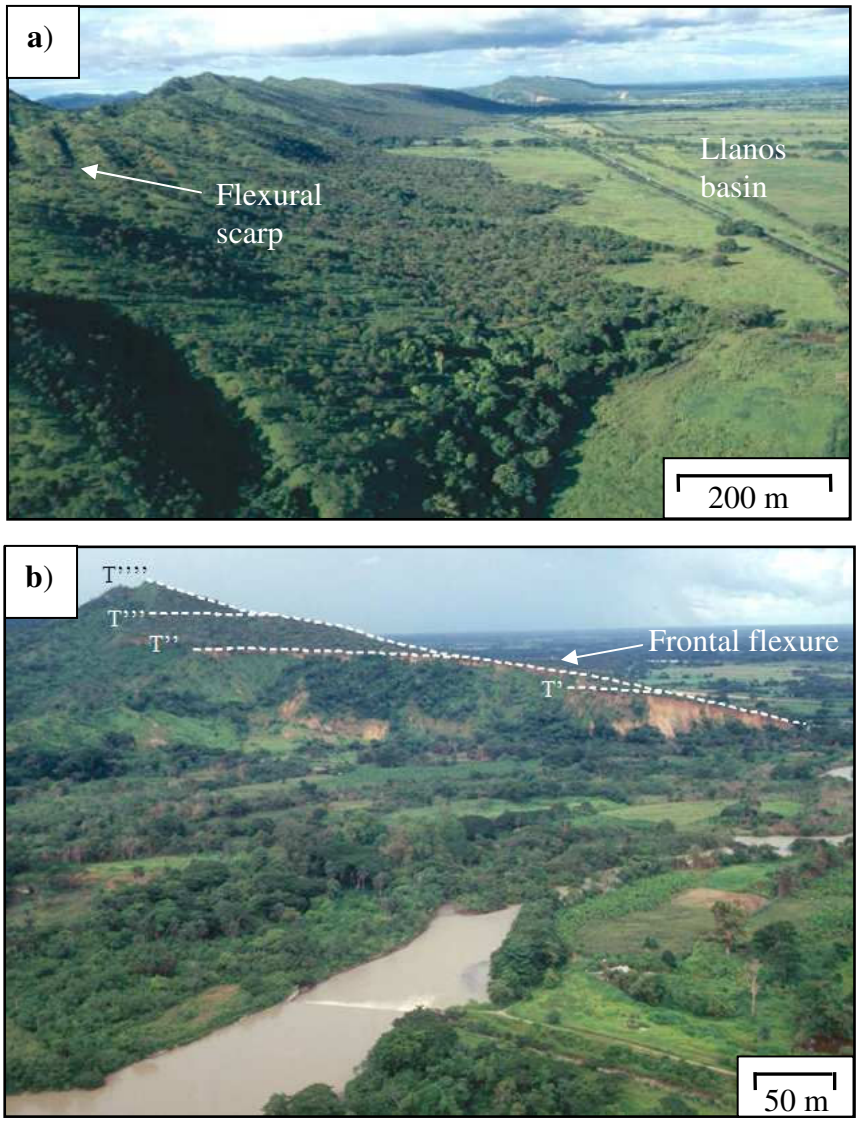

Figure III.8. *Geomorphic evidences of active faults along the Southern Andean Foothills thrust sytem.* ***a****) Flexural scarp of South Andean Frontal Flexure between Guanare and Barinas.* ***b****) Progressive tilting of at least four river terraces (T) along the Boconó river at Puente Páez, between Guanare and Barinas. The older and higher terrace (T'''') is the steeper one (adapted from Audemard, 2003).*

3.4. Climate and paleoclimate context of the Mérida Andes

- **Present-day climate**

Venezuela territory is entirely located in the tropics over the Equator between 0° and 12° N. Venezuelan climate varies from tropical humid conditions in the low elevation plains to glaciers tropical conditions in the highlands. This climatic zonation is sensitive to the seasonal migration of the Intertropical Convergence Zone (ITCZ), as a response to the annual insolation cycle (Poveda, et al., 2006). The ITCZ is a low-pressure tropical belt of maximum cloudiness and rainfall, and its position is determined by insolation and the convergence of the Northeast and Southeast tropical easterlies (McGregor and Nieuwolt, 1998). The ITCZ migration caused two distinct seasons in Venezuela: between December to March (when the ITCZ is South of Equator) a relatively cool and dry season with winds from the North is installed over Venezuela lands. While a period of heavy rainfall and hot conditions occurred between June and November (when the ITCZ migrates northward near to Venezuelan coast) (Hastenrath, 1984; Rull et al., 2010). This general pattern is locally modified by the topography of the MA. The Southeast side (also referred to as the "wet" side) is under the influence of wet trade winds that provide higher precipitation (~1500–2300 mm/a) than in the Northwest or "dry" side (~700–900 mm/a), which is in rainshadow. On the wet side, precipitation shows dependence on altitude; maximum values occur at ~2400 m elevation and decline above and below, a phenomenon not observed on the dry side (Monasterio and Reyes, 1980).

The maximum difference between the average temperature of the hottest and the coolest month of the year is around 2˚C or less (McGregor and Nieuwolt, 1998). The average annual temperature depends on the altitude, and ranges from 24 to 27˚C at sea level to slightly below 0˚C in the higher Andean summits (Monasterio and Reyes, 1980). In the MA, the temperature decreases at a rate of approximately 0.6 ˚C/100 m of elevation (Salgado-Labouriau, 1979; Huber, 1995). In contrast with the low seasonal temperature variability, the diurnal changes are remarkably high, especially in the high mountain environments (e.g. the MA), where they may reach 25°C between the daily maximum and minimum temperatures (Azocar and Monasterio, 1980).

- P**aleoclimatic setting**

The longest paleoclimate record for Venezuela was obtained in the Cariaco basin. This basin is located in the Northeastern continental shelf of Venezuela (around 1000 km eastward

to the MA) (**figure III.1**). Palynological and geochemical analysis of the marine and terrestrial record of this basin has been used for the reconstruction of climate variability for the last ~90 ka. (**figures III.9, 10**) (e.g. Hughen et al., 1996, 2000, Peterson et al., 2000a, 2000b; González et al., 2008). High-resolution reflectance measurements of the interval 90–25 ka, corresponding to Marine Isotopic Stage 3 (MIS 3), have clearly documented the abrupt stadial-interstadial shifts that characterized the Dansgaard-Oeschger (D/O) cycles and Heinrich Events (HE) described in North Atlantic marine cores and Greenland ice records (Hughen et al., 2004). In Cariaco basin, the interstadials events (warmings) are characterized by enhanced marine productivity, and increased precipitation and river discharge (as deduced from the elevated Ti and Fe content), as well as expansion of semi-deciduous forests. Stadials events (coolings) show the opposite trends (Peterson et al., 2000a, 2000b; Haug et al., 2001; Peterson and Haug, 2006; González et al., 2008) (**figure III.9**). Heinrich events are characterized by light color sediments and lower terrigenous input, prevailing cold and dry contitions almost indistinguishable from stadials (Haug et al., 2001; Peterson and Haug, 2006). The Last Glacial Maximun (LGM – Clark et al., 2009) and the Younger Dryas (YD – Muscheler et al., 2008) have been also documented in the Cariaco sea surface temperature reconstruction as cooling and dry periods, occurring between 23 and 21 cal ka BP and 13 and 11.8 cal ka BP, repectively (**figure III.10**). The last one was followed by a period of increased precipitation and riverine discharge that occurred during the Holocene thermal maximum (10.50 to 5.40 cal ka BP) (Haug et al. 2001; Lea et al., 2003; Hughen et al., 2004). Based on the previous results, the Cariaco paleoclimatologists concluded that the climate record of the Cariaco Basin is closely synchronous with the climatic events in the Northern hemisphere even with the rapid climate changes as D/O cycles and Heinrich events.

In another way, Van Daele et al. (2011) through seismostratigraphic analysis proposed a sea/lake level curve for the last ~130 ka of the Gulf of Cariaco (200 km eastward to the Cariaco basin) (**figure III.1**). The very good fit of this curve with the eustatic sea-level curves (Siddall et al., 2003; Waelbroeck et al., 2002) (both in terms of amplitude and of timing) seems to suggest that this curve respond to regional climatic variation, and therefore can be used as a paleoclimatic proxy (**figure III.11**).

In the MA no direct paleoclimatic information is available for times prior to the LGM (~18 ka). The only climatic evidence comes from glacial and fluvial sequences that have been dated and interpreted in terms of climatic variations (e.g. Schubert and Valastro, 1980; Salgado Labouriau, 1984; Mahaney et al., 2000; Dirszowsky et al., 2005; Rull, 2005). These data were recently compiled by Kalm and Mahaney (2011), in an attempt to reconstruct the

Late Quaternary glacial history of the MA (**figure III.12**). Here, a brief review of these data is presented with emphasis in the well documented climate/environment events and trends.

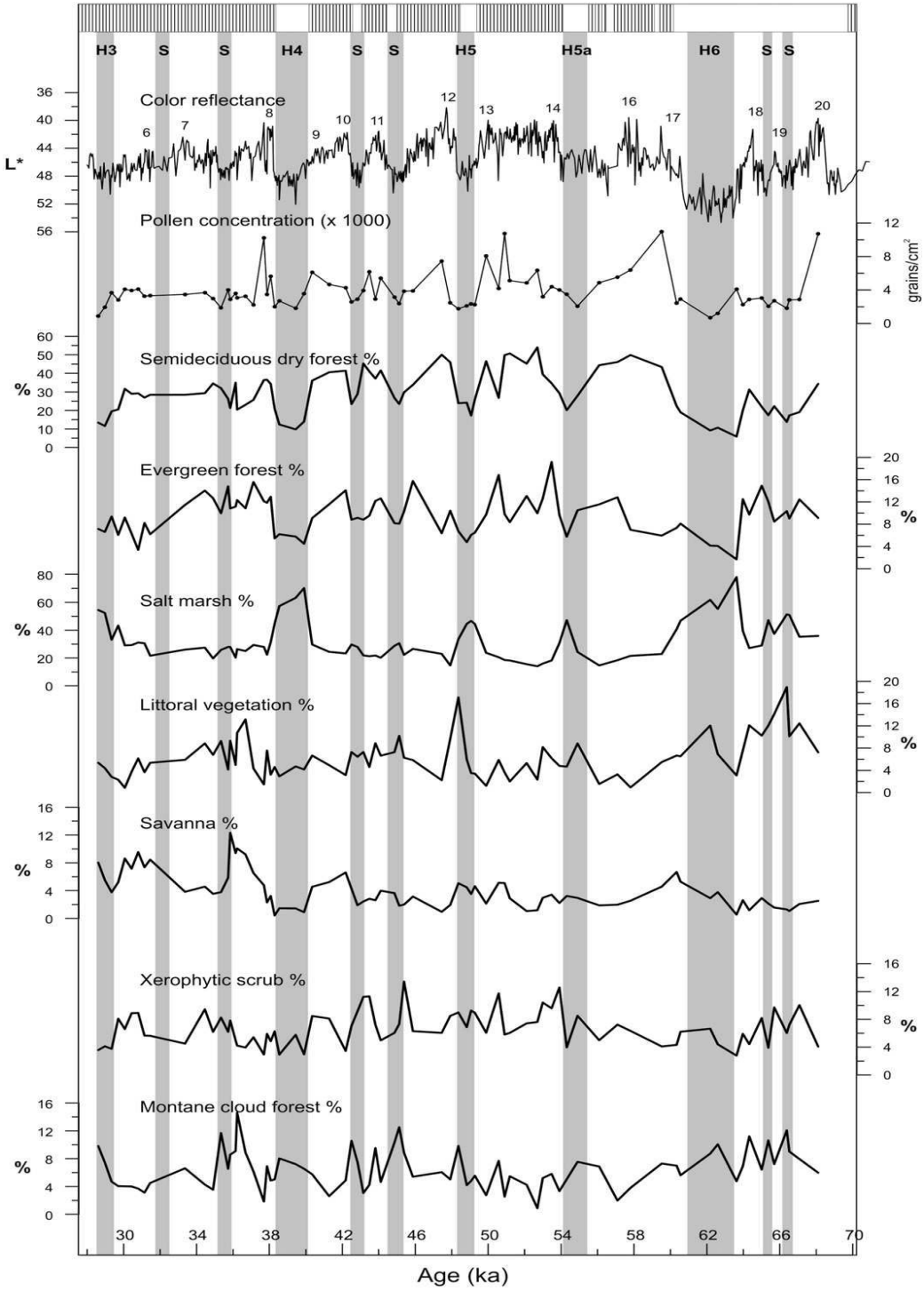

Figure III.9. *Cariaco basin reflectance and pollen records for the period between 70 and 30 ka from the core MD03-2622 (from González et al., 2008). Gray bars denote stadials (S) and Heinrich events (H). Heinrich events (H3–H6) are denoted according to cited ages (Rashid et al., 2003; Hemming, 2004), and interstadials are numbered as in ice core GISP 2.*

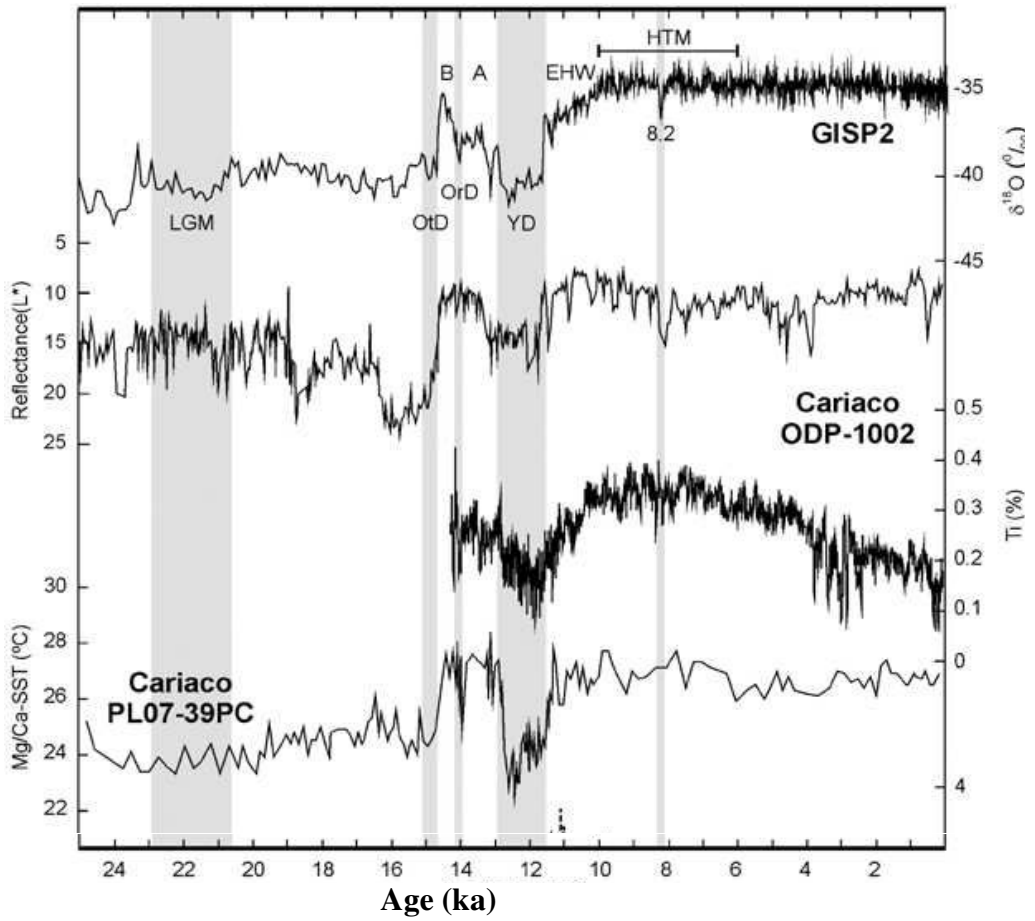

Figure III.10. *Summary of paleoclimate data since the LGM to the present, in Cariaco basin (from Rull et al., 2010). The oxygen-isotopic curve of the Greenland GISP2 ice core is shown for reference. Stadials and interstadials are from Stuiver et al. (1995):. (B) Bølling; (A) Allerød; (OtD) Oldest Dryas; (OrD) Older Dryas; (YD) Younger Dryas. Early Holocene warming (EHW) and Holocene thermal maximum (HTM) according to Haug et al. (2001), Bjöcrk et al. (2002), Kaufman et al. (2004), and Kaplan and Wolfe (2006).*

Schubert (1974), based on the presence of two moraines complexes located at different elevations, differentiates an early stage of Mérida glaciation, with ice reaching 2600 – 2800 m a.s.l. from a later stage with ice reaching 2900 – 3500 m a.s.l. The age for the Early Stage is poorly constrained. Indeed, only few chronological data are avalaible (Mahaney et al., 2001; Dirszowsky et al., 2005). These data set a lower limiting age at > 60 ka for the Early Mérida Stage. The age of the Late Mérida Stage is better constrained. In fact, this stage approximately coincides with the global LGM between 24 and 18 ka (Schubert, 1974; Schubert and Valastro, 1980; Schubert and Clapperton, 1990; Mahaney and Kalm, 1996; Rull, 2005). Temperatures estimation based on the elevation of representative moraines and reconstruction of the LGM Equilibrium Line Altitude (ELA) suggested a decrease in average temperature of at least 8.8 ±

2° C with respect to the present (Stansell et al., 2007). Lacustrine sediments with buried peat layers between sediments of Early and Late Mérida Stage at the El Pedregal section in central of the MA suggest interstadial condition (called El Pedregal Interstade) (relatively warmer and wetter climate), although with fluctuating climatic conditions during the period between < 60 ka and the LGM (Mahaney et al., 2001; Dirszowsky et al., 2005; Rull, 2005).

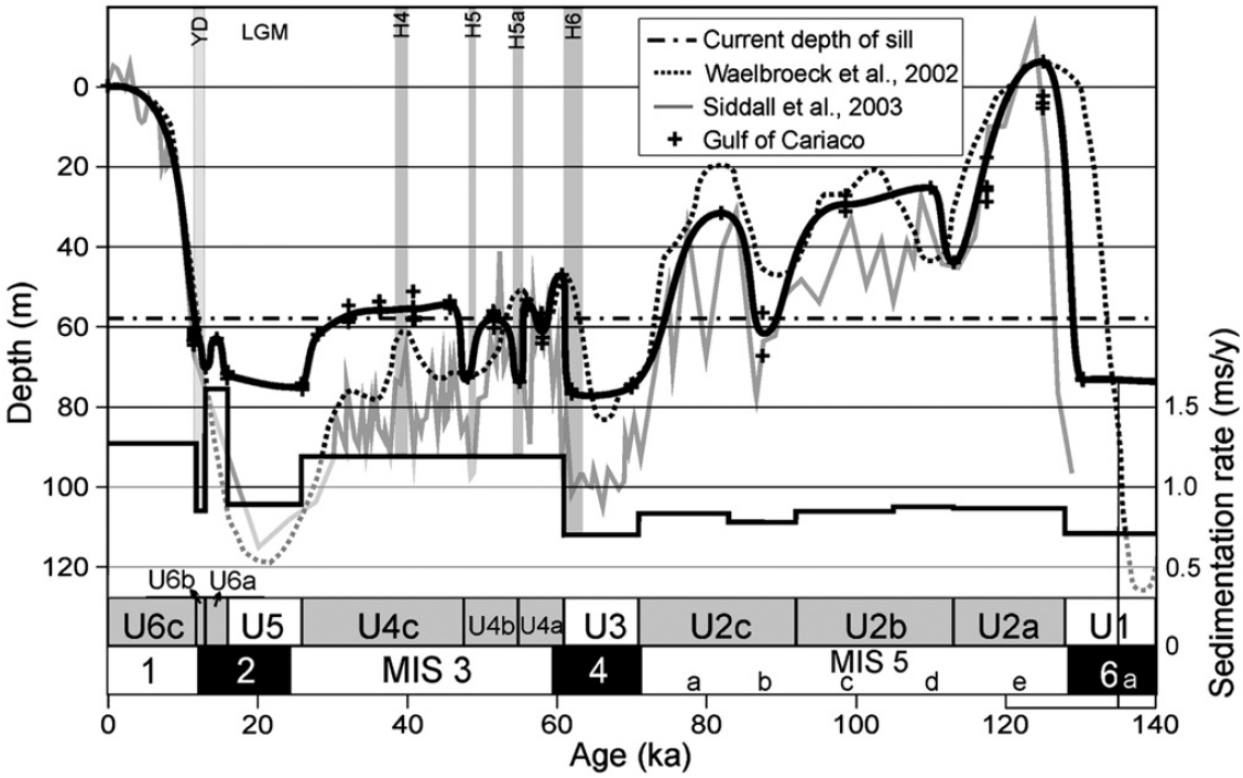

Figure III.11. *Sea/lake level curve for the last ~130 ka of the Gulf of Cariaco proposed by Van Daele et al. (2011). This curve is tuned to the eustatic sea level curve (Waelbroeck et al., 2002; Siddall et al., 2003) and to Marine isotope Stages (MIS 2–MIS 4). Also Heinrich Events (HE) recorded in the Cariaco Basin (Hughen et al., 2004; González et al., 2008) are indicated (grey bars).*

The climate history of the MA after LGM is largely based on pollen studies, which have yielded qualitative and quantitative estimates of past temperature and precipitation fluctuations (Salgado-Labouriau 1984; Salgado-Labouriau and Schubert 1976, 1977; Salgado-Labouriau et al., 1977, 1988, 1992; Rull 1998, 2005; Rull et al., 1987, 2005, Mahaney et al., 2008). Among the well-documented climatic periods are: a cold and dry phase between 12.65 and 11.50 ka (Salgado Laboriau, 1989; Carrillo, 2006; Carrillo et al., 2006; Mahaney et al., 2008). This cold and dry period can be correlated with the Younger Dryas cold event of Europe and North Atlantic region (c.a. 12.90 – 12.70 ka). A warm and humid phase between 9.4 and 6.3 ka (called Miranda warm phase), a cold and dry phase between 6.00 – 5.30 ka

(called La Culata dry phase) and a warm and humid phase between 3.64 – 2.45 ka (called Miranda warm phase II) (**figure III.12**). Two warm and humid periods dated by Mahaney et al., (2000) at around 1.48 and 0.92 ka

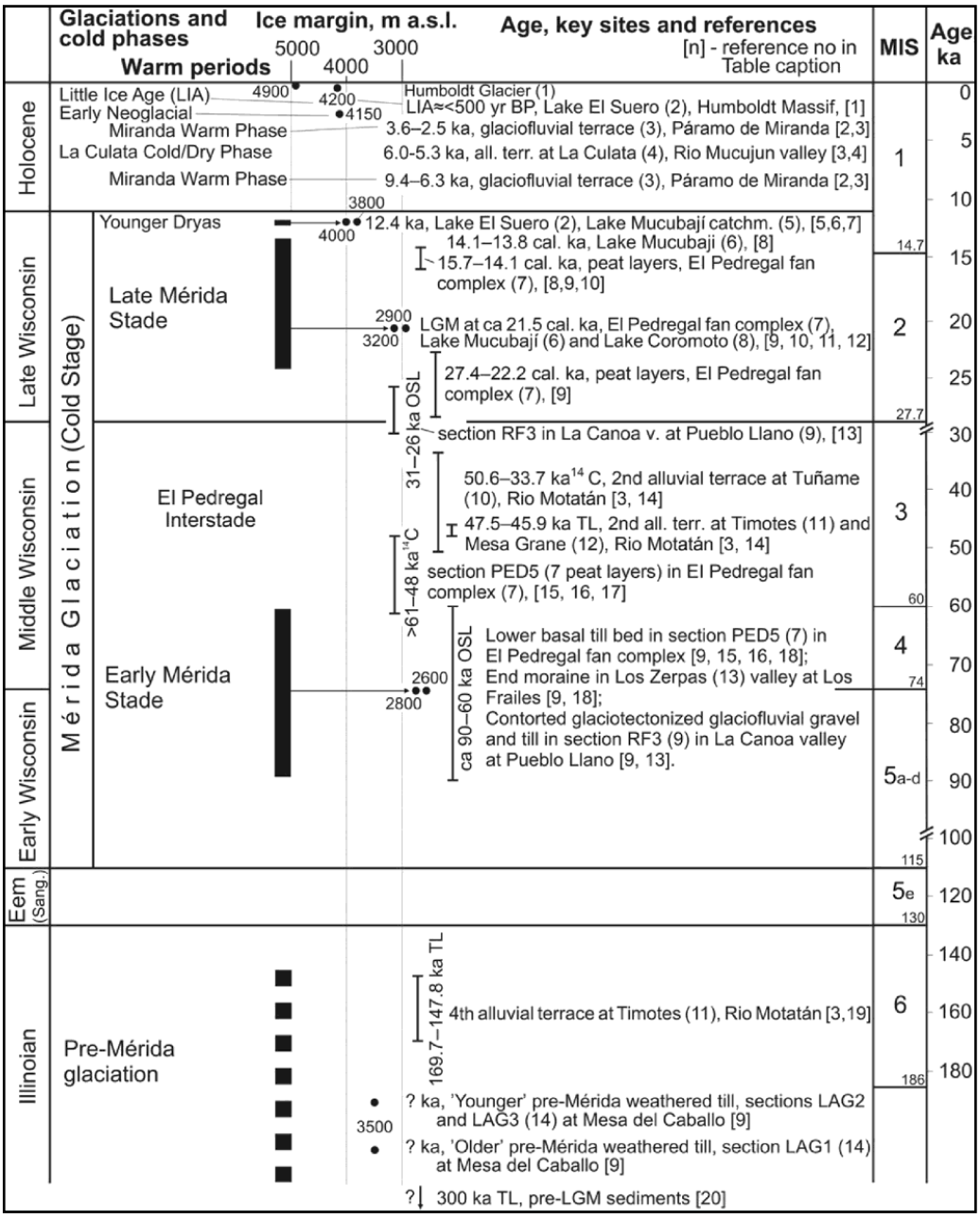

Figure II.12. *Glacial stratigraphy for the MA proposed by Kalm and Mahaney (2011). Dating and geomorphic data are compiled from different sources. They are indicated in the original figures with numbers in Square Brackets. See Kalm and Mahaney (2011) for full references.*

3.5. Pueblo Llano and Santo Domingo rivers system

- **General description**

At the core of the MA, the Pueblo Llano and Aracay rivers are the main tributaries of the Santo Domingo river. In this part of the chain, the upper reaches of Santo Domingo flows parallel to the axis of the chain, with a main direction from WSW to ENE (**figures III.2b, c, 6**). In this area, the upper and middle reaches of the Pueblo Llano river flow also parallel to the axis of the chain, but in an opposite direction from ENE to WSW. The lower reaches flow mainly from NNW to SSE in direction semi-orthogonal to the structural trend of the chain toward the confluence with the Aracay and Santo Domingo rivers in the Gral. José Antonio Páez dam. Then, the name of Santo Domingo is retained, and this river flows mainly orthogonal to the structural trend from WNW to ESE. Therefore, the lower reaches of the Pueblo Llano and Santo Domingo rivers, together constitute a rivers system that crosses orthogonally the MA, as well as active faults (**see subsection 3.2.2**). This system drains this part of the Southeastern flank of the chain.

Pueblo Llano and Santo Domingo rivers system (PLSDS) has a catchment surface of 1250 km^2 upstream to Barinas city. This system passes from a maximal elevation around 3500 m a.s.l. at the core of the chain to a minimum elevation around 200 m a.s.l. at the Southeastern flank in a distance of approximately 80 km. In the upper reaches (> 2700 m a.s.l.), glacial landforms and deposits have been reported (Vivas, 1979; Bezada, 1990; Mahaney et al., 2001), while in the middle and lower reaches, river terraces are the main landforms. The origin of these terraces have been mainly associated with Pleistocene paleoclimatic fluctuations (e.g. Zinck, 1980; Vivas, 1984; Schubert and Vivas, 1993), in particular with glacial/interglacial cycle (Tricart and Millies-Lacroix, 1962; Tricart and Michel, 1965; Tricart, 1966). For other terraces reported in rivers located along the axial part of the chain, a tectonic origin associated with the uplift of the chain has also been proposed (Shagam, 1972; Giegengack, 1984; Audemard, 2003). Nonetheless the lack of absolute ages in the river terraces of MA constitutes a weakness in the argumentation for the two hypotheses.

- **Morphometric analysis**

Longitudinal river profile of the PLSDS and the crest profile of the valley achieved in this thesis, put in evidence at least three morphostructural units. The first one belongs to the Andes Chain. It is located from the source of the system to km 50 downstream (**figure III.13**). In this unit the relief is between 600 and 3700 m a.s.l. with a mean elevation of 2550 m a.s.l.

The second unit, located between km 50 and km 70 from the source, correspond to the Southern foothills unit. The relief ranges in altitude between 200 and 600 m a.s.l. with a mean elevation of 430 m a.s.l. The last morphostructural unit corresponds to the flat relief of the Llanos basin.

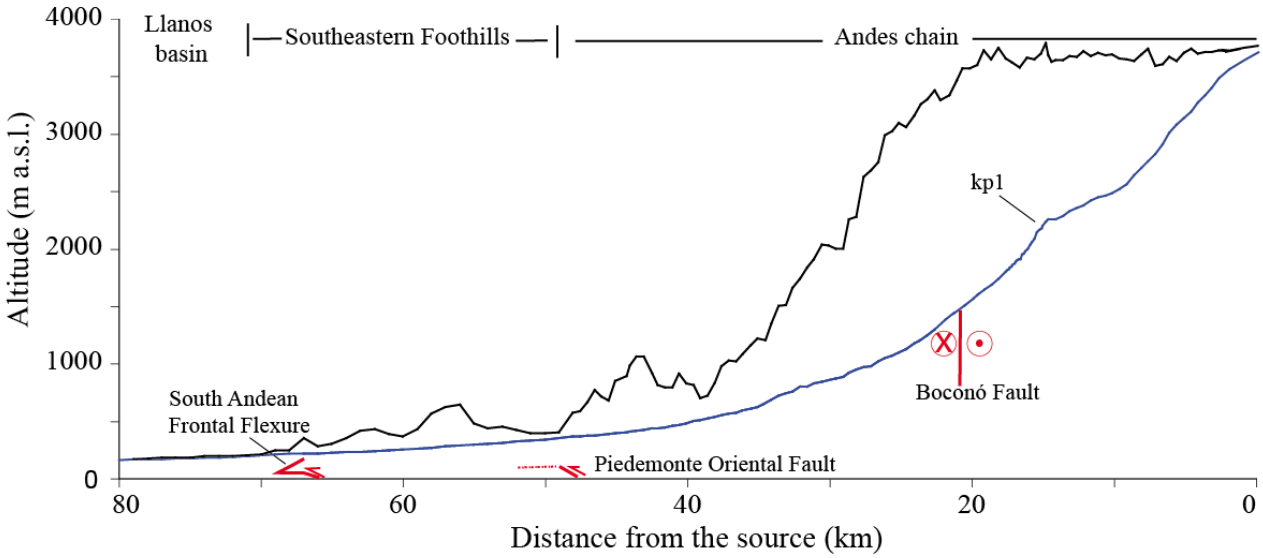

Figure III.13. *Morphometric curves of the Pueblo Llano and Santo Domingo rivers system. Blue and black lines represent the longitudinal river profile and the right crest profile along the valley, respectively. (kp) knickpoint. The geometry of the South Andean Frontal Flexure and Piedemonte Oriental Fault are extrapolated from the seismic profile of* ***figure III.7****, but the depth projections are not at scale.*

Topography disruptions observed in the right crest profile of the valley between the Andes Chain and Foothills units (between km 40 and km 50 from the source) puts in evidence the active deformation of the Southern Andean Foothills thrust system (**figure III.13**). Along the Foothills unit, the relief is dominated by river terraces, which are tectonically deformed according to their structural positition. Terraces located near the South Andean Frontal Flexure are progressively tilted, thus the highest terrace is the steeper one. This terrace forms the surface of the frontal flexure; the other terraces crop out upstream of the flexure (**figure III.8b**). By contrast, the surface of river terraces located between km 50 and km 65 from the source are mainly flat and evidences of localized tectonic deformation are not present (**figure II.3**).

Into the Andes chain unit, the PLSDS shows two different behaviours. At the upper reaches (upstream of km 38 from the source), a straight river shows an average high channel

gradient of approximately 4°, whereas at the lower reaches (between km 40 and km 50 from the source), a braided river has an average low channel gradient of approximately 1° (**figure III.13)**. In the foothills, the average channel gradient decreases to 0.3°. A knickpoint at 2250 m a.s.l. (kp1) is detected at the upper reaches of the system (**figure III.13)**. Knickpoints are also present in the longitudinal river profiles of the Aracay and the upper reaches of the Santo Domingo rivers. In the Aracay river, the knickpoint is located at 2750 m a.s.l. (kpAr). In the case of the upper Santo Domingo, the knickpoint is located at 3200 m a.s.l. (kpSD) (**figure III.14**)

- **Knickpoint origin**

The knickpoint identified in the PLSDS at 2250 m a.s.l. (kp1) would be associated either 1) to the transition of the glacial to the fluvial domain or 2) to the retreat of a knickpoint produced by the activity of the Boconó Fault. In the second case, kp1 and the knickpoints identified in the Aracay (kpAr) and upper Santo Domingo rivers (kpSD) could have the same origin. These knickpoints are located at different distances from the confluence (around 5, 10 and 20 km for kp1, kpAr and kpSD, respectively). Their elevations are different in each case (2250, 2750 and 3200 m a.s.l.). These differences can be produced by the diverse propagation speeds of the knickpoint in each river. However, the elevation of these knickpoints corresponds approximately to the minimal elevations reached by the glaciers during the Mérida glaciation in each catchment (e.g. Schubert, 1974; Vivas, 1979; Bezada, 1990; Schubert and Clapperton, 1990, Schubert and Vivas, 1993). Moreover, the comparison of the hypsometry curves of the three catchments seems to suggest that the drainage evolution is almost similar in the three rivers (**figure III.15**), regardless of the orientation of the catchment and/or the minimal elevation that could reach the glacier in each catchment. Therefore, we argue that kp1, kpAr and kpSD are associated to local base levels of each catchment, and probably are the evidence of transition between the glacial and fluvial deposits domain in the three valleys.

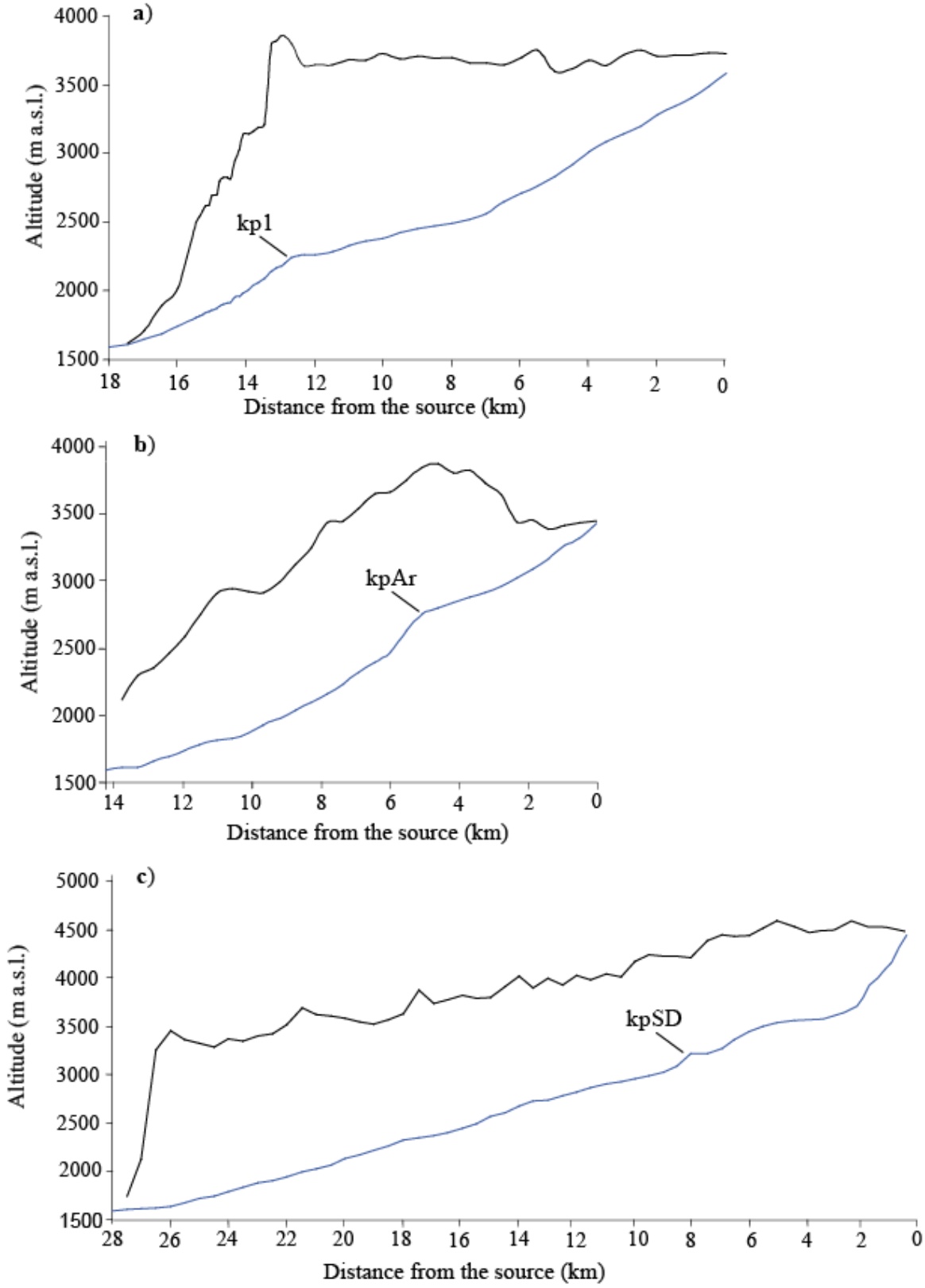

Figure III.14. *Morphometric curves of the:* ***a****) Pueblo Llano river.* ***b****) Aracay river.* ***c****) Upper reaches of the Santo Domingo river. Blue and black lines represent the longitudinal river profile and the right crest profile along the valley, respectively. In each profile a knickpoint (kp) is detected (see text for discussion).*

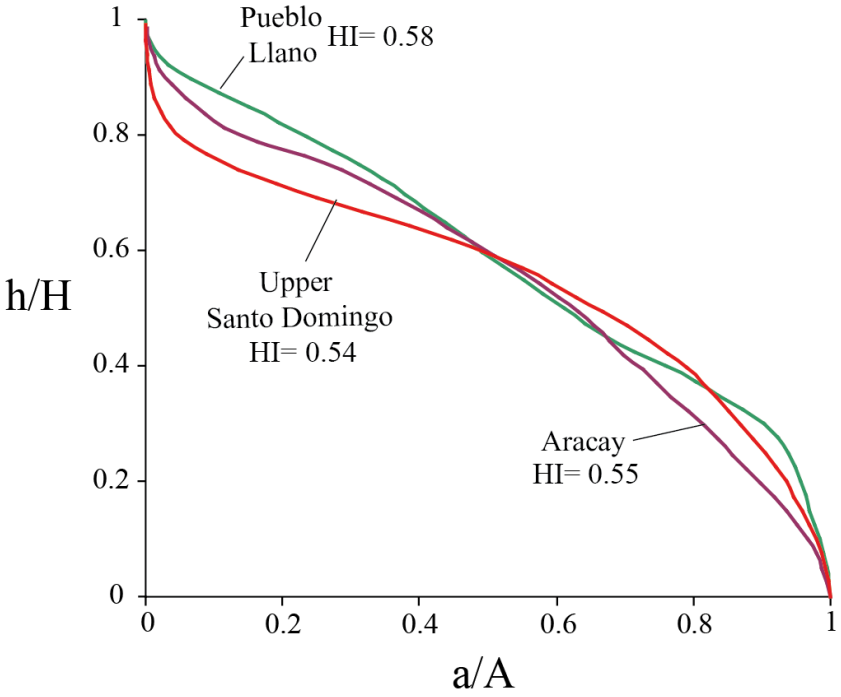

Figure III.15. *Hypsometric curves of Pueblo Llano, Aracay and Upper Santo Domingo rivers. The morphology of the curves is similar with a high hypsometric integral (HI), which suggests that the drainage evolution in the three catchments is almost similar.*

For the reasons discussed above, I argue that the geologic, geomorphic and paleoclimatic setting of the PLSDS appears as a suitable context to study the effects of tectonic and climatic variations in the process of terraces formation. Thus, I apply a morphotectonic analysis coupled with *in situ* produced ^{10}Be dating, in an attempt to understand the process of terrace formation along of this system. Firstly, I focus on the lower reaches of the system, within the foothills unit, where the river terraces are sufficiently far from the deformation front to suffer tectonic deformation. In this setting, I use the river terraces as geodetic markers, in order to constrain the uplift rate of the Southeastern flank of the MA. Moreover, I make a first correlation between paleoclimate context and processes of terraces formation. This study is presented as an article published in Journal of South American Earth Sciences in the following.

3.6. ^{10}Be dating of river terraces of Santo Domingo river, on Southeastern flank of the Mérida Andes, Venezuela: tectonic and climatic implications

Journal of South American Earth Sciences 48 (2013) 85–96

Contents lists available at ScienceDirect

Journal of South American Earth Sciences

journal homepage: www.elsevier.com/locate/jsames

^{10}Be dating of river terraces of Santo Domingo river, on Southeastern flank of the Mérida Andes, Venezuela: Tectonic and climatic implications

Oswaldo Guzmán [a, b, *], Riccardo Vassallo [b], Franck Audemard [c, d], Jean-Louis Mugnier [b], Javier Oropeza [c], Santiago Yepez [a, e], Julien Carcaillet [f], Miguel Alvarado [g], Eduardo Carrillo [h]

[a] Departamento de Ciencias de la Tierra, Universidad Simon Bolivar, 89000, Caracas 1081-A, Venezuela
[b] ISTerre, Université de Savoie, CNRS, F-73376 Le Bourget du Lac, France
[c] Departamento de Ciencias de la Tierra – Fundacion Venezolana de Investigaciones Sismologicas, Caracas, Venezuela
[d] Escuela de Geología, Minas y Geofísica, Facultad de Ingeniería, Universidad Central de Venezuela, Caracas, Venezuela
[e] Fundacion Instituto de Ingenieria – CPDI, Sartenejas, Venezuela
[f] ISTerre, Université de Grenoble 1, CNRS, F-38041 Grenoble, France
[g] Universidad de Los Andes, Mérida, Venezuela
[h] Instituto de Ciencias de La Tierra, Universidad Central de Venezuela, Venezuela

ARTICLE INFO

Article history:
Received 1 May 2013
Accepted 3 September 2013

Keywords:
Venezuela
Mérida Andes
River terraces
Climatic control
Uplift rate
In situ produced ^{10}Be

ABSTRACT

In this study, we discuss the first cosmogenic ^{10}Be dating of river terraces located in the lower reaches of the Santo Domingo river (Southeastern flank of the Mérida Andes, Western Venezuela). The geomorphic observations and dating allowed the restoration of the temporal evolution of incision rate, which was analysed in terms of tectonic, climatic and geomorphic processes. The long-term incision rate in the area has been constantly around 1.1 mm/a over the last 70 ka. Taking into account the geologic and geomorphologic setting, this value can be converted into the Late Pleistocene uplift rate of the Southeastern flank of the Mérida Andes. Our results show that the process of terraces formation in the lower reaches of the Santo Domingo river occurred at a higher frequency (10^3–10^4 years) than a glacial/interglacial cycle (10^4–10^5 years). According to the global and local climate curve, these terraces were abandoned during warm to cold transitions.

1. Introduction

River terraces are paleotopographic markers, the genesis of which results from tectonics, climatic changes, eustatic variations and geomorphic processes at the catchment scale (Pazzaglia, 2013). The geometrical and sedimentological analysis of river terraces coupled with numerical ages have been widely used in order to decipher and quantify the role of each process (e.g. Maddy et al., 2001; Antoine et al., 2007; Wegmann and Pazzaglia, 2009; Lewin and Gibbard, 2010). The Mérida Andes (MA) is an active tectonic range, located in Western Venezuela (Fig. 1), where several rivers (e.g. Chama, Santo Domingo, Motatán, Guanare, Mocotíes, Tucaní) provide a wide record of river terraces. The origin of these terraces has been mainly associated with Pleistocene paleoclimatic fluctuations (e.g. Zinck, 1980; Vivas, 1984; Schubert and Vivas, 1993), in particular with glacial/interglacial cycles (Tricart and Millies-Lacroix, 1962; Tricart and Michel, 1965; Tricart, 1966). For the terraces located along the axial part of the chain, a tectonic origin associated with the uplift of the chain has also been proposed (Shagam, 1972; Giegengack, 1984; Audemard, 2003). Nonetheless the lack of numerical ages in the river terraces of the MA constitutes a weakness in the argumentation for these two hypotheses.

This study focuses on the Southeastern flank of the MA. The study area is located in the lower reach of Santo Domingo river between the Barinitas city and El Charal village (Fig. 1). In this region, the river presents a series of well-preserved strath terraces, thus the incision rate can be estimated at different time scales. In this reach, the river is orthogonal to the structural trend of the chain; therefore the effect of localized active deformation in the

* Corresponding author. Departamento de Ciencias de la Tierra, Universidad Simon Bolivar, 89000, Caracas 1081-A, Venezuela.
E-mail addresses: oswaldojoseguzman@gmail.com, guzmano@usb.ve (O. Guzmán).

0895-9811/$ – see front matter © 2013 Elsevier Ltd. All rights reserved.
http://dx.doi.org/10.1016/j.jsames.2013.09.004

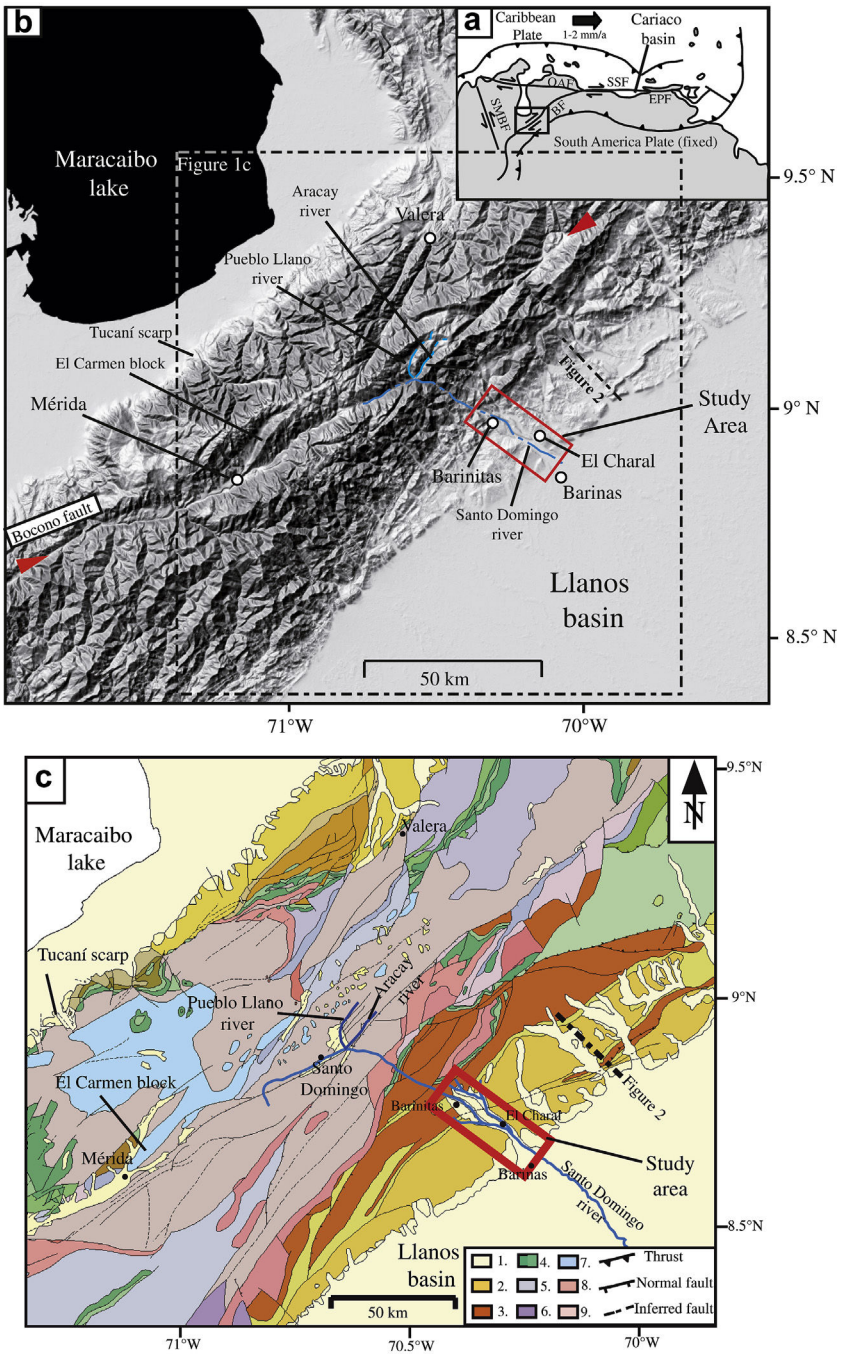

Fig. 1. Geodynamic and morphological settings of the study area. **a**) simplified main present-day active tectonics of Northern South America (from Audemard and Audemard, 2002). (SMBF) Santa Marta Bucaramanga Fault; (OAF) Oca-Ancón Fault; SSF) San Sebastián Fault; (EPF) EL Pilar Fault; (BF) Boconó Fault. Location of the Cariaco basin is shown. **b**) Shaded relief map of the MA based on SRTM. Location of the study area is shown by a red square. Main active trace of the Boconó Fault is located between the two red arrows. **c**) Geological map of the study area from Hackley et al. (2005). 1. Pleistocene to Holocene alluvial sediments; 2. Oligocene, Miocene and Pliocene conglomerates and sandstones; 3. Paleocene to Eocene shales and sandstones; 4. Jurassic to Cretaceous (Undifferentiated) limestones and sandstones; 5. Carboniferous to Permian phylites and limestones; 6. Ordovician to Silurian shales and silstones; 7. Upper Paleozoic to Mesozoic intrusives rocks; 8. Upper to Lower Paleozoic intrusives rocks, phyllites, schist and gneiss; 9. Proterozoic gneiss, schist and granites. Location of Tucaní scarp (Wesnousky et al., 2012) and El Carmen block (Kohn et al., 1984) are also shown. (For interpretation of the references to colour in this figure legend, the reader is referred to the web version of this article.)

process of terraces formation can be quantified. Additionally, the river is far from the sea (more than 1500 km), then the effect of eustatic variation can be neglected. Hence, in this study a morphotectonic analysis is coupled with *in situ* produced ^{10}Be dating (^{10}Be dating, in the text), in order to reconstruct the temporal evolution of the incision rate, which will be analysed in terms of impact of the different processes.

2. Geological setting

The MA is situated in the Western part of Venezuela. This range is around 400 km long with an SW-NE direction from the Colombian-Venezuelan border in the Southwest to Barquisimeto city in the Northeast. The mean elevation of the MA is about 2024 m a.s.l. and culminates at 4978 m a.s.l. at Pico Bolivar, located in the

central part of the chain. The range is bounded on both flanks by the lowlands of the Maracaibo and Llanos basins at the Northwest and Southeast, respectively. Two prominent forebergs are clearly distinguishable along both flanks even if the Southeastern one is better developed (Fig. 1).

The mountain building of MA is related to a complex geodynamic interaction between the Caribbean, South America and Nazca plates and other minor continental blocks (Taboada et al., 2000; Audemard and Audemard, 2002; Bermudez, 2009; Monod et al., 2010). This interaction of plates leads to the oblique convergence between the Maracaibo Triangular Block and South America Plate, and is responsible for the present MA build-up (Colletta et al., 1997; Audemard and Audemard, 2002). This geodynamic setting produces: 1) strain partitioning along the chain, with the NW – SE shortening component accommodated mostly along the two fronts, whereas the dextral component is accommodated along the axis of the range by the Boconó fault (Audemard and Audemard, 2002; Pérez et al., 2011); and 2) tectonic escape process in the central part of the MA (Dhont et al., 2005; Backé et al., 2006).

Current seismicity along the MA occurs within a broad zone, involving the main lineation of the Boconó fault and the entire width of the MA (Audemard and Audemard, 2002). Focal mechanism solutions show mainly a right-lateral faulting along the Boconó fault, left lateral faulting along the North–South trending faults to the North of the MA, and compression along the foothills thrust structures (Audemard, 2003; Colmenares and Zoback, 2003; Corredor, 2003; Cortés and Angelier, 2005). The compression component is distributed through time on different sub-parallel foothills thrusts (e.g. Soulas, 1985; De Toni and Kellogg, 1993; Colletta et al., 1997; Duerto et al., 1998; Audemard, 1999).

Audemard (2003) used the depths of formation of the igneous and metamorphic rocks (8–10 km), located in the highest summits of the chain (~5000 m a.s.l.), to propose a total uplift in the order of 12–15 km for the last 3–5 Ma, and to estimate a rough uplift rate of 2–5 mm/a. Cooling ages derived from apatite fission track analysis of samples from different part of the chain suggest that the long term uplift is diachronic across the MA from Southeast to Northwest (Kohn et al., 1984; Shagam et al., 1984; Bermudez, 2009; Bermudez et al., 2011). It is controlled by the reactivation of pre-existing faults and structures, and the inversion of Jurassic grabens (Kellogg and Bonini, 1982; Colletta et al., 1997; Audemard and Audemard, 2002; Bermudez, 2009). Recently, ^{10}Be dating of boulders on a faulted alluvial fan along the Northwestern foothills (Tucaní scarp – Fig. 1) yielded a Late Pleistocene uplift rate for the Northwestern Andes of ~1.7 ± 0.7 mm/a (Wesnousky et al., 2012).

The MA uplift corresponds to a positive vertical movement of the MA with respect to the Maracaibo and Llanos basins, which are the base levels of the NW and SE running drainage systems, respectively (Fig. 1). This leads to vertical incision by rivers draining the range and consequent formation of fluvial terraces along the rivers located within the chain. These rivers are predominantly oriented in two directions with respect to the axis of the chain: i) Sub-parallel, mainly in the core of the range, and ii) Sub-orthogonal, towards the NW and SE fronts. The Santo Domingo river, located in the central part of MA is flowing along the Southeastern flank from the axis of the chain to the Llanos basin (Fig. 1); in the lower reaches, the Santo Domingo river is orthogonal to the geological structures, thus allowing the study of the late Quaternary incision through them.

3. Paleoclimatic setting

In the MA paleoclimatic information for times prior to the Last Glacial Maximum (~18 ka) comes from glacial and fluvial sequences that have been dated and interpreted in terms of climatic variations (e.g. Schubert and Valastro, 1980; Salgado Labouriau, 1984; Mahaney et al., 2000; Dirszowsky et al., 2005; Rull, 2005). Schubert (1974), based on the presence of two moraine complexes located at different elevations, differentiates an Early and a Late Stage of Mérida glaciation. The age for the Early Stage is poorly constrained. Indeed, only few chronological data are available and they set a lower limiting age at 60 ka (Mahaney et al., 2001; Dirszowsky et al., 2005). The age of the Late Mérida Stage is better constrained. This stage approximately coincides with the global Last Glacial Maximum between 24 and 18 ka (Schubert, 1974; Schubert and Valastro, 1980; Schubert and Clapperton, 1990; Mahaney and Kalm, 1996; Rull, 2005). Lacustrine sediments with buried peat layers between sediments of Early and Late Mérida Stage at the El Pedregal section in central MA suggest interstadial condition (called El Pedregal Interstade). This period is relatively warm and humid, although affected by fluctuating climatic conditions (Mahaney et al., 2001; Dirszowsky et al., 2005; Rull, 2005).

At the scale of Venezuela, the longest paleoclimate record has been obtained in the sediments of Cariaco basin, located in Eastern Venezuela at around 1000 km from the MA (Fig. 1a). Palynological and geochemical analysis of the marine and terrestrial record of this basin (Hughen et al., 1996, 2000; Peterson et al., 2000a, 2000b; González et al., 2008) clearly document the abrupt stadial-interstadial shifts that characterize the Dansgaard/Oeschger cycles (D/O) (Dansgaard et al., 1993) and the Heinrich Events (HE) (Heinrich, 1988) described in North Atlantic marine cores and Greenland ice records over the last ~90 ka. In Cariaco basin, the interstadial warm events are characterized by enhanced marine productivity, increased precipitation and increased river discharge. Stadials cool events show the opposite trends (Peterson et al., 2000a, 2000b; Haug et al., 2001; Peterson and Haug, 2006; González et al., 2008). Heinrich events are characterized by few sediments and lower terrigenous input, with cold and dry conditions almost indistinguishable from stadials (Haug et al., 2001; Peterson and Haug, 2006). The Last Glacial Maximun (LGM – Clark et al., 2009) and the Younger Dryas (YD – Muscheler et al., 2008) have been also documented in the Cariaco basin as cooling and dry periods, occurring between 23 and 21 ka and 13 and 11.8 ka, repectively (Haug et al., 2001; Lea et al., 2003; Hughen et al., 2004). Based on these results, paleoclimatologists concluded that the climate evolution of the Cariaco basin is closely synchronous with the climatic events in the Northern hemisphere even with the rapid climate changes as D/O cycles and Heinrich events.

4. Methods

Field observations, topographic maps at 1:25000 scale (Dirección de Cartografia Nacional, 1976), satellite imagery (Google Earth, 2005) and a 30–m digital elevation model based on the Shuttle Radar Topographic Mission (SRTM) were used to identify and characterize river terraces in the lower reaches of the Santo Domingo river. Alluvial deposit thicknesses and heights of the terraces above the current riverbed were measured using a measuring tape and a laser distancemeter (vertical accuracy ± 0.5 m). Terrace logitudinal profiles were constructed from the digital elevation model and GPS navigator (Etrex®).

The ages of the terraces have been determined by ^{10}Be dating in siliceous rich sand, cobbles or boulders (Lal, 1991; Brown et al., 1991). Six samples were collected from a depth-profile in terrace T2. This sampling strategy allowed the estimation of the ^{10}Be inherited from prior exposure (Anderson et al., 1996; Repka et al., 1997). ^{10}Be inherited component was also estimated from the concentration of ^{10}Be in sediment of active stream bed (Repka et al., 1997; Hancock et al., 1999; Hetzel et al., 2002). This last approach assumes that the inherited concentration is similar to the current

riverbed concentration. For the terraces T3 and T2, we sampled the first 5 cm of the upper part of the siliceous surface boulders (gneiss, granite, pegmatite, sandstone) partly embedded in the alluvial deposit of the terrace and therefore not remobilized since their deposition (five and three sample were taken for dating T3 and T2, respectively).

Beryllium oxide targets were extracted following the chemical procedures of Brown et al. (1991) and Merchel and Herpers (1999). The extractions were made in the Cosmogenic Laboratory of Institut de Sciences de la Terre (ISTerre, France). ^{10}Be concentrations were measured at the accelerator mass spectrometry facility ASTER (CNRS, France) (Arnold et al., 2010). They were calibrated against NIST Standard Reference Material 4325 using its assumed ^{10}Be/^{9}Be ratio of $2.79 \pm 0.03 \times 10^{-11}$, and a ^{10}Be half-life of 1.387 ± 0.012 Ma (Chmeleff et al., 2010; Korschinek et al., 2010). Production rates were calculated following Stone (2000) using the modified scaling functions of Lal (1991) and a ^{10}Be production rate in quartz of 4.5 ± 0.3 at/g/a at sea level and high latitude. Geomorphic scaling factors were calculated following Dunne et al. (1999). All ^{10}Be age calculations were performed using attenuation lengths of 150, 1500 and 5300 g/cm^2 with associated relative contributions to the total production rate of 97.85%, 1.50% and 0.65% for neutrons, slow muons and fast muons, respectively (Braucher et al., 2003).

Methods and factors of correction for paleomagnetic effects remain a matter of debate and uncorrected ages do not significantly differ from intensity-corrected ages (e.g. Dunai, 2001; Carcaillet et al., 2004; Masarik et al., 2001; Pigati and Lifton, 2004), so in this study paleomagnetic intensity correction was not applied. Thus, numerical ages are given in ^{10}Be ka in order to allow straightforward correction for future refinements in production rates histories and paleomagnetic intensity corrections.

The incision rates were estimated from the ratio between the heights of the terrace surfaces above the current riverbed and the ^{10}Be exposure ages. These estimations were made in river terraces located sufficiently far from the deformation front not to suffer tectonic deformation (Figs. 2–4). In the lower reaches of the Santo Domingo river, the strath levels outcrop only in a few localized sites; thus, in order to homogenize the estimation of incision rates, the surfaces of the terraces were always taken as reference levels. The possible repercussions that this approach may generate in the estimation of the incision rate (e.g. overestimation) in the study area can be neglected for the following reasons: 1) the surfaces of the terraces have not been modified by post-depositional colluvia or tributary alluvial fan; 2) in most cases, the alluvial deposit is only few meters thick (Fig. 5a, b), which is negligible with respect to the incision of the terraces (more than 29 m, height of the lowest one); 3) the surfaces of the terraces are in general flat, which suggests that they have been little modified by denudation processes, or that the modifications have been uniform over the terrace surface (tread) (Fig. 5a); 4) in the few sites where strath levels can be observed, they are parallel to the surface of the corresponding terrace (Fig. 5a, b).

5. Geomorphic analysis and age calculations

5.1. General river description

The Santo Domingo river is located in the central part of the MA, and drains the Southeastern flank of the chain. Its catchment has a surface of 1250 km^2 upstream to Barinas city. Its source was glaciated during the Las Glacial Maximum (LGM) (Clarck et al., 2009), as suggested by well-preserved glacial features (e.g. Schubert and Vivas, 1993; Mahaney and Kalm, 1996; Carrillo, 2006). It flows over 200 km from the Mucubaji lake at 3570 m a.s.l. to the Apure river in the Llanos basin, with an outlet around 200 m a.s.l. The river in the upper reaches of the Santo Domingo flows from WSW to ENE for around 24 km along the Boconó fault and the axial part of the chain. In these reaches, the river flows over crystalline and metamorphic Paleozoic rocks (granite, gneiss and pegmatite) (Fig. 1c) (Hackley et al., 2005). Then it bends abruptly and flows from NW to SE downstream toward the front of the Southeastern flank. In this part, the river is orthogonal to the structural trend of the chain. It flows over crystalline-metamorphic Palaeozoic, calcareous Cretaceous, siliciclastic Neogene rocks and alluvial Quaternary alluvial sediments (Fig. 1c) (Hackley et al., 2005). The river crosses Quaternary faults, among which the POF and the SAFF, which belong to the Southeastern Foothills thrust system (Audemard et al., 2000; Audemard, 2009). In the lower reaches, the Santo Domingo river continues into the Llanos basin toward the Apure river, then into the Orinoco river, which reaches the Atlantic Ocean at more than 1500 km from the study area.

This work is geographically focused on the lower reach of Santo Domingo river, where river terraces have been studied since the first half of the XXth century (e.g. Liddle, 1928; Mackenzie, 1937; Pierce, 1960; Tricart and Millies-Lacroix, 1962; Zinck and Stagno, 1966). However, previous studies lack of detailed geomorphological analyses and numerical ages for these terraces. We therefore characterized terrace geometry (longitudinal and lateral extension, slope, height on the river, deposits thickness), stratigraphy, sedimentology, and dated their abandonment.

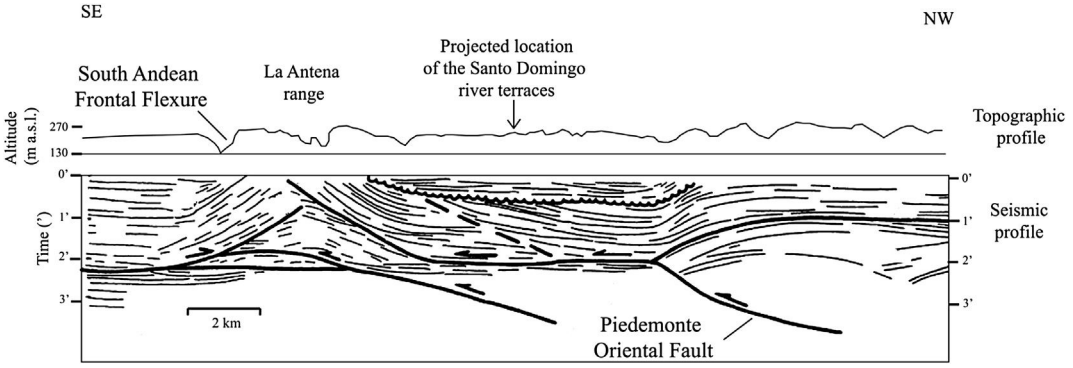

Fig. 2. Structural interpretation from seismic and topographic profiles across the Southeastern foothills of the MA (Funvisis, 1997; Duerto et al., 1998; Audemard, 1999). The faults exhibit ramp-flats geometry. Note the good matchinh between subsurface (seimic data) and surface deformation (topographic data). In the middle part of the section, the geometry of the Piedemonte Oriental Fault (POF) (low-dipping fault plane) causes a rising almost horizontally of the ground surface of his hangingwall block, where the river terraces located in the lower reaches of Santo Domingo river (object of this study and projected in this section) are located. In this part of the section, the POF has not produced surface deformation. Location of this section is shown in Fig. 1.

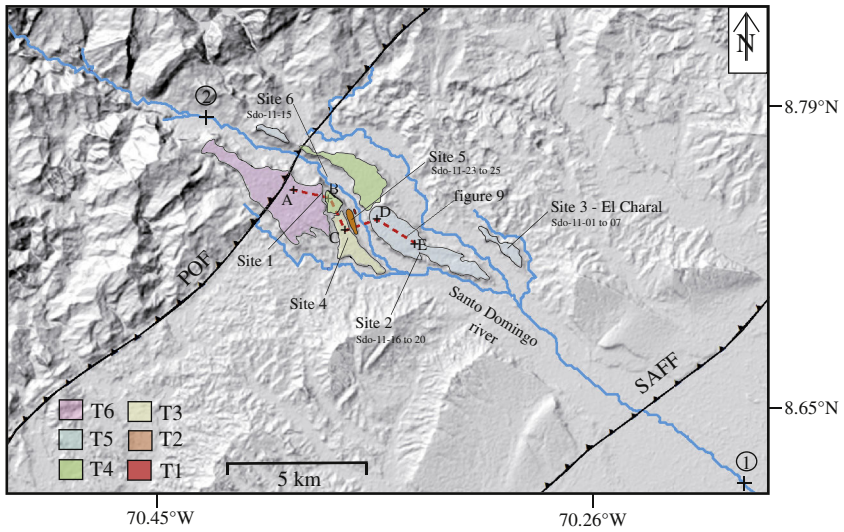

Fig. 3. Geomorphologic map of the lower Santo Domingo river. Surface projection of the POF and SAFF location are based on Audemard et al. (2000). Longitudinal river profile of the Fig. 4 was constructed in the lower reaches of the river between the point 1 and 2. The studied sites and the sampling locations are also shown. Location of the Fig. 9 is shown with red dashed line. (For interpretation of the references to colour in this figure legend, the reader is referred to the web version of this article.)

5.2. Terrace geometry

On the basis of geomorphic and stratigraphical analysis, six well preserved strath terraces were mapped in the lower reaches of the Santo Domingo river between Barinitas city and El Charal villages (Figs. 3 and 4). These terraces are called in the following T6 to T1, from the oldest to the youngest. They have an average downstream slope between 1.1° and 0.4°, decreasing with age of the terrace and downstream. Average slope of the present riverbed is 0.4° (Fig. 4). In general, the alluvial deposits of the terraces overlay detritic poorly lithified Neogene rocks (conglomerate, sandstone or mudstone), and their stratigraphy is relatively similar. Alluvial deposits present a lower unit of fine gravelled sand matrix supported conglomerate, where the clasts are composed of stratified well-rounded pebbles and cobbles (2–10 m thick), deposited in a fluvial environment. The clasts are constituted mainly of gneiss, granite and sandstones. This unit is overlain by a fine alluvial sand and clay unit that represented floodplain facies (50–150 cm thick).

All the river terraces analysed in this study are located sufficiently far from the deformation front not to suffer tectonic deformation. Moreover, most of the terraces are in the same structural block, except T6, which is traversed by the inferred projection of the POF (Fig. 2) (Audemard et al., 2000). Nevertheless, this fault has not produced surface deformation since the abandonment of T6, as proven by the absence of fault scarp at the surface of this terrace (Fig. 4). Therefore, no local structural control except at the front exists over the fluvial incision. The flat surface of the terraces when they cross two different lithological bedrock units and the absence of knickpoint in the current longitudinal river profile (Fig. 4) suggest that the fluvial incision is not dependent on

Surface	Average slope of the surface (°)	Height of surface above the current riverbed at Po (m)
T6	1.1	130 ± 0.5 *
T5	0.6 - 0.8	92 ± 0.5
T4	0.9	82 ± 0.5
T3	0.8	69 ± 0.5
T2	0.5	42 ± 0.5
T1	0.4	29 ± 0.5 *
river	0.4	-

* Extrapolated from the minimal elevation above the present riverbed

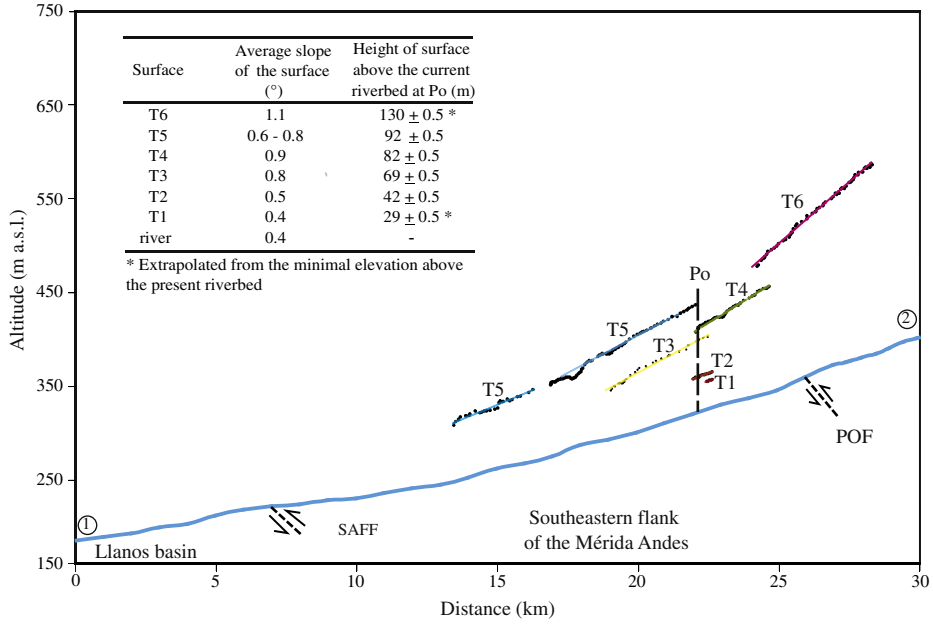

Fig. 4. Longitudinal profiles of the lower Santo Domingo river and terraces. The table in the upper left corner summarizes the geometry of the terraces. The localization of Po is shown in the figure. The height of the terraces T6 and T1 above the current riverbed at Po, were extrapolated from the minimal elevation of these terraces. Location of the POF and SAFF are based on Audemard et al. (2000).

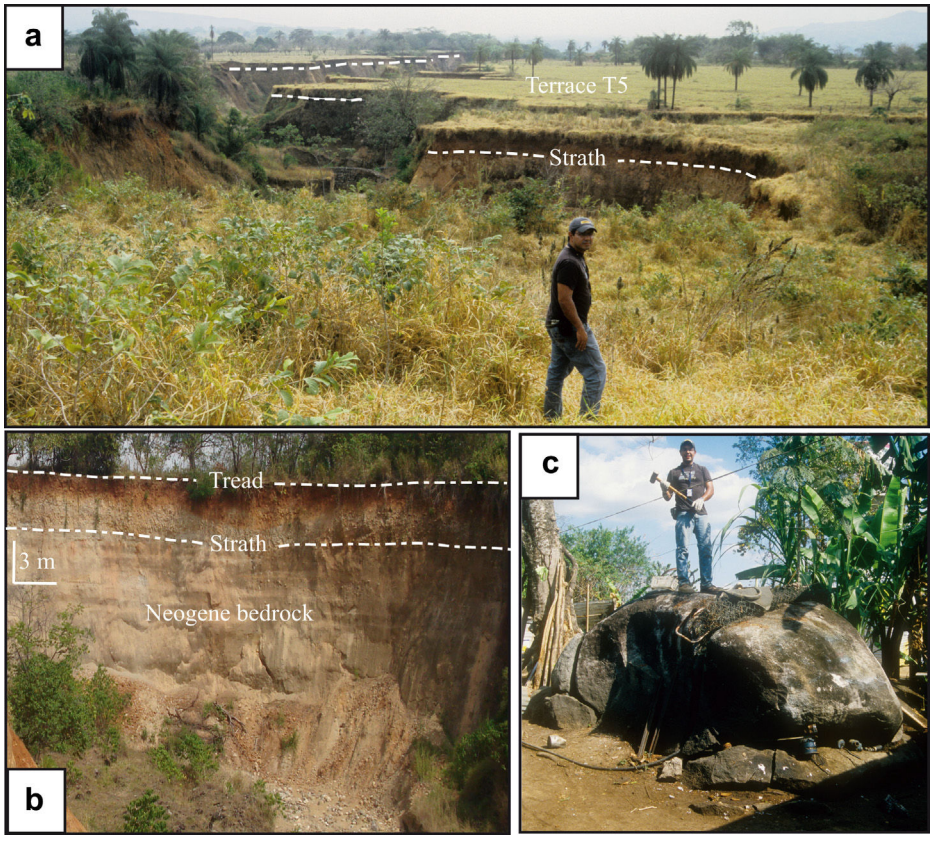

Fig. 5. Morphology of river terraces in the study area. **a**) Flat surface of the terrace T5 (site 2). **b**) Alluvial deposit of T5 composed of a basal unit of stratified cobbles and pebbles and an upper unit of red sand and silt. This deposit cut the sandstone Neogene bedrock. The surface of the terrace is parallel to the strath surface (site 2). **c**) Plurimetric rounded boulder partially embedded into the alluvial deposit of terrace T3 (site 4). Pictures by R. Vassallo (a, c) and M. Alvarado (b).

the lithology of Neogene bedrock. The effect of the growth of the drainage network over the fluvial incision is evidenced by the longitudinal upstream incision increase, which produces vertically divergent terraces upstream (Fig. 4). This effect is therefore lowest toward the outlet of the catchment. In order to minimize and homogenize this effect, we evaluate the fluvial incision at a single point (Po in the text) of the current riverbed in the lower part of the catchment, where most of the terraces are present (Fig. 4). Consequently, the long term fluvial incision rate in the lower reach of the Santo Domingo river is mainly controlled by mountain uplift. Hence the quantification of the incision rate allows the estimation of the uplift rate for the Southeastern flank of the MA.

In the following, we discuss the individual geometry and stratigraphy-sedimentology of the terraces. T6 is a river terrace located on the right bank of the Santo Domingo river, on which the city of Barinitas has settled (Fig. 6). The surface of this terrace has an average downstream slope of 1.1°. This terrace, as well as the other terraces, has a higher slope than the current riverbed (Fig. 4). The development of Barinitas city on the terrace inhibits the characterization of the original surface and the alluvial deposit. However, in a natural section located toward the Southern border of the terrace (site 1 – Figs. 3 and 6), T6 has an irregular surface with a mean rugosity around 50 cm. In this site the alluvial deposit of T6 is made of a gravel-sand matrix supported conglomerate. The clasts are composed by stratified rounded pebbles and cobbles (~400 cm thick).

Terrace T5 was studied at two sites along the study area. Despite this terrace is largely used for agriculture, there are places where the original surface of the terrace is well preserved. The surface of T5 is mainly flat with a variable downstream slope between 0.8° and 0.6° (Fig. 5a). At site 2 (Figs. 3 and 6), the alluvial deposit of T5 is around 4 m thick. It contains a basal unit of stratified rounded pebbles and cobbles. Thickness of the basal unit varies laterally (in a context of fluvial channels and bars sedimentation) from 0 to 350 cm, and is overlain by a red sand unit, which is 50–400 cm thick. At this site, the alluvial deposit of T5 is above a strath surface, located at the top of the sandstone Neogene bedrock (Fig. 5b).

T5 was also studied, in a pit-soil of 2 × 3 × 2 m located to the Southeast of the studied area (site 3 – Fig. 3). At this site, the surface of the terrace is relatively flat, with a maximal rugosity around 10 cm. The lower unit of the alluvial deposit of T5 is a 150 cm thick roughly stratified bed. This unit contains well-rounded pebbles and cobbles. An intermediate unit of 10 cm is made of coarse sand. The upper unit shows 40 cm of unsorted fine sand, silt and clay (Fig. 7).

Terrace T4 was observed on both banks of the river (Figs. 3 and 6). On the left bank, T4 is better preserved. T4 has a flat surface with an average downstream slope of 0.9° (Fig. 4). The alluvial deposit of T4 comprises a lower unit of stratified rounded pebbles and cobbles, which is at least 10 m thick. An upper thin ~60 cm thick sandy unit is observed.

T3 is preserved on the right bank of the river (Figs. 3 and 6). The surface of terrace T3 is mainly flat with an average downstream slope of 0.8° (Fig. 3). The alluvial deposit of T3 exhibits a lower unit of stratified well-rounded pebbles and cobbles at least 100 cm thick, and an upper thin fine sand and clay unit, not thicker than ~70 cm. Additionally, plurimetric rounded boulders composed of crystalline rocks, with an average diameter of ~200 cm and a maximal size of 400 cm, are embedded into the alluvial material. The top of these boulders are exposed >100 cm above ground surface (Fig. 5c).

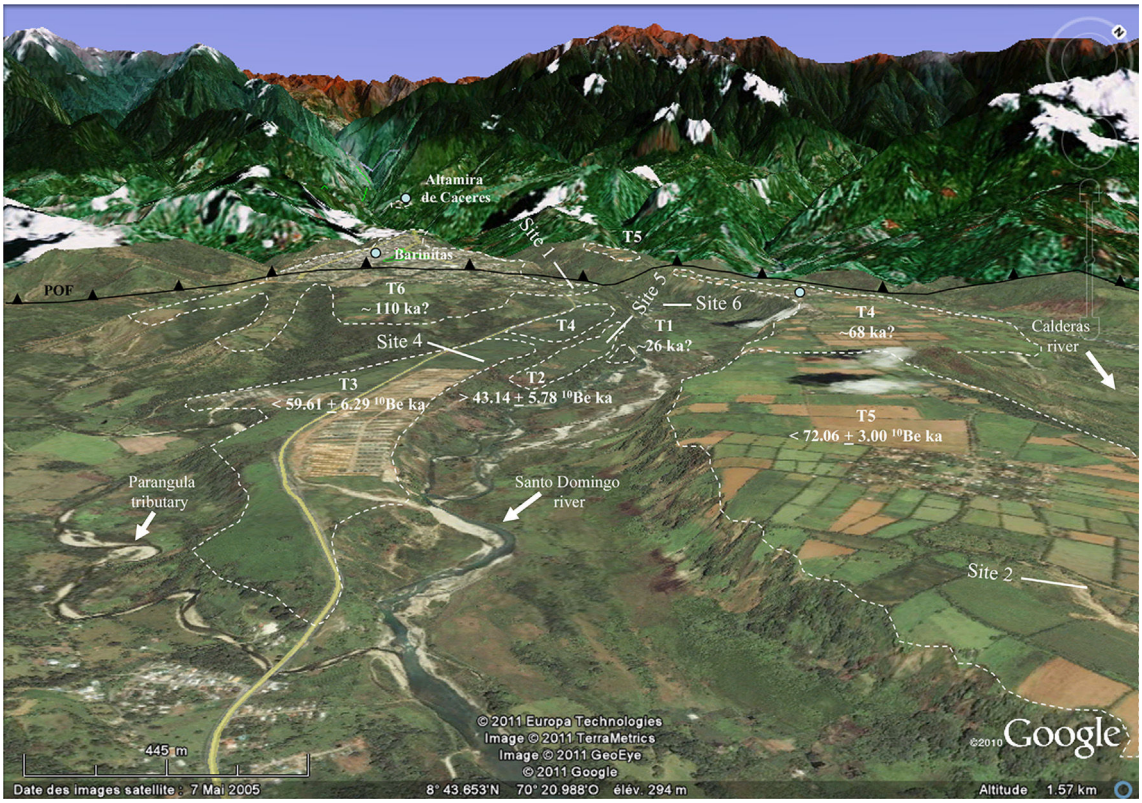

Fig. 6. Panoramic view of terraces from satellites images (Google earth, 2005). The estimated and extrapolated ages calculated in the present study are assigned to the terraces. The studied sites are also shown. Surface projection of the POF location are based on Audemard et al. (2000).

Terraces T2 and T1 are located on the right bank of the river. These terraces are the lowest and smallest preserved terraces in the study area (Figs. 3 and 6). The surfaces of these terraces are roughly irregular, with a rugosity that can reach 30 cm. They have a downstream slope of 0.5° (T2) and 0.4° (T1) (Fig. 5). The alluvial deposit of both terraces contains a lower unit of ~100 cm thick of stratified well-rounded pebbles and cobbles, and a ~150 cm thick upper unit of fine sand and clay. Into this unit, few pluri-decimetric exposed boulders, with an average diameter of 40 cm can be found.

5.3. Age calculations

In order to determine the exposure ages of the terraces identified in the lower reaches of the Santo Domingo river, the concentrations of ^{10}Be in samples taken in terraces T5, T3 and T2 were analysed. The results are discussed from oldest to youngest.

Terrace T5 was sampled at site 3 (Fig. 3). A cosmogenic depth profile was made along a 200 cm deep pit-soil (Fig. 7). At the sampling site, the small roughness of the surface of T5 suggests that

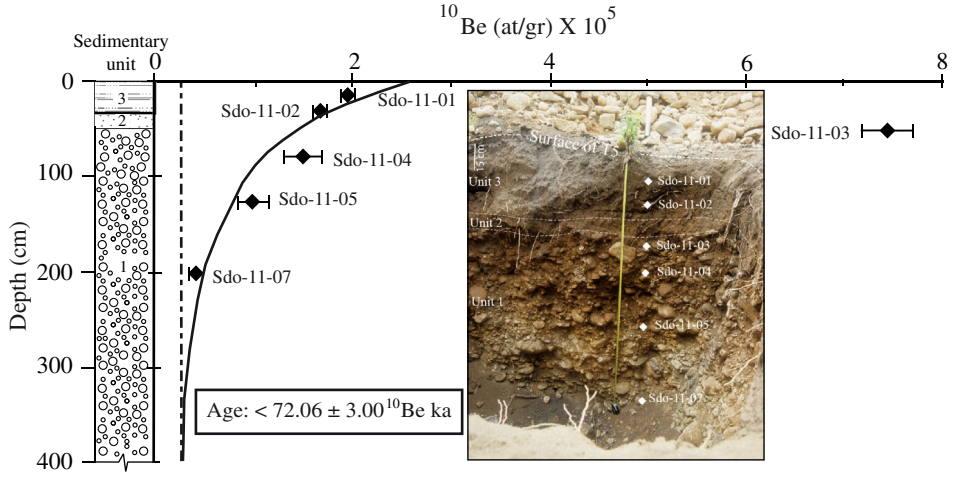

Fig. 7. Depth profile of the ^{10}Be concentration within the alluvial deposit of the terrace T5 at site 3. The depth-production best fit using a chi-square inversion is in solid line. The dashed line shows the inherited ^{10}Be concentration. Details of the exposure age calculations are in Table 1. On the picture we can see the soft rugosity in the surface of terrace T5 and the stratigraphy of the alluvial deposit. It is composed of three units. Unit 1: roughly stratified well-rounded pebbles and cobbles. Unit 2: coarse sand. Unit 3: fine sand, silts and clay. Picture by R. Vassallo.

a denudation process could have only slightly modified the original surface of the terrace. The local loss of alluvial material probably does not exceed the maximum rugosity of the surface irregularities (~10 cm). This upper-bound value was taken into account for the data inversion to determine a maximum age (Arboleya et al., 2008; Schmidt et al., 2011). The four lower samples are individual cobbles, coming from the coarse unit (see Section 5.2). The two other samples are constituted of fine sand from the upper unit (Fig. 7). The distribution of ^{10}Be concentration shows an exponential decrease with depth, except for the sample Sdo-11-03 (Fig. 7). This sample shows a high grade of weathering with respect to the other samples with similar lithology, and suggests a longer pre-exposure history. Thus, this sample was not considered for the age estimation. A mathematical model was used, in order to estimate the ^{10}Be in surface and consequently the exposure age of the terrace T5. Using a chi-square inversion to minimize the difference between observed and modeled ^{10}Be data (e.g. Braucher et al., 2003; Ritz et al., 2006) and assuming a density of 2.4 g/cm^3, the maximum inherited concentration was estimated at 0.30 ± 0.03 × 10^5 at/g (Fig. 7). This value is consistent with the inherited component estimated from the sediments of the active stream (Sdo-11-15 – Table 1). This result yields a maximum exposure age of 72.06 ± 3.00 ^{10}Be ka (Table 1).

To date terrace T3, five samples were taken from the pluri-metric boulders partially embedded into the alluvial deposit of the terrace (Sdo-11-16 to 20 – Table 1) (see Section 5.2). ^{10}Be concentrations are similar and range between 2.14 ± 0.12 and 2.51 ± 0.20 × 10^5 at/g (Table 1). The height of the boulder tops above ground surface of the terrace (some of them >80 cm) suggests that the samples have not been shielded by any matrix even if a slight denudation of the surface of the terrace occurred. Despite the difficulty to know the amount of inheritance in each boulder, the fact that these boulders are only present in terrace T3 and their homogeneous ^{10}Be concentrations suggest that these boulders have a similar simple and short pre-exposure history. This assumption gives a maximum exposure age estimate for this terrace that cluster around 59 and 70 ka. Therefore, the apparent age given by the boulder with the smallest concentration should be the closest to the true age (Vassallo et al., 2011). Sample Sdo-11-16 is the one with the lowest concentration with 2.14 ± 0.12 × 10^5 at/g, and yields a maximum exposure age of 59.21 ± 6.29 ^{10}Be ka (Table 1).

For terrace T2, we applied the same strategy used for terrace T3. Three surface samples were taken from pluri-decimetric well-rounded boulders, which outcrop at different heights above the ground. Two of them have similar ^{10}Be concentration (Sdo-11-23 and Sdo-11-25 – Table 1). At the sampling site, the surface of T2 has an irregular slope toward the axis of the valley, which suggests a bad preservation of the original surface. Therefore the samples could have suffered shielding since deposition. In this case, it is also difficult to know the amount of inheritance in each boulder. However, the impact in the estimation of the age that could be caused by the loss of thickness of this terrace of at least 30 cm (maximum rugosity of the surface –see subsection 5.2), is likely higher than the impact caused by the amount of inheritance. Therefore, we use the highest concentration for the age estimation, which corresponds to a minimum value. Sample Sdo-11-23 is the one with the highest concentration with 1.53 ± 0.15 × 10^5 at/g, which yields a minimum age of 43.14 ± 5.78 ^{10}Be ka (Table 1).

Table 1
Results of the ^{10}Be analysis. Calibration against NIST Standard Reference Material 4325. ^{10}Be concentrations uncertainties include analytical errors from the counting statistics and blank correction, whereas the ages uncertainties also include the errors of the production rate introduced by the scaling model of Lal (1991) – Stone (2000) and the errors of the ^{10}Be decay constant (Chmeleff et al., 2010; Korschinek et al., 2010). (*) Age estimated from ^{10}Be depth profile assuming a maximum erosion of 10 cm and a density of 2.4 g/cm^3.

Sample	Type of sample	Lithology	Latitude (N)	Longitude (E)	Altitude (m a.s.l.)	depth (cm)	Height above the ground (cm)	Surface P_0 (at/g/y)	Shielding factor	^{10}Be concentration (10^5 at/g)	^{10}Be age (ka)	Terrace
Site 3 – El Charal			−70.2903	8.7302	321			3.50 ± 0.23	1			T5
Sdo-11-01	Sand	Heterogeneous				15				1.95 ± 0.10	72.06 ± 3.00*	
Sdo-11-02	Sand	Heterogeneous				30				1.66 ± 0.10		
Sdo-11-03	Cobble	Gneiss				53				7.44 ± 0.39		
Sdo-11-04	Cobble	Granite				80				1.49 ± 0.21		
Sdo-11-05	Cobble	Gneiss				125				0.97 ± 0.17		
Sdo-11-07	Cobble	Granite				200				0.39 ± 0.06		
Site 4 – Santo Domingo			−70.3696	8.738	380			3.66 ± 0.24	1			T3
Sdo-11-16	Metric boulder	Pegmatite					70			2.14 ± 0.12	59.61 ± 6.29	
Sdo-11-17	Metric boulder	Granite					50			2.52 ± 0.08	70.18 ± 6.71	
Sdo-11-18	Metric boulder	Granite					40			2.51 ± 0.20	70.08 ± 8.37	
Sdo-11-19	Metric boulder	Granite					86			2.45 ± 0.13	68.33 ± 7.19	
Sdo-11-20	Metric boulder	Granite					180			2.34 ± 0.15	65.18 ± 7.28	
Site 5 – Los Platanos			−70.3711	8.7486	361			3.60 ± 0.24	1			T2
Sdo-11-23	Pluri-centimetric boulder	Sandstone					15			1.53 ± 0.15	43.14 ± 5.78	
Sdo-11-24	Pluri-centimetric boulder	Granite					8			0.82 ± 0.05	23.14 ± 2.60	
Sdo-11-25	Pluri-centimetric boulder	Sandstone					15			1.43 ± 0.07	40.17 ± 4.13	
Site 6 – Barinesa bridge			−70.389	8.7701	348							
Sdo-11-15	Sand	Heterogeneous					0			0.32 ± 0.02		river

6. Discussion

6.1. Incision rates and tectonic uplift

The incision rates were estimated for terraces T5, T3 and T2 at a single point (Po in Fig. 4), where most of the terraces are present. The results are summarized in the Table 2.

These estimations allow concluding that the long-term incision rate close to the mountain front in the lower Santo Domingo river averages around 1.1 mm/a over the last 70 ka. Taking into account the geologic and geomorphologic setting of the study area (see subsection 5.2.), this incision rate represents the uplift rate of the Southeastern flank of the MA. This estimation of the uplift rate is in the same range of the recent estimation ($\sim 1.7 \pm 0.7$ mm/a) done by Wesnousky et al. (2012) for the Northwestern flank over the Late Pleistocene. Additionally, this value is similar to the exhumation rate of 0.8 mm/a for the last 800 ka, proposed by Kohn et al. (1984) from cooling ages derived from apatite fission track of samples located in El Carmen Block, in the central part of the MA (Fig. 1). These results give a more detailed and broader picture of the uplift rate of the MA. In fact, they seem to indicate that the two flanks of the MA (NE and SW) uplift at a similar rate and that this rate is probably unchanged over several 100 ka. Nonetheless a more extensive analysis and dating of river terraces located in the valleys along the axis of the chain (e.g. Chama, Upper Santo Domingo, Upper Mocotíes and Pueblo Llano valleys), as well as in the Northwestern and Southeastern flanks (e.g. Lower Motatán, Guanare, Escalante and Uribante valleys) are required to constrain the spatial distribution of the uplift rate of the chain.

6.2. Terrace formation vs climate

From the extrapolation of the average incision rate performed in this study (~ 1.1 mm/a) and the height of the terraces at Po above the current riverbed, the ages of terraces T6, T4 and T1 were estimated at around 110, 68 and 26 ka, respectively (Fig. 8, Table 2). These results coupled with the exposure ages directly estimated for T5, T3 and T2 (see subsection 5.3) show that the process of terraces formation in the lower reach of Santo Domingo river occurred at a much higher frequency than an interglacial/glacial cycle (10^4–10^5 years) (Fig. 9).

Our dating also shows that all of the terraces younger than Early Mérida Glaciation in the lower Santo Domingo river were formed during the El Pedregal Interstade (between ~ 65 and 22 ka). During this period the climatic conditions were relatively warm and humid (Dirszowsky et al., 2005; Rull, 2005; Kalm and Mahaney, 2011). The comparison of our dating with the high resolution paleoclimatic record of the Cariaco basin (Peterson et al., 2000; González et al., 2008), show a correlation between the ages of abandonment of terraces T5, T3 and T2 and short periods of cold and dry conditions around 74, 60 and 43 ka (i.e. stadial (S) and Heinrich event (H6) conditions – Fig. 10). Therefore this correlation shows that the abandonment of the terraces occurred during a long-term warm and humid stage, but was triggered by short and rapid climatic variations from warm to cold conditions (Fig. 10). Hence, we argue that the process of river terraces formation in the lower reaches of Santo Domingo river was probably controlled by climatic variations. During the warm and humid periods of the El Pedregal Interstade (Dirszowsky et al., 2005; Rull, 2005; Kalm and Mahaney, 2011) the river attained an equilibrium between incision and aggradation. Consequently strath surfaces were developed. Then, during short period of cold and dry conditions equilibrium was interrupted by vertical fluvial incision triggered by the decrease in the transport capacity. Additionally, the signature of an instantaneous high energy aggradations event is put in evidence by the presence of the pluri-metric boulders at the surface of terrace T3. These boulders are embedded into the alluvial deposits and were probably transported and deposited by debris flow climatically or tectonically triggered in a context of high water discharge and sediment supply. In the case of climate controlled events, these events could have been similar to those occurring today in the Mérida Andes (Olivero et al., 2005a,b).

This climatic-driven formation model is opposed to the glacial/interglacial model previously proposed for the terraces of MA by Tricart and Millies-Lacroix (1962) (published well before that the recent advance in Quaternary geochronology and paleoclimatology) that associated the abandonment of the terraces to interglacial conditions. Our results show that this model is not applicable in the lower reaches of the Santo Domingo river. In fact, no river terraces have been formed in the study area during the end of the maximum extension of ice sheets through the Last Glacial period (LGM; Clark et al., 2009), which is well documented in glacial sediments in the core of the MA and dated at 21.5 ka (Kalm and Mahaney, 2011). This comparison also suggests that the process of terraces formation could be different in the upper catchment of the river. Thus, an analysis of river terraces in the upper part of the Santo Domingo catchment, close to the interaction with glacial fluctuations, could allow a better understanding of this issue.

Table 2
Summary of Santo Domingo river terraces ages and incision rates. The extrapolated ages for the terraces T6, T4 and T1 are also shown. Details of the extrapolated age calculations are in subsection 5.2.

Terrace	Height of surface above the current riverbed at Po (m)	Exposure age (ka)	Extrapolated age (ka)	Incision rate at Po (mm/a)
T6	130 ± 0.5[a]	–	110	–
T5	92 ± 0.5	72.06 ± 3.00	–	1.27 ± 0.06
T4	82 ± 0.5	–	68	–
T3	69 ± 0.5	59.61 ± 6.29	–	1.16 ± 0.12
T2	42 ± 0.5	43.14 ± 5.78	–	0.98 ± 0.13
T1	29 ± 0.5*	–	26	–

[a] Extrapolated from the minimal elevation above the current riverbed.

7. Conclusion

This study established a river terrace chronology based on cosmogenic ages for the lower reaches of the Santo Domingo river. The six well-preserved Late Pleistocene strath terraces identified allowed reconstructing the history and the dynamics of the incision as a response to climatic and tectonic inputs.

We estimated maximum exposure ages for terraces T5 and T3 at 72.06 ± 3.00 and 59.61 ± 6.29 ^{10}Be ka, respectively, and a minimum

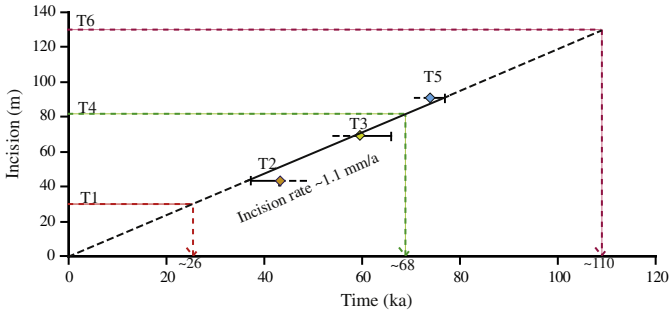

Fig. 8. Incision rate of lower Santo Domingo reaches calculated from the ratio between the height of terraces T5, T3 and T2 and the exposure ages estimated in this work. Extrapolated ages for T6, T4 and T1 were estimated assuming a constant incision rate over the last 120 ka. Maximum and minimum ages performed are plotted with their uncertainty associated and a dashed line toward younger and older times (maximum and minimum ages, respectively).

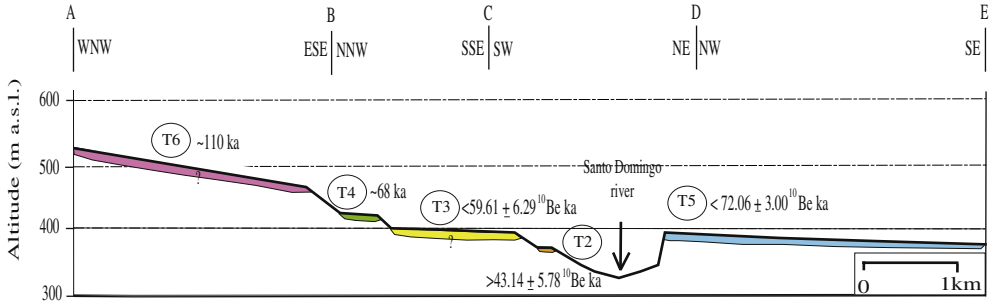

Fig. 9. Cross section trough the river terraces of the lower reaches of the Santo Domingo river. The ages of the terraces correspond to the numerical ages and extrapolation ages proposed in this work. Red-dashed line in Fig. 3 indicates location of this profile. Note that T5, on the left bank, is located downstream with respect to the other terraces.

exposure age for terrace T2 at 43.14 ± 5.78 ^{10}Be ka. These results and the elevations of terraces above the present riverbed yield a long-term constant incision rate around 1.1 mm/a over the last 70 ka.

The analysis of the geologic and geomorphologic setting allowed proposing that the long-term fluvial incision in the lower Santo Domingo river is mainly controlled by mountain uplift. Therefore we consider that the value estimated for the incision rate (~1.1 mm/a) can be converted into the Late Pleistocene uplift rate of the Southeastern flank of the MA. This value is in the same range of the uplift rate on the same period of the Northwestern flank (Wesnousky et al., 2012), showing that the MA may be being symmetrically uplifting on both flanks.

From the extrapolation of the long-term average incision rate estimated in this study, the ages of the terraces T6, T4 and T1 were estimated at around 110, 68 and 26 ka, respectively. This result shows that the process of terraces formation on the Southeastern flank of the MA occurred with a higher frequency than a glacial/interglacial cycle. In particular terraces seem to have been abandoned during warm to cold transitions and are therefore climatically controlled. However, the impact of the climatic input in terraces formation remains to be quantified, while other parameters such as seismic activity within the MA could play a significant role.

Acknowledgments

The authors thank the Fondo Nacional de Ciencia, Tecnología e Innovación – Venezuela (FONACIT) and the Fundación Gran

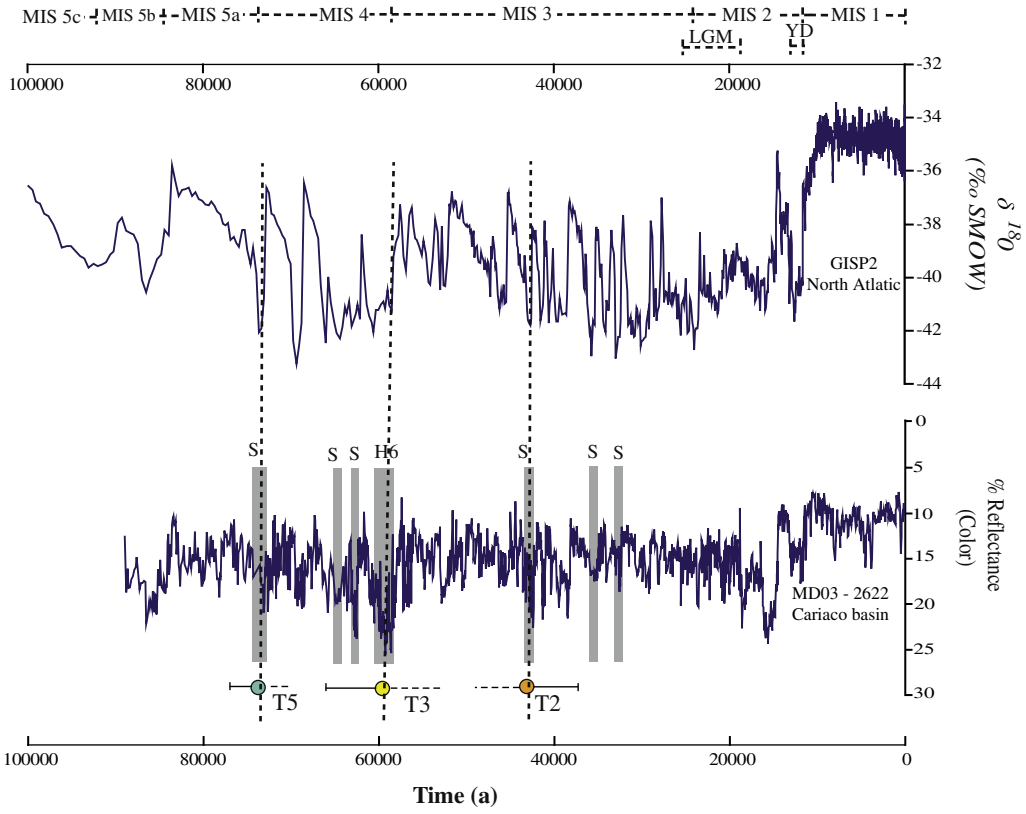

Fig. 10. Comparison of ages of abandonment of the lower Santo Domingo river terraces with: **a**) δ^{18}O record from the GISP2 ice core (Grootes et al., 1993; Stuiver et al., 1995). **b**) Color reflectance curve of Cariaco basin (Peterson et al., 2000). The gray rectangles represent short periods of cold and dry conditions identified by Peterson et al. (2000) and González et al. (2008) in the Cariaco basin. (S) stadial. (H6) Heinrich event 6. (MIS) Marine Isotope stage (Aitken and Stokes, 1997; Wright, 2000; Shackleton 1987); (LGM) Last Glacial Maximum (Clark et al., 2009); (YD) Younger Dryas (Berger, 1990).

Mariscal de Ayacucho by funded otorgated through the ECOS Nord project PI-2007001823 to O.G. and R.V. during field work. We also thank the Fundación Venezolana de Investigaciones Sismológicas (FUNVISIS) by the aerial photos and topographic maps of the study area, and the logistical support given during the field work. We thank the Fundación Instituto de Ingeniería – Laboratorio de Procesamieno Avanzado de Imagenes Satelitales – LPAIS – of Venezuela by supporting in construction of the DEM of the study area. We thank the Aster team (Mrs. Arnold M., Aumaitre, G. and Keddadouche, K.) for the isotopic mesures of the samples. This publication was also made possible through support provided by the IRD-DPF to O.G. We thank V. regard and an anonymous reviewer for their constructive comments that allowed us to significantly improve the quality of the paper.

References

Aitken, M.J., Stokes, S., 1997. Chapter 1. In: Taylor, R.E., Aitken, M.J. (Eds.), Chronometric Dating in Archaeology. Birkhäuser, ISBN 0-306-45715-6. ISBN 978-0-306-45715-9, google books.

Anderson, R.S., Repka, J.L., Dick, G.S., 1996. Explicit treatment of inheritance in dating depositional surfaces using *in situ* ^{10}Be and 26Al. Geology 24, 47–51.

Antoine, P., Limondin, N.L., Chaussé, C., Lautridou, J.-P., Pastrea, J.-F., Auguste, P., Bahaine, J.-J., Falguères, C., Galehb, B., 2007. Pleistocene fluvial terraces from Northern France (Seine, Yonne, Somme): synthesis, and new results from interglacial deposits. Quat. Sci. Rev. 26, 2701–2723.

Arboleya, M.-L., Babault, J., Owen, L., Teixell, A., Finkel, R., 2008. Timing and nature of quaternary fluvial incision in the Ouarzazate foreland basin, Morocco. J. Geol. Soc. 165, 1059–1073.

Arnold, M., Merchel, S., Bourles, D., Braucher, R., Benedetti, L., Finkel, R.C., Aumaitre, G., Gottdang, A., Klein, M., 2010. The French accelerator mass spectrometry facility ASTER: Improved performance and developments. Nucl. Instrum. Methods Phys. Res. Sect. B: Beam Interac. Mater. Atoms 268, 1954–1959.

Audemard, F.A., 1999. Morpho-structural expression of active thrust fault systems in humid tropical foothills of Colombia and Venezuela. Z. für Geomorphologie 118, 1–8.

Audemard, F.A., 2003. Geomorphic and geologic evidence of ongoing uplift and deformation in the Mérida Andes, Venezuela. Quat. Int. 101–102, 43–65.

Audemard, F.A., 2009. Flexura Frontal sub-andina, Venezuela (VE-07). In: Servicio Nacional de Geología y Minería (Ed.), Atlas de las deformaciones cuaternarias de Los Andes, Proyecto multinacional andino: Geociencia para las comunidades andinas, pp. 300–311. Publicacion Geológica nacional N° 7.

Audemard, F.A., Machette, M., Cox, J., Dart, R., Haller, K., 2000. Map and Database of Quaternary Faults in Venezuela and Its Offshore Regions. US Geological Survey Open-File Report 00-0018. Include map at scale 1:2,000,000 and 78-page report.

Audemard, F.E., Audemard, F.A., 2002. Structure of the Mérida Andes, Venezuela: relations with the South America-Caribbean geodynamic interaction. Tectonophysics 345, 299–327.

Backé, G., Dhont, D., Hervouët, Y., 2006. Spatial and temporal relationships between compression, strike–slip and extension in the Central Venezuelan Andes: clues for Plio–Quaternary tectonic escape. Tectonophysics 425, 25–53.

Berger, W.H., 1990. The Younger Dryas cold spell – a quest for causes. Glob. Planet. Change 3 (3), 219–237.

Bermúdez, M., 2009. Cenozoic Exhumation Patterns across the Venezuelan Andes: Insights from Fission-track Thermochronology. Ph.D. thesis. Joseph Fourier University, France, p. 305.

Bermúdez, M., van der Beek, P., Bernet, M., 2011. Asynchronous Miocene-Pliocene exhumation of the central Venezuelan Andes. Geology 39 (2), 139–142.

Braucher, R., Brown, E.T., Bourlès, D.L., Colin, F., 2003. *In situ* produced ^{10}Be measurements at great depths: implications for production rates by fast muons. Earth Planet. Sci. Lett. 211, 251–258.

Brown, E.T., Edmond, J.M., Raisbeck, G.M., Yiou, F., Kurtz, M.D., Brook, E.J., 1991. Examination of surface exposure ages of moraines in Arena Valley, Antarctica, using *in situ* produced ^{10}Be and ^{26}Al. Geochim. Cosmochim. Acta 55, 2269–2283.

Carcaillet, J., Bourlès, D.L., Thouveny, N., 2004. Geomagnetic dipole moment and ^{10}Be production rate intercalibration from authigenic ^{10}Be/^{9}Be for the last 1.3 Ma. Geochem. Geophys. Geosystem. 5. http://dx.doi.org/10.1029/2003GC000641.

Carrillo, E., 2006. L'Enregistrement sédimentaire de la sismicité récente le long de la frontière sudoccidentale de la plaque caraïbe 'Faille de Boconó): Modalités et chronologie. Contribution à l'estimation de l'aléa sismique régional. Ph.D. thesis. Université de Savoie, France, p. 335.

Chmeleff, J., Von Blanckenburg, F., Kossert, K., Jakob, D., 2010. Determination of the ^{10}Be half-life by multicollector ICP-MS and liquid scintillation counting. Nucl. Instruments Methods Phys. Res. Sect. B: Beam Interac. Mater. Atoms 268, 192–199.

Clark, Peter U., Dyke, Arthur S., Shakun, Jeremy D., Carlson, Anders E., Clark, Jorie, Wohlfarth, Barbara, Mitrovica, Jerry X., Hostetler, Steven W., 2009. The last glacial maximum. Science 325 (5941), 710–714.

Colletta, B., Roure, F., De Toni, B., Loureiro, D., Passalacqua, H., Gou, Y., 1997. Tectonic inheritance, crustal architecture, and contrasting structural styles in the Venezuelan Andes. Tectonics 16 (5), 777–794.

Colmenares, L., Zoback, M.D., 2003. Stress field and seismotectonics of Northern South America. Geology 31, 721–724.

Corredor, F., 2003. Eastward extent of the Late Eocene-Early Oligocene onset of deformation across the Northern Andes: constraints from the Northern portion of the Eastern Cordillera fold belt, Colombia. J. South Am. Earth Sci. 16, 445–457.

Cortés, M., Angelier, J., 2005. Current states of stress in the Northern Andes as indicated by focal mechanisms of earthquakes. Tectonophysics 403, 29–58.

Dansgaard, W., Johnsen, S.J., Clausen, H.B., Dahl-Jensen, N.S., Gundestrup, N.S., Hammer, C.U., Hvidberg, C.S., Steffensen, J.P., Sveinbjörnsdottir, A.E., Jouzel, J., Bond, J., 1993. Evidence for general instability of past climate from a 250-kyr ice-core record. Nature 364, 218–220.

De Toni, B., Kellogg, J., 1993. Seismic evidence for blind thrusting of the Northwestern flank of the Venezuelan Andes. Tectonics 12 (6), 1393–1409.

Dhont, D., Backé, G., Hervouët, Y., 2005. Plio–Quaternary extension in the Venezuelan Andes: mapping from SAR JERS imagery. Tectonophysics 399, 293–312.

Dirección de Cartografía Nacional, 1976. Mapas Topograficos a Escala 1:25000. Hojas, Barinitas, Rio Calderas, Qda. Seca, Campo Azul, La yuca.

Dirszowsky, R.W., Mahaney, W.C., Hodder, K.R., Milner, M.W., Kalm, V., Bezada, M., Beukens, R.P., 2005. Lithostratigraphy of the Mérida (Wisconsinan) glaciation and Pedregal interstade, Mérida Andes, NorthwesternVenezuela. J. South Am. Earth Sci. 19, 525–536.

Duerto, L., Audemard, F.E., Lugo, J., Ostos, M., 1998. Síntesis de las principales zonas triangulares en los frentes de montana del occidente venezolano. In: IX Congreso Venezolano de Geofisica (CDRom; paper # 25).

Dunai, T.J., 2001. Influence of secular variation of the geomagnetic field on production rates of *in situ* produced cosmogenic nuclides. Earth Planet. Sci. Lett. 193, 197–212.

Dunne, J., Elmore, D., Muzikar, P., 1999. Scaling factors for the rates of production of cosmogenic nuclides for geometric shielding and attenuation at depth on sloped surfaces. Geomorphology 27, 3–11.

Funvisis, 1997. Estudio neotectónico y geología de fallas activas en el piedemonte surandino de los Andes venezolanos (Proyecto INTEVEP 95–061). unpublished report for INTEVEP, S.A. Funvisis', p. 155. ± appendices.

Giegengack, R., 1984. Late Cenozoic tectonic environments of the central Venezuelan Andes. In: Bonini, W., Hargraves, R., Shagam, R. (Eds.), The Caribbean-south American Plate Boundary and Regional Tectonics, Memoir – Geological Soc. of America, vol. 162, pp. 343–364.

González, C., Dupont, L.M., Behling, H., Wefer, G., 2008. Neotropical vegetation response to rapid climate changes during the last glacial: palynological evidence from the Cariaco basin. Quat. Res. 69, 217–230.

Google earth V 6.1.0.5001, Mai 7, 2005. Barinitas City, Mérida Andes. 8° 43.653'N, 70° 20.988'W, Eye Alt 1.57 Km. SIO, NOAA, U.S. Navy, NGA, GEBCO. GeoEye. http://www.googleearth.com.

Grootes, P.M., Stuiver, M., White, J., Johnson, S., Jouzel, J., 1993. Comparison of oxygen isotope records from the GISP2 and GRIP Greenland ice cores. Nature 366, 552–554.

Hackley, P.C., Urbani, F., Karlsen, A.W., Garrity, C.P., 2005. Geologic Shaded Relief Map of Venezuela. U.S. Geological Survey Open File Report 2005–1038.

Hancock, G.S., Anderson, R.S., Chadwick, O.A., Finkel, R.C., 1999. Dating fluvial terraces with ^{10}Be and ^{26}Al profiles: application to the Wind River, Wyoming. Geomorphology 27, 41–60.

Haug, G.H., Hughen, K.A., Sigman, D.M., Peterson, L.C., Rohl, U., 2001. Southward migration of the Intertropical Convergence Zone through the Holocene. Science 293, 1304–1308.

Heinrich, H., 1988. Origin and consequences of cyclic ice rafting in the Northeast Atlantic Ocean during the past 130,000 years. Quat. Res. 29, 142–152.

Hetzel, R., Niedermann, S., Tao, M.X., Kubik, P.W., Ivy-Ochs, S., Gao, B., Strecker, M.R., 2002. Low slip rates and long-term preservation of geomorphic features in Central Asia. Nature 417, 428–432.

Hughen, K.A., Overpeck, J.T., Peterson, L.C., Trumbore, S.E., 1996. Rapid climate changes in the tropical Atlantic during the last deglaciation. Nature 380, 51–54.

Hughen, K.A., Southon, J.R., Lehman, S.J., Overpeck, J.T., 2000. Synchronous radiocarbon and climate shifts during the last deglaciation. Science 290, 1951–1954.

Hughen, K.A., Eglinton, T.I., Xu, L., Makou, M., 2004. Abrupt tropical vegetation response to rapid climate changes. Science 304, 1955–1959.

Kalm, V., Mahaney, W.C., 2011. Late Quaternary glaciation in the Venezuelan (Mérida) Andes developments in Quart. Science 15, 835–841.

Kellogg, J., Bonini, W., 1982. Subduction of the Caribbean Plate and basement uplifts in the overriding South-American Plate. Tectonics 1 (3), 251–276.

Kohn, B., Shagam, R., Banks, P., Burkley, L., 1984. Mesozoic–Pleistocene fission track ages on rocks of the Venezuelan Andes and their tectonic implications. Geol. Soc. America. Memoir. 162, 365–384.

Korschinek, G., Bergmaier, A., Faesterman, T., Gerstmann, U.C., Knie, K., Rugel, G., Wallner, A., Dillmann, I., Dollinger, G., Lierse von Gostomski, C., Kossert, K., Maiti, M., Poutivsev, M., Remmert, A., 2010. A new value for the half-life of ^{10}Be by heavy-Ion elastic recoil detection and liquid scintillation counting. Nucl. Instrum. Methods Phys. Res. B 268 (2), 187–191.

Lal, D., 1991. Cosmic ray labeling of erosion surfaces: *in situ* nuclide production rates and erosion models. Earth Planet. Sci. Lett. 104, 424–439.

Lea, D.W., Pak, D.K., Peterson, L.C., Hughen, K.A., 2003. Synchroneity of tropical and high-latitude Atlantic temperatures over the last glacial termination. Science 301, 1361–1364.
Lewin, J.A., Gibbard, P.L., 2010. Quaternary river terraces in England: forms, sediments and processes. Geomorphology 120, 293–311.
Liddle, R.A., 1928. The Geology of Venezuela and Trinidad. MacGowan, Fort Worth, p. 552.
Mackenzie, A.N., 1937. Sección geológica de la región de Barinas: Distritos Barinas, Bolívar y Obispos del Estado Barinas, Venezuela. Bol. Geol. Y Min., Caracas 1 (2–4), 269–293.
Maddy, D., Bridgland, D., Westaway, R., 2001. Uplift-driven valley incision and climate-controlled river terrace development in the Thames Valley, UK. Quat. Int. 79, 23–36.
Mahaney, W.C., Kalm, V., 1996. In: Field Guide for the International Conference on Quaternary Glaciation and Paleoclimate in the Andes Mountains, June 21–July 1, 1996. Quaternary Surveys Ltd, Toronto, Canada, p. 79.
Mahaney, W.C., Milner, M.W., Voros, J., Kalm, V., Hütt, G., Bezada, M., Hancock, R.G.V., Aufreiter, S., 2000. Stratotype of the Mérida glaciation at Pueblo Llano in the Northern Venezuelan Andes. J. South Am. Earth Sci. 13, 761–774.
Mahaney, W.C., Russell, S.E., Milner, M.W., Kalm, V., Bezada, M., Hancock, R.G.V., Beukens, R.P., 2001. Paleopedology of middle Wisconsin/Weichselian Paleosols in the Mérida Andes. Venezuela. Geoderma 104, 215–237.
Masarik, J., Frank, M., Schäfer, J.M., Wieler, R., 2001. Correction of in situ cosmogenic nuclide production rates for geomagnetic field intensity variations during the past 800000 years. Geochim. Cosmochim. Acta 65 (3–4), 515–521.
Merchel, S., Herpers, U., 1999. An update on radiochemical separation techniques for the determination of long lived radionuclides via Accelerator Mass Spectrometry. Radiochim. Acta 84, 215–219.
Monod, B., Dhont, D., Hervouët, Y., 2010. Orogenic float of the Venezuelan Andes. Tectonophysics 490, 123–135.
Muscheler, R., Kromer, B., Björck, S., Svensson, A., Frieddich, M., Kaiser, K.F., Southon, J., 2008. Tree rings and ice cores reveal ^{14}C calibration uncertainties during the Younger Dryas. Nat. Geosci. 1, 263–267.
Olivero, M.L., Aguirre, J., Moncada, A., 2005a. Phenomena related to the movement of mud and debris occurred in the Páramo zone of Mérida in June 2003. Revista Forestal Venezolana 49 (2), 131–141.
Olivero, M.L., Aguirre, J., Moncada, A., 2005b. Technical information about the movement of mud and debris occurred in the Páramo zone of Mérida in june 2003. Revista Forestal Venezolana 49 (2), 143–151.
Pazzaglia, F.J., 2013. Fluvial terraces. In: Shroder, J.F. (Ed.), Treatise on Geomorphology, vol. 9. Academic Press, San Diego, pp. 379–412.
Pérez, O.J., Bilham, R., Sequera, M., Molina, L., Gavotti, P., Codallo, H., Moncayo, C., Rodriguez, C., Velandia, R., Guzmán, M., Molnar, P., 2011. GPS derived velocity field in Western Venezuela: dextral shear component associated to the Boconó fault and convergent component normal to the Andes. Interciencia 36, 39–44.
Peterson, L.C., Haug, G.H., Hughen, K.A., Rohl, U., 2000a. Rapid changes in the hydrologic cycle of the tropical Atlantic during the last glacial. Science 290, 1947–1951.
Peterson, L.C., Haug, G.H., Murray, R.W., Yarincik, K.M., King, J.W., Bralower, T.J., Kameo, K., Rutherford, S.D., Pearce, R.B., 2000b. Late Quaternary stratigraphy and sedimentation at ODP Site 1002, Cariaco basin (Venezuela). Proc. Ocean Drilling Project: Scientific Results 165, 85–99.
Peterson, L.C., Haug, H.G., 2006. Variability in the mean latitude of the Atlantic Intertropical Convergence Zone as recorded by riverine input of sediments to the Cariaco basin (Venezuela). Palaeogeogr. Palaeoclimatol. Palaeoecol. 234, 97–113.
Pierce, G.R., 1960. Geología de la cuenca de Barinas: Boleltín de Geología. In: Publicación Especial N° 3, 1, pp. 214–276.
Pigati, J.S., Lifton, N.A., 2004. Geomagnetic effects on time-integrated cosmogenic nuclide production with emphasis on *in situ* ^{14}C and ^{10}Be. Earth Planet. Sci. Lett. 226 (1–2), 193–205.
Repka, J.L., Anderson, R.S., Finkel, R.C., 1997. Cosmogenic dating of fluvial terraces, Fremont river, Utah. 794 Earth Planet. Sci. Lett. 152, 59–73.
Ritz, J.-F., Vassallo, R., Braucher, R., Brown, E.T., Carretier, S., Bourlès, D.L., 2006. Using in situ-produced ^{10}Be to quantify active tectonics in the Gurvan Bogd mountain range (Gobi-Altay, Mongolia). In: Siame, L., Bourlès, D.L., Brown, E.T. (Eds.), Special Paper 415 *in Situ*-produced Cosmogenic Nuclides and Quantification of Geological Processes. Geological Soc.. of America, pp. 87–110.
Rull, V., 2005. A middle Wisconsin interstadial in the Northern Andes. J. South Am. Earth Sci. 19, 173–179.
Salgado-Labouriau, M.L., 1984. Late-Quaternary palynological studies in the Venezuelan Andes. Erdwissenschaftliche Forschung 18, 279–293.
Schmidt, S., Hetzel, R., Kuhlmann, J., Mingorance, F., Ramos, V., 2011. A note of caution on the use of boulders for exposure dating of depositional surfaces. Earth Planet. Sci. Lett. 302, 60–70.
Schubert, C., 1974. Late Pleistocene Mérida glaciation, Venezuelan Andes. Boreas 3, 147–152.
Schubert, C., Valastro, S., 1980. Quaternary Esnujaque formation, Venezuelan Andes: preliminary alluvial chronology in a tropical mountain range. Z. der Deutschen Geologischen Gesellschaft 131, 927–947.
Schubert, C., Clapperton, C.M., 1990. Quaternary glaciations in the Northern Andes (Venezuela, Colombia and Ecuador). Quat. Sci. Rev. 9, 123–135.
Schubert, C., Vivas, L., 1993. El Cuaternario de la Coordillera de Mérida – Andes Venezolanos. Universidad de Los Andes-Fundacion Polar, Mérida, Venezuela, p. 345.
Shackleton, N.J., 1987. Oxygen isotopes, ice volume and sea level. Quat. Sci. Rev. 6, 183–190.
Shagam, R., 1972. Andean research project, Venezuela: principal dat and tectonic implications. Geol. Soc. America. Memoir. 132, 449–463.
Shagam, R., Kohn, B., Banks, P., Dasch, L., Vargas, R., Rodríguez, G., Pimentel, N., 1984. Tectonic implications of Cretaceous–Pliocene fission track ages from rocks of the circum-Maracaibo Basin region of Western Venezuela and Eastern Colombia. Geol. Soc. America. Memoir. 162, 385–412.
Soulas, J.-P., 1985. Neotectonica del flanco occidental de los Andes de Venezuela entre 701300 y 711000W (Fallas de Bocon o, Valera, Pinango y del Piedemonte). In: Memorias del VI Congreso Geológico Venezolano, Caracas, pp. 2690–2711.
Stone, J.O., 2000. Air pressure and cosmogenic isotope production. J. Geophys. Res. 105 (B10), 753–759.
Stuiver, M., Grootes, P.M., Braziunas, T.F., 1995. The GISP2 18O climate record of the past 16,500 years and the role of the sun, ocean and volcanoes. Quat. Res. 44, 341–354.
Taboada, A., Rivera, L.A., Fuenzalida, A., Cisternas, A., Philip, H., Bijwaard, H., Olaya, J., Rivera, C., 2000. Geodynamic of the Northern Andes: subductions and intracontinental deformation (Colombia). Tectonics 19 (5), 787–813.
Tricart, J., 1966. Paléoclimats et terrasses quaternaires: C.R. Somm. seances. Societé Géologique de France, pp. 202–203 (Fasc. 5).
Tricart, J., Millies-Lacroix, A., 1962. Les terrasses quaternaires des Andes vénézueliennes. Bull. Soc. Géol. France, 7e Sér. 4, 201–219.
Tricart, J., Michel, M., 1965. Monographie et carte geomorphologique de la region de Lagunillas (Andes Vénézuéliennes). Revue de Geomorphologie Dynamique 15, 1–33.
Vassallo, R., Ritz, J.F., Carretier, S., 2011. Control of geomorphic processes on ^{10}Be concentrations in individual clasts: complexity of the exposure history in Gobi-Altay range (Mongolia). Geomorphology. http://dx.doi.org/10.1016/j.geomorph.2011.07.023.
Vivas, L., 1984. El Cuaternario. La Imprenta, Mérida, p. 266.
Wegmann, K.W., Pazzaglia, F.J., 2009. Late Quaternary fluvial terraces of the Romagna and Marche Apennines, Italy. Quat. Sci. Rev. 28, 137–165.
Wesnousky, S.G., Aranguren, R., Rengifo, M., Owen, L., Caffee, M.W., Krishna, M., Pérez, O.J., 2012. Toward quantifying geomorphic rates of crustal displacement, landscape development, and the age of glaciation in the Venezuelan Andes. Geomorphology 141-142, 99–113.
Wright, J.D., 2000. Global climate change in marine stable isotope records. In: Noller, J.S., Sowers, J.M., Lettis, W.R. (Eds.), Quaternary Geochronology: Methods and Applications, vol. 4. American Geophysical Union Reference Shelf, pp. 427–433.
Zinck, A., Stagno, P., 1966. Estudio edafologico de la zona de Santo Domingo-Pagüey, Estado Barinas: Division de Obras Hidraulicas. Ministerio de Obras Publicas, Caracas.
Zinck, A., 1980. Valles de Venezuela. Cuadernos Lagoven, p. 150.

3.7. River terraces along the Pueblo Llano river

In order to complete the morphogeochronologic analysis of the PLSDS, in this subsection, I discuss the results of the morphotectonic analysis and ^{10}Be dating made in the lower reaches of the Pueblo Llano river. This part of the river is located in the core of the Mérida Andes, thus the results presented here, added to those of the lower reaches of the Santo Domingo river, give a regional picture of the processes of terrace formation at the scale of a catchment in an active tectonic setting.

- ***General river description***

The Pueblo Llano and the Aracay rivers are the main tributaries of the Santo Domingo river in the central part of the MA. The three rivers flow independently and in different directions down to their confluence around Las Piedras village. Then, the Santo Domingo river, flowing from WNW to ESE, crosses a deep gorge of 15 km long in its way towards the Southeastern flank of the MA (**figure III.26**).

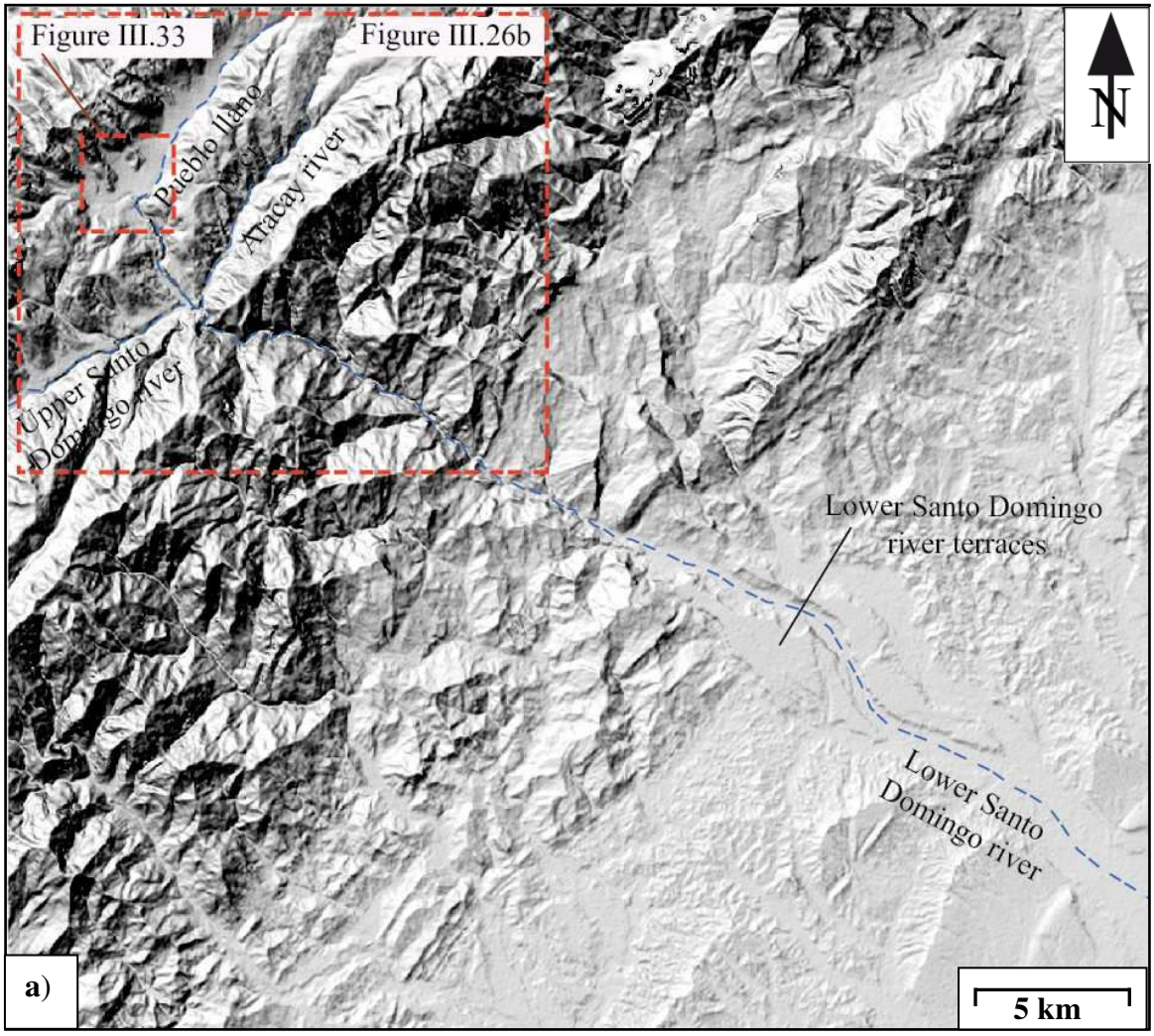

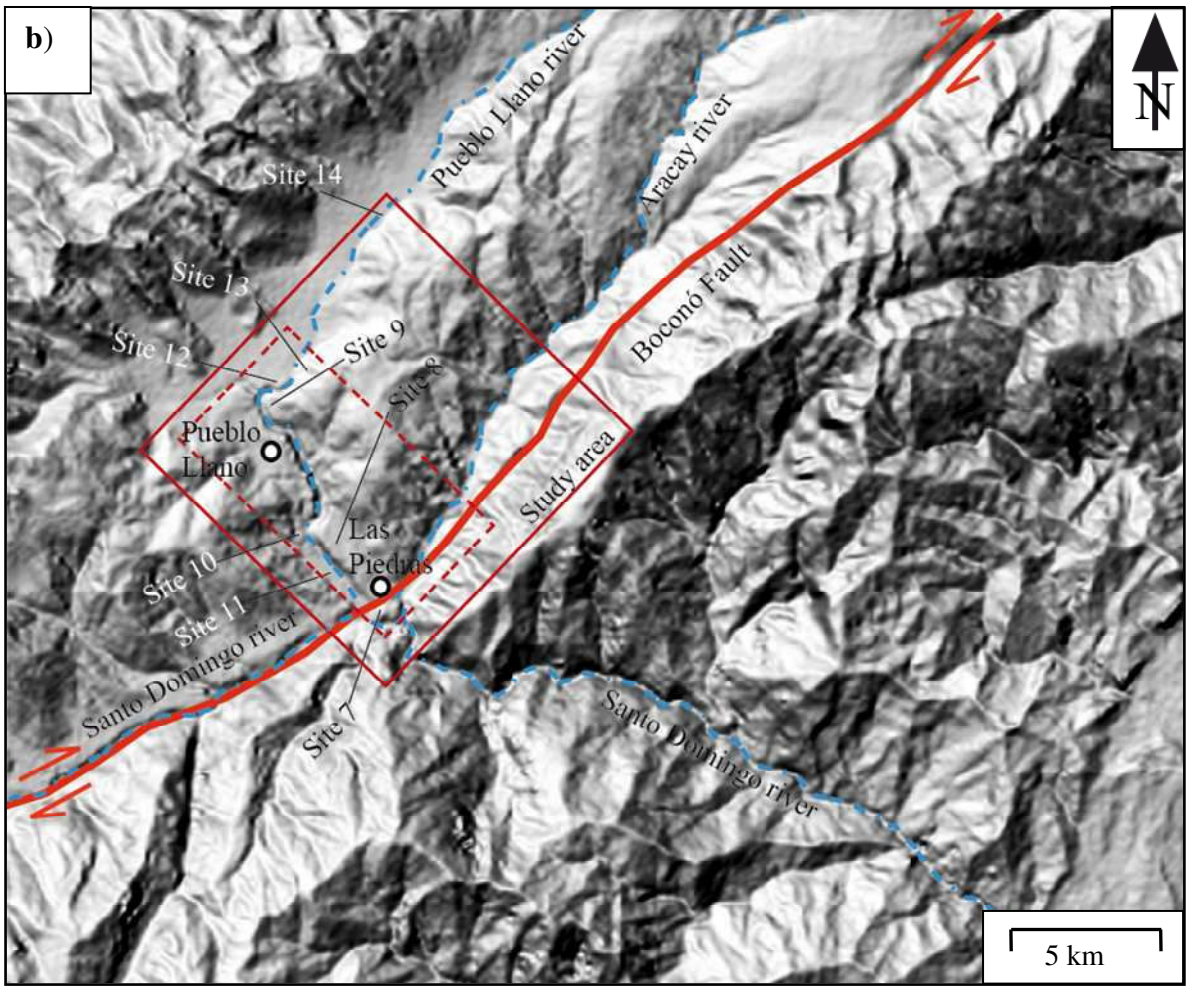

Figure III. 26. a*) Regional location of the study area. The Pueblo Llano river is located at the core of the MA. Location of the lower Santo Domingo river terraces analyzed in subsection 3.5 is shown. Location of* ***figures III.26b*** *and* ***III.33*** *are indicated by a red square.* ***b****) Study area at Pueblo Llano river. The study sites, as well as the Pueblo Llano and Las Piedras villages are shown. Location of the* ***figure III.27*** *is indicated by a red dashed square.*

The Pueblo Llano river catchment has a surface around 100 km^2. It flows over 18 km from its source at 3470 m a.s.l. to the Gral. José Antonio Páez dam at 1600 m a.s.l. The upper and middle reaches of the Pueblo Llano river flow from NNE to SSW (sub-parallel to the axis of the chain) for around 12 km, over crystalline and metamorphic Paleozoic rocks (granite, gneiss and pegmatite) (**figure III.16b**) (Hackley et al., 2005). Then, around 2300 m a.s.l. (near to Pueblo Llano village) (**figure III.26**) it bends abruptly and flows mainly from NNW to SSE in direction sub-orthogonally to the structural trend of the chain for around 6 km toward the confluence. In its lower reaches, the river cuts crystalline and metamorphic

Paleozoic rocks and Quaternary sediments (Hackley et al., 2005) and crosses the Boconó Fault (Audemard et al., 2000).

This analysis focuses on the lower reaches of the Pueblo Llano river, where Quaternary landforms, specially river terraces have been documented (e.g. Vivas, 1979; Bezada, 1990; Schubert and Vivas, 1993) The lack of absolute ages in these studies is a weakness for the correlation and genesis proposed for the alluvial deposits in the area. We therefore determined terraces and moraine geometry (longitudinal and lateral extension, slope, height on the river), sedimentology, and dated their abandonment.

- **Geomorphic analysis**

On the basis of geomorphic and sedimentological analysis three types of Quaternary landforms are recognized and mapped in the study area (**figure III.27**). These landforms were classified as river terraces, frontal moraines and alluvial fans. According to the objectives of this work, we focus our analyses on the river terraces and frontal moraines, however the relationship between all these landforms will be considered.

- *River terraces*

Six fill river terraces were mapped in the lower reaches of the Pueblo Llano river between Pueblo Llano and Las Piedras village (**figures III.26, 27**). These terraces are called in the following $T6_{PL}$ to $T1_{PL}$, from the oldest to the youngest. Most of the terraces are located in the same structural block, except $T6_{PL}$, which is situated to the South of the Boconó Fault. The terraces have an average downstream slope between 6 and 1°. In general, the surfaces of the terraces are flat. The thickness of the alluvial deposit varies according to the terraces from a maximal thickness of 80 m for the oldest terrace ($T6_{PL}$) to 18 m for the youngest one ($T1_{PL}$). The alluvial deposit is roughly stratified, and composed of very angular to rounded boulders, cobbles and pebbles, constituted of gneiss, granite and pegmatite, which are supported by a coarse sand matrix. The boulders size varies between centimetres to meters, with an average diameter of 100 cm and a maximal size of 1700 cm. These boulders are embedded into the alluvial material, but they can outcrop > 250 cm above the ground.

In the following, the individual geometry and sedimentology of the terraces will be discused from the oldest to the youngest one. For $T6_{PL}$ was only recognized a little remnant of terrace located near the Gral. José Antonio Páez dam (Site 7 – Las Piedras cemetery – **figures III.26, 27, 28**). This remnant (~1740 m a.s.l.) is correlatable with a peneplaned surface located around 300 m downstream of the river. From this point, the river enters into a canyon,

where no river terraces were developed (**figures III. 27, 29**). The small extention of the $T6_{PL}$ remnant (< 2000 m^2) and the anthropogenic modification of the terrace surface do not allow the characterization of the slope of this terrace. The incision of this terrace is around 150 ± 5 m (**figure III. 28**). The maximal thickness of the alluvial deposit of $T6_{PL}$ is around 80 m. This alluvial material overlains crystalline and metamorphic Paleozoic rocks. At site 7, the upper 200 cm of the alluvia are composed of roughly stratified very angular to rounded boulders, cobbles and pebbles, which are supported by a coarse sand matrix. The boulders have an average diameter of 20 cm and a maximum size of 70 cm (**figure III. 30**). The first 15 cm of the deposit have been locally reworked during graves digging.

$T5_{PL}$ was observed in the middle and lower section of the study area, and is preserved on the left bank of the river (**figure III.27**). On the eastern border of the remnant located in the middle section, this terrace is overlain by a lateral alluvial fan. By contrast, on the western border, the surface of the terrace is mainly flat with an average downstream slope between 6 and 4°. The incision of this terrace increases upstream from 83 to 115 m. The thickness of the alluvial deposit of $T5_{PL}$ is at least 30 m (**figure III. 28**). Plurimetric angular to rounded boulders composed of crystalline rocks with an average diameter of ~200 cm and a maximal size of 1700 cm are embedded into the alluvial material, but they can outcrop > 250 cm above the ground (**figure III.31**).

$T4_{PL}$ was mapped in the upper section of the study area (**figure III.27**). This terrace is preserved on both banks of the river. However, on the right bank remnants of the terrace are frequently overlain by lateral alluvial fans, and no pristine surface of the terrace is preserved. A remnant located on the left bank (Site 9 -La Laguna- **figure III.27**) has a flat surface with an average downstream slope of 4°. The incision of this terrace increases downstream from 57 to 111 m. As for the alluvial deposit of terrace $T5_{PL}$, plurimetric angular to rounded boulders are embedded into the alluvial material of terrace $T4_{PL}$, but in this case the boulders are smaller with an average diameter of ~100 cm and a maximum size of 300 cm (**figure III.32**).

$T3_{PL}$ was recognized in the upper part of the study area (**figure III.27**). In the only remnant identified, the surface of the terrace is mainly flat with some irregularities downward of the terrace top. $T3_{PL}$ has an average downstream slope of 5°. The incision of this terrace increases downstream from 70 to 100 m. The alluvial deposit of $T3_{PL}$ has a maximum thickness around 20 m. The boulders embedded into the alluvial material of this terrace have the same characteristics of the boulders of terrace $T4_{PL}$.

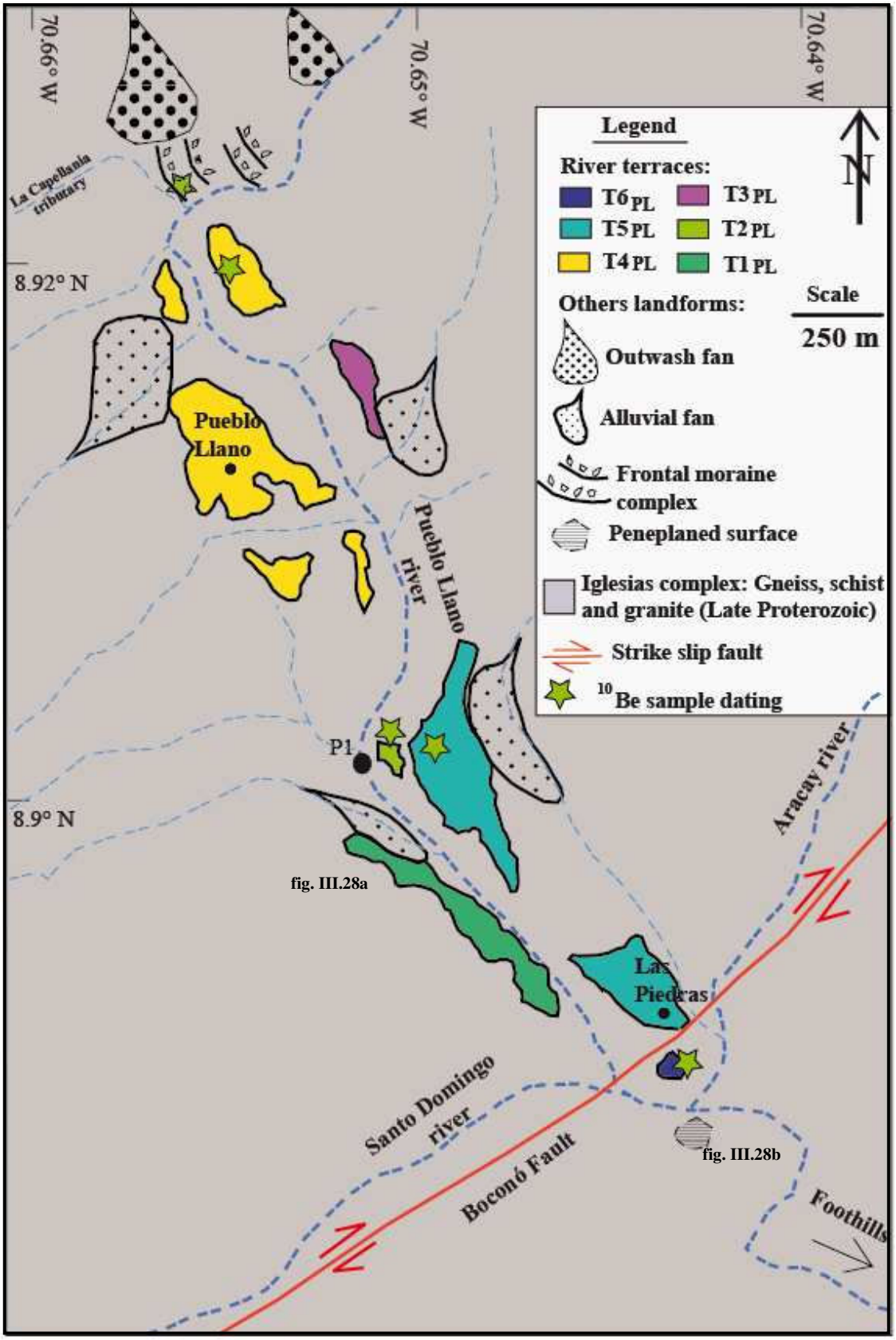

Figure III.27. *Geomorphic map of the lower reaches of the Pueblo llano river, just before its confluence with the Santo Domingo river. The geographical locations of the samples and the study sites are shown in the map. Position of sections of* ***figure III.28*** *are also shown.*

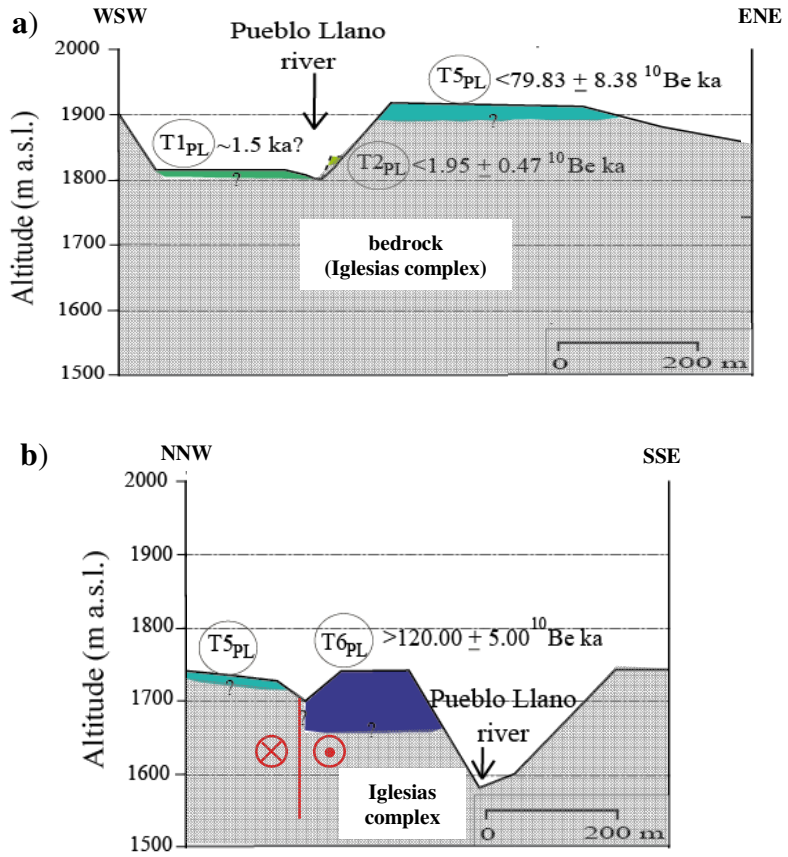

Figure III.28. *Cross section through the river terraces of the lower reaches of the Pueblo Llano river. The ages of the terraces correspond to the numerical ages and extrapolated ages proposed in this work. See* ***figure III.27*** *for location of section* ***a*** *and* ***b****.*

For terrace $T2_{PL}$ we only identified a remnant located in the middle section. This remnant has a surface mainly flat with an average downstream slope of 2° (Site 10 – **figure III.27**). The incision of this terrace is around 29 ± 1 m (**figure. III.28**). $T1_{PL}$ represents the lowest terrace in the study area. This terrace is located on the right bank of the Pueblo Llano river. Terrace $T1_{PL}$ is largely used for agriculture. Additionally, at the upstream border of this terrace, a lateral alluvial fan lies on top of the alluvial deposit of $T1_{PL}$. Nonetheless, remnants of the pristine surfaces of $T1_{PL}$ were observed on the terrace downward (Site 11 – **figure III.27**). In this part, $T1_{PL}$ has a flat surface with an average downstream slope of 3°. The incision of $T1_{PL}$ is around 18 ± 1 m (**figure. III.28**). Plurimetric rounded boulders with similar characteristics to those identified into the alluvial deposit of terrace $T4_{PL}$ were also observed within the alluvial deposit of these two youngest terraces.

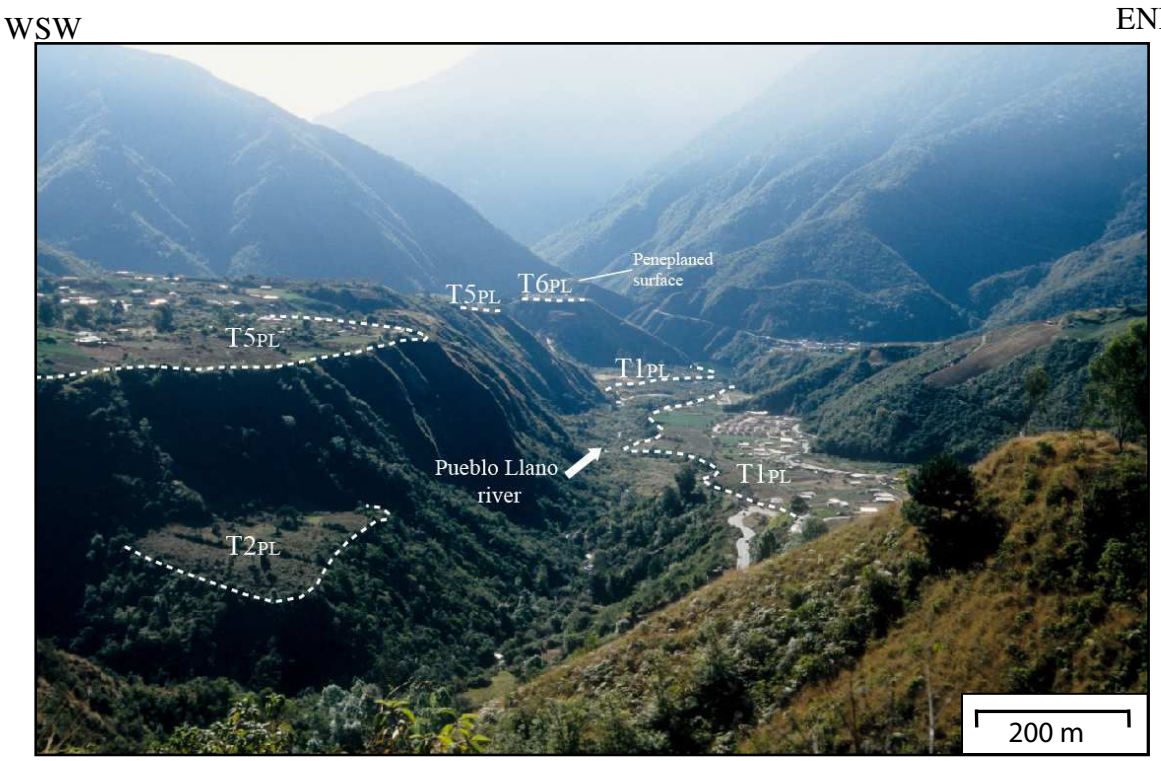

Figure III.29. *Panoramic view of river terraces along the lower reaches of the Pueblo Llano river. Picture by R. Vassallo.*

Figure III.30. *Pit-soil within the alluvial deposit of terrace $T6_{PL}$ at Site 7. The alluvial deposit is composed of very angular to rounded boulders, cobbles and pebbles, which are supported by a coarse sand matrix. Picture by R. Vassallo.*

Figure III.31. *Exposed boulders at surface of terrace $T5_{PL}$. The boulders are indicated by white arrows. Note the extraordinary size of the largest boulder. The top of this boulder is around 3 m above the ground. Picture by R. Vassallo.*

Figure III.32. *Terrace $T4_{PL}$ identified in both flank of the river. On the left bank the surface of the terrace is better preserved. On this bank, exposed boulders are indicated by white arrows. Picture by R. Vassallo.*

- *Frontal moraine complex*

At the confluence between the Pueblo Llano river and La Capellania tributary around 2300 m a.s.l. (Site 12 – **figures III.26b, 27, 33**), a frontal moraine complex was identified. Morphologically, the complex consists of a series of small ridges and depressions between them. The ridges can reach elevation of 15 m with respect to the depressions, and this pattern decreases upstream leaving place to a flat bottom valley (**figure III.33**). The ridges are mainly oriented NNW –SSE (orthogonal to the axis of the middle and upper reaches of the Pueblo Llano valley) with a stronger slope on their upstream flank. Sedimentologically, the ridges are composed of matrix-supported massive diamicton. The coarse material mainly consists of plurimetric very angular to angular boulders of crystalline and metamorphic Paleozoic rocks, with an average diameter of 150 cm and a maximal size of 330 cm. These boulders are embedded into the diamicton, but they can outcrop > 100 cm above ground surface (**figure III.33**).

Previous studies in this area interpreted these landforms as the distal part of a north-south oriented lateral outwash fan, which was produced by the process of ice melting in the high parts of the north hillslope of the Pueblo Llano valley (Vivas, 1979; Bezada, 1990) (**figure III.34**). The morphological expression of this fan is clear and notable on the right flank of the valley. However, his frontal extension was probably overestimated, because in the frontal part of this fan are included the ridge complex identified in the present work. We argue against the statement that these ridges were formed by the outwash fan for the following reasons:

1) The longitudinal profile of the outwash fan decreases in elevation from its apex outwards. Nonetheless, the ridges located in the frontal part are around 15 m higher than the supposed more proximal zone of the fan. Moreover, no constant drainage network over the surface of this deposit exists. This observation allows suggesting that either the relief does not have suffered any modifications or the modification is negligible. In any case, the observed relief must be close to the original. Therefore the ridges identified in this work could not be remnants of paleo-fans;

2) No plurimetric angular boulders are observed at the surface of the intermediate and distal part of the outwash fan, whereas several exposed plurimetric angular boulders are observed on the surface of the ridges. Thus, we argue that different sedimentary dynamics were responsible for these deposits;

3) The most distal ridge has NNW-SSE orientation. This orientation is sub-parallel to the main axis of the outwash fan. But it is orhtogonal to the longitudinal direction of the

Pueblo Llano valley. Thus, the ridges observed could have been formed by the frontal advance of a glacier coming from the Pueblo Llano valley;

4) Diamicton deposits identified in a lateral position of the valley (Site 13), around 500 m upstream to the most distal ridge are also probably glacial deposits. This supports the hypothesis of a glacier advance occurred in this area of the valley;

5) At around 1000 m upstream of the distal ridge, the fluvial incision is negliglibe (< 1 m). Conversely, at this point and toward the upper reaches, the Pueblo Llano valley is much wider and smoothed. This allows suggesting that the valley was not modelled by fluvial processes.

All these reasons strongly suggest that the ridges located around 2300 m a.s.l in the Pueblo Llano valley were formed by the advance of a glacier that flowed into this valley. Hence, these ridges constitute the terminal moraine complex that records the maximum advance of a glacier. This advance could correspond to the Late or to the Early Mérida Stage (see subsection 3.4). This result has important implications in terms of local and regional paleogeography, as will be discussed in subsection 3.8.

- *Alluvial fan*

Lateral alluvial fans were also recognized along the lower Pueblo Llano valley. The present alluvial fans are constructed over river terraces (**figure III.27**). This process was likely similar over the past 100 ka. Therefore, the alluvial fan deposits probably interfinger with the terraces alluvia, and form part of the alluvial deposit of the terraces that was modeled by the longitudinal action of the river.

SSW NNE

WNW ESE

SSW NNE

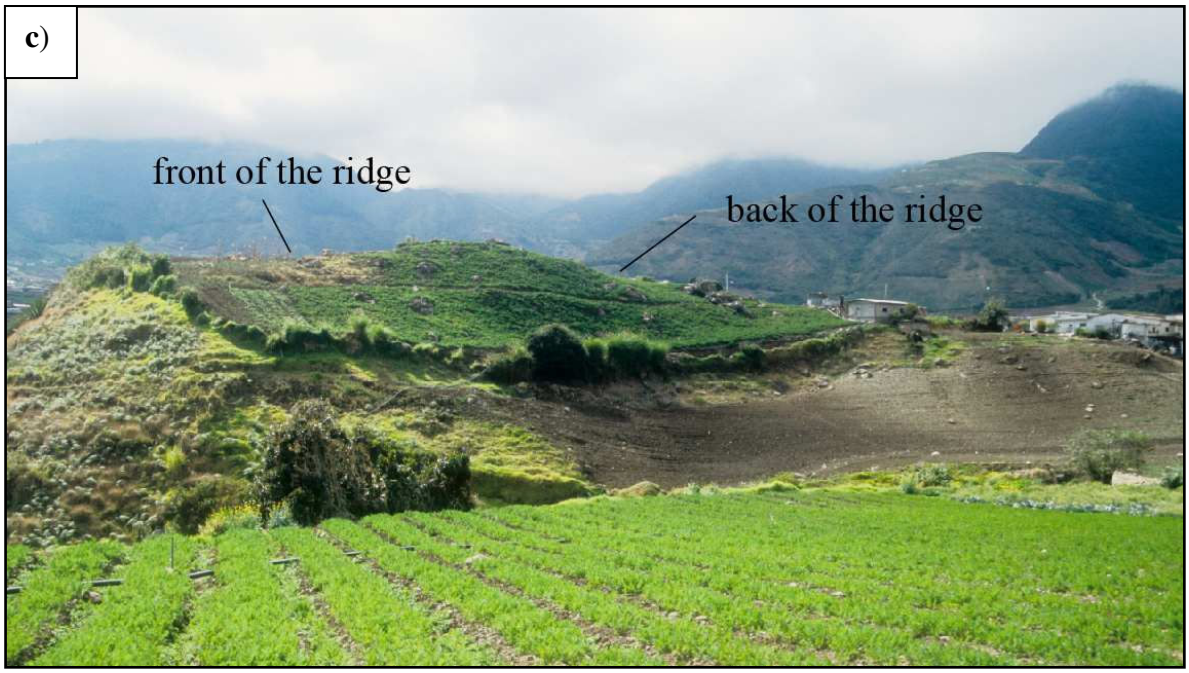

Figure III.33. *Morphology of the frontal moraine complex.* ***a****) Relation between outwash fan identified by Bezada (1990) and the frontal moraines complex identified in this study. Red dashed lines indicated the axis of the ridges that compose the moraine complex.* ***b****) Surface of the distal ridge. Note the elevation of the surface with respect to the surface of the fan. Exposed plurimetric boulders are indicated by white arrows.* ***c****) Morphology of the distal ridge. Note that the slope of the upstream side is stronger than the downstream one. Pictures by M. Alvarado (a) and R. Vassallo (b, c).*

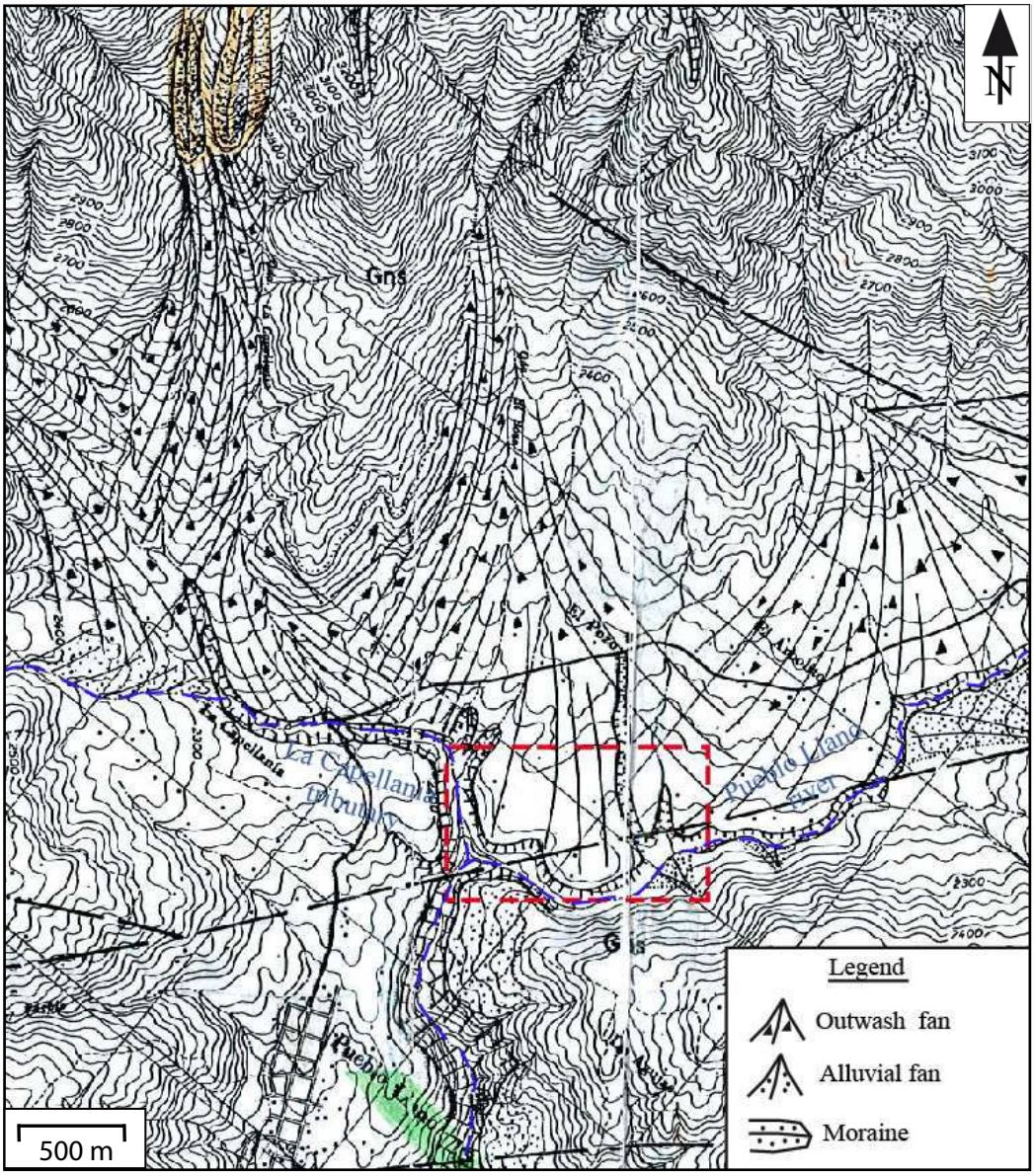

Figure III.34. *Extract of geomorphic map of the lower Pueblo Llano river by Bezada (1990). The zone where the frontal moraine complex identified in this study is indicated by a red square. Note the prolongation towards this zone of the outwash fan proposed by Bezada (1990). Location of this figure is shown in the* ***figure III.26a****.*

- **Age calculations**

In order to determine the exposure ages of the terraces and the frontal moraine complex identified in the lower reaches of the Pueblo Llano river, the concentration of *in situ* produced ^{10}Be in samples collected in terraces $T6_{PL}$, $T5_{PL}$, $T4_{PL}$, $T2_{PL}$ and in the moraine complex were analysed. The results are discussed next in this order: firtstly the terraces from the oldest to the youngest and lastly the moraine complex.

Terrace $T6_{PL}$ was sampled at Site 7 (**figures III.26b, 27).** Five samples (Pll-11-07 to 11) were collected from a cosmogenic depth profile made along a 200 cm deep pit-soil of (**figure III.35**). This sampling strategy allowed the estimation of the ^{10}Be inherited from prior exposure (Anderson et al., 1996; Repka et al., 1997). At the sampling site, the first 15 cm are remobilized material from digging (**figure III.35)**. Taken into account this thickness, the first sample was taken at 15 cm below the terrace surface. Each sample is formed by one fragment of siliceous rocks (gneiss). The two lower and the two upper samples were taken in two boulders, but at different depths (**figure III.35**). The distribution of ^{10}Be concentration shows an exponential decrease with depth. Assuming no denudation and using a chi-square inversion to minimize the difference between observed and modeled ^{10}Be data, we estimate a maximum inherited concentration of $0.34 \pm 0.03 \times 10^5$ at/g. These results yield a minimum exposure age of 120.00 ± 5.00 ^{10}Be ka (**Table III.3**).

To date $T5_{PL}$, four samples were taken at surface from the uppermost 5 cm of the siliceous plurimetric boulders partially embedded into the alluvial deposit of the terrace (Pll-11-21 to 24 – **Table III.3**). ^{10}Be concentration range between 8.33 ± 0.46 and $8.54 \pm 0.29 \times 10^5$ at/g (**Table III.3**). The height of the boulders tops above the surface of the terrace (some of them > 180 cm), suggests that the samples have not been shielded by any matrix, even if a slight denudation of the surface of the terrace occurred. Little scattering of their ^{10}Be concentrations suggests that these boulders have a similar and simple pre-exposure history. However the inherited component could not be estimated. This gives a maximum exposure age for this terrace, as well for the terraces $T4_{PL}$ and $T2_{PL}$, where the same dating strategy was used. Therefore, the apparent age, given by the boulder with the smallest concentration, should be the closest to the true age (Vassallo et al., 2011). For terrace $T5_{PL}$, sample Pll-11-21 is the one with the lowest concentration with $8.33 \pm 0.46 \times 10^5$ at/g, and yields a maximum exposure age of 79.03 ± 8.38 ^{10}Be ka (**Table III.3**).

In the case of terrace $T4_{PL}$, two surface samples were taken from plurimetric boulders. They have similar ^{10}Be concentrations: 2.31 ± 0.11 and $2.59 \pm 0.22 \times 10^5$ at/g (Pll-11-15 and 17, respectively – **Table III.3**). As for terrace $T5_{PL}$, the height of the boulder tops above the surface of the terrace (> 170 cm), suggests that the samples have not been shielded by any matrix. Sample Pll-11-15 is the one with the lowest concentration, and yields a maximum exposure age of 17.66 ± 1.81 ^{10}Be ka (**Table III.3**).

Four samples were taken to estimate the exposure age of terrace $T2_{PL}$ (Pll-11-18, 19, 19b and 20 – **Table III.3**). ^{10}Be concentration are similar, and they are comprises between 0.20 ± 0.04 and $0.23 \pm 0.05 \times 10^5$ at/g (**Table III.3**). In this case, sample Pll-11-20 is the one

with the lowest concentration with 0.20 ± 0.04 x 10^5 at/g, and yields a maximum exposure age of 1.95 ± 0.47 ^{10}Be ka (**Table III.3**).

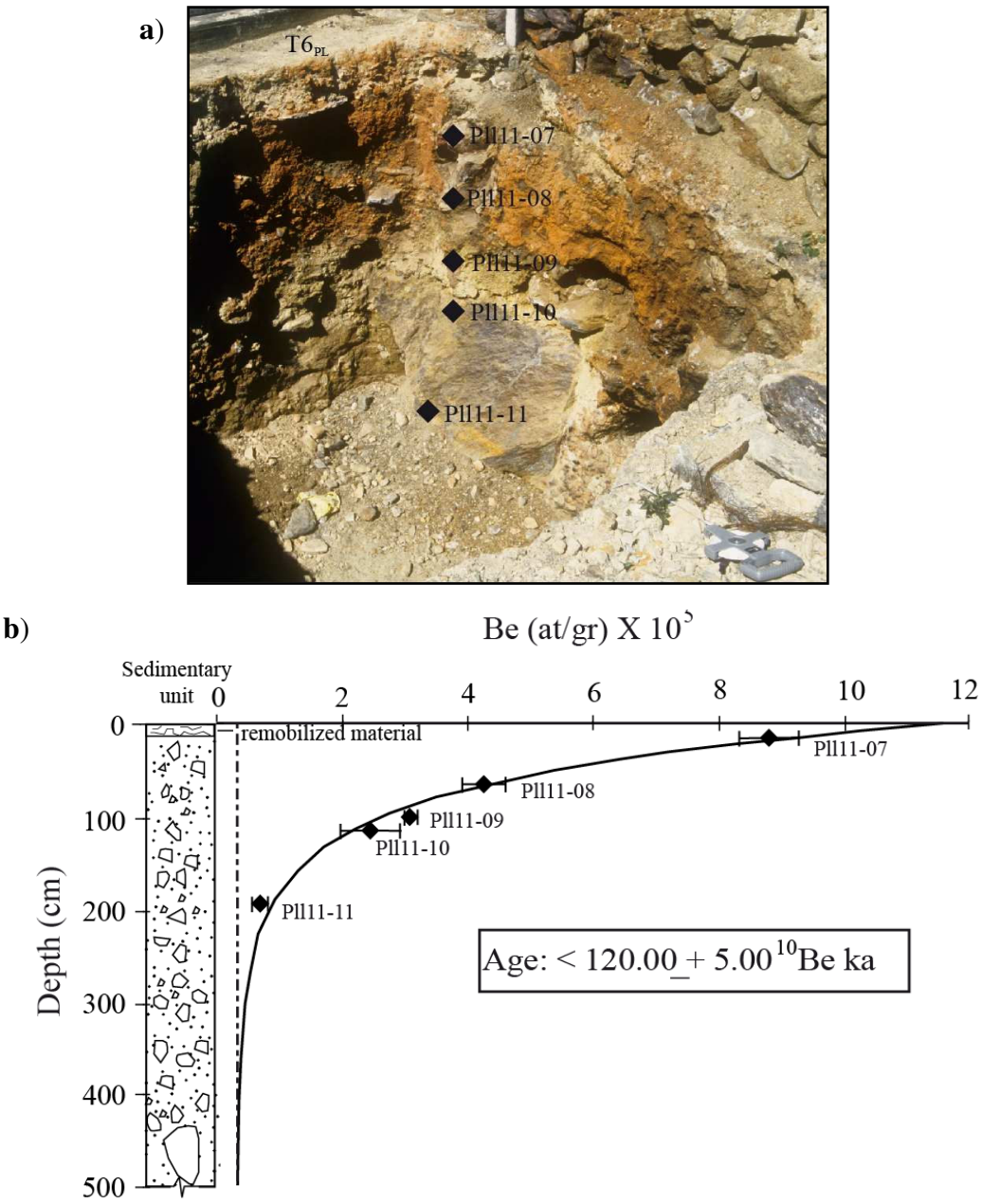

Figure III.35. *Depth profile of the ^{10}Be concentration within the alluvial deposit of the terrace $T6_{PL}$ at Site 7.* ***a****) Sample location in the pit-soil at Site 7.* ***b****) Depth profile of the ^{10}Be. The depth production best fit using a chi-squared inversion is in solid line. The dashed line shows the inherited ^{10}Be concentration. Detail of exposure ages calculations are in* ***Table III.3****.*

To date the frontal moraine complex, three samples were taken from the distal and highest ridge of the complex (Site 12 – **figures III.27, 33**). In the same way as for the terraces, the samples were taken at surface from the first 5 cm of the plurimetric boulders partially embedded into the diamicton (Pll-11-1, 2 and 5 – **Table III.3**). ^{10}Be concentration

varies between 2.40 ± 0.10 and 2.52 ± 0.09 x 10^5 at/g (**Table III.3**). The height of the boulder tops above the surface of the ridge (some of them > 100 cm), suggests that the samples have not been shielded by any matrix even if a slight denudation of the surface occurred. Very little scattering of their ^{10}Be concentrations and the glacial origin of the material allow suggesting that the inherited concentration in these boulders is probably negligible and the apparent exposure age, that we consider as a maximum, should be close to the true age. Therefore, the apparent age given by the boulder with the smallest concentration should be viewed as a maximum deglaciation age. Sample Pll-11-01 is the one with the lowest concentration with 2.40 ± 0.10 x 10^5 at/g, and yields an exposure age of 17.37 ± 1.72 ^{10}Be ka (**Table III.3**).

- **Temporal incision rates**

The incision rates were calculated as a result of the ratio between the height of the terrace above the current riverbed and the ^{10}Be ages estimate for terrace $T6_{PL}$, $T5_{PL}$, $T4_{PL}$ and $T2_{PL}$. Along the lower reaches of the Pueblo Llano river the remnants of these terraces are located at different localities, thus a single point where all the terraces are present does not exist. However, the incision rates for terraces $T5_{PL}$ and $T2_{PL}$ can be evaluated at the same point (P1 – see **figure III.27** for location), where both terraces are present and the fluvial incision is maximum. We also evaluate the incision rates for terraces $T6_{PL}$ and $T4_{PL}$ at the sites with maximum fluvial incision. These sites are located approximately 2 and 3 km down and upstream of P1, respectively.

In the case of terrace $T6_{PL}$, the maximum elevation of the terrace above the current riverbed is 150 ± 5 m. For this terrace, a minimum exposure age of 120 ± 5.00 ^{10}Be ka was estimated. The calculation yields a maximum incision rate of 1.25 ± 0.09 mm/a (**Table III.4**).

Terrace $T5_{PL}$ is 115 ± 0.5 m above the current riverbed. In this case, a maximum exposure age of 79.03 ± 8.38 ^{10}Be ka was estimated. Therefore the calculation yields a minimum incision rate of 1.45 ± 0.15 mm/a (**Table III.4**).

$T4_{PL}$ is located 111 ± 0.5 m above the present riverbed. A maximum exposure age of 17.66 ± 1.81 ^{10}Be ka was estimated for this terrace. The calculation yields a minimum incision rate of 6.28 ± 0.64 mm/a (**Table III.4**).

The maximum elevation of terrace $T2_{PL}$ is 30 ± 0.5 m above the present riverbed. A maximum exposure age of 1.95 ± 0.47 ^{10}Be ka was estimated. The calculation yields a minimum incision rate of 15.38 ± 3.72 mm/a (**Table III.4**).

Sample	Type of sample	Lithology	Latitude (N)	Longitude (E)	Altitude (m a.s.l.)	Depth (cm)	Height above the ground (cm)	Surface P_0 (at/g/y)	Shielding factor	^{10}Be concentration (10^5 at/g)	^{10}Be age (ka)	Terrace
Site 7 - Las Piedras			- 70.6378	8.8866	1738			9.75 ± 0.65	0.991		120.00 ± 5.00	$T6_{PL}$
Pll-11-07	Cent. boulder	Gneiss				15				8.23 ± 0.42		
Pll-11-08	Cent. boulder	Gneiss				65				4.24 ± 0.36		
Pll-11-09	Cent. boulder	Gneiss				100				3.08 ± 0.11		
Pll-11-10	Cent. boulder	Gneiss				115				2.44 ± 0.48		
Pll-11-11	Cent. boulder	Gneiss				195				6.63 ± 0.10		
Site 8 - Jaciri			- 70.6482	8.8989	1896			10.83 ± 0.72	0.993			$T5_{PL}$
Pll11-21	Cent. boulder	Gneiss					186			8.33 ± 0.46	79.03 ± 8.38	
Pll11-22	Cent. boulder	Granite					184			8.54 ± 0.29		
Pll11-23	Cent. boulder	Granite					170			8.41 ± 0.41		
Pll11-24	Cent. boulder	Gneiss					170			8.45 ± 0.29		
Site 9 - Laguna			- 70.6589	8.9245	2223			13.35 ± 0.89	0.986			$T4_{PL}$
Pll11-15	Metric boulder	Gneiss					197			2.31 ± 0.11	17.66 ± 1.81	
Pll11-17	Metric boulder	Granite					170			2.59 ± 0.22		
Site 10 - Las vacas			- 70.6509	8.9018	1851			10.51 ± 0.70	0.972			$T2_{PL}$
Pll11-18	Metric boulder	Gneiss					100			0.21 ± 0.04		
Pll11-19	Metric boulder	Gneiss					160			0.21 ± 0.08		
Pll11-19b	Metric boulder	Gneiss					160			0.23 ± 0.05		
Pll11-20	Metric boulder	Gneiss					110			0.20 ± 0.04	1.95 ± 0.47	
Site 12 - Moraine			- 70.6594	8.9286	2297			13.97 ± 0.93	0.994			$M1$
Pll11-01	Metric boulder	Pegmatite					105			2.52 ± 0.09		
Pll11-02	Plurimetric boulder	Gneiss					80			2.43 ± 0.19		
Pll11-05	Plurimetric boulder	Gneiss					91			2.40 ± 0.10	17.37 ± 1.72	
Site 14			- 70.6367	8.9605	2467							river
Pll-11-12	Sand	Heterogeneous				0				0.88 ± 0.11		

Table III.3. *Results of the ^{10}Be analysis for the lower reaches of the Pueblo Llano river. Calibration against NIST Standard Reference Material 4325. ^{10}Be concentrations uncertainties include analytical errors from the counting statistics and blank correction, whereas the ages uncertainties also include the errors of the production rate introduced by the scaling model of Lal (1991) - Stone (2000) and the errors of the ^{10}Be decay constant (Chmeleff et al., 2010; Korschinek et al., 2010).*

These results show that the mean incision rates in the lower reaches of Pueblo Llano river varies from 1.25 to 15.38 mm/a. The mean long-term incision rates estimated from the geometries of the terraces older than ~ 80 ka ($T6_{PL}$ and $T5_{PL}$) are quite similar and around 1.3 mm/a. Instead, the mean short-term incision rates estimated from the terraces abandoned after ~18 ka are at least five and ten times higher ($T4_{PL}$ and $T2_{PL}$, respectively). These differences include temporal and spatial variations and put clearly in evidence that the short-term incision rates are tipically faster than the long-term incision rates along the Pueblo Llano river.

Table III.4. *Summary of Lower Pueblo Llano river terraces ages and incision rates.*

Terrace	Height of surface above the current riverbed at P1 (m)	Exposure age (ka)	Incision rate (mm/a)
$T6_{PL}$	150 ± 5.0 *	120.00 ± 5.00	1.25 ± 0.09
$T5_{PL}$	115 ± 0.5	79.03 ± 8.38	1.45 ± 0.15
$T4_{PL}$	111 ± 0.5	17.66 ± 1.81	6.28 ± 0.64
$T2_{PL}$	30 ± 0.5 *	1.95 ± 0.47	15.38 ± 3.72

* Height in a point of maximal incision

3.8. Pueblo Llano and Santo Domingo rivers system (PLSDS)

In the previous subsections (3.5 and 3.6) we have identified and dated different river terraces along the PLSDS. Here, these results are analysed together, in order to better understand the impact of the external controls in the process of terraces formation in the whole system.

- **Correlation of terraces**

Our geomorphic observations and ^{10}Be dating show that all the terraces identified in the whole system were abandoned at different times. Thus, despite of the strong genetic relation between the terraces of the upper and lower reaches of the system (see discussion below), we argue that each terrace corresponds to an individual formation event. Thus, a total of twelve river terraces were identified for the whole system.

In the previous section, we used a local nomenclature for the individual analysis of each reach of the river. Here, an integrated nomenclature according to the chronostratigraphy framework of the system is presented (**Table III.5**), and used in the following.

Table III.5. *Chronostratigraphy framework of the Pueblo Llano and Santo Domingo system.*

Ages (ka) / River	~1.5?	1.95 ± 0.47	~10?	17.66 ± 1.81	17.37 ± 1.72	~26?	43.14 ± 5.78	59.61 ± 6.29	~68?	72.06 ± 3.00	79.03 ± 8.38	~110?	120.00 ± 5.00
Pueblo Llano	$T1_{PL}$	$T2_{PL}$	$T3_{PL}$	$T4_{PL}$	M1						$T5_{PL}$		$T6_{PL}$
Santo Domingo						T1	T2	T3	T4	T5		T6	
Whole system	Qt1	Qt2	Qt3	Qt4	M1	Qt5	Qt6	Qt7	Qt8	Qt9	Qt10	Qt11	Qt12

- **Terraces formation vs climate**

According to our ^{10}Be dating discussed in the sub-sections 3.5 and 3.6, river terraces along the PLSDS were abandoned during the last ~130 ka. Here, we compare the paleoclimatic proxies available for Venezuela with our terraces dating in order to decipher the impact of the climate in terraces formation (**figure III.37**).

The age of abandonment of the two oldest terraces (~120 and ~80 ka; Qt12 and Qt10, respectively) (**Table III.5**) located in the upper reaches of the system seem to correlate with a period of high sea/lake level in the Gulf of Cariaco centred at 125 and 83 ka, respectively

(Van Daele et al., 2011). These high levels correspond to the global warm condition of the MIS 5e (Eemian interstadial) and MIS 5a (Odderate interstadial) (e.g. James, 2000; Shackleton et al., 2003). Moreover, we argue that the age of abandonment of the terrace Qt10 at ~80 ka allow to better constrain the lower boundary of the El Pedregal Interstade previously defined as < 65 ka by Dirswosky et al. (2005), Rull (2005) and Kalm and Mahaney (2011).

Another terrace, Qt4, dated in the upper reaches, shows an age of abandonment that correlates with the end of the LGM in the MA (~18 ka), when the climatic conditions become relatively warmer. The youngest terrace dated in the upper reaches, Qt2, has a minimum age of abandonment of ~2 ka, which can also be correlated with a warm climatic phase, proposed for the MA by Rull (1998), and called Miranda Warm Phase (3 – 4 cal ka BP). Palynological and geochemical record of the Cariaco basin put in evidence that the interstadials were warm periods with an increase in the precipitations and river discharge (Peterson et al. 2000a, 2000b; Haug et al. 2001; Peterson and Haug 2006; González et al. 2008). Therefore, as Audemard (2003) and Audemard et al. (2007), we argue that the period of alluviation of these fill terraces can be related to cold and dry conditions, while the incision and abandon were triggered when the climate became relatively warm and humid.

The age of abandonment of strath terraces dated in the lower reaches (~74, ~60 and ~43; Qt9, Qt7 and Qt6, respectively) (**Table III.5**) correlate with short period of cold and dry conditions around 73, 59 and 43 ka identified in the paleoclimatic proxies of Cariaco basin (stadial and Heinrich event 6 **- figure III.36**) (Peterson et al. 2000a, 2000b; Haug et al. 2001; Peterson and Haug 2006; González et al. 2008). This suggests that the process of strath formation and the aggradation of alluvial deposits in the lower reaches of the system was developed during warm and humid conditions while the vertical incision and abandoment of the terraces was triggered by the transition to short cold and dry conditions.

These results suggest that climate-related changes in catchment hydrology and sediment availaibility would be the primary control for the formation of fluvial terraces in the PLSDS over periods of 10^3-10^4 years. However the MA uplift and the strike slip of Boconó Fault parrallely play a main role in the preservation of terraces and in the development of the alluvial deposit of the oldest terrace in the upper reaches (Qt12), as shown by the following discussion.

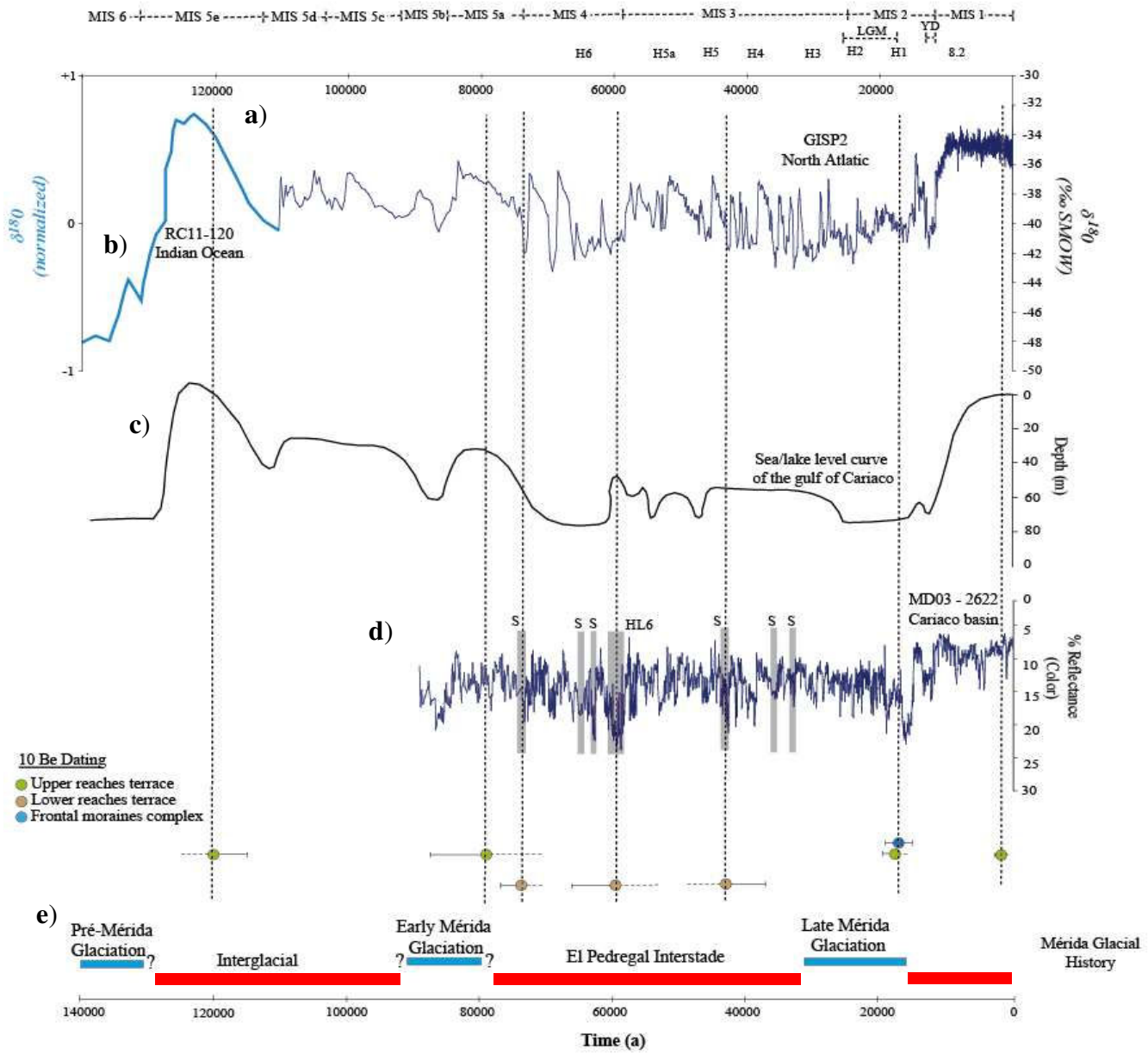

Figure III.36. *Ages of abandonment of river terraces for the last 120 ka along the PLSDS compared with:* ***a****)* $\delta^{18}O$ *record from the GISP2 ice core (Grootes et al., 1993; Stuiver et al., 1995).* ***b****)* $\delta^{18}O$ *normalized record from the deep sea sediment of Southwestern Indian Ocean (Martison et al., 1987)* ***c****). Sea/lake level curve for the last 140 ka of the Gulf of Cariaco (Van Daele et al., 2011).* ***d****) Color reflectance curve of Cariaco basin (Peterson et al., 2000a). The gray rectangles represent short periods of cold and dry conditions identified by Peterson et al (2000a) and González et al. (2008) in the Cariaco basin. (S) stadial; (H6) Heinrich event 6.* ***e****) Glacial history of Mérida Andes summarized from Dirswosky et al. (2005), Rull et al (2010) and Kalm and Mahaney (2011). The blue rectangles represent periods of glacial conditions (cold/dry) while the red rectangles representsinterglacial conditions (warm/humid). The timing of Heinrich events H1-H6 is according to Hemming (2004) and Rashid et al., (2003). (MIS) Marine Isotope stage (Aitken and Stokes, 1997; Wright, 2000; Shackleton, 1987). (LGM) Last Glacial Maximum (Clark et al., 2009). (YD) Younger Dryas (Berger, 1990).*

- **Dynamics of terraces formation**

The hypothesis that the rivers should respond to climatic change during the past 200 ka through vegetation-related variations in runoff and sediment supply was originally proposed by Bull and Knüpfer (1987) and Bull (1990) for the temperate river systems located in North Atlantic and New Zealand. Several records of river terraces around the world have reported the relation between the terrace formation and climate (e.g. Fuller et al., 1998; Macklin et al., 2002; Brighland and Westaway, 2008). In Venezuela, we argue that the formation of most of the terraces for the last ~130 ka mainly responds to climatic variations as well. Nevertheless, the type of response is highly related to the altitude of the site and the glacier infuence. Indeed, in the upper reaches of the Pueblo Llano and Santo Domingo rivers system, where the elevations vary between 2300 and 1600 m a.s.l. the aggradation phases are synchronized with cold and dry to warm and humid climatic periods, while the lower reaches of the system located around 300 m a.s.l. show the opposite pattern.

González et al. (2008) using the pollen record of the Cariaco basin showed that the vegetation in Eastern Venezuela is sensitive to the rapid climates changes, such as Stadial, Dansgaard–Oeschger and Heinrich events. In the MA, palynological analyses in the MA showed as well that the vegetation is sensitive to rapid climate changes (e.g. Salgado-Labouriau, 1979, 1989; Salgado-Labouriau and Schubert, 1976). Van der Hammen (1974), based also on pollen record analysis of the MA reported that the tree line descended from 3500 m a.s.l. to 2000 m a.s.l. during the coldest part of the Last Glacial period. Therefore, we propose that transitions from warm and humid to cold and dry periods destabilize hillslope's colluvia as a result of the decrease of the vegetative cover (e.g. Paramo ecosystems). Consequently, fluvial systems undergo significant variations in the transport capacity and sediment supply. High sediment fluxes combined with dry conditions leads to aggradation phases (cold and dry periods), while a developed tree cover associated to a reduced hillslope runoff, limits the sediment transport and favors fluvial incision (warm and humid periods) (e.g., Fuller et al., 1998; Macklin et al., 2002; Wegmann and Pazzaglia, 2009). In the lower reaches of the system, the process of terraces formation seems to be different. During warm and humid conditions, the material coming from the erosion of the upper part of the catchment is transported toward the lower reaches. In this zone the increase in sediment supply and water discharge makes the river attaining a graded condition (Mackin, 1948; Knok, 1975; Leopold and Bull, 1979). During this phase channel vertical incision and deposition are at a minimum. Lateral erosion is more important, thus a wide and continuous erosional surface (strath) is developed. These conditions are interrupted by vertical fluvial

incision and abandonment of river terraces triggered by the decrease in the transport capacity caused by short periods of cold and dry conditions (e.g. stadial) (**figure III.37**).

The spatial variability in the processes of river terraces formation along the PLSDS could be associated to the orographic precipitation pattern observed in the Southeatern flank of the MA (Monasterio and Reyes, 1980). Indeed, González et al. (2008) proposed for Eastern Venezuela the coexistence of two contrasting hydrological regimes during particular climatic conditions. For example, during stadial, colder and possibly more humid conditions dominated in the mountains regions whereas drier conditions dominated in the lowland. A similar pattern probably characterized the MA, and could explain the absence of terraces development during the stadial conditions in the upper reach of the rivers system. These complex hydrological regimes are clearly expressed in the dyachronism between the formation of terraces in the upper and the lower reaches.

Two other processes play a role in terrace formation. The signature of instantaneous high energy aggradations events is put in evidence by the presence of the pluri-metric boulders, with an average diameter up to ~500 cm, at the surface of terraces (e.g. Qt11, Qt7). These boulders are embedded into the alluvial deposits and were probably transported and deposited by debris flow climatically or tectonically triggered in a context of high water discharge and sediment supply. In the case of climate controlled events, these events could have been similar to those occurring today (Olivero et al., 2005a, b). These instantaneous deposits are intercalated with the normal sedimentation of the river and constitues an important part of the terraces deposit.

The second process is related to the neotectonic activity of the Boconó Fault. As mentioned above (see subsection 3.6), most of the identified terraces in the upper reaches of the system are localized to the North of the Boconó Fault. Considering the lateral right slip rate estimated for this fault between 5.5 and 9 mm/a in a site located around 20 km westward of the study area (e.g. Audemard et al., 2008; Wesnousky et al., 2012), and the exposure age of the terrace Qt12 (~120 ka), the structural block located to the South of the fault has been displaced at least 700 m westward over the last 120 ka. Before this configuration, a strong aggradation phase occurred as proven by the thickness of the alluvial deposit of Qt12 (≤ 80 m). These data must be associated with the following geomorphic observations: 1) a peneplaned surface probably modeled by fluvial erosion located around 300 m downstream of the terrace Qt12; 2) a deep and narrow gorge downstream of the peneplaned surface. Altogether these results suggest that the aggradation of alluvial deposit of terrace Qt12 would be a combined result of a dammed configuration at the confluence of the main drainages

(Santo Domingo, Pueblo Llano and Aracay rivers) led by neotectonic activity of the Boconó Fault, and the high sediment flux caused by climatic effect.

As discussed earlier, the upper reaches of the Pueblo Llano and Santo Domingo rivers system were affected by glacial conditions. We have discussed the effect that these conditions could have produced over the vegetation and the variations in runoff and sediment supply. Nonetheless, could we establish any relation between the glacial activity and the development of the river terraces? The age of abandoment of terraces Qt4 and the frontal moraine M1 are around 18 ka. These ages match with the end of the LGM. Older moraines with a maximal age of 81 ± 15 TL ka had been also reported in this catchment (Mahaney et al., 2000). This age is close to the abandonment of the terrace Qt10 reported in this study (~79 ka), which is situated just downstream of the M1. These data suggests that the alluvial materials of the terraces were deposited contemporarily to the glacier advance, while the vertical incision of the terraces and their abandoment match with the onset of the glacier melting. Thus, we argue that the following two scenarios were possible: 1) during the glacial condition all the material eroded by the glacier advance fed directly the river channel network and formed part of the terraces deposits; 2) during the glacier melting, the glacial sediments were rapidly transported to the fluvial system, and due to the large transport capacity of the river (humid conditions and glacier melting), the sediments were transported along the river.

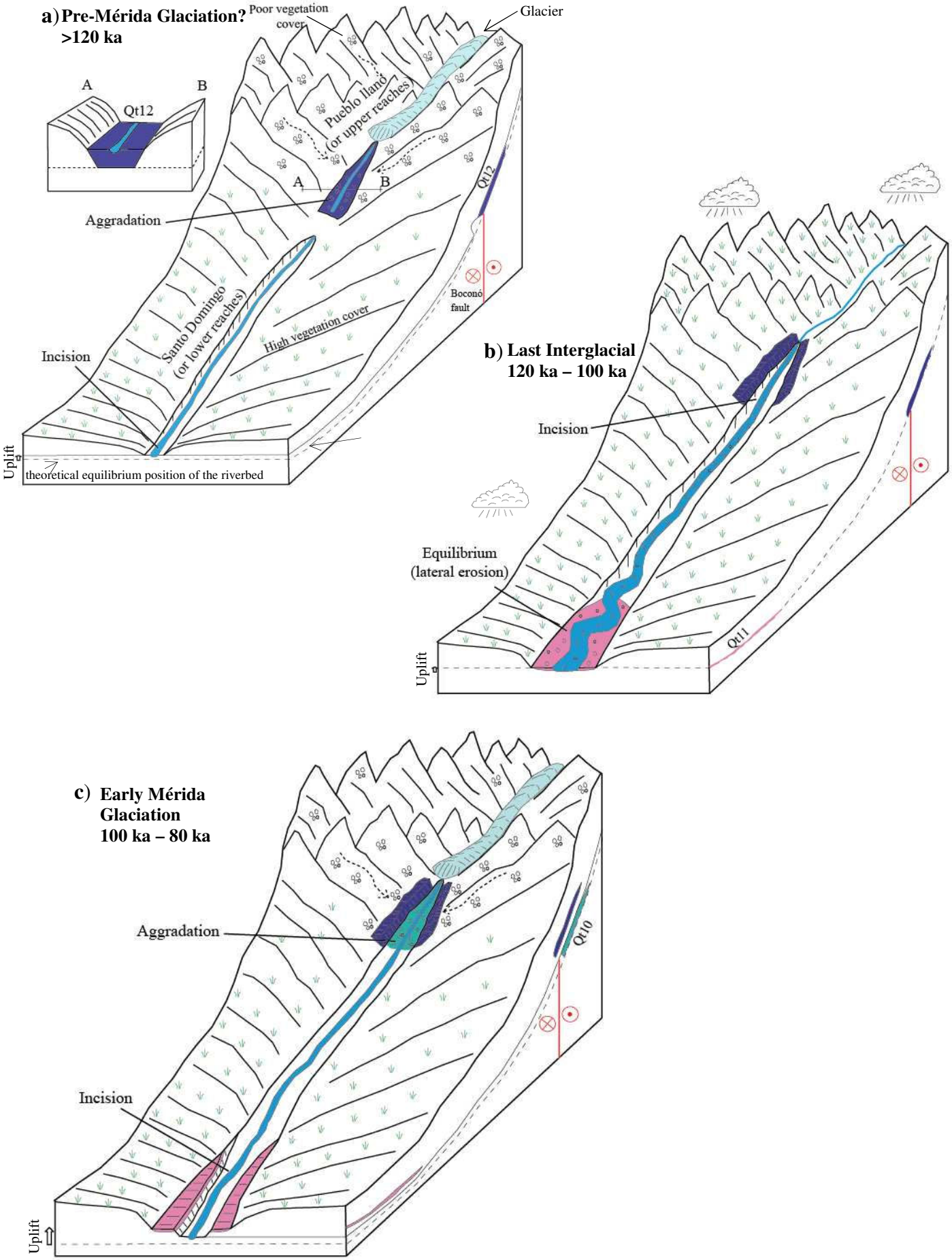
a) Pre-Mérida Glaciation?
>120 ka
Poor vegetation cover
Glacier
A
B
Qt12
Pueblo llano
(or upper reaches)
A
B
Qt12
Aggradation
Santo Domingo
(or lower reaches)
High vegetation cover
Boconó
fault
Incision
Uplift
theoretical equilibrium position of the riverbed
b) Last Interglacial
120 ka – 100 ka
Incision
Equilibrium
(lateral erosion)
Qt11
Uplift
c) Early Mérida
Glaciation
100 ka – 80 ka
Aggradation
Qt10
Incision
Uplift

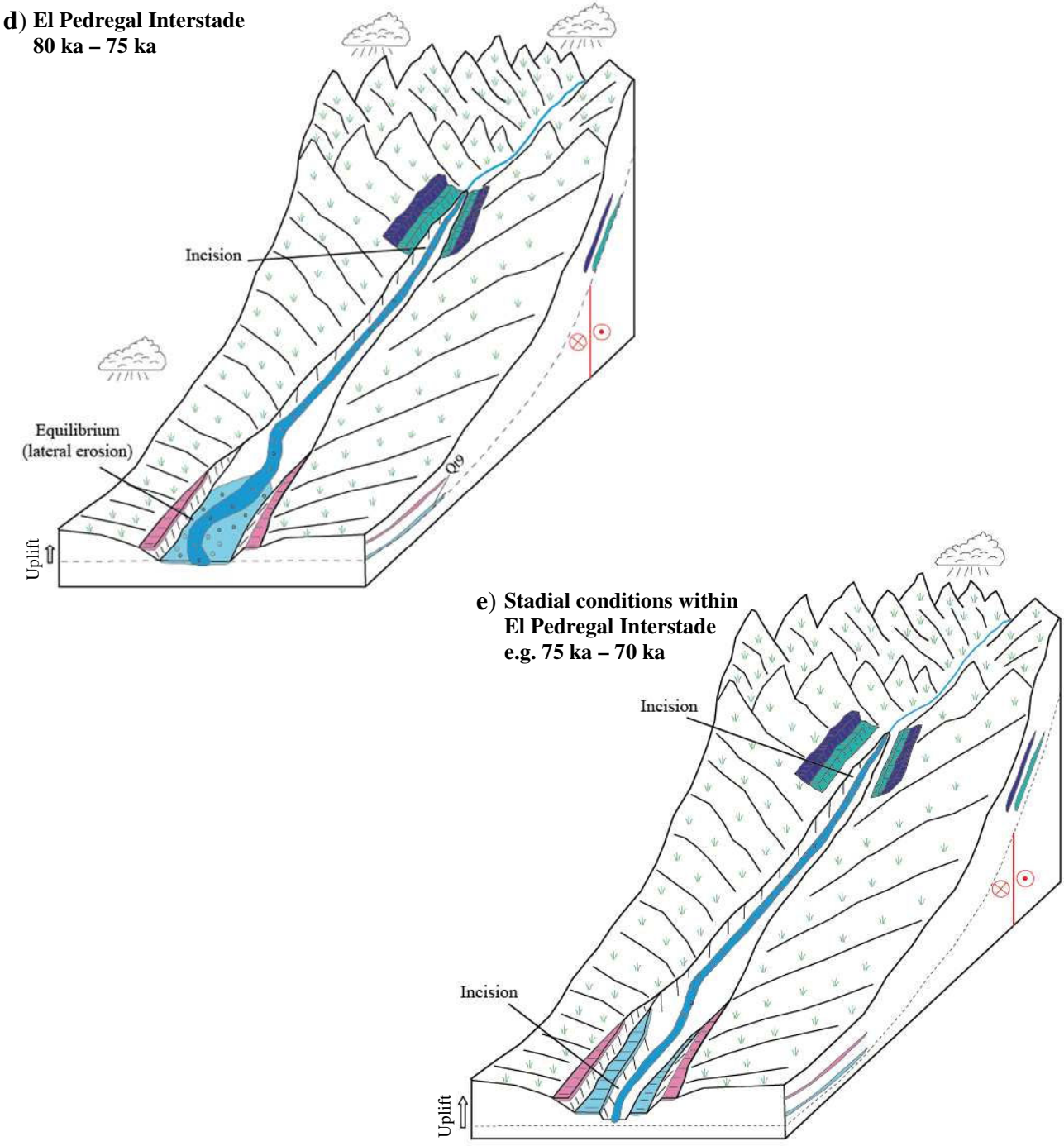

Figure III.37. *Block-diagrams showing possible relationships between vegetation cover, hillslope-channel coupling and aggradation–incision cycles during typical hydro-climatic conditions along the PLSDS. Frontal glacier position in different periods is speculative.* ***a****) Cold and dry conditions during Pre-Mérida Glaciation.* ***b****) Warm and humid conditions during interglacial periods.* ***c****) Cold and dry conditions during Early Mérida Glaciation.* ***d****) Warm and humid conditions during El Pedregal Interstade period.* ***e****) Cold and humid conditions dominated the upper reaches of the system, whereas drier conditions dominated in the lowland during stadial conditions within El Pedregal Interstade. See text for discussion.*

- **Reconstruction of the morphology of the PLSDS**

Based on the terraces formation model, the chronostratigraphy framework and the neotectonic of the area, the following Quaternary evolution is proposed for the PLSDS (**figure III. 37**):

1) During Pre-Mérida glaciation (>130 ka; Mahaney et al., 2010; Kalm and Mahaney, 2011), the outlet of the Santo Domingo, Pueblo Llano and Aracay rivers were dammed by a tectonic configuration controlled by the activity of the Boconó Fault. This fact, combined with a high sediment flux and the decrease of the stream power caused by the cold and dry glacial conditions, led to an aggradation phase at the upper reaches of the system (**figure III. 37a**). 2) At the interglacial period MIS 5e (~130 - 115 ka; Wright, 2000): enhanced stream power caused by the wetter climate triggers the vertical fluvial incision and the abandonment of the terrace Qt12 (~120 ka). The material removed was transported downstream toward the lower reaches. In this part of the system, this material beveled the bedrock, and was partially deposited constituting the alluvial deposit of terrace Qt11, which was abandoned by the decrease of stream power during the stadial 5d (~115-105 ka; Wright, 2000). (**figure III. 37b**). 3) During Early Mérida Glaciation (~90-65 ka; Mahaney et al., 2000, 2010), cold and dry conditions led to an aggradation phase at the upper reaches of the system (**figure III. 37c**). 4) Relatively warm and humid conditions during interstadial 5a (~84 – 74; Wright, 2000) caused fluvial incision and the abandonment of the terrace Qt10 (~79 ka) at the upper reaches of the system. 5) During El Pedregal Interstade (< 65 – 25 ka; Dirszowsky et al., 2005; Rull, 2005; Kalm and Mahaney, 2011), the material eroded was transported and deposited into the lower reaches of the system, where short climatic variations to cold and dry conditions (e.g. stadial conditions between Dansgaard–Oeschger events; Bond and Lotti, 1995) reduced the stream power and caused the incision and abandonment of the terraces Qt9 to Qt5 (~72, ~68, ~59 ka, ~43 and ~26 ka) (**figure III. 37d, e**). These climatic variations seem not to have produced any changes in the incision regime of the upper reaches of the system. 6) During Late Mérida Stage (~25-13 ka; e.g. Schubert and Valastro, 1980; Mahaney and Kalm, 1996; Rull, 2005), and specifically at LGM, the main glacier of the Pueblo Llano valley reached its maximum advance. The frontal moraine complex of Pueblo Llano was formed (M1, ~18 ka). In front of the glacier, within the fluvial domain, outwash sediments were deposited during cold and dry conditions (similar conditions of the **figure III.37c**). These sediments were incised when the melting post-LGM increases the stream power, forming the terrace Qt4 (~17 ka). 7) During the Younger Dryas (~13.60 – 12.40 ^{14}C cal ka BP; Mahaney et al., 2008; Kalm and Mahaney, 2011) cold and dry conditions caused the aggradation of the

alluvial deposit of Qt3. The transition to warm and humid conditions of Miranda Warm phase (~9.40 – 6.30 ka, Salgado-Labouriau et al., 1988; Schubert and Vivas, 1993) led to the vertical incision and abandonment of the terrace Qt3 at the upper reaches of the system (similar conditions of the **figure III.37b**). 8) Holocene transition from relative cold and dry conditions of Culata phase (6.00 – 5.30 ^{14}C ka, Salgado-Labouriau and Schubert, 1976) to warm and humid conditions of Miranda Warm phase II (3.64 – 2.45 ka; Salgado-Labouriau et al, 1988; Schubert and Vivas, 1993) led to the formation of terrace Qt2 (~2 ka). 9) Since 2 ka to the Present, another terrace called Qt1 was formed at the upper reaches of the system. This terrace could be an evidence of the climatic variations of the two last millennia in the MA (issue studied in detail by Polissar, 2005). Thus, the abandonment of this terrace could correspond with one of the two warm and humid periods dated by Mahaney et al. (2000) at around 1.48 and 0.92 ka. However a high influence of the anthropogenic effect over the fluvial dynamics in the formation of the last terrace is not discarded.

The Quaternary reconstruction of the PLSDS discussed above could be modelled analogically or numerically in order to reinforce and quantify the dynamic model, as well as the relation aggradation/incision in the system.

- **Implication of frontal moraine complex at Pueblo Llano valley in the reconstruction of Mérida Glaciation**

The first evidences of glaciation in the Venezuela Andes were described by Sievers (1886) and Jahn (1925, 1931). Later, Schubert spent more than 20 years to document in detail the extent and location of moraines and associated deposits in the region (Schubert, 1970, 1974; 1975, 1984, Schubert and Valastro, 1980; Schubert and Clapperton, 1990; Schubert and Vivas, 1993). Then, Mahaney and Kalm (1996) and Mahaney et al. (2000, 2001, 2008 and 2010) continued this work for other 15 years. These authors (among others) described for the MA two main moraine system complexes. The first is generally limited to elevations of 2600 to 2800 m a.s.l., and the second between 2900 and 3500 m a.s.l. These complexes have been associated with the two main glacial stages of the Mérida Glaciation (Schubert, 1974, 1976). The lowest complex is associated to the Early Mérida Stage of the last glaciation. Its age is poorly constrained and is assumed to be younger than MIS 5e (Shackleton et al., 2003) or approximately < 90 ka (Kalm and Mahaney et al., 2011), with a minimum age of ~ 60 ^{14}C cal ka BP (Mahaney et al., 2001; Dirszowsky et al., 2005). The highest complex is associated to the Late Mérida Stage (Schubert, 1974). It is estimated to have formed between 25 and 13 ka (Schubert, 1974, Schubert and Valastro, 1980, Schubert and Clapperton, 1990, Mahaney and

Kalm, 1996, Rull, 2005, Kalm and Mahaney, 2011), with a maximum ice advance between 23 and 19 ka, which has been correlated to the LGM (Schubert and Rinaldi, 1987; Mahaney and Kalm, 1996).

Along the Pueblo Llano valley, landforms and sediments associated to the Mérida Glaciation have been reported. For the upper and the middle part of the valley, specifically on the right hillslope, cirques and hanging valleys closed by terminal moraines are the main evidences of the glacial activity. Cirques are located at an average elevation of 3700 m a.s.l., while the moraines can reach a minimum elevation of 2700 m a.s.l. (Bezada, 1990). This author also reported outwash glacial fans located at the outlet of the cirques or hanging valley, which are interpreted as glacio-torrential deposits associated to the process of ice melting. TL dating of the fluvio-glacial sediment located at the valley floor of one of the glacial hanging valley (Canoa Valley at ~2800 m a.s.l.) yields an age of 18.00 ± 2.1 TL ka, therefore this landform has been correlated with the LGM (Bezada, 1990). At this site, based on sedimentology and OSL dating, Mahaney et al. (2000) also reported that the LGM till is overlying glaciotectonized diamict with an age of ~81 ka, which these authors correlated with the Early Mérida Stage.

In this study, a frontal moraine complex located at elevation of 2300 m a.s.l. was identified (see subsection 3.6). Our ^{10}Be dating of exposed boulders yields an exposure age of 17.37 ± 1.72 ka (Pll-11-05; **Table III.3**). Therefore, this moraine complex was formed during the Late Mérida Stage and puts in evidence the maximum advance of the glaciers in the Pueblo Llano valley during the LGM. Bezada (1990) had already reported that the glaciers of the Late Mérida Stage in this valley reached elevations 400 m lower than in other areas of the MA. However this author only takes into account lateral glaciers that produced moraine complex, which are hanging around 500 m above the bottom of the Pueblo Llano valley, and not the frontal moraine complex located identified and dated in this study.

This result highlights the fact that the glacier advance during the LGM in other areas of the MA could have also reached elevation lower than those reported in previous studies. A careful analysis and dating of other glacial landforms in the MA would be therefore necessary to reconstruct the real extension of the Late Mérida Glaciation.

- **Meaning of the ^{10}Be concentrations in sediments of the active stream bed**

Throughout this thesis, the ages of terraces have been determined mainly by radiocarbon and cosmogenic dating. In the case where the second methodology was applied a precise geomorphic, stratigraphic and sedimentologic characterization of the terrace and its

alluvial deposit appears absolutely fundamental. This characterization is necessary to constrain the different processes involved in the pre and post-deposit ^{10}Be production (e.g. exhumation, sediments transport, surface denudation), and formulate adapted hypothesis to interpret ^{10}Be concentrations correctly in terms of exposure ages.

Pre-deposit processes determine the inherited ^{10}Be concentration in the sample (^{10}Be accumulated during prior exposure), which could causes apparent exposure ages to be several times higher than true ones (e.g. Heyman et al, 2011; Vassallo et al., 2011). In this work, in order to characterize ^{10}Be inheritance along the PLSDS, two sampling strategies were applied. Following Anderson et al. (1996) and Repka et al. (1997), two concentrations depth profiles were constructed along the alluvial deposits of the terraces Qt12 and Qt9. In both cases, the ^{10}Be concentration describes an exponential decrease. Thus, ^{10}Be inherited concentrations were estimated from the asymptotic value towards which the exponential concentration model tends. These values are almost similar in both terraces even if the ages of these ones are different and even if they are situated in the higher and lower reaches, respectively (0.34 ± 0.03 and 0.30 ± 0.03 x 10^5 at/g, for terraces Qt12 and Qt9, respectively). This component was also estimated from the concentration of ^{10}Be in sediment of active stream bed (Repka et al., 1997; Hancock et al., 1999; Hetzel et al., 2002). This last approach assumes that the inherited concentration is similar to the current riverbed concentration. In this case, two samples of sand were taken. One was collected in the upper reaches of the system, where the fluvial incision is negligible (Pll-11-12) and the other in the lower reaches of the system (Sdo-11-15). The ^{10}Be concentration estimate in the sample Sdo-11-15 (0.30 ± 0.03 x 10^5 at/g; **Table III.1**) is close to those estimated from the concentration depth profiles. Thus, this concentration seems to validate this approach to estimate inherited concentration. We should expect a similar concentration in the sample Pll-11-12 took at the upper reach. On the contrary, a higher concentration was found (0.88 ± 0.11 x 10^5 at/g; **Table III.3**). We are aware that more measurements would be necessary to have a better statistics. Nevertheless, these results seem to suggest that the concentration of ^{10}Be in sand of active stream beds are highly controlled by the altitude of the sample in the system and their local production rate. In fact, the concentration of the sample Pll-11-12 located at the upper reaches is around three times higher that the concentration of Sdo-11-15. This difference is observed between the production rate of the two sites (~4 and ~14 at/g/a, for the lower and upper reaches samples respectively). This means that:

1) In the upper reaches the present exhumation/transport of sedimentary material is larger/slower than during the phases of aggradation that produced the deposits of the terraces;

2) the fluvial transport at the catchment scale is not responsible of the variations in ^{10}Be concentrations within the riverbed. If it were, we should observe an increase of these concentrations towards the lower reaches; 3) Most of the sand at one site of the river probably comes from proximal sources, as shows the strong correlation in ratios between concentrations and local production rates; 4) ^{10}Be concentrations in the present riverbeds cannot be systematically taken to estimate an inheritance value in post-deposits.

Chapter IV:

Geomorphologic Analysis of River terraces on Eastern Balkan, Albania

Panoramic view along the middle reaches of the Devoll river in Albania.

4.1. Overview of chapter IV

Albania is located in the central part of the Dinaric-Albanic-Hellenic Alpine fold belt. Albania is tectonically active and its seismicity is associated with the uplift of the Albanides mountain range (Aliaj, 2000; Sulstarova et al., 2000, 2003). This uplift leads to vertical incision of the mountain range by the fluvial systems and formation of river terraces along of the Albanian rivers. These terraces were initially documented by the pioneering studies of Melo (1961) and Prifti (1984). Numerical ages have been reported for these terraces since the beginning of the 90's (Lewin et al., 1991), with more emphasis on the last decade (Hamlin et al., 2000, Woodward et al., 2001, 2008; Koçi, 2007; Carcaillet et al., 2009). However, most of these studies were concentrated on Southern Albania.

Albanian rivers are mainly oriented orthogonal to the structural trend and the rivers flow from the extensional domain in the East to the compressional domain in the West, crossing several active faults. These rivers developed fluvial terraces on a vast area from mountainous regions to coastal plains at less than 20 km from the sea, and all of these rivers flow to the Adriatic Sea. Albania is affected by a long-term uplift (Aliaj, 1991, 2000; Carcaillet et al., 2009), hence the spatial and temporal reconstruction of the incisions allows a quantification of the fluvial evolution at a higher resolution than a glacial-interglacial cycle. For the previous reasons, Albanian rivers appear as one of the most suitable context in the Mediterranean domain to study the effect of the tectonic, climatic and eustatic variations in the processes of river terraces formation. Thus, we apply a morphotectonic analysis coupled with ^{14}C and *in situ* produced ^{10}Be dating, in attempt to understand the process of terraces formation in Albanian rivers.

In this chapter, firstly a brief synthesis of the geological, climatic and paleoclimatic setting of the Albania is discussed. Then, I focus the analysis in three rivers located in Central and Northern Albania (i.e. Shkumbin, Devoll and Mat rivers). New geomorphologic and geochronological data are integrated with published data coming from other rivers (i.e. Vjosa -called Voidomatis in Greece-, Osum and Erzen rivers) in order to propose a regional homogeneous stratigraphic/chronologic framework, applicable to terrace formation in Albania for the last 200 ka. From this framework the timing of formation of eleven regional river terraces over the last 200 ka was established. The correlation between the age of abandonment of Pleistocene-Early Holocene terraces and climatic proxies shows that the process of formation of Albanian terraces was mainly controlled by climatic variations through unsteady discharge of water and sediments. Lateral erosion and/or aggradation occur during cold and

dry conditions and the vertical incision and abandonment of terrace are triggered by warm and humid conditions. Nonetheless, our data also show that these geomorphic responses of the fluvial systems were probably modulated by the size of the catchments and by eustatic variations. For the pre-Marine Isotope stage 2 (MIS 2) period, during cold and dry conditions, the highlands of the large catchments were probably more heavily affected by hillslope processes and a greater volume of sediments was delivered to the main channel. This fact coupled with the diminished transport capacity of the river (dry conditions) favored the development of fill terraces in the large catchments. On the contrary, in the small catchments, the equilibrium between sediment supply and transport capacity favored the development of strath terraces. For the period after the beginning of the MIS 2, a complex relation between climatic and eustatic variations favored the development of strath terraces everywhere along the Albanian rivers. The results obtained in this analysis are presented in this chapter as an article to submit to Geomorphology.

Finally, the spatial and temporal variations of incision rate in the Shkumbin, Devoll, Osum and Vjosa rivers (Southern Albania and Northwestern Greece) are estimated from the geomorphological mapping, the measurement and the dating of the terraces. From this quantification, local shifts in the regional trend of incision rates were identified. These shifts are linked to the vertical slip of the active faults when they coincide with the presence of faults already mapped by previous authors. Vertical slip rates for eight active faults in Southern Albania were thus estimated for the last 19 ka and vary from ~0.1 to ~2 mm/a. These results are presented in this chapter as an article *in press* in a Special Issue in "Earthquake Geology" of Annals of Geophysics.

4.2. Resumé du chapitre et principaux résultats

L'Albanie est située dans la partie centrale de la chaîne alpine qi s'etend des Dinarides à Helléniques. L'Albanie est tectoniquement active et sa sismicité est associée au soulèvement des Albanides (Aliaj, 2000; Sulstarova et al., 2000, 2003). Ce soulèvement conduit à l'incision verticale de la chaîne de montagnes par les systèmes fluviaux et la formation de terrasses fluviales le long des rivières de l'Albanie. Ces terrasses ont d'abord été documentées par les études pionnières de Melo (1961) et Prifti (1984). Des âges numériques ont été obtenus pour ces terrasses depuis le début des années 90 (Lewin et al., 1991), avec une concentration plus importante sur la dernière décennie (Hamlin et al., 2000, Woodward et al., 2001, 2008; Koçi 2007; Carcaillet et al., 2009). Cependant, la plupart de ces études se concentraient sur l'Albanie du Sud.

Les rivières de l'Albanie sont principalement orientées perpendiculairement au grain structurale, et les rivières coulent depuis le domaine en extension à l'Est jusqu'au domaine en compression à l'Ouest, traversant plusieurs failles actives. Ces rivières développent des terrasses fluviales sur un vaste territoire, depuis les régions montagneuses jusqu'aux plaines côtières à moins de 20 km de la mer, et toutes ces rivières débouchent dans la mer Adriatique. L'Albanie est affectée par un soulèvement long-terme (Aliaj 1991, 2000, Carcaillet et al., 2009), ainsi la reconstruction spatiale et temporelle des incisions permet une quantification de l'évolution fluviale à une résolution supérieure à celle d'un cycle glaciaire-interglaciaire. Pour les raisons précédentes, les rivières de l'Albanie offrent un des contextes les plus appropriés dans le domaine méditerranéen pour étudier l'effet des variations tectoniques, climatiques et eustatiques dans les processus de formation des terrasses fluviales. Ainsi, nous avons appliqué une analyse morphotectonique couplée avec la datation ^{14}C et ^{10}Be *in situ*, pour tenter de comprendre le processus de formation des terrasses le long de ces rivières.

Dans ce chapitre, une breve synthèse du contexte géologique, climatique et paléoclimatique de l'Albanie est presenté dans un premier temps. Ensuite, des nouvelles données géomorphologiques et géochonologiques de la partie centrale et nord de l'Albanie (rivieres Shkumbin, Devoll et Mat) sont intégrées avec les données publiées provenant d'autres rivières (Vjosa -appelé Voidomatis en Grèce-, Osum et Erzen) afin de proposer un cadre stratigraphique et chronologique homogène à l'échelle régional, applicable à la formation des terrasses fluviales en Albanie pour les derniers 200 ka. Dans ce cadre, le moment de la formation de onze terrasses fluviales régionales au cours des derniers 200 ka a été établi. La corrélation entre l'âge d'abandon des terrasses Pléistocène-Holocène et les

reconstructions climatiques montre que le processus de formation des terrasses en Albanie a été contrôlé principalement par les variations climatiques. Notre modèle de formation des terrasses propose que l'érosion latérale et/ou l'aggradation fluviatile se produit pendant les périodes froides et sèches, tandis que l'incision verticale et l'abandon de terrasse est déclenchés par des conditions chaudes et humides. Néanmoins, nos données montrent aussi que les réponses géomorphologiques des systèmes fluviaux ont probablement été modulées par la taille des bassins versants et les variations eustatiques. Pour la période pré-MIS 2, dans des conditions froides et sèches les parties supérieures des grands bassins ont probablement été plus fortement touchée par les processus de versants et un plus grand volume de sédiments ont été livrés au principal chenal de la rivière. Ce fait, combiné avec la capacité de transport réduit de la rivière (conditions sèches), a favorisé le développement des terrasses de remplissage dans les grands bassins versants. Au contraire dans les petits bassins versants, l'équilibre entre l'apport de sédiments et la capacité de transport a favorisé le développement de terrasses d'abrasion. Pour la période après le début du MIS 2, une relation complexe entre les variations climatiques et eustatiques a favorisé le development des terrasses d'abrasion partout en Albanie. Les résultats obtenus dans cette analyse sont présentés dans ce chapitre sous forme d'un article à soumettre à Geomorphology.

Enfin, les variations spatiales et temporelles des taux d'incision dans les rivières Shkumbin, Devoll, Osum et Vjosa (Albanie du Sud et Nord-Ouest de la Grèce) sont estimées à partir de la cartographie, la mesure et la datation des terrasses. A partir de cette quantification, les changements locaux dans la tendance régionale des taux d'incision ont été identifiés. Ces changements sont interprétés comme liés à la composante verticale des failles actives quand ils coïncident avec la presence de failles déjà cartographiées dans des études antérieures. Les taux de glissement vertical pour huit failles actives dans le sud de l'Albanie ont donc été estimés pour les derniers 19 ka et varient de 0.1 à ~2 mm/an. Ces résultats sont présentés dans ce chapitre sous forme d'un article sous presse dans un volume spécial du "*Earthquake Geology*" d'Annals of Geophysics.

4.3. Geodynamics and structural context of Albania

Albania is located in the Eastern part of the Balkan region. Albania constitutes a segment of the wide Circum-Mediterranean-Peri-Tethyan Thrust Belts. Specifically, Albania is located on the central part of the Dinaric-Albanic-Hellenic Alpine fold belt, which has been thrusted westward over the Adriactic foreland during the Alpine orogeny. Thus, the Albanides thrust belt is associated to the convergence between the Apulia and Eurasia tectonic plates and the closure of the Thethys ocean (Sorel et al., 1992; Robertson and Shallo, 2000; Carminati et al., 2004; Roure et al., 2004) **(figure IV.1**).

The structural trend of the Albanides is mainly oriented NNW-SSE and the Albanides are traditionally divided in Internal and External Albanides. The Internal Albanides can be divided in a Central Belt (Mirdita zone) and an Eastern Continental Internal Complex (Gashi, Korabi and Rubiku zones), both mainly composed of Jurassic ophiolitic and Mesozoic carbonates, on top of which Cenozoic sedimentary basins have been developed (e.g. Burrel and Korcë basins; **figures IV.2, 3**) (Meço et al., 2000; Robertson and Shallo, 2000; Carminati et al., 2004; Muceku et al., 2006). The External Albanides are dissected by a major transfer zone: the Vlora-Elbassan-Dibra transfer zone, which is NE-SW oriented. The Northern part of the External Albanides comprises the Periadriatic depression in the West, where only the Neogene molasse of the foredeep crops out at the surface; and the Kruja and Krasta-Cukali zones in the East, which exhibits thrust anticlines of Mesozoic platform carbonates covered by Oligocene to Miocene and Cretaceous to Eocene flysch, respectively (Robertson and Shallo, 2000; Roure et al., 2004) (**figures IV.2, 3**). The Southern part of the External Albanides is divided in four thrust zones that are, from East to West: the Krasta-Cukali zone, the Kruja zone, the Ionian zone (constituted by Berati, Kurvaleshi and Cika belts) and the Sazani zone. The composition of the Kruja and Krasta-Cukali zones are much similar in the southern and northern parts of the External Albanides. The Ionian zone is composed of Triassic evaporites, Triassic to Paleogene platform and pelagic carbonates, and covered by Oligocene to Miocene flysch. The Sazani zone is made up of Triassic to Paleogene platform carbonates (Robertson and Shallo, 2000; Niewland, 2001; Roure et al., 2004) (**figures IV.2, 3**).

Geological and geophysiscal data evidence a present-day geodynamic context characterized by the subduction of the Adriatic oceanic plate beneath the foreland domain (Muço, 1994; Papazachos et al., 2002; Carminati et al., 2004) (**figure IV.4)**. Seismic tomographic data show a gently eastward-dipping slab below the Dinaric-Albanic-Hellenic

Alpine fold belt, and also indicate eastward thickening of the Albanian crust from about 30 km in Western Albania to 50 km in the East (Papazachos et al., 2002). This context produces contrasting relief with a flexural basin filled with Plio-Quaternary deposits, forming a flat coastal plain in the foreland (Roure et al., 2004), a thin skinned fold and thrust belt in the midland (Carminati et al., 2004) and a synorogenic Neogene-Quaternary graben system in the hinterland that crosscuts the previous thrust system (Aliaj, 1991) (**figure IV.3, 4, 5).**

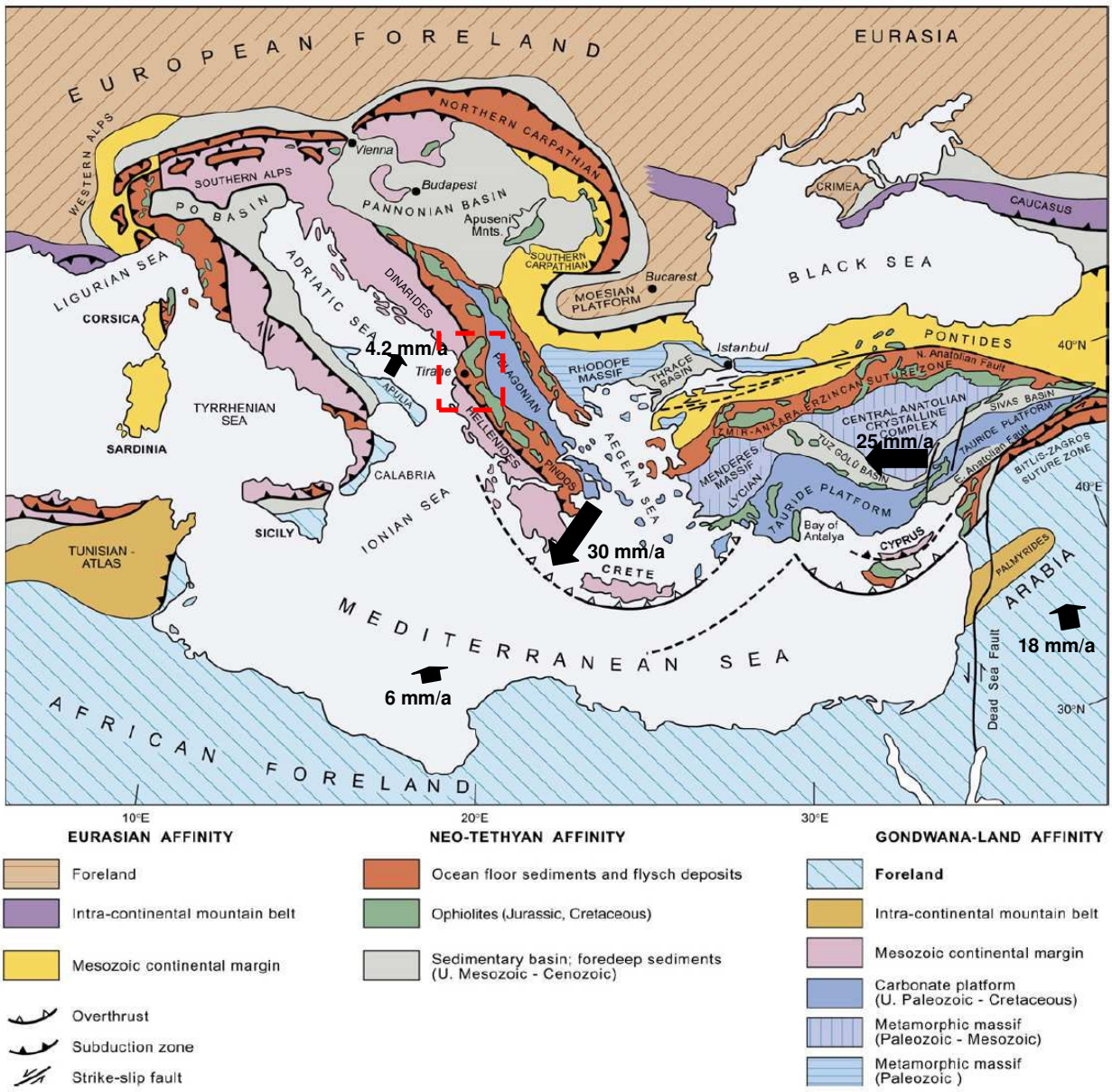

Figure IV.1. *Albania with respect to the geodynamics setting of the Mediterranean region. The map shows the main plate boundaries, orogenic belts, and tectonic units of Eurasian, Neo-Tethyan and Gondwana-Land affinities (from Dilek et al., 2008). Black arrows indicate direction of the motion relative to Eurasia. The values are shown near each arrow (from McClusky et al., 2000 for Arabian, Anatolian and Aegean plate; and from D'Agostino et al., 2008 for the Apulia plate). Location of* ***figure IV.2*** *is indicated by a dashed red box.*

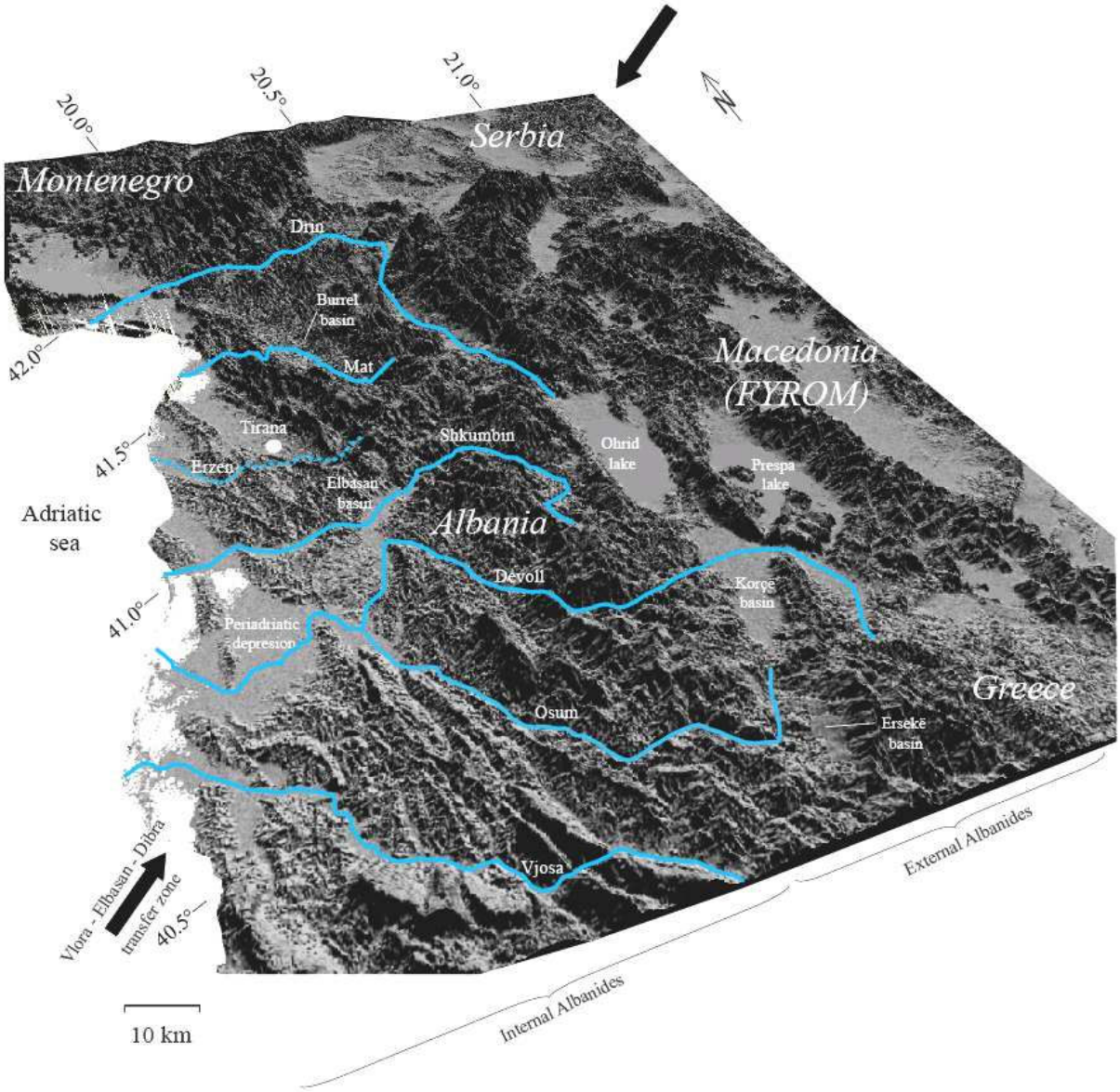

Figure IV.2. *Digital elevation model (DEM) of the Albania and neighboring areas from SRTM data. The regional morphology of the Internal and External Albanides is visible. Black arrows indicate the direction of Vlora-Elbasan-Dibra transfer zone. The seven main Albanian rivers are shown.*

Albania is one of the most seismically active countries in Europe with damage intensities reaching degree IX on MSK-64 scale. The strongest historical earthquakes occurred along three well-defined seismic belts (Aliaj, 1988; Muço, 1998; Sulstarova et al., 2003; Kiratzi, 2011): a) The Ionian-Adriatic coastal earthquake belt at the Western margin of the European plate, which trends NW-SE to NNW-SSE. It is the most seismically active zone in the country and is characterized by dip-slip to oblique-slip compressional thrust faults; b) The Peshkopia-Korçë earthquake belt, in the Internal Albanides, which trends NNW-SSE, characterized by normal faults; c) The Vlora-Elbasan-Dibra transverse earthquake belt, which trends NNE-SSW across the former two. This belt is characterized by normal faults (**figures IV.6, 7**).

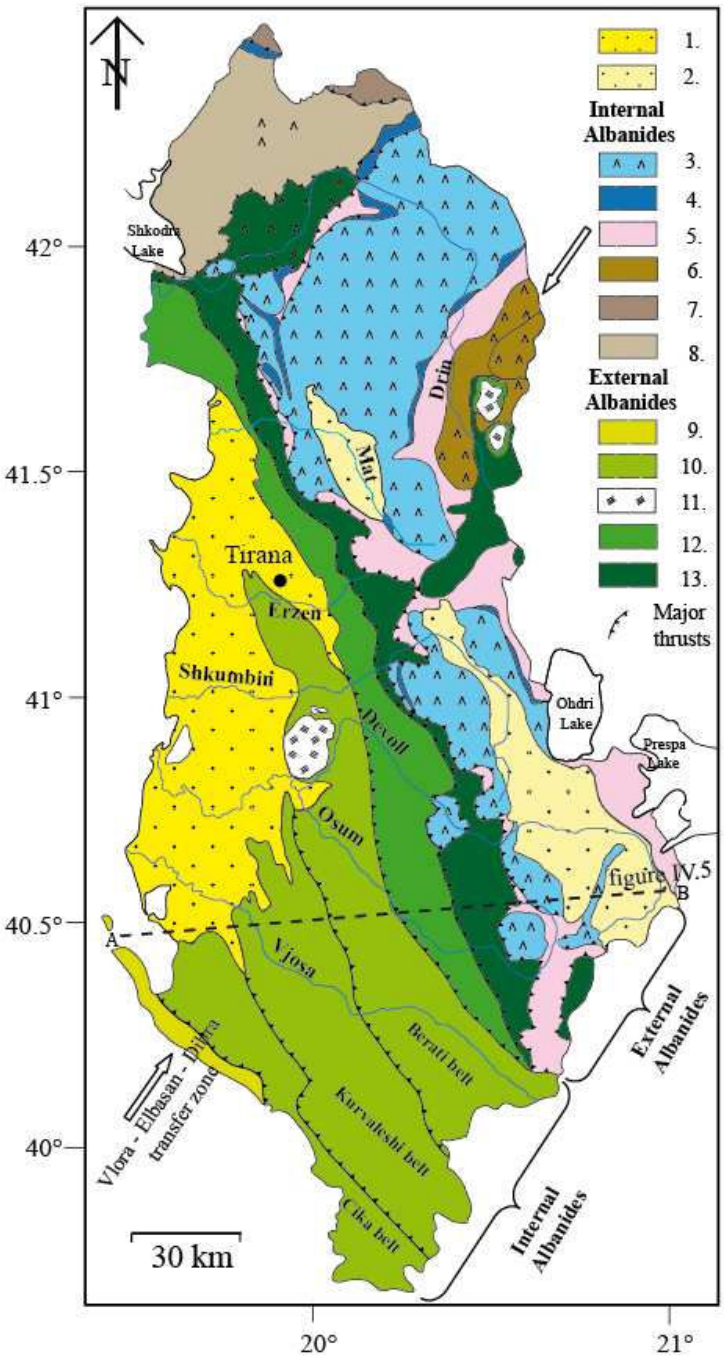

Figure IV.3. *Simplified geologic map of Albania showing main tectonostratigraphic units (modified from Robertson and Shallo, 2000, SHGJSH, 2003 and Muceku et al., 2008). Map legende: 1. Periadriatic depression (Neogene to Quaternary siliciclastic sediments); 2. Neogene-Quaternary graben system (Neogene to Quaternary siliciclastic sediments) 3. Mirdita (Jurassic ophiolites); 4. Rubiku (Triassic shallow water carbonates); 5. Korabi (Triassic to Jurassic ophiolitic melange, flysch and debris flow); 6. Korabi (Paleozoic ophiolitic melange, flysch and debris flow); 7. Gashi (Paleozoic to Triassic melange); 8. Valbona (Mesozoic platform carbonates and Cretaceous to Paleogene flysch); 9. Sazani (Triassic to Paleogene platform carbonates); 10. Ionian (Triassic to Paleogene platform and pelagic carbonates covered by Oligocene to Miocene flysch); 11. Ionian (Triassic evaporites) 12. Kruja (Mesozoic platform carbonates covered by Oligocene to Miocene flysch); 13. Krasta-Cukali (Mesozoic platform carbonates covered by Cretaceous to Eocene flysch). Location of* ***figure IV.4*** *is indicated.*

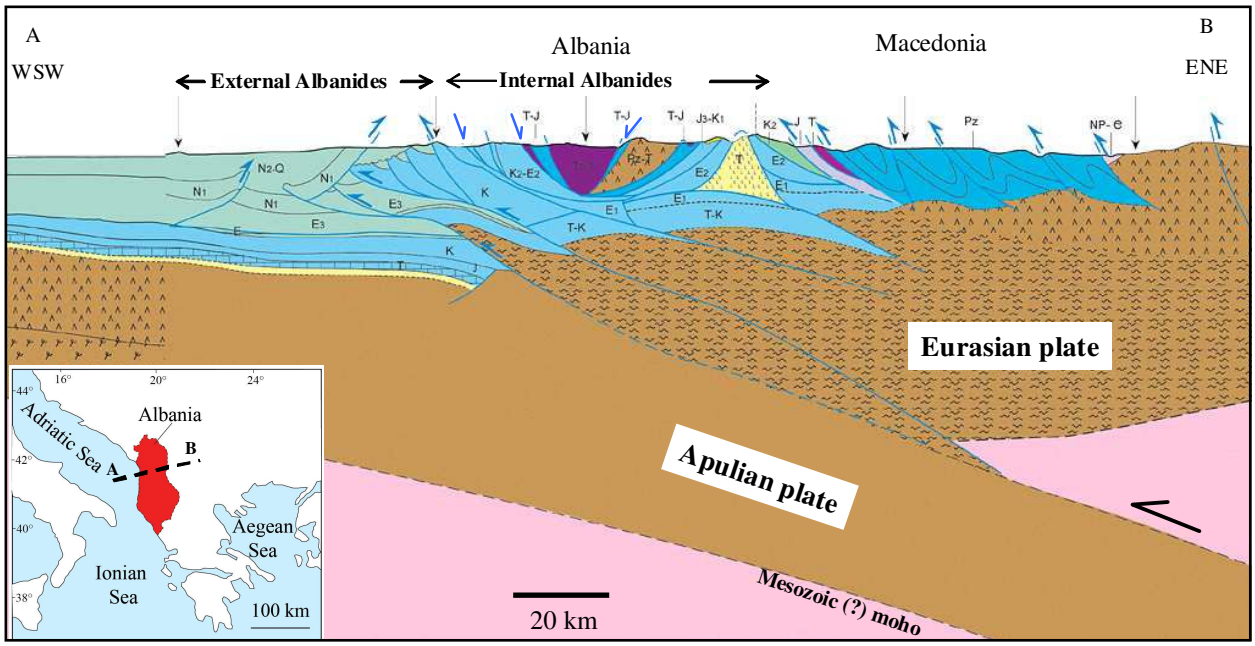

Figure IV.4. *Lithosphere-scale cross-section of the Dinaric-Albanic-Hellenicalpine fold belt at the latitude of central Albania (adapted from Cavazza et al., 2004).*

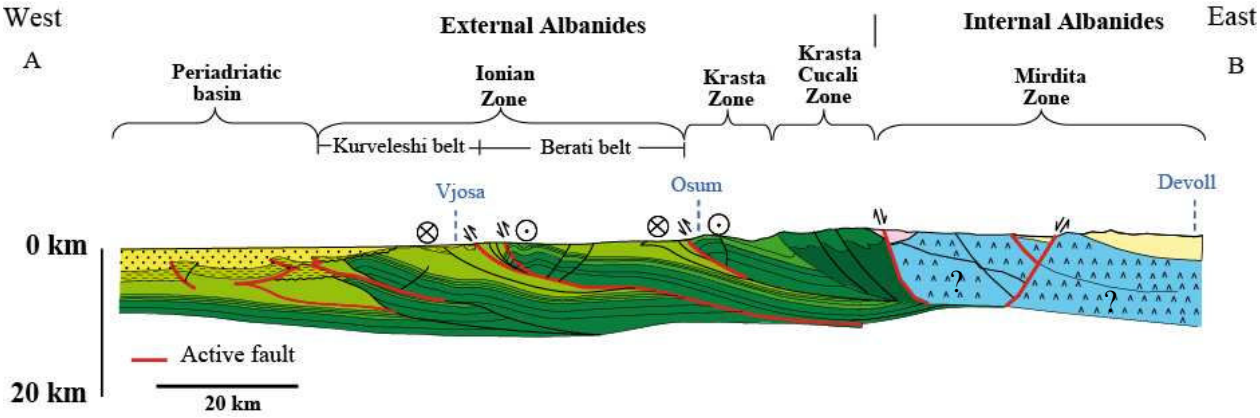

Figure IV.5. *Simplified structural cross-section through the Southern Albanides adapted from, the Geological Map of Albania (SHGJSH, 2003), Kilias et al. (2001), Roure et al. (2004) and Carcaillet et al. (2009). The neotectonic framework is modified from Aliaj et al. (1996, 2000) and the strike-slip component deduced from GPS network (Jouanne, et al., 2012). See* ***figure IV.3*** *for location and code lithologic colour code.*

In order to constrain the neotectonic stress field of Albania, these seismogenic belts have been studied via earthquake focal-mechanism solutions, micro-structural slickenslides analysis and geodetic measurement. All these studies suggest a compressional regime in the Western part, where the average axis of compression is oriented N 45° and an extensional regime in the eastern part of Albania, where the average axis of extension varies from N90° close to the Ohrid and Prespa lakes to N 160° at the Southern end of the Ersekë basins (**figure IV.8**) (Aliaj, 1988; Sulstarova, 1986, Jouanne et al., 2012). The compression in the Western

part is related to subduction of the Adriatic lithosphere. Two different mechanisms have been proposed to explain the presence of normal faulting within the Albania orogenic belt: 1) Roll-back of the subducted slab leads to a westward migration of the entire system, producing normal faulting in the Eastern part (Wortel and Spakman, 2000); and 2) A higher gravity potential energy in the Eastern part (mountain zone) in respect to the Western part (lowland). In such situation, crustal shortening tends to concentrate in the lowlands on the margins of the mountain belt, and the high mountains have a tendency to extend (Copley et al., 2009).

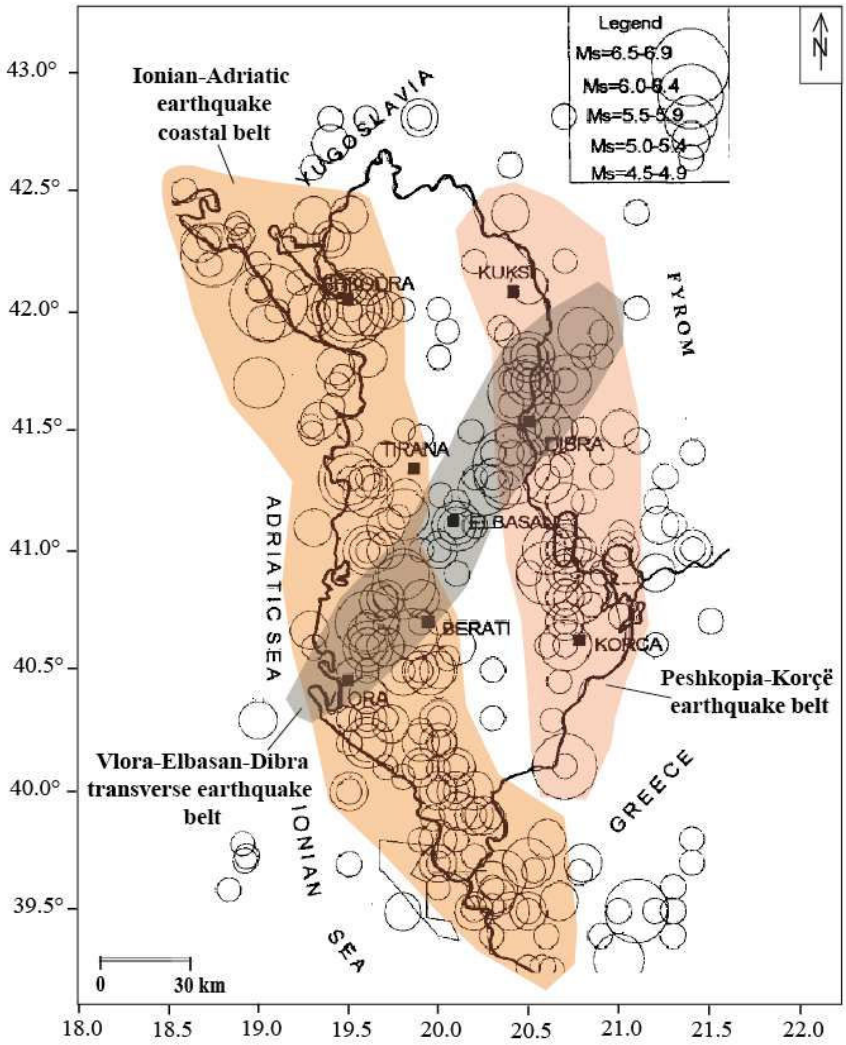

Figure IV.6. *Epicentral map of earthquakes in Albania and neighboring areas for the period 1901–1995 with Ms ≥ 4.5, from Sulstarova et al. (2000). The three earthquake belts are clearly identified by polygon of different colors.*

The long term exhumation deduced from fission tracks data is characterised by a phase of rapid exhumation of the Eastern Internal Albanides around 6-4 Ma, while the Western Internal Albanides record slower continuous exhumation since the Eocene (Muceku et al., 2008). The Quaternary uplift inferred from fluvial incision is in the order of 0.5 mm/a in the

Western internal domain (Carcaillet et al., 2009). The Quaternary increase of the uplift could be provoked by lateral migration of the rupture of the Adriatic slab in the lithosphere beneath Albania (Wortel and Spakman, 2000) or to the thermal regime of the lithosphere above the subduction (Copley et al., 2009).

This uplift corresponds to a positive vertical movement of the Albanides with respect to the Adriatic-Ionian sea level. This leads to vertical incision by rivers draining the range and consequent formation of river terraces along the seven main rivers of Albania, which are from South to North the Vjosa, the Osum, the Devoll, the Shkumbin, the Erzen, the Mat and the Drin rivers (**figure IV.8**).

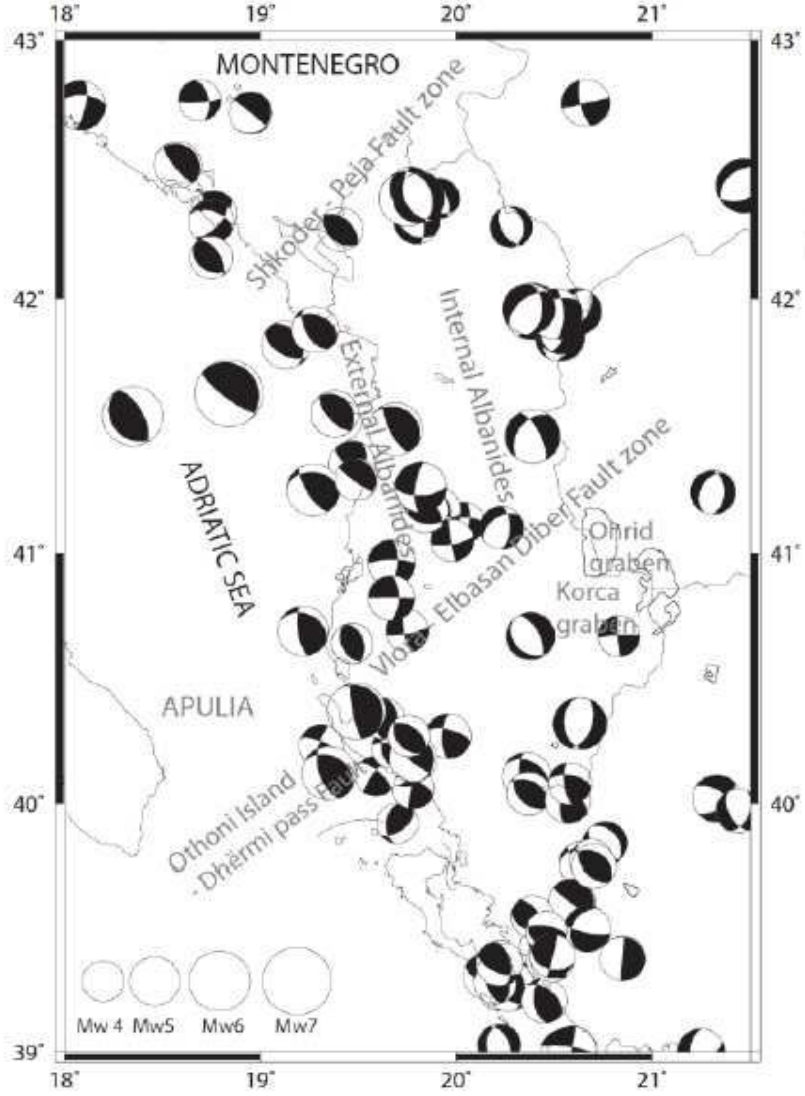

Figure IV.7. *Focal mechanism solutions for earthquake with Mw > 4.0 for the Albania and neighboring areas (from Jouanne et al., 2012). Different fault-rupture mechanisms can be identified: reverse/thrust faulting in the Western part (Ionian-Adriatic earthquake belt);~ N-S trending normal faulting in the Eastern and part (Peshkopia-Korcë earthquake belt); and strike-slip faulting (Vlora-Elbasan-Dibra transverse earthquake belt) in the Central part of Albania.*

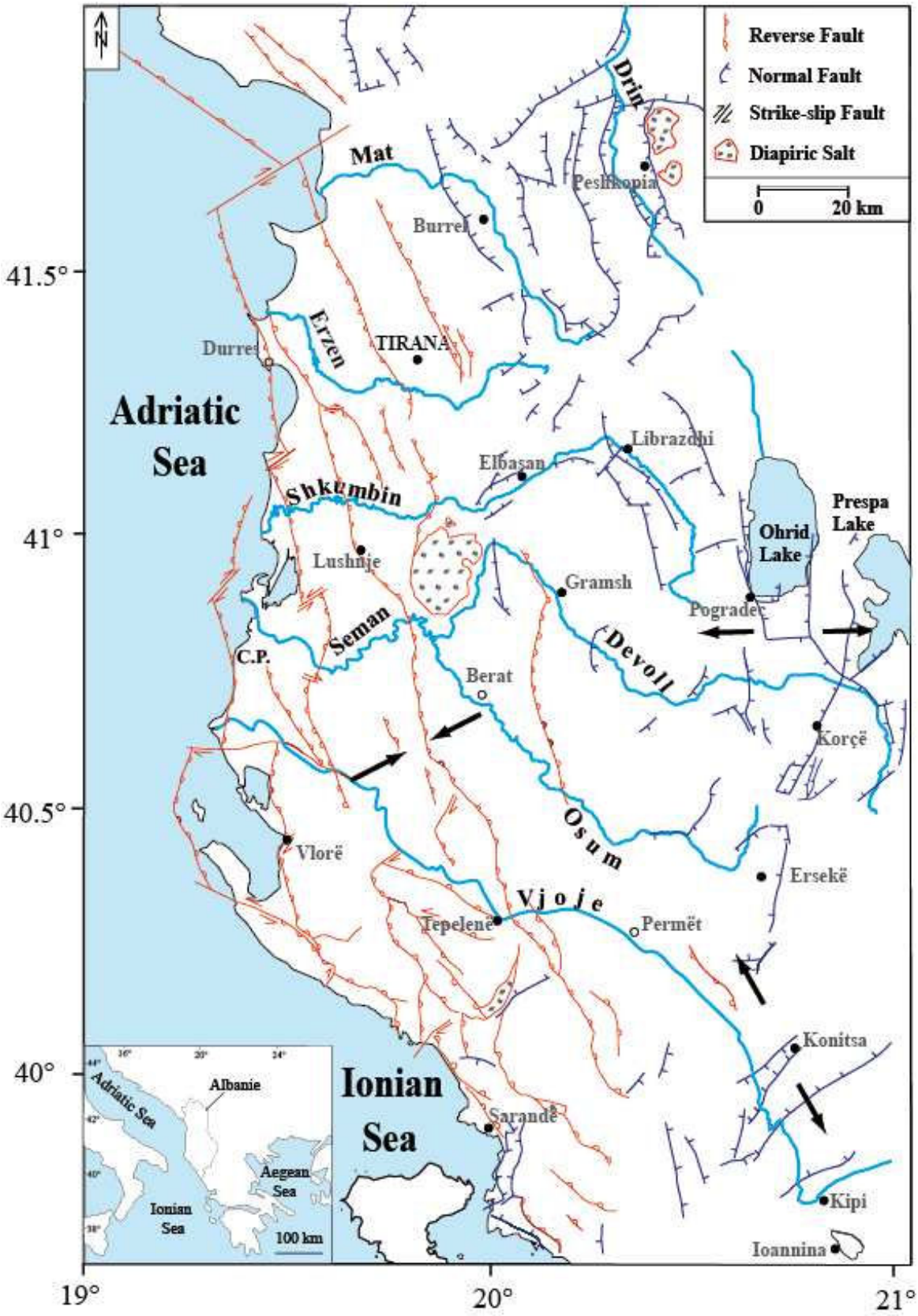

Figure IV.8. *Neo-tectonic map of the Albania and North-Western Greece (modified from Aliaj et al., 1996, 2000 and Carcaillet et al, 2009). Fault types are described in the picture caption and the overall current tectonic deformation (derived from GPS measurements) is represented by black arrows (from Jouanne et al., 2012).*

4.4. Climate and paleoclimate context of Albania

➢ Present-day climate

Albania is located in the Mediterranean region between 40 and 43° N. Its climate varies from typical Mediterranean weather in the coastal lowlands to Mediterranean continental climate in the highlands. In both, the weather varies markedly with seasons. During summer, all the country is dominated by subtropical high pressure cells, with dry sinking air capping a surface marine layer of varying humidity and making rainfall impossible or unlikely except for the occasional thunderstorm. Instead, during winter the polar jet stream and associated periodic storms reach into the lower latitudes of the Mediterranean zones, bringing rain, with snow at higher elevations. As a result, areas with this climate receive almost all of their precipitation (95%) during the winter season, while no significant precipitation occurs during the 4-6 months of summer (Akin, 1991; Kottek, et al., 2006; Peel et al., 2007).

In the lowland, the average dayly temperatures are around 24 and 7 °C for the summer and winter, respectively. While in the highland, the average temperatures vary between 15 to -5 °C from summer to winter. Precipitation is also affected by the relief. The lowland annual precipitation average is around 1000 mm/a with the higher level reaching 1500 mm/a located in the north. In the highland, the annual precipitation is around 1800 mm/a, with the higher level reaching 2550 mm/a in the north (Institute of Hydrometeorology Albania, 1984; World Metereological Organization, 1998).

➢ Paleoclimatic setting

Quaternary paleoclimatic research in the wide circum-Mediterranean have evidenced that the climatic evolution of the region strongly depends on that of the North Atlantic domain, even at the millennial scale change (e.g. Allen et al., 1999; Cacho et al., 1999; Sánchez Goñi et al., 2002, Tzedakis et al., 2004). The longest paleoclimatic record for the Balkan region has been obtained in Ioannina lake in Northwest of Greece (around 50 km Southward to the Albanian border). In this record, changes in arboreal pollen frequencies for the last 130 ka appear to correspond with low and high frequency climatic variations indicated in the Greenland ice core isotope record (Dansgaard et al., 1993), in the variations in $\delta^{18}O$ composition of planktonic foraminifera in marine core from Portuguese margin and in the derived sea surface temperatures in the Mediterranean Sea (**figures IV.9, 10**) (Cacho et al., 1999; Sánchez Goñi et al., 2002).

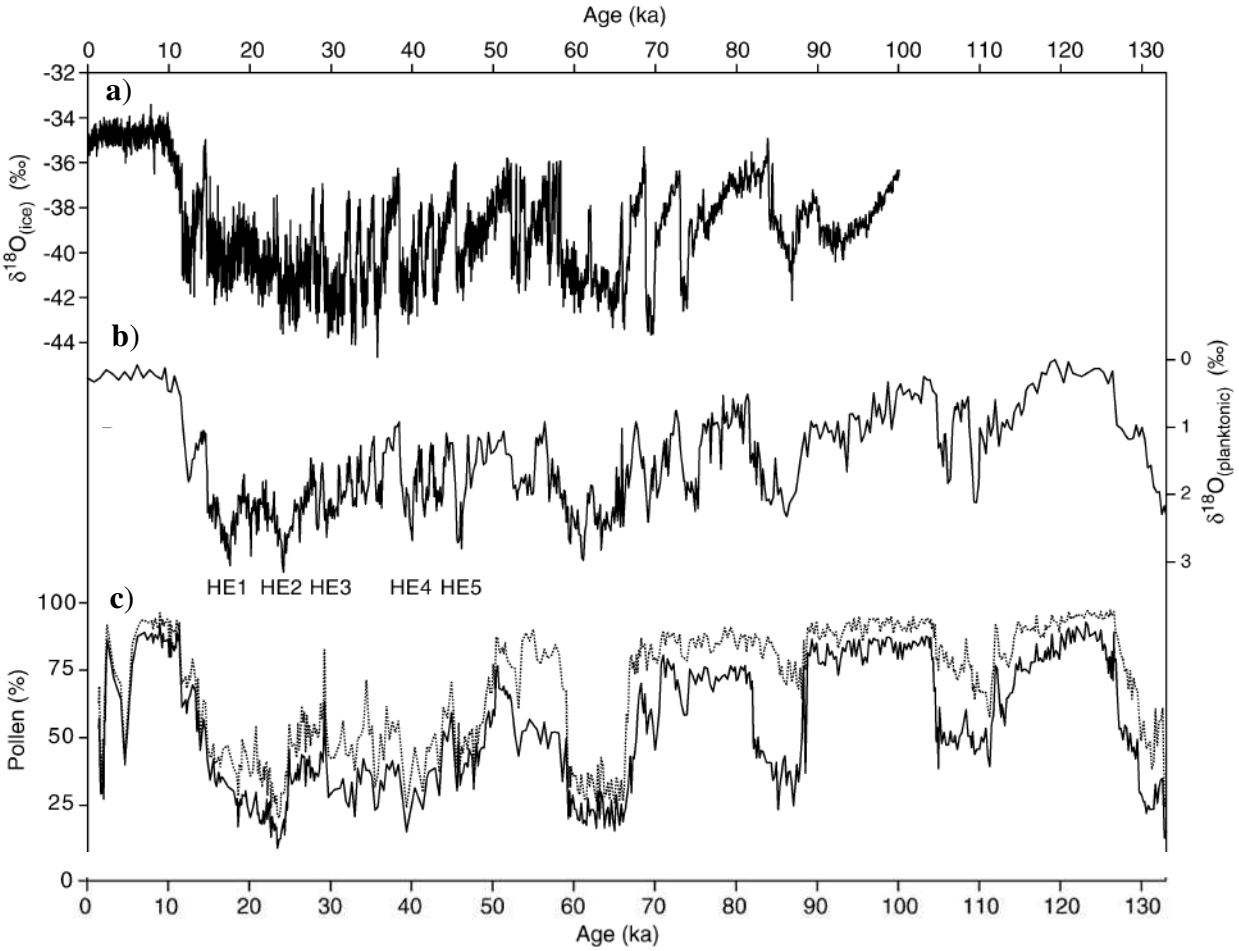

Figure VI.9. *Comparison of paleoenviromental records of Greenland, Portuguese margin and Ioanina Lake for the last 130 ka (from Tzedakis et al., 2004).* ***a****) Variations in* $\delta^{18}O$ *composition of ice in Greenland Ice Sheet Project 2 (GISP2) record (Grootes and Stuiver, 1997).* ***b****) Variations in* $\delta^{18}O$ *composition of planktonic foraminifera in marine core MD95-2042 from Portuguese margin (Shackleton et al., 2000). Labels HE1–HE5 represent positions of Heinrich events.* ***c****) Summary pollen percentage curves from Ioanina lake (I-284 sequence). Dashed line, total arboreal pollen, while solid line Juniperus 1 Pinus.*

Colder sea surface temperatures in the Mediterranean during the last cold stage appear to have been closely related to Heinrich Events in the North Atlantic, when polar waters entered the Mediterranean Sea through the Straits of Gibraltar (Cacho et al., 1999). The effects of such incursions appear to have penetrated throughout the Mediterranean Sea. For example, evidence from the Southern Aegean Sea suggests that short term climate changes in this area over the last 48 ka are closely associated with events in the North Atlantic region (Geraga et al., 2005). In fact, many climate events recorded in the North Atlantic have also been recognised in terrestrial (speleothem and lake level) records as far east as Israel (Bar-Matthews et al., 1999; Bartov et al., 2003). Cooler sea surface temperatures during Heinrich

events and Dansgaard–Oeschger stadials would have inhibited moisture supply to the atmosphere leading to a decline in precipitation. Thus, these high frequency events induce rapid changes in catchment hydrology and hillslope vegetation. This response is reflected in pronounced reductions in arboreal pollen frequencies in western Greece during these periods (Tzedakis et al., 2004) (**figure IV. 10**). Lacustrine sediments of the Prespa and Ohrid lakes, both located in eastern Albania also, recorded this response by a high concentration of the Manganese (Mn) and Total Inorganic Carbon (TIC) peaks in the Prespa lake (Wagner et al., 2010), and with relative high values in the ratio Zirconium/Titanium (Zr/Ti) of the Ohrid lake (Wagner et al., 2009; Vogel et al., 2010) (**figure IV.11**).

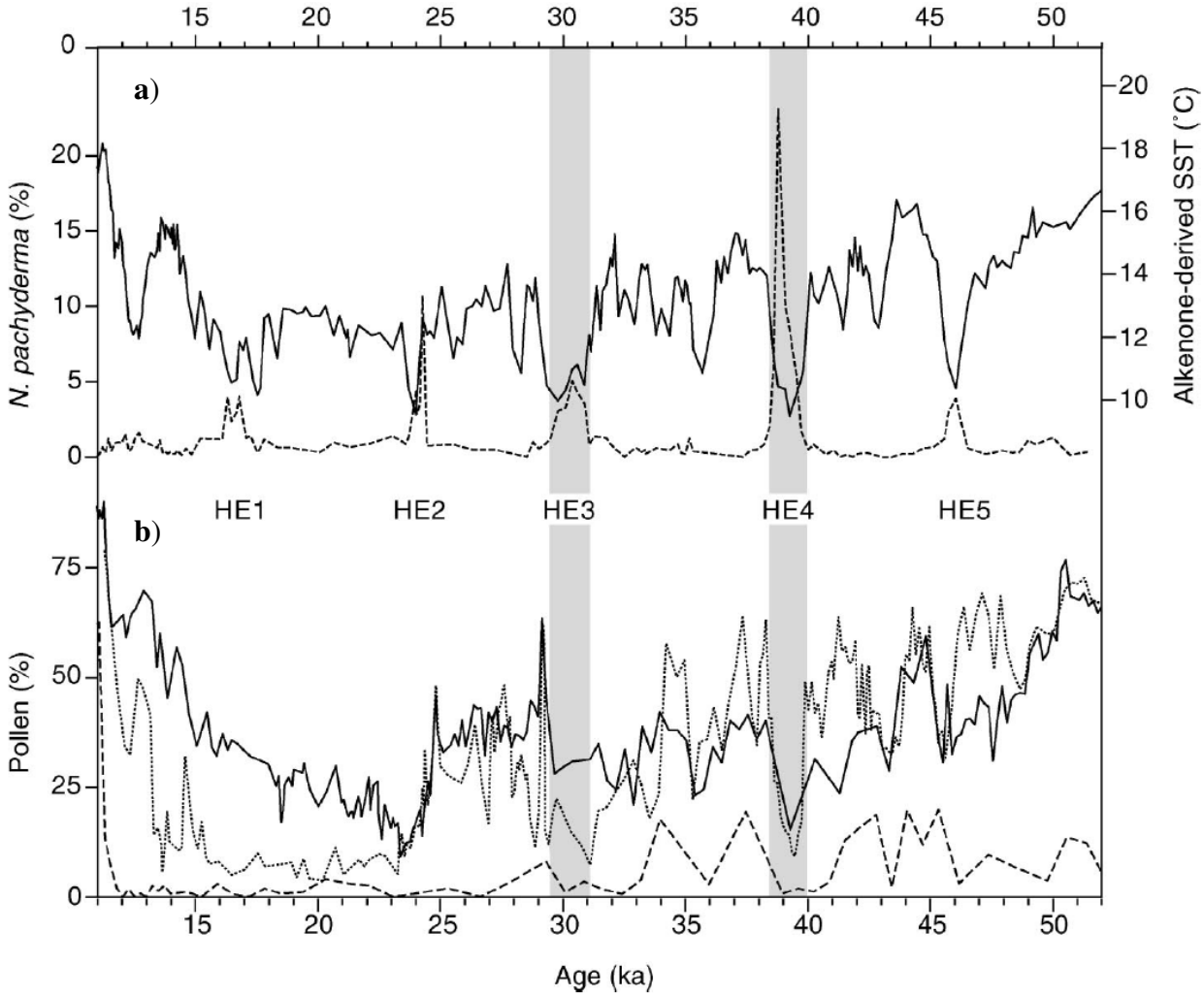

Figure IV.10. *Paleoenviromental records of Alboran Sea and Ioanina Lake for the last 50 ka (from Tzedakis et al., 2004).* ***a****) Variations in percentage of Neogloboquadrina pachyderma (sinestral) (dashed line) and derived sea-surface temperatures (SST; solid line) in marine core MD95- 2043 from Alboran Sea.* ***b****) Summary arboreal pollen, percentage curves from Ioannina I-284 (solid line), Kopais K93 (dotted line), and Tenaghi Philippon TF II (dashed line). Shaded vertical bars highlight two examples of Heinrich events (HE).*

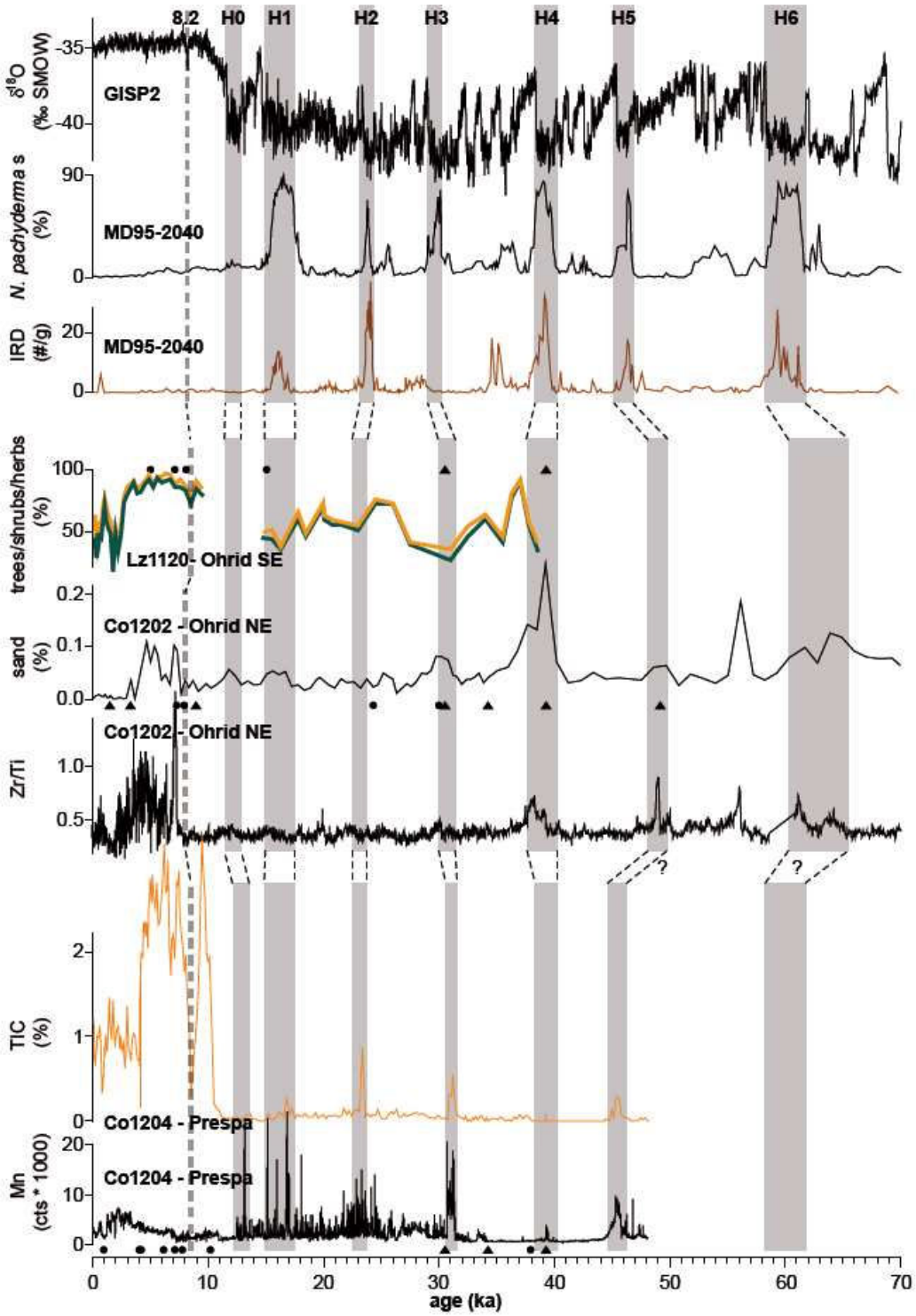

Figure IV.11. *Palaeoenvironmental records from Prespa lake (core Co1204) and Ohrid lake (cores Lz1120 and Co1202; Wagner et al., 2009; Vogel et al., 2010a) compared with the number of Ice-Rafted Debris (IRD) and the cold water thriving foraminifera N. pachyderma in marivne core MD95-2040 from the western Iberian margin (de Abreu et al., 2003) and with the $\delta^{18}O$ record from the GISP2 ice core (Grootes et al., 1993). The timing and thickness of Heinrich events H1–H6 is according to de Abreu et al. (2003) (from Wagner et al., 2010).*

4.5 Chronostratigraphy and incision of Albanian river terraces over the last 200 ka and their climatic implications

(To submit to Geomorphology)

Oswaldo Guzmán[a,b,*], Jean-Louis Mugnier[b], Riccardo Vassallo[b], Rexhep Koçi[c], Julien Carcaillet[d], François Jouanne[b], Eric Fouache[e]

[a] Departamento de Ciencias de la Tierra, Universidad Simon Bolivar, 89000, Caracas 1081-A, Venezuela
[b] ISTerre, Université de Savoie, CNRS, F-73376 Le Bourget du Lac, France
[c] Institute of Seismology of Albania, Rr. "Dom Bosko" 60, Tirana, Albania
[d] ISTerre, Université de Grenoble 1, CNRS, F-38041 Grenoble, France
[e] Université de Paris 10, Nanterre, UMR 8591, EA435 Gecko, France

[*] Corresponding author:
Oswaldo Guzmán - ISTerre, Université de Savoie, 73376 Le Bourget du Lac, France
Tel: ± 33 4 79 75 86 76 - Fax: ± 33 4 79 75 87 77 - E-mail adresse: Guzmáno@usb.ve.

Abstract

New dating and geomorphological studies of fluvial terraces from the Devoll, Shkumbin and Mat rivers are combined with published data from Vjosa, Osum and Erzen rivers (Albania) in order to build a regional chronostratigraphic framework for the last 200 ka. Two Holocene river terraces are recognized (T1 and T2). Seven regional terraces (T3 to T9) are identified for the last glacial stage (Tymphian stage). Two older interglacial and glacial stages terraces (T10 and T11) are dated in this study by ^{10}Be analysis. The correlation between the age of abandonment of late Quaternary terraces and climatic proxies show that the formation of Albanian terraces was mainly controlled by climatic variations through variable discharge of water and sediments. Lateral erosion and/or aggradation occur during cold and dry conditions, while the vertical incision and abandonment of terrace is triggered by warm and humid conditions. Nonetheless, our data also show that these geomorphic responses of the fluvial systems were modulated by the size of the catchments and eustatic variations. During cold and dry conditions of the period before the Marine Isotope Stage 2 (MIS 2), fill terraces were developed in the large catchments (more than 1250 km^2), while in the small catchments the equilibrium between sediment supply and transport capacity favored the development of strath terraces. The higher part of the large catchments was probably weakely vegetated and therefore heavily affected by hillslope processes that delivered a volume of sediments greater to the main channel than the transport capacity of the river, which diminished due to the dry conditions. For the period after the beginning of the MIS 2, a complex relation between climatic and eustatic drop favored the attainement of graded conditions, consequently strath terraces were developed everywhere.

Long-term incision rates are quite variable in space from less than 0.09 mm/a in the upper reaches of the Vjosa river (Southern Albania) to 1 mm/a along the Mat river (Northern Albania). The incision rate has increased since 25 ka in the large catchments. This climate-dependent suggests that an estimate of the uplift rate in these areas needs to integrate the incision over a glacial - interglacial cycle. For the small catchments, the average long-term incision rate seems to be uniform and steady through time and may be converted in an uplift rate.

Keywords: Albania, river terraces, incision rate, climatic control, eutatism, *in situ* produced ^{10}Be, ^{14}C.

1. Introduction (see also Fuller et al., 1998,

In a fluvial system characterized by dynamic equilibrium, the long-term incision rate of the rivers should equal the uplift rate (Hack, 1957). Thus, for a system characterized by: a) constant long-term uplift; b) no base level fluctuations; and c) a cyclic alternation of glacial and interglacial periods, a periodical formation of terraces vertically separated by a constant height difference would be expected. However, in most of the active mountain ranges, at least one of these conditions is not realized and the equilibrium is rarely attained. This could be due to: **1**) the propagation of a base level perturbation – tectonic or eustatic – through the system (e.g. Hancock and Anderson, 2002; Carretier and Lucazeau, 2005; Wegman and Pazzaglia, 2009; Craddock et al., 2010); **2**) the effect over the the river system of climatic oscillation at a shorter scale than a glacial/interglacial cycle (Fuller et al., 1998; Wegmann and Pazzaglia, 2009; Macklin et al., 2012; **3**) climate variations between the lower and the higher reaches of the range (e.g. Vanderberghe, 1995; Blum and Törnqvist, 2000); **4**) finally, the system can evolve in size by river capture or simple retrograde erosion of the drainage network (e.g. Kooi and Beaumont, 1996; van der Beek et al., 2002; Vassallo et al., 2007; Silva et al., 2008a). In such no steady-state contexts, river incision can decelerate or accelerate through time, even exceeding the uplift rate (Carretier et al., 2009), and river terraces pattern results more complex. When several of the above processes act together within an active range, little is known on the relative impact of each of them on river geomorphology.

The aim of this study is to decipher the different inputs –tectonic, eustatic, climatic - associated with river terraces formation in an uplifting area. In the Mediterranean region, Albanian rivers system appears as one of the most suitable context for this task. Firstly, several Quaternary terraces of different ages are widely preserved on a vast area from mountainous regions to coastal plains along the Albanian rivers (Melo, 1961; Prifti, 1984; Lewin et al., 1991; Koçi, 2007, Carcaillet et al., 2009). Secondly, the region is affected by a moderate and long-term uplift (Aliaj, 1991, 2000; Carcaillet et al., 2009), hence the spatial and temporal reconstruction of the incisions allows a quantification of the fluvial evolution at a higher resolution than a glacial-interglacial cycle (on the scale 10^3-10^5 years). Thirdly, since all these rivers flow into to the same sea (Adriatic Sea), thus the effect of the eustatism in the fluvial dynamics can be evaluated.

Despite several studies on Albanian rivers, there is a lack of numerical ages for the river terraces preserved in the central part of Albania (Devoll and Shkumbin rivers) (**figures IV.1, 2**). In this paper, new dating and geomorphological data about this part of Albania are reported. These data are integrated with published data coming from other rivers in order to

propose a homogeneous stratigraphic/chronologic framework, applicable to terraces formation in Albania for the past 200 ka.

2. Geological setting

The Albanian mountains form part of the Dinaric-Albanic-Hellenic fold belt, which have been thrusted westward over the Adriatic foreland during the Alpine orogeny (Sorel et al., 1992). The Albanian mountains are traditionally divided in Internal and External Albanides (**figure IV.1**). The Internal Albanides have a relatively simple linear geometry and consist mainly of Jurassic Ophiolites and Mesozoic carbonates (e.g. Mirdita zone), on top of which Cenozoic sedimentary basins have been developed. The External Albanides are divided in four thrust zones that are from East to West, the Krasta-Cukali, the Kruja, the Ionian and the Sazani zones (**figure IV.1**). These external zones are characterized by carbonate deposits covered by flysch deposits, except for the Sazani zone, which is composed of Triassic to Paleogene platform carbonates (Robertson and Shallo, 2000; Niewland, 2001; Roure et al., 2004).

The geodynamic context is characterized by a subduction of the Adriatic Sea plate beneath the foreland domain and produces contrasted reliefs: a foreland flexural basin filled with Plio-Quaternary deposits forms a flat costal plain (Roure et al., 2004); a thin skinned fold and thrust belt develops in the foothills (Carminati et al., 2004) and synorogenic Neogene-Quaternary grabens crosscut the previous thrust system in the hinterland (Aliaj, 1991; Roure et al., 2004). Neotectonics is still active in Albania (Aliaj, 1988); the external domain is affected by a compression oriented N 45°, whereas the internal domain is affected by an extension that varies from N 90° close to the Ohrid and Prespa lakes (Aliaj, 1988) to N 160° at the Southern end of the Ersekë basins (Jouanne et al., 2012) (**figure IV.2**).

A long-term exhumation is deduced from fission tracks data, with a slow continuous exhumation in the Western Internal Albanides since the Eocene and a phase of rapid exhumation around 6-4 Ma in the Eastern Internal Albanides (Muceku et al., 2008). The Quaternary uplift rate inferred from fluvial incision is in the order of 0.5 mm/a in the internal domain (Carcaillet et al., 2009) and is faster than the rapid uplift rate inferred between 6-4 Ma (Muceku et al., 2008). The Quaternary increase of the uplift rate could be linked to the thermal regime of the lithosphere above the Adriatic subduction (Copley et al., 2009) or to the lateral migration of a rupture of the Adriatic lithospheric slab beneath Albania (Wortel and Spakman, 2000).

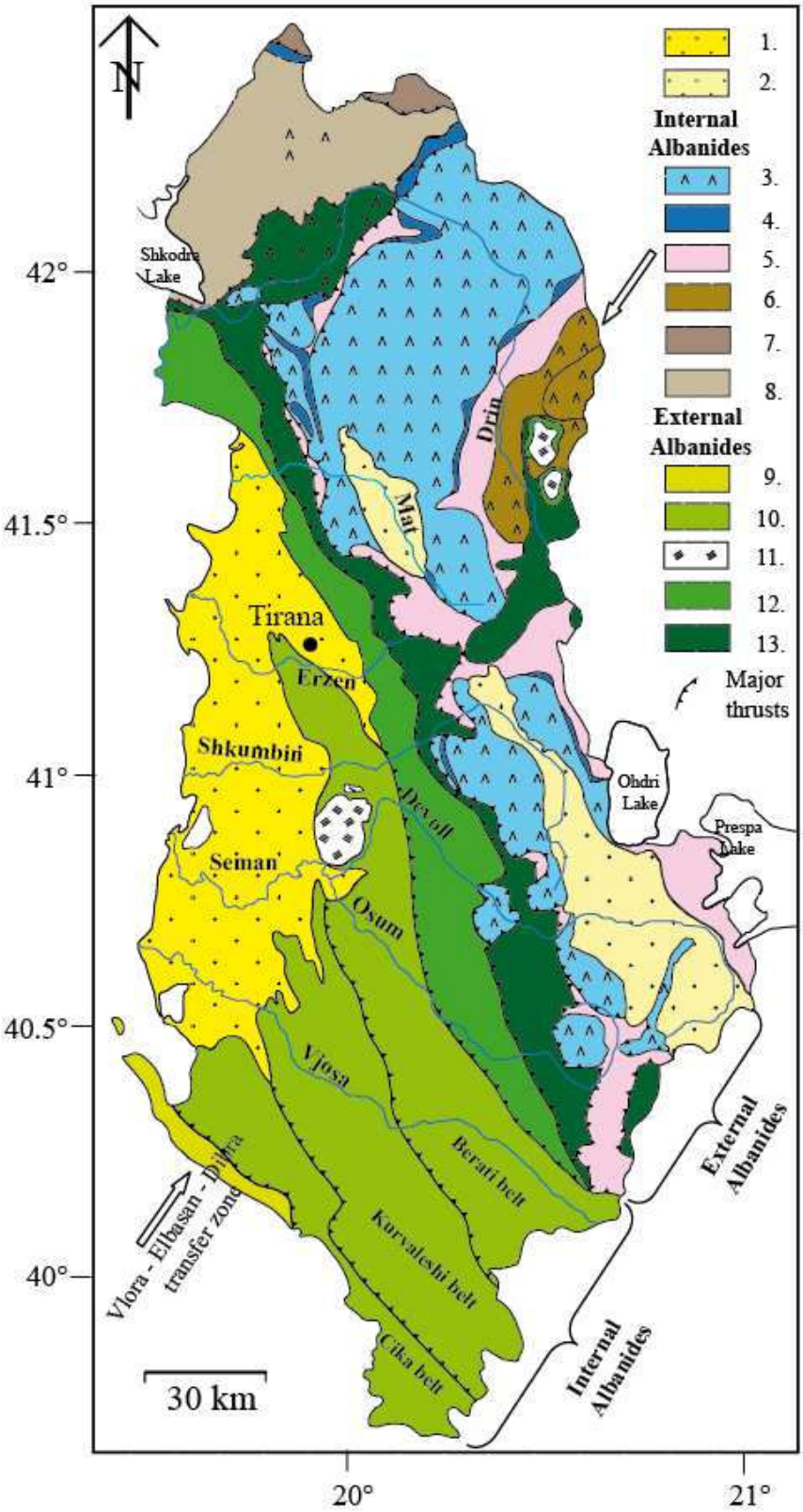

Figure IV.1. *Simplified geologic map of Albania showing main tectonostratigraphic units (modified from Robertson and Shallo, 2000, SHGJSH, 2003 and Muceku et al., 2008). The main Albanian rivers are shown. Map legend: 1. Periadriatic depression (Neogene to Quaternary siliciclastic sediments); 2. Neogene-Quaternary graben system (Neogene to Quaternary siliciclastic sediments) 3. Mirdita (Jurassic ophiolites); 4. Rubiku (Triassic shallow water carbonates); 5. Korabi (Triassic to Jurassic*

ophiolitic melange, flysch and debris flow); 6. Korabi (Paleozoic ophiolitic melange, flysch and debris flow); 7. Gashi (Paleozoic to Triassic melange); 8. Valbona (Mesozoic platform carbonates and Cretaceous to Paleogene flysch); 9. Sazani (Triassic to Paleogene platform carbonates); 10. Ionian (Triassic to Paleogene platform and pelagic carbonates covered by Oligocene to Miocene flysch); 11. Ionian (Triassic evaporites) 12. Kruja (Mesozoic platform carbonates covered by Oligocene-Miocene flysch); 13. Krasta-Cukali (Mesozoic platform carbonates covered by Cretaceous to Eocene flysch).

This uplift leads to vertical incision of the mountain range by the fluvial systems and formation of river terraces along of the Albanian rivers. We studied and compared the terraces along six of the seven main rivers of Albania. They are, from South to North, the Vjosa, the Osum, the Devoll, the Shkumbin, the Erzen and the Mat rivers (**figures IV.1, 2**); we excluded only the Drin river because of the numerous dam-lakes located along its middle and lower reaches. A comparison of the ages of the terraces along these six rivers is meaningful because they cross the same structures, have a common base level (Adriatic Sea) and their catchments undergo the same regional climatic oscillations. Nonetheless, the Mat and the Erzen rivers, located in northern Albania have smaller catchments area (900 and 1215 km^2, respectively, **figure IV.2**, **Table IV.1**) than the rivers located in Central and Southern Albania: the Vjosa, the Osum, the Devoll and Shkumbin rivers (catchment areas varies between 2230 to 6700 km^2**, figure IV.2**, **Table IV.1**). Additionally, the smaller catchments reach lower altitudes (maximum altitude 2246 m a.s.l. in the Mat catchment) than the larger catchments (maximum altitude 2523 m a.s.l. in the Vjosa catchment).

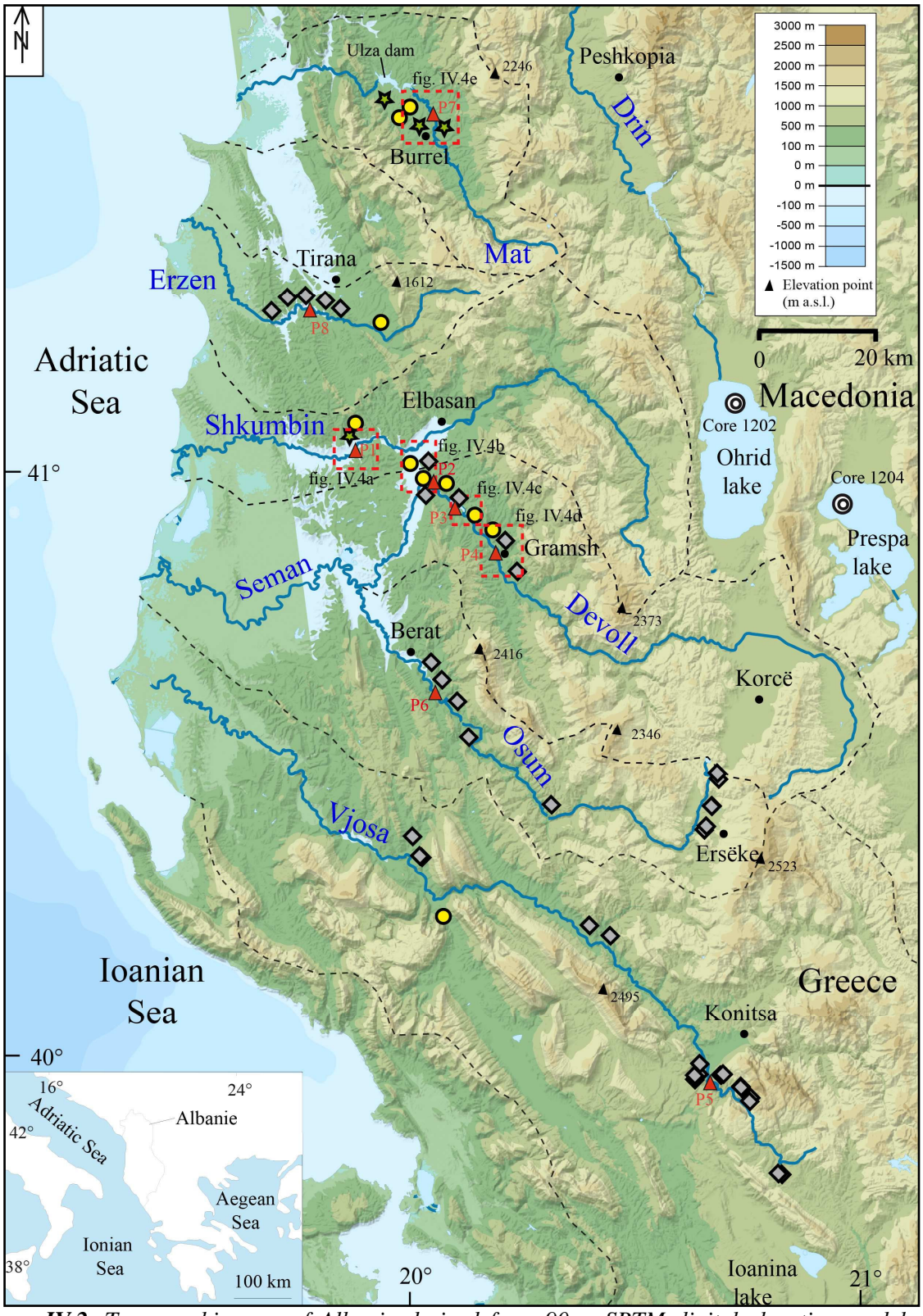

Figure IV.2. *Topographic map of Albania derived from 90-m SRTM digital elevation model. The seven main Albanian rivers are shown. Watersheds of the catchments are indicated by black dashed lines. Dark grey diamonds indicate published data (Lewin et al., 1991; Hamlin et al., 2000; Woodward et al., 2001; Koçi, 2007; Carcaillet et al., 2009), yellow circles (^{14}C dating) and green stars (^{10}Be dating) indicate data obtained in the present study.Red triangles indicate incision rate sites of the* ***figure IV.10****. The boxes show the location of the* ***figures IV.4a to e****. Location of Core 1202 and 1204 in Ohrid and Prespa lakes are shown (Wagner et al., 2009, 2010). Ioanina lake is also shown.*

Table IV.1. *Morphologic parameters of the Albanian rivers. Data was extracted from 30-m SRTM digital elevation model. Marine slope was extracted from Cushman-Roisin et al. (2001) and Savini et al. (2011).*

Morphologic parameters	**River**					
	Vjosa	Osum	Devoll	Shkumbin	Erzen	Mat
Catchment area (km^2)[a]	6700	2230*	3100*	3070	900	1215
Length of the river (km)[b]	272	120[$]	160[$]	130	75	85
Altitude at the source (m a.s.l.)	1600	1100	1100	1150	1300	1200
Maximum altitude in the catchment (m a .s.l.)	2523	2523	2416	2373	1612	2246
Average slope of the river close to the sea (°)	~0.2	~0.2	~0.2	~0.2	~0.2	~0.2
Average slope of the marine shelf (°)	~2.9	~2.9	~2.9	~2.7	~2.3	~2.3
Surface above 2174 m a.s.l. (km^2)[c]	~120	~12	~14	~11	0	~0.3

[a] Catchment area: (*) from the source to the confluence between Devoll and Osum rivers.
[b] Length of the river: ([$])from the source to the confluence between Devoll and Osum rivers. After this point Seman river continues for 70 km toward the Adriatic Sea
[c] Surface above 2174 m a.s.l.: This altitude corresponds to the ELA altitude in the area for the Thymphian stage (Hughes, 2004, Hughes et al., 2006)

3. Paleoclimatic setting

Quaternary paleoclimatic research in the wide Mediterranean circum have evidenced that the climatic evolution of the region strongly depends on that of the North Atlantic domain, even at the millennial scale change (e.g. Allen et al., 1999; Cacho et al., 1999; Sánchez Goñi et al., 2002, Tzedakis et al., 2004). The longest paleoclimatic record for the Balkan region was obtained in Ioannina lake in Northwest of Greece (around 50 km southward of the Albanian border, see **figure IV.2** for location). In this record, changes in arboreal pollen frequencies for the last 130 ka appear to correspond with: 1) low and high frequency climatic variations indicated in the Greenland ice core isotope record (Dansgaard et al., 1993); 2) variations in $\delta^{18}O$ composition of planktonic foraminifera in marine core from Portuguese margin, and 3) derived sea surface temperatures in the Mediterranean Sea (Cacho et al., 1999; Sánchez Goñi et al., 2002; de Abreu et al., 2003).

Colder sea surface temperatures in the Mediterranean during the last cold stage appear to have been closely related to events of ice rafting in Northeast Atlantic, called Heinrich Events (HE) (Heinrich, 1988). These short events (500 ± 250 years, Bond et al., 1992; Hemming, 2004) occurred at the end of cold periods and were always followed by warm and humid periods (Rahmstorf, 2002). During the HE, polar water entered in the Mediterranean

Sea through the Strait of Gibraltar with climatic effects that affected the whole region (Cacho et al., 1999). For example, evidence from the Southern Aegean Sea suggests that short-term climate changes in this area over the last 48 ka are closely associated with events in the North Atlantic region (Geraga et al., 2005). In fact, many climatic events recorded in the North Atlantic have also been recognised in terrestrial (speleothemes and lakes level) records as far East as Israel (Bar-Matthews et al., 1999; Bartov et al., 2003). Cooler sea surface temperatures during the HE and Dansgaard–Oeschger stadials would have inhibited moisture supply to the atmosphere leading to a decline in precipitation. Thus, these high frequency events induce rapid changes in catchment hydrology and hillslope vegetation. This response is reflected in pronounced reductions in arboreal pollen frequencies in Western Greece during these periods (Tzedakis et al., 2004). Lacustrine sediments of the Prespa and Ohrid lakes, both located in Eastern Albania also recorded this response by a high concentration of the Manganese (Mn) and Total Inorganic Carbon (TIC) peaks in the Prespa lake (Wagner et al., 2010), and with relative high values in the ratio Zirconium/Titanium (Zr/Ti) of the Ohrid lake (Wagner et al., 2009; Vogel et al, 2010).

4. Methods

Field observations, topographic maps at 1:25000 scale (Institutin Topografik te Ushtrise Tirane, 1959-1990), satellite imagery and a 30-m digital elevation model (based on SRTM data) were used to identify and characterize fluvial terraces in the Devoll and Shkumbin rivers. Alluvial deposits thicknesses and elevations of the terraces above the present river bed were measured using a measuring tape and a laser range distancemeter (vertical precision ± 0.5m).

The terraces correlation along the Devoll and Shkumbin valley was deduced from the map relationships and through deposit sedimentology and stratigraphy. The fieldwork correlation was reinforced by geochronological data. We correlated these terraces with those of Vjosa, Osum, Erzen and Mat rivers in order to better understan the processes of formation of river terraces at a regional scale.

The ages of the terraces were determined using radiocarbon (^{14}C) and *in situ* produced ^{10}Be dating (**Tables IV.2, 3**). Material used for ^{14}C dating consists of organic residues collected from clay lenses, which are located close to the base of the fine sediment level standing above or within the coarse material. This implies that most of the collected materials were deposited during the ultimate phase of river alluviation and these ages are close to the ages of the abandonment of the river terraces. ^{14}C dating was performed at the accelerator

mass spectrometer of the Poznan radiocarbon Laboratory (Poland). ^{14}C ages lower than ~40 ka were calibrated using the OxCal program version 4.1 (Ramsey, 2009), based on the IntCal09 data set (Reimer et al., 2009) and reported as intercept ages with two sigma (95%). Calibrated ages (cal ka BP) are given as a time interval linked to the related probability. ^{14}C ages older than ~40 ka were corrected using the polynomial calibration of Bard et al. (2004). The previously published ^{14}C ages (Lewin et al., 1991; Woodward et al., 2001, Koçi, 2007; Carcaillet et al., 2009) were calibrated following the same procedure (**Table IV.2**).

^{10}Be exposure ages (Lal, 1991; Brown et al., 1991) have been determined by the analysis of concentrations in siliceous rich pebbles or cobbles collected along depth-profiles. This sampling strategy allowed the estimation of the ^{10}Be inherited from prior exposure (Anderson et al., 1996; Repka et al., 1997). The deepest sample was thus collected deep enough to evaluate the geological blank. In the case where the outcrop does not allow profile realization, several individual exposed cobbles and/or pebbles were taken from the surface of the terrace, and were analyzed as a single sample. In absence of boulders at surface, this strategy allowed homogenize the ^{10}Be concentrations, in contexts where the scattering of the concentrations may be due to problems of inheritance.

Beryllium oxide targets were extracted following the chemical procedures of Brown et al. (1991) and Merchel and Herpers (1999). The extractions were made in the Cosmogenic Laboratory of Institut des Sciences de la Terre (ISTerre, France). ^{10}Be concentrations were measured at the accelerator mass spectrometry facility ASTER (CNRS, France) (Arnold et al., 2010). They were calibrated against NIST Standard Reference Material 4325 using its assumed $^{10}Be/^{9}Be$ ratio of $2.79 \pm 0.03 \times 10^{-11}$, and a ^{10}Be half-life of 1.387 ± 0.012 Ma (Chmeleff et al., 2010; Korschinek et al., 2010). Production rates were calculated following Stone (2000) using the modified scaling functions of Lal (1991) and a ^{10}Be production rate in quartz of 4.5 ± 0.3 at/g/a at sea level and high latitude. Geomorphic scaling factors were calculated following Dunne et al. (1999). All ^{10}Be age calculations were performed using attenuation lengths of 150, 1500 and 5300 g/cm^2 with associated relative contributions to the total production rate of 97.85%, 1.50% and 0.65% for neutrons, slow muons and fast muons, respectively (Braucher et al., 2003). There is no record of the thickness and duration of snow cover for the last 200 ka; however, at the altitude of the studied sites (< 500 m) and close to the Adriatic Sea, a null correction for recurrent snow cover is reasonable.

Table IV.2. *Numeric ages from fluvial terraces of Albania.*

Sample[a]	Material[b]	Latitude (°N)[c]	Longitude (°E)[c]	Elevation of sample above the river (m)	Methods[d]	Lab-Code Reactor Reference	^{14}C Ages (yr BP)	Calibrated interval Cal yr BP (Probability=0,95)	Concentration ^{10}Be (10^5 at/g)[e]	Ages (ka)[f]	Local terrace name or alluvial unit	Propose terrace name	Source[g]
Vjosa													
A153	C	40.2076	20.3875	17.3	^{14}C	SacA 16001	190 ± 30	4 - 302	-	0.15 ± 0.15	-	colluvium	(1)
A150	C	40.2084	20.0934	9.5	^{14}C	SacA 15998	330 ± 30	308 - 474	-	0.40 ± 0.08	-	colluvium	(2)
A28	Vd	40.3354	19.9921	12	^{14}C	Poz-8824	705 ± 30	564 - 691	-	0.63 ± 0.06	colluvium	colluvium	(1)
A155	Vd	40.3611	19.2907	13.4	^{14}C	SacA 16002	3870 ± 60	4094 - 4436	-	4.26 ± 0.17	-	colluvium	(2)
OxA-192	C	39.97(ç)	20.66(ç)	~4.5	^{14}C	OxA-192	800 ± 100	560 - 928	-	0.74 ± 0.18	U2(vjosa)	T1	(3, 4)
OxA-191	C	40.87(ç)	21.65(ç)	~4.5	^{14}C	OxA-191	1000 ± 50	788 - 1052	-	0.92 ± 0.13	U2(vjosa)	T1	(3, 4)
OxA-5246	C	39.96(ç)	20.65(ç)	~10.6	^{14}C	OxA-5246	13810 ± 130	16632 - 17224	-	16.93 ± 0.30	U3(vjosa)	T3	(5, 4)
Beta-109162	C	39.96(ç)	20.65(ç)	~10.6	^{14}C	Beta-109162	13960 ± 260	16591 - 17812	-	17.20 ± 0.61	U3(vjosa)	T3	(5, 4)
Beta-109187	C	39.96(ç)	20.65(ç)	~10.4	^{14}C	Beta-109187	14310 ± 200	16935 - 17924	-	17.43 ± 0.50	U3(vjosa)	T3	(5, 4)
VOI24	S	39.94(ç)	20.71(ç)	~9.7	TL	VOI24	-	-	-	19.60 ± 3.00	U3(vjosa)	T3	(5, 4)
Tributary site	Cc	39.95(ç)	20.68(ç)	~10.5	U/Th	-	-	-	-	21.25 ± 2.50	U3(vjosa)	T3	(6, 4)
Old Klithonia	Cc	39.96(ç)	20.65(ç)	~8.2	U/Th	-	-	-	-	24.00 ± 2.00	U4(vjosa)	T4	(6, 4)
571c	Dt	38.96(ç)	20.65(ç)	~12.4	ESR	571c	-	-	-	24.30 ± 2.60	U4(vjosa)	T4	(3, 4)
571a	Dt	38.96(ç)	20.65(ç)	~12.4	ESR	571a	-	-	-	25.00 ± 0.50	U4(vjosa)	T4	(3, 4)
Old Klithonia	Cc	39.96(ç)	20.65(ç)	~8.2	U/Th	-	-	-	-	25.00 ± 2.00	U4(vjosa)	T4	(6, 4)
571b	Dt	38.96(ç)	20.65(ç)	~12.4	ESR	571b	-	-	-	26.00 ± 1.90	U4(vjosa)	T4	(3, 4)
A151	C	40.2140	20.3842	21.7	^{14}C	SacA 15999	24070 ± 150	28457 - 29352	-	29.35 ± 0.89	U5(vjosa)	T5	(This study)
Konitsa1	Cc	39.86(ç)	20.77(ç)	~8	TL	-	-	-	-	53.00 ± 4.00	U6(vjosa)	T8	(4)
Konitsa2	Cc	39.58(ç)	20.39(ç)	~8	U/Th	-	-	-	-	56.50 ± 5.00	U6(vjosa)	T8	(4)
Konitsa3	Cc	39.58(ç)	20.39(ç)	~11	U/Th	-	-	-	-	74.00 ± 6.00	U7(vjosa)	T9	(4)
Konitsa4	Cc	39.58(ç)	20.39(ç)	~9	U/Th	-	-	-	-	80.00 ± 7.00	U7(vjosa)	T9	(4)
Konitsa5	Cc	39.58(ç)	20.39(ç)	~12	U/Th	-	-	-	-	113.00 ± 6.00	U8(vjosa)	T10	(4)
VOI26	S	39.86(ç)	20.77(ç)	~56	TL	VOI26	-	-	-	>150	U9(vjosa)	T12	(3)
Osum													
A17	Vd	40.4508	30.2900	17	^{14}C	Poz-10576	9990 ± 50	11262 - 11705	-	11.48 ± 0.22	T8(osum)	T2	(1)
Par-0 (*)	Sr	40.5200	20.7200	70	^{10}Be	-	-	-	2.60 ± 3.10 (&)	≥18.75 ± 1.41	T7(osum)	T3	(1)
Quaf-0 (*)	Sr	40.5500	20.6900	29	^{10}Be	-	-	-	4.44 ± 0.50(&)	≥19.80 ± 1.56	T7(osum)	T3	(1)
A16	Vd	40.6400	20.0600	24	^{14}C	Poz-10575	29900 ± 1300	31622 - 38026	-	34.82 ± 3.20	T5(osum)	T6-5	(1)
A83	C	40.6800	20.0200	14.8	^{14}C	Poz-13850	37000 ± 300	41380 - 42366	-	41.87 ± 0.50	T4(osum)	T7	(1)
A18	Vd	40.5600	20.1400	53	^{14}C	Poz-10578	45300 ± 1600	-	-	50.70 ± 1.80($)	T3(osum)	T8	(1)
A14	Vd	40.6400	20.0600	33.8	^{14}C	Poz-10574	49000 ± 2500	-	-	54.40 ± 2.78($)	T3(osum)	T8	(1)
Grem-0(*)	Sr	40.5560	20.7383	50	^{10}Be	-	-	-	6.23 ± 0.55(&)	≥52.59 ± 3.20	T3(osum)	T8	(1)

Continue **Table IV.2**

Paleo-Devoll													
A05	Vd	40.9092	20.1393	34	^{14}C	Poz-10572	119.5 ± 0.3 pMC	-	-	modern		colluvium	This study
Cer-08	C	41.0275	19.9817	8.4	^{14}C	Poz-39495	30 ± 80	278 - 8	-	0.14 ± 0.13	-	colluvium	(2)
Dev-02	C	40.9910	10.0165	16.6	^{14}C	Poz-39496	540 ± 130	726 - 307	-	0.52 ± 0.21	-	colluvium	(2)
Shk-06	Vd	41.0663	19.8800	52.8	^{14}C	Poz-34987	162 ± 0.46 pMC	-	-	Modern	-	colluvium	This study
Shk-22	C	41.0649	19.8714	6.3	^{14}C	Poz-39201	90 ± 30	266 - 22	-	0.14 ± 0.12	-	colluvium	This study
Cer-01	C	41.0100	20.0083	8.4	^{14}C	Poz-39197	5400 ± 40	6020 - 6293	-	6.16 ± 0.14	-	T2	This study
Shk-10(*)	Sr	41.0618	19.8685	14.7	^{10}Be	-	-	-	0.77 ± 0.07	≥16.15 ± 1.00		T3	This study
A60	C	40.9676	20.0526	19	^{14}C	Poz-12223	17640 ± 160	20477 - 21455	-	20.97 ± 0.49	-	T3	This study
A58	C	40.9214	20.1292	15.7	^{14}C	Poz-12116	21850 ± 150	25793 - 26810	-	26.30 ± 0.51	-	T4	This study
A100	C	40.9660	20.0636	24	^{14}C	Poz-17242	22780 ± 200	26825 - 28060	-	27.44 ± 0.68	-	T4	This study
A8	Vd	40.8271	20.2154	42,5	^{14}C	Poz-9838	23760 ± 150	28031 - 29109	-	28.57 ± 0.54	-	T6-5	This study
A1	Vd	40.8836	20.1773	42	^{14}C	Poz-8816	25500 ± 300	29603 - 30915	-	30.26 ± 0.66	-	T5	This study
A61	C	40.9414	20.1089	41,2	^{14}C	Poz-12117	38900 ± 700	42214 - 44365	-	43.29 ± 1.07	-	T7	This study
A56A	C	40.8834	20.1764	41	^{14}C		> 52000	-	-	> 52	-	T8	This study
Erzen													
A41	C	41.2697	19.8400	3	^{14}C	Poz-8826	170 ± 30	291 - -4	-	0.14 ± 0.14	colluvium	colluvium	(7)
A11	C	41.2900	19.7100	3.4	^{14}C	Poz-8818	200 ± 30	305 - - 4	-	0.15 ± 0.15	colluvium	colluvium	(7)
A81	C	41.2866	19.7094	23.4	^{14}C	Poz-13849	275 ± 35	152 - 458	-	0.30 ± 0.15	colluvium	colluvium	(7)
A65	C	41.3088	19.7544	29	^{14}C	Poz-12784	500 ± 30	501 - 618	-	0.56 ± 0.06	colluvium	colluvium	(7)
A76	Vd	41.2800	19.8300	11.7	^{14}C	Poz-13847	3075 ± 35	3212 - 3374	-	3.39 ± 0.08	colluvium	colluvium	(7)
A63B	C	41.2870	19.7197	17	^{14}C	Poz-12118	3700 ± 35	3926 - 4150	-	4.04 ± 0.11	colluvium	colluvium	(7)
A13	C	41.2700	19.6400	9	^{14}C	Poz-8823	1660 ± 30	1422 - 1691	-	1.56 ± 0.13	T1(erzen)	T1	(7)
A12	C	41.2700	19.6400	9	^{14}C	Poz-10573	1730 ± 30	1560 - 1710	-	1.63 ± 0.07	T1(erzen)	T1	(7)
A42	Vd	41.2700	19.8000	12	^{14}C	Poz-8827	6840 ± 60	7578 - 7818	-	7.67 ± 0.12	T2(erzen)	T2	(7)
A115	C	41.2844	19.9683	17	^{14}C	Poz-17243	26600 ± 500	30310 - 31946	-	31.13 ± 0.82	T3(erzen)	T5	This study
A67	C	41.2700	19.6400	9.4	^{14}C	Poz-12120	30400 ± 300	34536 - 36189	-	35.36 ± 0.83	T4(erzen)	T6	(7)
A69	C	41.2900	19.6400	41	^{14}C	Poz-12121	31500 ± 400	35070 - 36695	-	35.88 ± 0.81	T4(erzen)	T6	(7)
A64	C	41.2700	19.7100	24.8	^{14}C	Poz-12224	33400 ± 500	36758 - 39361	-	38.06 ± 1.30	T4(erzen)	T6	(7)
A79	C	41.2900	19.7100	26.5	^{14}C	Poz-13848	44200 ± 1600	-	-	49.59 ± 1.76($)	T6(erzen)	T8	(7)
A70	C	41.2900	19.6000	22	^{14}C	Poz-12785	48000 ± 2000	-	-	53.40 ± 2.22($)	T6(erzen)	T8	(7)
Mat													
Ma-05	C	41.6178	20.0294	24.3	^{14}C	Poz-34984	1075 ± 30	931- 1056	-	1.00 ± 0.62	-	colluvium	This study
Ma-18	C	41.6245	19.9978	7,00	^{14}C	Poz-39198	1725 ± 30 BP	1557 - 1708	-	1.63 ± 0.75	T1(mat)	T1	This study
Ma-21	C	41.6246	19.9970	10.3	^{14}C	Poz-39199	5100 ± 40 BP	5745 - 5923	-	5.83 ± 0.90	T2(mat)	T2	This study
Ma-24	C	41.6273	19.9968	26	^{14}C	Poz-39200	14850 ± 80	17782 - 18516	-	18.15 ± 0.37	T3(mat)	T3	This study
Ma-04	Sr	41.5920	20.0336	100	^{10}Be	-	-	-	5.63 ± 0.16	≥110.70 ± 11.18	T8(mat)	T10	This study
Ma-03(*)	Sr	41.6748	19.9166	94	^{10}Be	-	-	-	4.40 ± 0.14	≥114.00 ± 6.00	T8(mat)	T10	This study
Ma-06	Sr	41.6042	20.0130	190	^{10}Be	-	-	-	10.46 ± 0.40	≥188.84 ± 18.54	T9(mat)	T11	This study

[a] Samples: (*) for cosmogenic depth profile only the surface sample is in this table.
[b] Type of material dated: C= Charcoal, Vd= Vegetal debris, Cc= Calcite cement, S= Sediment, Dt= Deer tooth, Sr= Siliceous rock.
[c] Geographical location: (ç) Location estimated.
[d] Dating method: ^{14}C= Radiocarbon, TL= Termoluminicense, U/Th= Uranium series, ESR= Electron spin resonance, ^{10}Be= Cosmogenic in situ produced.
[e] Concentration of ^{10}Be: (&) Average concentration of surface samples from Carcaillet et al. (2009).
[f] Numerical ages: ($) Sample corrected using the polynomial calibration of Bard et al. (2004).
[g] Source: (1) Carcaillet et al. (2009), (2) Guzmán et al. (Submitted) (3) Lewin et al. (1991), (4) Woodward et al. (2008), (5) Woodward et al. (2001) (6) Hamlin et al. (2000), (7) Koçi (2007).

Methods and factors of correction for paleomagnetic effects remain a matter of debate and uncorrected ages do not significantly differ from intensity-corrected ages (e.g. Dunai, 2001; Masarik et al., 2001; Carcaillet et al., 2004, Pigati and Lifton, 2004), so in this study paleomagnetic intensity correction was not applied. Thus, numerical ages are given in ^{10}Be ka (**Table IV. 3**) in order to allow straightforward correction for future refinements in production rates histories and paleomagnetic intensity corrections.

According to the sampling strategy applied in this study, ^{10}Be ages represent the surface exposure ages of the terraces since their abandonment (Gosse and Phillips, 2001). ^{14}C ages and the other ages achieved in previous studies, using others methods and strategies (U series (U/Th), electron spin resonance (ESR) and thermoluminescense (TL)) (Lewin et al., 1991; Woodward et al., 2001, 2008), represent the timing of deposition or formation of a particular sediment or material within the alluvial deposit of the terrace (Noller et al., 2000). Most of the ^{14}C samples collected in this study, and also the material used in previous dating studies (e.g. calcite cement, deer tooth) were taken from the sediment that corresponds to the ultimate phase of river aggradation. These samples date thus this event. Nonetheless, due to the uncertainty associated with each dating methods, we are not able to distinguish between the last aggradation phase and definitive abandonment of the river terrace, which are separated by less than few thousand years. Therefore, taking into account the objective of this study, the ages coming from different methods are used indistinctively and are analysed as ages of abandonment of the terraces.

Table IV.3. *Results of the ^{10}Be analysis in the Albanian rivers. Calibration against NIST Standard Reference Material 4325. ^{10}Be concentrations uncertainties included analytical errors from the counting statistics and blank correction, whereas the ages uncertainties also include the errors of the production rate introduced by the scaling model of Lal (1991) - Stone (2000) and the errors of the ^{10}Be decay constant (Chmeleff et al., 2010; Korschinek et al., 2010).*

Sample	Type of sample	Lithology	Latitude (N)	Longitude (E)	Altitude (m)	Depth (cm)	Surface P_0 (at/g/y)	Shielding factor	^{10}Be concentration (10^5 at/g)	^{10}Be age (ka)	Terrace
Site 1- Lower paleo-Devoll											
Shk-10	Cobble	Quarzite	41.0618	19.8685	65	30	4.36	0.998	0.77 ± 0.07	16.15 ± 1.00	T3
Shk-11	Cobble	Granite				47			0.21 ± 0.05		
Shk-12	Amalgamated pebbles	Heterogeneous				75			0.61 ± 0.03		
Shk-14	Cobble	Granite				157			0.47 ± 0.06		
Shk-16	Cobble	Granite				240			0.66 ± 0.05		
Site 2 - Mat river - Uzal Dam											
Ma-03	Amalgamated pebbles	Heterogeneous	41.6748	19.9166	183	10	4.92	0.998	4.40 ± 0.14	114.00 ± 6.00	T9
Ma-09	Amalgamated pebbles	Heterogeneous				285			0.52 ± 0.06		
Ma-08	Amalgamated pebbles	Heterogeneous				495			0.27 ± 0.02		
Ma-07	Amalgamated pebbles	Heterogeneous				590			0.26 ± 0.01		
Site 3- Mat river											
Ma-04	Amalgamated pebbles	Heterogeneous	41.5920	20.0336	262	0	5.29	1	5.63 ± 0.16	110.70 ± 11.18	T9
Site 4 - Mat river - Burrel											
Ma-06	Amalgamated pebbles	Heterogeneous	41.6042	20.0130	322	0	5.59	1	10.04 ± 0.40	188.84 ± 18.54	T10

5. Devoll and Shkumbin terraces

5.1. Rivers geometry

The Devoll and Shkumbin rivers are two nearby rivers. Their catchments areas are respectively 3100 km^2 and 3070 km^2 (**Table IV.1**). The two rivers flow from the extensional domain of the Internal Albanides to the compressional domain of the External Albanides, crossing the ophiolites of the Mirdita zone, the flysch and carbonate deposits of the Krasta-Cukali, Kruja and Ionian zones, and the Quaternary sediments of the Periadriatic basin (**figure IV.1**) (SHGJSH, 2003).

The source of the Devoll is located close to the Greek border at an elevation of 1100 m a.s.l. The river flows over 160 km and connects with the Osum river in the flat plain downstream the city of Berat. This confluence forms the Seman river that flows for 70 km toward the Adriatic Sea. The Seman river and its tributaries form the longest drainage system of Albania (230 km) (**figure IV.2, Table IV.1**). The upper reach of the Devoll river flows through the plain of Korçë, which was a lake until the beginning of the XX^{th} century (Denefle et al., 2000).

The Shkumbin river is 130 km long and originates in the mountains to the Southwest of Lake Ohrid, at an elevation of 1150 m a.s.l. (**Table IV.1).** In the upper reaches, the Shkumbin flows from Southeast to Northwest and then it flows mainly from East to West. It crosses Elbasan town before reaching the Adriatic Sea.

5.2. Relations between the Devoll and Shkumbin rivers

The Devoll and Shkumbin rivers are separated close to Cërrik village by a plain of approximately 20 km^2 that dips ~ 0.1° toward the Northwest (**figure IV.3**). Nowadays no river flows through the Cërrik plain, but river terraces were identified along the Eastern border. The Cërrik plain is located above a thick deposit (at least 12 m from a natural section close to Gostimë village) formed of pebbles of variable sizes, supported by a sandy to silty matrix with interstratified lenticular bodies of sand. Paleocurrent data, obtained in this study from imbricate clasts and cross stratification, indicate a flow direction around N300°, close to Gostimë, and N340° close to Cërrik village (**figure IV.3b**, **Table IV.4**). It suggests, as proposed by Melo (1961), that the Paleo-Devoll river flowed toward the North, and connected to the Shkumbin river; afterwards, the Devoll river was captured toward the Southwest (**figure IV.3b**), probably due to the local subsidence caused by diapiric salt activity in this area (Roure et al., 2004). The absence of encased river terraces along the present-day Devoll river downstream of Gostimë village is consistent with the capture hypothesis.

Thus, the lower reaches of the Shkumbin corresponds to the Paleo-Devoll river. Hence, the terraces located along the middle reaches of the Devoll and the lower reaches of the Shkumbin along a distance of more than 100 km form the most extended terrace system of Albania. These two rivers are analyzed together in the following part under the name of Paleo-Devoll.

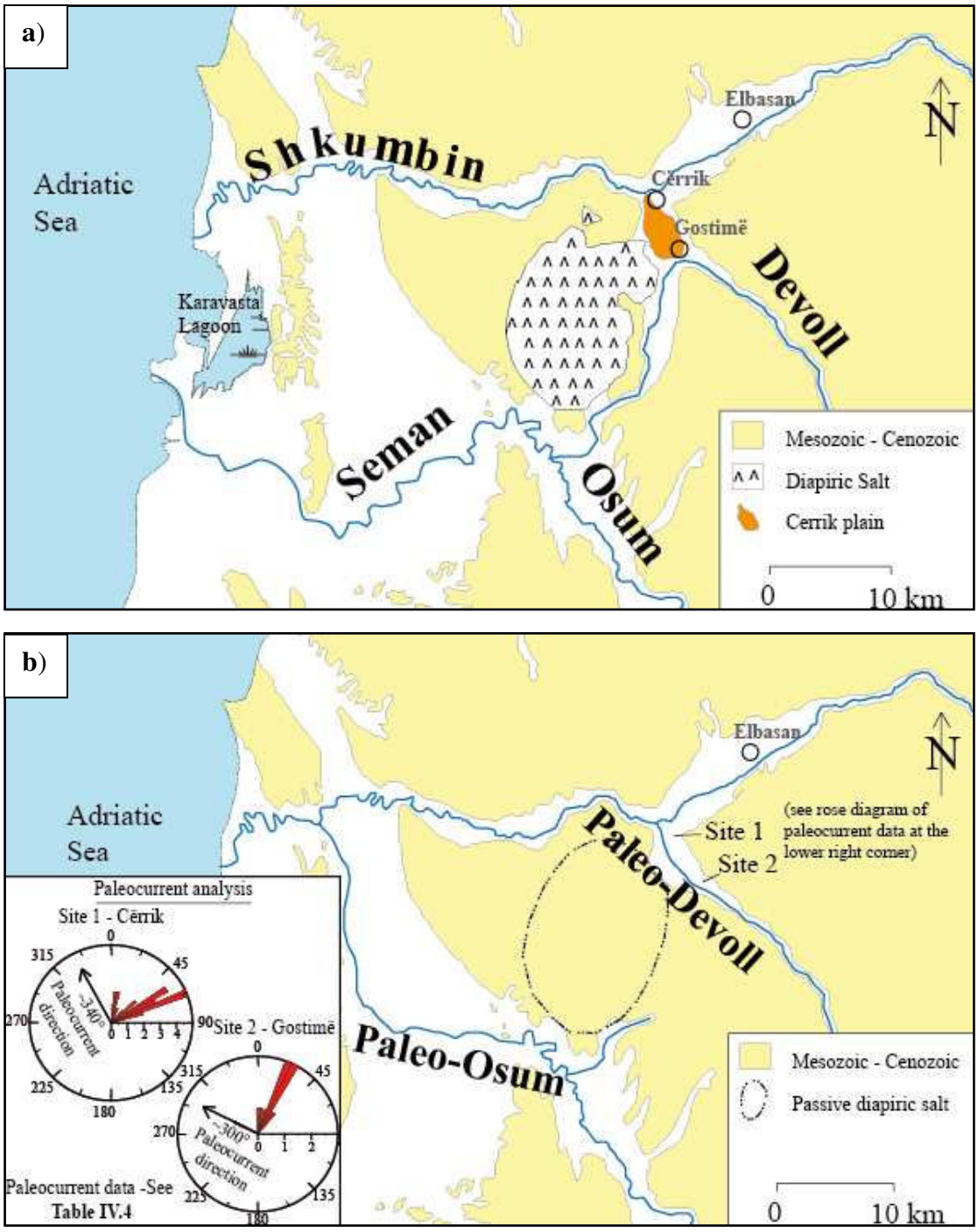

Figure IV.3. *Schema of changing course of Devoll, Osum and Shkumbin rivers.* ***a****) Present- day configuration.* ***b****) Ancient configuration. Course of Paleo-Osum from Chabreyrou (2006). The paleocurrent data from* ***Table IV.4*** *are represented here as a rose diagrams.*

Table IV.4. *Paleocurrent data from Gostimë-Cërrik plain. The rose diagrams with the results are represented in the* ***figure IV.3b****.*

Site	Azimuth	Dip	Sedimentary structure
Gostimë 40°59'33"N 20°00'32"E	25	40 SE	Imbricated clast
	20	30 SE	Imbricated clast
	25	50 SE	Imbricated clast
	32	45 SE	Imbricated clast
	29	30 SE	Imbricated clast
	40	40 SE	Imbricated clast
	5	40 SE	Imbricated clast
	25	20 SE	Imbricated clast
	27	25 N	Imbricated clast
	30	10 SE	Imbricated clast
	10	30 SE	Imbricated clast
	300	12 W	Cross stratification
Cërrik 41°01'39"N 19°58'54"E	10	45 E	Imbricated clast
	60	25 SE	Imbricated clast
	50	45 SE	Imbricated clast
	67	25 SE	Imbricated clast
	70	30 E	Imbricated clast
	15	25 E	Imbricated clast
	60	40 SE	Imbricated clast
	65	30 SE	Imbricated clast
	60	35 SE	Imbricated clast
	65	30 SE	Imbricated clast
	74	30 E	Imbricated clast
	68	22 E	Imbricated clast
	6	20 E	Imbricated clast
	60	40 SE	Imbricated clast
	15	1 E	Imbricated clast
	75	15 E	Imbricated clast
	65	30 SE	Imbricated clast
	70	25 SE	Imbricated clast
	50	25 SE	Imbricated clast
	25	25 SE	Imbricated clast
	45	40 SE	Imbricated clast
	70	55 SE	Imbricated clast

5.3. Characteristics of the Paleo-Devoll terraces

Shkumbin and Devoll rivers were studied by Melo (1961) and Prifti (1984). These authors respectively identified four and six terraces (**Table IV.5**), but no numerical ages were reported. In this study, we have mapped eleven river terraces between Kodovjati village and the lower part of the Shkumbin river (**figures IV.4a to d**). These terraces are called in the following T12 to T1, from the oldest to the youngest terrace. It is worth mentioning that this nomenclature is based on the regional framework of Albanian terraces proposed later in this study (see subsection 6). Then, terrace T9 was not identified along the Paleo-Devoll river.

Most of the terraces have rather flat surfaces and can be separated in fill and strath terraces. The seven higher terraces are fill terraces, while the four lower are strath terraces. Generally, fill terraces (T12, T11, T10, T8, T7, T6 and T5) are formed by a thick basal unit

(with an average thickness for each terrace that varies between 10 and 32 m) and usually lie above a rather flat strath surface. The thickness of this basal unit is positively correlated with the relative age of the terraces (**figure IV.6a, b**). This unit is constituted of rounded pebbles, cobbles and boulders, composed mainly of igneous rock (especially ultrabasic rocks), carbonates and flysch fragments, and the unit is supported by a gravel and sand matrix. The size of the coarse material decreases upward in the sedimentary column, while the percentage of the matrix increases. The basal unit is overlain by a thin sedimentary unit (0.5-1 m) composed of clay, siltstone, fine sand and organic material. This unit can reach a thickness more than 2 m for the higher terraces (T12 to T10). These sedimentary facies suggest that the alluvial deposits that composed the fill terraces of the Paleo-Devoll river were probably deposited in a meandering environment.

Strath terraces (T4, T3, T2 and T1) are composed of a thin basal unit (with a mean thickness for each terrace that varies between 4 and 6 m), located above an extended strath surface (**figure IV.6b, c**). The basal unit is constituted of cross stratified rounded pebbles, cobbles and boulders levels that alternate with horizontal stratified, fine to coarse sand levels. The coarse material has a composition similar to that of the fill terraces and is also overlain by a thin layer (0.4 to 1 m) composed of clay, siltstone, fine sand and organic material. The sediments covering the straths terraces were probably deposited in braided alluvial systems similar to the present-day river. In both fill and strath terraces, terrace alluvia are frequently overlain by post-terrace colluvia and alluvial fan deposits that tend to increase in thickness with terrace age and proximity to tributary mouths and valley margins.

The mean elevation of terrace T1 above the annual flow channel of the present Shkumbin and Devoll rivers is 4 ± 2 m. In some localities the base of the alluvial deposit that composes this terrace is lower than the flow channel. Thus, we considered that this terrace could still be affected by the present river dynamics (lateral erosion or recovering by flooding), and it is not analyzed in detail in this study.

Paleo-Devoll river terraces generally present a configuration of stepped terraces, where the substrata are composed of bedrock, and the risers are composed of the new alluvial material and bedrock. Nonetheless, close to the Kodovjati village, in the upper middle reaches of the river, we observed that the alluvial deposit of terraces T6 and T5 are superimposed (**figure IV.6.d**), forming only one surface terrace. This configuration was also documented in the Osum river by Carcaillet et al. (2009), and is called in the following terrace T6-5 in the Paleo-devoll sequence.

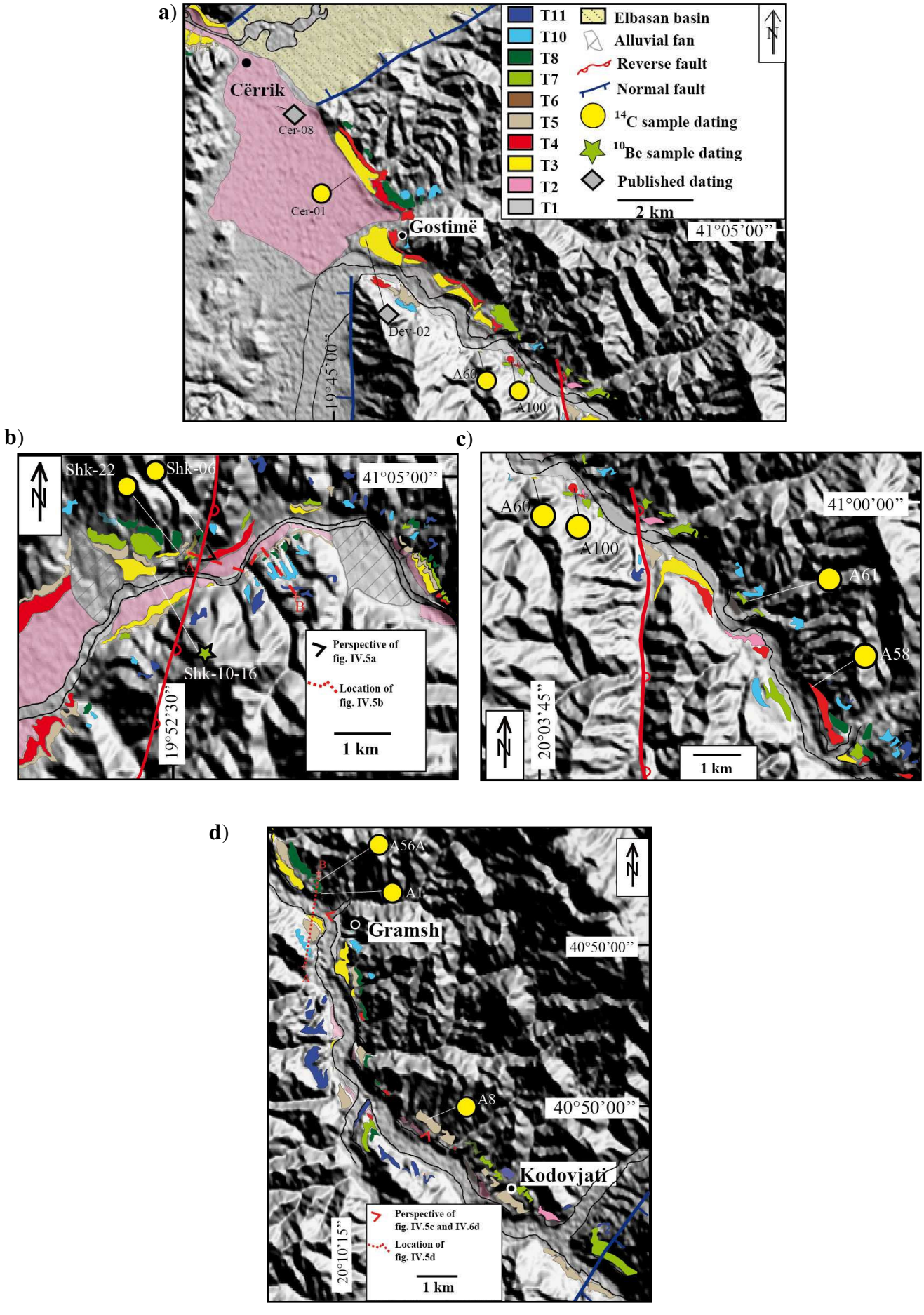
a)
Cërrik
Cer-08
Cer-01
Gostimë
Dev-02
A66
A100
19°45'00"
T11
T10
T8
T7
T6
T5
T4
T3
T2
T1
Elbasan basin
Alluvial fan
Reverse fault
Normal fault
14C sample dating
10Be sample dating
Published dating
2 km
41°05'00"
b)
Shk-22
Shk-06
Shk-10-16
41°05'00"
19°52'30"
A
B
Perspective of fig. IV.5a
Location of fig. IV.5b
1 km
c)
A60
A100
A61
A58
41°00'00"
20°03'45"
1 km
d)
A56A
A1
Gramsh
40°50'00"
A8
40°50'00"
Kodovjati
20°10'15"
Perspective of fig. IV.5c and IV.6d
Location of fig. IV.5d
1 km

e)

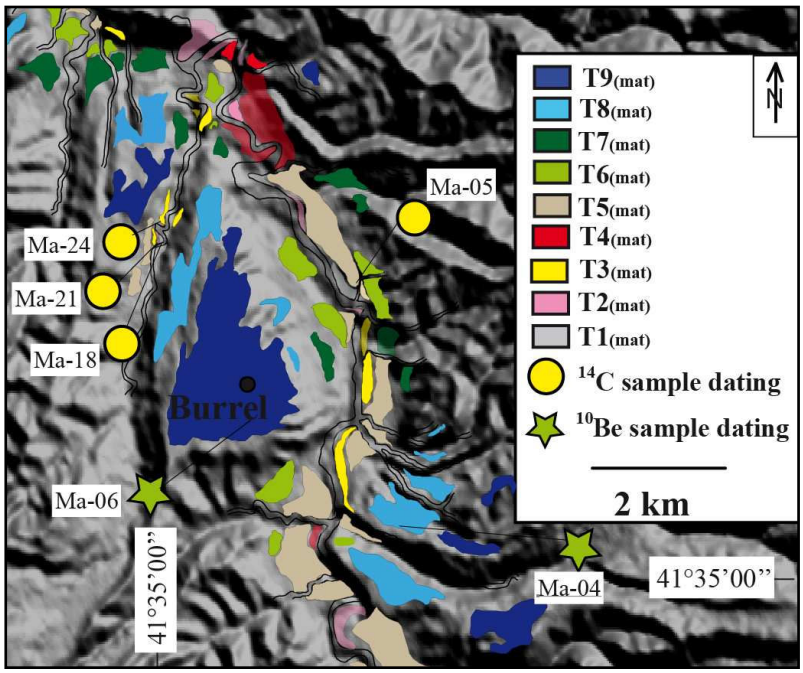

Figure IV.4. *Extract of geomorphic maps of Albanian river performed in this study:* ***a****) the Cërrik plain (Paleo-Devoll). b) Lower reaches of the Paleo-Devoll (present-day Shkumbin river).* ***c****) Middle reaches of the Devoll river.* ***d****) Upper middle reaches of the Devoll river.* ***e****) Middle reaches of the Mat river. The entire legend of the maps* ***a****,* ***b****,* ***c*** *and* ***d*** *is only shown in* ***a****. The terrace T6-5 was mapped within the terrace T5. The geographical locations of the samples dating are shown in the maps. Locations of others figures are also indicated in the maps. See* ***supplementary data A*** *for the entire map of the Paleo-Devoll river.*

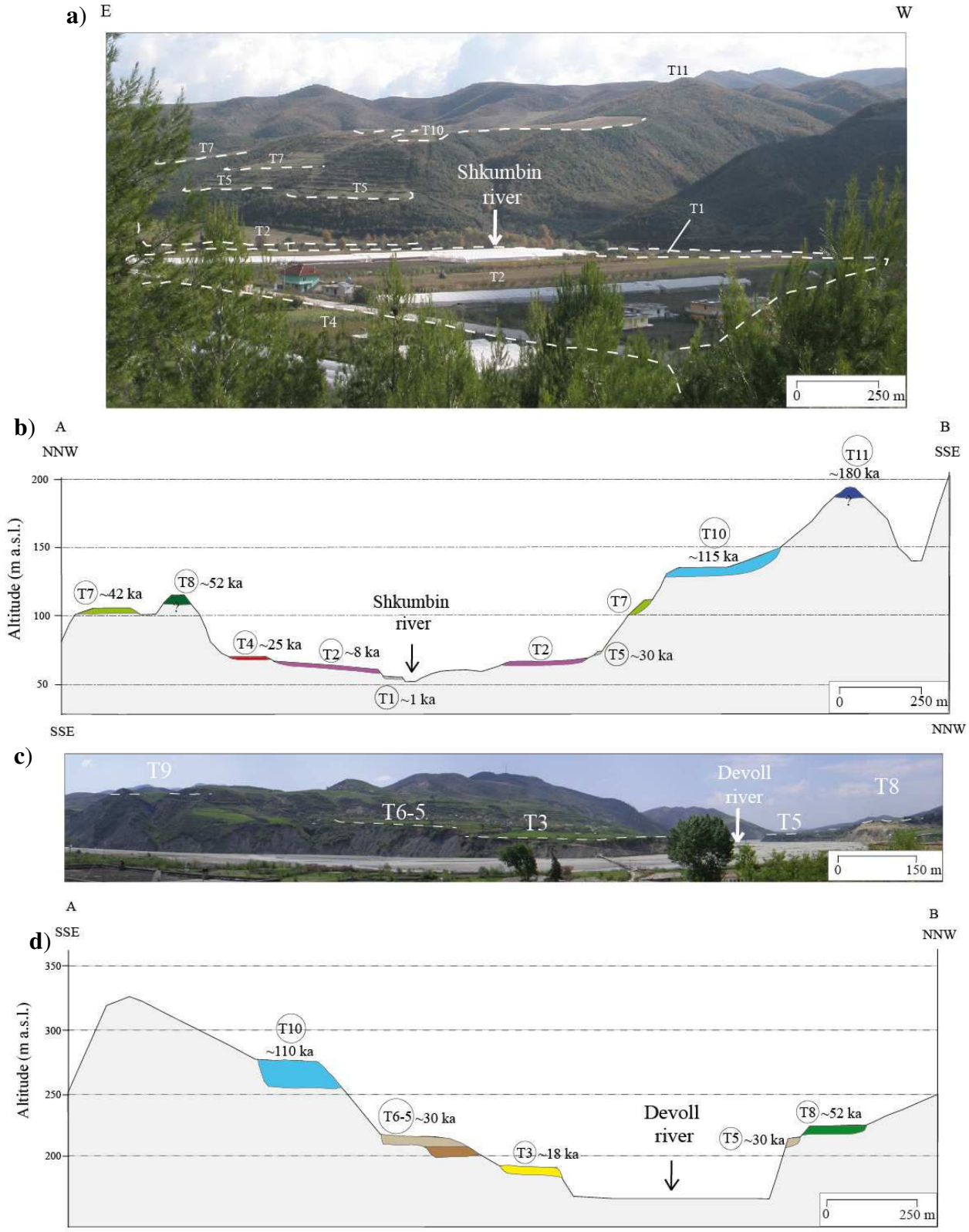

***Figure IV.5. a**) Panoramic view along the lower reaches of the Paleo-Devoll showing the location of terraces above the present-day Shkumbin river. The numbers refer to the nomenclature proposed in the present study. **b**) Cross section through the incised terraces of the lower Paleo-Devoll. The age of terrace corresponds to the most likely age of abandonment proposed in this study. **c**) Panoramic view along the upper middle reaches of the Paleo-Devoll river showing the location of terraces above the*

present-day Devoll. ***d****) Cross section through the incised terraces along the upper middle reaches of the Paleo-Devoll. See* ***figures IV.4b, d*** *and for location*

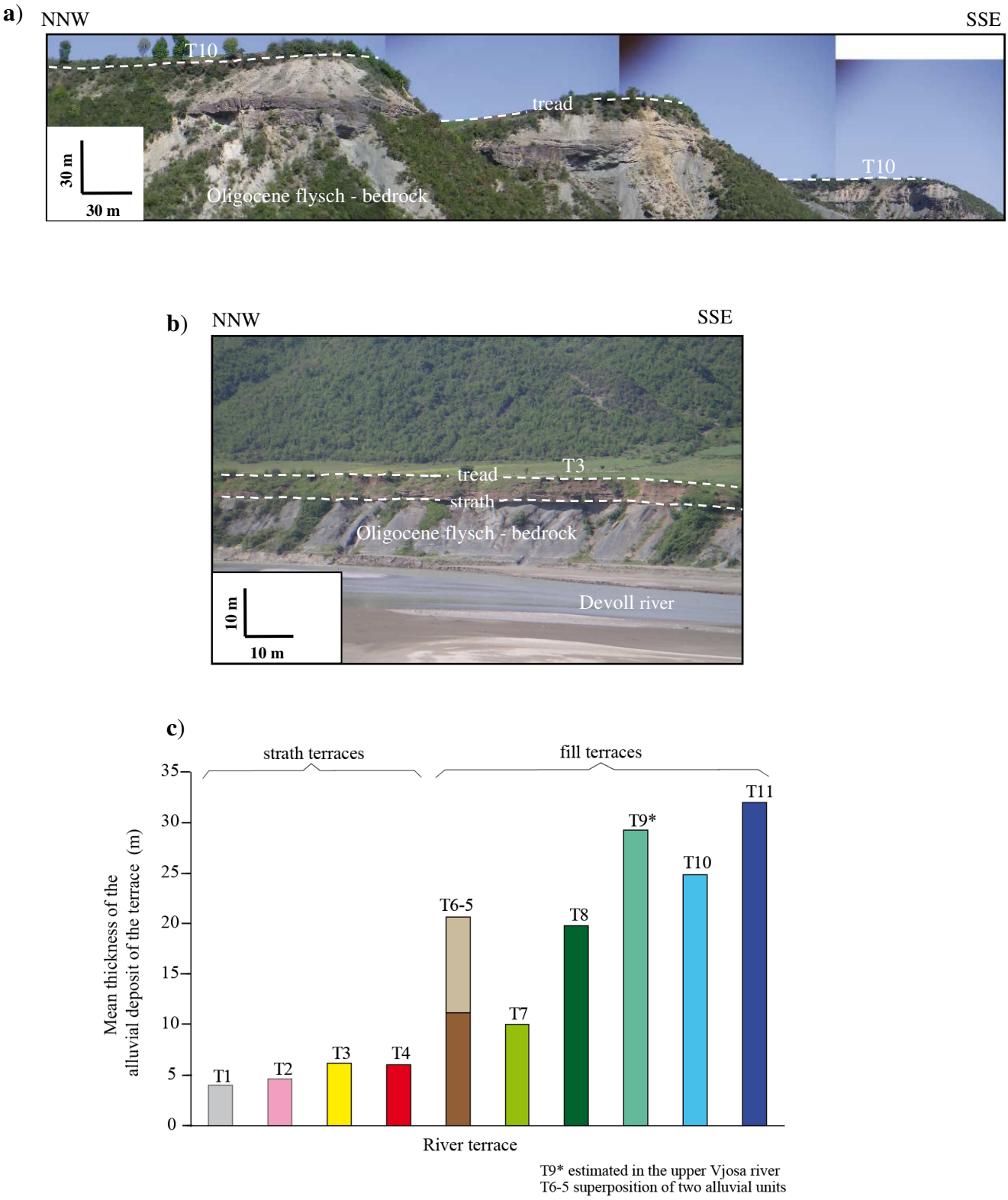

d)

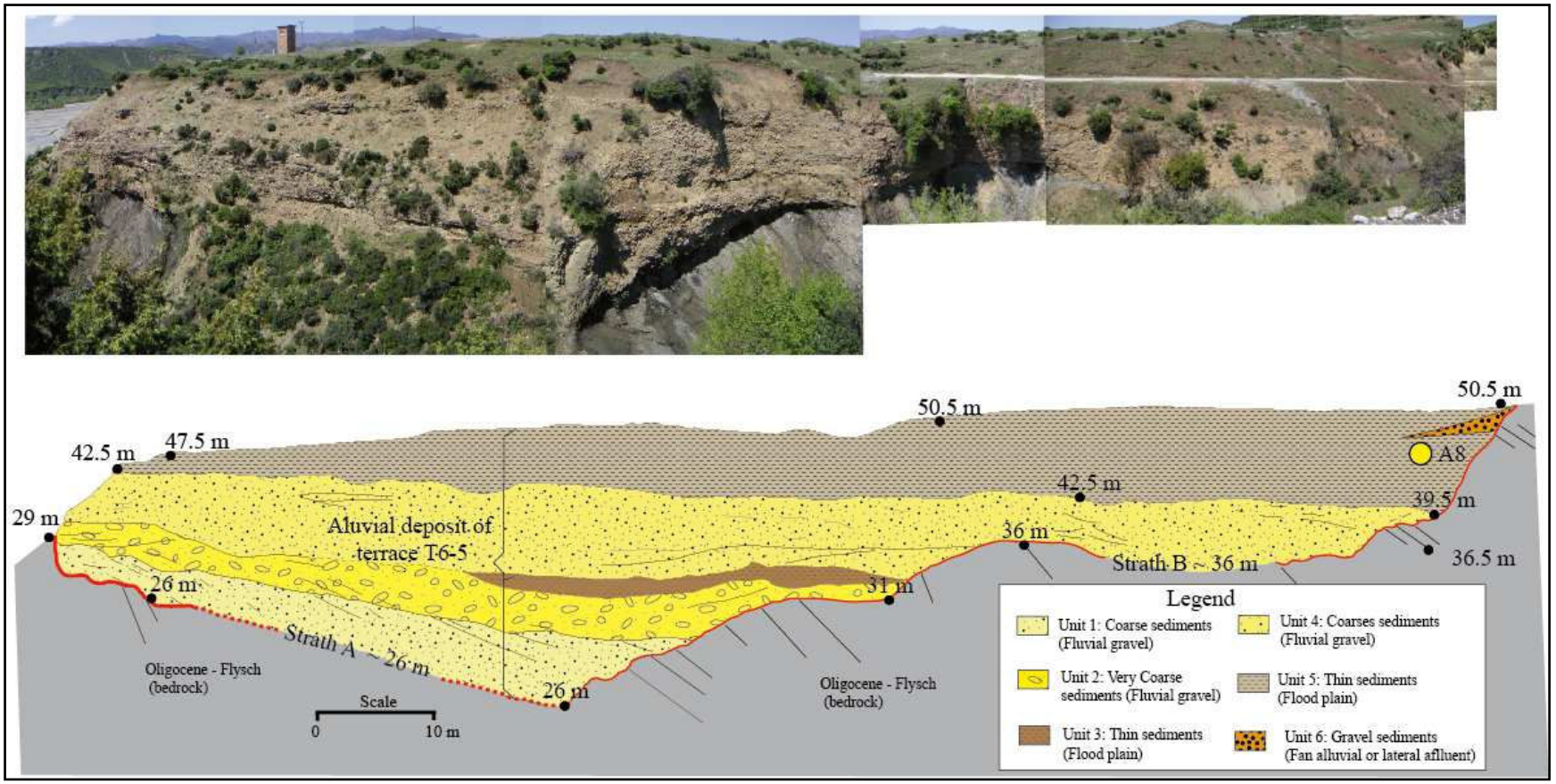

Figure IV.6. *River terraces along the Devoll river.* ***a****) Thick fill river terrace (T10).* ***b****) Strath terrace (T2).* ***c****) Mean thickness of the alluvial deposits of the Devoll terraces. Mean thickness of alluvial deposit of T9 is from the upper reaches of the Vjosa river (Woodward et al., 2008). T6-5 represents the superposition of two terraces, that constitutes an only surface terrace along the upper middle reaches of the Devoll river (see* ***d*** *for sedimentary detail of T6-5).* ***d****) Alluvial deposit of the terrace T6-5 located in the upper middle reaches of the Devoll river (see text for discussion). Two strath surfaces are identified at the top of the substratum, the first one at 26 m (strath A) and the second one at 36 m (strath B) above the present day river bed. The alluvial deposit is divided in at least 6 sedimentary units (see legend of the figure for description). This sedimentary arrangement put in evidence the superposition of the alluvial deposit equivalent to those of T6 and T5 terraces in the lower reaches of the Devoll. A8 refers to the location of a charcoal dated at 28.57 ± 0.54 cal ka BP.*

6. Chronology and correlation of Albanian terraces

The nomenclatures used in previous literature to describe fluvial terraces along the main rivers of Albania are based on both numerical and relative ages applied to the terraces identified in a single river catchment. This leads to local nomenclature and produces considerable confusion to achieve a direct inter-basin correlation due to the different numbers of terraces identified in each river. In this section, a review of types of preserved terraces and numerical dating for the six rivers is presented from South to North (**figure IV.7**, **Table IV.2**). New dating (twenty-one ^{14}C samples and eleven ^{10}Be samples) (**Tables IV.2, 3**) are included and a database of sixty-seven ages is obtained. A chronologic scheme for the Albanian terraces is proposed by correlating the "local" terraces (called in the following $Tx_{(river)}$) of each river (**figure IV.7**) to a regional frame. The correlation is based on: 1) synchronous ages deduced from the numerical dates of the terraces; 2) sedimentological and stratigraphic characteristic of their alluvial deposits; and 3) geometric relationship with respect to dated terraces for terrace levels where no dating has been performed.

6.1. Types and numerical ages of the Albanian terraces

In the upper reaches of the Vjosa river (called Voidomatis river in Greece) (**figures IV.1, 2**), four late Quaternary alluvial units that form four river terraces were firstly identified by Lewin et al. (1991), Hamlin et al. (2000) and Woodward et al. (2001). These units were called Kipi, Aristi, Vikos and Klithi units. Recently, Woodward et al. (2008) based on new and more extended geomorphological and geochronological data of the area identified seven alluvial units and their correlative river terraces. These units were called U8 to U2 and the present-day river channel was called U1. U8 and U7 alluvium are at least 23 and 26 m thick, respectively. Thus the terraces formed by these deposits were classified as fill terraces (Lewin et al., 1991; Woodward et al., 2008). The terraces comprised between the alluvial units U6 to U4 represent much smaller aggradations phases during a general process of down-cutting within the U7 alluvium. Thus, these terraces can be classified as fill-cut terraces. Finally, the U3 unit, contains large scale erosional channel forms and has a maximum thickness of 8.3 m, thus this terrace is classified as a strath terrace (Lewin et al., 1991). Independently, Prifti (1981) mapped five terraces along the middle reaches of the Vjosa river. In our field work, an additional terrace with respect to those recognized by Woodward et al. (2008) was identified and dated along the middle reaches of the Vjosa river. Hence, a total of nine river terraces can be identified along of the Vjosa river ($U9_{(vjosa)}$ to $U1_{(vjosa)}$, from oldest to youngest) and eight of them were dated using several dating methods (^{14}C, U/Th, ESR, TL). The ages of $U9_{(vjosa)}$,

$U8_{(vjosa)}$, $U7_{(vjosa)}$, $U6_{(vjosa)}$, $U5_{(vjosa)}$, $U4_{(vjosa)}$, $U3_{(vjosa)}$, $U1_{(vjosa)}$ are respectively > 150.00 ka, 113.00 ± 6.00 ka, between 68.00 and 87.00 ka, between 49.00 and 61.50 ka, between 22.00 and 27.90 ka, between 16.63 and 23.75 ka, and between 0.54 and 1.75 ka (**figure IV.7a**, **Table IV.1**). Based on lithologic criteria, Woodward et al. (2008) suggested that $U9_{(vjosa)}$ predates the Skamnellian Glaciation (Hughes et al., 2006) and is therefore more than 350 ka old.

Along the Osum river, (**figures IV.1, 2**), Carcaillet et al. (2009) mapped nine terraces ($T1_{(osum)}$ to $T9_{(osum)}$, from oldest to youngest), although remnants of another higher and older terrace are locally more than 150 m above the present-day river. These authors documented that the alluvial deposits of terraces $T5_{(osum)}$ and $T6_{(osum)}$ are superimposed close to the locality of Vertop and Fushe in the middle reaches of the Osum river, and form a single terrace surface. In this study, this terrace is referred as $T5\text{-}6_{(osum).}$ Carcaillet et al. (2009) reported that terraces older than ~35 ka along the upper reaches of the Osum river are composed of alluvial deposits of a thickness > 11 m. Hence, they classified these terraces as fill terraces.

For the lower reaches of the Osum, the same authors also identified two strath terraces ($T4_{(osum)\ and}$ $T7_{(osum),}$ according to their nomenclature). Using ^{14}C and ^{10}Be dating methods, they dated the abandonment of four of them ($T3_{(osum)}$, $T4_{(osum)}$, $T7_{(osum)}$ and $T8_{(osum)}$) respectively between 49.50 and 57.18 ka, 41.87 ± 0.50 cal ka BP, between 17.34 and 21.36 ^{10}Be ka, and 11.48 ± 0.22 cal ka BP, and propose an age of 34.84 ± 3.20 cal ka BP for the basal alluvial unit of $T5\text{-}6_{(osum)}$ (**figure IV.7b**, **Table IV.2**).

In this study, eleven river terraces were identified along the Paleo-Devoll river. They are T12 to T1, from oldest to youngest, and the name T9 is not used in order to fit the Paleo-Devoll terraces succession with the regional sucession defined in section 6.3 (**figure IV.4a to d**). Two alluvial deposits that form independent terraces in the lower reaches of the river are superimposed close to the Kodovjati village in the upper middle reaches (**figure IV.4d**). In this case, the resulting terrace is called T6-5. As discussed earlier, terraces older than T4 are fill terraces, while younger terraces (including T4) are strath terraces. Thirteen radiocarbon samples allowed to date six of them (T8, T7, T5, T4, T3 and T2, from oldest to youngest) at > 52.00 ka, 43.29 ± 1.07 cal ka BP, 30.26 ± 0.66 cal ka BP, between 28.12 and 24.79 ka, 20.97 ± 0.49 cal ka BP and 6.16 ± 0.14 cal ka BP (**figure IV.7c**, **Table IV.2**). A cosmogenic depth profile was made (**figure IV.8a**) through the alluvial deposit of the terrace T3 in the lower reaches of the Paleo-Devoll (**see appendix 1** for cosmogenic profile analysis). This profile yields a minimum exposure age of 16.15 ± 1.00 ^{10}Be ka. Moreover, a ^{14}C sample (A8, **Table**

IV.2) taken close to the surface of terrace T6-5 allows dating the abandonment age of this terrace at 28.57 ± 0.54 cal ka BP (**figure IV.6.d**).

The first study of the Erzen river in Central Albania was performed by Koçi (2007). He mapped five levels of terraces (**figure IV.7d)** and dated four of them using ^{14}C dating. All terraces are strath terraces with alluvial deposits ≤ 5 m. During our fieldwork, two other strath terraces were recognized along the Erzen river and one of them was dated. In total, seven strath terraces were identified ($T7_{(erzen)}$ to $T1_{(erzen)}$, from oldest to youngest) and five of them were dated. The ages of $T6_{(erzen)}$, $T4_{(erzen)}$,$T3_{(erzen)}$, $T2_{(erzen)}$ and $T1_{(erzen)}$ are respectively between 48.83 and 55.62 cal ka BP, between 34.54 and 39.36 cal ka BP, at 31.13 ± 0.82 cal ka BP, between 7.55 and 7.79 cal ka BP and between 1.43 and 1.70 cal ka BP. (**Table IV.2**).

In Northern Albania, five terraces were previously mapped along the middle reaches of the Mat river (Melo, 1996) but no numerical ages were reported. Nine strath terraces were mapped during our fieldwork (**figures IV.4e, 7e**). At the outcrop scale, each terrace consists of a planar bedrock strath surface, above which are 3-5 m (except for the alluvial deposit of $T9_{(mat)}$ that can reach 8 m) of upward fining alluvial gravel and sand, overlained by 0.5-1 m of mixed horizon composed of fine grained and organic materials. The three younger terraces were dated by radiocarbon samples at 1.63 ± 0.75, 5.83 ± 0.90 and 18.15 ± 0.37 cal ka BP (respectively $T1_{(mat)}$,$T2_{(mat)}$ and $T3_{(mat)}$).

The two older terraces of the Mat river were dated with ^{10}Be dating method. A cosmogenic depth profile (**figure IV.8b**) was made within the alluvial deposits of the terrace $T8_{(Mat)}$ and yields a minimum exposure age of 114.00 ± 6.00 ^{10}Be ka (**see appendix 1** for cosmogenic profile analysis). A sample collected on the surface of $T8_{(Mat)}$ and formed of amalgamated pebbles (Ma-04 in **Table IV.3**) also furnishes a minimum exposure age of 110.70 ± 11.18 ^{10}Be ka. An amalgamated pebbles sample (Ma-06 in **Table IV.3**) was taken at the surface of terrace $T9_{(Mat)}$ and furnishes a minimum exposure age of 188.86 ± 18.54 ^{10}Be ka.

Stratified post-terrace colluvial and/or alluvial fan deposits are frequently located in the proximity of tributary outlets and valley margins above the terraces alluvium of the main Albanian rivers. Some of them were dated in order to obtain a chronostratigraphic control with respect to the main river alluvia. We obtained ^{14}C ages between 0.14 ± 0.13 (Cer-08 in **Table IV.2**) and 0.52 ± 0.21 cal ka BP (Dev-02 in **Table IV.2**) for the colluvium above T2 along the Paleo-Devoll. Colluvia deposits were also dated in Vjosa, Erzen (Koçi, 2007) and Mat rivers and their ages are between 0.14 ± 0.14 (A41 in **Table IV.2)** and 1.00 ± 0.62 cal ka BP (Ma-05 in **Table IV.2)**. Thus, this historic colluvial event seems to have occurred along

most of Albanian catchments. Another colluvial event was also dated around 4 ka (A76, A63B, A155 in **Table IV.2)** along the Erzen and lower Vjosa rivers.

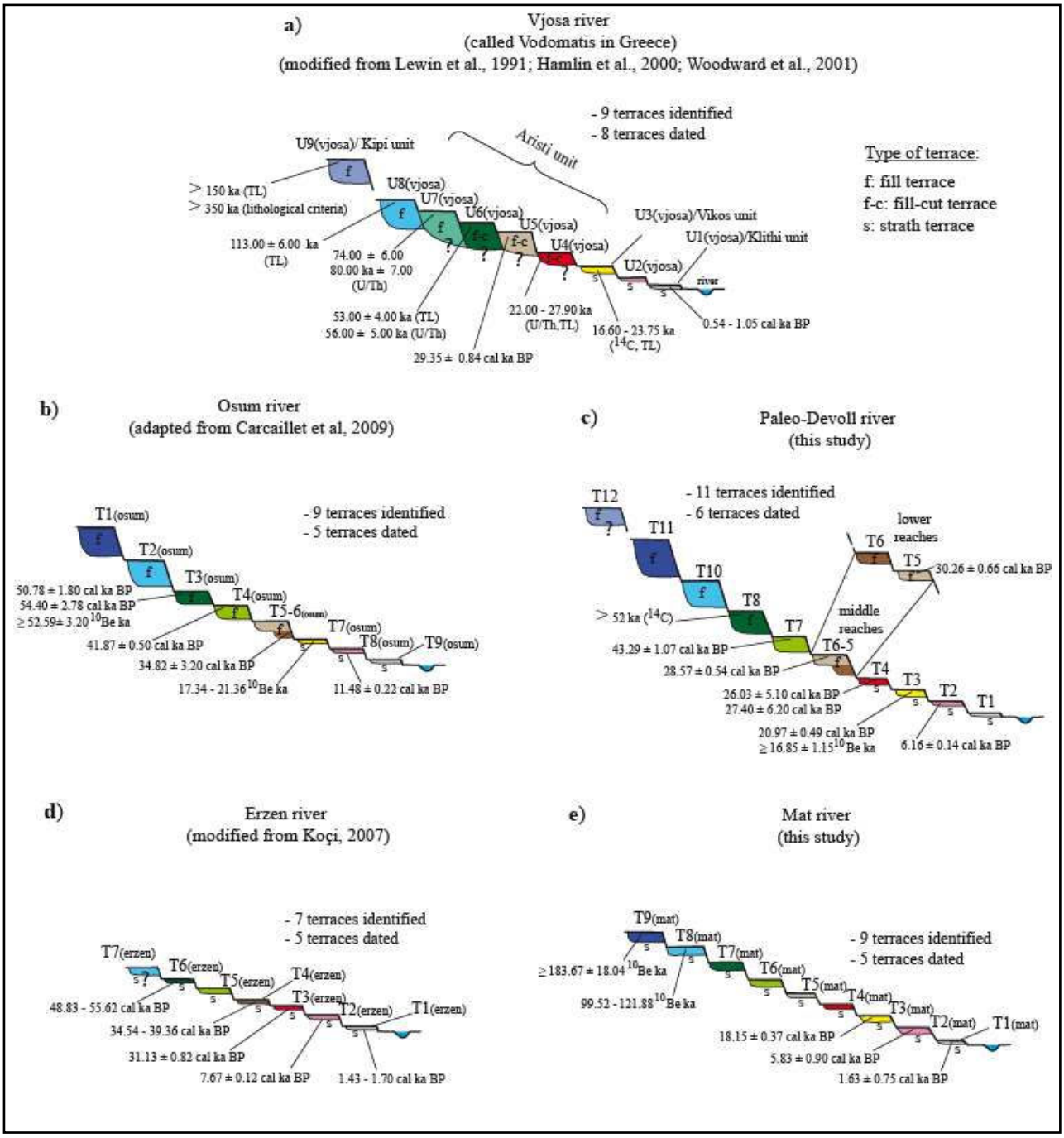

Figure IV.7. *Simplified scheme of terraces geometry identified along six main Albanian rivers. This scheme was constructed taking into consideration the relative position and the ages of the terrace. Horizontal and vertical axis are not at scale, although the relative thicknesses of the alluvial deposits were considered. Types of terraces are indicated. Each river shows a local terrace nomenclature adapted from previous studies (**Table IV.5**). For previous studies, if there is more than three ages for one level, the age of terrace formation is shown as an interval. For Paleo-Devoll and Mat rivers, we show all the individual ages computed in this study.*

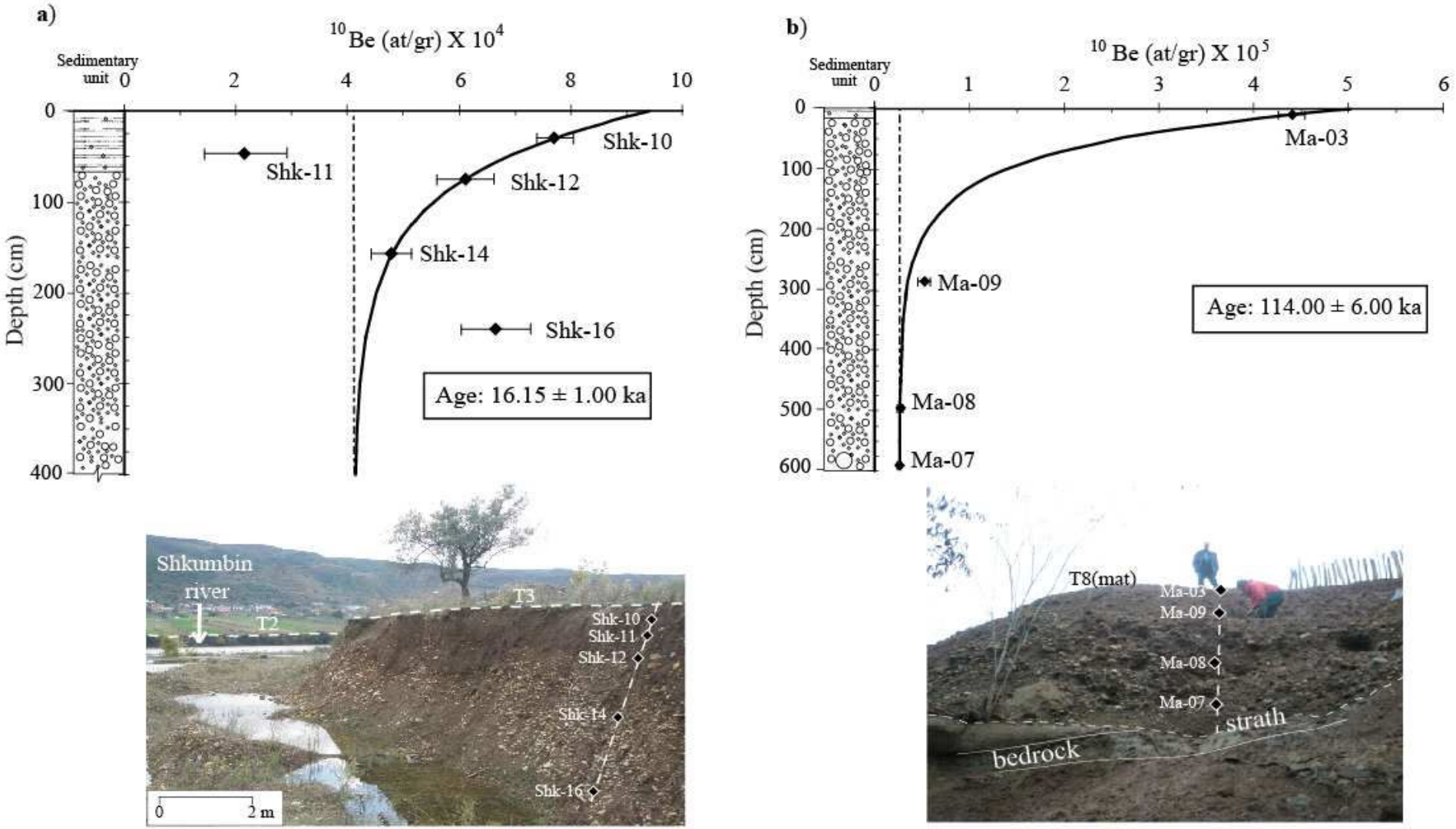

Figure IV.8. *Depth profiles of the ^{10}Be concentration.* ***a****) Lower reaches of the Paleo-Devoll river.* ***b****) Middle reaches of the Mat river. The depth-production best-fits using a chi-square inversion are in solid lines. The dashed line shows the inherited ^{10}Be concentrations. Details of the exposures age calculations are in* ***Table IV.3*** *and* ***appendix 1****.*

6.2. A regional correlation of the terraces younger than 60 ka

In this subsection, a regional chronologic scheme for the abandonment of Albanian river terraces is proposed from our new and the published geochronological data (**Table IV.1**). Firstly, the forty-five available dating for the terraces younger than 60 ka are analyzed. Scaterring of the ages for each terrace is reconciled by a summation of the normal distribution of individual calibrated ages and their associated two sigma errors (95%) using the cumulative probability command within OxCal 4.1 calibration program (Ramsey, 2009). The result is a probability density plot of all the ages (**figure IV.9**), a representation already used in similar studies with large set of dates (Meyer et al., 1995; Wegmann and Pazzaglia, 2002, 2009). From this probability density plot, a succession of seven high probability ages is found (except for the scattered data of terrace T2 –see discussion below) and this succession furnishes a chronologic framework for the river terraces in Albania for the last 60 ka.

A comparison between these numerical ages and the relative ages (T8-T1, from oldest to youngest) found along the Paleo-Devoll river and the other rivers is performed in the following.

Terrace T8 is a rather continuous terrace along the Paleo-Devoll (**figures IV.4**, **5**) and the dating of a charcoal sample (A56A) gives an age of abandonment for this terrace > 52 ka (**Table IV.2**). From this age, T8 could be correlated with $T3_{(osum)}$ dated between 49.90 - 57.18 ka (Carcaillet et al., 2009), with $T6_{(erzen)}$ dated between 48.83 and 55.62 cal ka BP (Koçi, 2007) and with the terrace $U6_{(vjosa)}$ dated between 49 and 61 ka (Woodward et al., 2008).

Terrace T7 (**figures IV.4**, **5**) was dated at 43.29 ± 1.07 cal ka BP (A61, charcoal). From this age, T7 correlates with $T4_{(osum)}$ dated at 42.2 ± 0.8 cal ka BP along the lower reaches of the Osum river by Carcaillet et al. (2009).

Terrace T6 has not been dated along the Paleo-Devoll river. Nonetheless, the abandonment of the terrace T6-5 identified along the middle reaches of the river was dated at 28.57 ± 0.54 cal ka BP (A8, vegetal debris - **figures IV.6d**). Taking into consideration that the same configuration was observed along the Osum river, where the basal unit was dated at 34.82 ± 3.20 cal ka BP (Carcaillet et al., 2009), we argue that the deposition of terrace T6-5 began around 38 ka and its abandoned occurred around 29 ka. In the areas where T5 and T6 are stepped terraces, the abandonment age of T6 would be around ~35 ka and can be correlated with T4(erzen), dated between 34.54 and 39.36 ka (Koçi, 2007) (**Table IV.2**).

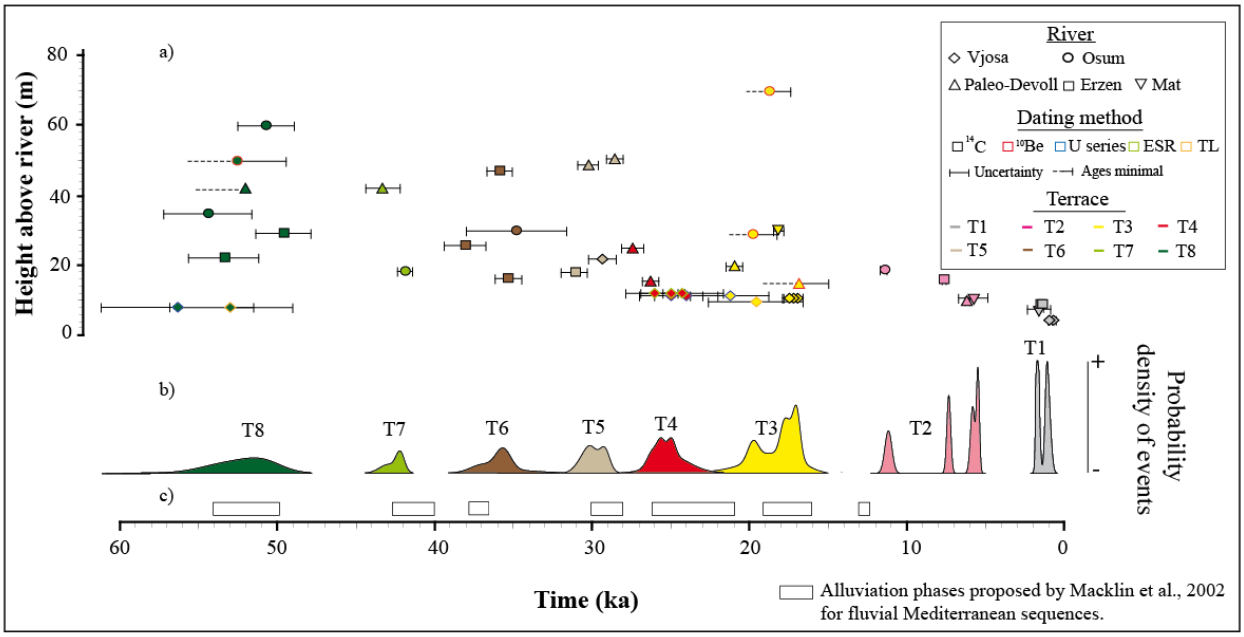

Figure IV.9. *Compilation of Albanian terraces ages for the last 60 ka (**Table VI.2**). a) Plot of individual terraces ages. Each terrace is represented by a symbol related to the river, the contour colour of the symbol corresponds to the dating methods, while the fill colour of the symbol corresponds to the terrace level. The horizontal axis corresponds to the age of abandonment of terrace while the vertical axis represents the height of the terrace above the present-day river. **b**) Probability density curves of age of terraces. The probability curves were produced by calculating calendar ages and their two sigma (95%) analytical errors and then summing the normal probabilities distribution defined for individual ages using the OxCal program version 4.1 (Ramsey, 2009). Minimum ages were not used in the construction of probability curves. **c**) Alluviation phases proposed for fluvial Mediterranean sequences by Macklin et al. (2002) are shown by white rectangles.*

T5 is dated along the Paleo-Devoll by a radiocarbon sample at 30.26 ± 0.66 cal ka BP (A1, vegetal debris samples). This terrace was also dated in the Vjosa and Erzen rivers where two radiocarbon analyses indicate 29.35 ± 0.39 and 31.13 ± 0.82 cal ka BP (respectively charcoal samples A151 and A115) (**Table IV.2**).

T4 was dated at 26.30 ± 5.1 (A58, charcoal) and 27.44 ± 0.68 cal ka BP (A100, charcoal) along the paleo-Devoll river (**figures IV.4**, **5**). Regionally, T4 is correlated with the terrace $U4_{(vjosa)}$ dated between 22 and 27.90 ka in the upper reaches of the Vjosa river (**figures IV.4**, **Table IV.1**) (Woodward et al., 2008).

For terrace T3 in the Paleo-Devoll river, radiocarbon dating of a charcoal sample (A60) yields an age of abandonment at 20.97 ± 0.49 cal ka BP (**figure IV.4**) and ^{10}Be dating yields a minimum exposure age of 16.15 ± 1.00 ^{10}Be ka. T3 is chronologically correlated with

$U3_{(vjosa)}$ (Vikos unit of Lewin et al., 1991), dated in the upper Vjosa river between 16.60 and 23.75 ka (Hamlin et al., 2000, Woodward et al., 2001, 2008), with $T7_{(osum)}$ dated between 17.34 and 21.36 ka (Carcaillet et al., 2009) and with $T3_{(mat)}$ in the Mat river, where a charcoal sample (Ma-24) yields an age of 18.15 ± 0.37 cal ka BP.

T2 is clearly identified along the Paleo-Devoll, where the large terrace developed at the water gap between the Shkumbin and Devoll rivers (Cërrik plain) is cartographically in continuity with the top of the terrace T2 (**figure IV.4a**). The sediments of this plain were deposited by the Paleo-Devoll river when it flowed northward (see subsection 4.2). A charcoal sample (Cer-01, **Table IV.2**), taken within a pit-soil located in the Cërrik plain was dated at 6.16 ± 0.14 cal ka BP and suggests that the capture of the Devoll river occurred around 6 ka. Regionally, T2 was correlated with $T2_{(mat)}$ dated in the Mat river at 5.80 ± 0.93 cal ka BP (Ma-21, charcoal) with $T2_{(erzen)}$ dated at 7.67 ± 0.62 cal ka BP (Koçi, 2007) and $T8_{(osum)}$ dated at 11.48 ± 0.22 cal ka BP (sample A17; Carcaillet et al., 2009). This last age is slightly older and inhibits the identification of a high probability age for this terrace in the probability density plot. However all the ages are close to a global cold climatic event at 8.2 ka identified by Kallel et al. (2000) in the Eastern Mediterranean and in the sediments of the Prespa lake located in the West border of Albania (Wagner et al., 2010). Hence, we argue that the age of abandonment of terrace T2 is around 8.2 ka.

T1 is located at a mean elevation of 4 ± 2 m above the present-day Devoll and Shkumbin rivers. Terrace T1 was not dated in both rivers. Nonetheless, this terrace correalates with the terrace $U1_{(vjosa)}$ (Klithi unit of Lewin et al., 1991) dated between 0.54 and 1.05 ka in the Greek part of the Vjosa river (Lewin et al., 1991), with the $T1_{(erzen)}$ dated between 1.43 and 1.70 ka (Koçi, 2007) and with the $T1_{(mat)}$ dated at dated at 1.63 ± 0.65 cal ka BP in this study (Ma-18, charcoal).

The above correlations confirms that the succession of high probability terraces ages for the last 60 ka deduced from the summation of normal distribution of individual calibrated ages fits with the correlation scheme based on the relative ages of the terraces, and allowed constraining the regional abandonment ages for the Albanian river terraces younger than 60 ka.

6.3. A regional correlation of the terraces older than 60 ka

For the Albanian river terraces older than 60 ka only seven numerical ages, with with high uncertainties are avalaible for all Albanian terraces. No numerical ages are available for this period along the Paleo-Devoll river. Nonetheless, a comparison between the dated

succession of the upper reaches of the Vjosa river (Woodward et al., 2008) and the Mat river (this study) is performed and used as a framework for the other rivers.

As discussed earlier, the alluvial deposits that form the highest terrace of the upper Vjosa river ($U9_{(vjosa)}$) was dated by a TL sample at > 150 ka (Lewin et al., 1991). Later, Woodward et al. (2008), based on lithologic criteria suggested that the deposit that form this terrace predate the Skamnellian Glaciation (Hughes et al., 2006) and is therefore older than 350 ka. Along the Paleo-Devoll, a unique outcrop of T12 was found more than 300 m above the present-day channel, and possibly correlates with the the terrace $U9_{(vjosa)}$ identified in the Vjosa river. Thus, this outcrop seems to be related the oldest preserved Albanian terrace.

In the middle reaches of the Mat river, minimum ages between 100 and 122 ^{10}Be ka and 188.84 ± 18.54 ^{10}Be ka were obtained for the highest terraces $T8_{(mat)}$ and $T9_{(mat)}$, respectively. $T8_{(mat)}$ could be correlated with the terrace that form $U8_{(vjosa)}$ in the upper reach of the Vjosa river, which was dated at 113 ± 6 ka. Moreover, $T8_{(mat)}$ and $T9_{(mat)}$, would be correlated with terraces T10 and T11 mapped but not dated along the middle reaches of the Paleo-Devoll river (**figure IV.7c**), and with the higher terraces of the Osum river, called $T2_{(osum)}$ and $T1_{(osum)}$. The highest terrace identified in the Erzen river $T7_{(erzen)}$ would be also correlated with $T8_{(mat)}$. Nonetheless, due to the scarce numerical ages for the terraces formed during this period, the correlation proposed here should be considered as a first attempt of inter-basin correlation.

Finally, the terrace $U7_{(vjosa)}$ identified along the upper reaches of the Vjosa river was dated between 68 and 87 ka (Woodward et al., 2008). Although we do not identify terraces in the same range of ages in the others Albanian rivers, we recognize the lack of ages for the older terraces, thus we consider this terrace into the regional framework of the Albanian rivers, and is called T9. The above correlations allow establishing a numerical chronology for at least eleven regional river terraces during the last 200 ka in the Albanian domain (**figure IV.9**, **Table IV.5**) although the succession at regional scale of the older terraces is difficult to establish.

6.4. Coparison between Mediterranean and Albanian river terraces

A comparison between the chronology proposed in this study and the alluviation phases defined by Macklin et al. (2002) in the Mediterranean domain (**figure IV.9c**) globally indicates a good correlation between the Mediterranean alluviation phases and the formation of Albanian terraces. In detail, alluvial deposits that compose the terraces T11 and T10 could be correlated with alluviation phases developed between ~88-111 and 179-183 ka in the

Mediterranean and Adriatic domain (see also Fuller et al., 1998, Wegmann and Pazzaglia, 2009). Alluvial deposits of terrace T9 defined by Woodward et al. (2008) can be correlated with an alluviation phase centred around 85 ka reported for the Western and Central Mediterranean (see also Harvey et al., 1995; Fuller et al., 1998, Mass et al., 1998). Alluvial deposits that form terraces T8 to T4 would correspond to alluviation phases described in the Northern Mediterranean around ~50 ka, ~40 ka, 36-38 ka, 28-30 ka and 23-26 ka, respectively. Alluvial deposits of T3 corresponds to a period of terrace development that was recorded in many Mediterranean rivers between 16 and 19 ka, at the end of the Last Glacial Maximum (LGM, Clark et al., 2009). Finally, the Early Holocene T2 terrace, could be correlated with river terraces reported in Spain and Northern Appenines for the period between 8-9 ka by Fuller et al. (1998) and Wegmann and Pazzaglia (2009), respectively.

In summary, eleven regional river terraces were identified along the Albanian rivers for the last 200 ka and an older one is also found. At a regional scale, the abandonment of each terrace was approximately synchronous (few thousand years), although the types of terraces developed and preserved were different from one river to another. In general, most of the terraces older than ~28 ka fed by large catchments (Vjosa, Osum, and Paleo-Devoll rivers) are fill terraces, while for the two smaller catchments (Erzen and Mat) only strath terraces were formed. After the beginning of MIS 2, strath terraces were formed everywhere. Hence, Albanian rivers provide a broad preserved record of alluviation phases that occurred in the Mediterranean context and are useful markers for incision and paleoclimatic studies.

7. Temporal evolution of the incision rate

In order to evaluate the temporal evolution of the incision rate in the Albanian rivers, we chosed sites where maximal numbers of river terraces are preserved and the effect of local deformation over the incision rate is minimal (i.e. far from the active faults). These sites are located in: 1) the lower reaches of the Shkumbin river; 2) the lower and middle reaches of the Devoll river; 3) the upper reaches of the Vjosa river; 4) the middle reaches of the Osum river; 5) the middle reaches of the Erzen; and 6) the middle reaches of the Mat river (see location in **figure IV.2**). The average long-term incision rate was deduced from a linear interpolation of the elevations of the terraces as a function of their ages. As terrace T1 is still exposed to the present fluvial dynamics, it was not taken into consideration for the reconstruction of the incision rate (**figure IV.10**).

Table IV.5. *Correlation of the local terrace nomenclature with a regional nomenclature, which is based on river terraces identified along the Albanian rivers. The regional ages of terrace abandonment is obtained from the numerical dating and the correlation with climatic events.*

River	Vjosa			Osum	Paleo-Devoll			Erzen		Mat		Regional nomenclature	Regional abandonment ages (ka)
Author	(Lewin et al., 1991; Hamlin et al., 2000; Woodward et al., 2001)	(Woodward et al., 2008)	(This study)	(Carcaillet et al., 2009)	(Melo, 1961 - Shkumbin river)	(Prifti, 1984 - Devoll river)	(This study)	(Koçi, 2007)	(This study)	(Melo, 1961 in Aliaj et al., 1996)	(This study)		
Terrace	Kipi unit	U8	U9(vjosa)				T12						>350
				T1(osum)		Terrace VI	T11			V	T9(mat)	T11	~180
		U7	U8(vjosa)	T2(osum)	Terrace IV	Terrace V	T10	T1(erzen)	T7(erzen)	IV	T8(mat)	T10	~115
		U6	U7(vjosa)									T9	~85
		U5	U6(vjosa)	T3(osum)	Terrace III	Terrace IV	T8	T2(erzen)	T6(erzen)		T7(mat)	T8	~52
				T4(osum)			T7		T5(erzen)	III	T6(mat)	T7	~42
				T5-6(Osum)			T6	T3(erzen)	T4(erzen)			T6	~35
			U5(vjosa)		Terrace II	Terrace III	T5/T6-5		T3(erzen)	II	T5(mat)	T5	~30
	Aristi unit	U4	U4(vjosa)				T4				T4(mat)	T4	~25
	Vikos unit	U3	U3(vjosa)	T7(osum)		Terrace II	T3			I	T3(mat)	T3	~17
		U2	U2(vjosa)	T8(osum)	Terrace I	Terrace I	T2	T4(erzen)	T2(erzen)		T2(mat)	T2	~8
	Klithi unit	U1-present	U1(vjosa)	T9(osum)			T1	T5(erzen)	T1(erzen)		T1(mat)	T1	~1-recent

The trends of the average long-term incision rate for the large catchments do not cross the incision axis at zero at present-day (**figure IV.10**). This fact puts in evidence that the long-term incision rate of the large Albania rivers have been non-uniform and unsteady through time. On the contrary, the trendss of the incision rate for the small catchments cross the zero at present-day. This fact suggests that the average long-term incision rates in the small catchment have been almost steady at around 1 mm/a for the Mat river and 0.7 mm/a for the Erzen river over several climatic periods (**figure IV.10**).

The results also show that the long-term incision rates depend on the tectonic context. They varies from 0.1 mm/a close to the Konitsa graben (Vjosa river) to 1 mm/a in the Mirdita zone (Mat river), passing through 0.5 mm/a in the Kruja zone (Devoll river), 0.4 mm/a in the Ionian zone (Osum and Shkumbin rivers) and 0.7 mm/a in the Periadriatic depression (Erzen river). The details of the spatial variation of the incision rate along the Southern Albania rivers are analyzed by Guzmán et al. (submitted) (subsection 4.6 of this thesis).

In order to evaluate the temporal variation of the incision rates along the large catchments, short-term incision rates were estimated for the period between 25 ka and present-day (**figure IV.11**) The results show that they varies from 0.3 mm/a in the Vjosa river to 0.8-1.0 mm/a along the Devoll river, with 0.7 to 0.8 mm/a in the Osum and Skhumbin rivers, respectively. Thus, the average short-term incision rates in the large catchments are double with respect to the average long-term incision rate. This increase seems to be related to the type of terraces along the rivers. Indeed, the Mat and Erzen rivers only formed strath terraces for the periods before ~25 ka, while the other rivers formed fill terraces. This increase would be the result of a fast vertical incision at the beginning of the last 25 ka through the thick alluvial deposit of the fill terraces in the Vjosa, Osum and Paleo-Devoll (Shkumbin and Devoll) rivers, while in the Mat and Erzen rivers the incision through the thin alluvial material of the strath terraces and the bedrock was almost constant. For Devoll river, the capture of the Paleo-Devoll by the tributary of the Osum river evidenced in this study (subsection 5.2) could have an effect, but it only occurred after 6-8 ka keeping the same length of the river before and after the capture. Then, we argue that it did not play a significant role in the incision rate the river, and is not analyzed in the following.

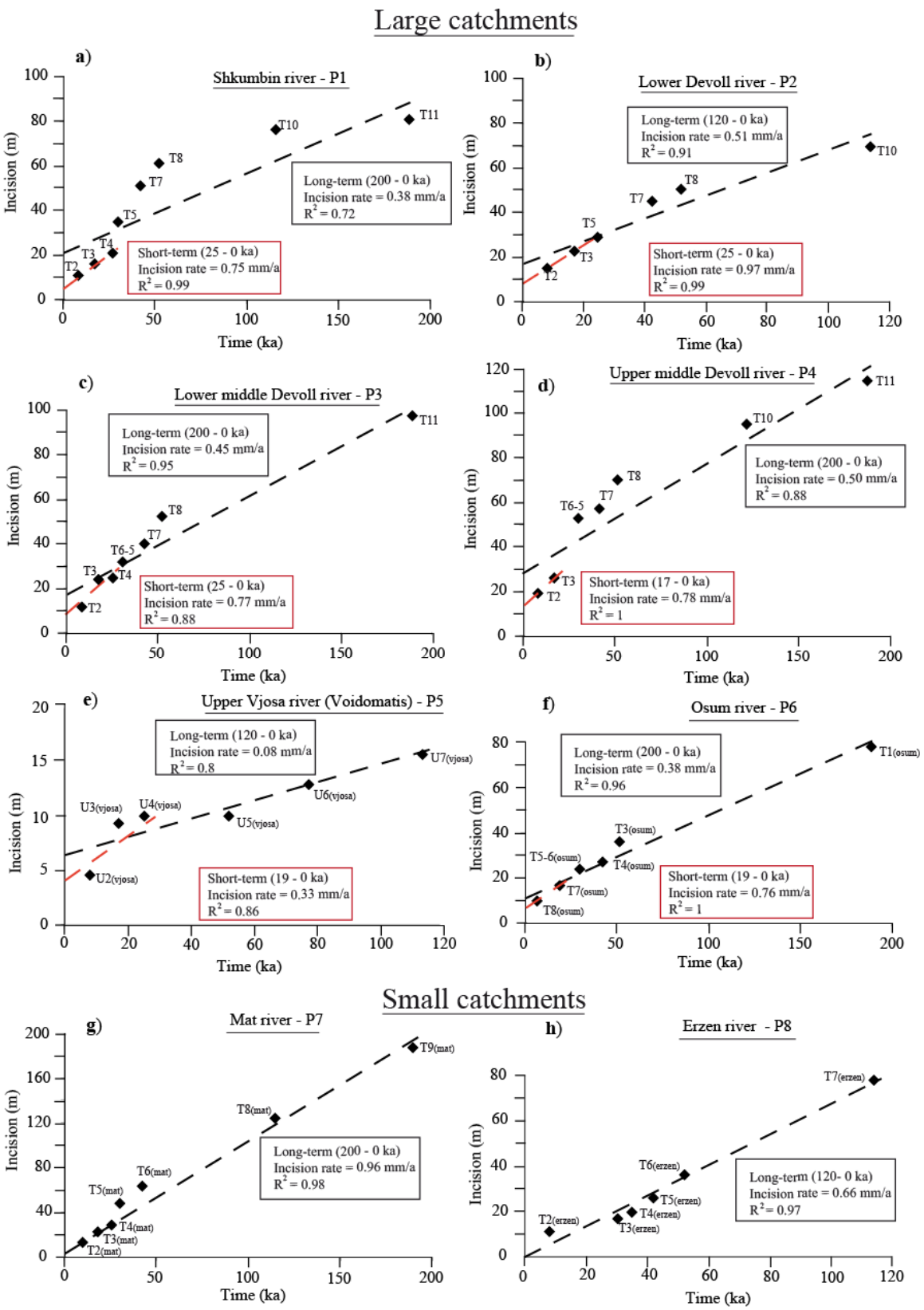

Figure IV.10. *Average long-term (last 200 ka, dashed black line) and short-term (last 25 ka, dashed red line) incision rates at single sites along the Albanian rivers. The coefficient of correlation (R^2) is shown in each case.* ***a****) Lower Shkumbin.* ***b****) LowerDevoll.* ***c****) Lower middle Devoll.* ***d****) Upper middle Devoll.* ***e****) Upper Vjosa (adapted from Woodward et al., 2008).* ***f****) Middle Osum (adapted from Carcaillet et al., 2009).* ***g****) Middle Mat.* ***h****) Middle Erzen (modified from Koci, 2007). The location of the sites is shown in the* ***figure IV.2****.*

8. Discussion

It is accepted that active tectonics, eustatism and climate interact together in terraces formation (e.g. Starkel, 1994; Vandenberghe, 1995; Blum and Törnqvist, 2000). Nevertheless, these factors operate at different time scales and their relative impact is variable in time, space and intensity (e.g. Vandenberghe and Maddy, 2000; Silva et al., 2008b). In order to evaluate these factors in the Albanian domain, the ages of terraces abandonment and the changes in the incision rates are compared with paleoenviromental proxies (Grootes et al., 1993; de Abreu et al., 2003; Wagner et al., 2009, 2010; Vogel et al., 2010) and the curve of sea level variations (Lambeck and Bard, 2000; Lambeck and Chappell, 2001) (**figure IV.11**).

8.1. Climatic control of river terraces

As previously described, the climatic evolution of the Mediterranean domain strongly depends on that of the North Atlantic domain (e.g. Allen et al., 1999; Cacho et al., 1999; Sánchez Goñi et al., 2002, Tzedakis et al., 2004). Thus, the $\delta\ ^{18}O$ record of the North Atlantic is used in this study as a proxy of temperatures (Grootes et al., 1993), together with paleoenviromental reconstruction of the Iberian margin (de Abreu et al., 2003) and Albanian lakes (Wagner et al., 2009, 2010; Vogel et al., 2010), in order to decipher the climatic variations impact in terraces formation (**figure IV.11**).

The most likely ages of abandonment of terrace T8, T5, T4 and T3 correlate with the ages of the Heinrich Events (H5a, H3, H2 and H1, respectively) (**figure IV.11)**. Therefore, we argue that the alluvial sediments that constitute the terraces T8, T5, T4 and T3 would be deposited during cold and dry conditions, while the beginning of the vertical incision and subsequent abandonment of terraces would be triggered when the climate becomes warmer and more humid.

For terrace T7, the most likely abandonment age at 42 ka also corresponds to a cooling event recorded in the distribution of foraminifera *N. pachyderma* on the Iberian margin (**figure IV.11b**) (de Abreu et al., 2003), which is followed by warm conditions reported from the temperature proxy of the GISP2 ice core (**figure IV.11a**) (Grootes et al., 1993). Therefore the abandonment of terrace T7 would also be linked to a transition from cold to warm climate. All available dates for terrace T2 are around a global cold event dated at 8.2 ka and followed by warm conditions (Meese et al., 1994). This event was identified by Kallel et al. (2000) in Eastern Mediterranean and correlated with cold and dry conditions. This cold event was also identified by a minimum of carbonate and organic matter in Prespa Lake (Wagner et al., 2010), and in lipid biomarker of sediments of Ohrid Lake (Holtvoeth et al., 2010). Thus, we

argue that the abandonment of terrace T2 would also be linked to a transition from cold to warm climate.

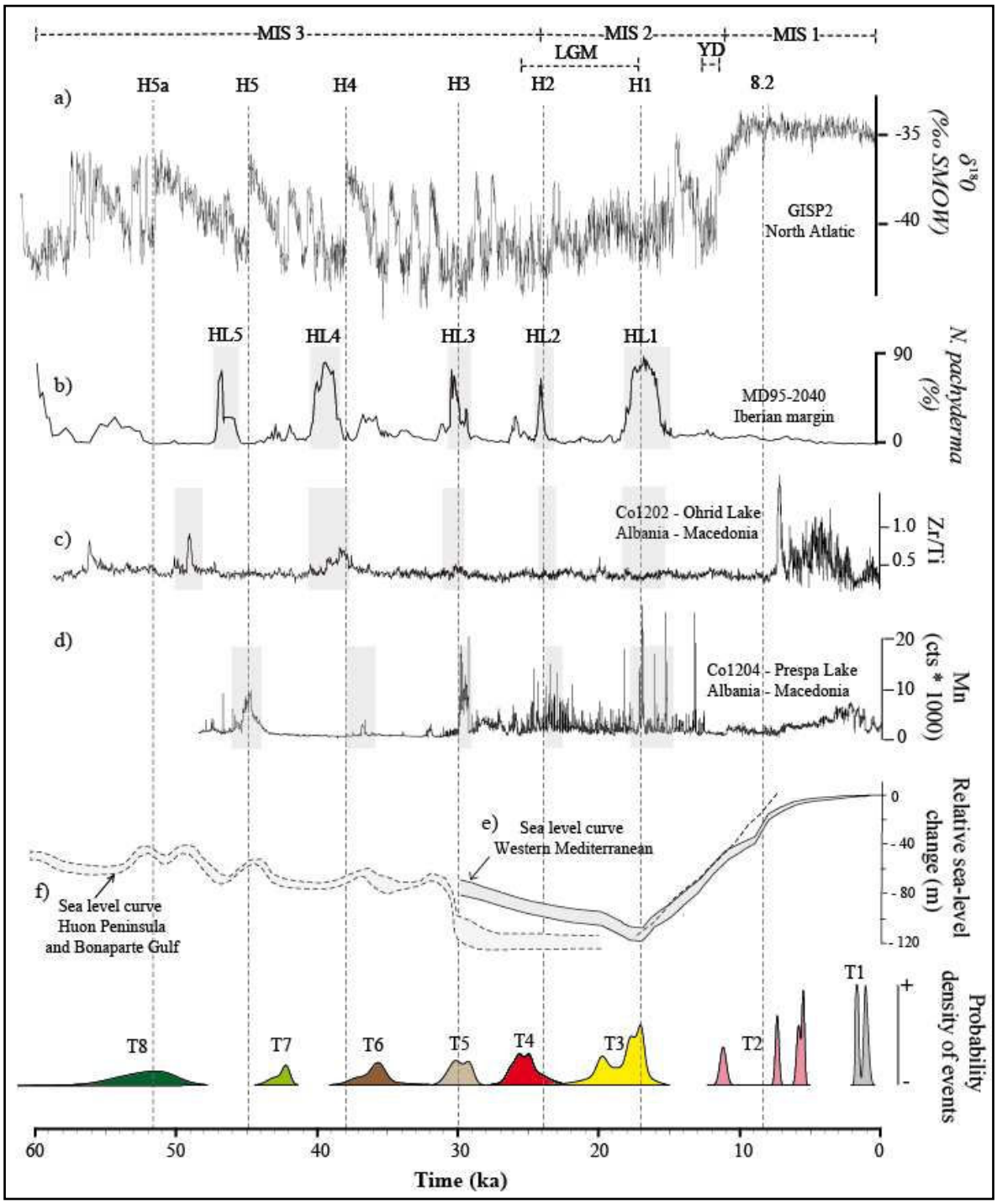

Figure IV.11. *Probability density curves for Albanian terraces ages for the last 60 ka compared with:* ***a****)* $\delta^{18}O$ *record from the GISP2 ice core (Grootes et al., 1993).* ***b****) The percentage of the cold water thriving foraminifera N. pachyderma from Iberian margin (de Abreu et al., 2003).* ***c****) Paleoenviromental record from Ohrid lake (Zirconium/Titanium -Zi/Ti-) (Core 1202; Wagner et al., 2009; Vogel et al., 2010).* ***d****) From Prespa lake (Manganese –Mn-) (Core 1204. Wagner et al., 2010);* ***e****) Sea level curve proposed for the Western Mediterranean for the last 30 ka (Lambeck and Bard,*

*2000.; and **f**) Sea level curve for the Huon Peninsula and Bonaparte Gulf (Lambeck and Chappell 2001). The timing of the Heinrich events H1-H5a is according to Rashid et al. (2003); Hemming (2004. The gray rectangles represents the Heinrich layers (HL) identified by the original authors of the curves **b**, **c**, **d**. (MIS) Marine Isotope Stage (Shackleton, 1987); (LGM) Last Glacial Maximum (Clark et al., 2009); (YD) Younger Dryas (Berger, 1990) are also shown.*

Despite the few available dating for the terraces older than 60 ka, we propose a first attempt of correlation between climatic variations and terraces formation. The abandonment of terrace T9, documented in the upper Vjosa river by Woodward et al. (2008), could be linked to a global cooling event between 82 and 88 ka and followed by warm conditions, evidenced in the pollen records of the Ioanina lake in Northwestern Greece (Tzedakis et al., 2004) and Grande di Monticchio lake in Southern Italy (Allen et al., 1999). The abandonment of T10 could be linked to a significant cooling episode around 115 ka also identified in the pollen records of the Ioanina and Grande di Monticchio lakes (Tzedakis et al., 2004, Allen and Huntley, 2009) and in the oxygen isotope record of foraminifera of Eastern Mediterranean domain (Kallel et al., 2000). The abandonment of T11 could also be linked to cooling episodes identified in the Eastern Mediterranean domain around ~179-183 ka by Kallel et al. (2000).

T6 is the only terrace not clearly synchronous with a climatic variation, and for T1 an anthropogenic impact is not discarded (Carcaillet et al., 2009).

8.2. Eustatic variations and river terraces

The influence of eustatic variations on the development of the river terraces in Albania is evaluated in this subsection. The Albanian coastal shelf is very narrow and its slope (average value between 2.3° and 2.9°) is greater than the slope of the coastal plain (average value of 0.2°) (**Table IV.1**) (Cushman-Roisin et al., 2001; Savini et al., 2011). These conditions would lead to an incision or an aggradation in the coastal plain domain from a fall or rise of the sea level (Summerfield, 1985; Schumm, 1993) and provoke the development of river terraces even upstream.

The sea level fluctuations for the last 30 ka is well studied for the Western Mediterranean Sea (Lambeck and Bard, 2000) (**figure IV.11e**). For older periods, the word-wide sea level curve (Lambeck and Chappell, 2001) (**figure IV.11f**) could applied to the Albanian coast, which was sufficiently far from the margins of the ice sheets to exclude important glacio-isostasy and therefore follows, in a first approximation, the eustatic changes

(Lambeck and Bard, 2000). During the two last dramatic global eustatic variations that occurred during the Late Pleistocene, the development of the Albanian terraces is the following:

Abandonment of terrace T5 (at ~30 ka) is nearly synchronous with the beginning of the 35 to 50 m sea level fall that occurred between ~30 ka and ~18 ka (Lambeck and Bard, 2000). A phase of main lateral fluvial erosion (strath terraces T4) occurred during this fall. An increase of the incision rate during this sea level fall ocurred for the large catchment but differs from one river to the other and its beginning is difficult to define. Nonetheless, the total incision estimated along the rivers during this period is always lower than the incision that would be produced by a sea level fall of 35 to 50 m.

A rapid rise of sea level of approximately 110 m in about 11 ka that began at the end of the LGM (at ~17 ka) corresponds to a period when few river terraces were formed. Indeed, terrace T3 formed at the transition between the fall and the rise of the sea level, and only T2 probably formed at the end of the rise of sea level (at ~8 ka). Both are strath terraces linked to lateral erosion.

These comparisons suggest that the sea level variations could have an impact in the processes of terraces formation along of the Albanian rivers, especially for the river terraces formed between ~30 and 18 ka, although this impact is complex and difficult to quantify with our morphotectonic approach. We argue that this impact is secondary with respect to climatic control, which is discussed in the model of terraces formation in the following.

8.3. Model for late Quaternary Albanian terraces

Bull and Knüpfer (1987) and Bull (1990, 1991) proposed that the rivers systems in the North Atlantic region respond to simultaneous variations of sediment supply, linked to vegetation changes, and runoff produced by climatic changes. During cold and dry periods, the forest-ecosystems decreases and the lack of vegetal cover leads to a destabilization of the hillslope's colluvia; high sediment fluxes combined with dry conditions (small runoff) leads to aggradation phases. During warm and humid periods, the water runoff increases whereas a development of a tree cover reduces hillslope productions and limits the sediment supply; this therefore favorizes the vertical fluvial incision. This response has been reported in Mediterranean fluvial systems, where Quaternary climatic variations induce rapid changes (< 0.2 kyears) in catchment hydrology and in hillslope vegetation (Tszedakis et al., 1997, 2004; Allen et al., 1999; Allen, 2003; Wohlfarth et al., 2008). In this domain, the succession of aggradation and incision phases are thus synchronized with the succession of cold-dry and

warm-humid periods (e.g., Fuller et al., 1998; Macklin et al., 2002; Wegmann and Pazzaglia, 2009). Our data show that the development of most of the Albanian terraces is mainly linked to a climatic control. Nonetheless, these data also suggest that the geomorphic responses of the fluvial system to the climatic variations were probably modulated by other processes, like the size of the catchments and eustatic variations.

The development of fill terraces in large catchments and strath terraces in smaller catchments for the periods before the MIS 2, could be the impact of the climatic contrast between the lower and the higher part of the range. Indeed, upper reaches of large catchments reach elevation around ~2500 m a.s.l. (**Table IV.1**). Then during cold and dry periods, these zones have even developed glaciers during the Tymphian stage (Hughes, 2004, Hughes et al., 2006) and surronding areas were probably free of continuous vegetal cover. Hence, the large catchments were more heavily affected by hillslope processes that furnished much greater volume of sediments to the main channel with respect to the small catchments. The high sediments production coupled with a decrease in the transport capacity of the river, caused by the dry conditions leads to the formation of the fill terraces in the large catchments. In the small catchments the equilibrium between a diminished sediment supply and transport capacity of the rivers leads to the formation of strath terraces. In this context the time interval represented by aggradation in the large catchments is the same time interval represented by strath carving in the small catchments. In contrast, vertical fluvial incision and abandonment of river terraces in both catchment types are simultaneous and occurs during cold-dry to warm-humid climatic transitions, although incision rates may be initially faster for the large catchments since they have a larger amount of sedimentary fill to incise.

Differences between types of climatic preserved terraces along catchments separated for less than 100 km were also reported for the Northern Appenines in Italy by Wegmann and Pazzaglia (2009). These authors proposed that the siliciclastic bedrocks of the Bidente catchment favorized the development of strath terraces, due to the low weathering of the siliciclastic lithology that limits the hillslope production. On the contrary, in the Musone catchment, the weathering is more intense in the carbonate bedrocks, and here much greater volumes of sediments were furnished in this case to the channel bedload leading to the development of fill terraces. The bedrock lithology of the Albanian catchments varies from the ophiolitic rocks in the upper reaches of the rivers to the intercalation of carbonates and siliciclastic lithology in the middle and lower reaches. Moreover, despite of the local variations in the lithology of the clast of the the alluvial deposits of the terraces, the conglomeratic material of both the strath and fill terraces are almost similar with a higher

percentage of igneous rock (mainly ultrabasic) and carbonates rocks and a lower percentage of flysch fragments. Thus, the bedrock lithology does not influence the type of terraces along of the Albanian rivers.

For the period after the beginning of MIS 2, only strath terraces were developed in all Albanian catchments. The sea level fall that occurred between ~30 and 18 ka is consistent with the strath terraces developed during this period. Then, we expected that the rapid sea rise of 110 m between ~17 ka and 8 ka contributed to the development of aggradations phases and probably formation of fill terraces, however terraces developed during this period are linked to lateral erosion rather than aggradation. Thus, after ~17 ka, eustatic rise had less influence in the development of Albanian terraces. This supports the model that the climate-related changes in catchment hydrology and sediment supply would be the primary control for the formation of fluvial terraces in Albania over periods of 10^3-10^4 years. Then, for the period after the beginning of the MIS 2, strath terraces were developed everywhere as a result of the interaction between climatic induced changes (sediment supply and transport capacity), size of the catchments and eustatic drop.

8.4. Fluvial incision and uplift

Our results suggest that climate related changes affect the incision pattern at two scales: **1**) variations over periods 10^3-10^4 years produced by changes in the hydrology and sediment supply. These variations lead to the formation of Albanian river terraces; **2**) variations over periods of few 10^4 years driven by eustatic lowering and increase of transport capacity of the river after the Tymphian stage. These results do not disminish the main role that Albania uplift has in the process of preservation of terraces. Indeed, the moderate uplift of Albania provides the long-term potential for vertical incision and preservation of the river responses to low and high frequency climatic variations. Moreover, it determines the spatial variation of the incision rates along the rivers according to the Quaternary fault activity (Carcaillet et al, 2009; Guzmán et al., submitted). Nonetheless, in order to estimate the Albanian uplift from incision rates, the above incision variations should be taken into account. Determination of the uplift rate in the large catchments should be approached by the average incision rate estimated on a very long period including at least one glacial and one interglacial stage. For the small catchments, the average long-term incision rate seems to be uniform and steady through time. This suggests that the river profiles are close to the steady state and that the incision rate is equivalent to the uplift rate.

9. Conclusions

This study synthesizes new and published chronostratigraphical data concerning the morphology and the chronostratigraphy of river terraces along Albania and Northwestern Greece. The timing of the formation of eleven terraces is established over the last 200 ka in a coherent regional framework. Two Holocene river terraces are recognized (T1 and T2). Seven regional terraces (T3 to T9) are identified for the Last Glacial period (Tymphian stage). For the older interglacial and glacial stages, the remnants of the oldest terraces are discontinuous and difficult to date and correlate at a regional scale. Nonetheless ^{10}Be dating performed in this study improves their dating. Terrace T10 is dated between 100 and 122 ^{10}Be ka. The minimum age for the oldest terrace T11 is 188.84 ± 18.54 ^{10}Be ka whereas remnants of oldest terraces are probably older than 350 ka. Additionally, the capture of the Devoll by the Osum river was documented and dated at ~6 ka.

The correlation between the age of abandonment of late Quaternary terraces and climatic proxies show that the formation of Albanian terraces was mainly controlled by climatic variations. Nonetheless, this study also shows that the geomorphic responses of the fluvial system to the climatic variations were probably modulated by other processes, like the size of the catchments and the eustatic variations. In fact, we argue that during the cold and dry conditions of the period before the MIS 2, the higher part of the large catchments were more heavily affected by hillslope processes, wich led that greater volume were delivered to the the main channel. This fact coupled with the diminished transport capacity of the river (caused by dry conditions) favored the development of fill terraces in the large catchments. In the small catchments the equilibrium between sediment supply and transport capacity favored the development of strath terraces. For the period after the beginning of the MIS 2, a complex relation between climatic and eustatic variation led to the ocurrence of graded conditions, therefore strath terraces were developed everywhere.

Long-term incision rates are quite variable in space from less than 0.09 mm/a in the upper reaches of the Vjosa river (Southern Albania) to 1 mm/a along the Mat river (Northern Albania). Moreover, the incision rates increased since 25 ka in the large catchments. This variability of the incision rate at the scale of interglacial and glacial stages suggests that an estimate of the uplift rate in these areas needs to integrate the incision at least at a glacia/interglacial cycle. For the small catchments, the average long-term incision rates seems to be uniform and steady through time and would be near to the late Quaternary uplift rate.

Acknowledgements
The authors thank the NATO SFP 977993 and the Science for Peace team to have supported this work. This publication was also made possible through support provided by the IRD-DPF. We warmly thank the staff of the AMS facility ASTER at Centre Européen de recherche et d'Enseignement des geosciences de l'Environnement (CNRS, France) for technical assistance during ^{10}Be measurements.

References

Aliaj, S.,1988. Neotectonic and seismotectonic of Albania. Ph.D. Thesis, Archive of Institute of Seismology, Tirana, Albania. (in Albanian).

Aliaj, S., 1991. Neotectonic structure of Albania. Albanian J. of Nat. Technol Sci. 4, 79-98.

Aliaj, S., 2000. Neotectonics and seismicity in Albania. In: Melo, S., Aliaj, S., Turku, I. (Eds.), Geology of Albania, Beitrage zur regionalen Geologie der Erde. Gebruder Borntrager, Berlin, 28, pp. 135–178.

Aliaj, Sh., Melo, V., Hyseni, A., Skrami, J., Mëhillka, Ll. Muço, B., Sulstarova, E., Prifti, K., Pashko, P., Prillo, S., 1996. Neo-tectonic map of Albania in scale 1:200000. Archive of seismology Institute, Tirana, Albania (in Albanian).

Allen, H.D., 2003. Response of past and present Mediterranean ecosystems to environmental change. Progress in Phys. Geography 27(3), 359-377.

Allen, J.R.M., Brandt, U., Brauer, A., Hubberten, H., Huntley, B., Keller, J., Kraml, M., Mackensen, A., Mingram, J., Negendank, J.F.W., Nowaczyk, N.R., Oberhänsli, H., Watts, W.A., Wulf, S., Zolitschka, B., 1999. Rapid environmental changes in southern Europe during the last glacial period. Nature 400, 740–743.

Allen, J.R.M., Huntley, B., 2009. Last Interglacial palaeovegetation, palaeoenvironments and chronology: a new record from Lago Grande di Monticchio, southern Italy. Quat. Sci. Rev. 28,1521–1538.

Anderson, R.S., Repka, J.L., Dick, G.S., 1996. Explicit treatment of inheritance in dating depositional surfaces using *in situ* ^{10}Be and 26Al. Geology 24, 47–51.

Arnold, M., Merchel, S., Bourles, D., Braucher, R., Benedetti, L., Finkel, R.C., Aumaitre, G., Gottdang, A., Klein, M., 2010. The French accelerator mass spectrometry facility ASTER: Improved performance and developments. Nucl. Instruments and Methods in Phys. Res. Sect. B: Beam Interac. with Mater. and Atoms 268, 1954-1959.

Bard, E., Rostek, F., Ménot-Combes, G., 2004. Radiocarbon calibration beyond 20,000 ^{14}C yr BP by means of planktonic foraminifera of the Iberian Margin. Quat. Res. 61, 204-214.

Bar-Matthews, M., Ayalon, A., Kaufman, A., Wasserburg, G.J., 1999. The Eastern Mediterranean palaeoclimate as a reflection of regional events: Soreq Cave, Israel. Earth and Planet. Sci. Lett. 166, 85–95.

Bartov, Y., Goldstein, S.L., Stein, M., Enzel, Y., 2003. Catastrophic arid episodes in the Eastern Mediterranean linked with the North Atlantic Heinrich Events. Geology 31, 439–442.

Berger, W. H., 1990. The younger dryas cold spell—a quest for causes. Global and Planetary Change. Vol. 3, Issue 3, 219–237.

Blum M.D., Törnqvist, T.E., 2000. Fluvial responses to climate and sea-level change: a review and look forward. Sedimentology 47, 2-48.

Bond, G., Heinrich, H., Broecker, W., Labeyrie, L., Mcmanus, J., Andrews, J., Huon, S., Jantschik, R., Clasen, S., Simet, C., 1992. Evidence for massive discharges of icebergs into the North Atlantic ocean during the last glacial period. Nature 360, 245–249.

Braucher, R., Brown, E. T., Bourlès, D. L. Colin, F., 2003. In situ produced ^{10}Be measurements at great depths: implications for production rates by fast muons. Earth Planet. Sci. Lett., 211, 251-258.

Brown, E.T., Edmond, J.M., Raisbeck, G.M. Yiou F., Kurtz M.D., Brook E.J., 1991. Examination of surface exposure ages of moraines in Arena Valley, Antarctica, using *in situ* produced ^{10}Be and ^{26}Al. Geochimica Cosmochimica Acta 55, 2269-2283.

Bull, W.B., 1990. Stream-terrace genesis: Implications for soil development. In: Knüpfer, P.L.K., McFadden, L.D. Ž. (Eds.), Soils and Landscape Evolution. Geomorphology3, pp. 351–367.

Bull, W.B., 1991. Geomorphic Responses to Climatic Change. Oxford Univ. Press, New York, NY.

Cacho, I., Grimalt, J. O., Pelejero, C., Canals, M., Sierro, F. J., Flores, J. A., Shackleton, N. J., 1999. Dansgaard–Oeschger and Heinrich event imprints in Alboran Sea paleotemperatures. Paleoceanography 14, 698–705.

Carcaillet J., Bourlès D. L., Thouveny N., 2004. Geomagnetic dipole moment and 10Be production rate intercalibration from authigenic 10Be/9Be for the last 1.3 Ma. Geochem., Geophys., Geosystem, 5, DOI 10.1029/2003GC000641.

Carcaillet, J., Mugnier, J.L., Koçi, R., Jouanne, F., 2009. Uplift and active tectonics of southern Albania inferred from incision of alluvial terraces. Quat. Res. 71, 465-476.

Carminati, E., Doglioni, C., Argnani, A., Carrara, G., Dabovski, C., Dumurdzanov, N., Gaetani, M., Georgiev, G., Mauffret, A., Nazai, S., Sartori, R., Scionti, V., Scrocca, D., Séranne, M., Torelli, L., Zagorchev, I., 2004. TRANSMED Transect III. In Cavazza, W., Roure, F., Spakman, W., Stampfli, G.M., Siegle, P. (Eds.), The TRANSMED Atlas – The Mediterranean region from Crust to Mantle. Springler, Berlin Heidelberg.

Carretier, S., Lucazeau, F., 2005. How does alluvial sedimentation at range fronts modify the erosional dynamics of mountain catchments?. Basin Res. 17, 361– 381.

Carretier, S., Poisson, B., Vassallo, R., Pepin, E., Farias, M., 2009. Tectonic interpretation of transient stage erosion rates at different spatial scales in an uplifting block, J. of Geophys. Res. 114, F02003, doi:10.1029/2008JF001080.

Chabreyrou, J., 2006. Morphologie fluviale et structures tectoniques actives en albanie. Master thesis, Université Joseph Fourier, France.

Chmeleff, J., Von Blanckenburg, F., Kossert, K., Jakob, D., 2010. Determination of the ^{10}Be half-life bymulticollector ICP-MS and liquid scintillation counting. Nucl. Instruments and Methods in Phys. Res. Sect. B: Beam Interac. with Mater. and Atoms 268, 192-199.

Clark, P. U., Dyke, A. S., Shakun, J. D., Carlson, A. E., Clark, J., Wohlfarth, B., Mitrovica, J. X., Hostetler, S. W., 2009. The Last Glacial Maximum. Sci. 325 (5941), 710-4.

Copley, A., Boait, F., Hollingsworth, J., Jackson, J., McKenzie, D., 2009. Subparallel thrust and normal faulting in Albania and the roles of gravitational potential energy and rheology contrasts in mountain belts. J. of Geophys. Res. 114, B05407, doi:10.1029/2008JB005931

Craddock, W.H., Kirby, E., Harkins, N. W., Zhang, H., Shi, X., Liu, J., 2010. Rapid fluvial incision along the Yellow River during headward basin integration. Nature Geosci. 3, 209-213.

Cushman-Roisin, B., Gačić, M., Poulain, P. M., Artegiani. A., 2001. Physical Oceanography of the Adriatic Sea: Past, Present and Future, Springer, New York. 304 pp.

Dansgaard, W., Johnsen, S. J., Clausen, H. B., Dahl-Jensen, D., Gundestrup, N. S., Hammer, C. U., Hvidberg, C. S., Steffensen, J. P., Sveinbjörnsdottir, A. E., Jouzel, J., Bond, G..1993. Evidence for general instability of past climate from a 250,000- year ice-core record.Nature364 , 218–20.

de Abreu, L., Shackleton, N. J., Schönfeld, J., Hall, M. A., Chapman, M.R., 2003. Millenial-scale oceanic climate variability off the Western Iberian margin during the last two glacial periods. Mar. Geol., 196, 1–20.

Denefle, M., Lézine, A.M., Fouache, E, Dufaure, J.J, 2000. A 12 000-Year pollen record from lake Maliq, Albania. Quat. Res. 54, 423-432.

Dunai, T.J., 2001. Influence of secular variation of the geomagnetic field on production rates of in situ produced cosmogenic nuclides. Earth Planet. Sci. Lett. 193, 197–212.

Dunne, J., Elmore, D., Muzikar, P., 1999. Scaling factors for the rates of production of cosmogenic nuclides for geometric shielding and attenuation at depth on sloped surfaces. Geomorphology 27, 3–11.

Fuller, I.C., Macklin, M.G., Lewin, J., Passmore, D.G., Wintle, A.G., 1998. River response to high-frequency climate oscillations in southern Europe over the Past 200 k.y. Geology 26(3), 275-278.

Gardner, T.W., Jorgensen, D.W., Schuman, C., Lemieux, 1987. Geomorphic and tectonic process rates: effects of measured time interval. Geology 15, 259–261.

Geraga, M., Tsaila-Monopolis, S., Ioakim, C., Papatheodorou, G., Ferentinos, G., 2005. Short-term changes in the southern Aegean Sea over the last 48,000 years. Palaeoceanoraphy, Palaeoclimatology, Palaeoecology 220, 311–332.

Gosse, J., Phillips, F., 2001. Terrestrial in situ cosmogenic nuclides: theory and application. Quat. Science review. 20, 1475-1560.

Grootes, P. M., Stuiver, M., White, J., Johnson S., Jouzel, J., 1993. Comparison of oxygen isotope records from the GISP2 and GRIP Greenland ice cores. Nature 366, 552-554.

Guzmán, O., Mugnier, J.L., Vassallo, Koçi, R., Jouanne, F. Vertical slip rate of major active faults of southern Albania inferred from river terraces. (submitted to Annals of Geophysics).

Hack, J.T., 1957. Studies of longitudinal stream profiles in Virginia and Maryland. U.S. Geological Survey Professional Paper 294-B, 45–97.

Hamlin, R.,Woodward, J., Black, S., Macklin, M.G., 2000. Sediment fingerprinting as 580 a tool for interpreting long-term river activity: the Voidomatis basin, NW Greece. In: 581 Foster, I.D.L. (Ed.), Tracers in Geomorphology. Wiley, Chichester, pp. 473–501.

Hancock, G., Anderson, R., 2002. Numerical modeling of fluvial strath-terrace formation in response to oscillating climate. Geological Soc. of America Bull. 114(9), 1131-1142.

Harvey, A.M., Miller, S.Y., Wells, S.G., 1995. Quaternary soil and river terrace sequences in the Aguas/Feos river systems Southeast Spain. In: Lewin, J., Macklin, M.G., Woodward, J.C. (Eds.) Mediterranean Quaternary River Environments. Balkema, Rotterdam, pp. 263–281.

Heinrich, H., 1988. Origin and consequences of cyclic ice rafting in the Northeast Atlantic Ocean during the past 130,000 years. Quat. Res. 29, 142-152.

Hemming, S. R., 2004. Heinrich events: Massive Late Pleistocene detritus layers of the North Atlantic and their global climate imprint. Rev. Geophys. 42, RG1005, doi:10.1029/2003RG000128.

Holtvoeth, J., Vogel, H., Wagner, B., Wolff, G. A., 2010. Lipid biomarkers in Holocene and glacial sediments from ancient Lake Ohrid (Macedonia, Albania). Biogeosci. Discuss. 7, 4607– 4640.

Hughes, P.D., 2004. Quaternary Glaciation in the Pindus Mountains, Northwest Greece. Ph.D. thesis, University of Cambridge. 341 pp.

Hughes, P.D.,Woodward, J.C., Gibbard, P.L.,Macklin,M.G., Gilmour, M.A.,Smith, G.R., 2006. The glacial history of the PindusMountains, Greece. J. of Geology 114, 413–434

Institutin Topografik te Ushtrise Tirane, 1959-1990. Topographic maps of Socialist Republic of Albania in scale: 1:25000. Archive of Institute of Seismology, Tirana, Albania. (in Albanian).

Jouanne, F., Mugnier, J.L., Koci, R., Bushati, S., Matev, K., Kuka, N., Shinko, I., Kociu, S., Duni, L., 2012. GPS constraints on current tectonics of Albania. Tectonophysics. doi: 0.1016/j.tecto.2012.06.008

Kallel, N., Duplessy, J.C., Labeyrie, L., Fontugne, M., Paterne, M., Montacer, M., 2000. Mediterranean pluvial periods and Sapropel formation over the last 200,000 years. Palaeogeography, Palaeoclimatology, Palaeoecology 157, 45–58.

Koçi, R., 2007. Geomorphology of quaternary deposits of Albanian rivers. Ph.D. Thesis. Archive of Institute of Seismology, Tirana, Albania. (in Albanian).

Kooi, H., Beaumont, C., 1996. Large-scale geomorphology: classical concepts reconciled and integrated with contemporary ideas via surface processes model. J. Geophys. Res. 101, 3361-3386.

Korschinek, G., Bergmaier, A., Faesterman, T., Gerstmann, U.C., Knie, K., Rugel, G., Wallner, A., Dillmann, I., Dollinger, G., Lierse von Gostomski, C., Kossert, K., Maiti, M., Poutivsev, M., Remmert, A., 2010. A new value for the half-life of ^{10}Be by heavy-Ion elastic recoil detection and liquid scintillation counting. Nucl. Instrum. Methods Phys. Res. B268 (2), 187-191.

Lal, D., 1991. Cosmic ray labeling of erosion surfaces: *in situ* nuclide production rates and erosion models. Earth and Planet. Sci. Lett. 104, 424–439

Lambeck, K., Bard, E., 2000. Sea-level change along the French Mediterranean coast since the time of the Last Glacial Maximum. Earth and Planet. Sci. Lett. 175, 203–222.

Lambeck, K., Chappell, J., 2001. Sea-level change through the last glacial cycle. Sci. 292, 679–686.

Lewin, J., Macklin, M.G., Woodward, J.C., 1991. Late Quaternary fluvial sedimentation in the Voidomatis basin, Epirus, Northwest Greece. Quat. Res. 35, 103-115.

Maas, G.S., Macklin, M.G., Kirkby, M.J., 1998. Late Pleistocene and Holocene river development in Mediterranean steepland environments, southwest Crete. In: Benito, G., Baker, V.R., Gregory, K.J. (Eds.), Palaeohydrology and Environmental Change. Wiley, Chichester, pp. 153–166

Macklin, M.G., Fuller, I.C., Lewin, J., Maas, G.S., Passmore, D.G., Rose, J., Woodward, J.C., Black, S., Hamlin, R.H.B., Rowa, J.S., 2002. Correlation of fluvial sequences in the Mediterranean basin over last 200 ka and their relationship to climate change. Quat. Sci. Rev. 21, 1633-1641.

Macklin, M.G., Lewin, J., Woodward, J.C 2012. The fluvial record of climate change. Phil. Trans. R. Soc. A **370**, 2143–2172. doi:10.1098/rsta.2011.0608

Masarik, J., Frank, M., Schäfer, J. M., and Wieler, R., 2001. Correction of in situ cosmogenic nuclide production rates for geomagnetic field intensity variations during the past 800000 years: Geochim. Cosmochim. Acta, 65 (3-4), 515-521.

Meese, D. A., Gow, A. J., Grootes, P., Mayewski, P. A., Ram, M., Stuiver, M., Taylor, K. C., Waddington, E. D., and Zielinski, G. A., 1994, The accumulation record from the GISP2 Core as an indicator of climate change throughout the Holocene: Science, v. 266, p. 1680–1682.

Melo, V. 1961. Neotectonic in the Elbassan-Peqin area from Shkumbin terraces –. Bul. Univ. Sht. Shkencave Natyrore II. (in Albanian).

Melo, V. 1996. The terraces of the Mat river. In: Aliaj, Sh., Melo, V., Hyseni, A., Skrami, J., Mëhillka, Ll. Muço, B., Sulstarova, E., Prifti, K., Pashko, P., Prillo, S. (Eds.), Neo-tectonic map of Albania in scale 1:200000, Archive of seismology Institute, Tirana, Albania. (in Albanian).

Merchel, S., Herpers, U., 1999. An update on radiochemical separation techniques for the determination of long-lived radionuclides via Accelerator Mass Spectrometry. Radiochimia. Acta 84, 215-219.

Meyer, G.A., Wells, S.G., Jull, A.J.T., 1995. Fire and alluvial chronology in Yellowstone National Park: climate and intrinsic controls on Holocene geomorphic processes. Geological Soc. of America Bull. 107, 1211–1230.

Muceku, B., Van der Beek, P., Bernet, M., Reinerrs, P., Mascle, G., Tashko, A., 2008. Thermochronological evidence for Mio-Pliocene late orogenic extension in the north-eastern Albanides (Albania). Terra Nova 20, 180-187.

Niewland, D.A., Oudemayer, B.C., Valbona, U., 2001. The tectonic development of Albania: explanation and prediction of structural styles. Marine and Petroleum Geology 18, 161-177.

Noller, Jay S., Sowers, Janet M., Lettis, William R. 2000. Quaternary geochronology: methods and applications. American Geophysical Union. Vol. 4, 582 pp.

Pigati, J. S., and Lifton, N. A., 2004. Geomagnetic effects on time-integrated cosmogenic nuclide production with emphasis on in situ 14C and 10Be. Earth Planet. Sci. Lett., 226 (1-2), 193-205.

Prifti, K., 1981. Formation of the quaternary valley of the upper Vjosa river . Archive of Institute of Seismology, Tirana, Albania. (in Albanian).

Prifti, K., 1984. Geomophology of quaternary deposits of the Devoll river. Buletini I Shkencave Gjeologjike 2, 43- 59. (in Albanian).

Rahmstorf, S., 2002. Ocean circulation and climate during the past 120 000 years. Nature 419, 207-214.

Ramsey, B., 2009. Bayesian analysis of radiocarbon dates. Radiocarbon 51(1), 337-360.

Rashid, H., Hesse, R., Piper, D.J., 2003. Evidence for an aditional Heinrich event between H5 to H6 in the Labrador Sea. Paleoceanogr. 18, 4, 1077-1091.

Reimer, P.J., Baillie, M.G.L., Bard, E., Bayliss, A., Beck, J.W., Blackwell, P.G., Bronk Ramsey, C., Buck, C.E., Burr, G.S., Edwards, R.L., Friedrich, M., Grootes, P.M., Guilderson, T.P., Hajdas, I., Heaton, T.J., Hogg, A.G., Hughen, K.A., Kaiser, K.F., Kromer, B., McCormac, F.G., Manning, S.W., Reimer, R.W., Richards, D.A., Southon, J.R., Talamo, S., Turney, C.S.M., van der Plicht, J., (2009). IntCal09 and Marine09 Radiocarbon Age Calibration Curves, 0–50,000 Years cal BP, Radiocarbon, 51(4), 1111-1150

Repka, J.L., Anderson, R.S., Finkel, R.C., 1997. Cosmogenic dating of fluvial terraces, Fremont River, Utah. Earth Planet. Sci. Lett., 152, 59–73

Robertson, A., Shallo, M. 2000. Mesozoic-Tertiary tectonic evolution of Albania in its regional Eastern Mediterranean context. Tectonophysics 316(3), 197-254.

Roure, F., Nazaj, S., Mushka, K., Fili, I., Cadet, J.P., Bonneau, M., 2004. Kinematic evolution and petroleum systems - An appraisal of the Outer Albanides. In: McClay K.R. (Ed.), Thrust tectonics and hydrocarbon systems AAPG memoir 82, pp. 474-493.

Sánchez Goñi, M.F., Cacho, I., Turon, J.-L., Guiot, J., Sierro, F.J., Peypouquet, J.-P., Grimalt, J.O., Shackleton, N.J., 2002. Synchroneity between marine and terrestrial responses to millennial scale climatic variability during the last glacial period in the Mediterranean region. Climate Dynamics 19, 95–105.

Savini, A., Corselli, C., Durmishi, C., Marku, S., Morelli, D., Tessarolo, C., 2011. Geomorphology of the Vlora Gulf Seafloor: Results from Multibeam and High-Resolution Seismic Data. J. of Coastal Research, Special Issue 58, 6-16.

Schumm, S.A., 1993. River response to base-level change: implications for sequence stratigraphy. J. of Geology 101, 279–294.

Shackleton, N.J., 1987. Oxygen isotopes, ice volume and sea level. Quat. Sci. Rev. 6, 183-190.

SHGJSH., 2003. Geological Map of Albania in scale 1:200000. Geological Service of Albania, Tirana, Albania, 2nd edn (in Albanian).

Silva, P.G., Badají, T., Calmel-Avila, M., Goy, J.L., Zazo, C., 2008a. Transition from alluvial to fluvial systems in the Guadalentín Depression (SE Spain) during the Holocene: Lorca Fan versus Guadalentín River. Geomorphology 100, 140-153.

Silva, P.G., Audemard, F.A., Mather, A.E., 2008b. Impact of active tectonic and uplift on fluvial landscapes and drainage development. Geomorphology 102 (1). 204 pp.

Sorel, D., Bizon, G., Aliaj, S., Hasani, L., 1992. Calage stratigraphique de l'âge et de la durée des phases compressives des Hellenéides externs (Grèce nord-occidentales et Albanie), du Miocène à l'actuel, Bull. Soc. Geol. France, t. 163, 447-454.

Starkel, L., 1994. Reflection of the Glacial-Interglacial Cycle in the evolutiuon of the Vistula River Basin, Poland. Terra Nova 6, 486–494.

Stone, J.O., 2000. Air pressure and cosmogenic isotope production. J. of Geophys. Res. 105(B10), 23,753-759.

Summerfield, M. A., 1985. Plate tectonics and landscape development on the African continent. In Morisawa, M., Hack, J. (Eds.), Tectonic Geomorphology, Allen and Unwin, Boston, pp. 27-51.

Tzedakis, P.C., Andrieu, V., de Beaulieu, J-L., Crowhurst, S., Follieri, M., Hooghiemstra, H., Magri, D., Reille, M., Sadori, L., Shackleton, N.J., Wijmstra, T.A., 1997. Comparison of terrestrial and marine records of changing climate of the last 500,000 years. Earth and Planet. Sci. Lett. 150, 171–176

Tzedakis, P.C., Frogley, M. R., Lawson, I. T., Preece, R. C., Cacho, I., de Abreu, L., 2004. Ecological thresholds and patterns of millennial-scale climate variability: The response of vegetation in Greece during the last glacial period.Geology 32, 109–12

Vandenberghe, J., 1995. Timescales, climate and river development. Quat. Sci. Rev. 14, 631–638.

Vandenberghe, J., Maddy, D., 2000. Quaternary Fluvial Archives. Geomorphology, 33 (3-4).

van der Beek, P., Summerfield, M.A., Braun, J., Brown, R.W., Fleming, A., 2002. Modeling postbreakup landscape development and denudational history across the southeast African (Drakensberg Escarpment) margin, J. Geophys. Res., 107(B12), 2351-2369.

Vassallo, R., Ritz, J.-F., Braucher, R., Jolivet, M., Carretier, S., Larroque, C., Chauvet, A., Sue, C., Todbileg, M., Bourles, D., Arzhannikova, A., Arzhannikov, S., 2007. Transpressional tectonics and stream terraces of the Gobi-Altay, Mongolia. Tectonics 26 (5), TC5013.

Vogel, H., Wagner, B., Zanchetta, G., Sulpizio, R., Rosén, P., 2010. A paleoclimate record with tephrochronological age control fort he last glacial-interglacial cycle from Lake Ohrid, Albania and Macedonia, J. Paleolimnol. 44, 295–310.

Wagner, B., Lotter, A. F., Nowaczyk, N., Reed, J. M., Schwalb, A., Sulpizio, R., Valsecchi, V., Wessels, M., Zanchetta, G., 2009. A 40,000-year record of environmental change from ancient Lake Ohrid (Albania and Macedonia), J. Paleolimnol. 41, 407–430.

Wagner, B., Vogel, H., Zanchetta, G., Sulpizio, R., 2010. Enviromental change within the Balkan region during the past ca. 50 ka recorded in the sediments from lakes Prespa and Ohrid. Biogesciences 7, 3187–3198.

Wegmann, K.W., Pazzaglia, F.J., 2002. Holocene strath terraces, climate change, and active tectonics; the Clearwater River basin, Olympic Peninsula, Washington State. Geological Soc. of America Bull. 114 (6), 731–744.

Wegmann, K.W., Pazzaglia, F. J., 2009. Late Quaternary fluvial terraces of the Romagna and Marche Apennines, Italy. Quat. Sci. Rev. 28, 137-165.

Wohlfarth, B., Veres, D., Ampel, L., Lacourse, T., Blaauw, M., Preusser, F., Andrieu-Ponel, V., Kéravis, D., Lallier- ergès, E., Björk, S., Davies, S. M., de Beaulieu, J.-L., Risberg, J., Hormes, A., Kasper, H. U., Possnert, G., Reille, M., Thouveny, N., Zander, A., 2008. Rapid ecosystem response to abrupt climate changes during the last glacial period in western Europe, 40–16 ka. Geology 36, 407–410.

Woodward, J.C., Hamlin, R.B.H., Macklin, M.G., Karkanas, P., Kotjabopoulou E., 2001. Quantitative sourcing of slackwater deposits at Boila rockshelter: A record of late-glacial flooding and palaeolithic settlement in the Pindus Mountains, Northern Greece. Geoarchaeology 16(5), 501-536.

Woodward, J.C., Hamlin, R.H.B., Macklin, M.G., Hughes, P.D., Lewin, J., 2008. Glacial activity and catchment dynamics in northwest Greece: long-term river behaviour and the slackwater sediment record for the last glacial to interglacial transition. Geomorphology 101, 44–67.

Wortel, M. J. R, Spakman, W., 2000. Subduction and Slab Detachment in the Mediterranean-Carpathian Region. Sci. 290, 1910-1917.

APPENDIX 1

Cosmogenic dating:

In the lower reaches of the Paleo-Devoll catchment, a cosmogenic depth profile was made through the alluvial deposit of T3 strath terrace (**figure IV.8a**). Each sample was formed by one cobble of siliceous rock (e.g. granite, quartzite) except Shk-12, which was constituted by an amalgamation of small siliceous pebbles, collected in a depth interval of 10 cm. The sampled terrace is nowadays used for agriculture, thus the upper 25 cm was assimilated as the ploughing depth. The first sample (Shk-10 in **Table IV.3**) was taken at 30 cm below surface. This sample has a ^{10}Be concentration of 7.70 ± 0.72 x 10^4 at/g. In spite of no clear attenuation trend with depth in the ^{10}Be concentration for all of the samples, three of them (Shk-10, 12, 14) allowed drawing a possible exponential curve assimilated to the theoretical evolution of production with depth. Assuming no denudation, assigning a material density of 2.2 g/cm^3 to the alluvial material and using a chi-squared inversion to minimize the difference between observed and modelled ^{10}Be data, a maximum inherited concentration of 4.03 ± 0.32 x 10^4 at/g was estimated. These results yield a minimum exposure age of 16.15 ± 1.00 ^{10}Be ka. The unexpected high ^{10}Be concentration of sample Shk-16 can be explained by a provenance from a neighbour tributary stream shed leading to a different pre-exposure history. Chemical problems during sample preparation could have caused the low concentration measured for sample Shk-11.

In the middle reaches of the Mat river, a cosmogenic depth profile was made through the alluvial deposits of terrace $T8_{(Mat)}$ close to the Ulza dam (**figure IV.8b,** for location see **figure IV.2**). Each sample was formed by an amalgamation of small siliceous pebbles. The first sample (Ma-03 in **Table IV.3**) was collected at 10 cm of the terrace surface. This sample has a concentration of 4.40 ± 0.14 x 10^5 at/g surface. Assuming no denudation, assigning a material density of 2.4 g/cm^3 to the alluvial material and considering the concentration of the lower sample collected at 590 cm as the inherited ^{10}Be concentration (0.26 ± 0.01 x 10^5 at/g), this profile yields a minimum exposure age of 114.00 ± 6.00 ^{10}Be ka. Other sample (Ma-04 in **Table IV.3**) formed by an amalgamation of small siliceous pebbles was also taken in the terrace surface of a remnant of the terrace $T8_{(Mat)}$, located ~20 km upstream of the previous site and at 100 m above the river. This sample has a concentration of 5.63 ± 0.16 x 10^5 at/g and allowed estimateing a minimum exposure age for this remnant of 110.70 ± 1.18 ^{10}Be ka.

Finally, along the middle reaches of the Mat rivers, an heterogeneous siliceous (e.g. radiolarites, chert, quartz) amalgamated pebbles surface sample (Ma-06 in **Table IV.2**) was taken in the highest terrace $T9_{(Mat)}$ located at 190 m above the present day river (**figure IV.4g**.

This sample has a ^{10}Be concentration of 10.46 ± 0.40 x 10^5 at/g, which allowed the estimation of a minimum exposure age of 183.67 ± 18.04 ka.

Supplementary data

A. Geomorphologic map in detail of the Shkumbin and Devoll rivers system. **a**) lower reaches; **b**) middle reaches; **c**) upper middle reaches. The geographical locations of the samples dating are shown in the map.

a)

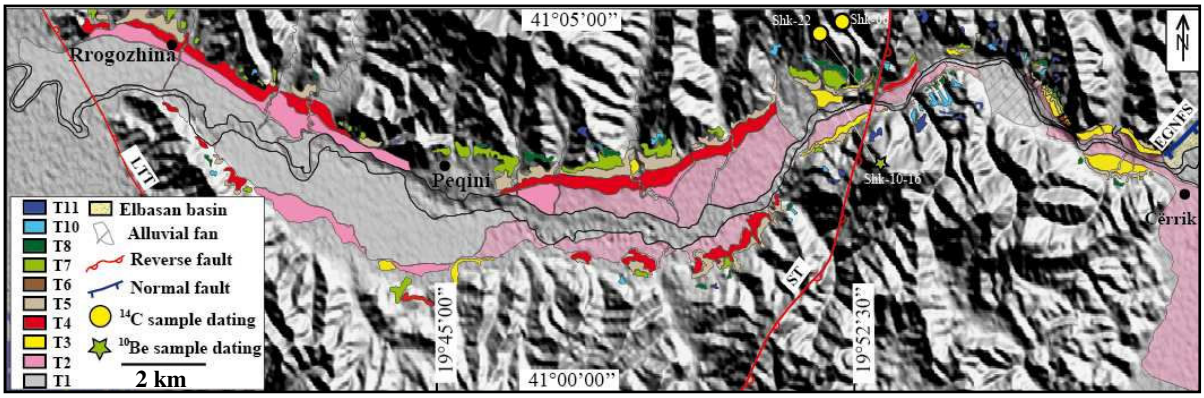

b)

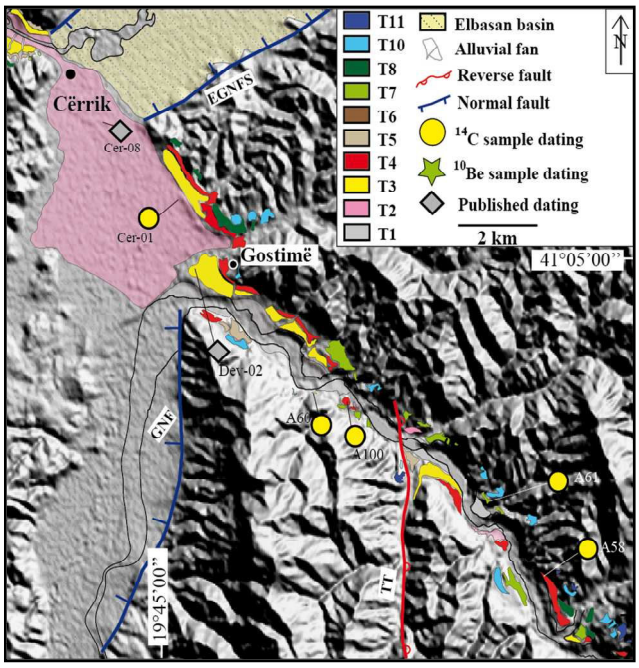

c)

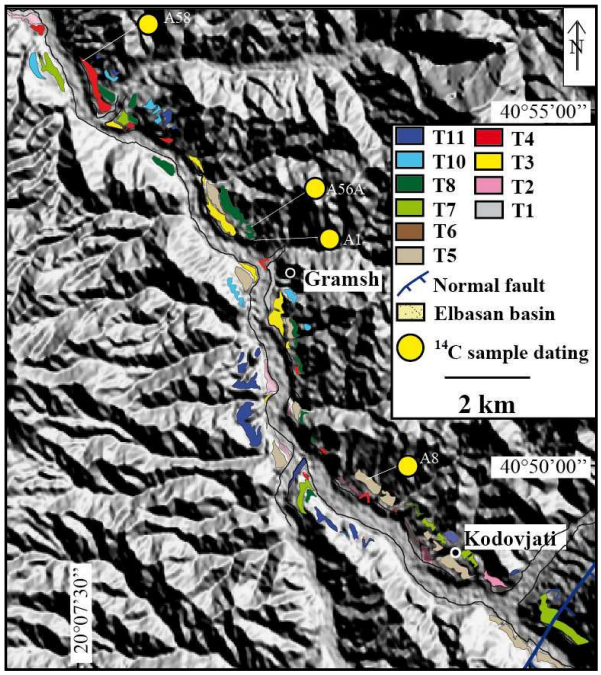

4.6. Vertical slip rates of active faults of Southern Albania inferred from river terraces.

(In press in a special issue of "Earthquake Geology" of Annals of Geophysics)

Oswaldo Guzmán[a,b,*], Jean-Louis Mugnier[b], Riccardo Vassallo[b], Rexhep Koçi[c], François Jouanne[b]

[a] Departamento de Ciencias de la Tierra, Universidad Simon Bolivar, 89000, Caracas 1081-A, Venezuela
[b] ISTerre, Université de Savoie, CNRS, F-73376 Le Bourget du Lac, France
[c] Institute of Seismology of Albania, Rr. "Dom Bosko" 60, Tirana, Albania

[*] Corresponding author:
Oswaldo Guzmán - ISTerre, Université de Savoie, 73376 Le Bourget du Lac, France
Tel: ± 33 4 79 75 86 76 - Fax:± 33 4 79 75 87 77 - E-mail Adresse: guzmano@usb.ve.

Abstract. Fluvial terraces of Shkumbin, Devoll, Osum and Vjosa rivers (Southern Albania and Northwestern Greece) are studied in order to quantify the vertical slip rates of the large active faults of the Dinaric-Albanic-Hellenic Alpine fold belt. The spatial and temporal variations of the incision rates along these rivers were estimated from the geomorphological mapping of the Quaternary sediments, the geometry and the dating of the terraces. Eleven terraces levels were identified in Albania from 67 geochronological ages already published or acquired for this work. The five lower terraces of the four studied rivers are well dated (10 new and 22 already published ages). These terraces are younger than 30 ka and their remnants are numerous. Their restoration allows estimating the regional trend of incision rate and the identification of local shifts. We argue that these shifts are linked to the active tectonics when they coincide with the faults already mapped by previous authors. Vertical slip rates for eight active faults in Southern Albania are thus estimated for the last 19 ka and vary from ~0.1 to ~2 mm/a. The Lushnje Tepelene Thrust, that extends more than 120 kilometers, has a throw rate that varies from 0.2 to 0.8 mm/a, whereas the active faults of the extensional domain are segmented but are very active, with throw rates reaching locally 2 mm/a.

Keywords: Albania, Albanides, river terraces, incision rate, active faults, vertical slip rate.

1-. Introduction

Albania is one of the most seismically active countries in Europe with damage intensities reaching degree IX of MSK-64 scale. The strongest historical earthquakes occurred along three well-defined seismic belts (Aliaj, 1988; Muço, 1998; Sulstarova et al., 2003; Kiratzi, 2011): a) The Ionian-Adriatic coastal earthquake belt at the Western margin of the European plate, which trends NW-SE to NNW-SSE. It is the most seismically active zone in the country and it is characterized by dip-slip to oblique-slip compressional thrust faults. b) The Peshkopia-Korca earthquake belt, in the internal Albanides, which trends NNW-SSE, characterized by normal faults. c) The Elbasan-Dibra transverse belt, which trends NNE-SSW across the former two. This belt is characterized by normal faults (**figure IV.24**).

In these belts, several studies of earthquake focal-mechanism solutions, micro-structural slickenslides analysis and geodetic measures have been made (e.g. Sulstarova, 1986, Aliaj, 1988; Tagari, 1993; Muço, 1994, Kiratzi, 2011; Jouanne et al., 2012). Therefore a precise characterization of the seismotectonic stress field and its comparison with GPS velocities is available. However, the characterization of the individual activity of the Albanian active faults is poorly known, and no hierarchy is currently proposed for the neotectonic features (Fig. 1). One of the means to characterize the activity of faults is to determine their long-term slip rates by studying the offset of morphological markers like alluvial fans, moraines, fluvial and marine terraces (e.g. Carozza and Delacaillau, 1999,Vassallo et al., 2005; Mason et al., 2006; Caputo et al., 2008; 2010; Wegmann and Pazzaglia, 2009; Wesnousky et al., 2012).

The Shkumbin, Devoll, Osum and Vjosa rivers, in Southern Albania, flow from East to West, crossing several active faults (**figures IV.24, 25**), and are characterized by the formation of numerous Quaternary terraces (Melo, 1961; Prifti, 1981). The morphological mapping of these fluvial terraces (**figure 26**, **supplementary data A**), combined with new and published geochronological data (**Table IV.5**) (Lewin et al., 1991; Hamlin et al., 2000; Woodward et al., 2001; 2008; Koçi, 2007; Carcaillet, et al., 2009), are used in order to reconstruct the spatial and temporal variation of fluvial incision along these rivers. The regional trend of incision is related to regional uplift whereas local shifts are interpreted in terms of vertical motion along active faults.

The aim of this paper is to compare the pattern of the incision rate with the existing active tectonic map in order to detect the most active faults and quantify their vertical slip rates.

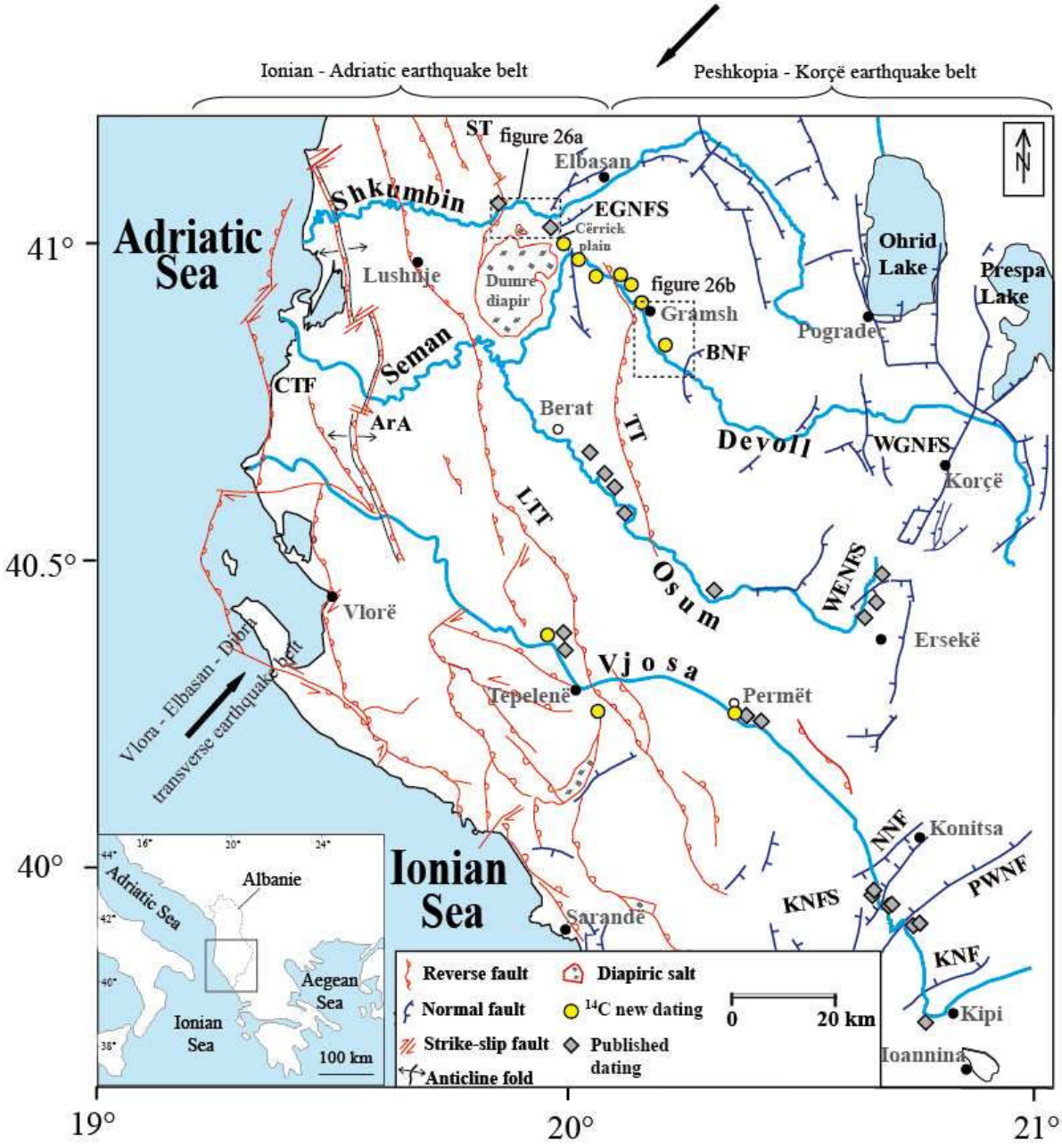

Figure IV.24. *Neo-tectonic map of the Albania and North-Western Greece (modified from Aliaj et al., 1996, 2000 and Carcaillet et al, 2009). Dark grey diamond indicate published data (Lewin et al., 1991; Hamlin et al., 2000; Woodward et al., 2001; Koçi, 2007; Carcaillet et al., 2009) and yellow circles indicate data computed in the present study. Fault types are described in the picture caption. Location of* ***figures IV.26a, b*** *are shown in the map. (CTF) Coastal Thrust Fault; (ArA) Ardenica Anticline; (LTT) Lushnje - Tepelenë Thrust; (ST) Shkumbin Trust; (TT) Tomorrica Thrust; (BNF) Bulcar Normal Fault; (EG) Elbasan Graben Normal Fault System; (NNF) Nerotrivi Normal Fault; (KNFS.) Konitsa Normal Fault System; (PWNF) Papingo West Normal Fault; (KNF) Kipi Normal Fault; (WGNFS) West Graben Normal Fault System; (WENFS) West Ersekë Normal Fault System. These abbreviations are kept unchaged for all figures and text.*

2-. Geological Setting

Albania is located on the central part of the Dinaric-Albanic-Hellenic Alpine fold belt, which was thrusted westward over the Adriatic foreland during the Alpine orogeny (Sorel et al., 1992). The Albanian mountains are traditionally divided in Internal and External Albanides (**figure IV.24**). The Internal Albanides display a relatively simple linear geometry and consist partly of ophiolites (i.e. The Mirdita zone). The External Albanides are divided in three thrust zones that are, from East to West, the Krasta-Cukali zone, the Kruja zone and the Ionian zone. All of these zones are characterized by carbonate deposition in syn-rift and post-rift settings, covered by flysch deposits (Roure et al., 2004; Niewland et al., 2001; Robertson and Shallo, 2000) (**figure IV.25**).

The geodynamic context is characterized by the subduction of the Adriatic plate beneath the foreland domain. This produces contrasting relief with a flexural basin filled with Plio-Quaternary deposits, forming a flat coastal plain in the foreland (Roure et al., 2004), a thin skinned fold and thrust belt in the midland (Carminati et al., 2004) and a synorogenic Neogene-Quaternary graben system in the hinterland that crosscuts the previous thrust system (Aliaj, 1991).

Neotectonics stress field has been studied via micro-structural analysis of slicken-slides (Aliaj, 1988; Tagari, 1993) and earthquake focal-mechanism solutions (Sulstarova, 1986; Muço, 1994), which were compared with GPS velocities (Jouanne et al., 2012). In the external domain, the average axis of compression is oriented N 45°, whereas in the internal domain the average axis of extension varies from N90° close to the Ohrid and Prespa lakes to N 160° at the Southern end of the Ersekë basins (**figure IV.24**) (Aliaj, 1988; Sulstarova, 1986, Jouanne et al., 2012).

The study area is tectonically active and produces both permanent microseismicity and stronger historical earthquakes reaching (Aliaj, 2000; Sulstarova et al., 2000, 2003). This seismicity is associated with the uplift of the Albanides mountain range (Aliaj, 2000). This uplift corresponds to a positive vertical movement of the Albanides with respect to the Adriatic-Ionian sea level. This leads to vertical incision by rivers draining the range, and together with Quaternary climatic variation cause the formation of river terraces along their paths.

This study is focused on the structures crossed by Shkumbin, Devoll, Osum and Vjosa rivers, which are four of the six main rivers of Albania. They flow from the SE to the NW, crossing all the structural domains of the internal and external Albanides and most of the currently active structures.

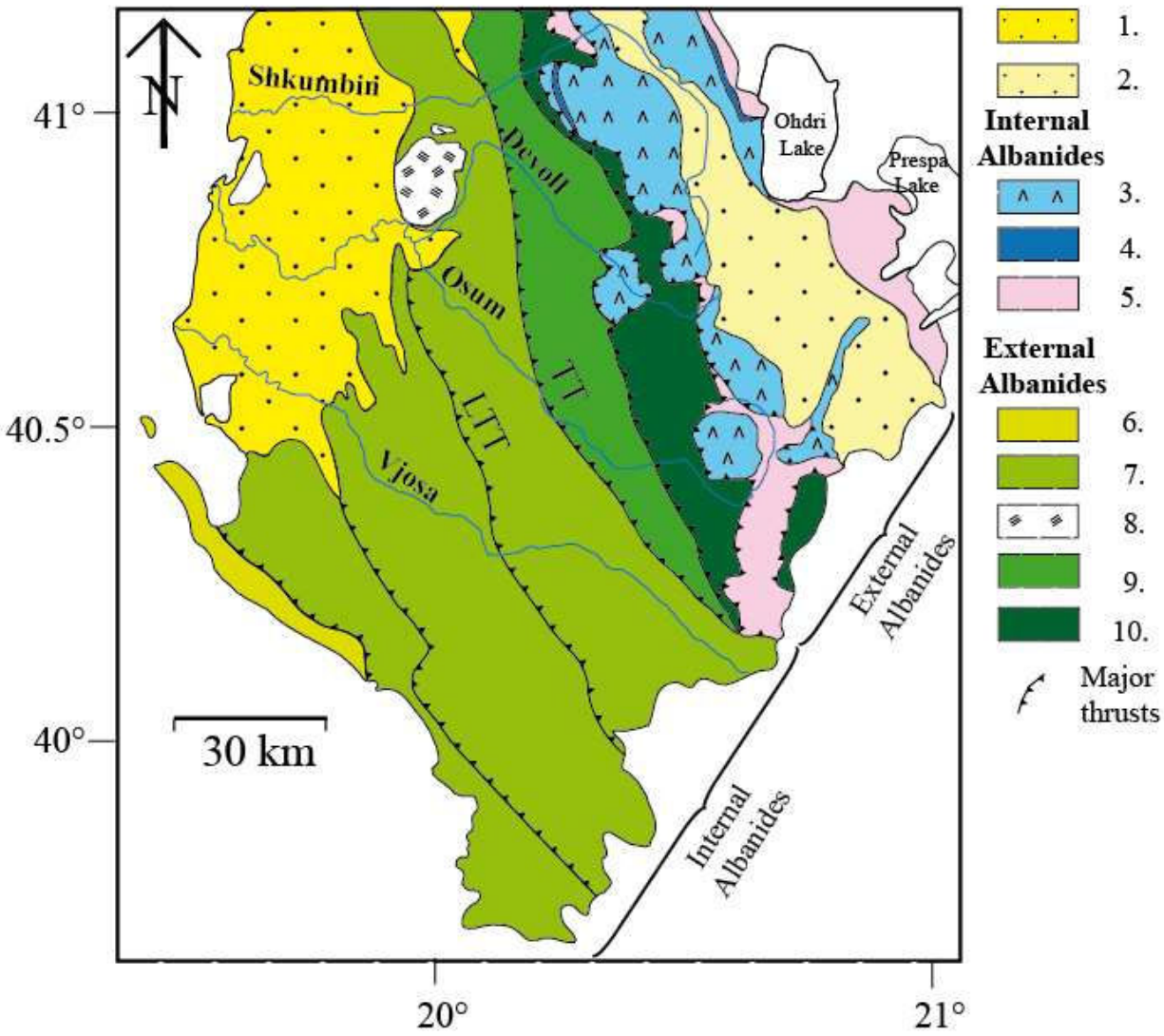

Figure IV.25. *Simplified geologic map of Albania showing main tectonostratigraphic units (modified from Robertson and Shallo, 2000, SHGJSH, 2003 and Muceku et al., 2008). Map legende: 1. Periadriatic depression (Neogene – Quaternary siliciclastic sediments); 2. Neogene - Quaternary graben system (Neogene – Quaternary siliciclastic sediments) 3. Mirdita (Jurasssic ophiolites); 4. Rubiku (Triassic shallow water carbonates); 5. Korabi (Triassic – Jurassic ophiolitic melange/ flysch/ debris flow); 6. Sazani (Triassic to Paleogene platform carbonates); 7. Ionian (Triassic to Paleogene platform and pelagic carbonates covered by Oligocene to Miocene flysch); 8. Ionian (Triassic evaporites). 9. Kruja (Mesozoic platform carbonates covered by Oligocene-Miocene); 10. Krasta-Cukali (Mesozoic platform carbonates covered by Cretaceous to Eocene flysch)*

Table IV.5. Numerical ages of Albanian river terraces.

Sample[a]	Material[b]	Latitude (°N)[c]	Longitude (°E)[c]	Elevation of sample above the river (m)	Methods[d]	Lab-Code Reactor Reference	^{14}C Ages (yr BP)	Calibrated interval Cal yr BP (Probability=0,95)	Concentration ^{10}Be (10^5 at/g)[e]	Ages (ka)	Local terrace name or alluvial unit	Propose terrace name	Source[f]
Vjosa													
A153	C	40.2076	20.3875	17.3	^{14}C	SacA 16001	190 ± 30	4 - 302		0.15 ± 0.15	-	Colluvium	(1)
A150	C	40.2084	20.0934	9.5	^{14}C	SacA 15998	330 ± 30	308 - 474		0.40 ± 0.08	-	Colluvium	This study
A28	Vd	40.3354	19.9921	12	^{14}C	Poz-8824	705 ± 30	564 - 691		0.63 ± 0.06	Colluvium	Colluvium	(1)
A155	Vd	40.3611	19.2907	13.4	^{14}C	SacA 16002	3870 ± 60	4094 - 4436		4.26 ± 0.17	-	Colluvium	This study
OxA-192	C	39.97(ç)	20.66(ç)	~4.5	^{14}C	OxA-192	800 ± 100	560 - 928		0.74 ± 0.18	U2(vjosa)	T1	(2, 3)
OxA-191	C	40.87(ç)	21.65(ç)	~4.5	^{14}C	OxA-191	1000 ± 50	788 - 1052		0.92 ± 0.13	U2(vjosa)	T1	(2, 3)
OxA-5246	C	39.96(ç)	20.65(ç)	~10.6	^{14}C	OxA-5246	13810 ± 130	16632 - 17224		16.93 ± 0.30	U3(vjosa)	T3	(4, 3)
Beta-109162	C	39.96(ç)	20.65(ç)	~10.6	^{14}C	Beta-109162	13960 ± 260	16591 - 17812		17.20 ± 0.61	U3(vjosa)	T3	(4, 3)
Beta-109187	C	39.96(ç)	20.65(ç)	~10.4	^{14}C	Beta-109187	14310 ± 200	16935 - 17924		17.43 ± 0.50	U3(vjosa)	T3	(4, 3)
VOI24	S	39.94(ç)	20.71(ç)	~9.7	TL	VOI24	-	-		19.60 ± 3.00	U3(vjosa)	T3	(4, 3)
Tributary site	Cc	39.95(ç)	20.68(ç)	~10.5	U/Th	-	-	-		21.25 ± 2.50	U3(vjosa)	T3	(5, 3)
Old Klithonia	Cc	39.96(ç)	20.65(ç)	~8.2	U/Th	-	-	-		24.00 ± 2.00	U4(vjosa)	T4	(5, 3)
571c	Dt	38.96(ç)	20.65(ç)	~12.4	ESR	571c	-	-		24.30 ± 2.60	U4(vjosa)	T4	(2, 3)
571a	Dt	38.96(ç)	20.65(ç)	~12.4	ESR	571a	-	-		25.00 ± 0.50	U4(vjosa)	T4	(2, 3)
Old Klithonia	Cc	39.96(ç)	20.65(ç)	~8.2	U/Th	-	-	-		25.00 ± 2.00	U4(vjosa)	T4	(5, 3)
571b	Dt	38.96(ç)	20.65(ç)	~12.4	ESR	571b	-	-		26.00 ± 1.90	U4(vjosa)	T4	(2, 3)
A151	C	40.2140	20.3842	21.7	^{14}C	SacA 15999	24070 ± 150	28457 - 29352		29.35 ± 0.89	U5(vjosa)	T5	This study
Osum													
A17	Vd	40.4508	30.2900	17	^{14}C	Poz-10576	9990 ± 50	11262 - 11705		11.48 ± 0.22	T8(osum)	T2	(1)
Par-0 (*)	Sr	40.5200	20.7200	70	^{10}Be	-	-	-	2.60 ± 3.10 (&)	≥18.75 ± 1.41	T7(osum)	T3	(1)
Quaf-0 (*)	Sr	40.5500	20.6900	29	^{10}Be	-	-	-	4.44 ± 0.50(&)	≥19.80 ± 1.56	T7(osum)	T3	(1)
Paleo-Devoll													
A05	Vd	40.9092	20.1393	34	^{14}C	Poz-10572	119.5 ± 0.3 pMC	-		modern		Colluvium	(6)
Cer-08	C	41.0275	19.9817	8.4	^{14}C	Poz-39495	30 ± 80	278 - 8		0.14 ± 0.13	-	Colluvium	This study
Dev-02	C	40.9910	10.0165	16.6	^{14}C	Poz-39496	540 ± 130	726 - 307		0.52 ± 0.21	-	Colluvium	This study
Shk-06	Vd	41.0663	19.8800	52.8	^{14}C	Poz-34987	162 ± 0.46 pMC	-		Modern	-	Colluvium	(6)
Shk-22	C	41.0649	19.8714	6.3	^{14}C	Poz-39201	90 ± 30	266 - 22		0.14 ± 0.12	-	Colluvium	(6)
Cer-01	C	41.0100	20.0083	8.4	^{14}C	Poz-39197	5400 ± 40	6020 - 6293		6.16 ± 0.14	-	T2	(6)
Shk-10(*)	Sr	41.0618	19.8685	14.7	^{10}Be	-	-	-	0.77 ± 0.07	≥16.15 ± 1.00		T3	(6)
A60	C	40.9676	20.0526	19	^{14}C	Poz-12223	17640 ± 160	20477 - 21455		20.97 ± 0.49	-	T3	This study
A58	C	40.9214	20.1292	15.7	^{14}C	Poz-12116	21850 ± 150	25793 - 26810		26.30 ± 0.51	-	T4	This study
A100	C	40.9660	20.0636	24	^{14}C	Poz-17242	22780 ± 200	26825 - 28060		27.44 ± 0.68	-	T4	This study
A8	Vd	40.8271	20.2154	42,5	^{14}C	Poz-9838	23760 ± 150	28031 - 29109		28.57 ± 0.54	-	T5	This study
A1	Vd	40.8836	20.1773	42	^{14}C	Poz-8816	25500 ± 300	29603 - 30915		30.26 ± 0.66	-	T5	This study

[a] Samples: (*) for cosmogenic depth profile; only the surface sample is in this table.

[b] Type of material dated: C= Charcoal, Vd= Vegetal debris, Cc= Calcite cement, S= Sediment, Dt= Deer tooth, Sr= Siliceous rock.
[c] Geographical location: (ç) Location estimated.
[d] Dating method: ^{14}C= Radiocarbon, TL= Termoluminiscense, U/Th = Uranium series, ESR= Electron spin resonance, ^{10}Be= Cosmogenic in situ produced.
[e] Concentration of ^{10}Be: (&) Average concentration of surface samples from Carcaillet et al., 2009.
[f] Source: (1) Carcaillet et al. (2009); (2) Lewin et al. (1991); (3) Woodward et al. (2008); (4) Woodward et al. (2001); (5) Hamlin et al. (2000); (6) Guzmán et al. (in preparation).

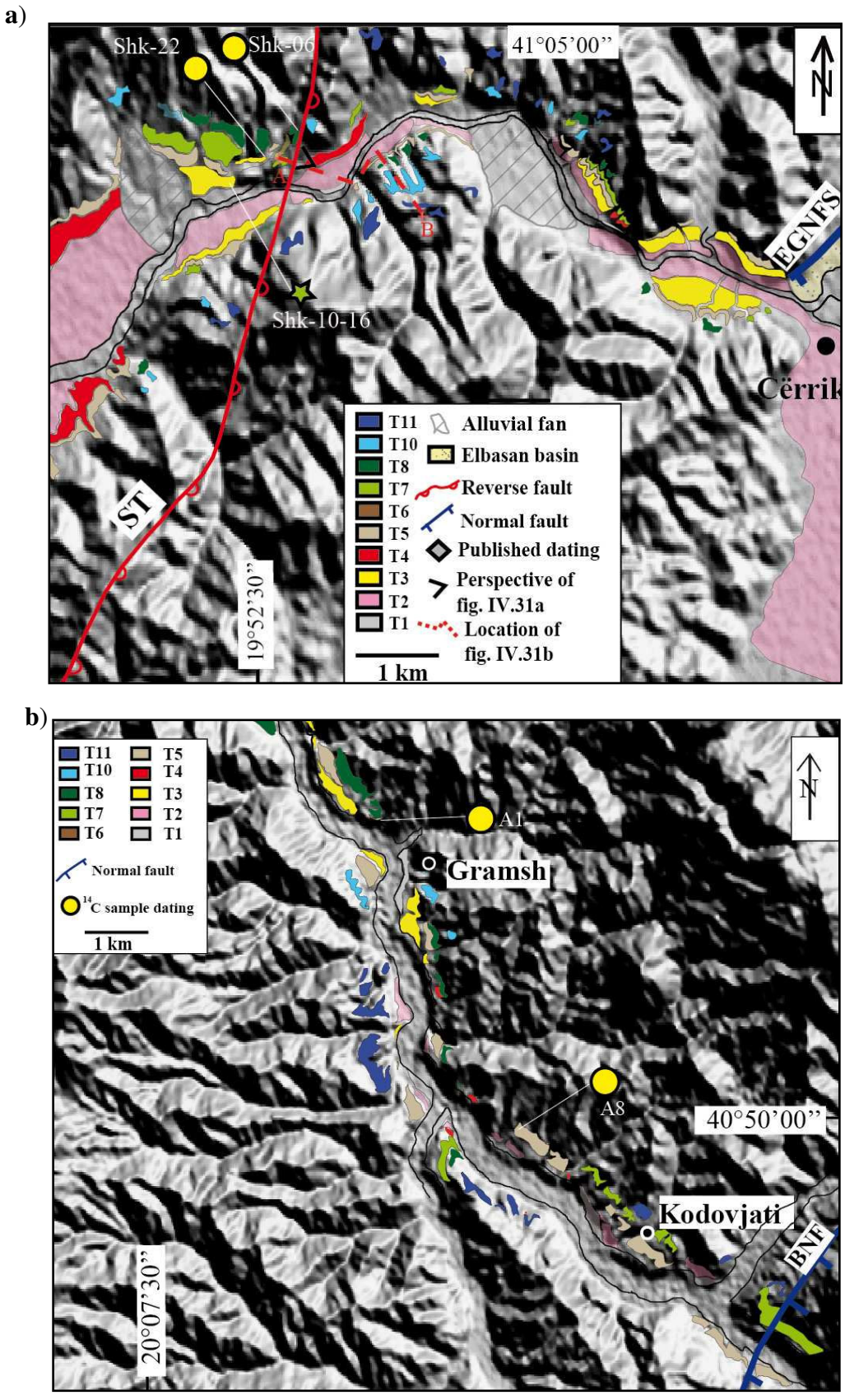

Figure IV.26. *Geomorphic map extracts of the Shkumbin (a) and Devoll (b) rivers. Samples and geographical location mentioned in the text are shown. Location of the* ***figure IV.31*** *is also shown. See* ***supplementary data A*** *for a regional geomorphic map.*

The mapping of active faults has began in 1920 (Fourcart, 1921) and numerous active faults were mapped by the Albanian geologists between 1948 and 2000 (e.g. Aliaj 1988, 1991; Aliaj et al., 1996). The NATO project n° 972342 "Seismotectonic and Seismic Albania Hazard Assessment in Albania 1998-2003"compiled all these studies in a seismotectonic map at scale 1:500000 (**figure IV.24**) and a more than 1000 pages report (Aliaj et al., 2000, summarized by Aliaj, 2000, 2004). The geological evidences in the field allowed distinguishing three tectonics phases: Middle Pleistocene to Holocene, Pliocene to lower Pleistocene and pre-Pliocene to Pliocene. This map is now used as a base for tectonic and seismogenic models of this part of the Adriatic basin (e.g. Copley et al., 2009, Basili et al., 2013 – within EU-FP7 project "Seismic Hazard Harmonization in Europe" (SHARE)). Nonetheless, this map does not give a hierarchy of the faults and all the pre-Pliocene faults are not necessarily still active. Furthermore the Aliaj et al. (2000) work is geographically restricted to the Albanian territory.

In our study, the following structures are analysed (**figure IV.24**): **1**) A large extensional system located in Eastern Albania, frequently considered as a half graben with a major NNE-oriented fault that dips towards the East (e.g. Dumurdzanov et al., 2005; Fouache, et al., 2010a; Kastelic et al., 2012); however several faults affecting its hanging wall have been documented from the initial mapping of Fourcart (1921), from the work of Tagari et al. (1993), and modified from our personal field work (Carcaillet et al., 2009). This system is separated in the following in the West Graben Normal Fault System (WGNFS) and West Ersekë Normal Fault System (WENFS); **2**) A transverse extensional fault system located in the central part of Albania, mainly oriented NE-SW. The study of this system is based on the work of Melo (1961), Aliaj (1999) and Sulstarova et al. (2000), and it is named in the following Elbasan Graben Normal Fault System (EGNFS); **3**) Two compressional faults located from the central to southern part of Albania, roughly trending NNE-SSW. These faults are named in the following the Tomorrica Thrust (TT) and Lushnje-Tepelenë Thrust (LTT). They are major geological contacts (SHGJSH, 2003), and represent the thrust at the footwall of the Kruja zone and at the footwall of the Berati belt (within Ionian zone), respectively. These thrusts are considered as locally reactivated by Aliaj et al. (2000); **4**) Another compressional fault also located in the central part of Albania between the TT and LTT, with a main orientation of NNE-SSW. The study of this fault is based on the work of Melo (1961) and Aliaj et al., (2000), and it is named in the following Shkumbin Thrust (ST); **5**) Two other compressional structures also oriented NNE-SSW and located in Western Albania, have been studied in details with hydrocarbon (Aliaj, 1971, 2006) and archaeological objectives

(Fouache et al., 2010b). These structures are respectively named Ardenica Anticline (ArA) and Coastal Thrust Fault (CTF); **6**) For the active tectonics of North-Western Greece, the work of Waters (1993) is used to define the cartography of Kipi Normal Fault (KNF), Papingo West Normal Fault (PWNF), Konitsa Normal Fault System (KNFS) and Nerotrivi Normal Fault (NNF); and **7**) The Bulcar Normal Fault (BNF) is an active fault that reactivates the base of the Mirdita zone in the middle reaches of the Devoll river. It has been detected during our field work from faulting and slicken-slide that affect the alluvial deposits of the terrace T7 (**figure IV.27**).

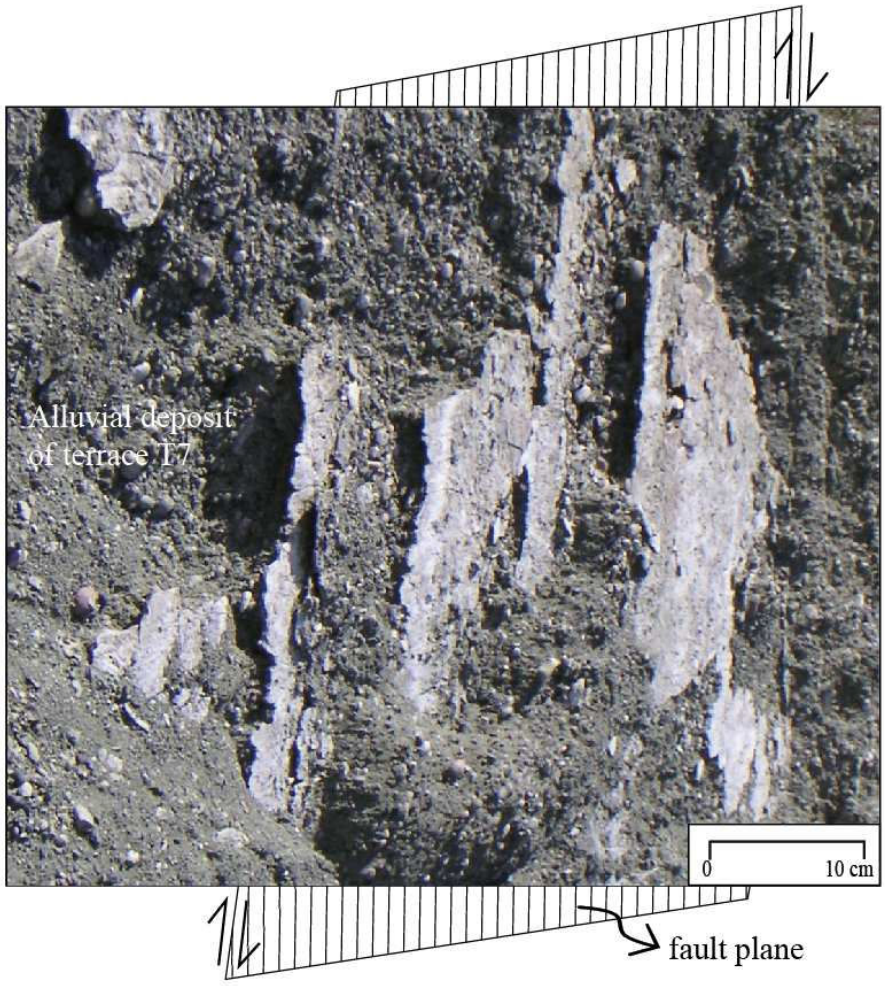

Figure IV.27. *Fault plane of the Burcal Normal Fault through the alluvial deposit of terrace T7 at the middle reaches of the Devoll river. See figure 1 for location of the fault.*

3-. Methods

Field observations, topographic maps at 1:25000 scale (Institutin Topografik te Ushtrise Tirane, 1959-1990), satellite imagery, and a 30-m digital elevation model based on the Shuttle Radar Topographic Mission (SRTM) were used to identify and characterize fluvial

terraces in the study rivers. Alluvial deposits thicknesses and elevations of the terraces above the present river-bed were measured using a measuring tape and a laser range distancemeter (vertical precision ± 0.5 m).

The remnants of the river terraces found along the rivers were correlated from the map relationship (**figure IV.26**, **supplementary data A**) and through the sedimentological and stratigraphic analysis of their alluvial deposit characteristics. This fieldwork correlation was reinforced by morphogeochronological data, obtained from data previously published by Lewin et al. (1991), Hamlin et al. (2000), Woodward et al. (2001), Carcaillet et al. (2009), as well as radiocarbon (^{14}C) dating performed specifically for this study (**Table IV.5**). The incision rates were determined by calculating the ratio between the heights of the terraces above the river and the age of the terraces (Burbank and Anderson, 2001; Pazzaglia and Brandon, 2001; Caputo et al., 2008; Weggman and Pazzaglia, 2009). Moreover, our mapping correlation takes also into account the encased pattern of several terraces. In fact, the use of a diagram representing incision rate rather than terraces heights above the riverbed, allows a further checking for terraces correlation (**figure IV.28**). Distant and solitary terraces are found in the upper reaches of the Devoll (between the km 110 and 145), in the middle reaches of the Osum (around km 141) and in the lower reaches of the Vjoja (between the km 70 to 110 and km 120 to 145), and their correlation is not clear. In other cases, the available dating for the upper and lower reaches allowed the correlation of the terraces between distant reaches.

Vertical slip rates were deduced from the local shifts in the average regional trends of the incision rates (**figure IV.29**). This approach avoids the possible effect produced by the roughness of the terrace surfaces. In most cases the terraces are not preserved above the fault trajectory, preventing the direct observation of fault scarps (Avouac, 1993), and direct estimation of slip rate. We thus used the altitude of the closest terrace remnants and the general trend of the incision rate in order to estimate the rate. Where rivers cross an aggrading domain, we are unable to know the terrace reference level within the sedimentation domain. In these cases, a minimum vertical slip rate was estimated considering the height of the present river as a reference level (**figure IV.29b**).

4-. Age of terraces

A succession of at least eleven regional terraces has been identified in Albanian rivers (Aliaj et al., 2000; Woodward et al., 2001, 2008, Carcaillet et al., 2009, Guzmán et al., in preparation). Even though not all theses terraces are found along each individual river, the Shkumbin and Devoll rivers exhibit a quite complete record (ten terraces). Most of the high

terraces are thick fill terraces (8 – 30 m-thick) whereas the lower terraces are thin strath terraces (1 – 5 m-thick) (**figures IV.26, 30, 31**).

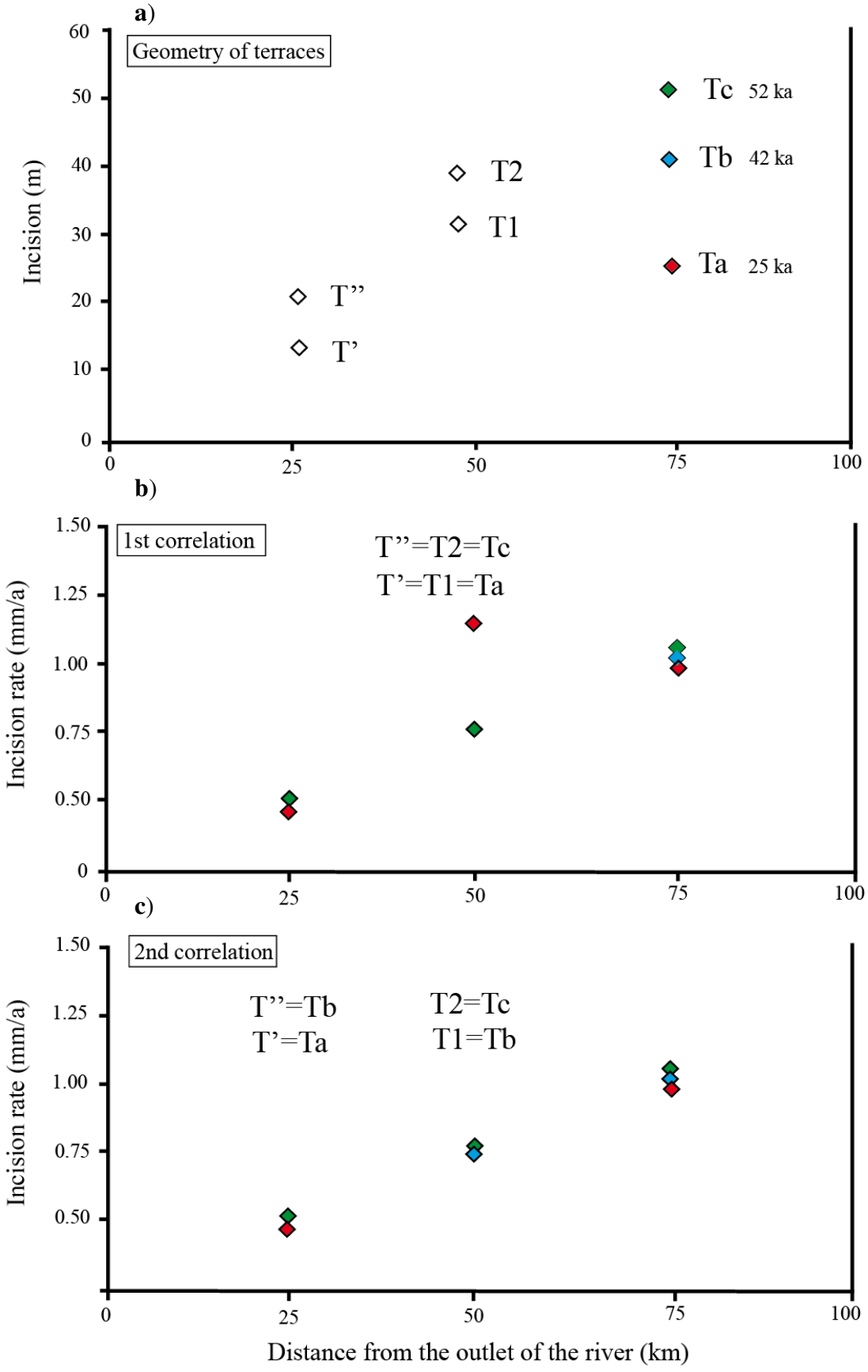

Figure IV.28. *Idealized correlation of remnants of river terraces between distant reaches of the river using an incision rate diagram. In this idealized example, the river does not cross active faults, homogeneous bedrock is present along the river valley and the incision rates at the different reaches have been different but constant over the analyzed time.* ***a****) Geometry of terraces. Different numbers of terraces are identified along the river valley. Terrace ages are provided for the three terraces located at km 75.* ***b****) In the first correlation, terraces located at km 25 and 50 are correlated with the highest and lowest terraces of km 75. Anomalous value for the incision rate of the terrace T2 located at km 50 allow identifying that the correlation proposed is probably erroneous.* ***c****) In the second correlation, terraces located at km 25 are correlated with the highest and lowest terraces located at km 75, while terraces located at km 50 are correlated with the intermediate and the lowest terraces located at km 75. The similarities between the values of the incision rates in the diferent reaches indicate that the correlation proposed is coherent.*

Sixty-seven numerical ages are available for all the Albanian terraces dated along six rivers. There is a lack of numerical ages for the highest identified terraces. By contrast, sixty-one datings allow constraining the ages of the eight lower terraces. Ten new numerical ages are provided in this study and forty-four are provided by previous studies (in order to simplify the presentation of ages, in this study, we only show the ages for the terraces used for the incision rate reconstruction (T5 to T1), for all dating **see supplementary data B**) (Lewin et al., 1991; Hamlin et al., 2000; Woodward et al., 2001; Koçi, 2007; Carcaillet et al., 2009, Guzmán et al., in preparation). These ages result from analytical measurements coming from different parts of the river catchments, from different rivers or from different dating methods (i.e. ^{14}C, ^{10}Be, U series (U/Th), electron spin resonance (ESR), thermoluminescense (TL) – **Table IV.1**).

According to the strategy used by Carcaillet et al (2009) and Guzmán et al. (in preparation), ^{10}Be ages used in this study represent the surface exposure ages of the terraces (Gosse and Phillips, 2001). ^{14}C ages and the others ages achieved in previous studies, using others methods and strategies (U/Th, ESR, TL) (Lewin et al., 1991; Woodward et al., 2001, 2008), represent the timing of deposition or formation of a particular sediment or material within the alluvial deposit of the terrace (Noller et al., 2000). ^{14}C samples taken in this study, and also the material used in previous dating studies (e.g. calcite cement, deer tooth) were taken from the sediments that correspond to the ultimate phase of river aggradation (**figure IV.30**). These ages thus represent a maximum age of abandonment of the river terrace. Despite the different meaning of the samples dated, a good agreement between most of the ages analysed in this study, either new or published, allow suggesting that the process of

formation of each terrace in Albania occurs in a maximum time span of few thousand years (**figure IV.32**). Thus, considering the uncertainties on the ages and the aim of this study, we assumed that the formation of each Albanian terrace is synchronous at the spatial scale of the river catchments.

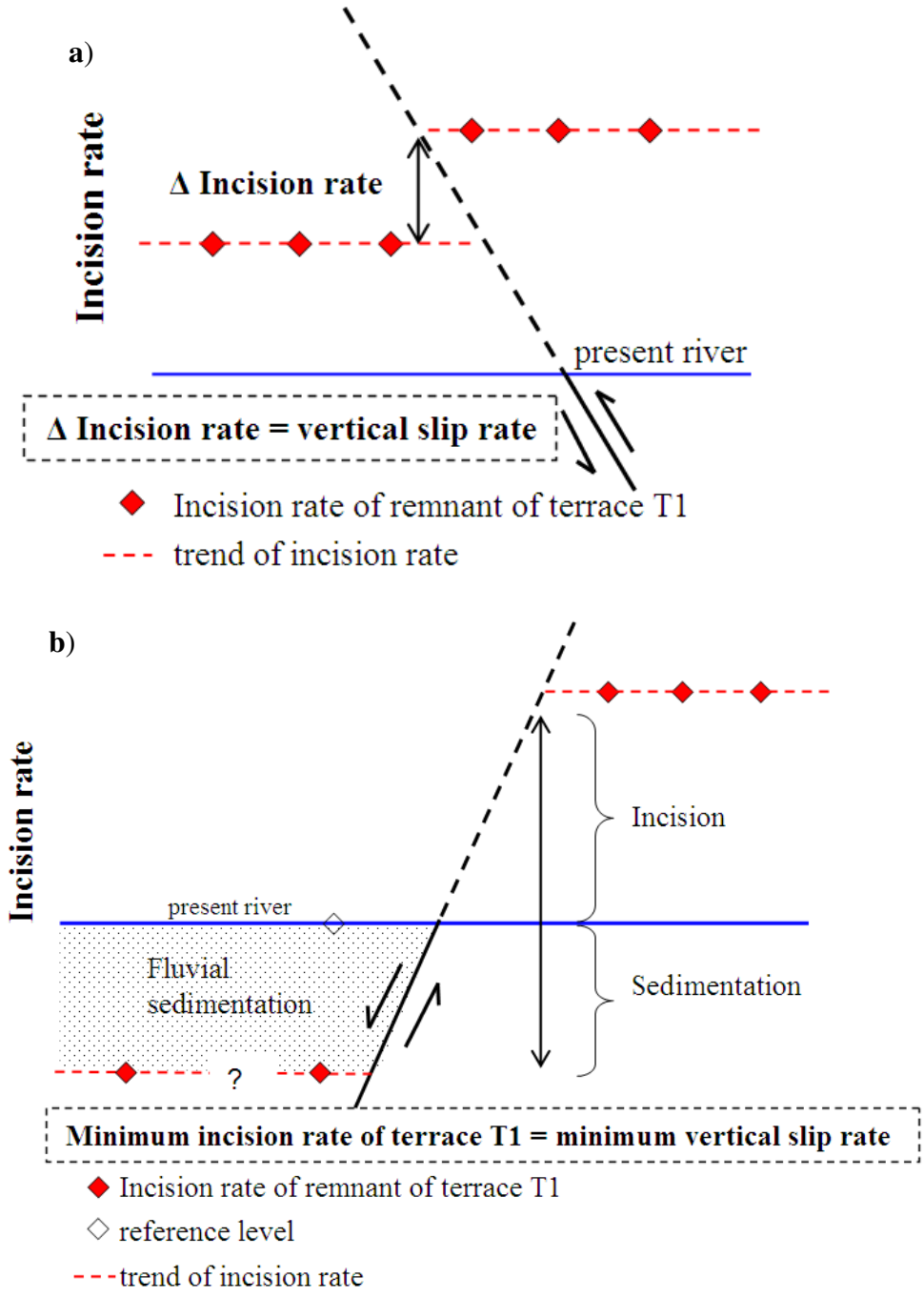

Figure IV.29. *Definition of fluvial incision and vertical slip rate in a context of:* ***a****) without sedimentation;* ***b****) with sedimentation in the footwall block. In case b, the level of the present river is taken as a reference level in the footwall block. The incision and the vertical slip rates estimated are thus minimal.*

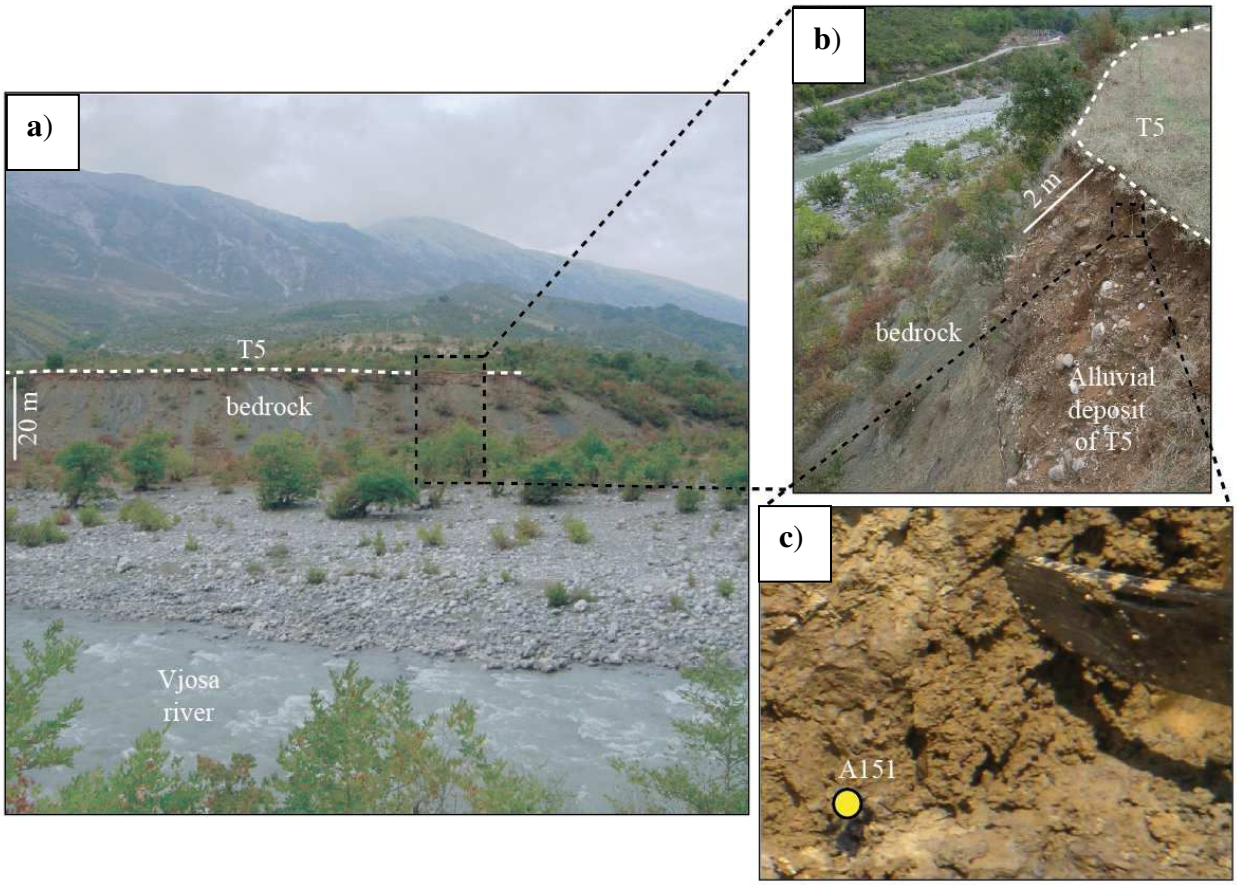

Figure IV.30. *Example of a thin strath terrace above the Vjosa river.* ***a****) General view: the top of the terrace is 22 m above the low flow of the river.* ***b****) View of the alluvial deposit located above the strath surface. The deposit is around 2 m thick. It is constituted by gravels and pebbles embedded in a clay and silt matrix. Radiocarbon sample was taken close to the top of the terrace.* ***c****) View of a sampled organic material (sample A151, in* ***Table IV.5****) that gives an age of abandonment of 29.35 ± 0.89 cal ka BP ka for this terrace (terrace T5).*

The age of each terrace is determined from the normal distribution of individual calibrated ages and their associated two sigma errors (95%) using the cumulative probability command within OxCal 4.1 calibration program (Ramsey, 2009). The result is a probability density plot of all the ages (**figure IV.32**), a representation already used in similar studies of large set of dates (Meyer et al., 1995; Wegmann and Pazzaglia, 2002, 2009). This gives six high probability ages for the period between 60 to 12 ka: 51.8 ± 2.4 ka; 41.8 ± 0.5 ka; 34.8 ± 3.2 ka; 29.4 ± 0.8 ka; 24.8 ± 1.8 ka; 18.7 ± 2.1 ka from T8 to T3. All these ages are coherent with climatic river terrace ages documented along the wide Mediterranean domain (e.g. Fuller et al., 1998, Macklin et al., 2002, Wegmann and Pazzaglia, 2009) and dicussed in detail by Guzmán et al. (2011) and Guzmán et al. (in preparation). Available datings for terrace T2 are more scattered. Nevertheless all of them are close to a global cold climatic event at 8.2 ka

identified by Kallel et al. (2000) in the Eastern Mediterranean and in the sediment of the Prespa lake located in the West border of Albania (Wagner et al., 2010). Hence, we argue that the age of abandonment of terrace T2 is around 8.2 ka. T1 is the lower terrace and in some localities the base of the alluvial deposit that composed this terrace is lower than the flow channel. Thus, we considered that this terrace could still be affected by the river dynamics. The most probable ages discussed here are combined with our mapping correlation, to estimate the incision rates for all terrace remnants along the Shkumbin, Devoll, Osum and Vjosa rivers.

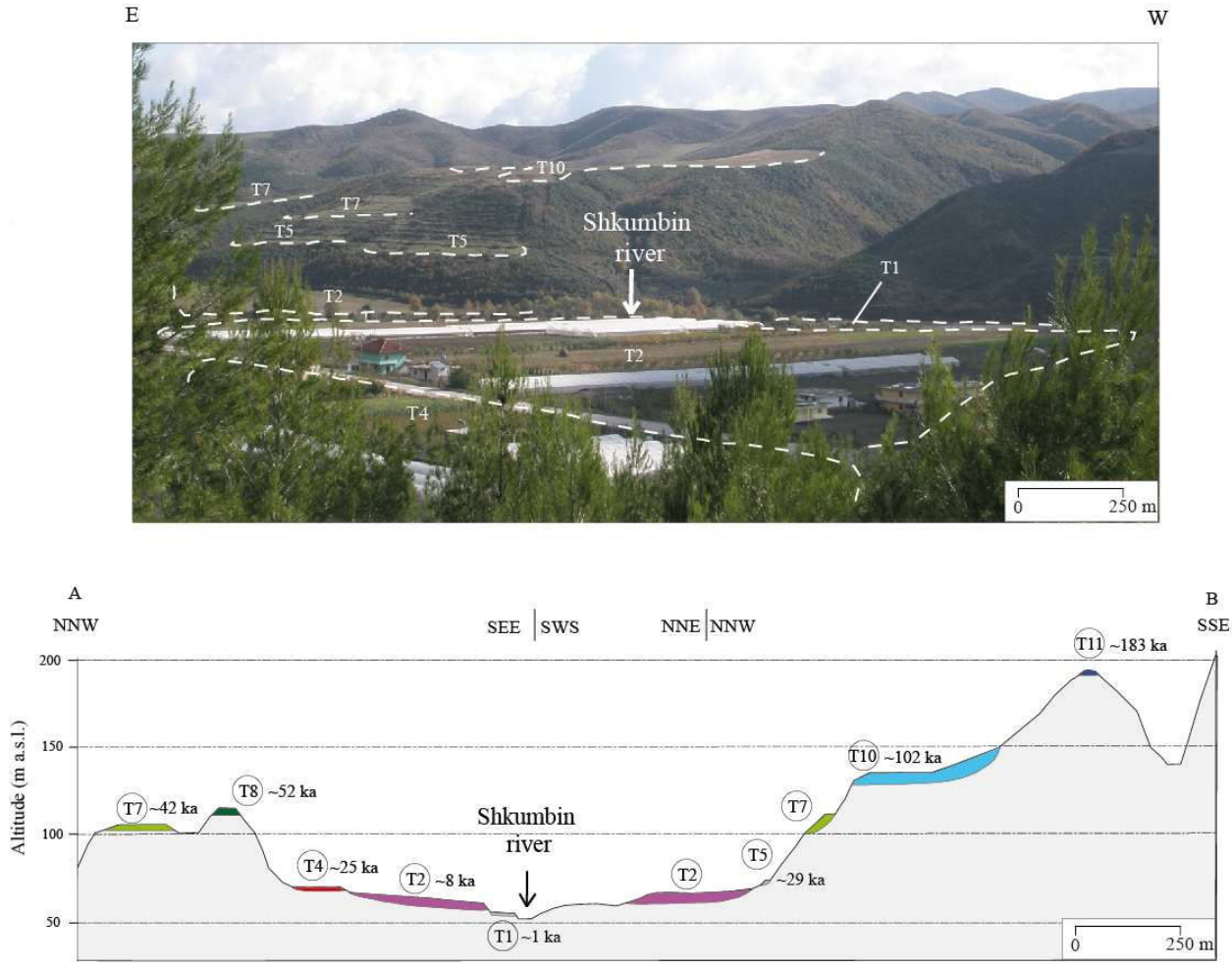

***Figure IV.31. a**) Panoramic view of the lower Paleo-Devoll river showing the location of terraces. The numbers refer to the nomenclature proposed in Guzmán et al (in preparation). The present Shkumbin river is shown in the figure. **b**) Cross section through the encased terraces in the lower Paleo-Devoll. The ages of the terraces from previous studies are indicated (Lewin et al., 1991; Hamlin et al., 2000; Woodward et al., 2001; Koçi, 2007; Carcaillet et al., 2009, Guzmán et al., in preparation)*

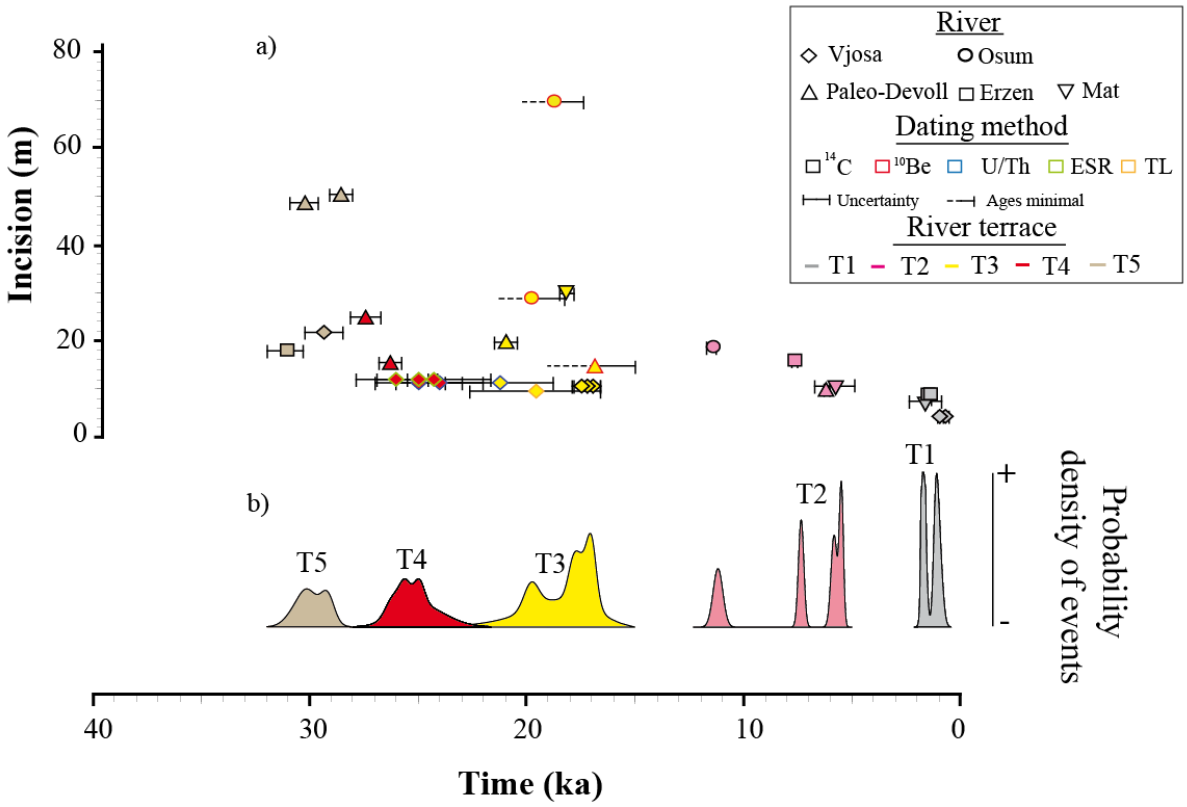

Figure IV.32. *Compilation of Albanian terraces ages for the last 30 ka (**Table IV.5**). **a**) Plot of incision versus terraces ages. Each terrace is represented by a symbol related to the river, the fill of the symbol corresponds to the dating method. **b**) Probability density curves of age of terraces. The probability curves was produced by calculating calendar ages and their two sigma (95%) analytical errors and then summing the normal probabilities distribution defined by individual ages using the OxCal program version 4.1 (Ramsey, 2009).*

5. Morphological analysis

5.1. Shkumbin and Devoll system

These two rivers are located in the central part of Albania (**figures IV.24, 25**). Nowadays, the Shkumbin and Devoll rivers flow in two different catchments. However geomorphologic and sedimentologic evidence around the Cërrik plain (Melo, 1961; Guzmán, et al., 2011) suggest that the downstream part of the Shkumbin corresponds to the Paleo-Devoll river (**figure IV.24**). This divergence occurred around ~6 ka (Guzmán, et al., 2011). As a consequence, terraces developed along the upper and middle Devoll and lower Shkumbin can be analysed together along the Paleo-Devoll profile.

The dominance of sedimentation against incision along the last 25 km (close to the sea) of the Paleo-Devoll (Fouache et al., 2010b) prevents the preservation of terraces in this area. On the other hand, ten river terraces were identified along the section located between

25 and 165 km from the Adriatic Sea. Among these, remnants of the terraces T4 and T2, dated respectively around ~25 and 8.2 ka, are the best preserved and are nearly continuous along almost all the section (**figure IV.33**). Hence, the geometries of these two terraces were used for the study of fault activity.

In **figure IV.33**, we plotted together: 1) the modern river profile, 2) the Quaternary active faults (adapted from Aliaj et al., 1996, 2000), 3) the river incision rates estimated for each remnant of terrace and 4) the average regional trend of the incision rates for each tectonic block. This plot shows a regional upstream increment of the incision rate of the two terraces until km 112 of the valley, where the incision rate starts decreasing. However, the number of preserved remnants of terraces T2 and T4 in this area is limited; therefore the trend of the incision rate in the upper reaches of the river remains uncertain. The river incision rate estimated from T2 is higher than the incision rate deduced from T4, a trend already evidenced and discussed by Carcaillet et al. (2009).

Local shifts in the incision rate are identified at km 35, 68, 73, 92, 110 and 149 of the valley (**figure IV.33**). These shifts are situated close to the emergence of the following faults: LTT, EGNFS, TT, BNF and WGNFS (**figures IV.24, 32**). No lithological changes occur at these points, except at km 110 (**figure IV.25**). Therefore, we argue that the local shifts in the incision rate observed along of the Devoll and Shkumbin rivers are induced by the Quaternary activity of the mentioned faults. Assuming a constant vertical motion of the faults since at least 25 ka, we estimated a vertical slip rate for LTT between 0.7 and 1 mm/a, for EGNFS > 1 mm/a, for TT ~0.4 mm/a, for BNF ~0.3 mm/a and for WGNFS > 0.8 mm/a (**figure IV.33**, **Table IV.6**). No local shift in the regional trend of the incision rate is observed close to the emergence of the ST. Hence, either the activity of this fault does not influence the evolution of the river profile or this fault has been inactive since 25 ka.

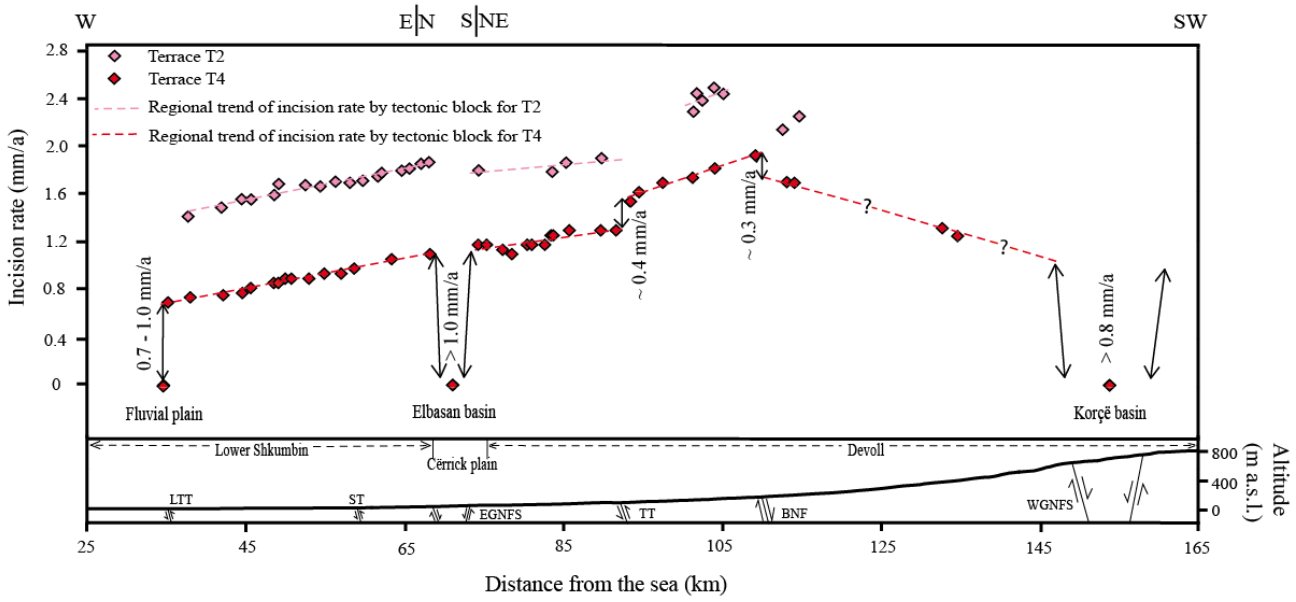

Figure IV.33. *Evolution of the incision rate along the combined river profile of the lower Shkumbin and Devoll (Paleo-Devoll river). Left axis is the calculated incision rate; right axis is the elevation of the present-day river bed. Colour of the diamonds refers to the different terraces units. Into the lower box, appear the present-day river profile, on which are indicated the active faults. In the sedimentation zones (Fluvial plain, Elbasan and Korçë basins) the correlative deposits of terrace T4 are located in the present river-bed. In the river profile are located the Lushnje - Tepelenë Thrust (LTT),Shkumbin Trust (ST), Tomorrica Thrust (TT), the Burcal Normal Fault (BNF) and the West Graben Normal Fault System (WGNFS).*

5.2-. Osum river

This river is located in Southern Albania (**figure IV.24**), flows over 160 km, and connects with the Devoll river in the fluvial plain downstream of the city of Berat. This confluence forms the Seman river, which together with its tributaries forms the longest drainage system of Albania.

In this study, we analyzed the reaches of the Osum river located between 120 and 220 km from the Adriatic Sea, where the preservation of nine river terraces (Carcaillet et al., 2009) allows the estimation of the effect of faults activity. As for the Shkumbin and Devoll, due to the objectives of the present study, we only present the incision rate of the two most frequently observed terraces developed around ~19 and 8.2 ka (T3 and T2, respectively) that are presented in **figure IV.34**.

A regional upstream increment in the incision rate for the two terraces is observed. An abrupt local shift in the trend of the incision rate of terrace T3 is identified at km 217 of the valley. Another shift is recognizable from the slope-break in the regional trend of incision rate

of the terrace T2. This shift is located between 175 and 192 km from the Adriatic Sea. A third shift located between 150 and 166 km is less evident, but it can be identified from the extrapolation of the regional trend of incision rate of terrace T3. The emergence of the TT (at km 164) and WENFS (at km 190 and 217) are located in the zones where these shift are observed (**figure IV.34**). Therefore, we propose that the local shifts in the trend of the incision rate are associated with Quaternary activity of the TT and WENFS. We estimate that at least for the last 19 ka the vertical slip rate of the TT is ~0.3 mm/a, while it varies between 1.3 and 2 mm/a for the West and East segment of WENFS, respectively (**figure IV.34**, **Table IV.6**). These last values agree with the estimation (2.2 mm/a) done by Carcaillet et al. (2009) for the East segment.

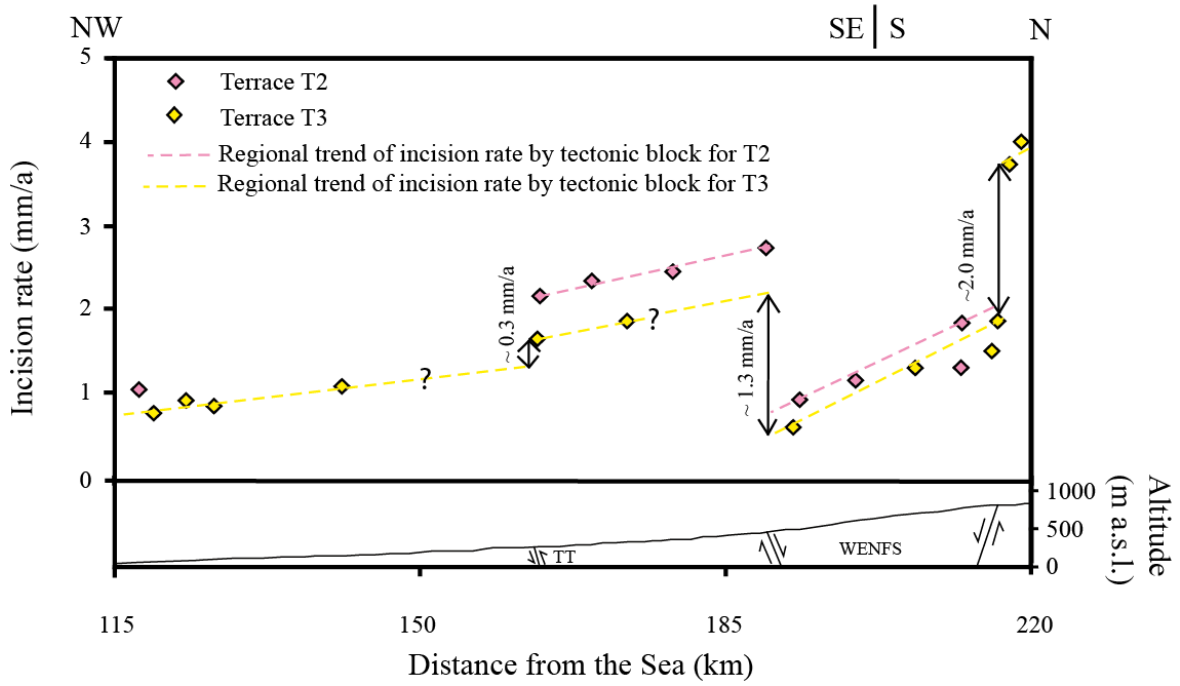

Figure IV.34. *Evolution of the incision rate along the river profile of the Osum. Bold lines represent normal faults belonging to West Ersekë Normal Fault System (WENFS) and Tomorrica Thrust (TT).*

5.3. Vjosa river

The Vjosa river, called Voidomatis in Greece, flows towards NW for around 272 km from the Greek land to the Adriatic Sea (**figure IV.24**). The Vjosa flows in an atypical catchment in the Mediterranean zone: its upper part was glaciated during the Last Glacial Maximum (LGM) (Clark et al., 2009), as suggested by well-preserved glacial features (Lewin et al., 1991).

Five river terraces for the section of Vjosa located between 60 and 165 km from the Adriatic Sea were identified (**figure IV.35**). These terraces are located in small reaches and the information about the spatial evolution of the incision rate is limited. However, the continuity of the terraces T4 and T3 between the km 109 and 117 allow evaluating the activity of the fault in this zone with a good degree of confidence. A local shift of the incision rate observed at km 112 is probably associated with the Quaternary activity of the LTT. Thus, we estimate at least for the last 25 ka a vertical slip rate of ~ 0.3 mm/a for this fault.

Additionally, the extrapolation of the regional trend of the incision rate towards the Konitsa basin, allows estimating a slip rate of > 0.4 mm/a for the NNF and KNFS (**figure IV.35**, **Table IV.6**).

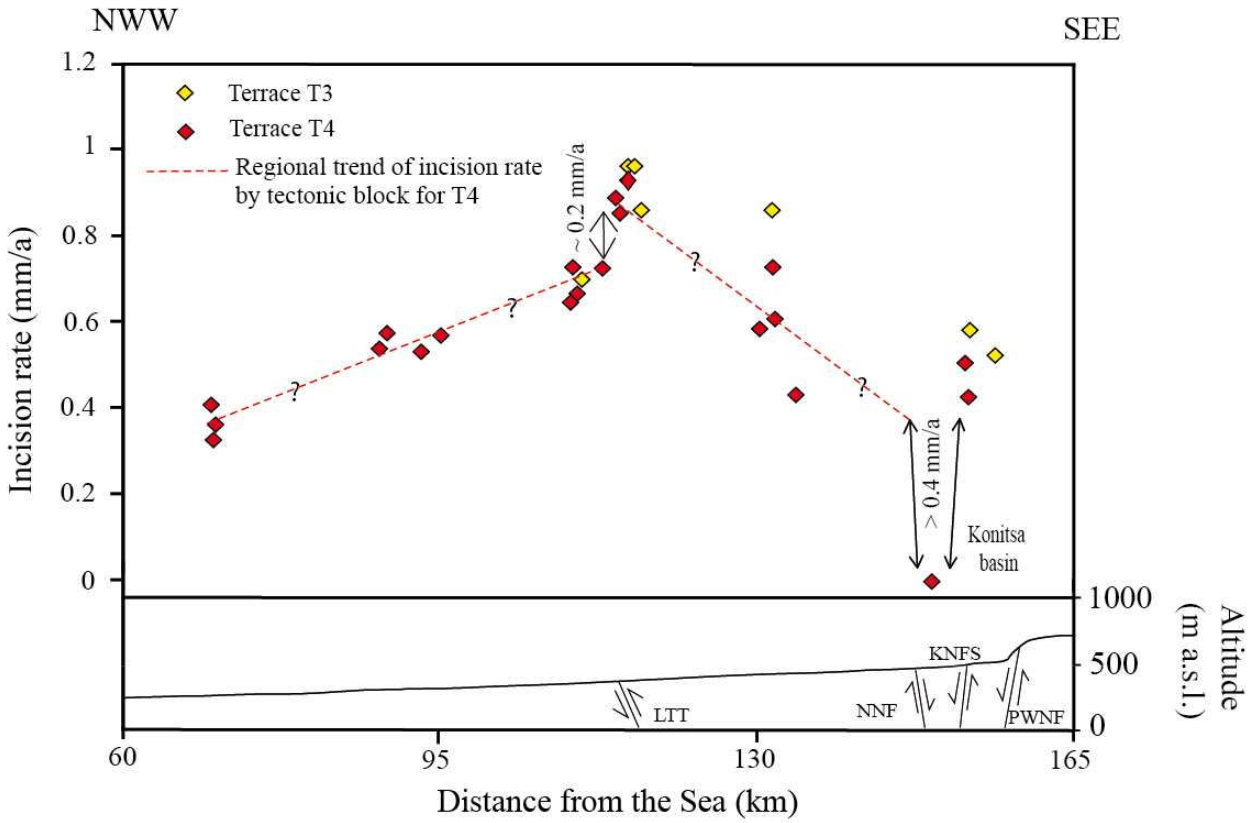

Figure IV.35. *Evolution of the incision rate along the river profile of the Vjosa. In the Konitsa basin the correlative deposit of terrace T4 is located in the present river-bed. In the river profile are located the Lushnje-Tepelenë Thrust (LTT), Nerotrivi Normal fault (NNF), Konitsa Normal Fault System (KNFS) and Papingo West Normal Fault (PWNF).*

Table IV.6. Vertical slip rate of active structures in Albania, analyzed from the incision of river terraces of Paleo-Devoll, Osum and Vjosa rivers.

Structure name	Acronyme (in text)	River	Vertical slip rate (mm/a)[a]	Active fault length (km)		
				Aliaj et al. (2000)	Waters (1993)	This study[b]
Coastal Thrust Fault	CTF	Paleo-Seman	~ 0.1 (1)	≥ 80	-	-
Ardenica Anticline	ArA	Paleo-Seman	~ 0.1 (1)	-	-	-
Lushnje-Tepelenë Thrust	LTT	Paleo-Devoll	0.7 – 1.0	~ 100	-	> 120
Lushnje - Tepelenë Thrust	LTT	Vjosa	< 0.2		-	
Tomorica Thrust	TT	Paleo-Devoll	~ 0.4	~ 20	-	≥ 50
Tomorica Thrust	TT	Osum	~ 0.3		-	
Elbasan Graben Normal Fault Systems	EGNFS	Paleo-Devoll	> 1.0	≥ 5	-	≥5
Burcal Normal Fault	BNF	Paleo-Devoll	~ 0.3	-	-	~ 10
West Ersekë Normal Fault Systems	WENFS	Osum	1.3 – 2.0	~ 10	-	> 20
West Graben Normal Fault Systems	WGNFS	Paleo-Devoll	> 0.8	≤ 20	-	> 20
Nerotrivi Normal Fault	NNF	Vjosa	> 0.4	-	15	≥ 15*
Konitsa Normal Fault Systems	KNFS	Vjosa	> 0.4	-	15	≥ 15*

[a] Vertical slip rate: (1) Fouache et al. (2010b).
[b] Active fault length: (*) Length for one segment of the system.

5.4. Comparison between seismotectonics and Quaternary fault activity at regional scale

In order to evaluate the extent of the major faults in Southern Albania, the vertical slip rates of the faults evidenced in this study and those estimated in previous published works were plotted together on a regional map (**figure IV.36**) (Carcaillet et al., 2009, Fouache et al., 2010 - **Table IV.6**). The neotectonic map of Albania (Aliaj et al., 1996, 2000) and Northwestern Greece (Waters, 1993) were used as a base for mapping the faults. In this map, the line thickness is proportional to the vertical slip rate of each fault. The results suggest that: a) the largest vertical slip rate of the active faults is associated to the extensional domain in the Eastern part of Southern Albania; b) the normal faulting linked to the E-W extension of the Eastern Albanian graben systems seems more active than the normal faulting linked to the NW-SE extension that affect the NW part of Greece; c) the Elbasan Graben Normal Fault System is also very active.

As there are no significant differences between geodetic strain rates and seismological derived strain rates (Jouanne et al., 2012), it is suggested that no aseismic deformation occurs in Albania and active faulting is expected to be linked to a succession of earthquakes. The comparison between the seismic activity of the three well-defined seismic belts (Aliaj, 1988, 2000; Muço, 1998; Sulstarova et al., 2003) and the slip rate of the faults confirms the superficial activity of the faults in the Peshkopia-Korçë earthquake belt and the Vlora-Elbasan-Dibra transverse belt. For the Ionian-Adriatic coastal earthquake belt there is a

discrepancy between the high seismic activity and the small evidences of fault activity from our morphotectonic approach. This discrepancy could either be due to a bias induced by the dominance of sedimentation and the absence of preservation of terraces in the zone, or to compressional earthquakes that do not cross the upper part of the crust. Thus, other geophysical or geodetic approach should be used to better constrain this issue.

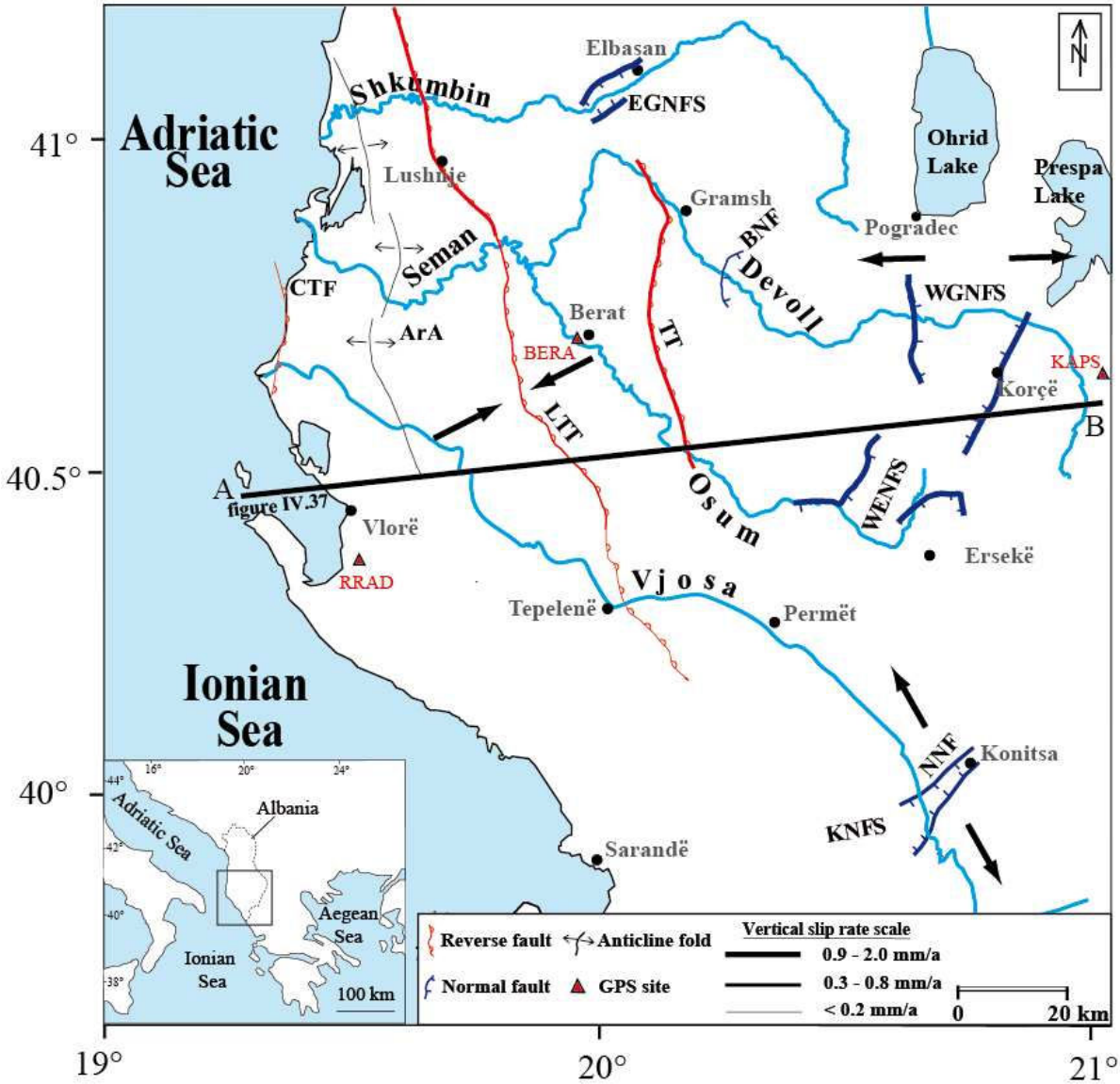

Figure IV.36. *Regional map showing the vertical slip rates of the active faults inferred from incision of river terraces (the whole neotectonic structures inferred in Albania are shown on* ***figure IV.24****). Thickness of the fault traces is proportional to the valuse of vertical slip rate. Black arrow represents the orientation of the maximum extension and shortening of the present day deformation field of Albania (from Jouanne et al., 2012).Location of the* ***figure IV.37*** *is also shown in the map.*

5.5-. Comparison between present-day deformation and Quaternary fault activity at regional scale

An estimate of the current displacement along the faults from GPS measurements is not possible due to the small number of GPS sites at the vicinity of the faults and their elastic loading during seismic cycle. Nonetheless the present-day deformation rates deduced from GPS velocities (Jouanne et al., 2012) and our study outline the major role of the LTT: this fault is more than 120 km long (**Table IV.6**) and is also the present-day boundary between the Western domain affected by the Apulia/Albanide collision and the Eastern domain affected by a displacement with a component toward the South (Jouanne et al., 2012). Our geomormophological study and GPS data also confirm the major activity of the normal fault system of Eastern Albania.

A comparison between the displacements of three GPS sites (**Table IV.7**) located on the three domains limited by the LTT and the normal fault system of Albania allows the following considerations:

On a regional West-East cross-section (**figure IV.37**), the GPS measurements indicate: 1) a displacement component towards the East of 1.3 mm/a between the Western coast (RRAD site) and a station located at the hanging-wall of the LTT (BERA site); 2) a displacement component towards the East of 2.6 mm/a between the Internal Albanides (KAPS site) and the BERA station. The horizontal shortening associated with the active thrust faults along this cross section can also be estimated by using the slip rate inferred from the incision rate and a mean dip of 30° for the thrusts of ArA and LTT, and a dip of 60° for the normal faults of WENFS; we found a shortening of ~0.6 mm/a between the coast and Berat city, and an extension between 0.9 and 1.3 mm/a associated with the normal fault systems of Eastern Albania. As there are no significant differences between geodetic strain rates and seismological derived strain rates (Jouanne et al., 2012), the discrepancies between GPS measurements and geomorphological estimates do not mean that the interseismic velocities of the Albania active faults are unsteady throughout the seismic cycle. These differences could be caused by the under-estimation of vertical slip rates in the sedimentation zones in this study, or by the distribution of the deformation on other active structures not analyzed in this study.

North-South components of displacement evidenced by the three GPS stations are larger than the East-West components, implying a dextral oblique slip component along most of the active faults. These dextral components cannot be estimated from the vertical incision of the river, and no faults clearly horizontally offset the river profiles.

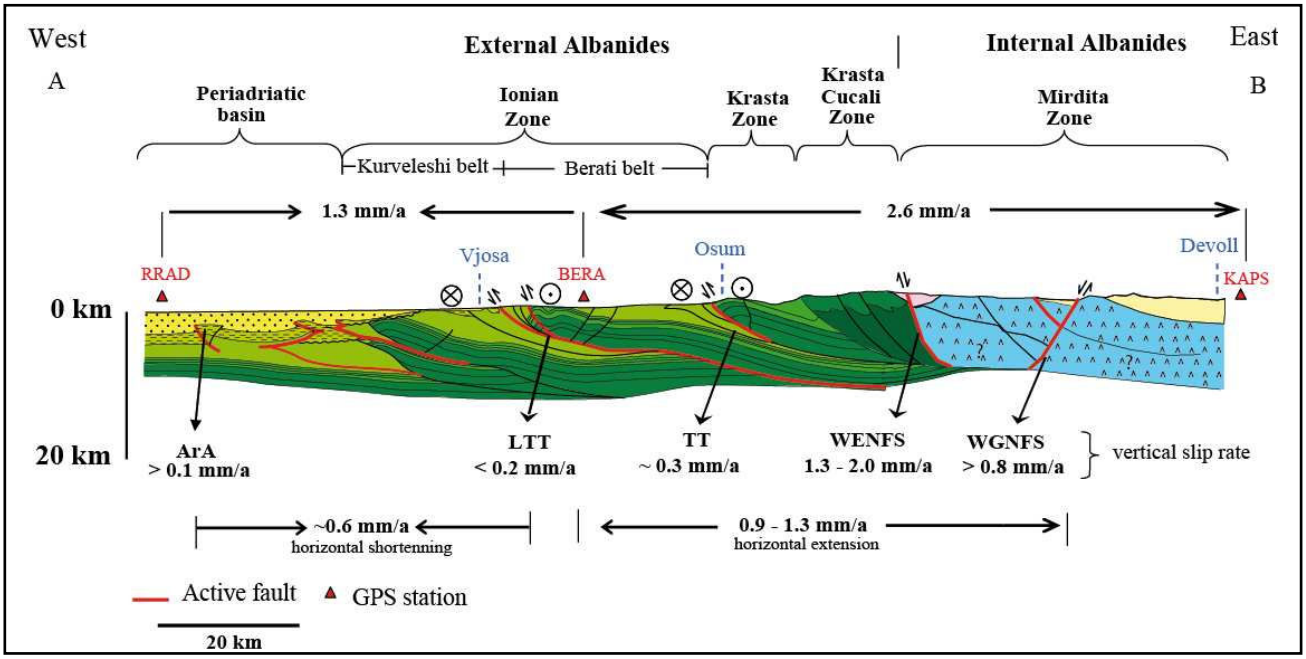

Figure IV.37. *Simplified structural cross-section through the Southern Albanides adapted from, the Geological Map of Albania (SHGJSH, 2003), Kilias et al. (2001), Roure et al. (2004) and Carcaillet et al. (2009). The neotectonic framework is modified from Aliaj et al. (1996, 2000) and the strike-slip component deduced from GPS network (Jouanne, et al., 2012). Values of relative displacements between GPS sites are indicated above GPS stations. Vertical slip rates calculated in the present study are shown, as well as, the horizontal shortening and extension estimated from the slip rate.*

Table IV.7. *Velocities of GPS sites in a ITRF2005 (Altamimi et al., 2007) (from Jouanne et al., 2012). Ve and Vn are respectively the component of velocity towards E and N. See text for discussion of the velocity with respect to BERA at the hanging wall of the LTT.*

GPS site	Geographical location	Latitude (°N)	Longitude (°E)	Ve (mm/a) respect to ITRF2005 (Altamimi et al., 2007)	Ve (mm/a) respect to ITRF2005 (Altamimi et al., 2007)	Ve (mm/a) respect to BERA site	Ve (mm/a) respect to BERA site
RRAD	Sea border	19.4938	40.3654	23.748	17.168	1.3	2.0
BERA	Berat	19.9455	40.7082	22.405	15.181	0.0	0.0
KAPS	Greek border	21.0404	40.6226	25.005	10.365	2.6	4.8

6. Conclusion

In this study, we quantified the spatial and temporal evolution of the incision rate along four rivers in Southern Albania. From this quantification, we identified local shifts in the regional trend of incision rates associated with Quaternary faults. These incision rate shifts allowed the quantification of the vertical slip rate of eight active faults in the area. Most of them were already considered as potential seismogenic sources (Aliaj et al., 2000; Sulstarova

et al., 2003; Basili et al., 2013 and the SHARE database) and this study furnishes more precisions: 1) the thrust at the footwall of the Berati belt (LTT) is active on a length of more than 120 kilometers and its vertical slip rate is ~ 0.8 mm/a close to Lushnje in the North and strongly decreases towards the South; 2) the Tomorica Thrust (TT) at the base of one of the highest summit of Albania is active with a vertical slip rate of 0.3 mm/a and on a length of at least 50 km; 3) the Elbasan Graben Normal Fault System (EGNFS) has a vertical slip rate ≥ 1 mm/a on a fault segment of at least 5-km-long; 4) the Graben system of Southeastern Albania is very active on its western side. The fault system is formed by several segments with a length of at least 20 km. The vertical slip rates of the segments located West of Ersekë (WENFS) vary between 1.3 and 2.0 mm/a, while that for the segments located West of Korçë (WGNFS) are ≥ 0.8 mm/a; 5) the vertical slip rate of the normal fault system of Northwestern Greece (NNF and KNFS) is ≥ 0.4 mm/a along fault segments of at least 15 km lenght. Finally our field work has detected an unknown active fault that reactivates the base of the Mirdita zone in the middle reach of the Devoll river (BNF). The vertical slip rate of this fault is ~0.3 mm/a.

Finally, the results of this study also put in evidence that the fluvial incision is maximal at the transition between the domains of extensional and compressional tectonics, suggesting that the regional uplift is maximal in this zone and reaches more than 1 mm/a.

7. Acknowledgements

The authors thank the NATO SFP 977993 and the Science for Peace team to have supported this work. This publication was also made possible through support provided by the IRD-DPF. O.G. thanks to INQUA - Terpro for the grant to participate in the 2nd INQUA-ICGP 567 International Workshop on Active Tectonics, Earthquake Geology, Archaeology and Engineering.

8-. References

Aliaj, Sh., 1971. Adriatic depression and its structures in the light of geophysical dta. Bul. USHT, Ser. Shk. Nat. 3, 25-41 (In Albanian).

Aliaj, Sh.,1988. Neotectonic and seismotectonic of Albania. Ph.D. Thesis, Archive of Institute of Seismology, Tirana, Albania. (in Albanian).

Aliaj, S. H., 1999. Transverse fault in Albania Orogen front. Albania journal of Natural and technical sciences 6, 121-132.

Aliaj, Sh., 1991. Neotectonic structure of Albania. Albanian J. of Nat. Technol Sci. 4, 79-98.

Aliaj, Sh., 2004. Seismic source zones in Albania. NATO Sciences for peace programme, Project N° 972342 "Seismotectonis and Seismic hazard Assesment in Albania" Final report.

Aliaj, Sh., 2006. The Albanian Orogen: Convergence zone between Eurasia and the Adria microplate. In: Pinter, N., Grenerczy, G., Weber, J., Stein, S., Medak., D. (Eds), The Adria Microplate: GPS Geodesy, Tectonics and hazards. NATO Science Series. IV/61 Earth and Environmental Sciences. 133-149.

Aliaj, Sh., 2000. Neotectonics and seismicity in Albania. In: Melo, S., Aliaj, S., Turku, I. (Eds.), Geology of Albania, Beitrage zur regionalen Geologie der Erde. Gebruder Borntrager, Berlin, 28, pp. 135–178.

Aliaj, Sh., Melo, V., Hyseni, A., Skrami, J., Mëhillka, Ll. Muço, B., Sulstarova, E., Prifti, K., Pashko, P., Prillo, S., 1996. Neo-tectonic map of Albania in scale 1:200000. Archive of seismology Institute, Tirana, Albania (in Albanian).

Aliaj, S., Sulstarova, E., Muço, B., Koçiu, S., 2000. Seismotectonic map of Albania in scale 1: 500000. Archive of Institute of Seismology, Tirana, Albania. (in Albanian).

Altamimi Z.. Collilieux X.. Legrand J.. Garayt B.. Boucher C., 2007. ITRF2005: A new release of the International Terrestrial Reference Frame based on time series of station positions and Earth Orientation Parameters. J. of Geophys. Res.. VOL. 112, B09401, doi:10.1029/2007JB004949/.

Avouac, J-P., 1993. Analysis of scarp profiles: evaluation of errors in morphologic dating. J. of Geophys. Res. 98, 6745 – 6754.

Basili, R., Kastelic, V., Demircioglu, M. B., Garcia Moreno, D., Newser, E., S., Petricca, P., Sboras, S. P., Besana-Ostma, G. M., Cabral, J., Camelbeeck, T., Caputo, R., Danciu, L., Dornac, H., Fonseca, J., Garcia-Mayordomo, J., Giardini, D., Glavatovic, B., Gulen, L., Ince, Y., Pavlides, S., Sesetyan, K., Tarabusi, G., Tiberti, M. M., Utkucu, M., Valensise, G., Vanneste, K., Vilanova, S., Wössner, J., 2013. The European Database of Seismogenic Faults (EDSF) compiled in the framework of the Project SHARE. http://diss.rm.ingv.it/share-edsf/, doi: 10.6092/INGV.IT-SHARE-EDSF.

Burbank, D.W., Anderson, R.S., 2001. Tectonic Geomorphology. Blackwell, Great Britain. 274 pp.

Caputo, R., Salviulo, L., Bianca., M., 2008. Late Quaternary activity of the Scorciabuoi Fault (Southern Italy) as inferred from morphotectonic investigations and numerical modelling Tectonics 27, TC3004, doi:10.1029/2007TC002203.

Caputo, R., Bianca, M., D'Onofrio, R., 2010. Ionian marine terraces of Southern Italy: Insights into the Quaternary tectonic evolution of the area. Tectonics TC4005, doi:10.1029/2009TC002625.

Carcaillet, J., Mugnier, J.L., Koçi, R., Jouanne, F., 2009. Uplift and active tectonics of Southern Albania inferred from incision of alluvial terraces. Quat. Res. 71, 465-476.

Carminati, E., Doglioni, C., Argnani, A., Carrara, G., Dabovski, C., Dumurdzanov, N., Gaetani, M., Georgiev, G., Mauffret, A., Nazai, S., Sartori, R., Scionti, V., Scrocca, D., Séranne, M., Torelli, L., Zagorchev, I., 2004. TRANSMED Transect III. In Cavazza, W., Roure, F., Spakman, W., Stampfli, G.M., Siegle, P. (Eds.), The TRANSMED Atlas – The Mediterranean region from Crust to Mantle. Springler, Berlin Heidelberg.

Carozza, J.-M., Delcaillau, B., 1999. Geomorphic record of Quaternary tectonic activity by Alluvial terraces: example from the Tet basin (Roussillon, France). Earth and Planetary Sciences, 329, 735-740.

Clark, Peter U., Dyke, Arthur S., Shakun, Jeremy D., Carlson, Anders E., Clark, Jorie, Wohlfarth, Barbara, Mitrovica, Jerry X., Hostetler, Steven W., 2009. The Last Glacial Maximum. Sci. 325 – 5941, 710–714.

Copley, A., Boait, F., Hollingsworth, J., Jackson, J., McKenzie, D., 2009. Subparallel thrust and normal faulting in Albania and the roles of gravitational potential energy and rheology contrasts in mountain belts. J. of Geophys. Res. 114, B05407, doi:10.1029/2008JB005931.

Dumurdzanov, N., Serafimovski, T., Burchfiel, B. C., 2005. Cenozoic tectonics of Macedonia and its relation to the South Balkan extensional regime. Geosphere 1-1, 1-22.

Fouache, E., Desruelles, S., Magny, M., Bordon, A., Oberweiler, C., Coussot, C., Touchais, G., Lera, P., Lézine, A-M., Fadin, L., Roger, R., 2010a. Paleogeographical reconstruction of Lake Maliq (Korça Basin, Albania) between 14000 BP and 2000 BP. J. of Archaeological Sci. 37, 525-535

Fouache, E., Vella, E., Dimo, L., Gruda, G., Mugnier, J-L., Dènefle, M., Monnier, O., Hotyat, M., Huth, E., 2010b. Shoreline reconstruction since the Middle Holocene in the vicinity of the ancient city of Apollonia (Albania, Seman and Vjosa deltas). Quat. International 216, 118-128.

Fourcart J. 1921. Carte Geologique des confines Albanais. 1/200 000. Published by the service géographique de l'armée française.

Fuller, I.C., Macklin, M.G., Lewin, J., Passmore, D.G., Wintle, A.G., 1998. River response to high-frequency climate oscillations in Southern Europe over the Past 200 k.y. Geology 26(3), 275-278.

Gosse, J. C., Phillips, F. M., 2001. Terrestrial in situ cosmogenic nuclides: theory and application. Quat. Sci. Rev. 20, 1475-1560.

Guzmán, O., Mugnier, J-L., Koçi, R., Vassallo, R., Carcaillet, J., Jouanne, F., Fouache, E., 2011. Active tectonics of Albania inferred from fluvial terraces geometries. 2nd INQUA-ICGP 567 International Workshop on Active Tectonics, Earthquake Geology, Archaeology and Engineering. Proceedings Volume 2, 2011

Guzmán, O., Mugnier, J-L., Koçi, R., Vassallo, R., Carcaillet, J., Jouanne, F., Fouache, E. Chronostratigraphy and incision of Albanian river terraces over the last 200 ka and their climatic implications. (In preparation).

Hamlin, R.,Woodward, J., Black, S., Macklin, M.G., 2000. Sediment fingerprinting as a tool for interpreting long-term river activity: the Voidomatis basin, NW Greece. In: 581 Foster, I.D.L. (Ed.), Tracers in Geomorphology. Wiley, Chichester, pp. 473–501.

Institutin Topografik te Ushtrise Tirane, 1959-1990. Topographic maps of Socialist Republic of Albania in scale: 1:25000. Archive of Institute of Seismology, Tirana, Albania. (in Albanian).

Jouanne, F., Mugnier, J.L., Koçi, R., Bushati, S., Matev, K., Kuka, N., Shinko, I., Kociu, S., Duni, L., 2012. GPS constraints on current tectonics of Albania. Tectonophysics. doi: 0.1016/j.tecto.2012.06.008.

Kallel, N., Duplessy, J.C., Labeyrie, L., Fontugne, M., Paterne, M., Montacer, M., 2000. Mediterranean pluvial periods and Sapropel formation over the last 200,000 years. Palaeogeography, Palaeoclimatology, Palaeoecology 157, 45–58.

Kastelic, V., Basili, R., Duni, L., Koçi, R., 2012. Contributions to European Database of Seismogenic fauts, within the EU-FP7 Project "Seismic hazard harmonization in Europe (SHARE)". http://diss.rm.ingv.it/share-edsf/.

Kilias, A., Tranos, M., Mountrakis, D., Shallo, M., Marto, A., Turku, I., 2001. Geometry and kinematics of deformation in the Albanian orogenic belt during the Tertiary. Journal of Geodynamics 31 (2), 169–187.

Kiratzi, A., 2011. The 6 September 2009 Mw5.4 earthquake sequence in Eastern Albania, Turkish Journal of Earth Sciences, in press.

Koçi, R., 2007. Geomorphology of quaternary deposits of Albanian rivers. Ph.D. Thesis. Archive of Institute of Seismology, Tirana, Albania. (in Albanian).

Lewin, J., Macklin, M.G., Woodward, J.C., 1991. Late Quaternary fluvial sedimentation in the Voidomatis basin, Epirus, Northwest Greece. Quat. Res. 35, 103-115.

Macklin, M.G., Fuller, I.C., Lewin, J., Maas, G.S., Passmore, D.G., Rose, J., Woodward, J.C., Black, S., Hamlin, R.H.B., Rowa, J.S., 2002. Correlation of fluvial sequences in the Mediterranean basin over last 200 ka and their relationship to climate change. Quat. Sci. Rev. 21, 1633-1641.

Mason, D., Little, T., Van Dissen, R.., 2006. Rates of active faulting during late Quaternary fluvial terrace formation at Saxton River, Awatere fault, New Zealand. Bulletin Geological Society of America. 118. 1431-1446.

Melo, V., 1961. Neotectonic in the Elbasan-Peqin area from Shkumbin terraces –. Bul. Univ. Sht. Shkencave Natyrore II. (in Albanian).

Meyer, G.A., Wells, S.G., Jull, A.J.T., 1995. Fire and alluvial chronology in Yellowstone National Park: climate and intrinsic controls on Holocene geomorphic processes. Geological Soc. of America Bull. 107, 1211–1230.

Muceku, B., Van der Beek, P., Bernet, M., Reinerrs, P., Mascle, G., Tashko, A., 2008. Thermochronological evidence for Mio-Pliocene late orogenic extension in the north-eastern Albanides (Albania). Terra Nova 20, 180-187.

Muço, B., 1994. Focal mechanism solutions of earthquakes for the period 1964-1988. Tectonophysics, 231,

Muço, B., 1998. Catalogue of ML ≥ 3 earthquakes in Albania from 1976 to 1995 and distribution of seismic energy released. Tectonophysics, 29é, 311-319.

Niewland, D.A., Oudemayer, B.C., Valbona, U., 2001. The tectonic development of Albania: explanation and prediction of structural styles. Marine and Petroleum Geology 18, 161–177.

Noller, J. S., Sowers J. M., Lettis, W. R., 2000. 'Quaternary geochronology. Methods and applications.' AGU Reference Shelf 4. American Geophysical Union, Washington DC.

Pazzaglia, F.J., Brandon, M.T., 2001. A fluvial record of long-term steady-state uplift and erosion across the Cascadia forearc high, Western Washington state. American Journal of Science 301, 385–431.

Prifti, K., 1981. Formation of the quaternary valley of the upper Vjosa river . Archive of Institute of Seismology, Tirana, Albania. (in Albanian).

Ramsey, B., 2009. Bayesian analysis of radiocarbon dates. Radiocarbon 51(1), 337-360.

Robertson, A., Shallo, M. 2000. Mesozoic-Tertiary tectonic evolution of Albania in its regional Eastern Mediterranean context. Tectonophysics 316(3), 197-254.

Roure, F., Nazaj, S., Mushka, K., Fili, I., Cadet, J.P., Bonneau, M., 2004. Kinematic evolution and petroleum systems - An appraisal of the Outer Albanides. In: McClay K.R. (Ed.), Thrust tectonics and hydrocarbon systems AAPG memoir 82, pp. 474-493.

SHGJSH, 2003. Geological Map of Albania in scale 1:200000. Geological Service of Albania, Tirana, Albania, 2nd edn (in Albanian).

Sorel, D., Bizon, G., Aliaj, Sh., Hasani, L., 1992. Calage stratigraphique de l'âge et durée des phases compressives des Hellenéides extrens (Grèce nord-occidentales et Albanie), du Miocène à l'actuel. Bull. Soc. Geologique France 163, 447-454.

Sulstarova, E., 1986. Mechanism of earthquakes and field of present-day tectonic stresses in Albania. Ph.D. Thesis. Archive of Institute of Seismology, Tirana. (in Albanian).

Sulstarova, E., Peçi, V., Shuteriqi, P., 2000. Vlora-Elbasani-Dibra (Albania) transversal fault zone and its seismic activity. Journal of Seismology 4, 117-131.

Sulstarova E, Kociaj S, Muco B, Peci V., 2003. "The Albanian earthquakes catalogue for historical and instrumental data with magnitude Mš4.5." Internal Report (behalf on NATO Project "Seismotectonic and Seismic Hazard Assessment in Albania", 1999-2002), Seismological Institute, Tirana, Albania.

Tagari, Dh., 1993. Etude neotectonique et seismotectonique des Albanides: Analyse des deformations et geodynamique du Langhien a l'actuel. Ph.D. Thesis. Univ. Paris-Sud, Orsay, France.

Tagari, Dh., Vergely, P., Aliaj, Sh., 1993. Tectonique polyphasée plio-quaternarire en Albanie orientale (région de Korçë-Pogradeci). Bull. Soc. Géol. France 164-5, 727-737.

Vassallo, R., Ritz, J-F., Braucher, R., Carretier, S., 2005. Dating faulted alluvial fans with cosmogenic 10Be in the Gurvan Bogd mountain range (Gobi-Altay, Mongolia): climatic and tectonic implications. Terra Nova. 17, 278-285.

Wagner, B., Vogel, H., Zanchetta, G., Sulpizio, R., 2010. Enviromental change within the Balkan region during the past ca. 50 ka recorded in the sediments from lakes Prespa and Ohrid. Biogesciences 7, 3187–3198.

Waters, D. W., 1993, The tectonic evolution of Epirus, N.W. Greece. PhD thesis ,Univ. of Cambridge, Cambridge, England.

Wegmann, K.W., Pazzaglia, F.J., 2002. Holocene strath terraces, climate change, and active tectonics; the Clearwater River basin, Olympic Peninsula, Washington State. Geological Soc. of America Bull. 114 (6), 731–744.

Wegmann, K.W., Pazzaglia, F. J., 2009. Late Quaternary fluvial terraces of the Romagna and Marche Apennines, Italy. Quat. Sci. Rev. 28, 137-165.

Wesnousky, S.G., Aranguren, R., Rengifo, M., Owen, L. A., Caffe, M. W., Murari, M. K., Pérez, O., 2012. Toward quantifying geomorphic rates of crustal displacement, landscape development, and the age of glaciation in the Venezuelan Andes. Geomorphology 141-142, 99-113.

Woodward, J.C., Hamlin, R.B.H., Macklin, M.G., Karkanas, P., Kotjabopoulou E., 2001. Quantitative sourcing of slackwater deposits at Boila rockshelter: A record of late-glacial flooding and palaeolithic settlement in the Pindus Mountains, Northern Greece. Geoarchaeology 16(5), 501-536.

Woodward, J.C., Hamlin, R.H.B., Macklin, M.G., Hughes, P.D., Lewin, J., 2008. Glacial activity and catchment dynamics in Northwest Greece: long-term river behaviour and the slackwater sediment record for the last glacial to interglacial transition. Geomorphology 101, 44–67.

Supplementary data

A. *Geomorphologic map in detail of the Shkumbin and Devoll rivers system.* ***a****) Lower reaches;* ***b****) middle reaches;* ***c****) upper middle reaches. The geographical location of the dating samples are shown in the map.*

a)

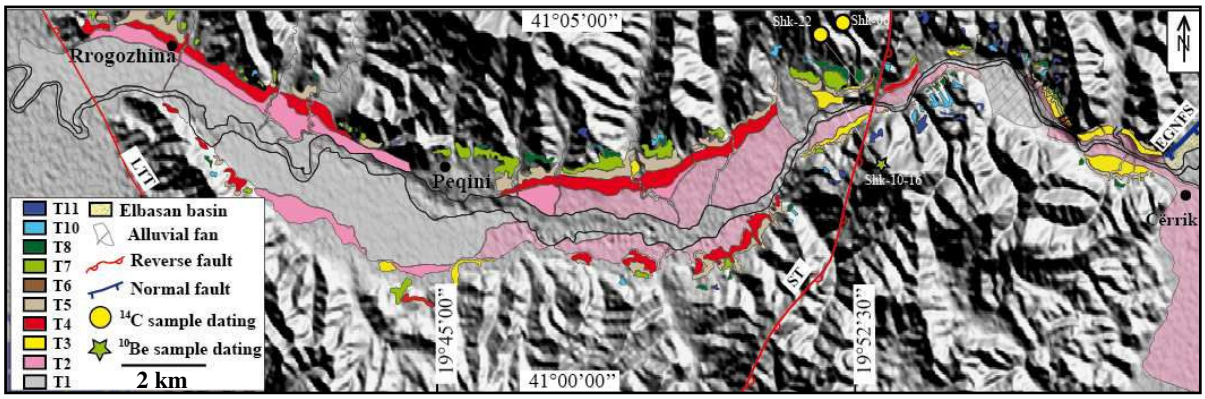

b)

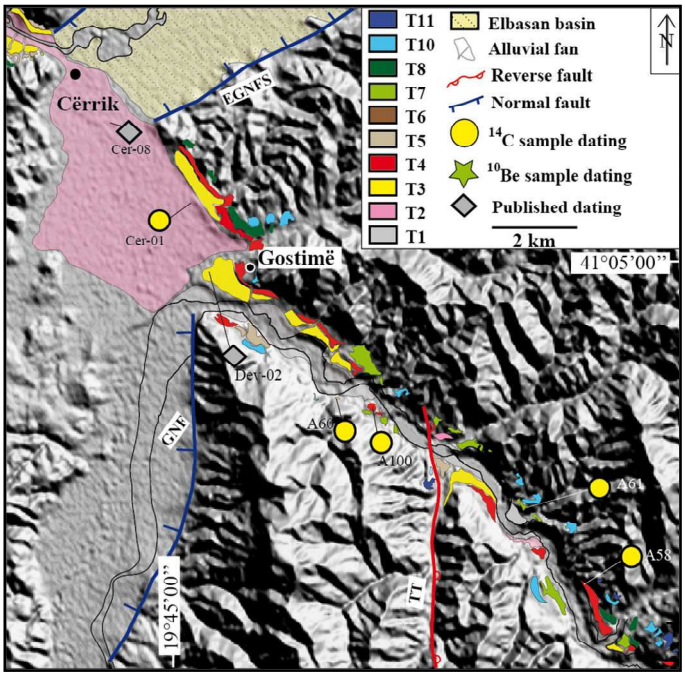

c)

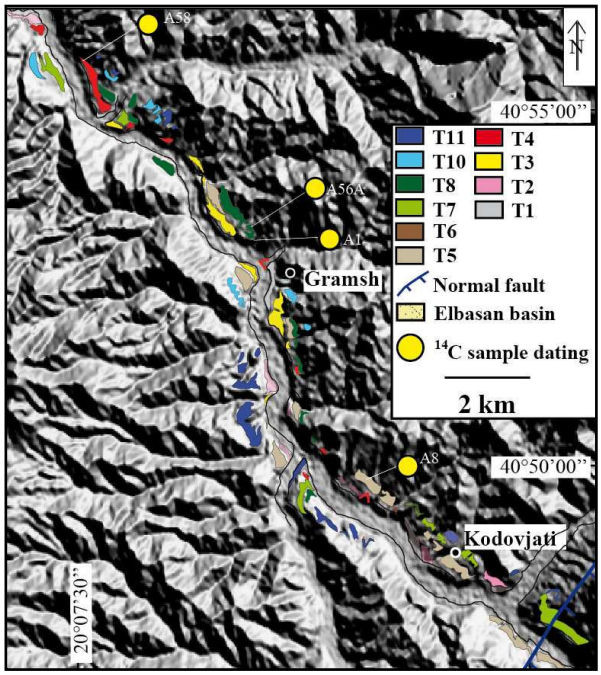

B. Table B1. *Numeric ages from river terraces of Albania.*

Sample[a]	Material[b]	Latitude (°N)[c]	Longitude (°E)[c]	Elevation of sample above the river (m)	Methods[d]	Lab-Code Reactor Reference	^{14}C Ages (yr BP)	Calibrated interval Cal yr BP (Probability=0,95)	Concentration ^{10}Be (10^5 at/g)[e]	Ages (ka)[f]	Local terrace name or alluvial unit	Proposed terrace name	Source[g]
Vjosa													
A153	C	40.2076	20.3875	17.3	^{14}C	SacA 16001	190 ± 30	4 - 302	-	0.15 ± 0.15	-	colluvium	(1)
A150	C	40.2084	20.0934	9.5	^{14}C	SacA 15998	330 ± 30	308 - 474	-	0.40 ± 0.08	-	colluvium	This study
A28	Vd	40.3354	19.9921	12	^{14}C	Poz-8824	705 ± 30	564 - 691	-	0.63 ± 0.06	colluvium	colluvium	(1)
A155	Vd	40.3611	19.2907	13.4	^{14}C	SacA 16002	3870 ± 60	4094 - 4436	-	4.26 ± 0.17	-	colluvium	This study
OxA-192	C	39.97(ç)	20.66(ç)	~4.5	^{14}C	OxA-192	800 ± 100	560 - 928	-	0.74 ± 0.18	U2(vjosa)	T1	(2, 3)
OxA-191	C	40.87(ç)	21.65(ç)	~4.5	^{14}C	OxA-191	1000 ± 50	788 - 1052	-	0.92 ± 0.13	U2(vjosa)	T1	(2, 3)
OxA-5246	C	39.96(ç)	20.65(ç)	~10.6	^{14}C	OxA-5246	13810 ± 130	16632 - 17224	-	16.93 ± 0.30	U3(vjosa)	T3	(4, 3)
Beta-109162	C	39.96(ç)	20.65(ç)	~10.6	^{14}C	Beta-109162	13960 ± 260	16591 - 17812	-	17.20 ± 0.61	U3(vjosa)	T3	(4, 3)
Beta-109187	C	39.96(ç)	20.65(ç)	~10.4	^{14}C	Beta-109187	14310 ± 200	16935 - 17924	-	17.43 ± 0.50	U3(vjosa)	T3	(4, 3)
VOI24	S	39.94(ç)	20.71(ç)	~9.7	TL	VOI24	-	-	-	19.60 ± 3.00	U3(vjosa)	T3	(4, 3)
Tributary site	Cc	39.95(ç)	20.68(ç)	~10.5	U/Th	-	-	-	-	21.25 ± 2.50	U3(vjosa)	T3	(5, 3)
Old Klithonia	Cc	39.96(ç)	20.65(ç)	~8.2	U/Th	-	-	-	-	24.00 ± 2.00	U4(vjosa)	T4	(5, 3)
571c	Dt	38.96(ç)	20.65(ç)	~12.4	ESR	571c	-	-	-	24.30 ± 2.60	U4(vjosa)	T4	(2, 3)
571a	Dt	38.96(ç)	20.65(ç)	~12.4	ESR	571a	-	-	-	25.00 ± 0.50	U4(vjosa)	T4	(2, 3)
Old Klithonia	Cc	39.96(ç)	20.65(ç)	~8.2	U/Th	-	-	-	-	25.00 ± 2.00	U4(vjosa)	T4	(5, 3)
571b	Dt	38.96(ç)	20.65(ç)	~12.4	ESR	571b	-	-	-	26.00 ± 1.90	U4(vjosa)	T4	(2, 3)
A151	C	40.2140	20.3842	21.7	^{14}C	SacA 15999	24070 ± 150	28457 - 29352	-	29.35 ± 0.89	U5(vjosa)	T5	This study
Konitsa1	Cc	39.86(ç)	20.77(ç)	~8	TL	-	-	-	-	53.00 ± 4.00	U6(vjosa)	T8	(3)
Konitsa2	Cc	39.58(ç)	20.39(ç)	~8	U/Th	-	-	-	-	56.50 ± 5.00	U6(vjosa)	T8	(3)
Konitsa3	Cc	39.58(ç)	20.39(ç)	~11	U/Th	-	-	-	-	74.00 ± 6.00	U7(vjosa)	T9	(3)
Konitsa4	Cc	39.58(ç)	20.39(ç)	~9	U/Th	-	-	-	-	80.00 ± 7.00	U7(vjosa)	T9	(3)
Konitsa5	Cc	39.58(ç)	20.39(ç)	~12	U/Th	-	-	-	-	113.00 ± 6.00	U8(vjosa)	T10	(3)
VOI26	S	39.86(ç)	20.77(ç)	~56	TL	VOI26	-	-	-	>150	U9(vjosa)	T12	(2)
Osum													
A17	Vd	40.4508	30.2900	17	^{14}C	Poz-10576	9990 ± 50	11262 - 11705	-	11.48 ± 0.22	T8(osum)	T2	(1)
Par-0 (*)	Sr	40.5200	20.7200	70	^{10}Be	-	-	-	2.60 ± 3.10 (&)	≥18.75 ± 1.41	T7(osum)	T3	(1)
Quaf-0 (*)	Sr	40.5500	20.6900	29	^{10}Be	-	-	-	4.44 ± 0.50(&)	≥19.80 ± 1.56	T7(osum)	T3	(1)
A16	Vd	40.6400	20.0600	24	^{14}C	Poz-10575	29900 ± 1300	31622 - 38026	-	34.82 ± 3.20	T5(osum)	T6-5	(1)
A83	C	40.6800	20.0200	14.8	^{14}C	Poz-13850	37000 ± 300	41380 - 42366	-	41.87 ± 0.50	T4(osum)	T7	(1)
A18	Vd	40.5600	20.1400	53	^{14}C	Poz-10578	45300 ± 1600	-	-	50.70 ± 1.80($)	T3(osum)	T8	(1)
A14	Vd	40.6400	20.0600	33.8	^{14}C	Poz-10574	49000 ± 2500	-	-	54.40 ± 2.78($)	T3(osum)	T8	(1)
Grem-0(*)	Sr	40.5560	20.7383	50	^{10}Be	-	-	-	6.23 ± 0.55(&)	≥52.59 ± 3.20	T3(osum)	T8	(1)

Continue **Table B1**

Paleo-Devoll													
A05	Vd	40.9092	20.1393	34	^{14}C	Poz-10572	119.5 ± 0.3 pMC	-	-	modern		colluvium	This study
Cer-08	C	41.0275	19.9817	8.4	^{14}C	Poz-39495	30 ± 80	278 - 8	-	0.14 ± 0.13	-	colluvium	This study
Dev-02	C	40.9910	10.0165	16.6	^{14}C	Poz-39496	540 ± 130	726 - 307	-	0.52 ± 0.21	-	colluvium	This study
Shk-06	Vd	41.0663	19.8800	52.8	^{14}C	Poz-34987	162 ± 0.46 pMC	-	-	Modern	-	colluvium	This study
Shk-22	C	41.0649	19.8714	6.3	^{14}C	Poz-39201	90 ± 30	266 - 22	-	0.14 ± 0.12	-	colluvium	This study
Cer-01	C	41.0100	20.0083	8.4	^{14}C	Poz-39197	5400 ± 40	6020 - 6293	-	6.16 ± 0.14	-	T2	This study
Shk-10(*)	Sr	41.0618	19.8685	14.7	^{10}Be	-	-	-	0.77 ± 0.07	≥16.15 ± 1.00		T3	This study
A60	C	40.9676	20.0526	19	^{14}C	Poz-12223	17640 ± 160	20477 - 21455	-	20.97 ± 0.49	-	T3	This study
A58	C	40.9214	20.1292	15.7	^{14}C	Poz-12116	21850 ± 150	25793 - 26810	-	26.30 ± 0.51	-	T4	This study
A100	C	40.9660	20.0636	24	^{14}C	Poz-17242	22780 ± 200	26825 - 28060	-	27.44 ± 0.68	-	T4	This study
A8	Vd	40.8271	20.2154	42,5	^{14}C	Poz-9838	23760 ± 150	28031 - 29109	-	28.57 ± 0.54	-	T6-5	This study
A1	Vd	40.8836	20.1773	42	^{14}C	Poz-8816	25500 ± 300	29603 - 30915	-	30.26 ± 0.66	-	T5	This study
A61	C	40.9414	20.1089	41,2	^{14}C	Poz-12117	38900 ± 700	42214 - 44365	-	43.29 ± 1.07	-	T7	This study
A56A	C	40.8834	20.1764	41	^{14}C		> 52000	-	-	> 52	-	T8	This study
Erzen													
A41	C	41.2697	19.8400	3	^{14}C	Poz-8826	170 ± 30	291 - -4	-	0.14 ± 0.14	colluvium	colluvium	(6)
A11	C	41.2900	19.7100	3.4	^{14}C	Poz-8818	200 ± 30	305 - - 4	-	0.15 ± 0.15	colluvium	colluvium	(6)
A81	C	41.2866	19.7094	23.4	^{14}C	Poz-13849	275 ± 35	152 - 458	-	0.30 ± 0.15	colluvium	colluvium	(6)
A65	C	41.3088	19.7544	29	^{14}C	Poz-12784	500 ± 30	501 - 618	-	0.56 ± 0.06	colluvium	colluvium	(6)
A76	Vd	41.2800	19.8300	11.7	^{14}C	Poz-13847	3075 ± 35	3212 - 3374	-	3.39 ± 0.08	colluvium	colluvium	(6)
A63B	C	41.2870	19.7197	17	^{14}C	Poz-12118	3700 ± 35	3926 - 4150	-	4.04 ± 0.11	colluvium	colluvium	(6)
A13	C	41.2700	19.6400	9	^{14}C	Poz-8823	1660 ± 30	1422 - 1691	-	1.56 ± 0.13	T1(erzen)	T1	(6)
A12	C	41.2700	19.6400	9	^{14}C	Poz-10573	1730 ± 30	1560 - 1710	-	1.63 ± 0.07	T1(erzen)	T1	(6)
A42	Vd	41.2700	19.8000	14	^{14}C	Poz-8827	6840 ± 60	7578 - 7818	-	7.67 ± 0.12	T2(erzen)	T2	(6)
A115	C	41.2844	19.9683	17	^{14}C	Poz-17243	26600 ± 500	30310 - 31946	-	31.13 ± 0.82	T3(erzen)	T5	This study
A67	C	41.2700	19.6400	9.4	^{14}C	Poz-12120	30400 ± 300	34536 - 36189	-	35.36 ± 0.83	T4(erzen)	T6	(6)
A69	C	41.2900	19.6400	41	^{14}C	Poz-12121	31500 ± 400	35070 - 36695	-	35.88 ± 0.81	T4(erzen)	T6	(6)
A64	C	41.2700	19.7100	24.8	^{14}C	Poz-12224	33400 ± 500	36758 - 39361	-	38.06 ± 1.30	T4(erzen)	T6	(6)
A79	C	41.2900	19.7100	26.5	^{14}C	Poz-13848	44200 ± 1600	-	-	49.59 ± 1.76($)	T6(erzen)	T8	(6)
A70	C	41.2900	19.6000	22	^{14}C	Poz-12785	48000 ± 2000	-	-	53.40 ± 2.22($)	T6(erzen)	T8	(6)
Mat													
Ma-05	C	41.6178	20.0294	24.3	^{14}C	Poz-34984	1075 ± 30	931- 1056	-	1.00 ± 0.62	-	colluvium	This study
Ma-18	C	41.6245	19.9978	7,00	^{14}C	Poz-39198	1725 ± 30 BP	1557 - 1708	-	1.63 ± 0.75	T1(mat)	T1	This study
Ma-21	C	41.6246	19.9970	10.3	^{14}C	Poz-39199	5100 ± 40 BP	5745 - 5923	-	5.83 ± 0.90	T2(mat)	T2	This study
Ma-24	C	41.6273	19.9968	26	^{14}C	Poz-39200	14850 ± 80	17782 - 18516	-	18.15 ± 0.37	T3(mat)	T3	This study
Ma-04	Sr	41.5920	20.0336	100	^{10}Be	-	-	-	5.63 ± 0.16	≥110.70 ± 11.18	T8(mat)	T10	This study
Ma-03(*)	Sr	41.6748	19.9166	94	^{10}Be	-	-	-	4.40 ± 0.14	≥114.00 ± 6.00	T8(mat)	T10	This study
Ma-06	Sr	41.6042	20.0130	190	^{10}Be	-	-	-	10.46 ± 0.40	≥188.84 ± 18.54	T9(mat)	T11	This study

[a] Samples: (*) for cosmogenic depth profile only the surface sample is in this table.
[b] Type of material dated: C= Charcoal, Vd= Vegetal debris, Cc= Calcite cement, S= Sediment, Dt= Deer tooth, Sr= Siliceous rock.
[c] Geographical location: (ç) Location estimated.
[d] Dating method: ^{14}C= Radiocarbon, TL= Termoluminicense, U/Th = Uranium series, ESR= Electron spin resonance, ^{10}Be= Cosmogenic in situ produced.
[e] Concentration of ^{10}Be: (&) Average concentration of surface samples from Carcaillet et al. (2009).
[f] Numerical ages: (£) Have not been taken into account for the probability density curves due to its large uncertainty.
[g] Source: (1) Carcaillet et al. (2009) ; (2) Lewin et al. (1991) ; (3) Woodward et al. (2008); (4) Woodward et al. (2001); (5) Hamlin et al. (2000); (6) Koçi (2007).

Chapter V: Synthesis of the Main Results

This study provides new geomorphologic, as well as geochronological data, of river terraces developed in active tectonics contexts with moderate uplift (0.1 – 2.0 mm/a) and different geological, climatic and geomorphological setting: Venezuela (Mérida Andes) and Albania. The state of the art of the river terraces analyses in these areas are at different stages. For this reason, our study strategy was different, but the results in terms of impact of the different processes in river terraces formation are comparable.

In Venezuela, despite the fact that several river terraces have been early studied along the Mérida Andes (e.g. Tricart and Millies-Lacroix, 1962; Tricart and Michel, 1965, Zinck, 1980), geochronological analyses are at an initial stage with only some numerical ages (six ages for terraces older than the Holocene) scattered along of the 400 km of the chain (Schubert and Vivas, 1993, Wesnousky et al., 2012). Moreover, these studies are restricted to localized zones of the rivers. Thus, our efforts were directed to provide the first detailed geomorphologic and geochonological analysis of river terraces in an entire river (from the upper to the lower reaches) for the last 200 ka in the Mérida Andes. We focused our work on one system of rivers located in the Southeastern flank of the Mérida Andes, which is the Pueblo Llano and Santo Domingo rivers system (PLSDS).

The Albanian river terraces were initially documented by the pioneering studies of Melo (1961) and Prifti (1984). Numerical ages have been reported for these terraces since the beginning of the 90's (Lewin et al., 1991), with more emphasis on the last decade (Hamlin et al., 2000, Woodward et al., 2001, 2008; Koçi, 2007; Carcaillet et al., 2009). However, most of these studies were concentrated on Southern Albania. In this thesis we intend to provide a regional chronostratigraphy framework for the Albanian terraces for the last 200 ka. Hence, terraces located in three rivers of the central and Northern Albania, along the Paleo-Devoll rivers system (includes Shkumbin and Devoll rivers) and Mat river were studied, respectively. Then, the results obtained were correlated with previously published data (i.e. Vjosa -called Voidomatis in Greece-, Osum and Erzen rivers).

In this chapter, the main results obtained in this thesis are compiled and synthesized (**Tables V.1, 2**). These results provide the basis for the general discussion and conclusions presented in chapter VI.

Table V.1. *Main morphologic parameters of Venezuelan and Albania rivers analyzed in this study.*

Morphologic parameters	Venezuelan river	Albanian river					
	Pueblo Llano-Santo Domingo	Vjosa	Osum	Devoll	Shkumbin	Erzen	Mat
Catchment area (km^2)[a]	1250[#]	6700	2230*	3100*	3070	900	1215
Length of the river (km)[b]	80	272	120[$]	160[$]	130	75	85
Altitude at the source (m a.s.l.)	3470	1600	1100	1100	1150	1300	1200
Maximum altitude in the catchment (m a .s.l.)	3820	2523	2523	2416	2373	1612	2246
Mean slope of the river (°)	0.04	0.01	0.01	0.01	0.01	0.02	0.01
Mean slope of the river within alluvial plain (°)	~0.001	~0.2	~0.2	~0.2	~0.2	~0.2	~0.2
Mean slope of the marine shelf (°)	-	~2.9	~2.9	~2.9	~2.7	~2.3	~2.3
Surface above ELA LGM: - 3220 m a.s.l (km^2) - Venezuela[c] - 2174 m a.s.l. (km^2) - Albania[d]	~246	~120	~12	~14	~11	0	~0.3

[a] Catchment area: (#) for the Pueblo Llano and Santo Domingo rivers systems (*) from the source to the confluence between Devoll and Osum rivers.
[b] Length of the river: from the source to the confluence between Devoll and Osum rivers. After this point Seman river continue for 70 km towards the Adriatic Sea
Surface above ELA altitude for the LGM: (c) Venezuelan ELA LGM (Late Mérida Stage - Stansell et al., 2007). (d) Albanian ELA LGM (Thymphian stage - Hughes, 2004, Hughes et al., 2006).

- **Morphologic characteristics of Venezuelan and Albanian rivers**

In **Table V.1**, the main morphologic parameters of the rivers studied in this thesis are synthetized. The catchment areas of the rivers vary from 900 to 6700 km^2. Lengths of the rivers are similar and vary between 75 and 160 km, except for the Vjosa river, which has a total length of 272 km. Venezuelan riverw and the large catchments of Albania contains areas that were exposed to glacial activity. These parameters show that Venezuelan and Albanian rivers are morphologically comparable, and we discuss the river terraces characteristics together in the following.

- **General characterization of river terraces**

In Venezuela, twelve river terraces and one frontal moraine complex were identified along the Pueblo Llano and Santo Domingo rivers system. Types of terraces can be grouped according to the reaches of the system. Fill terraces were developed in the upper reaches, while only strath terraces were developed in the lower reaches (**Table V.2, figures V.1. 2**). In Albania, eleven and nine terraces were identified along of the Paleo-Devoll and Mat rivers, respectively. However, based on the regional correlation, eleven regional river terraces were developed and preserved in Albania over the last 200 ka. During the pre-Marine Isotope Stage

2 (MIS 2) period, fill terraces were developed in the large and lithologically variable bedrock catchments (Vjosa, Osum, Devoll and Shkumbin catchments), while only strath terraces were developed in the small catchment and siliciclastic bedrock (Erzen and Mat catchments). After the beginning of the MIS 2, strath terraces were developed everywhere (**Table V.2, figure V.3**).

Table V.2. *Main results of the river terraces analysis performed in this thesis.*

Main results / Area	Rivers studied	Number of terraces	Regional river terraces	Types of terraces	Ages of terraces and others: Samples ^{10}Be	Samples ^{14}C	New numerical ages	Incision rate
Venezuela	Pueblo Llano and Santo Domingo system	12	12	**Upper reaches:** Fill terraces **Lower reaches:** Strath terraces	35	-	- River terraces: 7 - Frontal moraine: 1	**Upper reaches:** variable from~1.3 to ~15.40 mm/a **Lower reaches:** constant ~1.1 mm/a
Albania	Paleo-Devoll system (large catchment)	11	12	**pre-MIS 2:** - *Large catchments:* Fill terraces - *Small catchments:* strath terraces **MIS 2 and post-MIS 2:** Strath terraces everywhere	11	17	- River terraces: 17 - Coluvial deposits: 9	**Long-term (last 200 ka):** Unsteady in space and varies from 0.1 mm/a to 1.1 mm/a **Short-term (last 25 ka):** - *Large catchments:* two times greater than long-term - *Small catchments:* similar to long-term **Fault activities:** - Leads local pulses of incision rates
	Mat (small catchment)	9						

- **Ages of terraces**

In Venezuela, the analysis of ^{10}Be concentration of thirty five samples performed in this thesis provided for the first time exposure ages for seven terraces and for one frontal moraine complex (**Table V.2**). Exposure ages of river terraces at >120.00 $\pm$ 5.00 ^{10}Be ka; <79.03 ± 8.38 ^{10}Be ka, <72.06 ± 3.00 ^{10}Be ka, <59.61 ± 6.29 ^{10}Be ka; >43.14 ± 5.78 ^{10}Be ka; >17.66 ± 1.81 ^{10}Be ka and >1.95 ± 0.47 ^{10}Be ka, were estimated for Qt12, Qt10, Qt9, Qt7, Qt6, Qt4 and Qt3, respectively. Exposure age at 17.14 ± 2.00 ^{10}Be ka was estimated for the frontal moraine complex M1 (**figure V.1**).

In Albania, seventeen ^{14}C and eleven ^{10}Be samples achieved in this thesis provided new fifteen numerical terrace ages for the Paleo-Devoll and Mat rivers, one for the Vjosa river and one for the Erzen river (**Table V.2**). These ages complete and refine the chronological record of Albanian terraces. Particularly, the precision of the numerical ages of the two oldest terraces (T10 and T11) was improved. The minimum age for terrace T11 was

refined from > 150 TL ka to 188.84 ± 18.54 ^{10}Be ka and a minimum age for terrace T8 between ~ 100 and ~120 ^{10}Be ka was obtained (**figure V.3**).

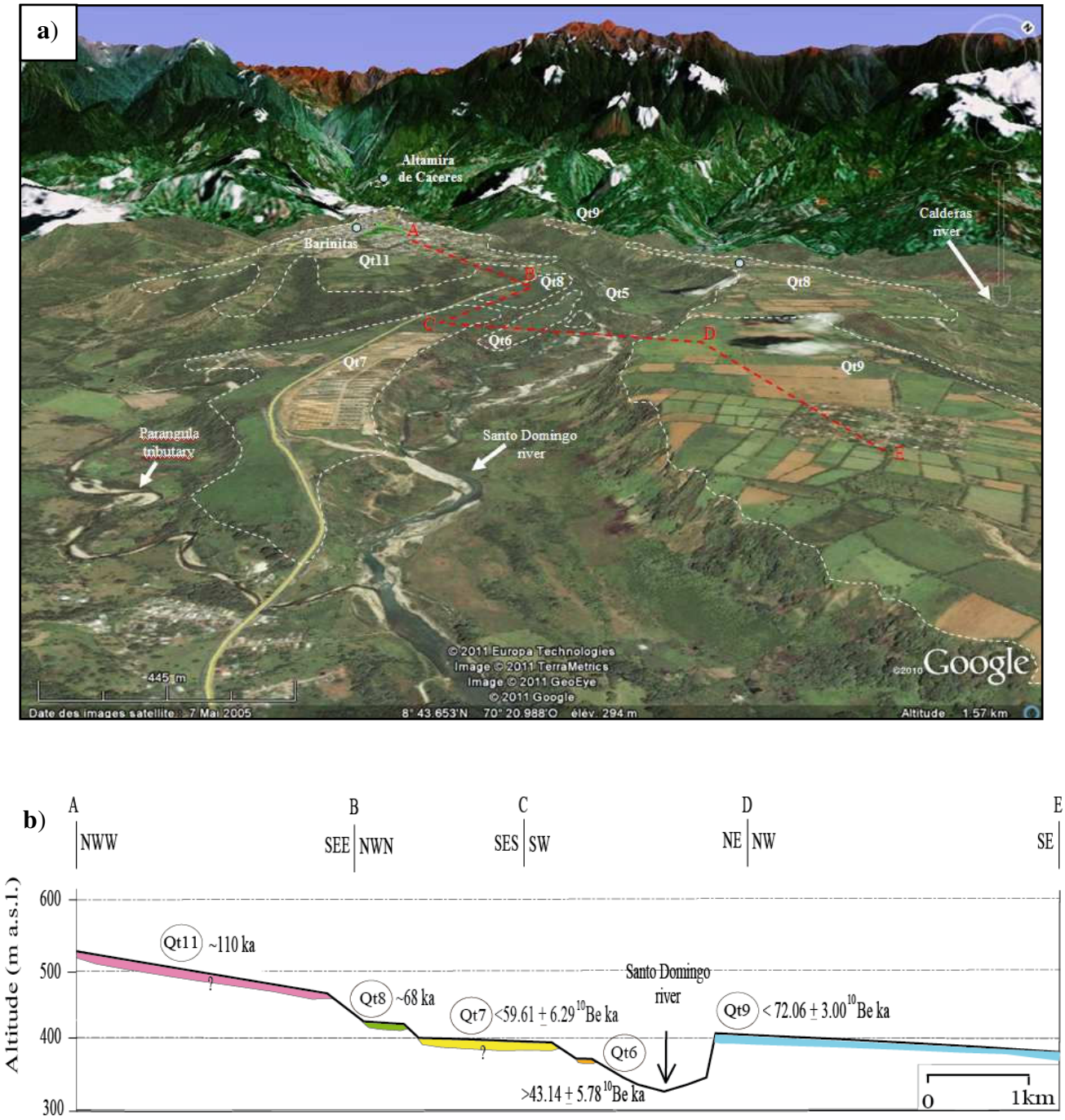

Figure V.1. *Synthesis of the main geomorphic and geochronological results obtained along of the lower reaches of the PLSDS – Western Venezuela.* ***a****) Satellite image with river terraces mapped in which red line represents the cross section of the* ***figure V.1b****.* ***b****) Cross section through the stepped terraces. Notice that the terrace ages correspond to the numerical ages and to the extrapolation ages proposed in this thesis. Qt9, on the left bank, is located downstream with respect to the other terraces.*

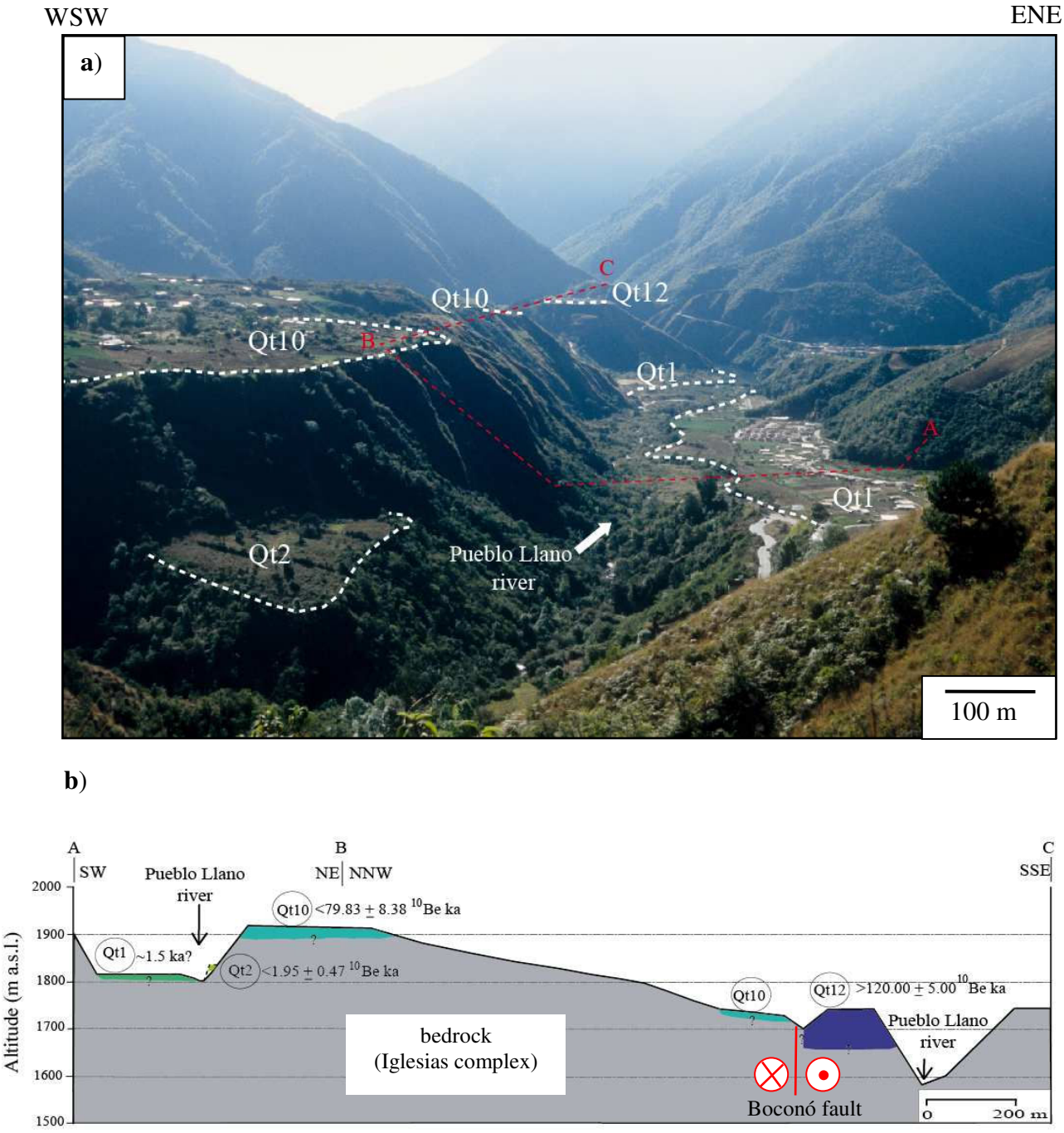

Figure V.2. *Synthesis of the main geomorphic and geochronological results obtained along of the upper reaches of the PLSDS – Western Venezuela.* ***a****) Panoramic view of the upper reach. Red line represents the cross section of the* ***figure V.2b****.* ***b****) Cross section through the terraces. Terrace Qt2 was projected in the cross section. The terrace ages correspond to the numerical ages and extrapolation ages proposed in this thesis.*

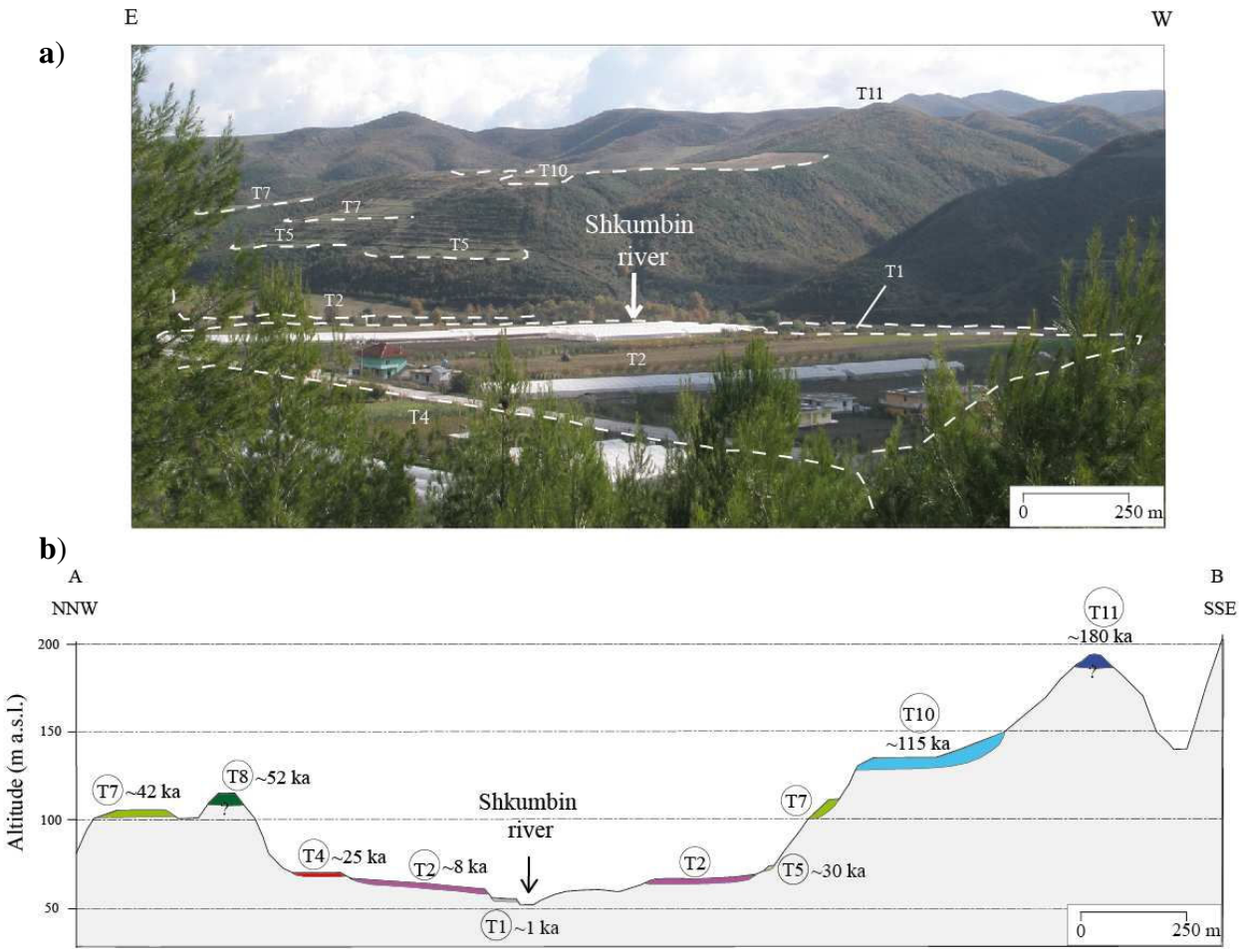

Figure V.3*. Synthesis of the main geomorphic and geochronological results obtained along of the lower reaches of the Paleo-Devoll river – Central Albania. The results are represented in a single section where most of the regional Albanian river terraces were identified.* ***a****) Panoramic view of the lower Paleo-Devol. The present-day Shkumbin river is shown in the figure.* ***b****) Cross section trough the stepped terraces in the lower paleo-Devoll. The ages of the terraces were obtained from the numerical dating and the correlation with climatic events.*

- **Incision rate**

The morphochronologic analysis of the river terraces applied in this study also allowed the reconstruction of the temporal and spatial incision rates in both study areas. Considering the geological and geomorphological context of PLSDS and Albania rivers, uplift rates and vertical slip rates of the main faults were estimated.

In the lowest reaches of the Pueblo Llano and Santo Domingo system, a constant incision rate of ~1.1 mm/a over the last 70 ka can be converted in the Late Pleistocene uplift rate of the Southeastern flank of the MA. This value is close to the recent estimation of the

uplift rate of ~1.7 ± 0.7 mm/a done by Wesnousky et al. (2012) for the Northwestern flank over the Late Pleistocene. Additionally, this value is similar to the exhumation rate of 0.8 mm/a proposed by Kohn et al. (1984) for the core of the MA over the last 800 ka. These results give a more detailed and broader picture of the uplift rate of the MA. In fact, they seem to indicate that the two flanks of the MA (NE and SW) uplift at a similar rate and that this rate is probably unchanged over several 100 ka. In the upper reaches of PLSDS, the incision rate varies from ~1.3 mm/a for the older terraces Qt12 and Qt10 (~120 and ~80 ka, respectively) to ~6.3 and 15.4 mm/a for the younger terrace Qt3 and Qt1 (~17.5 and ~2 ka, repectively).

In the case of Albanian rivers, long-term incision rates are quite variable in space from less than 0.1 mm/a in the upper reaches of the Vjosa river (Southern Albania) that flows through an extensional zone to 1 mm/a along the Mat river (Northern Albania). The incision rate increases recently (at least for the last 25 ka) in the large catchments (Vjosa, Osum, Devoll and Shkumbin rivers), while in the small catchments (Erzen and Mat rivers) it seems to be constant through time. Spatial and temporal evolution of the incision rates along four rivers in Southern Albania allowed identifying local shifts in the regional trend of incision rates associated with Quaternary faults. The fluvial incision is more strongly controlled by normal faults than thrust faults. These incision rate shifts were used for the quantification of the vertical slip rate of eight active faults in the area. The vertical slip rates appear to decrease from ~2 to ~0.1 mm/a from the extensional domain in the Eastern Albania to the compressional domain in Western Albania. Nonetheless in this last domain, more analysis using other approaches and methods are needed to study the structures hidden by the recent sedimentation, and also to quantify the strike-slip components of the faults along the whole Albanian domain.

- **Frontal moraine at Pueblo Llano river**

In this thesis, a frontal moraine complex was identified at an elevation of 2300 m a.s.l. in the upper reach of PLSDS. This complex was dated around 18 ka. Therefore, this moraine was formed during the Late Mérida Glaciation and represents the maximum advance of glaciers in the Pueblo Llano valley during the LGM. Previous studies have described for the MA two main phases of moraine formation: one is generally limited to elevations of 2600 to 2800 m a.s.l., and another between 2900 and 3500 m a.s.l. (e.g. Schubert, 1970, 1974, 1976; Schubert and Clapperton, 1990; Mahaney and Kalm, 1996; Mahaney et al., 1996, 2000, 2010). Based on well constrained ages the highest complex has been associated to the Late

Mérida Glaciation (Schubert, 1974). It is estimated to have occurred between 25 and 15 ka (Schubert, 1974; Schubert and Valastro, 1980; Schubert and Clapperton, 1990; Schubert and Vivas, 1993; Mahaney and Kalm, 1996; Rull, 2005; Kalm and Mahaney, 2011; Carrillo, 2006; Carrillo et al., 2006). The maximal ice advance of this stage has been correlated with the LGM proposed for the MA between 23 and 19 ka (Schubert and Rinaldi, 1987; Mahaney and Kalm, 1996). By contrast, there is a lack of ages for the lowest moraine complex. Based on their position below moraines dated as Late Mérida Stage and their morphological characteristics (outcrop limited to disperse patches of diamicton eroded by runoff), the lowest deposits have been ascribed to the Early Mérida Glaciation (Schubert, 1974, 1976). Nevertheless, the results of this study put in evidence that those criteria are not enough to correlate glacial deposits and landforms in the MA. Hence, numerical dating in the lowest deposits is needed to reconstruct the glacial history of the area. In fact, the glacier advance during the LGM, in other areas of the MA, could also have reached elevations lower than those previously reported between 2900 and 3500 m a.s.l. These results might have relevant implications in the paleoclimatic reconstruction of the Mérida Andes, and these paleoclimatic implications could have strongly influence the development of the fluvial system along the area.

Chapter VI: General Discussions and Conclusions

The morphochronological analysis of river terraces performed in this thesis along Venezuelan (Mérida Andes) and Albanian rivers, have brought to a better understanding of the main role that play the external controls, such as climate and/or base level variation (tectonic or eustatic) in the processes of terraces formation. In fact, our analysis put in evidence that in both areas the process of vertical incision and consequently abandonment of terraces is both a response to the uplift and climatic variation, while the eustatic variation and morphologic parameters (e.g. size of the catchments, altitude) appears to modulate the rivers response to climate changes. In the following we discuss the role of each variable, as well as our general conclusions:

1) Climatic transition as a trigger of terrace formation

Recently, Bridgland and Westaway (2008) summarized the three main models around the world for terraces formation in response to climatic variations (**figure I.4**). However, do the Venezuelan and Albanian terraces fit in this scheme? The comparison done in this thesis of regional and local paleoclimatic proxies with the age of abandonment of Venezuelan and Albania terraces allowed better understanding the relationships between climate variations and the processes of terraces formation.

In Albania and more generally in the Mediterranean context, the abandonment ages of almost all terraces correlate with Quaternary global climatic changes. These changes correspond to the transition from cold and dry to warm and humid conditions (**figure VI.1**). These climate variations induce rapid changes (< 0.2 ka) in catchment hydrology and in hillslope vegetation (Tzedakis et al., 1997; Allen et al., 1999; Allen, 2003; Wohlfarth et al., 2008), which control the phases of aggradation as well as incision of river terraces. In particular, during cold and dry conditions the hillslope's colluvia are destabilized as a result of the change in vegetative cover (e.g. from forest-dominated ecosystems (warm and humid) to steppe-dominated ecosystem (cold and dry)). Consequently, fluvial systems undergo significant variations in the transport capacity and sediment supply. Hence, high sediment fluxes combined with dry conditions, lead to aggradation phases during cold and dry periods. Then, transition from cool and dry to warm and humid conditions leads to the return of tree cover in response to increasing temperature. This vegetation cover reduces hillslope erosion by runoff and limits the sediment transport. This fact coupled with the increasing transport

capacity of the river (due to new humid conditions) provokes the vertical fluvial incision and abandonment of the river terrace during warm and humid periods (**figure VI.2)**. This fluvial response to climate changes was originally proposed by Bull and Knüpfer (1987) and Bull (1990, 1991) for the river systems in the temperate climate of the Rocky Mountains in Western United States and the Southern Alps of New Zealand over the last 200 ka. This response has also been documented in temperate maritime climate of northwestern European rivers (e.g. van der Berg, 1996, Bridgland, 2000; Bridgland et al., 2004), in several Mediterranean terraces record (e.g., Fuller et al., 1998; Macklin et al., 2002; Wegmann and Pazzaglia, 2009), in semid-arid climate of central Asia (Vassallo et al.; 2007), and recently in the sub-Saharan climate within the subtropical high pressure system of the central High Atlas mountains in Morocco (Arboleya et al., 2008).

In Venezuela, the ages of abandonment of the Pleistocene Pueblo Llano and Santo Domingo river terraces seem to have a good correlation with global climate change (**figure VI.1**) (González et al., 2008; Van Daele et al., 2011; Rull et al., 2010). Like in the Albanian context, these climatic variations also produce rapid changes in catchment hydrology and hillslope vegetation in Venezuela (Peterson et al., 2000a, 2000b; Haugh et al., 2001; Peterson and Haugh, 2006; González et al., 2008). These changes modulate the phases of deposits and incision of river, although geomorphic observations indicate that other processes also play a role in the deposition of alluvial materials (e.g. glacial outwash at the upper reach of the system, instantaneous catastrophic climatic events, neotectonic activity of Boconó fault).

2) Size of the catchment and orographic precipitation

This study shows that the geomorphic responses of the Albanian fluvial system induced by the climatic variations were probably modulated by other processes, like the size of the catchments and eustatic variations. As a matter of fact, we argue that during the cold and dry conditions of the pre-MIS 2 periods, the higher part of the large catchments were more heavily affected by hillslope processes, which determined the fact that much greater volumes of sediments delivered to the main channel. This fact coupled with the diminished transport capacity of the river (caused by dry conditions) favored the development of fill terraces in the large catchments. In the small catchments of the Albania, the equilibrium between sediment supply and transport capacity favored the development of strath terraces rather than fill terraces.

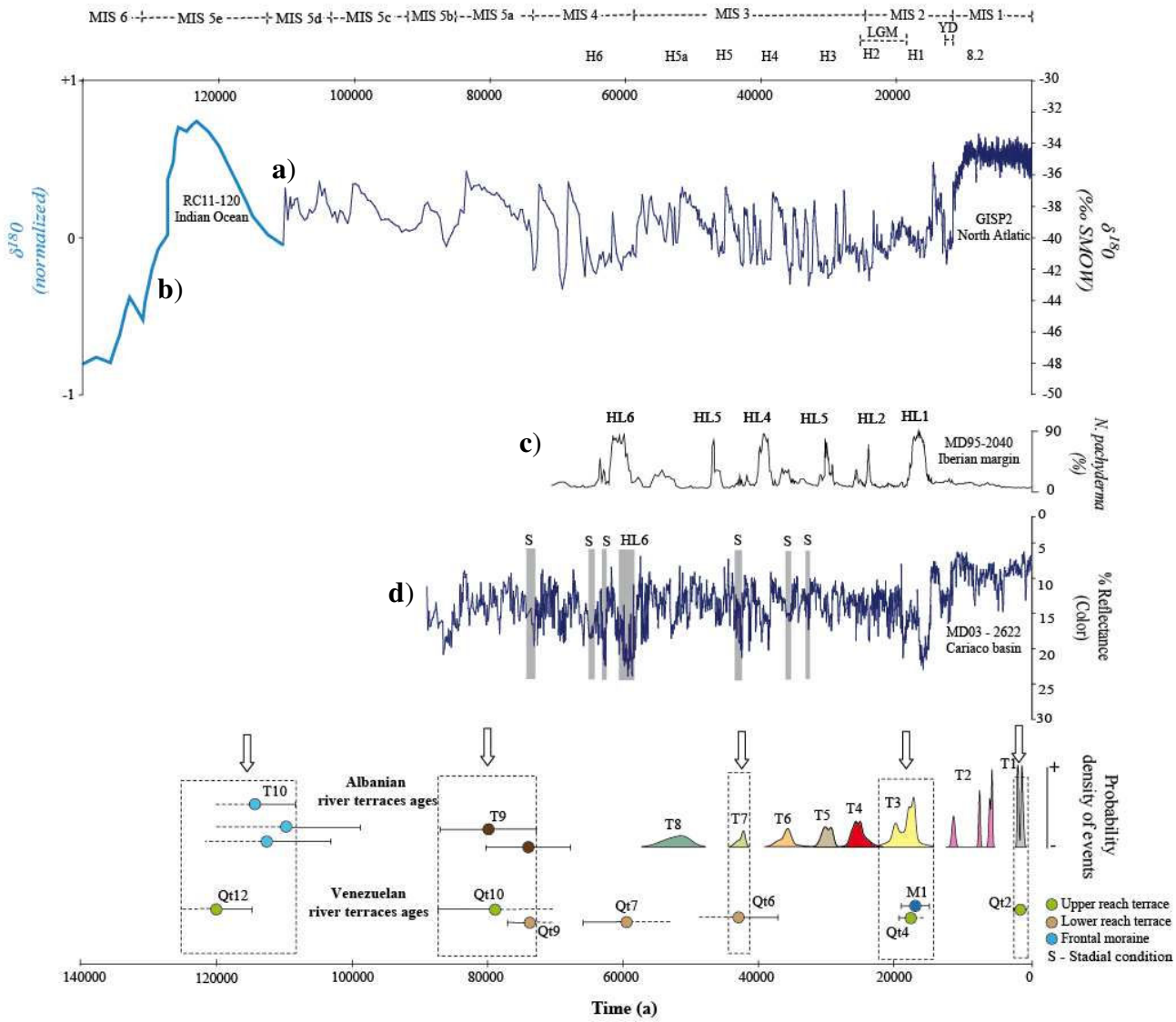

Figure VI.1. *Ages of abandonment of Venezuela and Albania river terraces for the last 120 ka compared with:* ***a****)* $\delta^{18}O$ *record from the GISP2 ice core (Grootes et al., 1993; Stuiver et al., 1995).* ***b****)* $\delta^{18}O$ *normalized record from the deep sea sediment of Southwestern Indian Ocean (Martison et al., 1987)* ***c****) The percentage of the cold water thriving foraminifera N. pachydermata from Iberian margin (de Abreu et al., 2003).* ***d****) Color reflectance curve of Cariaco basin (Peterson et al., 2000a). The gray rectangles represent short periods of cold and dry conditions identified by Peterson et al. (2000a) and González et al. (2008) in the Cariaco basin. (S) stadial. (HL6) Heinrich event 6. Dashed rectangles and white arrows represent the possible correlation between Venezuelan and Albania river terraces. The timing of Heinrich events H1-H6 is according to Hemming (2004) and Rashid et al., (2003). (MIS) Marine Isotope stage (Aitken and Stokes, 1997; Wright, 2000; Shackleton, 1987. (LGM) Last Glacial Maximum (Clark et al., 2009). (YD) Younger Dryas (Berger, 1990). (HL) Heinrich layers identified by the original authors of the curves* ***c****,* ***d*** *are also shown.*

In Venezuela differently to Albania, the river response to a climate variation and the processes of terraces formation seem to be highly controlled by the altitude of the reaches.

In fact, in the upper reaches of the PLSDS, where the elevations vary between 2300 and 1600 m a.s.l and only fill terraces are recognized, the ages of abandonment of the terraces correspond to cold-dry/warm-humid transition. On the contrary, in the lower reaches of the system, where the elevations are around 300 m a.s.l. and only strath terraces are identified, the ages of the abandonment of the terraces seem to correspond to short period of cold and dry conditions (e.g. stadial), within a large relatively warm and humid period (e.g. El Pedregal Interstade - Dirszowsky et al., 2005; Rull, 2005; Kalm and Mahaney, 2011). Therefore, we propose that the fill terraces located in the upper reaches of the system were formed in a similar way to the Albanian fill terraces. Cold and dry periods lead to aggradation phases, while warm and humid conditions cause the incision and abandonment of the terraces. During warm and humid conditions, the material eroded at the upper reaches is transported towards the lower reaches, where the increase in the sediment supply and water discharge determines that the river attains graded conditions (Mackin, 1948; Knox, 1975; Leopold and Bull, 1979); under these conditions, channel vertical incision and deposition are at a minimum; lateral erosion is more important, thus wide and continuous erosional surface (strath) is developed. This lateral erosion in the lower reaches of the system is interrupted by vertical fluvial incision triggered by the decrease in the transport capacity of the system caused by short period of cold and dry conditions. Thus, in this moment, a strath terrace is abandoned at the lower reach of the river (**figure VI.2**). Similar fluvial river response to climatic variations was reported for Stara planina valley in Bulgaria (Mishev, 1964 in Starkel, 2003). In this valley a high sediment supply during cold stages caused aggradation only in the upper river reaches, which is absent downstream in vegetated foothills, where a simultaneous incision took place.

The spatial variability in the processes of river terraces formation along the PLSDS could be associated to the orographic precipitation pattern observed in the Southeastern flank of the Mérida Andes (MA) (Monasterio and Reyes, 1980). In fact, González et al. (2008) proposed for Eastern Venezuela, the coexistence of two contrasting hydrological regimes during particular climatic conditions. For example, during stadial conditions, colder and possibly more humid conditions dominated in the mountain regions whereas drier conditions dominated in the lowland. A similar context occurring in the MA could be the explanation the fact that there is no terrace development during the stadial conditions in the upper reach of the rivers system. Moreover, the total record of river terraces in the PLSDS could reflect these complex hydrological regimes along the MA. However, more temporal and spatial data of river terraces along other rivers of MA (e.g., Motatan, Chama, Mocotíes and Guanare) are needed to better understanding the terraces development at the chain scale.

Figure VI.2. *Cartoon demonstrating possible relationships between vegetation cover, hillslope-channel coupling and aggradation–incision cycles during typical hydro-climatic conditions in the Albanian rivers and Venezuelan rivers. (MIS 2) Marine Isotope Stage 2.*

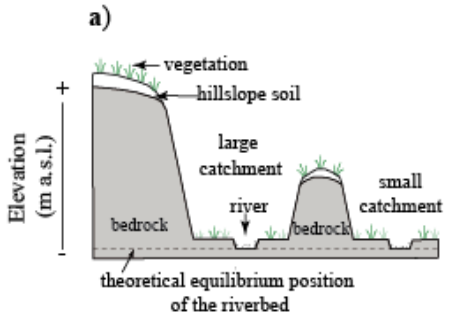

Hydro-climatic condition	Albanian terraces record		Venezuelan terraces record	
	Large catchment	Small catchment	Upper reaches	Lower reaches
Late warm and humid (1) * High vegetation cover * Stable hillslopes * Reduced sediment supply to the river channel * High transport capacity of the river	Vertical and lateral incision phase: * Strath surfaces of T12 toT5	Vertical and lateral incision phase	Vertical and lateral incision phase: * Strath surfaces of Qt12, Qt10, Qt4 to Qt1	Lateral incision phase: * Strath surfaces of Qt11, Qt9, Qt8 to Qt5
Cold and dry (1) Higher elevation * Poor vegetation cover * Unstable hillslopes * Increased sediment supply to the river channel * Reduced transport capacity of the river Lower elevation * Moderate vegetation cover * Stable hillslopes * Reduced transport capacity of the river Upper reaches in Venezuela During short cold and dry contitions (e.g. stadial, heinrich event), humid conditions prevailed in this part of the river (see text for discussion)	Case 1- pre-MIS 2 Aggradation phase: * Alluvial deposits of T12 to T5 Case 2- after the beginnig of MIS 2 Lateral incision phase: * Strath surfaces of T4 to T1	Lateral incision phase: * Strath surfaces of T11 to T1	Case 1- Long cold and dry conditions Aggradation phase: * Alluvial deposits of Qt12, Qt10, Qt4 to Qt1 Case 2- Short cold and dry conditions vertical incision of previous phase continues	Vertical incision phase: * Abandonment of terraces Qt11, Qt9, Qt8 to Qt5 note 1: the process is similar to that represented for the small catchment in **c)**
Early warm and humid (2) * High vegetation cover returns to hillslope and river valley * Reduced sediment supply to the river channel * Increased transport capacity of the river	Vertical incision phase: * Abandonment of terraces T12 to T1	Vertical incision phase: * Abandonment of terraces T11 to T1	Vertical incision phase: * Abandonment of terraces Qt12, Qt10, Qt4 to Qt1	Lateral incision phase note 2: the process is similar to that represented for the small catchment in **b)**

3) Eustatic influence

Geological and geomorphological settings of Albania rivers provide the geometrical conditions, in which the eustatic variations influence river terraces formation. Actually, we argue that the strath terraces developed in all Albanian rivers since the beginning of the MIS 2 are linked to a complex relation between climatic variation (hillslope processes, catchment hydrology) and eustatic drop. We recommend quantifying via analogical and numerical modeling these interactions.

4) Tectonic influence

Some of the Venezuelan and Albanian terraces could also be formed as a response of a base level tectonic perturbation. However, there is no record yet of sudden tectonic uplift or an increased uplift rate in both areas that can lead to a river terrace formation. In contrast, the incision rate of the river terraces of the lower PLSDS estimated in this thesis indicates a constant uplift rate over at least the last 70 ka in the Southeastern flank of the MA (see discussion subsection 3.5). These data together with the strong correlation between climatic variations and ages of terrace abandonment seem to suggest that the hypothesis of the purely tectonic river terraces is unlikely. We argue that the large record of the Venezuelan and Albanian terraces was possible due to the constant and moderate uplift that affected both areas. As expected, this setting provided the potential for vertical incision and preservation of the river responses to low and high frequency climatic variations.

This consideration bring us to the next question: can we estimate uplift rates from the river incision rate in any geological and geomorphological conditions? Incision rate estimated in this thesis are highly variable along the reaches of the studied rivers. For example, in Albanian rivers, the incision rate increases from the lower to the upper reaches. Mean long-term incision rates (last 200 ka) are quite variable from one river to another. Moreover, they were unsteady in the large catchments, while in the small catchments were constant. Additionally, Quaternary fault activity leads to local pulses of vertical incision rates. In Venezuela, the incision rate in the lower reaches of the river studied have been constant over the last 70 ka. Conversely, in the upper reaches the younger terraces (~18 and ~2 ka) show incision rates at least five times faster than the incision rate of the older terraces (~120 and ~79 ka). These results evidence that the estimation of the uplift rate from fluvial incision rate should consider the geological and geomorphological context of the area. Specifically, this analysis should be realized at least in a point of the catchment where the incision rate can be estimated for several periods, far enough from local fault deformation, with a homogeneous

lithology and minimizing the effects of incision induced by the evolution of the drainage network.

5) Glacial activity vs river terraces

Two of the seven rivers studied in this thesis were affected in the headwater by glacial activity (Vjosa and Pueblo Llano rivers, in Albania and Venezuela respectively). For the Vjosa river, Woodward et al. (2008), based on a morphochronological and sedimentological glacial and fluvial database along the upper reaches of the river, propose a model of long-term fluvial response to headwater glaciation. In this model, glacial activity during the Middle and Late Pleistocene shifted the boundary conditions for fluvial activity in the Vjosa catchment, because the location and volume of the glaciers changed markedly between cold stages. This shifted the main routes for meltwater runoff and sediment delivery. Material eroded by the large glaciers during the Marine Isotope Stage 6 (MIS 6) was partially delivered to the river channel network and constitutes the coarse material of the alluvial deposit of the terrace developed during this period (T10 in our integrated nomenclature of Albania terraces). Another part of this material was stored in the hillslope catchment. While during the last cold stage (MIS 5d to 2), the glaciers in the area were much smaller than their Middle Pleistocene counterparts, in this case, the direct delivery of the glacial coarse sediment to the fluvial system via meltwater floods, was likely to have been more reduced because of the restricted size of the glaciated areas. However, during this period, meltwater floods could have transported coarse sediments inherited from the large sediment fluxes associated with the Middle Pleistocene glaciations, and this material form part of the alluvial deposit of the terraces developed during the last cold stage in the upper reaches of the Vjosa river (T9, T8 and T4).

In Venezuela, our morphochronological analysis of the Pueblo Llano river gives some detail of the probable relations between glacial activity and fluvial system behavior. As a matter of fact, the age of abandonment of terraces Qt4 and Qt10 (~18 and ~79 ka) matches with the onset of the glacial melting of the Late and Early Mérida Glaciations in the PLSDS (~18 and ~81 ka, this study and Mahaney et al., 2000, respectively). These data allow suggesting that the material that constitutes the river terraces was deposited contemporarily to the glacier advance, while the vertical incision of the terraces and their abandonment match with the onset of the glacier melting. Thus, we argue that the following two scenarios were possible: 1) during the glacial condition all the material eroded by the glacier advance fed directly the river channel network and formed part of the terraces deposits; 2) during the

glacier melting, the glacial sediments were rapidly transported to the fluvial system, and due to the large transport capacity of the river (humid conditions and glacier melting), the sediments were transported along the river. Hence, more geomorphologic, dating analysis and analogical and numerical modeling along the fluvial system affected by headwater glaciation in the MA (e.g. upper reaches of: Santo Domingo, Chama, Mocotíes rivers) are required to better constrain theses scenarios.

6) The potential of river terraces record

In spite of the differences between the processes of river terraces formation in Albania and Venezuela, both terrace records put in evidence river response to global Quaternary climatic variations. Moreover, five of the seven ages of terrace abandonment of Venezuela could correspond to five of the Albanian ones (**figure VI.1**). This correlation highlights the potential of terrace record in global paleoclimatic reconstructions.

Though the terraces formation is mainly linked to climatic conditions, our results show that the long-term incision rate highly depends from the regional uplift and local change of incision rates are produced by the fault activity. Therefore, both terraces record put in evidence that this kind of study should strongly take into account the geological, geomorphological, tectonic and climatic context of the study area, which should be coupled with a set of precise numerical dating.

Chapitre VI: Discussions générales et conclusions

L'analyses morpho-chronologiques de terrasses fluviales effectuées dans cette thèse le long des rivières du Vénézuéla (Andes de Mérida) et de l'Albanie, ont amené à une meilleure compréhension du rôle principal que jouent les contrôles externes, tels que le climat et la variation du niveau de base (soit tectonique ou eustatique) dans les processus de formation des terrasses. Notre analyse met en évidence que le processus d'incision verticale et par conséquent l'abandon des terrasses, dans les deux domaines, est à la fois une réponse au soulèvement et aux variations climatiques, tandis que la variation eustatique et les paramètres morphologiques (par exemple la taille des bassins versants, l'altitude) semblent moduler la réponse des rivières aux changements climatiques. Dans ce qui suit, nous discuterons le rôle de chaque variable, ainsi que nos conclusions générales:

1) La transition climatique comme un déclencheur de la formation de terrasse

Récemment, Bridgland et Westaway (2008) ont résumé les trois principaux modèles dans le monde pour la formation des terrasses en réponse aux variations climatiques (**figure I.4**). Cependant, les terrasses du Vénézuéla et de l'Albanie s'inscrivent-ils dans ce schéma? La comparaison faite dans cette thèse entre les courbes paléoclimatiques régionales et locales avec l'âge de l'abandon des terrasses du Vénézuéla et de l'Albanie a permis de mieux comprendre les relations entre les variations climatiques et les processus de formation des terrasses.

En Albanie, et plus généralement dans le contexte méditerranéen, l'âge d'abandon de presque toutes les terrasses sont en corrélation avec les changements climatiques globaux quaternaires. Ces changements correspondent à la transition des conditions froides et sèches aux conditions chaudes et humides (**figure VI.1**). Ces variations climatiques entraînent des changements rapides (<0.2 ka) dans l'hydrologie et la végétation du bassin versant (Tzedakis et al., 1997; Allen et al., 1999; Allen, 2003; Wohlfarth et al., 2008), qui contrôlent les phases d'aggradation ainsi que l'incision de terrasses fluviales. En particulier, dans des conditions froides et sèches, des colluvions du versant sont déstabilisées à la suite de la modification de la couverture végétale (par exemple des écosystèmes forestiers dominés (des conditions chaude et humide) à l'écosystème steppique dominé (des conditions froides et sèches)). En conséquence, les systèmes fluviaux subissent des variations importantes dans la capacité de

transport et d'approvisionnement des sédiments. Les flux élevés de sédiments associés à des conditions sèches, conduisent à des phases d'alluvionnement pendant les périodes froides et sèches. Puis, à partir de la transition des conditions froides et sèches à des conditions chaudes et humides, la couverture végétale revient en réponse à une température croissante. Cette couverture végétale réduit l'érosion du versant par le ruissellement et limite le transport des sédiments. Ce fait, combiné avec la capacité de transport croissante de la rivière (en raison des nouvelles conditions humides) induisent l'incision fluviale et l'abandon de la terrasse pendant les périodes chaudes et humides (**figure VI.2**). Cette réponse fluviale aux changements climatiques a été initialement proposé par Bull et Knüpfer (1987) et Bull (1990, 1991) pour les systèmes fluviaux dans le climat tempéré des montagnes Rocheuses dans l'ouest des États-Unis et les Alpes du Sud de Nouvelle-Zélande au cours des dernières 200 ka. Cette réponse a également été documentée en climat tempéré maritime des rivières du nord-ouest européens (par exemple van der Berg, 1996 Bridgland, 2000; Bridgland et al., 2004), dans plusieurs enregistrement des terrasses méditerranée (par exemple, Fuller et al., 1998; Macklin et al, 2002; Wegmann et Pazzaglia, 2009), dans le climat semi-arides de l'Asie centrale (Vassallo et al., 2007), et plus récemment dans le climat sub-saharien du système de haute pression subtropicale des montagnes de Haut Atlas central au Maroc (Arboleya et al., 2008).

Au Vénézuéla, l'âge de l'abandon des terrasses fluviales du système des rivières Pueblo Llano et Santo Domingo semblent avoir une bonne corrélation avec le changement climatique (**figure VI.1**) (González et al., 2008; Van Daele et al., 2011; Rull et al., 2010). Comme dans le contexte albanais, ces variations climatiques produisent également des changements rapides dans l'hydrologie et la végétation des bassins versants au Venezuela (Peterson et al., 2000a, 2000b; Haugh et al., 2001; Peterson et Haugh, 2006; González et al., 2008). Ces changements modulent les phases d'aggradations et incision de la rivière, bien que les observations géomorphologiques indiquent que d'autres processus jouent également un rôle dans le dépôt de matériaux alluvionnaires (par exemple l'épandage glaciaire en amont du système, les événements climatiques catastrophiques instantanées, l'activité néotectonique de la faille du Boconó).

2) Taille du bassin versant et précipitations

Cette étude montre que les réponses géomorphologiques du système fluvial albanais induits par les variations climatiques ont probablement été modulées par d'autres processus, comme la taille des bassins versants et des variations eustatiques. En fait, nous pensons que pendant les conditions froides et sèches de la période pré-MIS 2, les parties supérieures des

grands bassins versants ont été plus fortement touchée par les processus des versants. Ces derniers ont déterminé le fait qu'une plus grande quantité de sédiments ont été délivrés au canal principal de la rivière. Ce fait, combiné avec la capacité de transport réduite de la rivière (causée par des conditions sèches) a favorisé le développement des terrasses de remplissage dans les grands bassins. Dans les petits bassins versants de l'Albanie, l'équilibre entre l'apport de sédiments et la capacité de transport de la rivière a favorisé le développement de terrasses d'abrasion plutôt que de terrasses de remplissage.

Au Venezuela, autrement qu'en Albanie, la réponse de la rivière à une variation du climat et les processus de formation des terrasses semblent être fortement contrôlées par l'altitude de la partie. En fait, dans la partie supérieure du système des rivières Pueblo Llano et Santo Domingo, où les altitudes varient entre 2300 et 1600 m au dessus du niveau de la mer et où des terrasses de remplissage sont reconnues, l'âge d'abandon des terrasses correspond à la transition des conditions froides et sèches à des conditions chaudes et humides. Au contraire, dans la partie inférieure du système, où l'altitude est d'environ 300 m au dessus du niveau de la mer et où des terrasses d'abrasion sont identifiées, l'âge de l'abandon des terrasses semblent correspondre à des courtes périodes de temps froid et sec (par exemple stadiaire), dans une grande période de temps relativement chaud et humide (par exemple El Pedregal Interstade - Dirszowsky et al., 2005; Rull, 2005; Kalm et Mahaney, 2011). Par conséquent, nous proposons que les terrasses de remplissages situées dans la partie supérieure du système ont été formées de manière similaire aux terrasses de remplissage de l'Albanie. Les périodes froides et sèches conduisent à des phases d'alluvionnement, tandis que les conditions chaudes et humides induisent l'incision et l'abandon des terrasses. Pendant des conditions chaudes et humides, le matériau érodé de la partie supérieure est transporté vers le cours inférieur, où l'augmentation simultanée du débit et de l'apport de sédiments mettent la rivière en condition d'équilibre (*graded condition*) (Mackin, 1948; Knox, 1975; Léopold et Bull, 1979); dans ces conditions, l'incision verticale et l'aggradation sont réduits au minimum; l'érosion latérale est plus importante, donc une surface large et continue d'abrasion latérale (*strath*) est développé. Cette abrasion latérale dans le cours inférieur du système est interrompue par une incision verticale causée par la diminution de la capacité de transport de la riviere provoquée par une courte periode de temps froid et sec. Ainsi, en ce moment, une terrasse d'abrasion est abandonnée à la partie inférieure de la rivière (**figure VI.2**). Une réponse similaire des rivières aux variations climatiques a été signalée pour la vallée de Stara Planina en Bulgarie (Mishev, 1964 à Starkel, 2003). Dans cette vallée, un apport de sédiments élevé pendant une phase froide a causé une aggradation seulement dans la partie supérieure de la rivière, bien

qu'un processus d'incision verticale se soit produit simultanément dans la partie inférieure de la rivière, qui est couverte par la végétation.

La variabilité spatiale dans les processus de formation des terrasses de rivière le long du sytème des rivières Pueblo Llano et Santo Domingo pourrait être associée à la configuration des précipitations observées dans le flanc sud-est des Andes de Mérida (Monasterio et Reyes, 1980). En fait, González et al. (2008) ont proposé pour l'Est du Vénézuéla, la coexistence de deux régimes hydrologiques contrastés lors de conditions climatiques particulières. Par exemple, dans des periodes stadiaires, des conditions plus froides et humides dominent dans les régions de montagne, tandis que des conditions plus sèches dominent dans la plaine. Un contexte similaire survenu dans les Andes de Mérida pourrait explique l'absence de développement des terrasse pendant les conditions stadiaire dans la partie supérieur du système des rivières. En outre, le total record de terrasses fluviales dans le sytème des rivières Pueblo Llano et Santo Domingo pourrait refléter ces régimes hydrologiques complexes le long des Andes de Mérida. Toutefois, plus de données temporelles et spatiales des terrasses fluviales le long d'autres rivières des Andes de Mérida (par exemple Motatan, Chama, Mocotíes et Guanare) sont nécessaires pour mieux comprendre le développement des terrasses à l'échelle de la chaîne.

3) L'influence Eustatique

Le cadre géologique et géomorphologique des rivières de l'Albanie fournit les conditions géométriques, dans laquelle la variation eustatique influence la formation des terrasses de la rivière. En fait, nous soutenons que les terrasses d'abrasion développées dans toutes les rivières d'Albanie depuis le début du MIS 2 sont liées à une relation complexe entre les variations climatiques (hydrologie des bassins versants) et la chute eustatique. Nous recommandons, pour la suite des recherches, de quantifier par modélisation analogique et numérique ces interactions.

4) L'influence Tectonique

Certaines des terrasses du Vénézuéla et de l'Albanie pourraient également avoir été formées comme une réponse d'une perturbation tectonique à un niveau de base. Cependant, il n'y pas encore trace de surrection soudaine ou d'une augmentation du taux de surrection dans les deux domaines qui peuvent conduire à une formation de terrasse fluviale. En revanche, le taux d'incision estimé dans cette thèse de la partie inférieurs du sytème des rivières Pueblo Llano et Santo Domingo indique un taux de surrection constante sur au moins les dernières 70

ka dans le flanc sud-est des Andes de Mérida. Ces données, ainsi que la forte corrélation entre les variations climatiques et les âges d'abandon des terrasses, semblent suggérer que l'hypothèse des terrasses fluviales purement tectoniques est peu probable. Nous soutenons que le large registre des terrasses du Vénézuéla et de l'Albanie a été possible grâce à la surrection constante et modérée qui a affecté les deux zones. Comme prévu, ce paramètre a fourni la possibilité d'incision verticale et la préservation des réponses de la rivière aux variations climatiques à basses et hautes fréquences.

Cette considération nous amène à la question suivante: peut-on estimer les taux de surrection à partir des taux d'incision de la rivière dans n'importe quelle contextes géologiques et géomorphologiques? Les taux d'incisions estimés dans cette thèse sont très variables le long du cours des rivières étudiées. Par exemple, dans les rivières d'Albanie, le taux d'incision augmente de la partie inférieure à la partie supérieure de la rivière. Les taux d'incisions moyens à long-terme (dernières 200 ka) sont très variables d'une rivière à l'autre. En outre, ils étaient variables dans les grands bassins versants, tandis que, dans les petits bassins versants, ils ont été constants. En outre, l'activité Quaternaire des failles conduit à l'augmentation locale des taux d'incisions verticale. Au Vénézuéla, le taux d'incision dans la partie inférieur de la rivière étudiée a été constant au cours des dernières 70 ka. Inversement, dans la partie supérieur les terrasses les plus jeunes (~18 à ~2 ka) montrent des taux d'incision au moins cinq fois plus rapide que le taux d'incision des terrasses anciennes (~120 et ~79 ka). Ces résultats mettent en évidence que l'estimation du taux de surrection à partir de taux d'incision fluviale doit tenir compte du contexte géologique et géomorphologique de la région. Plus précisément, cette analyse doit être réalisée au moins en un point du bassin versant où le taux d'incision peut être estimé pour plusieurs périodes, assez loin de la déformation locale induite par faille, sur une lithologie homogène, et se doit minimiser les effets de l'incision induits par l'évolution du drainage réseau.

5) L'activité glaciaire et les terrasses fluviales

Deux des sept rivières étudiées dans cette thèse ont été affectées dans la partie supérieur par l'activité glaciaire (des rivières Vjosa et Pueblo Llano, en l'Albanie et au Vénézuéla, respectivement). Pour la rivière Vjosa, Woodward et al. (2008), sur la base de données morphochronologiques et sédimentologiques glaciaire et fluviale le long de la partie supérieure de la rivière, ont proposé un modèle de réponse fluviale à long-terme, à la glaciation d'amont. Dans ce modèle, l'activité glaciaire au Pléistocène moyen et supérieur contrôle les conditions aux limites pour l'activité fluviale dans le bassin versant du Vjosa,

parce que l'emplacement et l'extension des glaciers ont considérablement changé entre les phases froides. Ces paramètres contrôlent les principales routes pour l'écoulement des eaux de fonte et de l'apport de sédiments. Les matériaux érodés par les grands glaciers au cours de la MIS 6 ont été partiellement délivrés au chenal de la rivière, et constituent la matière grossière du dépôt alluvial de la terrasse développé au cours de cette période (T10 dans notre nomenclature intégrée des terrasses de l'Albanie). Une autre partie de cette matière a été stockée dans les versants. Alors que pendant la dernière phase froide (MIS 5d à 2), les glaciers de la région étaient beaucoup plus petits que leurs homologues du Pléistocène moyen, l'apport direct des sédiments grossiers glaciaire au système fluvial par les inondations d'eau de fonte, a été probablement plus réduit en raison de la taille restreinte des zones glaciaires. Toutefois, pendant cette période, les inondations d'eaux de fonte auraient transporté les sédiments grossiers hérités des grands flux de sédiments associés aux glaciations du Pléistocène moyen, et cette matière fait partie du dépôt alluvial des terrasses développés au cours de la dernière étape de froid dans le cours supérieur de la rivière Vjosa (T9, T8 et T4).

Au Vénézuéla, notre analyse morpho-chronologique de la rivière Pueblo Llano donne quelques détails sur les relations probables entre l'activité glaciaire et le comportement du système fluvial. En fait, l'âge de l'abandon des terrasses Qt4 et QT10 (~18 et ~79 ka) correspond au début de la fonte des glaciers de la première et deuxieme période glaciaire de "Mérida" (*Early and Late Mérida Glaciation)* dans le valley du Pueblo Llano (~18 et ~81 ka, cette étude, et Mahaney et al., 2000, respectivement). Ces données permettent de penser que la matière qui constitue les terrasses fluviales a été déposée simultanément à l'avance des glaciers, tandis que l'incision verticale des terrasses et leur abandon correspondent avec le début de la fonte des glaciers. Ainsi, nous soutenons que les deux scénarios suivants sont possibles: 1) au cours de l'état glacial tout le matériel érodé par l'avance des glaciers a alimenté directement le réseau de canaux de la rivière et fait partie des dépôts de terrasses, 2) lors de la fonte des glaciers, les sédiments glaciaires ont été rapidement transportés vers le système fluvial, et en raison de la grande capacité de transport de la rivière (des conditions humides et de la fonte des glaciers), les sédiments ont été transportés le long de la rivière. Pour mieux comprendre ces processus, plus des données géomorphologiques et chronologiques, ainsi que la modélisation analogique et numérique le long des systèmes fluviales affecté par la glaciation dans les Andes de Mérida (par exemple partie supérieur des rivières: Santo Domingo, Chama et Mocotíes) sont nécessaires.

6) Le potentiel des terrasses fluviales

En dépit des différences entre les processus de formation des terrasses fluviales en Albanie et Vénézuéla, les deux registres des terrasses mettent en évidence la réponse des rivières aux variations climatiques globale du Quaternaire. Par ailleurs, cinq sur sept âges d'abandon des terrasses du Venezuela pourraient correspondre avec cinq des terrasses de l'Albanie (**figure VI.1**). Cette corrélation met en évidence le potentiel du registre de terrasses dans les reconstructions paléoclimatiques globale.

Bien que la formation des terrasses soit principalement liée aux conditions climatiques, nos résultats montrent que le taux d'incision à long-terme dépend fortement de la surrection regionale et que les changements locaux des taux d'incision est produits par l'activité de failles. Par conséquent, les deux registres des terrasses ont mis en évidence que ce type d'étude devrait fortement prendre en compte le contexte géologique, géomorphologique, tectonique et climatique de la zone d'étude, et doit être couplé avec des datations numériques précises.

References

A

Aitken, M. J., Stokes, S. 1997. Chapter 1. In: Taylor, R. E., Aitken, M. J., (Eds.), Chronometric dating in archaeology. Birkhäuser, ISBN 0-306-45715-6, ISBN 978-0-306-45715-9, google books.

Akin, W. E. 1991. Global Patterns: Climate, Vegetation, and Soils. University of Oklahoma Press, 52 pp.

Aliaj, Sh., 1971. Adriatic depression and its structures in the light of geophysical dta. Bul. USHT, Ser. Shk. Nat. 3, 25-41 (In Albanian).

Aliaj, S.,1988. Neotectonic and seismotectonic of Albania. Ph.D. Thesis, Archive of Institute of Seismology, Tirana, Albania. (in Albanian).

Aliaj, S., 1991. Neotectonic structure of Albania. Albanian J. of Nat. Technol Sci. 4, 79-98.

Aliaj, S. H., 1999. Transverse fault in Albania Orogen front. Albanian J. of Nat. Technol Sci. 6, 121-132.

Aliaj, S., 2000. Neotectonics and seismicity in Albania. In: Melo, S., Aliaj, S., Turku, I. (Eds.), Geology of Albania, Beitrage zur regionalen Geologie der Erde. Gebruder Borntrager, Berlin, 135–178.

Aliaj, Sh., 2004. Seismic source zones in Albania. NATO Sciences for peace programme, Project N° 972342 "Seismotectonis and Seismic hazard Assesment in Albania" Final report.

Aliaj, Sh., 2006. The Albanian Orogen: Convergence zone between Eurasia and the Adria microplate. In: Pinter, N., Grenerczy, G., Weber, J., Stein, S., Medak., D. (Eds), The Adria Microplate: GPS Geodesy, Tectonics and hazards. NATO Science Series. IV/61 Earth and Environmental Sci. 133-149.

Aliaj, Sh., Melo, V., Hyseni, A., Skrami, J., Mëhillka, Ll. Muço, B., Sulstarova, E., Prifti, K., Pashko, P., Prillo, S., 1996. Neo-tectonic map of Albania in scale 1:200000. Archive of seismology Institute, Tirana, Albania (in Albanian).

Aliaj, S., Sulstarova, E., Muço, B., Koçiu, S., 2000. Seismotectonic map of Albania in scale 1: 500000. Archive of Institute of Seismology, Tirana, Albania. (in Albanian).

Allen, H. D., 2003. Response of past and present Mediterranean ecosystems to environmental change. Progress in Phys. Geography 27(3), 359-377.

Allen, J. R. M., Brandt, U., Brauer, A., Hubberten, H., Huntley, B., Keller, J., Kraml, M., Mackensen, A., Mingram, J., Negendank, J.F.W., Nowaczyk, N.R., Oberhänsli, H., Watts, W.A., Wulf, S., Zolitschka, B., 1999. Rapid environmental changes in southern Europe during the last glacial period. Nature 400, 740–743.

Allen, J. R. M., Huntley, B., 2009. Last Interglacial palaeovegetation, palaeoenvironments and chronology: a new record from Lago Grande di Monticchio, southern Italy. Quat. Sci. Rev. 28,1521–1538.

Altamimi Z., Collilieux X., Legrand J., Garayt B., Boucher C., 2007. ITRF2005: A new release of the International Terrestrial Reference Frame based on time series of station positions and Earth Orientation Parameters. J. of Geophysical Res. 112, B09401, doi:10.1029/2007JB004949.

Anderson, R.S., Repka, J.L., Dick, G.S., 1996. Explicit treatment of inheritance in dating depositional surfaces using *in situ* ^{10}Be and ^{26}Al. Geology 24, 47–51.

Antoine, P., 1994. The Somme Valley terrace system (northern France); a model of river response to Quaternary climatic variations since 800000 BP. Terra Nova 6, 453–464.

Antoine, P., Lautridou, J.P., Laurent, M., 2000. Long-term fluvial archives in NW France: response of the Seine and Somme rivers to tectonic movements, climate variations and sea-level changes. Geomorphology 33, 183–207.

Antoine, P., Limondin, N.L., Chaussé, C., Lautridou, J-P., Pastrea, J-F., Auguste, P., Bahaine, J-J., Falguères, C., Galehb, B., 2007. Pleistocene fluvial terraces from Northern France (Seine, Yonne, Somme): synthesis, and new results from interglacial deposits. Quat. Sci. Rev. 26, 2701–2723.

Arboleya, M-L., Babault, J., Owen, L., Teixell, A., Finkel, R., 2008. Timing and nature of Quaternary fluvial incision in the Ouarzazate foreland basin, Morocco. J. of the Geological Soc. 165, 1059-1073.

Arnold, M., Merchel, S., Bourles, D., Braucher, R., Benedetti, L., Finkel, R.C., Aumaitre, G., Gottdang, A., Klein, M., 2010. The French accelerator mass spectrometry facility ASTER: Improved performance and developments. Nucl. Instrum. and Methods in Phys. Res. Sect. B: Beam Interac. with Mater. and Atoms 268, 1954-1959.

Audemard, F. A., 1993. Néotectonique, Sismotectonique et Aléa Sismique du Nordouest du Vénézuéla (Système de failles d'Oca-Ancón). Ph.D. Thesis, Université Montpellier II, France, 369 pp.

Audemard, F. A., 1998. Evolution Géodynamique de la Façade Nord Sud-américaine: Nouveaux apports de l'Histoire Géologique du Bassin de Falcón, Vénézuéla. XIV Caribbean Geological Conference, Trinidad-1995, 2, 327-340.

Audemard, F. A., 1999. Morpho-structural expression of active thrust fault systems in humid tropical foothills of Colombia and Venezuela. Zeitschrift für Geomorphologie 118, 1-8.

Audemard, F. A., 2003. Geomorphic and geologic evidence of ongoing uplift and deformation in the Mérida Andes, Venezuela. Quat. International 101-102C, 43-65.

Audemard, F. A., 2009. Flexura Frontal Sub-andina, Venezuela (VE-07). In: Servicio Nacional de Geología y Minería (Ed), Atlas de las deformaciones cuaternarias de Los Andes. Proyecto multinacional andino: Geociencia para las comunidades andinas. Publicacion Geológica nacional N° 7, 300-311.

Audemard, F. A., Romero, G., Rendón, H., 1999a. Sismicidad, Neotectónica y Campo de Esfuerzos del Norte de Venezuela. Funvisis unpublished Report for PDVSA-CVP, 221 pp.

Audemard, F. A., Pantosti, D., Machette, M., Costa, C., Okumura, K., Cowan, H., Diederix, H., Ferrer, C. and Sawop Participants, 1999b. Trench investigation along the Mérida sectión of the Boconó fault (central Venezuelan Andes), Venezuela. In: Pavlides, S., Pantosti, D., Peizhen, Z., (Eds.), Earthquakes, Paleoseismology and Active Tectonics. Selected papers to 29th General Assembly of the Association of Seismology and Physics of the Earth's Interior (IASPEI), Thessaloniki, Greece, August 1997. Tectonophysics 308, 1-21.

Audemard, F. A., Machette, M., Cox, J., Dart, R. Haller, K., 2000. Map and Database of Quaternary Faults in Venezuela and its Offshore Regions. US Geological Survey Open-File Report 00-0018. Include map at scale 1: 2.000,000 and 78-page report.

Audemard, F. A., Romero, G., Rendon, H., Cano, V., 2005. Quaternary fault kinematics and stress tensors along the southern Caribbean from fault-slip data and focal mechanism solutions. Earth Sci. Rev., 69, 181–233.

Audemard, F. A., Singer, A., Soulas, J. P., the Neotectonic section of the FUNVISIS Earth Sciences Department, Including Bellier, O., 2006. Quaternary faults and stress regime of Venezuela. Revista de la Asociacion Geológica Argentina 61, 480-491.

Audemard, F., Carrillo, E., Beck, C., 2007. Blind dip-slip faulting and strain partitioning in an active orogen: The Mérida Andes case, Venezuela. Fieldtrip Guidebook. International Workshop, 77 pp.

Audemard, F. A., Ollarves, R., Bechtold, M., Diaz, G., Beck, C., Carrillo, E., Pantosti, D., Diederix, H., 2008. Trench investigation on the main strand of the Boconó fault in its central section, at Mesa del Caballo, Mérida Andes, Venezuela. Tectonophysics 459, 38–53.

Audemard, F. E., 1991. Tectonics of Western of Venezuela. Ph.D. Thesis, Rice University, Texas, 245 pp + appendices.

Audemard, F. E., Audemard F. A., 2002, Structure of the Mérida Andes, Venezuela: relations with the South America-Caribbean geodynamic interaction. Tectonophysics 345, 299-327.

Autin, W. J., Burns, S. F., Miller, B. J., Saucier, R. T., Snead, J. I., 1991. Quaternary geology of the Lower Mississippi valley. In: Morrison, R. B (Ed.), Quaternary Nonglacial Geology: Counterminous U.S., Boulder, Colorado. Geological Society of America, Geology of North America k-2, 547-582.

Avé-Lallemant, H. G., 1997. Transpression, Displacement Partitioning, and Exhumation In The Eastern Caribbean/South American Plate Boundary Zone. Tectonics 16 (2), 272-289.

Avouac, J-P., 1993. Analysis of scarp profiles: evaluation of errors in morphologic dating. J. of Geophysical Res. 98, 6745 – 6754.

Azocar, A., Monasterio, M., 1980. Caracterización ecológica del clima en el Páramo de Mucubají. In: Monasterio, M. (Ed), Estudios ecológicos en los paramos andinos. Universidad de Los Andes, Mérida, 207–262.

B

Backé, G., Dhont, D., Hervouët, Y., 2006. Spatial and temporal relationships between compression, strike-slip and extension in the central Venezuelan Andes: Clues for Plio-Quaternary tectonic escape. Tectonophysics 425, 25-53.

Bagnold, R.A., 1960. Sediment discharge and stream power: a preliminary announcement. U. S. Geol. Surv. Bull. 421.

Bagnold, R.A., 1977. Bed-load transport by natural rivers. Water Resour. Res. 13, 303–312.

Balco, G., Stone, J.O., Lifton, N.A., Dunai, T.J., 2008. A complete and easily accessible means of calculating surface exposure ages or erosion rates from ^{10}Be and ^{26}Al measurements. Quat. Geochron. 3, 174–195.

Basili, R., Kastelic, V., Demircioglu, M. B., Garcia Moreno, D., Newser, E., S., Petricca, P., Sboras, S. P., Besana-Ostma, G. M., Cabral, J., Camelbeeck, T., Caputo, R., Danciu, L., Dornac, H., Fonseca, J., Garcia-Mayordomo, J., Giardini, D., Glavatovic, B., Gulen, L., Ince, Y., Pavlides, S., Sesetyan, K., Tarabusi, G., Tiberti, M. M., Utkucu, M., Valensise, G., Vanneste, K., Vilanova, S., Wössner, J., 2013. The European Database of Seismogenic Faults (EDSF) compiled in the framework of the Project SHARE. http://diss.rm.ingv.it/share-edsf/, doi: 10.6092/INGV.IT-SHARE-EDSF.

Bard, E., Hamelin, B., Fairbanks, R.G., Zindler, A., 1990. Calibration of the ^{14}C timescale over the past 30,000 years using mass spectrometric U-Thages from Barbados corals. Nature 345, 405-410.

Bard, E., Rostek, F., Ménot-Combes, G., 2004. Radiocarbon calibration beyond 20,000 ^{14}C yr BP by means of planktonic foraminifera of the Iberian Margin. Quat. Res. 61, 204-214.

Bar-Matthews, M., Ayalon, A., Kaufman, A., Wasserburg, G.J., 1999. The Eastern Mediterranean palaeoclimate as a reflection of regional events: Soreq Cave, Israel. Earth and Planet. Sci. Lett. 166, 85–95.

Bartov, Y., Goldstein, S.L., Stein, M., Enzel, Y., 2003. Catastrophic arid episodes in the Eastern Mediterranean linked with the North Atlantic Heinrich Events. Geology 31, 439–442.

Begin, Z. B., Meyer, D. F. Schumm, S. A., 1981. Develop- ment of longitudinal profiles of alluvial channels in response to base-level lowering. Earth Surf. Process. Landforms, 6, 49-68.

Beltrán, C., 1994, Trazas activas y síntesis neotectónica de Venezuela a escala 1:2.000.000. VII Congreso Venezolano de Geofísica, Caracas. Sociedad Venezolana de Ingenieros Geofísicos, 541- 547.

Bell, J., 1972. Geotectonic evolution of the Southern Caribbean area. Geological Soc. of America Memoir 132, 369–386.

Berger, W. H., 1990. The Younger Dryas cold spell – a quest for causes .*Glob.* and Planet. Change 3 (3). 219–237.

Bermúdez, M., 2009. Cenozoic exhumation patterns across the Venezuelan Andes: insights from fission-track thermochronology. Ph.D. Thesis, Université Joseph Fourier, France, 305 pp.

Bermudez, M., van der Beek, P., Bernet, M., 2011. Asynchronous Miocene-Pliocene exhumation of the central Venezuelan Andes. Geology 39, Issue 2, 139-142.

Bezada, M., 1990. Geología glacial del Cuaternario de la región de Santo Domingo-Pueblo Llano-Las Mesitas (Estado Mérida y Trujillo). Ph.D. Thesis, Centro de Estudios Avanzados, Instituto Venezolano de Investigaciones Científicas, Caracas, 245 pp.

Bierman P. R., 1994. Using in situ produced cosmogenic isotopes to estimate rates of landscape evolution: A review from the geomorphic perspective. J. Geophys. Res., 99 (B7), 13885-13896.

Björck, J., Th. Andren, S. Wastegard, G. Possnert, and K. Schoning. 2002. An event stratigraphy for the Last Glacial–Holocene transition in eastern middle Sweden: Results from investigations of varved clay and terrestrial sequences. Quat. Sci. Rev. 21, 1489–1501.

Blum, M. D., 1993. Genesis and architecture of incised valley fill sequences; a late Quaternary example from the Colorado River, Gulf Coastal Plain of Texas. In: Weimer, P., Posamentier, H. W. (Eds.), Siliciclastic sequence stratigraphy; recent developments and applications, AAPG Memoir 58, 259-283.

Blum, M. D., and Valastro, S. Jr., 1994. Late Quaternary sedimentation, lower Colorado River, Gulf Coastal Plain of Texas; with Suppl. Data 9420. Geological Society of America Bulletin, 106, 1002-1016.

Blum M.D., Törnqvist, T.E., 2000. Fluvial responses to climate and sea-level change: a review and look forward. Sedimentology 47, 2-48.

Bond, G., Heinrich, H., Broecker, W., Labeyrie, L., Mcmanus, J., Andrews, J., Huon, S., Jantschik, R., Clasen, S., Simet, C., 1992. Evidence for massive discharges of icebergs into the North Atlantic ocean during the last glacial period. Nature 360, 245–249.

Bond, G. C., Lotti, R., 1995. Iceberg Discharges into the North Atlantic on Millennial Time Scales During the Last Glaciation. Sci. 267 (5200): 1005–1010.

Braucher R., 1998. Utilisation du ^{10}Be cosmogénique produit in-situ pour l'étude de la dynamique des latérites en zone tropicale. Ph.D. Thesis, Université d'Aix-Marseille III , France, 117 pp.

Braucher, R., Bourlès, D.L., Brown, E.T., Colin, F., Muller, J.-P., Braun, J.-J., Delaune, M., Edou Minko, A., Lescouet, C., Raisbeck, G.M., Yiou, F., 2000. Application of in situ-produced cosmogenic ^{10}Be and ^{26}Al to the study of lateritic soil development in tropical forest: theory and examples from Cameroon and Gabon. Chemical Geology 170 – 2000, 95–111

Braucher, R., Brown, E. T., Bourlès, D. L. Colin, F., 2003. In situ produced ^{10}Be measurements at great depths: implications for production rates by fast muons. Earth Planet. Sci. Lett., 211, 251-258.

Bridgland, D.R., 2000. River terrace systems in north-west Europe: an archive of environmental change, uplift and early human occupation. Quat. Sci. Rev. 19, 1293–1303.

Bridgland, D.R., 2001. The Pleistocene evolution and Palaeolithic occupation of the Solent River. In: Wenban-Smith, F.F., Hosfield, R.T. (Eds.), Palaeolithic Archaeology of the Solent River. Lithic Studies Society. Occasional Paper 7. Lithic Studies Society, London, 15–25.

Bridgland, D.R., Maddy, D., Bates, M., 2004. River terrace sequences: templates for Quaternary geochronology and marineterrestrial correlation. J. of Quat. Sci. 19, 203–218.

Bridgland, D., Westaway, R., 2008. Climatically controlled river terrce staircases: A worldwide Quaternary phenomenon. Geomorphology 98, 285-315.

Brown, E.T., Edmond, J.M., Raisbeck, G.M., Yiou, F., Kurz, M.D., Brook, E.J., 1991. Examination of surface exposure ages of Antarctic moraines using in situ produced 10Be and 26Al: Geochimica et Cosmochimica Acta 55, 2269-2283.

Brown E. T., Brook, E. J., Raisbeck, G. M., Yiou, F., Kurz, M. D., 1992. Effective attenuation lengths of cosmic rays producing ^{10}Be and ^{26}Al in quartz: implication for exposure age dating. Geophys. Res. Let., 19 (4), 369-372.

Bull, W.B., 1979. Threshold of critical power in streams. Geol. Soc. Am. Bull. 90, 453–464.

Bull, W.B., Knüpfer, P.L.K., 1987. Adjustments by the Charwell River, New Zealand, to uplift and climatic changes. Geomorphology 1, 15–32.

Bull, W.B., 1990. Stream-terrace genesis: Implications for soil development. In: Knüpfer, P.L.K., McFadden, L.D. Ž. (Eds.), Soils and Landscape Evolution. Geomorphology 3, 351–367.

Bull, W.B., 1991. Geomorphic Responses to Climatic Change. Oxford Univ. Press, New York, NY.

Bull, W. B., 2009. Tectonically Active Landscapes. Wiley-Blackwell, 326 pp.

Burbank, D.W., Anderson, R.S., 2001. Tectonic Geomorphology. Blackwell, Great Britain. 274 pp.

Burke, K., Dewey, J. F., Cooper, C., Mann, P., Pindell, J. L., 1984. Caribbean tectonics and relative plate motions, Geological Soc. of America, Memoir 162, 31-63.

C

Cacho, I., Grimalt, J. O., Pelejero, C., Canals, M., Sierro, F. J., Flores, J. A., Shackleton, N. J., 1999. Dansgaard–Oeschger and Heinrich event imprints in Alboran Sea paleotemperatures. Paleoceanography 14, 698–705.

Caputo, R., Salviulo, L., Bianca., M., 2008. Late Quaternary activity of the Scorciabuoi Fault (Southern Italy) as inferred from morphotectonic investigations and numerical modelling Tectonics 27, TC3004, doi:10.1029/2007TC002203.

Caputo, R., Bianca, M., D'Onofrio, R., 2010. Ionian marine terraces of Southern Italy: Insights into the Quaternary tectonic evolution of the area. Tectonics TC4005, doi:10.1029/2009TC002625.

Carcaillet J., Bourlès D. L., Thouveny N., 2004. Geomagnetic dipole moment and ^{10}Be production rate intercalibration from authigenic ^{10}Be/^{9}Be for the last 1.3 Ma. Geochem., Geophys., Geosystem, 5, doi 10.1029/2003GC000641.

Carcaillet, J., Mugnier, J.L., Koçi, R., Jouanne, F., 2009. Uplift and active tectonics of southern Albania inferred from incision of alluvial terraces. Quat. Res. 71, 465-476.

Carminati, E., Doglioni, C., Argnani, A., Carrara, G., Dabovski, C., Dumurdzanov, N., Gaetani, M., Georgiev, G., Mauffret, A., Nazai, S., Sartori, R., Scionti, V., Scrocca, D., Séranne, M., Torelli, L., Zagorchev, I., 2004. TRANSMED Transect III. In Cavazza, W., Roure, F., Spakman, W., Stampfli, G.M., Siegle, P. (Eds.), The TRANSMED Atlas – The Mediterranean region from Crust to Mantle. Springler, Berlin Heidelberg.

Carozza, J.-M., Delcaillau, B., 1999. Geomorphic record of Quaternary tectonic activity by Alluvial terraces: example from the Tet basin (Roussillon, France). Earth and Planetary Sci. 329, 735-740.

Carretier, S., Lucazeau, F., 2005. How does alluvial sedimentation at range fronts modify the erosional dynamics of mountain catchments?. Basin Res. 17, 361– 381.

Carretier, S., Poisson, B., Vassallo, R., Pepin, E., Farias, M., 2009. Tectonic interpretation of transient stage erosion rates at different spatial scales in an uplifting block, J. of Geophys. Res. 114, F02003, doi:10.1029/2008JF001080.

Carrillo, E., 2006. L'Enregistrement sédimentaire de la sismicité récente le long de la frontière sudoccidentale de la plaque caraïbe 'Faille de Boconó) : Modalités et chronologie. Contribution à l'estimation de l'aléa sismique régional. Ph.D. Thesis, Université de Savoie, France, 335 pp.

Carrillo, E., Audemard, F., Beck, C., Cano, V., Castilla, R., Cousin, M., Jouanne, F., Melo, L., Villemin, T., 2006. A late Pleistocene sedimentary seismograph along the Boconó fault (Mérida Andes, Venezuela): Themoraine-dammed Los Zerpa paleo-lake. Bull. Soc. Géol. Fr. 177, 3-17.

Cediel, F., Shaw, R. P., Cáceres, C., 2003. Tectonic assembly of the Northern Andean Block. In: Bartolini, C., Buffler, R.T., Blickwede, J. (Eds), The Circum-Gulf of Mexico and the Caribbean: Hydrocarbon habitats, basin formation, and plate tectonics. AAPG Memoir 79, 815-848.

Chabreyrou, J., 2006. Morphologie fluviale et structures tectoniques actives en Albanie. Master Thesis, Université Joseph Fourier, France.

Chmeleff, J., Von Blanckenburg, F., Kossert, K., Jakob, D., 2010. Determination of the ^{10}Be half-life bymulticollector ICP-MS and liquid scintillation counting. Nucl. Instruments and Methods in Phys. Res. Sect. B: Beam Interac. with Mater. and Atoms 268, 192-199.

Clark, Peter U., Dyke, Arthur S., Shakun, Jeremy D., Carlson, Anders E., Clark, Jorie, Wohlfarth, Barbara, Mitrovica, Jerry X., Hostetler, Steven W., 2009. The Last Glacial Maximum. Sci. 325 – 5941, 710–714.

Colletta, B., Roure, F., De Toni, B., Loureiro, D., Passalacqua, H., Gou, Y., 1997. Tectonic inheritance, crustal architecture, and contrasting structural styles in the Venezuelan Andes. Tectonics 16 (5), 777-794.

Colmenares, L., Zoback, M. D, 2003. Stress field and seismotectonics of Northern South America. Geology 31, 721-724.

Copley, A., Boait, F., Hollingsworth, J., Jackson, J., McKenzie, D., 2009. Subparallel thrust and normal faulting in Albania and the roles of gravitational potential energy and rheology contrasts in mountain belts. J. of Geophys. Res. 114, B05407, doi:10.1029/2008JB005931.

Cordier, S., Harmand, D., Losson, B., Beiner, M., 2004. Alluviation of the Meurthe and Moselle valleys (Eastern Paris Basin, France): lithological contribution to the study of the Moselle capture and Pleistocene climatic fluctuations. Quaternaire 15, 65–76.

Cordier, S., Harmand, D., Frechen, M., Beiner, M., 2006. Fluvial system response to Middle and Upper Pleistocene climate change in the Meurthe and Moselle valleys (Eastern Paris Basin and Rhenish Massif). Quat. Sci. Rev. 25, 1460–1474.

Corredor, F., 2003. Eastward extent of the Late Eocene-Early Oligocene onset of deformation across the Northern Andes: constraints from the Northern portion of the Eastern Cordillera fold belt, Colombia. J. of South American Earth Sci. 16, 445-457.

Cortés, M., Angelier, J., 2005. Current states of stress in the Northern Andes as indicated by focal mechanisms of earthquakes. Tectonophysics 403, 29-58.

Craddock, W.H., Kirby, E., Harkins, N.W., Zhang, H., Shi, X., Liu, J., 2010. Rapid fluvial incision along the Yellow River during headward basin integration. Nature Geosci. 3, 209-213.

Craig, H., 1954. Carbon 13 in plants and the relationships between carbon 13 and car bon 14 variations in nature. J. Geol. 62, 115-149.

Cushman-Roisin, B., Gačić, M., Poulain, P. M., Artegiani. A., 2001. Physical Oceanography of the Adriatic Sea: Past, Present and Future, Springer, New York. 304 pp.

D

D'Agostino, N., Avallone, A., Cheloni, D., D'Anastasio, E., Mantenuto, S., Selvaggi, G. 2008. Active tectonics of the Adriatic region from GPS and earthquake slip vectors, J. Geophys. Res., 113, B12413.

Dansgaard, W., Johnsen, S. J., Clausen, H. B., Dahl-Jensen, D., Gundestrup, N. S., Hammer, C. U., Hvidberg, C. S., Steffensen, J. P., Sveinbjörnsdottir, A. E., Jouzel, J., Bond, G..1993. Evidence for general instability of past climate from a 250,000- year ice-core record. Nature 364, 218–20.

de Abreu, L., Shackleton, N. J., Schönfeld, J., Hall, M. A., Chapman, M.R., 2003. Millenial-scale oceanic climate variability off the Western Iberian margin during the last two glacial periods. Mar. Geol., 196, 1–20.

Delcaillau, B., 1986. Dynamique et évolution morpho-structurale du piémont frontal de l'Himalaya : les Siwalik de l'Himalaya du Népal oriental: Rev. Géogr. Phys. Géol. Dynam. 27, 319–337.

Delcaillau, B., 2004. Reliefs et Tectonique Récente. Paris, Vuibert. 259 pp.

Delcaillau, B., Deffontaines, B., Floissac, L., Angelier, J., Deramond, J., Souquet, P., Chu, H. T., Lee, J. F., 1998. Morphotectonic evidence from lateral propagation of an active frontal fold; Pakuashan anticline, foothills of Taiwan. Geomorphology 24, 263–290.

Delcaillau, B., Laville, E., Amrhar, M., Namous, M., Dugué, O., Pedoja, K., 2010. Quaternary evolution of the Marrakech High Atlas and morphotectonic evidences of the Tizi N'Test Faul activity, Morocco. Geomorphology 118, 262-279.

Denefle, M., Lézine, A.M., Fouache, E, Dufaure, J.J., 2000. A 12 000-Year pollen record from lake Maliq, Albania. Quat. Res. 54, 423-432.

De Toni, B., Kellogg, J., 1993. Seismic evidence for blind thrusting of the Northwestern flank of the Venezuelan Andes. Tectonics 12, 1393-1409.

Dhont, D., Backé, G., Hervouët, Y., 2005. Plio-Quaternary extension in the Venezuelan Andes: Mapping from SAR JERS imagery. Tectonophysics 399, 293-312.

Dilek, Y., Furnes, H., Shallo, M., 2008. Geochemistry of the Jurassic Mirdita Ophiolite (Albania) and the MORB to SSZ evolution of a marginal basin oceanic crust. Lithos 100, 174–209.

Dirección de Cartografía Nacional, 1976. Mapas Topograficos a escala 1:25000. Hojas: Barinitas, Rio Calderas, Qda. Seca, Campo Azul, La yuca.

Dirszowsky, R.W., Mahaney, W.C., Hodder, K.R., Milner, M.W., Kalm, V., Bezada, M., Beukens, R.P., 2005. Lithostratigraphy of the Mérida (Wisconsinan) glaciation and Pedregal interstade, Mérida Andes, NorthwesternVenezuela. J. of South American Earth Sci. 19, 525–536.

Duerto, L., Audemard, F. E., Lugo, J., Ostos, M., 1998. Síntesis de las principales zonas triangulares en los frentes de montaña del occidente venezolano. IX Congreso Venezolano de Geofísica (in CD-Rom; paper # 25).

Dumurdzanov, N., Serafimovski, T., Burchfiel, B. C., 2005. Cenozoic tectonics of Macedonia and its relation to the South Balkan extensional regime. Geosphere 1-1, 1-22.

Dunai, T.J., 2001. Influence of secular variation of the geomagnetic field on production rates of in situ produced cosmogenic nuclides. Earth Planet. Sci. Lett. 193, 197–212.

Dunai, T.J., 2010. Cosmogenic Nuclides. Principles, Concepts and Applications in the Earth Surface sciences. Cambridge, University Press. 187 pp.

Dunne, J., Elmore, D., Muzikar, P., 1999. Scaling factors for the rates of production of cosmogenic nuclides for geometric shielding and attenuation at depth on sloped surfaces. Geomorphology 27, 3–11.

E

Easterbrook, Don J., 1999. Surface Processes and Landforms, 2nd Edition. Upper Saddle River, NJ: Prentice Hall. ISBN 0-13-860958-6.

F

Fairbridge, R. W., 1968. Encyclopedia of Geomorphology. Reinhold Book Company, New York.

Ferrer, C., 1991. Características geomorfológicas y neotectónicas de un segmento de la falla de Boconó entre la ciudad de Mérida y la Laguna de Mucubají, Estado Mérida. Guía de la excursión. Escuela Latinoamericana de Geofísica, 25 pp.

Fouache, E., Desruelles, S., Magny, M., Bordon, A., Oberweiler, C., Coussot, C., Touchais, G., Lera, P., Lézine, A-M., Fadin, L., Roger, R., 2010a. Paleogeographical reconstruction of Lake Maliq (Korça Basin, Albania) between 14000 BP and 2000 BP. J. of Archaeological Sci. 37, 525-535

Fouache, E., Vella, E., Dimo, L., Gruda, G., Mugnier, J-L., Dènefle, M., Monnier, O., Hotyat, M., Huth, E., 2010b. Shoreline reconstruction since the Middle Holocene in the vicinity of the ancient city of Apollonia (Albania, Seman and Vjosa deltas). Quat. International 216, 118-128.

Fourcart J. 1921. Carte Geologique des confines Albanais. 1/200000. Published by the service géographique de l'armée française.

Freymueller, J. T., Kellogg, J. N., Vega, V., 1993. Plate motions in the North Andean region. J. of Geophys. Res. 98 (12), 21.853- 21.863.

Fuller, I.C., Macklin, M.G., Lewin, J., Passmore, D.G., Wintle, A.G., 1998. River response to high-frequency climate oscillations in Southern Europe over the Past 200 k.y. Geology 26(3), 275-278.

Funvisis, 1997. Estudio neotectónico y geología de fallas activas en el piedemonte surandino de los Andes venezolanos (Proyecto INTEVEP 95-061). Funvisis unpublished report for INTEVEP, S.A. 155 pp ± appendices.

G

Gardner, T.W., Jorgensen, D.W., Schuman, C., Lemieux, 1987. Geomorphic and tectonic process rates: effects of measured time interval. Geology 15, 259–261.

Gardner, T. W., Verdonck, D., Pinter, N. M., Slingerland, R. L., Furlong, K. P., Bullard, T. F., Wells, S. G., 1992. Quaternary uplift astride the aseismic Cocos Ridge, Pacific Coast, Costa Rica: Geological Soc. of America Bull., 104, 219-232.

Geraga, M., Tsaila-Monopolis, S., Ioakim, C., Papatheodorou, G., Ferentinos, G., 2005. Short-term changes in the southern Aegean Sea over the last 48,000 years. Palaeoceanoraphy, Palaeoclimatology, Palaeoecology 220, 311–332.

Giegengack, R. 1984. Late Cenozoic tectonic environments of the central Venezuelan Andes. In: Bonini, W., Hargraves, R. Shagam, R., (Eds), The Caribbean-South American plate boundary and regional tectonics. Memoir - Geological Soc. of America, 162, 343-364.

Gilbert, G. K., 1877, Report on the geology of the Henry Mountains [Utah]. Publication of the Powell Survey, U.S. Government Printing Office, Washington D.C., 160 pp.

Giraldo, C., 1985. Neótectonique et sismotectonique de la région d'El Tocuyo-San Felipe (Vénézuéla centro-occidental). Ph.D. Thesis, Université de Montpellier II, 130 pp.

González, C., Dupont, L. M., Behling, H., Wefer, G., 2008. Neotropical vegetation response to rapid climate changes during the last glacial: Palynological evidence from the Cariaco basin. Quat. Res. 69, 217–30.

Google earth V 6.1.0.5001 (Mai 7, 2005). Barinitas city, Mérida Andes. 8° 43.653'N, 70° 20.988'W, Eye alt 1.57 km. SIO, NOAA, U.S. Navy, NGA, GEBCO. GeoEye 2012. http://www.googleearth.com.

Gosse, J., Phillips, F., 2001. Terrestrial in situ cosmogenic nuclides: theory and application. Quat. Sci. Rev. 20, 1475-1560.

Grootes, P. M., Stuiver, M., White, J., Johnson S., Jouzel, J., 1993. Comparison of oxygen isotope records from the GISP2 and GRIP Greenland ice cores. Nature 366, 552-554.

Grootes, P.M., Stuiver, M., 1997. Oxygen 18116 variability in Greenland snow and ice with 10^3- to 10^5-year time resolution. J. of Geophys. Res. 102 (26) 455–26,470.

Guzmán, O., Mugnier, J-L., Koçi, R., Vassallo, R., Carcaillet, J., Jouanne, F., Fouache, E., 2011. Active tectonics of Albania inferred from fluvial terraces geometries. 2nd INQUA-IGCP 567 International Workshop on Active Tectonics, Earthquake Geology, Archaeology and Engineering. Proceedings Volume 2, 2011

Guzmán, O., Mugnier, J.L., Vassallo, R., Koçi, R., Jouanne, F. Vertical slip rate of major active faults of southern Albania inferred from river terraces. (Submitted).

Guzmán, O., Mugnier, J-L., Koçi, R., Vassallo, R., Carcaillet, J., Jouanne, F., Fouache, E.. Chronostratigraphy and incision of Albanian river terraces over the last 200 ka and their climatic implications. (In preparation)

H

Hack, J.T., 1957. Studies of longitudinal stream profiles in Virginia and Maryland. U.S. Geological Survey Professional Paper 294-B, 45–97.

Hackley, P. C., Urbani, F., Karlsen, A. W., Garrity, C. P., 2005. Geologic Shaded Relief Map of Venezuela. U.S. Geological Survey Open File Report 2005-1038.

Hajdas, I., Ivy, S., Beer, J., Bonani, G., Imboden, D., Lotted, A., Sturm, M., Suter, M., 1993. AMS radiocarbon dating and varve chronology of Lake Soppensee: 6000 to 12000 ^{14}C years BP. Climate Dynamics 9 (3), 107-116.

Hamlin, R.,Woodward, J., Black, S., Macklin, M.G., 2000. Sediment fingerprinting as a tool for interpreting long-term river activity: the Voidomatis basin, NW Greece. In: Foster, I. D. L., (Ed.), Tracers in Geomorphology. Wiley, Chichester, pp. 473–501.

Hancock, G.S., Anderson, R.S., Chadwick, O.A., Finkel, R.C., 1999. Dating fluvial terraces with ^{10}Be and ^{26}Al profiles: application to the Wind River, Wyoming. Geomorphology 27, 41–60.

Hancock, G.S., Anderson, R.S., 2002. Numerical modeling of fluvial strath-terrace formation in response to oscillating climate. GSA Bull. 114 (9), 1131–1142.

Harvey, A.M., Miller, S.Y., Wells, S.G., 1995. Quaternary soil and river terrace sequences in the Aguas/Feos river systems Southeast Spain. In: Lewin, J., Macklin, M.G., Woodward, J.C. (Eds.) Mediterranean Quaternary River Environments. Balkema, Rotterdam, 263–281.

Hastenrath, S., 1984. Interannual variability and the annual cycle: Mechanisms of circulation and climate in the tropical Atlantic sector. Monthly Weather Rev. 112, 1097-1107.

Haug, G. H., Hughen, K. A., Sigman, D. M., Peterson, L. C., Rohl, U., 2001. Southward migration of the Intertropical Convergence Zone through the Holocene. Sci. 293, 1304–1308.

Heinrich, H., 1988. Origin and consequences of cyclic ice rafting in the Northeast Atlantic Ocean during the past 130,000 years. Quat. Res. 29, 142-152.

Hemming, S. R., 2004. Heinrich events: Massive Late Pleistocene detritus layers of the North Atlantic and their global climate imprint. Rev. Geophys. 42, RG1005, doi:10.1029/2003RG000128.

Henneberg, H.G., Schubert, C. 1986. Geodetic networks along the Caribbean-South American plate boundary. Tectonophysics, 130, 77-94.

Hetzel, R., Niedermann, S., Tao, M.X., Kubik, P.W., Ivy-Ochs, S., Gao, B., Strecker, M.R., 2002. Low slip rates and long-term preservation of geomorphic features in Central Asia. Nature 417, 428–432.

Heyman, J., Stroeven, A. P., Harbor, J. M., Caffee, M. W. 2011. Too young or too old: Evaluating cosmogenic exposure dating based on an analysis of compiled boulder exposure ages. Earth and Planetary Sci. Letters 302, 71-80.

Holtvoeth, J., Vogel, H., Wagner, B., Wolff, G. A., 2010. Lipid biomarkers in Holocene and glacial sediments from ancient Lake Ohrid (Macedonia, Albania). Biogeosci. Discuss. 7, 4607– 4640.

Hospers, J., Van Wijnen, J., 1959. The gravity field of the Venezuelan Andes and adjacents basins. Verslag van de Gewone Vergadering van de Afdeling Natuurkunde, Koninklijke Nederlandse Akademie van Wetenschappen 23 (1), 1-95.

Huber, O., 1995. Geographical and physical features. In: Berry, P. E., Holst, B. K., Yatskievych, K. (Eds), Flora of the Venezuelan Guayana. Vol. 1.Missouri Botanical Garden Press, St. Louis, 1–61.

Hughen, K. A., Overpeck, J. T., Peterson, L. C., Trumbore, S. E., 1996. Rapid climate changes in the tropical Atlantic during the last deglaciation. Nature 380, 51–54.

Hughen, K. A., Southon, J. R., Lehman, S. J., Overpeck, J. T., 2000. Synchronous radiocarbon and climate shifts during the last deglaciation. Sci. 290, 1951–54.

Hughen, K. A., Eglinton, T. I., Xu, L., Makou, M., 2004. Abrupt tropical vegetation response to rapid climate changes. Sci. 304, 1955–59.

Hughes, P.D., 2004. Quaternary Glaciation in the Pindus Mountains, Northwest Greece. Ph.D. thesis, University of Cambridge. 341 pp.

Hughes, P.D.,Woodward, J.C., Gibbard, P.L.,Macklin,M.G., Gilmour, M.A.,Smith, G.R., 2006. The glacial history of the Pindus Mountains, Greece. J. of Geology 114, 413–434

I

Institute of Hydrometeorology Albania, 1984. The climate of Albania. IHM-Publication (in Albanian).

Institutin Topografik te Ushtrise Tirane, 1959-1990. Topographic maps of Socialist Republic of Albania in scale: 1:25000. Archive of Institute of Seismology, Tirana, Albania. (in Albanian).

Ishihara, T., Sugai, T., Hachinoe, S., 2012. Fluvial response to sea-level changes since the latest Pleistocene in the near-coastal lowland, central Kanto Plain, Japan. Geomorphology 147-148, 49-60.

J

Jácome, M., Audemard, F. E., Graterol, V., 1995. A Seismic, Gravimetric and Geologic Interpretation of a Transandean Profile Across the Venezuelan Andes. I Latinoamerican Geophys. Congress, Rio de Janeiro, Brasil, 15-18.

Jahn, A. 1925. Observaciones galaciologicas en los Andes Venezolanos. Cultura Venezolana 64, 265-280.

Jahn, A. 1931. Los Paramos venezolanos. Boletín de la Sociedad Venezolana de Ciencias Naturales 1 (3), 93-132.

James, K. H., 2000. The Venezuelan hydrocarbon habitat, part 1: tectonics, structure, palaeogeography and source rocks. J. of Petroleum Geology 23(1), 5-53.

Jordan, T., 1975. The present-day motions of the Caribbean plate. J. of Geophys. Res. 80, 4433– 4439.

Joanne, F., Audemard, F., Beck, C., van Welden, A., Ollarves, R., Reinoza, C., 2011. Present-day deformation along the El Pilar Fault in eastern Venezuela: Evidence of creep along a major transform boundary. J. of Geodynamics 51, 398-410.

Jouanne, F., Mugnier, J.L., Koci, R., Bushati, S., Matev, K., Kuka, N., Shinko, I., Kociu, S., Duni, L., 2012. GPS constraints on current tectonics of Albania. Tectonophysics. doi: 0.1016/j.tecto.2012.06.008

K

Kallel, N., Duplessy, J.C., Labeyrie, L., Fontugne, M., Paterne, M., Montacer, M., 2000. Mediterranean pluvial periods and Sapropel formation over the last 200,000 years. Palaeogeography, Palaeoclimatology, Palaeoecology 157, 45–58.

Kalm, V., Mahaney, W. C., 2011. Late Quaternary Glaciation in the Venezuelan (Mérida) Andes. Developments in Quart. Sci. 15. 835-841.

Kamen, M. D., 1963. Early History of Carbon-14: Discovery of this supremely important tracer was expected in the physical sense but not in the chemical sense. Science 140 (3567), 584–590

Kaniuth, K., Drewes, H., Stuber, K., Temel, H., Hernández, J. N., Hoyer, M., Wildermann, E., Kahle, H. G., Geiger, G., 1999. Position changes due to recent crustal deformations along the Caribbean-South American plate boundary derived from CASA GPS project. General Assembly of the International Union of Geodesy and Geophysics (IUGG), Birmingham, U.K. Poster at Symposium G1 of International Association of Geodesy.

Kaplan, M. R., Wolfe, A. P., 2006. Spatial and temporal variability of Holocene temperature in the north Atlantic region. Quat. Res. 65, 223–31.

Karlen, I., Olsson, I. U., Kallberg, P., Kilicci, S., 1966. Absolute determination of the activity of two ^{14}C dating standards: Arkiv Geofysik 6, 465-471.

Kastelic, V., Basili, R., Duni, L., Koçi, R., 2012. Contributions to European Database of Seismogenic fauts, within the EU-FP7 Project "Seismic hazard harmonization in Europe (SHARE)". http://diss.rm.ingv.it/share-edsf/.

Kaufman, D. S., Ager, T. A ., Anderson, N. J., Anderson, P. M., Andrews, J. T., Bartlein, P. J., Brubaker, L. B. , Coats, L. L., Cwynar, L. C., Duvall, M. L., Dyke, A. S., Edwards, M. E., Eisner, W. R., Gajewski, K. , Geirsdottir, A., Hu, F. S., Jennings, A. E., Kaplan, M. R., Kerwin, M. W., Lozhkin, A. V., MacDonald, G. M., Miller, G. H., Mock, C. J., Oswald, W. W., Otto-Bliesner, B. L., Porinchu, D. F., Ruhland, K., Smol, J. P., Steigd, E. J., Wolfe, B. B., 2004. Holocene thermal maximum in the western Arctic (0–18° W). Quat. Sci. Rev. 23, 529–60.

Kellogg, J., Bonini, W., 1982. Subduction of the Caribbean Plate and basement uplifts in the overriding South-American Plate. Tectonics 1(3), 251-276.

Kilias, A., Tranos, M., Mountrakis, D., Shallo, M., Marto, A., Turku, I., 2001. Geometry and kinematics of deformation in the Albanian orogenic belt during the Tertiary. Journal of Geodynamics 31 (2), 169–187.

Kiratzi, A., 2011. The 6 September 2009 Mw5.4 earthquake sequence in Eastern Albania, Turkish Journal of Earth Sciences, in press.

Knox, J.C., 1975. Concept of the graded stream. In: Melhorn, W.N., Flemal, R.C. Eds., Theories of Landform Development. A Proceedings Volume of the 6th Annual Geomorphology Symposia Series. Publications in Geomorphology, State University of New York, Binghamton, pp. 169–198.

Kohn, B., Shagam, R., Banks, P., Burkley, L., 1984. Mesozoic–Pleistocene fission track ages on rocks of the Venezuelan Andes and their tectonic implications. In: Bonini, W., Hargraves, R. Shagam, R., (Eds),

The Caribbean-South American plate boundary and regional tectonics. Memoir - Geological Soc. of America, 162, 366-384.

Koçi, R., 2007. Geomorphology of quaternary deposits of Albanian rivers. Ph.D. Thesis. Archive of Institute of Seismology, Tirana, Albania. (in Albanian).

Kooi, H., Beaumont, C., 1996. Large-scale geomorphology: classical concepts reconciled and integrated with contemporary ideas via surface processes model. J. Geophys. Res. 101, 3361-3386.

Korschinek, G., Bergmaier, A., Faesterman, T., Gerstmann, U.C., Knie, K., Rugel, G., Wallner, A., Dillmann, I., Dollinger, G., Lierse von Gostomski, C., Kossert, K., Maiti, M., Poutivsev, M., Remmert, A., 2010. A new value for the half-life of ^{10}Be by heavy-Ion elastic recoil detection and liquid scintillation counting. Nucl. Instrum. Methods Phys. Res. B268 (2), 187-191.

Kottek, M., Grieser, J., Beck C., Rudolf, B. & Rubel, F. 2006. World map of Köppen- Geiger climate classification updated. Meteorologische Zeitschrift 15, 259-263.

L

Lal, D., 1991. Cosmic ray labeling of erosion surfaces: *in situ* nuclide production rates and erosion models. Earth and Planet. Sci. Lett. 104, 424–439.

Lambeck, K., Bard, E., 2000. Sea-level change along the French Mediterranean coast since the time of the Last Glacial Maximum. Earth and Planet. Sci. Lett. 175, 203–222.

Lambeck, K., Chappell, J., 2001. Sea-level change through the last glacial cycle. Sci. 292, 679–686.

Lavé, J., Avouac, J. P., 2000. Active folding of fluvial terraces across the Siwaliks Hills, Himalayas of central Nepal. J. Geophys. Res. 105, 5735-5770.

Lea, D. W., Pak, D. K., Peterson, L. C., Hughen, K. A., 2003. Synchroneity of tropical and high-latitude Atlantic temperatures over the last glacial termination. Sci. 301, 1361–64.

Leopold, L. B., Wolman, M. G., Miller, J. P., 1964. Fluvial processes in geomorphology. San Francisco, Calif., W. H. Freeman and Company, 522 pp.

Leopold, L. B., Bull, W. B., 1979. Base level, aggradation, and grade. Proc. Am. Philos. Soc. 123, 168–202.

Lewin, J., Macklin, M. G., Woodward, J. C., 1991. Late Quaternary fluvial sedimentation in the Voidomatis basin, Epirus, Northwest Greece. Quat. Res. 35, 103-115.

Lewin, J. A., Gibbard, P.L., 2010. Quaternary river terraces in England: Forms, sediments and processes. Geomorphology 120, 293–311.

Libby, W F., 1955. Radiocarbon dating. University of Chicago press, 2nd edition, Chicago, 175 pp.

Liddle, R. A., 1928. The geology of Venezuela and Trinidad. MacGowan, Fort Worth, 552 pp.

M

Maas, G.S., Macklin, M.G., Kirkby, M.J., 1998. Late Pleistocene and Holocene river development in Mediterranean steepland environments, southwest Crete. In: Benito, G., Baker, V.R., Gregory, K.J. (Eds.), Palaeohydrology and Environmental Change. Wiley, Chichester, pp. 153–166.

Mackenzie, A. N., 1937. Sección geológica de la región de Barinas: Distritos Barinas, Bolívar y Obispos del Estado Barinas, Venezuela. Bol. Geol. y Min. 1 (2-4), 269-293.

Mackin, J.H., 1948. Concept of the graded stream. Geol. Soc. Am. Bull. 59, 463–512.

Macklin, M.G., Fuller, I.C., Lewin, J., Maas, G.S., Passmore, D.G., Rose, J., Woodward, J.C., Black, S., Hamlin, R.H.B., Rowa, J.S., 2002. Correlation of fluvial sequences in the Mediterranean basin over last 200 ka and their relationship to climate change. Quat. Sci. Rev. 21, 1633-1641.

Macklin, M.G., Lewin, J., Woodward, J.C 2012. The fluvial record of climate change. Phil. Trans. R. Soc. A 370, 2143–2172. doi:10.1098/rsta.2011.0608.

Maddy, D., 1997. Uplift-driven valley incision and river terrace formation in southern England. J. of Quat. Sci. 12, 539–545.

Maddy, D., Bridgland, D., Westaway, R., 2001. Uplift-driven valley incision and climate-controlled river terrace development in the Thames Valley, UK. Quat. International 79, 23 – 36.

Mahaney, W.C., Kalm, V., 1996. Field Guide for the International Conference on Quaternary Glaciation and Paleoclimate in the Andes Mountains, June 21-July 1, 1996. Quaternary Surveys Ltd, Toronto, Canada, 79 pp.

Mahaney, W. C., Milner, M. W., Voros, J., Kalm, V., Hütt, G., Bezada, M., Hancock, R. G. V., Aufreiter, S., 2000. Stratotype of the Mérida Glaciation at Pueblo Llano in the Northern Venezuelan Andes. J. of South American Earth Sci. 13, 761–774

Mahaney, W. C., Russell, S.E., Milner, M. W., Kalm, V., Bezada, M., Hancock, R.G.V., Beukens, R.P., 2001. Paleopedology of Middle Wisconsin/Weichselian Paleosols in the Mérida Andes. Venezuela. Geoderma 104, 215–237.

Mahaney, W. C., Milner, M. W., Kalm, V., Dirszowsky, R. W., Hancock, R. G. V., Beukens, R. P., 2008. Evidence for a Younger Dryas glacial advance in the Andes of worthWestern Venezuela. Geomorphology 96, 199–211.

Mahaney, W., Kalm, V., Menzies, J., Milner, M., 2010. Reconstruction of the Early Mérida, pre-LGM glaciation with comparison to Late Glacial Maximum till, northwestern Venezuelan Andes. Sedimentary Geology 226, 29–41.

Malfait, B., Dinkelman, M., 1972. Circum-Caribbean tectonic and igneous activity and the evolution of the Caribbean plate. Geological Society of America Bulletin 83 (2), 251– 272.

Marín, L., 1982. Mecanismo focal de algunos eventos sísmicos ocurridos en Venezuela. Undergraduate Thesis, Facultad de Ingeniería, Escuela de Ingeniería Geodésica, Universidad del Zulia, Maracaibo.

Martinson, D.G., Pisias, N.G., Hays, J. D., Imbrie, J., Moore, T. C., Jr., Shackleton, N. J., 1987, Age dating and the orbital theory of the Ice Ages: Development of a high resolution 0 to 300,000-year chronostratigraphy. Quat. Res. 27, 1-29.

Masarik, J., Frank, M., Schäfer, J. M., and Wieler, R., 2001. Correction of in situ cosmogenic nuclide production rates for geomagnetic field intensity variations during the past 800000 years. Geochim. Cosmochim. Acta, 65 (3-4), 515-521.

Mason, D., Little, T., Van Dissen, R.., 2006. Rates of active faulting during late Quaternary fluvial terrace formation at Saxton River, Awatere fault, New Zealand. Bull. Geological Soc. of America. 118. 1431-1446.

McClusky, S., Balassanian, S., Barka, A., Demir, C., Ergintav, S., Georgiev, I., Gurkan, O., Hamburger, M., Hurst, K., Kahle, H., Kasten, L., Kekelidze, G., King, R., Kotzev, V., Lenk, O., Mahmoud, S., Mishin, A., Nadariya, M., Ouzonis, A., Paradissis, D., Peter, Y., Prilepin, M., Reilinger, R., Sanli, I., Seeger, H., Tealeb, A., Toksöz, M. N., Veis, G., 2000. Global Positioning System constraints on plate kinematics and dynamics in the eastern Mediterranean and Caucasus. J. Geophys. Res. 105 (B3), 5695–5719.

McCormac, F.G., Hogg, A.G., Blackwell, P.G., Buck, C.E., Higham, T.F.G., Reimer, P.J., 2004. SHCal04 Southern hemisphere calibration 0–11.0 cal kyr BP. Radiocarbon 46, 1087–1092.

McGregor, G. R., Nieuwolt. S., 1998. Tropical climatology. 2nd ed. Chichester: J. Wiley and Sons, 339 pp.

Meço, S., Aliaj, SH., Turku, I., 2000. Geology of Albania. Gebruder Borntraeger, Berlin. Stuttgart (Beitrage zur Regionalen Geologie der Erde, Bd. 28), 246 pp.

Meese, D. A., Gow, A. J., Grootes, P., Mayewski, P. A., Ram, M., Stuiver, M., Taylor, K. C., Waddington, E. D., and Zielinski, G. A., 1994, The accumulation record from the GISP2 Core as an indicator of climate change throughout the Holocene: Science, v. 266, p. 1680–1682.

Melo, V. 1961. Neotectonic in the Elbassan-Peqin area from Shkumbin terraces –. Bul. Univ. Sht. Shkencave Natyrore II. (in Albanian).

Melo, V. 1996. The terraces of the Mat river. In: Aliaj, Sh., Melo, V., Hyseni, A., Skrami, J., Mëhillka, Ll. Muço, B., Sulstarova, E., Prifti, K., Pashko, P., Prillo, S. (Eds.), Neo-tectonic map of Albania in scale 1:200000, Archive of seismology Institute, Tirana, Albania. (in Albanian).

Merchel, S., Herpers, U., 1999. An update on radiochemical separation techniques for the determination of long lived radionuclides via Accelerator Mass Spectrometry. Radiochim. Acta 84, 215-219.

Meyer, G.A., Wells, S.G., Jull, A.J.T., 1995. Fire and alluvial chronology in Yellowstone National Park: climate and intrinsic controls on Holocene geomorphic processes. Geological Soc. of America Bull. 107, 1211–1230.

Mishev, K., 1964. Morfo"ogiya na terasite v dolinata na rieka Vidina (Res. La morphologie des terraces fluviales de la riviere Vidina). Izvestia na By"garsko Geograficko Dru'zstvo 4, 7–26.

Molin, P., Pazzaglia, F. J., Francesco, D., 2004, Geomorphic expression of active tectonics in a rapidly-deforming forearc, Sila Massif, Calabria, southern Italy. American J. of Sci. 304, 559-589.

Molnar, P., Sykes, L., 1969. Tectonics of the Caribbean and Middle America Regions from focal mechanisms and seismicity. Geological Soc. of America Bull. 80, 1639–1684.

Monasterio, M., Reyes, S., 1980. Diversidad ambiental y variación de la vegetación en los paramos de los Andes venezolanos. In: Monasterio, M. (Ed), Estudios ecológicos en los paramos andinos. Universidad de Los Andes, Mérida, 47–91.

Monod, B., Dhont, D., Hervouët, Y., 2010. Orogenic float of the Venezuelan Andes. Tectonophysics 490, 123–135.

Muceku, B., Mascle, G. Tashko, A. 2006. First results of fission-track thermochronology in the Albanides. In: Robertson, A. H. F., Mountrakis, D., (Eds.), Tectonic Development of the Eastern Mediterranean Region. Geol. Soc. London Spec. Publ., 260, 539–556.

Muceku, B., Van der Beek, P., Bernet, M., Reinerrs, P., Mascle, G., Tashko, A., 2008. Thermochronological evidence for Mio-Pliocene late orogenic extension in the north-eastern Albanides (Albania). Terra Nova 20, 180-187.

Muço, B., 1994. Focal mechanism solutions of earthquakes for the period 1964-1988. Tectonophysics, 231,

Muço, B., 1998. Catalogue of ML ≥ 3 earthquakes in Albania from 1976 to 1995 and distribution of seismic energy released. Tectonophysics, 29é, 311-319.

Muscheler, R., Kromer, B., Björck, S., Svensson, A., Frieddich, M., Kaiser, K. F., Southon, J., 2008. Tree rings and ice cores reveal 14C calibration uncertainties during the Younger Dryas. Nature Geoscience 1, 263-267.

N

Niewland, D.A., Oudemayer, B.C., Valbona, U., 2001. The tectonic development of Albania: explanation and prediction of structural styles. Marine and Petroleum Geology 18, 161–177.

Nesci, O., Savelli, D., 2003. Diverging drainage in the Marche Apennines (central Italy). Quaternary International, 101-102, 203-209.

Noller, Jay S., Sowers, Janet M., Lettis, William R. 2000. Quaternary geochronology: methods and applications. American Geophys. Union 4, 582 pp.

O

Oldow, J. S., Bally, A. W., Avé Lallemant, H. G., 1990, Transpression, orogenic float, and lithospheric balance. Geology 18, 991-994.

Olivero, M. L., Aguirre, J., Moncada, A., 2003a. Phenomena related to the movement of mud and debris occurred in the Páramo zone of Mérida in June 2003. Revista forestal Venezolana 49 (2), 131-141.

Olivero, M. L., Aguirre, J., Moncada, A., 2003b. Technical information about the movement of mud and debris occurred in the Páramo zone of Mérida in june 2003. Revista forestal Venezolana 49 (2), 143-151.

P

Paola, C. and Mohrig, D., 1996. Paleohydraulics revisited: paleoslope estimation in coarsegrained braided rivers. Basin Research, 8, 243-254.

Papazachos, C., Scordilis, E., Peci, V., 2002. P- & S-deep velocity structure of the southern Adriatic-Eurasia collision obtained by robust non-linear inversion of travel times. 50th ESC Assembly, Genoa, Extended Abstract, 8 pp.

Pazzaglia, F. J., 2013. Fluvial terraces, in Shroder, J. F., ed., Treatise on Geomorphology, Volume 9, 379-412, San Diego: Academic Press.

Pazzaglia, F. J., Gardner, T. W., Merrits, D. J., 1998. Bedrock fluvial incision and longitudinal profile development over geologic time scales determined by fluvial terraces. In: Tinkler, K. J.; Wohl, E. E., eds., Rivers over rock; fluvial processes in bedrock channels. Geophysical Monograph, 107, 207-235.

Pazzaglia, F.J., Brandon, M.T., 2001. A fluvial record of long-term steady-state uplift and erosion across the Cascadia forearc high, Western Washington state. American Journal of Science 301, 385–431.

Pedoja, K., Husson, L., Regard, V., Cobbold, P., Ostanciaux, E., Johnson, M., Kershaw, S., Saillard, M., Martinod, J., Furgerot, L., Weill, P., Delcaillau, B., 2011. Relative sea-level fall since the last interglacial stage: Are coasts uplifting worldwide? Earth-Science Rev. 108, 1–15.

Peel, M. C., Finlayson, B. L., McMahon, T. A., 2007. Updated world map of the Köppen-Geiger climate classification. Hydrology and Earth System Sciences 4 (2), 439–473.

Pérez, O. J., Bilham, R., Bendick, R., Velandia, J. R., Hernández, N., Moncayo, C., Hoyer, M., Kozuch, M., 2001. Velocity field accross the Southern Caribbean plate boundary and estimates of Caribbean/South-American plate motion using GPS geodesy 1994-2000. Geophys. Res. Lett. 28, 2987-2990.

Pérez, O. J., Bilham, R., Sequera, M., Molina, L., Gavotti, P., Codallo, H., Moncayo, C., Rodriguez, C., Velandia, R., Guzmán, M., Molnar, P., 2011. GPS derived velocity field in Western Venezuela: dextral shear component associated to the Boconó fault and convergent component normal to the Andes. Interciencia 36, 39–44.

Pérez-Peña, J. V., Azañon, M. J., Azor, A., 2009. Calypso: An ArcGis extensión to calculate hysometric curves and their statitical moments. Applications to dranaige basin analysis in SE Spain. J. Computer & Geosciences 35, 6, 1214-1223.

Personius, S. F., 1993. Age and Origin of Fluvial Terraces in the Central Coast Range, Western Oregon. U.S. Geological Survey Bulletin 2038, United Stated Government Printing Office, Washington, 46 pp.

Peterson, L. C., Haug, G. H., Hughen, K. A., Rohl, U., 2000a. Rapid changes in the hydrologic cycle of the tropical Atlantic during the last glacial. Sci. 290, 1947–51.

Peterson, L. C., Haug, G. H., Murray, R. W., Yarincik, K. M., King, J. W., Bralower, T. J., Kameo, K., Rutherford, S. D., Pearce, R. B., 2000b. Late Quaternary stratigraphy and sedimentation at ODP Site 1002, Cariaco basin (Venezuela). Proceedings of the Ocean Drilling Project: Scientific Results 165, 85–99.

Peterson, L. C., Haug. H. G., 2006. Variability in the mean latitude of the Atlantic Intertropical Convergence Zone as recorded by riverine input of sediments to the Cariaco basin (Venezuela). Palaeogeography, Palaeoclimatology, Palaeoecology 234, 97–113.

Phillips, F.M., Zreda, M.G., Gosse, J.C., Klein, J., Evenson, E.B., Hall, R.D., Chadwick, O.A., Sharma, P., 1997. Cosmogenic ^{36}Cl and ^{10}Be ages of Quaternary glacial and fluvial deposits of the Wind River Range, Wyoming. Geological Soc. of America Bull. 109 - 11, 1453–1463.

Pierce, G. R., 1960. Geología de la cuenca de Barinas: Boleltín de Geología. Publicación especial N° 3, 1: 214-276.

Pigati, J. S., and Lifton, N. A., 2004. Geomagnetic effects on time-integrated cosmogenic nuclide production with emphasis on *in situ* ^{14}C and ^{10}Be. Earth and Planet. Sci. Lett. 226 (1-2), 193-205.

Prifti, K., 1981. Formation of the quaternary valley of the upper Vjosa river . Archive of Institute of Seismology, Tirana, Albania. (in Albanian).

Prifti, K., 1984. Geomophology of quaternary deposits of the Devoll river. Buletini I Shkencave Gjeologjike 2, 43- 59. (in Albanian).

Pindell, J., Dewey, J., 1982. Permo-Triassic reconstruction of Western Pangea and the evolution of the Gulf of Mexico/Caribbean region. Tectonics 1 (2), 179–211.

Polissar, P. J. 2005. Lake records of Holocene climate change, Cordillera de Merida, Venezuela. Ph.D. Thesis, University of Massachusetts, USA, 207 pp.

Poveda, G., Waylen, P. R., Pulwarty, R.S., 2006. Annual and inter-annual variability of the present climate in Northern South America and Southern Mesoamerica. Palaeogeography, Palaeoclimatology, Palaeoecology 234, 3–27.

R

Rahmstorf, S., 2002. Ocean circulation and climate during the past 120 000 years. Nature 419, 207-214.

Raisbeck, G.M., Yiou, F., Bourlès, D.L., Lestringuez, J., and Deboffe, D., 1987. Measurements of ^{10}Be and ^{26}Al with a Tandetron AMS facility: Nuclear Instruments and Methods in Physics Research, 29, 22–26.

Ramsey, B., 2009. Bayesian analysis of radiocarbon dates. Radiocarbon 51(1), 337-360.

Rashid, H., Hesse, R., Piper, D.J., 2003. Evidence for an aditional Heinrich event between H5 to H6 in the Labrador Sea. Paleoceanogr. 18, 4, 1077-1091.

Reimer, P.J., Baillie, M.G.L., Bard, E., Bayliss, A., Beck, J.W., Blackwell, P.G., Bronk Ramsey, C., Buck, C.E., Burr, G.S., Edwards, R.L., Friedrich, M., Grootes, P.M., Guilderson, T.P., Hajdas, I., Heaton, T.J., Hogg, A.G., Hughen, K.A., Kaiser, K.F., Kromer, B., McCormac, F.G., Manning, S.W., Reimer, R.W., Richards, D.A., Southon, J.R., Talamo, S., Turney, C.S.M., van der Plicht, J., (2009). IntCal09 and Marine09 Radiocarbon Age Calibration Curves, 0–50,000 Years cal BP, Radiocarbon, 51(4), 1111-1150

Repka, J.L., Anderson, R.S., Finkel, R.C., 1997. Cosmogenic dating of fluvial terraces, Fremont River, Utah. Earth and Planet. Sci. Lett., 152, 59–73.

Ritter, D.F., Kochel, R.C., Miller, J.R., 1995. Process Geomorphology. 3rd edn. W.C. Brown Publishers, Dubuque, IA.

Ritz J-F., Brown, E. T., Bourlès, D. L., Philip, H., Schlupp, A., Raisbeck, G. M., Yiou, F., Enkhtuvshin, B., 1995. Slip rates along active faults estimated with cosmic-ray-exposure dates: Application to the Bogd fault, Gobi-Altaï, Mongolia. Geology, 23, 1019– 1022.

Ritz, J.-F., Vassallo, R., Braucher, R., Brown, E.T., Carretier, S., Bourlès, D.L., 2006. Using in situ-produced 10Be to quantify active tectonics in the Gurvan Bogd mountain range (Gobi-Altay, Mongolia). In: Siame, L., Bourlès, D.L., Brown, E.T., (Eds.), Geological Soc. of America Special Paper 415 "In Situ-Produced Cosmogenic Nuclides and Quantification of Geological Processes, 87–110.

Robertson, A., Shallo, M. 2000. Mesozoic-Tertiary tectonic evolution of Albania in its regional Eastern Mediterranean context. Tectonophysics 316 (3), 197-254.

Rockwell, T. K., Keller, E. A., Clark, M., N., Johson, D. L., 1984. Chronology and rates of faulting of Ventura River terraces, California**.** Geological Soc. of America Bull. 95, 12, 1466-1474,

Rod, E., 1958. Strike Slip Faults of Northern Venezuela. American Association of Petroleum Geologist Bull., 40(3), 457-475.

Roure, F., Nazaj, S., Mushka, K., Fili, I., Cadet, J.P., Bonneau, M., 2004. Kinematic evolution and petroleum systems - An appraisal of the Outer Albanides. In: McClay K. R., (Ed.), Thrust tectonics and hydrocarbon systems AAPG memoir 82, pp. 474-493.

Rull, V., 1998. Modern and Quaternary palynological studies in the Caribbean and Atlantic coasts of Northern South America: A palaeoecologically-oriented review. Boletín de la Sociedad Venezolana de Geologos 23, 5–24.

Rull, V., 2005. A Middle Wisconsin interstadial in the Northern Andes. J. of South American Earth Sci. 19, 173–79.

Rull, V., Salgado-Labouriau, M. L., Schubert, C., Valastro, S., 1987. Late Holocene temperature depression in the Venezuelan Andes: Palynological evidence. Palaeogeography, Palaeoclimatology, Palaeoecology 60, 109–21.

Rull, V., Abbott, M. B., Polissar, P., Wolfe, A. P., Bezada, M., Bradley, R. S., 2005. Late Quaternary paleoecology and paleolimnology of high-altitude tropical environment in the Venezuelan Andes. Quat. Res. 64, 308–17

Rull, V., Abbott, M. B., Vegas-Vilarrúbia, T., Bezada, M., Montoya, E., Nogué, S., González, C., 2010. Paleoenvironmental Trends in Venezuela during the Last Glacial Cycle. In: Sánchez-Villagra, M. R., Aguilera, O. A., Carlini, A. A. (Eds), Urumaco and Venezuelan paleontology: the fossil record of the Northern Neotropics. Indiana University Press, Bloomington, 52-83.

S

Sak, P. B., Fisher, D. M., and Gardner, T. W., 2004, Effects of subducting seafloor roughness on upper plate vertical tectonism; Osa Peninsula, Costa Rica: Tectonics, 23, 10.1029/2002TC001474.

Salgado-Labouriau, M. L., 1979. Modern pollen deposition in the Venezuelan Andes. Grana 18, 53–61.

Salgado-Labouriau, M. L., 1984. Late-Quaternary palynological studies in the Venezuelan Andes. Erdwissenschaftliche Forschung 18, 279–93.

Salgado-Labouriau, M. L., 1989. Late Quaternary climatic oscillations in the Venezuelan Andes. Biology International 18, 12–14.

Salgado-Labouriau, M. L., Schubert, C., 1976. Palynology of Holocene peat bogs from Central Venezuelan Andes. Palaeogeography, Palaeoclimatology, Palaeoecology 19, 147–56.

Salgado-Labouriau, M. L., Schubert. C., 1977. Pollen analysis of a peat bog from Laguna Victoria (Venezuelan Andes). Acta Cientifica Venezolana 28, 328–32.

Salgado-Labouriau, M. L., Schubert, C., Valastro, S., 1977. Palaeoecologic analysis of a Late Quaternary terrace from Mucubaji, Venezuelan Andes. J. of Biogeography 4, 313–25.

Salgado-Labouriau, M. L., Rull, V., Schubert, C., Valastro, S., 1988. The establishment of vegetation after Late Pleistocene deglaciation in the Paramo Miranda, Venezuelan Andes. Rev. of Palaeobotany and Palynology 55, 5–17.

Salgado-Labouriau, M. L., Bradley, R. S., Yuretich, R. F., Weingarten, B., 1992. Palaeoecological analysis of the sediments of Lake Mucubaji, Venezuelan Andes. J. of Biogeography 19, 317–27.

Sánchez Goñi, M.F., Cacho, I., Turon, J.-L., Guiot, J., Sierro, F.J., Peypouquet, J.-P., Grimalt, J.O., Shackleton, N.J., 2002. Synchroneity between marine and terrestrial responses to millennial scale climatic variability during the last glacial period in the Mediterranean region. Climate Dynamics 19, 95–105.

Savini, A., Corselli, C., Durmishi, C., Marku, S., Morelli, D., Tessarolo, C., 2011. Geomorphology of the Vlora Gulf Seafloor: Results from Multibeam and High-Resolution Seismic Data. J. of Coastal Research, Special Issue 58, 6-16.

Schmidt, S., Hetzel, R., Kuhlmann, J., Mingorance, F., Ramos, V., 2011. A note of caution on the use of boulders for exposure dating of depositional surfaces. Earth and Planet. Sci. Lett. 302, 60-70.

Schubert, C. 1970. Glaciation of the Sierra de Santo Domingo, Venezuelan Andes. Quaternaria 13, 232-261.

Schubert, C. 1974. Late Pleistocene Mérida glaciation, Venezuelan Andes. Boreas 3, 147–52.

Schubert, C. 1975. Glaciation and periglacial morphology in the northwestern Venezeualn Andes. Eiszeitalter und Gegenwart 26, 196-211.

Schubert, C., 1976. Definicion geológica de la Glaciación Mérida, Andes venezolanos. Boletín de Geología, Pub. Espe. 7 (2), 1181-1185.

Schubert, C., 1980a. Morfología neotectónica de una falla rumbo-deslizante e informe preliminar sobre la falla de Boconó, Andes merideños. Acta Científica Venezolana 31, 98-111.

Schubert C., 1980b. Late Cenozoic pull-apart basins, Boconó fault zone, Venezuelan Andes. J. of Structural Geology 2 (4), 463-468.

Schubert C., 1982. Neotectonics of the Boconó fault, Western Venezuela. Tectonophysics 85, 205-220.

Schubert, C. 1984. The Pleistocene and recent extent of the glaciers of the Sierra Nevada de Mérida, Venezuela. Erdwissenshaftliche Forshung 18, 269- 278

Schubert, C., Sifontes, R.S., 1970. Boconó-Fault, Venezuelan Andes - evidence of postglacial movement. Sci. 170, 66–69.

Schubert, C., Valastro, S., 1980. Quaternary Esnujaque Formation, Venezuelan Andes: Preliminary alluvial chronology in a tropical mountain range. Zeitschrift der Deutschen Geologischen Gesellschaft 131, 927–47.

Schubert, C., Rinaldi, M., 1987. Nuevos datos sobre la cronología del Estadio Tardio de la Glacicion Mérida, Andes Venezolanos. Acta Cientifica Venezolana 38, 135-136.

Schubert, C., Vaz, J. E., 1987. Edad termoluminiscente del complejo aluvial Cuaternario de Timotes, Andes venezolanos: Acta Cientifica Venezolana 38, 285-286.

Schubert, C., Clapperton, C. M., 1990. Quaternary glaciations in the Northern Andes (Venezuela, Colombia and Ecuador). Quat. Sci. Rev. 9, 123-135.

Schubert, C., Vivas, L., 1993. El Cuaternario de la cordillera de Mérida, Andes Venezolanos. 1º ed. ULA-Fundación Polar, 345 pp.

Schumm, S.A., 1977. The Fluvial System. Wiley, New York, 338 pp.

Schumm, S.A., 1993. River response to base-level change: implications for sequence stratigraphy. J. of Geology 101, 279–294.

Shackleton, N.J., 1987. Oxygen isotopes, ice volume and sea level. Quat. Sci. Rev. 6, 183-190.

Shackleton, N. J., Hall, M. A., Vincent, E., 2000. Phase relationships between millennial scale events 64,000 to 24,000 years ago. Paleoceanography15, 565–569.

Shackleton, N. J., Sánchez Goñi, M.F., Paillerc, D., Lancelot, Y., 2003. Marine Isotope Substage 5e and the Eemian Interglacial. Global and Planet. Change 36, 151-155.

Shagam, R., 1972. Andean research project, Venezuela: principal dat and tectonic implications. Geological Soc. of America. Memoir 132, 449-463.

Shagam, R., Kohn, B., Banks, P., Dasch, L., Vargas, R., Rodríguez, G., Pimentel, N., 1984. Tectonic implications of Cretaceous–Pliocene fission track ages from rocks of the circum-Maracaibo Basin region of Western Venezuela and Eastern Colombia. In: Bonini, W., Hargraves, R. Shagam, R., (Eds), The Caribbean-South American plate boundary and regional tectonics. Memoir - Geological Soc. of America 162, 385-412.

SHGJSH., 2003. Geological Map of Albania in scale 1:200000. Geological Service of Albania, Tirana, Albania, 2nd edn (in Albanian).

Sievers, W. 1886. Über Schneeverhältnisse in der Cordillere Venezuelas. Mitteeeilungen der Geographishen Gesellshaft München, Heft 10, 54-57.

Siddall, M., Rohling, E. J., Almogi-Labin, A., Hemleben, C., Meischner, D., Schmelzer, I., Smeed, D. A., 2003. sea-level fluctuations during the last glacial cycle. Nature 423 (6942), 853–858.

Silva, P.G., Badají, T., Calmel-Avila, M., Goy, J.L., Zazo, C., 2008a. Transition from alluvial to fluvial systems in the Guadalentín Depression (SE Spain) during the Holocene: Lorca Fan versus Guadalentín River. Geomorphology 100, 140-153.

Silva, P.G., Audemard, F.A., Mather, A.E., 2008b. Impact of active tectonic and uplift on fluvial landscapes and drainage development. Geomorphology 102 (1), 204 pp.

Singer, A., Audemard, F. A., 1997. Aportes de Funvisis al desarrollo de la geología de fallas activas y de la paleosismología para los estudios de amenaza y riesgo sísmico. Academia de las Ciencias Naturales, Matemáticas y Físicas. Publicación Especial 3, 25-38.

Sorel, D., Bizon, G., Aliaj, S., Hasani, L., 1992. Calage stratigraphique de l'âge et de la durée des phases compressives des Hellenéides externs (Grèce nord-occidentales et Albanie), du Miocène à l'actuel, Bull. Soc. Geol. France163, 447-454.

Soulas, J-P., 1985. Neotectónica del flanco occidental de los Andes de Venezuela entre 70º30' y 71º00'W (Fallas de Boconó, Valera, Piñango y del Piedemonte). VI Congreso Geológico Venezolano, Caracas, 4, 2690-2711.

Soulas, J-P., 1986. Neotectónica y tectónica activa en Venezuela y regiones vecinas. VI Congreso Geológico Venezolano Memorias, Septiembre-Octubre, Tomo X, p. 6639-6656.

Soulas, J-P., Rojas, C., Schubert, C., 1986. Neotectónica de las fallas de Boconó, Valera, Tuñame y Mene Grande. Excursión Nº 4. VI Congreso Geológico Venezolano, Caracas- 1985, 10, 6961-6999.

Stansell, N. D., Polissar, P. J. Abbott, M. B., 2007. Last Glacial Maximum Equilibrium-Line Altitude and paleo-temperature reconstructions for the Cordillera de Mérida, Venezuelan Andes. Quat. Res. 67, 115–27.

Starkel, L., 1994. Reflection of the Glacial-Interglacial Cycle in the evolutiuon of the Vistula River Basin, Poland. Terra Nova 6, 486–494.

Starkel, L., 2003. Climatically controlled terraces in uplifting mountain areas. Quat. Sci. Rev. 22, 2189–2198.

Stéphan, J-F., 1982. Evolution geodynamique du domaine caraibe Andes et chaines caraibe sur la transversele de Barquisimeto, Venézuéla. Ph.D. Thesis, Universitè Pierre et Marie Curie, Paris 1 and 2, 512 pp.

Stone, J.O., 2000. Air pressure and cosmogenic isotope production. J. of Geophys. Res. 105 (B10), 23,753-759.

Strahler, A. N., 1952. Hypsometric (area-altitude) analysis of erosional topography. Geological Soc. of America Bulletin 63(11), 1117-1142.

Strahler, A. N., 1957. Quantitative analysis of watershed geomorphology. Transactions of the American Geophys. Union 38 (6), 913–920.

Stuiver M, Polach H. A., 1977. Discussion: reporting of ^{14}C data. Radiocarbon 19 (3), 355–63.

Stuiver, M., Kra, R., 1986. Calibration issue. Radiocarbon 28 (2B), 805-1030.

Stuiver, M., Braziunas, T. F., Becker, B. and Kromer, B. 1991 Climatic, solar, oceanic, and geomagnetic influences on late-glacial and Holocene atmospheric $^{14}C/^{12}C$ change. Quat. Res. 35,1-24.

Stuiver, M., Long, A., Kra, R. S., 1993. Calibration. Radiocarbon 35 (1), 244 pp.

Stuiver, M., P.M. Grootes, Braziunas, T. F., 1995. The GISP2 18O climate record of the past 16,500 years and the role of the sun, ocean and volcanoes. Quat. Res. 44, 341-354.

Summerfield, M. A., 1985. Plate tectonics and landscape development on the African continent. In: Morisawa, M., Hack, J. (Eds.), Tectonic Geomorphology, Allen and Unwin, Boston, 27-51.

Sulstarova, E., 1986. Mechanism of earthquakes and field of present-day tectonic stresses in Albania. Ph.D. Thesis. Archive of Institute of Seismology, Tirana. (in Albanian).

Sulstarova, E., Peçi, V., Shuteriqi, P., 2000. Vlora-Elbasani-Dibra (Albania) transversal fault zone and its seismic activity. J. of Seismology 4, 117-131.

Sulstarova E, Kociaj S, Muco B, Peci V., 2003. "The Albanian earthquakes catalogue for historical and instrumental data with magnitude Mš4.5." Internal Report (behalf on NATO Project "Seismotectonic and Seismic Hazard Assessment in Albania", 1999-2002), Seismological Institute, Tirana, Albania.

Sykes, L., McCann, W., Kafka, A., 1982. Motion of Caribbean Plate during last 7 million years and implications for earlier Cenozoic movements. J. of Geophys. Res. 87 (B13), 10656– 10676.

T

Taboada, A., Rivera, L. A., Fuenzalida, A., Cisternas, A., Philip, H., Bijwaard, H., Olaya, J., Rivera, C., 2000. Geodynamic of the Northern Andes: Subductions and intracontinental deformation (Colombia). Tectonics 19(5), 787-813.

Tagari, Dh., 1993. Etude neotectonique et seismotectonique des Albanides: Analyse des deformations et geodynamique du Langhien a l'actuel. Ph.D. Thesis. Univ. Paris-Sud, Orsay, France.

Tagari, Dh., Vergely, P., Aliaj, Sh., 1993. Tectonique polyphasée plio-quaternarire en Albanie orientale (région de Korçë-Pogradeci). Bull. Soc. Géol. France 164-5, 727-737.

Taylor, J.A., Lloyd, J.L., 1992. Sources and sinks of atmospheric CO_2. Aust. J. Bot. 40, 407–418.

Tricart, J., 1966. Paléoclimats et terrasses quaternaires: C.R. Somm. seances. Societé Géologique de France (Fasc. 5). 202-203.

Tricart, J., Millies-Lacroix, A., 1962. Les terrasses quaternaires des Andes vénézueliennes. Bull. Soc. Géol. France, 7e Sér., 4, 201-219.

Tricart, J., Michel, M., 1965. Monographie et carte geomorphologique de la region de Lagunillas (Andes Vénézuéliennes). Revue de Geomorphologie Dynamique 15, 1-33.

Trenkamp, R., Kellogg, J., Freymueller, J., Mora, H., 2002. Wide plate margin deformation, Southern Central America and Northwestern South America, CASA GPS observations. J. of South American Earth Sci. 15, 157-171.

Trumbore, S; E., 2000. Constraints on below-ground carbon cycling from radiocarbon: the age of soil organic matter and respired CO2. Ecological Applications 10, 399-411.

Tzedakis, P.C., Andrieu, V., de Beaulieu, J-L., Crowhurst, S., Follieri, M., Hooghiemstra, H., Magri, D., Reille, M., Sadori, L., Shackleton, N.J., Wijmstra, T.A., 1997. Comparison of terrestrial and marine records of changing climate of the last 500,000 years. Earth and Planet. Sci. Lett. 150, 171–176.

Tzedakis, P.C., Frogley, M. R., Lawson, I. T., Preece, R. C., Cacho, I., de Abreu, L., 2004. Ecological thresholds and patterns of millennial-scale climate variability: The response of vegetation in Greece during the last glacial period. Geology 32, 109–12

V

Van Daele, M., van Welden, A., Moernaut, J., Beck, C., Audemard, F., Sánchez, J., Jouanne, F., Carrillo, E., Malavé, G., Lemus, A., de Batist, M., 2011. Reconstruction of Late-Quaternary sea- and lake-level changes in a tectonically active marginal basin using seismic stratigraphy: The Gulf of Cariaco, NE Venezuela. Marine Geology 279, 37-51.

van den Berg, M. W.,1996, Fluvial sequences of the Maas. Ph.D. Thesis, Landbouwuniversiteit, Netherlands, 181 pp.

Vandenberghe, J., 1995. Timescales, climate and river development. Quat. Sci. Rev. 14, 631–638.

Vandenberghe, J., Maddy, D., 2000. Quaternary Fluvial Archives. Geomorphology, 33, 3-4.

van der Beek, P., Summerfield, M.A., Braun, J., Brown, R.W., Fleming, A., 2002. Modeling postbreakup landscape development and denudational history across the southeast African (Drakensberg Escarpment) margin, J. Geophys. Res., 107(B12), 2351-2369.

van der Hammen, T. 1974. The Pleistocene changes of vegetation and climate in tropical South America. Journal of Biogeography 1, 3-26.

Vassallo, R., 2006. Chronologie et évolution des reliefs dans la région Mongolie-Sibérie: Approche morphotectonique et géochronologique. PhD. Thesis, Université Montpellier II, France, 280 pp.

Vassallo, R., Ritz, J.-F., Braucher, R., Jolivet, M., Carretier, S., Larroque, C., Chauvet, A., Sue, C., Todbileg, M., Bourles, D., Arzhannikova, A., Arzhannikov, S., 2007. Transpressional tectonics and stream terraces of the Gobi-Altay, Mongolia. Tectonics 26 (5), TC5013.

Vassallo, R., Ritz, J-F., Braucher, R., Carretier, S., 2005. Dating faulted alluvial fans with cosmogenic ^{10}Be in the Gurvan Bogd mountain range (Gobi-Altay, Mongolia): climatic and tectonic implications. Terra Nova. 17, 278-285.

Vassallo, R., Ritz, J.-F., Braucher, R., Jolivet, M., Carretier, S., Larroque, C., Chauvet, A., Sue, C., Todbileg, M., Bourles, D., Arzhannikova, A., Arzhannikov, S., 2007. Transpressional tectonics and stream terraces of the Gobi-Altay, Mongolia. Tectonics 26 (5), TC5013.

Vassallo, R.,Ritz, J.F., Carretier, S. 2011. Control of geomorphic processes on ^{10}Be concentrations in individual clasts: Complexity of the exposure history in Gobi-Altay range (Mongolia). Geomorphology, doi:10.1016/j.geomorph.2011.07.023.

Vignon, V., 2011. Activité hors séquence des chevauchements dans la syntaxe nord- ouest himalayenne : apports de la modélisation analogique et quantification quaternaire par analyse morphotectonique. PhD. Thesis, Université de Grenoble, France, 278 pp.

Villamil, T., Pindell, J. L., 1998. Mesozoic paleogeographic evolution of Northern South America: Foundations for sequence stratigraphic studies in passive margin strata deposited during non-glacial times. In: Pindell, J.L., Drake, C., (Eds), Paleogeographic Evolution and Non-glacial Eustacy: Northern South America. SEPM Special Publication, 283-318.

Vivas, L., 1979. Aracay y Pueblo Llano. Comparacion de las condiciones geomorfologicas de las cuencas de los rios Aracay y Pueblo Llano. Trabajo de ascenso inédito. Facultad de Ciencias Forestales. Universidad de Los Andes, 123 pp

Vivas, L., 1984. El Cuaternario. La Imprenta, Mérida, 266 pp.

Vogel, H., Wagner, B., Zanchetta, G., Sulpizio, R., Rosén, P., 2010. A paleoclimate record with tephrochronological age control fort he last glacial-interglacial cycle from Lake Ohrid, Albania and Macedonia, J. Paleolimnol. 44, 295–310.

W

Wadge, G., Burke, K., 1983. Neogene Caribbean plate rotation and associated central American tectonic evolution. Tectonics 2 (6), 633-643.

Waelbroeck, C., Labeyrie, L., Michel, E., Duplessy, J. C., McManus, J. F., Lambeck, K., Balbon, E., Labracherie, M., 2002. Sea-level and deep water temperature changes derived from benthic foraminifera isotopic records. Quat. Sci. Rev. 21 (1–3), 295–305.

Wagner, B., Lotter, A. F., Nowaczyk, N., Reed, J. M., Schwalb, A., Sulpizio, R., Valsecchi, V., Wessels, M., Zanchetta, G., 2009. A 40,000-year record of environmental change from ancient Lake Ohrid (Albania and Macedonia), J. Paleolimnol. 41, 407–430.

Wagner, B., Vogel, H., Zanchetta, G., Sulpizio, R., 2010. Enviromental change within the Balkan region during the past ca. 50 ka recorded in the sediments from lakes Prespa and Ohrid. Biogesciences 7, 3187–3198.

Waters, D. W., 1993. The tectonic evolution of Epirus, N.W. Greece. PhD thesis ,Univ. of Cambridge, Cambridge, England.

Weber, J.C., Dixon, T.H., DeMets, C., Ambeh, W.B., Jansma, P., Mattioli, G., Saleh, J., Sella, G., Bilham, R., Perez, O., 2001. GPS estimate of relative motion between the Caribbean and South American plates, and geologic implications for Trinidad and Venezuela. Geology 29, 75-78.

Wegmann, K.W., Pazzaglia, F.J., 2002. Holocene strath terraces, climate change, and active tectonics; the Clearwater River basin, Olympic Peninsula, Washington State. Geological Soc. of America Bull. 114 (6), 731–744.

Wegmann, K.W., Pazzaglia, F. J., 2009. Late Quaternary fluvial terraces of the Romagna and Marche Apennines, Italy. Quat. Sci. Rev. 28, 137-165.

Wesnousky, S. G., Aranguren, R., Rengifo, M, Owen, L., Caffee, M. W., Krishna, M., Pérez, O. J., 2012. Toward quantifying geomorphic rates of crustal displacement, landscape development, and the age of glaciation in the Venezuelan Andes. Geomorphology 141-142, 99-113.

Whipple, K. X., 2001. Fluvial landscape response time; how plausible is steady-state denudation? American J. of Sci., 301, 313-325.

Willet, S., Beaumount, C., Fullsack, P., 1993. Mechanical models for the tectonics of doubly vergent compressional orogens. Geology 21, 371-374.

Wohlfarth, B., Veres, D., Ampel, L., Lacourse, T., Blaauw, M., Preusser, F., Andrieu-Ponel, V., Kéravis, D., Lallier- ergès, E., Björk, S., Davies, S. M., de Beaulieu, J.-L., Risberg, J., Hormes, A., Kasper, H. U.,

Possnert, G., Reille, M., Thouveny, N., Zander, A., 2008. Rapid ecosystem response to abrupt climate changes during the last glacial period in western Europe, 40–16 ka. Geology 36, 407–410.

Woodward, J.C., Hamlin, R.B.H., Macklin, M.G., Karkanas, P., Kotjabopoulou E., 2001. Quantitative sourcing of slackwater deposits at Boila rockshelter: A record of late-glacial flooding and palaeolithic settlement in the Pindus Mountains, Northern Greece. Geoarchaeology 16(5), 501-536.

Woodward, J.C., Hamlin, R.H.B., Macklin, M.G., Hughes, P.D., Lewin, J., 2008. Glacial activity and catchment dynamics in northwest Greece: long-term river behaviour and the slackwater sediment record for the last glacial to interglacial transition. Geomorphology 101, 44–67.

Wright, J. D., 2000. Global Climate Change in Marine Stable Isotope Records. In: Noller, J. S., Sowers, J. M., Lettis, W. R. (Eds), Quaternary geochronology: methods and applications, American Geophysical Union Reference Shelf 4, 427-433.

World Meteorological Organisation, 1998. 1961-1990 global climate normals. Electronic resource. National Climatic Data Center, US: Asheville, NC.

Wortel, M. J. R, Spakman, W., 2000. Subduction and Slab Detachment in the Mediterranean-Carpathian Region. Sci. 290, 1910-1917.

Y

Yoris, F., Ostos, M., 1997. Well Evaluation Conference. Schlumberger Oilfield Services, Caracas, Venezuela, 1-40.

Z

Zaprowski, B. J., Evenson, E. B., Pazzaglia, F. J., Epstein, J. B., 2001. Knickzone propagation in the Black Hills and Northern High Plains; a different perspective on the late Cenozoic exhumation of the Laramide Rocky Mountains. Geology 29, 547-550.

Zinck, A., Stagno, P., 1966. Estudio edafologico de la zona de Santo Domingo-Pagüey, Estado Barinas: Division de Obras Hidraulicas, Ministerio de Obras Publicas, Caracas.

Zinck, A. 1980. Valles de Venezuela. Cuadernos Lagoven, 150 pp.